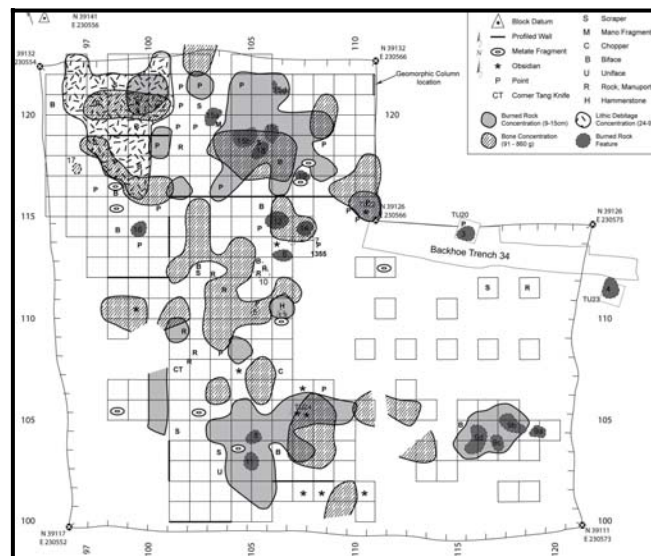
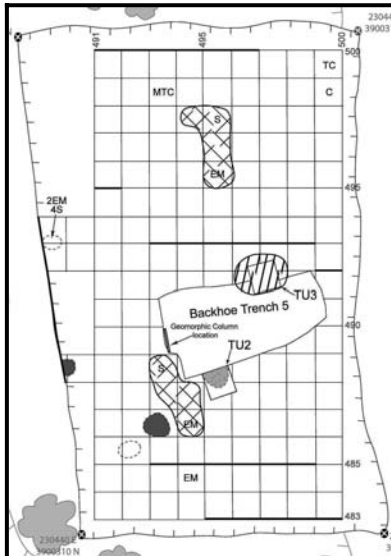


Landis Property: Data Recovery at Three Prehistoric Sites (41PT185, 41PT186, and 41PT245) in Potter County, Texas

Volume II: Appendices

By:

J. Michael Quigg, Charles D. Frederick, Paul M. Matchen, and Kendra G. DuBois



Prepared for:

Bureau of Land Management

Rio Puerco Field Office
Albuquerque, New Mexico

Prepared by:



TRC Environmental Corporation
Austin, Texas

TRC Report No. 150832

June 2010

**Landis Property: Data Recovery
at Three Prehistoric Sites (41PT185, 41PT186, and
41PT245) in Potter County, Texas
Volume II: Appendices**

By:

J. Michael Quigg, Charles D. Frederick, Paul M. Matchen, and Kendra G. DuBois

Prepared for:

**Bureau of Land Management
Rio Puerco Field Office
Albuquerque, New Mexico**

Prepared by:



**TRC Environmental Corporation
505 East Huntland Drive, Suite 250
Austin, Texas 78752**

**J. Michael Quigg, Principal Investigator
TRC Report No. 150832**

BLM Delivery Order Number NAD080024, Contract Number NAC050010

June 2010

TABLE OF CONTENTS VOLUME II

	<u>Page</u>
CHAPTERS 1-14.....	see Volume I
APPENDIX A BACKHOE TRENCH DESCRIPTIONS	617
APPENDIX B ARTIFACT DISTRIBUTIONS	671
APPENDIX C OBSIDIAN SOURCE ANALYSIS	685
APPENDIX D BIOSILICATE ANALYSIS AND PALYNOLOGY	695
APPENDIX E CHERT SOURCING IN THE TEXAS PANHANDLE: COMPOSITIONAL ANALYSES OF CHERT AND JASPER SOURCES AND ARTIFACTS, LANDIS PROPERTY PROJECT	735
APPENDIX F STARCH ANALYSES FROM THE BLM LANDIS PROPERTY	767
APPENDIX G ANALYSIS OF LIPIDS EXTRACTED FROM ARCHAEOLOGICAL BURNED ROCK AND POTTERY RESIDUES FROM SITES IN POTTER COUNTY, TEXAS	791
APPENDIX H STABLE ISOTOPE ANALYSIS ON BISON BONES	827
APPENDIX I PETROGRAPHIC ANALYSIS OF ABORIGINAL CERAMICS FROM THE BLM LANDIS PROPERTY, TEXAS PANHANDLE	833
APPENDIX J INSTRUMENTAL NEUTRON ACTIVATION ANALYSIS OF CLAYS AND CERAMICS FROM THE TEXAS PANHANDLE.....	857
APPENDIX K RADIOCARBON ASSAYS.....	873
APPENDIX L FUNCTIONAL ANALYSIS OF STONE TOOLS FROM BLM PROJECT - LANDIS PROPERTY IN THE TEXAS PANHANDLE (SITES 41PT186 AND 185/C).....	967
APPENDIX M LATE HOLOCENE PALEOENVIRONMENTAL HISTORY OF UPPER WEST AMARILLO CREEK VALLEY, TEXAS.....	995
APPENDIX N PLANT REMAINS FROM 41PT185/C, 41PT186, AND 41PT245	1035
APPENDIX O MULTI-INSTRUMENT GEOPHYSICAL INVESTIGATIONS AT 41PT185, 41PT186, AND 41PT245	1047
APPENDIX P DIATOM PALEOENVIRONMENTAL ANALYSIS OF SEDIMENTS FROM ARCHAEOLOGICAL SITE 41PT185/C, BLM PROJECT- LANDIS PROPERTY IN THE TEXAS PANHANDLE, POTTER COUNTY, TEXAS	1091
APPENDIX Q METRIC AND NON-METRIC DATA FOR ARTIFACTS FROM THE LANDIS PROPERTY SITES (41PT185, 41PT186, AND 41PT245) AND PROJECT ARTIFACT DATABASE.....	1119
APPENDIX R ORGANIC RESIDUE (FTIR) ANALYSIS OF BURNED ROCK, GROUNDSTONE, AND LITHIC SAMPLES FROM SITE 41PT185/C, POTTER COUNTY, TEXAS	1161

This page intentionally left blank.

APPENDIX A
BACKHOE TRENCH DESCRIPTIONS

BACKHOE TRENCH DESCRIPTIONS

Prepared for:



**TRC Environmental Corporation
505 East Huntland Drive, Suite 250
Austin, Texas 78752**

Prepared by:

**Charles D. Frederick, Ph.D.
Geosarcheological Consultant
Dublin, Texas**

TRENCH 1

Location: 0230420E 3900247N
 Core of T₁ surface on the right bank meander south of 41PT186

Geologic Units: Unit E resting unconformably upon a thin, truncated remnant of Unit D.

Cultural material: Broad ash bed between 7-10 cm, presumably clearance related; no other material observed.

Comments: Near channel overbank facies with multiple weakly developed buried soils.

Zone	Horizon	Depth (cm)	Description
1	C	0-7	Brown (7.5YR 4/3, m) loam, loose, weak fine subangular blocky structure, abrupt wavy boundary, violently effervescent; Unit E.
2	C	7-10	White (10YR 8/2, m) silt loam, loose, single grain, abrupt discontinuous boundary, violently effervescent, Ash, thin but extensive bed of ash, probably result of land clearance activity, with an oxidized rim beneath it in a few places.
3	C	10-28	Yellowish brown (10YR 5/4, m) silt loam, very friable, moderate medium subangular blocky structure, abrupt smooth boundary, violently effervescent, few granules throughout; Unit E.
4	Ab	28-50	Dark gray to dark grayish brown (10YR 4/1 to 4/2, m) loam, friable, moderate medium subangular blocky structure, gradual smooth boundary, violently effervescent, few bits of charcoal scattered throughout, buried soil; Unit E.
5	AC	50-81	Dark grayish brown (7.5YR 4/2, m) loam, firm, weak coarse prismatic structure, abrupt smooth boundary, violently effervescent; Unit E.
6	C	81-90	Brown-yellowish brown (10YR 5/3.5, m) slightly gravelly to gravelly loamy sand, loose, single grain, abrupt smooth boundary, violently effervescent, approximately 40% coarse fragments which are mostly sub-rounded caliche smaller than 1 cm in diameter, largest clast observed was 3 cm long; Unit E.
7	C	90-98	Yellowish brown (10YR 5/4, m) loam, hard, massive, clear to abrupt smooth boundary, violently effervescent, <1% coarse fragments; Unit E.
8	C	98-102	Brown (7.5YR 5/4, m) sand to loamy sand, slightly hard, weak medium subangular blocky structure, abrupt smooth boundary, violently effervescent, many (~50%) dark colored very dark gray to dark gray (10YR 3/1 to 4/1) worm casts, few granules throughout, original bed was a fairly clean sand prior to being run through by worms which resulted in a finer texture overall; Unit E.
9	2Ab	102-118	Dark gray (10YR 4/1, m) loam, hard, weak coarse subangular blocky structure, abrupt smooth boundary, violently effervescent, few (1-2%) coarse fragments.
10	2C	118-128	Brown (7.5YR 5/4, m) slightly gravelly loamy sand, slightly hard, massive, abrupt smooth boundary, violently effervescent, ~10-15% coarse fragments, numerous granules impart a speckled appearance; Unit E.
11	3Ab	128-145	Brown (7.5YR 5/4, m) loamy sand to sandy loam, hard, weak medium subangular blocky structure, abrupt smooth boundary, violently effervescent; Unit E.
12	3C	145-150	Brown (7.5YR 5/4, m) slightly gravelly loamy sand, slightly hard to loose, massive to weak very coarse subangular blocky structure, abrupt smooth boundary, violently effervescent, 5-15% coarse fragments; Unit E.
13	3C	150-167	Brown (7.5YR 5/3, m) sandy loam, hard, weak very coarse subangular blocky structure, abrupt smooth boundary, violently effervescent; Unit E.
14	3C	167-176	Brown (10YR 5/3, m) gravelly loamy sand, loose, single grain, abrupt smooth boundary, violently effervescent, 40-50% coarse fragments; Unit E.
15	3C	176-196	Brown (7.5YR 4/3, m) loamy fine sand, very friable, weak very coarse subangular blocky structure, abrupt smooth boundary, violently effervescent; Unit E.

Appendix A
Backhoe Trench Descriptions

Zone	Horizon	Depth (cm)	Description
16	3C	196-198	Brown (7.5YR 5/4, m) loamy sand, slightly hard, massive, abrupt smooth boundary, violently effervescent; Unit E.
17	3C	198-203	Brown (7.5YR 5/4, m) slightly gravelly to gravelly sand, loose, single grain, abrupt smooth boundary, violently effervescent, 15-30% coarse fragments; Unit E.
18	3C	203-225	Brown (7.5YR 5/3, m) loamy sand, slightly hard, weak medium subangular blocky structure, abrupt smooth boundary, violently effervescent; Unit E.
19	3C	225-231	Brown (7.5YR 5/4, m) sandy loam, slightly hard, massive, abrupt smooth boundary, violently effervescent, 5% coarse fragments, few calcium carbonate filaments; Unit E.
20	3C	231-250	Brown (7.5YR 5/4, m) loamy sand, friable, weak medium subangular blocky structure, abrupt smooth boundary, violently effervescent, few (1-3%) calcium carbonate filaments; Unit E.
21	3C	250-260	Brown (7.5YR 5/3, m) loam, hard, moderate to strong medium subangular blocky structure, abrupt smooth boundary, violently effervescent; Unit E.
22	3C	260-268	Brown (7.5YR 5/3, m) loamy sand, slightly hard, massive, abrupt smooth boundary, violently effervescent; Unit E.
23	3C	268-280	Pale brown (10YR 6/3, m) slightly gravelly sandy loam, very friable to loose, single grain, abrupt smooth boundary, violently effervescent; Unit E.
24	3C	280-308	Pale brown (10YR 6/3, m) sand, loamy sand and very fine sandy gravel, loose to very friable, single grain to massive, abrupt smooth boundary, violently effervescent, zone comprises several thin beds; Unit E.
25	4Ck	308-320	Brown (7.5YR 5/3, m) loam to silt loam, firm, moderate medium subangular blocky structure, abrupt smooth boundary, violently effervescent, few to common (5-7%) calcium carbonate filaments, a bulk sediment sample of this zone collected from 310-313 cm yielded an age of 2180 ± 40 years B.P. (Beta-328307); Unit D.
26	4C	320-330	Brown (7.5YR 4/4, m) very gravelly sand, loose, single grain, violently effervescent, 60-70% coarse fragments, mostly fine gravel, common strong brown 7.5YR 5/8 stains on gravel surfaces; few manganese stains on gravels as well; Unit D.

TRENCH 2

Location: 0230459E 3900214N
 Rear of T₁ surface on a slightly elevated (~1 m) bench
 Geologic Units: Middle and/or Late Holocene Colluvium
 Cultural material: None observed
 Comments: Numerous discontinuous gravelly lenses

Zone	Horizon	Depth (cm)	Description
1	A	0-60	Very dark grayish brown (10YR 3/2, m) sandy loam, very friable, weak coarse subangular blocky structure, diffuse smooth boundary, violently effervescent, many krotovina, few gravels throughout (matrix supported), 3-5% coarse fragments; Qc.
2	AC	60-120	Brown (7.5YR 5/3, m) slightly gravelly loamy sand to sandy loam, friable, massive, clear smooth boundary, violently effervescent, 5-7% coarse fragments, matrix supported; Qc.
3a	C	120-320	Brown (7.5YR 5/4, m) sandy loam, friable, weak coarse subangular blocky structure, clear smooth boundary, violently effervescent, few calcium carbonate filaments, 7-15% coarse fragments, matrix supported; Qc.
3b	C	120-320	Light brown (7.5YR 6/3, m) slightly gravelly loamy sand, loose, single grain, abrupt smooth boundary, violently effervescent, zone comprises numerous slightly westward dipping discontinuous beds of angular to subrounded caliche fragments.
4	R	>320	Massive indurated caliche, Ogallala Formation. Top of this deposit has been eroded and slopes to toward the valley axis.

TRENCH 3

Location: 0230399E 3900278N
Core of T₁ surface on the right bank meander south of 41PT186

Geologic Units: Unit B overlain by a thin veneer of Unit E.

Cultural material: An extensive scatter of FBR, a single Alibates flake and a few bone fragments between 0.8 and 2.2 m below the surface in the rubified Early or Middle Holocene alluvium.

Comments: This trench exposes a near channel overbank to medial overbank facies of the early-Middle Holocene alluvium. The A horizon is extensively bioturbated, and because it is considerably sandier, it may actually be a thin veneer of the Late Holocene alluvium.

Zone	Horizon	Depth (cm)	Description
1	A	0-80	Brown (7.5YR 5/4, m) sandy loam, very friable, weak coarse subangular blocky structure, gradual smooth boundary, violently effervescent, many krotovina; Unit E.
2	Bw	80-160	Brown (7.5YR 4/4, m) loam, firm, strong coarse prismatic structure, gradual smooth boundary, violently effervescent, common krotovina, few scattered FCR and bone fragments throughout; Unit B.
3a	Bk	160-230	Brown (7.5YR 5/4, m) loamy sand, very friable, massive, abrupt smooth boundary, violently effervescent, few (1-3%) calcium carbonate filaments, zone comprises four distinct sandy beds that pinch out to the west, within 2 m of the east trench end; basal sand bed has a small amount of gravel; Unit B.
3b	Bk	160-230	Brown (7.5YR 5/4.5, m) loam, friable, strong coarse subangular blocky structure, abrupt smooth boundary, violently effervescent, common (5-7%) calcium carbonate filaments, possibly a few calcium carbonate coats on ped faces, numerous FCR and few scattered bone fragments throughout; Unit B.
4	C	230-265	Brown (7.5YR 4/4, m) loamy sand to sandy loam, very friable, massive, abrupt smooth boundary, violently effervescent, few (1%) calcium carbonate filaments, appears to be at least 3 different beds but they were difficult to clearly discern, so described as a single zone; Unit B.
5	C	265-280	Brown (7.5YR 4/4,m) loamy sand, very friable, massive, violently effervescent; Unit B.

TRENCH 4

Location: 0230361E 3900323N
 Trench was placed on the T₀ surface, which in this location lies about 1.5 m above the channel floor.

Geologic Units: Recent (modern) alluvium, resting unconformably upon Unit E , which in turn rests unconformably upon an Unit D.

Cultural material: A rusted can was observed within the recent alluvium in the top 30 cm.

Comments: The recent alluvium was a thin veneer in most of the trench but in the northernmost 20 cm of this trench this unit dove to a depth of more than 1.2 m and probably upwards of 2 m just to the north of the trench. Numerous samples were collected from the older channel plug at depth.

Zone	Horizon	Depth (cm)	Description
1	AC	0-16	Brown (10YR 4/3, m) loamy sand, very friable to loose, weak medium subangular blocky structure, abrupt broken boundary, violently effervescent, many krotovina have left only fragments of original beds; modern.
2	C	16-23	Light yellowish brown (10YR 6/4, m) sand, loose, single grain, abrupt-broken boundary, violently effervescent, laminated in places, but most in this profile has been disturbed by rodents; modern.
3	C	23-47	Yellowish brown (10YR 5/4, m) sand to loamy sand, loose, single grain, abrupt smooth boundary, violently effervescent, <1% coarse fragments; modern.
4	C	47-60	Dark grayish brown-brown (10YR 4/2.5, m) slightly gravelly to gravelly sandy loam to loamy sand, slightly hard, weak medium subangular blocky structure, abrupt smooth boundary, violently effervescent, crudely laminated in places, 15-30% coarse fragments; Unit E.
5	AC	60-66	Very dark grayish brown-dark grayish brown (10YR 3.5/2, m) loamy sand to sandy loam, slightly hard, weak medium to coarse subangular blocky structure, abrupt smooth boundary, violently effervescent, looks to be very locally re-deposited zone 7 material, <3% coarse fragments; Unit E.
6	C	66-70	Brown (10YR 4/3, m) loamy sand, slightly hard, weak fine subangular blocky to massive structure, abrupt smooth boundary, violently effervescent, hints of bedding in places, 1-3% coarse fragments; Unit E.
7	3Ab	70-102	Dark brown-brown (10YR 3.5/3, m) sandy loam, slightly hard, moderate coarse subangular blocky structure, clear smooth boundary, violently effervescent, small fragments of charcoal are present in upper half of this zone; Unit E.
8	3C	102-121	Yellowish brown (10YR 5/4, m) slightly gravelly to gravelly sandy loam to loamy sand, loose, single grain, abrupt smooth boundary, violently effervescent, hints of bedding in places, 15-30% coarse fragments; Unit E.
9	4Ck1	121-145	Yellowish brown (10YR 5/4, m) sandy loam, friable, moderate very coarse subangular blocky structure, abrupt smooth boundary, violently effervescent, 15-20% calcium carbonate filaments; Unit E.
10	4Ck2	145-177	Gray (10YR 5/1, m) gravelly silty clay, friable, moderate coarse subangular blocky structure, abrupt smooth boundary, violently effervescent, 30-40% coarse fragments (<2cm subrounded caliche, matrix supported), common (5-7%) calcium carbonate filaments, few brown (7.5YR 5/4) medium distinct mottles; Unit E.
11	4Ck3	177-198	Pale brown (10YR 6/3, m) sand and slightly gravelly sand, slightly hard, massive, abrupt smooth boundary, violently effervescent, <15% coarse fragments, few (1-3%) calcium carbonate filaments, few brown (7.5YR 5/4) medium distinct mottles, several distinct alternating coarse and fine laminated thin beds, some appear contorted, possibly due to trampling; Unit D.

Zone	Horizon	Depth (cm)	Description
12	4Ckg1	198-234	Dark grayish brown (10YR 4/2, m) silty clay loam, firm, strong coarse angular blocky structure, abrupt smooth boundary, violently effervescent, common (5-7%) calcium carbonate filaments on ped faces, common fine distinct red (2.5YR 6/6) mottles and along bedding planes; Unit D.
13	4Ckg2	234-258	Very dark grayish brown to dark grayish brown (10YR 3/2 to 4/2, m) slightly gravelly silty clay, firm, strong coarse angular blocky structure, abrupt smooth boundary, violently effervescent, few fine faint (7.5YR 4/4) thread-like mottles, 15-20% coarse fragments (rounded caliche matrix supported), common (5-7%) calcium carbonate filaments on ped faces; Unit D.
14	4C	258-277	Yellowish brown (10YR 5/4, m) sand to loamy sand, friable, massive, abrupt wavy boundary, prominently laminated, few very dark gray (10YR 3/1) clay laminae the upper of which has a continuous <1 mm carbonate coat (travertine?), and a few other carbonate partings on bedding planes were present throughout this bed; Unit D.
15	4C	277-322	Dark grayish brown (10YR 4/2, m) loam to slightly gravelly loam, friable, moderate medium subangular blocky structure, abrupt smooth boundary, violently effervescent, few (1-3%) calcium carbonate filaments, zone comprises sever interbedded alternating coarse and fine beds, coarser beds have 15-25% coarse fragments, common medium faint olive yellow (2.5Y 6/8) irregular and thread-like mottles; Unit D.
16	4Cg	322-340	Brown (10YR 5/3, m) loam to slightly gravelly loam, very friable, moderate medium subangular blocky structure, abrupt smooth boundary, violently effervescent, few (1-3%) calcium carbonate filaments, common fine faint yellow (10YR 7/6) thread-like mottles; Unit D.
17	4Cg	340-350	Sandy gravel (hard to determine color), loose, single grain, abrupt smooth boundary, >80% coarse fragments, violently effervescent, common strong brown to dark reddish brown (7.5YR 5/8 to 5YR 3/4) iron stains on gravel surfaces; Unit D.
18	4C	350-360	(7.5YR 4/2, m) sandy clay, firm, strong medium subangular blocky structure, abrupt smooth boundary, few fine faint brownish yellow (10YR 6/8) thread-like mottles; Unit D.
19	4Cg	310-360	Very dark gray (2.5Y 3/1, m) clay, firm, strong coarse angular blocky structure, violently effervescent, 5-10% coarse fragments, common open cylindrical molds of reeds throughout, common sand coats on ped faces, common coarse prominent yellowish red (5YR 5/8) irregular shaped mottles on ped faces; Unit D.

TRENCH 5

Location: 0230-420E 3900314N
 This trench was placed upon the T_{1b} surface immediately south of the site, which is centered upon then T_{1a} surface.

Geologic Units: Unit E is 3 m deep here and appears to rest upon Unit D.

Cultural material: One prominent prehistoric occupation surface on the top of a buried soil (zone 7) which appears to have extremely well define activity areas as we uncovered an ash dump (a positive relief feature) and a thin bed of butchered bone, spatially offset from each other.

Comments: Exquisite buried occupation surface.

Zone	Horizon	Depth (cm)	Description
1	A	0-32	Brown (10YR 4/3, m) sandy loam, very friable, weak fine subangular blocky structure, clear smooth boundary, violently effervescent; Unit E.
2	C	32-52	Dark yellowish brown (10YR 4/4, m) sandy loam, very friable, massive, abrupt smooth boundary, violently effervescent, few to no (0-3%) coarse fragments, with one diffuse gravel scatter at ~40 cm which becomes more prominent to northeast in this trench; Unit E.
3	C	52-57	Brown (10YR 4/3, m) slightly gravelly to gravelly loamy sand, loose, single grain, abrupt smooth boundary, violently effervescent, 15-40% coarse fragments which are mostly fine subrounded caliche clasts reworked from the Ogallala Fm., this zone becomes more gravelly away from the cutbank; Unit E.
4	C	57-70	Brown (10YR 4/3, m) loam to a sandy loam, very friable, massive, abrupt smooth boundary, violently effervescent; Unit E.
5	C	70-75	Dark grayish brown to brown 10YR 4/2-4/3, m) loamy sand, very friable, weak medium to fine subangular blocky structure, abrupt smooth boundary, violently effervescent, becomes slightly gravelly to northeast away from the cutbank/channel; Unit E.
6	C	75-77	Ash dump. White (N8/0, m) silt, loose to very friable, massive, abrupt smooth boundary, violently effervescent, contains a few rounded aggregates of burned earth (7.5YR 6/6), clearly a positive relief dump of ash, a piece of charcoal from this ash was radiocarbon dated and yielded an age of 230 ± 40 years B.P. (Beta-235482), and a piece of butchered bison bone from the same stratigraphic position on the opposite side of the trench yielded an age of 210 ± 40 years B.P. (Beta-238317).
7	2Ab	77-112	Dark brown-brown (10YR 3.5/3, m) sandy loam, friable, moderate medium subangular blocky structure, abrupt broken boundary, violently effervescent, boundary with zone 8 disturbed by worm bioturbation, there is a prominent Protohistoric occupation on top of this zone; Unit E.
8	2C	112-118	Light yellowish brown (10YR 6/4, m) sand to sandy loam, very friable to loose, massive, abrupt broken boundary, violently effervescent, this was a discrete bed of clean sand but it has been seriously altered by worm bioturbation; Unit E.
9	3Ab	118-149	Brown-dark grayish brown (10YR 4/2.5, m) loam, very friable, weak to moderate coarse subangular blocky structure, abrupt broken boundary, violently effervescent, incipient A-horizon; Unit E.
10	3C	149-152	(10YR 6/4, m) sand, loose, single grain, abrupt broken boundary, violently effervescent, clean sand severely altered by worm bioturbation; Unit E.
11	3C	152-158	Brown (7.5YR 4/3, m) loam, very friable, massive, abrupt broken boundary, violently effervescent; Unit E.

Zone	Horizon	Depth (cm)	Description
12	3C	158-162	Light yellowish brown (10YR 6/4, m) sand to loam sand, loose to very friable, single grain to weak fine subangular blocky structure, abrupt broken boundary, violently effervescent, a relatively clean sand severely altered by worm bioturbation; Unit E.
13	3C	162-210	Brown (7.5YR 4/3, m) sandy loam, very friable, weak very coarse subangular blocky structure to massive, abrupt smooth boundary, violently effervescent, hints off thin beds/lamination throughout; Unit E.
14	3C	210-213	Light yellowish brown (10YR 6/4, m) loamy sand to sand, loose to very friable, single grained to massive, abrupt discontinuous boundary, violently effervescent; Unit E.
15	3C	213-233	Brown (10YR 4/3, m) loam, very friable, weak coarse subangular blocky structure, abrupt smooth boundary, violently effervescent; Unit E.
16	4A _{ck}	233-245	Very dark grayish brown (10YR 3/2, m) silty clay loam, friable, strong fine to medium subangular blocky structure, abrupt smooth boundary, violently effervescent, few (1-3%) calcium carbonate filaments, this bed dips and thickens to the west, where it exhibits some hints of internal bedding. Dark color of this bed may be detrital rather than pedogenic; Unit D.
17	4C	245-255	Pale brown (10YR 6/3, m) loamy sand, very friable, massive, abrupt smooth boundary, violently effervescent; Unit D.
18	5A _{ck}	255-264	Very dark grayish brown (10YR 3/2, m) silty clay loam, friable, strong medium angular blocky structure, abrupt wavy boundary, few (1-3%) coarse fragments, violently effervescent, few (3%) calcium carbonate filaments; Unit D.
19	6B _{kg}	264-300+	Gray (5Y 5/1, m) slightly gravelly loam to sandy clay loam, very friable, violently effervescent, many (25%) calcium carbonate filaments, few fine coarse distinct olive (5Y 5/6) mottles; Unit D.

TRENCH 6

Location: 0230417E 3900341N
This trench is located on the T₁ surface, south of the corral adjacent to the T₁ scarp overlooking the floodplain.

Geologic Units: A thin drape of Unit E (?) resting upon Unit B.

Cultural material: A small number of items were observed in the top 30 cm, but this part of the deposit is extensively bioturbated.

Comments: None.

Zone	Horizon	Depth (cm)	Description
1	Ap	0-7	Brown (10YR 4/3, m) sandy loam to loamy sand, very friable to loose, weak fine subangular blocky structure to single grain, abrupt smooth boundary, violently effervescent, <1% coarse fragments, appears to be recent rodent spoil, but possibly a veneer of recent alluvium; Unit E.
2	A	7-65	Very dark grayish brown (10YR 3/2, m) loam to sandy loam, firm, strong very coarse prismatic, gradual smooth boundary, violently effervescent, few coarse fragments (1%) most of which are granule to fine gravel sized clasts, notably slightly concentrated in the bottom 10 cm of the zone. This may be, at least partially, a thin drape of late Holocene alluvium; Unit E.
3	Bw	65-92	Brown (7.5YR 4/4, m) loam to silty clay loam, firm, strong coarse prismatic structure parting to medium subangular blocky structure, gradual smooth boundary, violently effervescent, common (5%) calcium carbonate filaments, few (3-5%) coarse fragments throughout, which are primarily 3-5 mm granules of reworked caliche, but a few looked like <i>in situ</i> pedogenic nodules; Unit B.
4	Bk	92-140	Brown (7.5YR 4/4, m) loam to silt loam, firm, strong medium to coarse subangular blocky structure, clear smooth boundary, violently effervescent, few (5%) coarse fragments in the lower 5 cm of the zone, common (7-15%) prominent white calcium carbonate filaments; Unit B.
5	2Ab?	140-157	Brown (7.5YR 4/2.5, m) silty clay, friable, strong coarse prismatic structure, clear smooth boundary, violently effervescent, few (1-3%) calcium carbonate filaments, possibly a very weak A horizon. A bulk sample was collected for radiocarbon dating from the top of this zone and it yielded an age of 8280 ± 50 years B.P. (Beta-235483); Unit B.
6	2Bk	157-198	Brown (7.5YR 4/4, m) silt loam to silty clay loam, friable, moderate medium subangular blocky structure, clear smooth boundary, violently effervescent, common (3-5%) calcium carbonate filaments; Unit B.
7	3Ab?	198-216	Dark brown-brown (7.5YR 4/2.5, m) silt loam, friable, moderate medium subangular blocky structure, diffuse smooth boundary, violently effervescent, possibly a very weakly developed A-horizon; Unit B.
8	3Bk	216-320	Brown (7.5YR 4/3, m) silty clay loam, firm, moderate to strong columnar structure, violently effervescent, common (3-5%) calcium carbonate filaments, and a few 5-10 mm irregular shaped diffuse edged calcium carbonate nodules, a bulk sample collected from 264-269 cm within this zone was radiocarbon dated and yielded an age of 9610 ± 50 years B.P. (Beta-235484); Unit B.

TRENCH 7

Location: 0230409E 3900381N
Trench was located on the north side of the T_{1a} surface adjacent to the cutbank, which was slightly lower than the core of the T_{1a} surface.

Geologic Units: Thin veneer of Unit E resting upon Unit B.

Cultural material: None observed.

Comments: None.

Zone	Horizon	Depth (cm)	Description
1	A	0-30	Very dark grayish brown (10YR 3/2, m) sandy loam, very friable, weak coarse subangular blocky structure, clear smooth boundary, violently effervescent, possibly a thin veneer of Unit E.
2	AB	30-60	Dark brown (7.5YR 3/3, m) silty clay loam, friable, strong medium to coarse prismatic structure, gradual smooth boundary, violently effervescent, few coarse fragments (1-3%), most of which are granules of reworked caliche throughout; Unit B.
3	Bk	60-135	Brown (7.5YR 4/4, m) silty clay, firm, strong medium to coarse prismatic structure, diffuse smooth boundary, violently effervescent, rare (<1%) 1-3 mm calcium carbonate nodules, common (3-5%) calcium carbonate filaments; Unit B.
4	Bk	135-190	Brown (7.5YR 4/4, m) silt loam to silty clay loam, very friable, moderate medium subangular blocky structure, clear smooth boundary, violently effervescent, common (5-7%) prominent white calcium carbonate filaments; Unit B.
5	Ab?	190-203	Brown (7.5YR 4/3, m) loam to silt loam, very friable, weak medium subangular blocky structure, violently effervescent, few (3%) calcium carbonate filaments, appears to be a very weakly developed A horizon; Unit B.
6	Bk	203-252	Brown (7.5YR 5/4, m) loam, very friable, weak to moderate medium subangular blocky structure, clear smooth boundary, few to common (3-5%) calcium carbonate filaments; Unit B.
7	C	252-270	Strong brown (7.5YR 5/6, m) sandy loam, very friable, weak coarse subangular blocky structure, violently effervescent, few cobbles at the top of this zone; Unit B.

TRENCH 8

Location: 0230361E 3900347N
 This trench was placed across the T_{1b} surface along the west side of site 41PT185 (?).
 Geologic Units: Unit E resting unconformably upon Unit D.
 Cultural material: At least one prehistoric occupation surface is present in the trench.
 Comments: Both of the units present have significant dips and lateral facies changes in the length of the trench, mostly from north to south across the floodplain; look like lateral accretion beds.

Zone	Horizon	Depth (cm)	Description
1	A	0-37	Dark grayish brown (10YR 4/2, m) sandy loam, friable, weak very coarse subangular blocky structure, clear smooth boundary, violently effervescent, few (1-3%) coarse fragments throughout, extensively bioturbated; Unit E.
2	C	37-61	Brown-dark yellowish brown (10YR4/3.5, m) loamy sand, very friable, moderate fine to medium subangular blocky structure, abrupt smooth boundary, violently effervescent, few (<3%) coarse fragments, extensively bioturbated; Unit E.
3	2Ab	61-95	Dark grayish brown-brown (10YR 4/2.5, m) sandy loam, slightly hard, moderate medium to coarse subangular blocky structure, clear smooth boundary, violently effervescent, few (1%) calcium carbonate filaments, few (1-3%) coarse fragments; Unit E.
4	2C	95-105	Brown (10YR 5/3, m) slightly gravelly to gravelly loam, hard, weak coarse subangular blocky structure, abrupt smooth boundary, violently effervescent, common (15-30% coarse fragments, mostly clast supported, this is a discontinuous bed which dips to the north and west; Unit E.
5	2C	105-117	Brown (10YR 5/3, m) loamy sand, firm, weak coarse subangular blocky structure, abrupt smooth boundary, violently effervescent; Unit E.
6	2C	117-128	Brown (10YR 5/3, m) loamy sand to (10YR 6/3, m) sand, very friable, weak to moderate coarse subangular blocky structure, abrupt smooth boundary, violently effervescent, multiple thin laminated beds, extensively worm bioturbated; Unit E.
7	3Akb	128-153	Very dark grayish brown to dark grayish brown(10YR 3/2 to 4/2, m) sandy clay, very firm, strong medium prismatic structure, clear smooth boundary, violently effervescent, common (5-7%) calcium carbonate filaments, few (1-5%) coarse fragments; Unit D.
8	3Akgb	153-175	Very dark gray-dark gray (10YR 3.5/1, m) sandy clay loam, firm to very firm, strong medium subangular blocky structure, abrupt smooth boundary, violently effervescent, many (15%) calcium carbonate filaments, few fine fine (2.5Y 5/6) mottles; Unit D.
9	3C	175-189	Yellowish brown (10YR 5/4, m) clayey gravel, firm, massive, abrupt smooth boundary, violently effervescent, 60-80% coarse fragments, prominent laterally discontinuous gravel bed; Unit D.
10	4Ab	189-198	Very dark gray (10YR 3/1, m) sandy clay, firm, strong fine prismatic structure, abrupt smooth boundary, few (1%) calcium carbonate filaments, 5-10% coarse fragments mostly matrix supported; Unit D.
11	4C	198-203	Brown (10YR 4/3, m) slightly gravelly sandy clay, hard, weak medium subangular blocky structure, abrupt smooth boundary, violently effervescent, 15-25% coarse fragments mostly matrix supported; Unit D.
12	5Ab	203-205	Very dark grayish brown (10YR 3/2, m) slightly gravelly clay, very hard, strong medium to coarse angular blocky structure, abrupt smooth boundary, violently effervescent, 5% matrix supported coarse fragments; Unit D.

TRENCH 9

Location: Trench runs east-west from the western edge of the Corral, down the axis of a meander of West Amarillo Creek, stopping just before the bike trail.

Geologic Units: Unit E, draping Units D, C and B.

Cultural material: Extensive amounts of cultural material in the Unit E veneer (which is very bioturbated), and small amounts of material in Unit C.

Comments: A very complex trench. No depths are listed as the descriptions refer to a long wall drawing.

Zone	Horizon	Depth (cm)	Description
1	A	--	Very dark grayish brown (10YR 3/2, m) loam to sandy loam, firm, weak very coarse prismatic structure in a few places, but mostly massive (owing to bioturbation), clear smooth boundary, violently effervescent, few coarse fragments (1%) most of which are granule to fine gravel sized clasts, a piece of bison bone recovered from the base of this unit where it drapes Unit C yielded an age of 600 ± 40 years B.P. (Beta-237020) and a sample of bulk soil collected from approximately the same position yielded an age of 2040 ± 40 years B.P. (Beta-235495) which is more likely close to the age of the immediately underlying Unit C; Unit E
2	2ACb	--	Dark gray to very dark gray (10YR 3.5/1, m) sandy clay loam, firm to very firm, strong medium subangular blocky structure, abrupt smooth boundary, violently effervescent, many (15%) calcium carbonate filaments, few fine (2.5Y 5/6) mottles; Unit D.
3	3Ck	--	Brown (10YR 5/3) loam (marl?), friable, weak medium subangular blocky structure, gradual smooth boundary, violently effervescent, abundant diffuse calcium carbonate, many (15-25%) calcium carbonate filaments, <1% coarse fragments; Unit C.
4	4Akb	--	Dark grayish brown (10YR 4/2) loam, friable, moderate to strong subangular blocky structure, clear smooth boundary, violently effervescent, many (10-15%) calcium carbonate filaments, abundant diffuse calcium carbonate, few fine faint light brownish gray (10YR 6/2) redox depletions, weak A horizon, a bulk sample of which collected from the top of the zone yielded an age of 2150 ± 40 years B.P. (Beta-235486) and a piece of charcoal collected from this zone was radiocarbon dated and yielded an age of 2490 ± 40 years B.P. (Beta-237021); Unit C.
5	4C	--	Brown (7.5YR 5/4) loam, friable, weak to moderate very coarse subangular blocky structure, gradual smooth boundary, violently effervescent, many (7-15%) calcium carbonate filaments; Unit C
6	4C	--	Gravelly sandy loam, loose, single grain, violently effervescent, 60-90% coarse fragments; Unit C
7	5Ab	--	Dark brown (7.5YR 3/3, m) silty clay loam, friable, strong medium to coarse prismatic structure, gradual smooth boundary, violently effervescent, few coarse fragments (1-3%), most of which are granules of reworked caliche throughout; Unit B.
8	5Bk	--	Brown (7.5YR 4/4, m) silty clay, firm, strong medium to coarse prismatic structure, diffuse smooth boundary, violently effervescent, rare (<1%) 1-3 mm calcium carbonate nodules, common (3-5%) calcium carbonate filaments; Unit B.

TRENCH 10

Location: 0230410E 3900486N
 Trench was placed on the T_{1b} surface on the downstream side of the meander.

Geologic Units: A thin veneer of Unit E over a northward thickening wedge of Unit D.

Cultural material: A hearth was discovered at a depth of 105-110 cm in the late Holocene clayey alluvium.

Comments: Both of the alluvial units in this trench dip and thicken to the north, and a rubified alluvial fill was exposed on the floor of the trench.

Zone	Horizon	Depth (cm)	Description
1	A1	0-14	Dark brown (7.5R 3/2, m) sandy loam, very friable, weak medium subangular blocky structure, clear smooth boundary, violently effervescent; Unit E.
2	A2	14-32	Brown-dark brown (7.5YR 3.5/2, m) loamy sand to sandy loam, friable, moderate medium subangular blocky structure, clear smooth boundary, violently effervescent; Unit E.
3	C	32-56	Brown (7.5YR 5/4, m) sandy loam, friable, moderate fine subangular blocky structure, abrupt smooth boundary, violently effervescent; Unit E.
4	2Ab	56-80	Very dark grayish brown (10YR 3/2, m) silty clay to sandy clay loam, firm, strong medium subangular blocky structure, gradual smooth boundary, violently effervescent, few to common (3-5%) calcium carbonate filaments, 1-3 % matrix supported coarse fragments; Unit D.
5	AC	80-154	Very dark gray (10YR 3/1, m) silty clay loam, friable, strong medium to very fine subangular blocky structure, abrupt discontinuous boundary, violently effervescent, common (7%) calcium carbonate filaments, few (1-3%) matrix supported coarse fragments; Unit D.
6	3Ab	154-155	Very dark grayish brown to very dark gray (10YR 3/1 to 3/2, m) slightly gravelly silty clay, friable, massive, abrupt discontinuous boundary, violently effervescent, few to common (3-5%) calcium carbonate filaments, 15-45% coarse fragments often clast supported, discontinuous gravelly bed; Unit D.
7	3AC	156-180	Very dark grayish brown (10YR 3/2, m) clay to silty clay, friable, strong coarse prismatic parting to strong fine subangular blocky structure, abrupt smooth boundary, violently effervescent, common (5-7%) calcium carbonate filaments; Unit D.
8	3Ab	>180	Brown (7.5YR 4/4, m) silt loam, friable, strong medium to fine subangular blocky structure, many (7-15%) calcium carbonate filaments, few (1%) 1-5 mm calcium carbonate nodules, common fine faint 10YR 5/6 mottles; Unit D.

TRENCH 11

Location: 0230549E 3900092N
Trench placed on colluvial slope at the edge of the alluvial valley just above a cutbank that exposes a buried soil which appears to be a Late Pleistocene alluvial fill (Unit A). Terrace appears to be the T₂ surface which lies about 6-7 m above the channel of West Amarillo Creek.

Geologic Units: Holocene colluvium over Unit A, over Ogallala Formation.
Cultural material: None observed
Comments: Prominent well-developed soil formed in the Late Pleistocene deposit, the top of which

Zone	Horizon	Depth (cm)	Description
1	A	0-20	Dark grayish brown (10YR 4/2, m) loamy sand, friable to very friable, weak medium subangular blocky structure, clear smooth boundary, violently effervescent, 10% coarse fragments scattered throughout the zone; Qc.
2	Bk	20-50	Brown (7.5YR 4/2.5, m) sandy loam, friable, moderate fine to medium subangular blocky structure, violently effervescent, , common to many (5-15%) calcium carbonate filaments, 3-5% coarse fragments scattered throughout the zone; Qc.
3	2Akb	50-90	Very dark grayish brown (10YR 3/2, m) sandy loam, friable, strong medium subangular blocky structure, gradual smooth boundary, weakly to moderately effervescent, many (7-15%) calcium carbonate filaments, 5% coarse fragments throughout; Unit A.
4	2Btkb	90-120	Brown (7.5YR 4/3, m) loam to sandy clay, friable, strong very coarse prismatic structure, diffuse smooth boundary, violently effervescent, many (7-15%) calcium carbonate filaments, many (50-90%) continuous prominent white calcium carbonate coats on ped faces, 5-10% coarse fragments throughout zone, more colluvial component to this zone than zone 5; Unit A.
5	2Btkb2	120-153	Brown (7.5YR 4/3, m) loam to sandy clay, friable, strong very coarse prismatic structure, gradual smooth boundary, violently effervescent, many (7-15%) calcium carbonate filaments, many (50-90%) continuous prominent white calcium carbonate coats on ped faces; Unit A.
6	3Akb	153-180	Very dark grayish brown (10YR 3/2, m) sandy loam, friable, strong medium to coarse prismatic structure, gradual smooth boundary, violently effervescent, common (5-7%) calcium carbonate filaments, many (25-90%) prominent white calcium carbonate coats on ped faces, base of zone has been blurred by krotovina, a bulk soil sample collected from the top of this zone yielded an age of 10,730 ± 70 years B.P. (Beta-238309); Unit A.
7	4Bk	180-260	Light yellowish brown (10YR 6/4, m) slightly gravelly loamy sand, very friable, strong very coarse prismatic structure, gradual smooth boundary, strongly effervescent, 10-20% coarse fragments scattered throughout; Ogallala Formation.
8	4Bk	260-290	Pink (7.5YR 7/4, m) sand, loose to very friable, single grain, violently effervescent, common (5-7%) calcium carbonate filaments, few fine (1-2mm) distinct 7.5YR 5/8 thread-like mottles; Ogallala Formation?.

TRENCH 12

Location: 0230469E 3900503N
 Located adjacent to cutbank on outside of meander on the T_{1a} surface.

Geologic Units: Thin veneers of late Holocene alluvium (Units C, D and/or E; 0-60 cm) resting upon Unit B (60-260+ cm).

Cultural material: Cultural material was observed widely scattered in the top 1.2 m, and a hearth was observed eroding from the cutbank immediately north of the trench.

Comments: Zones 1-6 increase in thickness from south to north in this trench, going from 62 cm at south end to 130 at the north end.

Zone	Horizon	Depth (cm)	Description
1	A	0-41	Very dark grayish brown (10YR 3/2, m) loamy sand to sandy loam, very friable, weak medium subangular blocky structure, gradual smooth boundary, violently effervescent, 1-5% coarse fragments, most of which are fine gravels widely dispersed in the matrix; Late Holocene.
2	A	41-84	Very dark grayish brown (10YR 3/2, m) sandy loam, very friable, weak coarse subangular blocky structure, gradual smooth boundary, few (<1%) coarse fragments, a small number of bone and FCR were found scattered in this zone; late Holocene.
3	2Bw	84-104	Brown (7.5YR 5/4 to 4/4, m) silt loam, very friable, weak coarse prismatic structure, clear smooth boundary, violently effervescent, few (1-3%) calcium carbonate filaments; Unit B.
4	2Bk	104-115	Brown (7.5YR 4/4, m) loam, firm, moderate to strong fine prismatic structure, clear smooth boundary, violently effervescent, common (5-7%) medium (2-5 mm) distinct white irregular shaped calcium carbonate nodules; Unit B.
5	3Akb	115-139	Brown (7.5YR 4/4, m) silt loam, firm, moderate medium subangular blocky structure, diffuse smooth boundary, violently effervescent, common (5-7%) medium (2-5 mm) distinct white irregular shaped calcium carbonate nodules; Unit B.
6	3Bkb1	139-186	Brown (7.5YR 5/4, m) loam to sandy loam, friable, moderate coarse prismatic parting to moderate medium to coarse subangular blocky structure, diffuse smooth boundary, violently effervescent, common (7-10%) medium (2-5 mm) distinct white irregular shaped calcium carbonate nodules; Unit B.
7	3Bkb2	186-230	Brown-light brown (7.5YR 5.5/4, m) sandy loam, friable, weak to moderate coarse prismatic structure, clear smooth boundary, violently effervescent, common (7-10%) medium (2-5 mm) distinct white irregular shaped calcium carbonate nodules; Unit B.
8	3C	230-250	Light brown (10YR 6/4, m) coarse sand, very friable to loose, single grained, abrupt smooth boundary, abrupt smooth boundary, violently effervescent, 5-10% coarse fragments; Unit B.
9	3Cg	250-260+	Light brown (7.5YR 6/4, m) medium sand, loose to very friable, single grain, violently effervescent, common medium distinct 7.5YR 5/8 cylindrical mottles; Unit B.

TRENCH 13

Location: 0230509E 3900009N
Trench was located close to leading edge of the T_{1b} surface.

Geologic Units: Unit E resting upon Unit D, which in turn rests on Unit B at the base of the trench.

Cultural material: A few scraps of bone were observed in the backdirt but none was observed in the trench.

Comments: Top half of this trench was extensively disturbed by rodents; a few large boulders were observed in the lower half of the trench in association with gravel beds.

Zone	Horizon	Depth (cm)	Description
1	A	0-10	Dark grayish brown (10YR 4/3, m) sandy loam, very friable, weak medium subangular blocky structure, clear smooth boundary, violently effervescent; Unit E.
2	A	10-40	Dark grayish brown (10YR 4/3 to 4/2, m) sandy loam, friable, moderate coarse subangular blocky structure, diffuse smooth boundary, violently effervescent., few (1-3%) coarse fragments throughout, extensively bioturbated; Unit E.
3	C	40-160	Dark grayish brown (10YR 4/2, m) loamy sand, very friable to loose, weak coarse subangular blocky structure to single grain, diffuse smooth boundary, violently effervescent, few (1-3%) coarse fragments, common krotovina; Unit E.
4	C	160-190	Yellowish brown (10YR 5/4, m) loam to silt loam, very friable, moderate fine subangular blocky structure, abrupt smooth boundary, violently effervescent. Few (1-3%) calcium carbonate filaments; Unit E.
5	C	190-200	Dark grayish brown (10YR 4/2, m) gravelly loamy sand, very friable to loose, single grain, abrupt smooth boundary, violently effervescent, 50-60% coarse fragments, a few isolated boulders were observed associated with this otherwise thin gravelly bed away from the measured section; Unit E.
6	2Ab	200-215	Very dark grayish brown (10YR 3/2, m) loam to silt loam, friable, moderate fine prismatic structure, abrupt smooth boundary, violently effervescent, few (1-3%) calcium carbonate filaments; Unit D.
7	2AC	215-220	Very dark grayish brown (10YR 3/2, m) gravelly silt loam, friable, massive, abrupt smooth boundary, violently effervescent; Unit D.
8	2Ab	220-270	Very dark grayish brown (10YR 3/2, m) silt loam, friable, moderate fine prismatic structure parting to moderate fine subangular blocky structure, gradual smooth boundary, violently effervescent; Unit D.
9	3Bw	270-290+	Strong brown (7.5YR 4/6, m) loamy sand, very friable, massive, violently effervescent, few 1-3% calcium carbonate filaments; Unit B.

TRENCH 14

Location: 0230525E 3900000N
 Trench was placed on the T_{1a} surface at rear of the floodplain.
 Geologic Units: Holocene colluvium resting upon a buried soil formed within what is suspected to be Unit B.
 Cultural material: None observed.
 Comments: None.

Zone	Horizon	Depth (cm)	Description
1	A	0-33	Dark brown (7.5YR 3/2, m) loamy sand, very friable, weak medium subangular blocky structure, very friable, clear smooth boundary, violently effervescent, few (1-2%) coarse fragments; Qc.
2	A	33-70	Dark brown (7.5YR 3/2, m) slightly gravelly sandy loam, friable, weak coarse subangular blocky structure, gradual smooth boundary, violently effervescent, common (7-10%) coarse fragments; Qc.
3	Bw	70-230	Brown (7.5Y 4/3, m) sandy loam, very friable, weak coarse prismatic structure, clear smooth boundary, violently effervescent, few (1%) calcium carbonate filaments, common (7-10%) coarse fragments scattered throughout; Qc.
4	2Akb	230-250	Brown (10YR 4/3, m) silt loam, friable, moderate to strong coarse prismatic structure, violently effervescent, common (3-5%) calcium carbonate filaments; Unit B.

TRENCH 15

Location: 0230488E 3900091N
 Geologic Units: Units E, D and B.
 Cultural material: None observed.
 Comments: Trench was placed across the T₀-T₁ scarp and encountered considerable stratigraphic complexity (see long wall drawing). No depths are listed here as the description is not from a vertical column.

Zone	Horizon	Depth (cm)	Description
1	A	--	Brown (7.5YR 4/3) sandy loam, very friable, weak medium subangular blocky structure, abrupt smooth boundary, violently effervescent.
2	C	--	Gravelly loamy sand (hard to determine color), loose, single grain, abrupt discontinuous boundary, violently effervescent, 40-60% coarse fragments.
3	Ab	--	Brown (7.5YR 4/2) loam to sandy loam, friable, moderate fine prismatic structure, abrupt smooth boundary, violently effervescent, few (1-3%) coarse fragments.
4	C	--	Very gravelly fine sand (hard to determine color), loose, single grain, abrupt smooth boundary, violently effervescent, 80% coarse fragments, mostly 1-4 mm reworked caliche nodules.
5	Akb	--	Very dark gray (10YR 3/1) silt loam, friable, strong medium prismatic structure, diffuse smooth boundary, violently effervescent, 5-7% calcium carbonate filaments, few thin discontinuous calcium carbonate coats on ped faces, few (1-3%) coarse fragments.
6	Akb	--	Dark brown (7.5YR 3/2) silt loam to silty clay loam, hard, strong very coarse prismatic structure, diffuse smooth boundary, violently effervescent, 1% calcium carbonate filaments, few (1-5%) coarse fragments.
7	Bw	--	Brown (7.5YR 5/4) silt loam, friable, moderate coarse prismatic structure, clear smooth boundary, violently effervescent, few (1-3%) coarse fragments scattered throughout.
7a	Ab	--	Brown (7.5YR 4/3) silty clay, extremely hard, strong fine prismatic structure, gradual smooth boundary, violently effervescent.
7b	Bk	--	Brown (7.5YR 4/4) silt loam, friable, strong extremely coarse prismatic structure, abrupt smooth boundary, 5-7% calcium carbonate filaments, common faint discontinuous calcium carbonate coats on ped faces.
8	Ab	--	Very dark grayish brown (10YR 3/2) to dark brown (7.5YR 3/2) sandy clay, friable strong fine columnar structure, abrupt smooth boundary, violently effervescent, 15-20% granules throughout zone.
9	C	--	White (~10YR 8/1) very gravelly sand, loose, single grain, abrupt smooth boundary, violently effervescent, ~60% coarse fragments, laminated with graded beds.
10	Akb	--	Brown (7.5YR 4/3) sandy loam, friable, weak very coarse prismatic structure, gradual smooth boundary, violently effervescent, 1-3% calcium carbonate filaments, few faint white discontinuous calcium carbonate coats on ped faces.
11	C	--	Brown (7.5YR 4/3) loamy sand, loose, single grain, abrupt smooth boundary, violently effervescent.
12	C	--	Brownish yellow (10YR 6/6) sandy gravel to gravelly loamy sand, loose, single grain, abrupt wavy boundary, violently effervescent, 40-80% coarse fragments.
13	C	--	Brown (7.5YR 5/4) loamy sand, very friable to loose, single grain, abrupt smooth boundary, violently effervescent, laminated.
14	C	--	White (~10YR 8/1) sand, loose, single grain, violently effervescent, laminated.

TRENCH 16

Location: 0230488E 3900091N
 Geologic Units: Unit B with a drape of younger sandy sediment (Unit E?)
 Cultural material: Two burned rocks were observed with ashy soil and charcoal flecks around 2.8-2.9 m below surface.
 Comments:

Zone	Horizon	Depth (cm)	Description
1	A	0-40	Very dark grayish brown (10YR 3/2) sandy loam, friable, moderate coarse subangular blocky structure, gradual smooth boundary, violently effervescent, few (1-2%) coarse fragments.
2	2Bw	40-78	Brown (7.5YR 5/4) sandy loam, friable, weak to moderate medium subangular blocky structure, gradual smooth boundary, violently effervescent, few (1%) calcium carbonate filaments, few (1-2%) coarse fragments.
3	3Ab	78-130	Brown (7.5YR 4/3) sandy loam to loam, friable, weak coarse subangular blocky structure, gradual smooth boundary, violently effervescent, few (1-3%) coarse fragments, a very faint and weakly developed A horizon.
4	3Bk	130-240	Brown (7.5YR 4/4) loam, friable, weak to moderate medium prismatic structure parting to strong fine angular blocky structure, clear smooth boundary, violently effervescent, 5-7% calcium carbonate filaments, few faint discontinuous calcium carbonate coats on ped faces, few (1-3%) coarse fragments.
5	3Bk	240-253	Strong brown (7.5YR 4/6) loam, friable, weak to moderate medium prismatic structure parting to moderate to strong fine angular blocky structure, clear smooth boundary, violently effervescent, 5% calcium carbonate filaments, few faint discontinuous calcium carbonate coats on ped faces, few (3-5%) coarse fragments.
6	4Akb	253-300	Brown (7.5YR 4/4) loam to silt loam, friable, moderate medium subangular blocky structure, violently effervescent, few (3%) calcium carbonate filaments, possibly a weak A horizon, two burned rocks were found between 280-290 cm, and this zone also contained flecks of charcoal and had an ashy feel in places.

TRENCH 17A

Location: 0230437E 3900678N
 Geologic Units: Thin veneer of late Holocene sediment resting upon Unit B
 Cultural material: Two levels of burned rock appear to be present in this trench, one around 35 cm below surface, and another around 52-60 cm.
 Comments: This trench is situated immediately west of the pavilion, adjacent to the point where the hike and bike trail crosses over the terrace scarp down to the channel of West Amarillo Creek. It was situated here on the basis of a shallowly buried hearth cropping out in the cutbank exposure.

Zone	Horizon	Depth (cm)	Description
1	A	0-65	Very dark gray to very dark grayish brown (10YR 3/1 to 10YR 3/2) sandy loam to loam, massive to moderate medium subangular blocky structure, gradual to abrupt smooth boundary, violently effervescent, two levels of burned rock were observed in this zone, one at about 35 cm, which was same as the hearth exposed on cutbank, and another around 52-60 cm.
2	2AB	65-72	Brown (7.5YR 5/4) slightly gravelly to gravelly loam, friable, massive to weak coarse subangular blocky structure, abrupt smooth boundary, violently effervescent, 14-40% coarse fragments, mostly fine (1-3 mm) gravels and granules.
3	2Bw	72-107	Strong brown (7.5YR 5/6) to brown (7.5YR 5/4) sandy clay loam, firm, strong coarse prismatic structure parting to strong coarse subangular blocky structure, abrupt smooth boundary, violently effervescent.
4	3Ab	107-174	Brown (7.5YR 4/3) loam to silt loam, very friable, moderate medium prismatic structure, clear smooth boundary, violently effervescent.
5	3Bk	174-224	Brown (7.5YR 4.5/4) sandy loam, firm, weak coarse subangular blocky structure, abrupt smooth boundary, violently effervescent, few (5%) calcium carbonate filaments).
6	3C	205-210	Brown (7.5YR 5/4) gravelly sand, very friable to loose, single grain, abrupt discontinuous boundary, violently effervescent, 50-60% coarse fragments, discontinuous gravel bed.
7	3C	224-240	Brown (7.5YR 5/4) very gravelly silt loam, friable, massive, abrupt smooth boundary, violently effervescent, many (70%) coarse fragments, mostly 1-2 cm subrounded reworked caliche fragments.
8	4Ab	240-265	Brown (7.5YR 4/4) silt loam, very friable, weak coarse prismatic structure, clear smooth boundary, violently effervescent, few (1%) calcium carbonate filaments, few (1%) coarse fragments.
9	4Bk	265-310+	Brown (7.5YR 5/4) loam to silt loam, very friable, weak coarse prismatic structure, violently effervescent, many (15%) calcium carbonate filaments, few (2%) coarse fragments.

TRENCH 17B

Location: 0230483E 3900031N
 Geologic Units: Thin veneer of late Holocene alluvium (Unit E?) over Unit B.
 Cultural material: Possible cultural deposit was observed around 259 cm in zone 7, consisting of ashy soil, and charcoal.
 Comments:

Zone	Horizon	Depth (cm)	Description
1	A	0-45	Very dark grayish brown (10YR 3/2) loam, friable, strong coarse subangular blocky structure, gradual smooth boundary, violently effervescent, common krotovina.
2	2Bw	45-82	Brown (7.5YR 5/4) loam to sandy loam, very friable, weak very coarse prismatic structure, abrupt smooth boundary, violently effervescent, few krotovina.
3	3Ab	82-120	Brown (7.5YR 4/3) loam to silt loam, friable, moderate to strong coarse subangular blocky structure, diffuse smooth boundary, violently effervescent, few thin discontinuous coats of calcium carbonate on ped faces, few (5-10%) coarse fragments.
4	3AB	120-170	Brown (7.5YR 4/3) loamy sand to sandy loam, very friable, weak medium to coarse subangular blocky structure, gradual smooth boundary, violently effervescent, few thin discontinuous coats of calcium carbonate on ped faces.
5	3C	170-216	Brown (7.5YR 5/4) loamy sand, very friable, weak coarse prismatic structure, abrupt smooth boundary, violently effervescent, a thin, discontinuous gravel stringer was present around 195-200 cm.
6	3C	216-255	Brown (7.5YR 4/4) slightly gravelly loam, very friable, massive, abrupt smooth boundary, abrupt smooth boundary, violently effervescent, few (1-3%) calcium carbonate filaments, 10-20% coarse fragments, few thin discontinuous gravel stringers.
7	4Ab	255-280*	Brown (7.5YR 5/4) loam to silt loam, very friable, weak to moderate medium prismatic structure parting to weak medium subangular blocky structure, violently effervescent, 5-7% calcium carbonate filaments, several charcoal fragments were observed, and soil has an ashy feel. No cultural objects were observed, although an anthropogenic component is suspected here.

TRENCH 18

Location: 0230428E 3900666N
 Geologic Units: Unit E overlying Unit C
 Cultural material: a scatter of burned rock was observed at the interface of the two deposits, and was thought in the field to be in Unit C, but radiocarbon dating of material from the cultural deposit clearly indicates that this material is in Unit E (430 ± 40 years B.P., Beta-238318)
 Comments: Depths are not listed as the descriptions relate to a long wall drawing.

Zone	Horizon	Depth (cm)	Description
1	A1	--	Very dark brown (10YR 2/2) loam, very friable, weak fine to medium subangular blocky structure, clear smooth boundary, violently effervescent, contains a discontinuous thin bed (to a scatter) of coal fragments within the top 20 cm, excluding coal this zone has < 2% coarse fragments.
2	A2	--	Dark brown (10YR 3/3) loam, very friable, massive, clear to gradual smooth boundary, violently effervescent, violently effervescent, < 2% coarse fragments, significantly bioturbated.
3	C	--	Brown (10YR 4/3) loamy sand, loose to very friable, massive, abrupt smooth boundary, violently effervescent, several large krotovina.
4	C	--	Brown (7.5YR 4/4) slightly gravelly loam, very friable, weak fine subangular blocky structure, abrupt smooth boundary, violently effervescent, 15-25% coarse fragments, this is a colluvial bed at rear of the Unit E deposit, adjacent to Unit B.
5	2Ab	--	Very dark gray to very dark grayish brown (10YR 3/1 to 10YR 3/2) loam to silt loam, very friable, moderate fine to medium prismatic structure, clear smooth boundary, violently effervescent, few (1%) calcium carbonate filaments.
6	2C	--	Brown (10YR 4.5/4) loam, friable to very friable, weak coarse subangular blocky structure, abrupt broken boundary, violently effervescent, many large krotovina.
7	2C	--	Brown (7.5YR 4/3) slightly gravelly loam to silt loam, friable, weak to moderate coarse subangular blocky structure, abrupt smooth boundary, violently effervescent, few (1-2%) calcium carbonate filaments, this is a colluvial bed that, like zone 4, is situated at the rear of the T ₀ surface, and pinches out a short distance from the Unit B exposure at the east end of this trench.
8	2C	--	Black (N 2/0) loamy sand, very friable, massive to weak fine subangular blocky structure, clear smooth boundary, violently effervescent, broad gently concave burned zone that extends almost entire length of the Unit E exposure in this trench (more than 6 m).
9	3Bk1	--	Yellowish brown (10YR 5/4) to brown (7.5YR 5/4) loam to silt loam, very friable, weak to moderate medium to coarse subangular blocky structure, abrupt smooth boundary, violently effervescent, truncated Unit B, hints of bedding in places, common 0.5 cm faint light olive brown (2.5Y 5/6) mottles, abundant diffuse calcium carbonate, many (10-15%) calcium carbonate filaments, marl, with a few burned rocks situated within 10 cm of the interface; a radiocarbon date from this cultural material yielded an age of 430 ± 40 years B.P., Beta-238318, suggesting that the cultural material was deposited on the eroded top of Unit C, and has been integrated into it by pedoturbation.
10	3Bk2	--	Brown (7.5YR 5/4) to strong brown (7.5YR 4/6) slightly gravelly silt loam, friable, moderate medium subangular blocky structure, violently effervescent, common (5-7%) calcium carbonate filaments; this deposit, which is unit B, was not described in detail here as Trench 17a is only a few meters away.

TRENCH 19

Location: 0230467E 3900711N
 Geologic Units: Thin veneer of Unit E on top of Unit D
 Cultural material: Two apparent occupations, one around 118 cm and another slightly deeper, around 130-134 cm.
 Comments: Most of this is a cumulic soil, formed from fine grained alluvium.

Zone	Horizon	Depth (cm)	Description
1	A	0-56	Very dark gray to very dark grayish brown (10YR 3/1.5) sandy loam, very friable, weak medium subangular blocky structure, clear smooth boundary, violently effervescent; Unit E.
2	2Ab	56-82	Very dark grayish brown (10YR 3/2) loam, friable, moderate medium coarse prismatic structure, clear smooth boundary, violently effervescent; Unit E.
3	2AC	82-105	Dark brown (10YR 3/3) loamy sand, very friable, weak medium subangular blocky structure, abrupt smooth boundary, violently effervescent; Unit E.
4	3Ab	105-135	Very dark grayish brown (10YR 3/2) slightly gravelly to gravelly loam, friable, moderate fine prismatic structure, abrupt smooth boundary, violently effervescent, 5-20% coarse fragments, two prehistoric occupations appear to be present in this zone, one at ~118 cm and a second around 130-134 cm, a bulk sediment sample collected near the top of this zone at 125-127 cm was radiocarbon dated and yielded an age of 1390 ± 40 years B.P. (Beta-237026) ; Unit D.
5	4Ab	135-150	Very dark gray (10YR 3/1) loam to silt loam, friable, moderate to strong coarse prismatic structure, abrupt smooth boundary, violently effervescent; Unit D.
6	4Ab	150-174	Very dark grayish brown (10YR 3/2) slightly gravelly to gravelly loam, firm, moderate to strong medium prismatic structure, abrupt smooth boundary, violently effervescent, common (3-5%) calcium carbonate filaments, 15-30% coarse fragments; Unit D.
7	4Ab	174-260	Very dark grayish brown (10YR 3/2) silty clay loam, friable, strong fine subangular blocky structure, violently effervescent, 1-5% coarse fragments, common (3-5%) calcium carbonate filaments; Unit D.

TRENCH 20

Location: 0230488E 3900719N
 Geologic Units: Unit E resting on top of Unit D
 Cultural material: None within the recorded section, but there were several bones observed within this long trench.
 Comments:

Zone	Horizon	Depth (cm)	Description
1	C	0-10	Very pale brown (10YR 7/4) loamy sand, loose, single grain, abrupt smooth boundary, violently effervescent, approximately 10% coarse fragments, introduced fill derived from Pleistocene or older alluvium.
2	2Ab	10-25	Dark brown (10YR 3/3) sandy loam, very friable, weak medium subangular blocky structure, gradual smooth boundary, violently effervescent, <3% coarse fragments; Unit E.
3	3Ab	Between zones 2 and 4	Very dark grayish brown (10YR 3/2) to brown (10YR 4/2) sandy loam, friable, weak to moderate subangular blocky structure, abrupt smooth boundary, violently effervescent, <3% coarse fragments, zone pinches out within the trench, being thickest at northwest end closest to the stream channel; Unit E.
4	3AC	25-60	Very dark grayish brown (10YR 3/2) sandy loam, very friable, massive, clear smooth boundary, violently effervescent; Unit E.
5	4Ab	60-85	Very dark gray to very dark grayish brown (10YR 3/1 to 10YR 3/2) loam, friable, moderate to strong coarse subangular blocky structure, clear smooth boundary, violently effervescent; Unit E.
6	4AC	85-105	Dark brown (10YR 3/3) loam, friable, moderate coarse subangular blocky structure, abrupt smooth boundary, violently effervescent, <2% coarse fragments; Unit E.
7	5Ab1	105-160	Very dark grayish brown (10YR 3/2) silty clay loam, firm, moderate to strong coarse prismatic structure, gradual smooth boundary, violently effervescent, few (1-3%) calcium carbonate filaments, 3-5% coarse fragments; Unit D.
8	5Ab2	160-215	Very dark grayish brown (10YR 3/2) silty clay loam, firm, strong coarse prismatic structure, clear smooth boundary, violently effervescent, many (5-10%) calcium carbonate filaments, few (1%) coarse fragments, a bulk sediment sample collected from 180 cm within this trench yielded an age of 1210 ± 40 years B.P. (Beta-237022); Unit D.
9	5Ab3	215-270	Very dark grayish brown (10YR 3/2) silty clay loam, firm, strong coarse prismatic structure parting to strong fine angular blocky structure, violently effervescent, few to common (1-5%) calcium carbonate filaments, 3% coarse fragments, a bulk sediment sample collected from 240 cm within this trench yielded an age of 1840 ± 40 years B.P. (Beta237023) ; Unit D.

TRENCH 21

Location: 0230450E 3900629N
 Geologic Units: Unit B resting upon Unit A.
 Cultural material: None observed.
 Comments: Two radiocarbon dates were obtained from this trench, one, a bulk sediment sample from 145-148 cm (zone 5), which yielded an age of **10,590 ± 40** years B.P. (Beta-238320) which appears to date the early phase of Unit B deposition in a floodplain facies. The second age was also obtained from a bulk sample within the A horizon at 271-274 cm (zone 7) and yielded an age of **10,850 ± 50** years B.P. (Beta-238319) which is a maximum age for the deposition of Unit A.

Zone	Horizon	Depth (cm)	Description
1	A	0-30	Very dark brown (10YR 2/2) sandy loam, very friable, massive to weak fine subangular blocky structure, abrupt smooth boundary, violently effervescent; Unit E?
2	2Bt	30-60	Brown (7.5YR 4/3) clay, firm to very firm, strong coarse prismatic structure, clear smooth boundary, strongly effervescent, few (1-5%) coarse fragments; Unit B.
3	2Btk1	60-90	Brown (7.5YR 4/3) clay, very firm, strong coarse prismatic structure, gradual smooth boundary, strongly effervescent, common to many (5-7%) calcium carbonate filaments, few (3%) irregular shaped white 7-12 mm calcium carbonate nodules; Unit B.
4	2Btk2	90-120	Brown (7.5YR 4/3 to 4/2) silty clay, firm, strong fine angular blocky structure, diffuse smooth boundary, violently effervescent, many (10-15%) calcium carbonate filaments, common (5-7%) irregular shaped white 7-12 mm calcium carbonate nodules; Unit B.
5	2Bk	120-185	Brown (7.5YR 4/3) silt loam, friable, moderate fine subangular blocky structure, abrupt smooth boundary, violently effervescent, many (15-20%) calcium carbonate filaments; Unit B.
6	3Akb1	185-230	Dark brown (7.5YR 3/2) silt loam, friable, moderate to strong medium to coarse prismatic structure, clear smooth boundary, violently effervescent, few (2%) calcium carbonate filaments (although dry sample may exhibit more), 3% coarse fragments, mostly fine gravel sized fragments of reworked Ogallala caliche, few thin black manganese coats lining pores; Unit A.
7	3Akb2	230-270	Very dark brown (10YR 2/2) silty clay, friable, moderate to strong medium to fine prismatic structure, violently effervescent, many (15%) calcium carbonate filaments, few thin black manganese coats lining pores; Unit A.

TRENCH 22

Location: 0230407E 3900614N
 Geologic Units: Unit E resting upon Unit D.
 Cultural material: Few scattered burned rock were observed between 45 and 55 cm.
 Comments: Upper 1.2 m appeared to be extensively pedoturbated.

Zone	Horizon	Depth (cm)	Description
1	A	0-28	Very dark grayish brown (10YR 3/2) sandy loam, very friable, massive, clear smooth boundary, violently effervescent, 1% coarse fragments; Unit E.
2	AC	28-65	Dark grayish brown (10YR 4/2) sandy loam, very friable, weak medium to fine subangular blocky structure, clear smooth boundary, violently effervescent, <3% coarse fragments, few large krotovina, few burned rocks scattered between 45 and 55 cm; Unit E.
3	2Ab	65-90	Very dark grayish brown (10YR 3/2) sandy loam, very friable, moderate medium prismatic structure, abrupt to clear smooth boundary, violently effervescent, <3% coarse fragments, common large krotovina, few burned rocks scattered between 45 and 55 cm; Unit E.
4	2AC	90-115	Brown (10YR 4/3) loam, very friable, weak to moderate prismatic structure, clear smooth boundary, violently effervescent, <3% coarse fragments, common large krotovina; Unit E.
5	3Ab	115-155	Dark grayish brown (10YR 4/2) sandy loam, friable, massive, abrupt smooth boundary, violently effervescent, 5-15 % coarse fragments; Unit D.
6	3C	155-170	Dark grayish brown (10YR 4/2) gravelly sandy loam, friable, massive to single grain (depending upon moisture), abrupt smooth boundary, violently effervescent, 30-70% coarse fragments; Unit D.
7	4AC	170-190	Brown (10YR 5/3) loam, friable, massive, abrupt wavy boundary, violently effervescent, ~5% coarse fragments; Unit D.
8	4C	190-215	White to brown (10YR 8/1 to 10YR 5/3) very gravelly loamy sand, loose to very friable, single grain, abrupt smooth boundary, violently effervescent, ~70% coarse fragments; Unit D.
9	4C	215-227	Very dark gray (10YR 3/1) silty clay and light yellowish brown (10YR 6/4) sand interlaminated, friable to loose, massive, abrupt smooth boundary, violently effervescent, 1-3% coarse fragments, mostly in sands; Unit D.
10	5Agb	227-285	Black (10YR 2/1) clay, firm, strong very coarse prismatic structure, abrupt smooth boundary, violently effervescent, numerous fine (1-3mm) gravels throughout (~3% coarse fragments), few to common aquatic snails and bivalves; Unit D.
11	5Cg	285-300	Dark gray-very dark gray (10YR 3.5/1) loam to sandy clay, friable, moderate medium prismatic structure, violently effervescent, few (3%) fine gravel sized fragments of reworked caliche throughout; Unit D.

TRENCH 23

Location: 0230563E 3901216N
 Geologic Units: Unit E (?) resting upon Unit B.
 Cultural material: Two zones of cultural material were apparent in the trench, one around 39-42 cm, and a second between 75 and 77 cm.
 Comments: This trench is within the confines of Site 41PT185, Locus B.

Zone	Horizon	Depth (cm)	Description
1	A	0-30	Very dark grayish brown (10YR 3/2) to dark brown (7.5YR 3/2) sandy loam, very friable, weak fine to medium subangular blocky structure, diffuse smooth boundary, violently effervescent; Unit E?
2	AC	30-55	Brown (7.5YR 4/3) loamy sand to sandy loam, very friable, weak medium subangular blocky structure to massive, abrupt smooth to wavy boundary, violently effervescent, few scattered burned rocks between 39 and 42 cm; Unit E?
3	2Ab	55-100	Dark grayish brown to very dark grayish brown (10YR 3.5/2) silty clay loam, very firm, strong extremely coarse prismatic structure, gradual smooth boundary, violently effervescent, 1-3% coarse fragments, few scattered burned rocks between 75 and 77 cm; Unit B.
4	2Bw	100-170	Brown (7.5YR 5/4) loam, friable, moderate medium prismatic structure, clear smooth boundary, violently effervescent, 3-5% coarse fragments; Unit B.
5	3Ab	170-200	Brown (7.5YR 4/3) loam to silt loam, friable, moderate medium subangular blocky structure, violently effervescent, 3-5% coarse fragments, very weak a horizon; Unit B.

TRENCH 24

Location: 0230600E 3901219N
 Geologic Units: Unit E (?) resting upon Unit B, which in turn rests upon an unidentified deposit, possibly Unit A, or an older, yet unidentified deposit.
 Cultural material: None observed.
 Comments: This trench is within the confines of Site 41PT185, Locus B. Zone 8, 9 and 11 are the very margin of a channel deposit that was present east of this trench, which was inferred from dramatic litho logical changes from one trench wall to the other.

Zone	Horizon	Depth (cm)	Description
1	A	0-37	Very dark grayish brown (10YR 3/2) sandy loam, very friable, weak fine to medium subangular blocky structure, clear smooth boundary, violently effervescent; Unit E?
2	AC1	37-60	Very dark grayish brown (10YR 3/2) sandy loam, friable, weak coarse subangular blocky structure, abrupt smooth boundary, violently effervescent; Unit E?
3	AC2	60-92	Brown (10YR 4/3) loam, friable, moderate medium to coarse subangular blocky structure, diffuse smooth boundary, violently effervescent, Unit B.
4	AC3	92-115	Brown (7.5YR 4/3 to 5/3) loam, friable, weak coarse subangular blocky structure, abrupt smooth boundary, violently effervescent, 1% coarse fragments; Unit B?
5	2Akb	115-148	Brown (7.5YR 4/3) clay to silty clay, firm, strong coarse prismatic structure, gradual smooth boundary, violently effervescent, common medium prominent white irregular shaped calcium carbonate nodules, common faint thin clay films on ped faces; former Btk horizon over printed with an A horizon; Unit A or older deposit.
6	2Bk	148-180	Light yellowish brown (10YR 6/4) loam, friable, strong coarse prismatic structure, gradual smooth boundary, violently effervescent, abundant diffuse calcium carbonate, common (20%) 0.5-1 cm diameter prominent white, irregular calcium carbonate nodules; Unit A or older deposit.
7	2Bkg	180-230	Brown (7.5YR 5/4) loam, friable, moderate medium subangular blocky structure, gradual smooth boundary, violently effervescent, 5-10% calcium carbonate filaments, common faint gray (2.5Y 6/1) redox depletions; Unit A or older deposit.
8	2Bkg	230-265	Light yellowish brown (10YR 6/4) loam, very friable, moderate medium subangular blocky structure, abrupt smooth boundary, violently effervescent, common (5-7%) calcium carbonate filaments, common faint gray (2.5Y 6/1) redox depletions; Unit A or older deposit.
9	2C	265-270	Light gray (2.5Y 7/2) sand, loose, single grain, abrupt smooth boundary, violently effervescent; Unit A or older deposit.
10	2Ckg	270-280	Light olive brown-light yellowish brown (2.5Y 5.5/3) loamy sand, very friable, massive to weak coarse subangular blocky structure, abrupt smooth boundary, violently effervescent, few (1-5%) calcium carbonate filaments, few fine faint gray (2.5Y 7/2) redox depletions; Unit A or older deposit.
11	2C	280-300	Light gray (2.5Y 7/2) sand, loose, single grain, violently effervescent, few coarse prominent black (N 2/0) manganese haloes (hypocoats) around pores and channels, few coarse brownish yellow (10YR 6/8) cylindrical mottles which are lined by manganese hypocoats.

TRENCH 25

Location: 0230566E 3901163N
 Geologic Units: Unit E.
 Cultural material: A burned rock and a bone were recovered from zone 9, but they appeared to be very isolated.
 Comments: This deposit is on the leading edge of the T₀ surface, and exposes a deposit that appears to be entirely Unit E, as there are no significant breaks in the column. The channel deposit represented by the lowest 3 zones was a channel that was offset from the modern channel by about 20-30 m, which suggests the channel location has shifted slightly throughout the period of Unit E deposition.

Zone	Horizon	Depth (cm)	Description
1	A	0-40	Very dark grayish brown (10YR 3/2) sandy loam, very friable, weak medium subangular blocky structure to massive, clear smooth boundary, violently effervescent, 5% coarse fragments; Unit E.
2	AC	40-55	Brown (10YR 4/3) sandy loam, loose to very friable, single grain to weak coarse subangular blocky structure, clear smooth boundary, violently effervescent, 5% coarse fragments; Unit E.
3	C	55-65	Brown (10YR 4/3) gravelly sand, loose, single grain, abrupt discontinuous boundary, violently effervescent, 20-40% coarse fragments, appears to be one (but possibly two) flood deposits; Unit E.
4	2Ab	65-90	Very dark grayish brown (10YR 3/2) loam to sandy clay, friable, moderate medium prismatic structure, clear smooth boundary, violently effervescent, 7-20% coarse fragments; Unit E.
5	2C	90-122	Brown (10YR 4/3) loamy sand, very friable, massive, clear smooth boundary, violently effervescent, <10% coarse fragments; Unit E.
6	2C	122-145	Brown (10YR 4/3) sandy loam to slightly gravelly sandy loam, loose to very friable, weak coarse subangular blocky structure, clear smooth boundary, violently effervescent, 5-25% coarse fragments; Unit E.
7	2C	145-172	Yellowish brown (10YR 5/4) loam, friable, weak very coarse subangular blocky structure, clear smooth boundary, violently effervescent, few (1%) calcium carbonate filaments, <5% coarse fragments; Unit E.
8	2C	172-200	Yellowish brown (10YR 5/4) sandy loam to loam, friable, weak coarse subangular blocky structure, clear smooth boundary, violently effervescent, few (1%) calcium carbonate filaments, 5-20% coarse fragments; Unit E.
9	2C	200-240	Brown (10YR 5/3) sandy loam, friable, massive, abrupt smooth boundary, violently effervescent, common (3-5%) calcium carbonate filaments, <1% coarse fragments; Unit E.
10a	2C	240-270	Grayish brown (10YR 5/2) sandy loam, very friable, massive, abrupt smooth boundary, violently effervescent, few (1-3%) calcium carbonate filaments, interbedded with zone 10b; Unit E.
10b	2C	240-270	Pale brown (10YR 6/3) loamy sand to sand, very friable, massive, abrupt smooth boundary, violently effervescent, few (1-3%) calcium carbonate filaments, entire suite of deposits (10a and 10b) dip slightly away from (to the west of) the then active channel, which was located immediately east of this trench; Unit E.
11	2C	270-290	White (10YR 8/1) sandy gravel, loose, single grain, violently effervescent, >90% coarse fragments most of which are reworked caliche with a small amount (~20%) reworked Triassic mud balls and sandstone fragments.

TRENCH 26

Location: 0230550E 3901127N
 Geologic Units: A drape of Unit E resting upon Unit D.
 Cultural material: None obvious.
 Comments: Depths are not listed owing to major lateral variation within the trench. Refer to the long wall drawing for the relative location of each zone. There is a sloping unconformity in the middle of this trench that is mantled with large rocks (boulders) which derive from the Triassic sandstone outcrop on the other side of the channel. It is hard to envision how these rocks got here without human assistance, but no evidence of cultural material was apparent within this deposit despite very slow excavation. At the very least this exposure suggests that there was some complexity to the deposition of Unit D.

Zone	Horizon	Depth (cm)	Description
1	A	--	Black (10YR 2/1) sandy loam, very friable, moderate medium subangular blocky structure, clear smooth boundary, violently effervescent, <3% calcium carbonate filaments; Unit E.
2	AC	--	Very dark grayish brown (10YR 3/2) slightly gravelly sandy loam, very friable to loose, weak coarse subangular blocky structure, clear smooth boundary, violently effervescent, 5-15% coarse fragments; Unit E.
3	C	--	Very dark grayish brown (10YR 3/2) to brown (10YR 4/3) slightly gravelly loam, loose, single grain, abrupt smooth boundary, violently effervescent, 30-40% coarse fragments; Unit E.
4	AC	--	Brown (10YR 4/3) loam, friable, moderate coarse subangular blocky structure, abrupt smooth boundary, violently effervescent, few (1%) calcium carbonate filaments, <1% coarse fragments; Unit E.
5	2Ab	--	Very dark gray(10YR 3/1) silty clay, friable, strong very coarse subangular blocky structure, abrupt smooth boundary, violently effervescent, few (1%) calcium carbonate filaments, few (1-7%) coarse fragments mostly fine gravel and granules throughout, few fine red mudballs of reworked Triassic muds, few fine faint reddish brown (5Y 5/4) mottles, aquatic invertebrates (snails and bivalves) throughout; Unit D.
6	3C	--	Dark reddish brown (5YE 3/4) and pale olive (5Y 6/1) flaggy rubble, loose, structureless, abrupt smooth boundary, zone consists of large 20-50+ cm diameter slabs of Triassic sandstone, mudstone and Ogallala caliche that armor an inclined unconformity within the Unit D deposit. This looks anthropogenic but we could find no cultural material associated with it.
7	4Ab1	--	Dark grayish brown (10YR 4/2) silty clay, friable, moderate coarse subangular blocky structure, clear smooth boundary, violently effervescent, common to many (7-10%) calcium carbonate filaments, few aquatic mollusks throughout; Unit D.
8	4Ab2	--	Very dark gray (10YR 3/1) silty clay, friable, strong coarse subangular blocky parting to strong fine subangular blocky structure, violently effervescent, common (7%) calcium carbonate filaments, few aquatic mollusks throughout; Unit D.

TRENCH 27

Location: 0230584E 3901129N
 Geologic Units: Unit E resting unconformably upon Unit B, which sits upon a truncated remnant of a much older deposit, possibly Unit A.
 Cultural material: A scatter of burned rock was observed within zone 2 at a depth of approximately 70 cm, and a radiocarbon date obtained from this material yielded an age of **2640 ± 40** years B.P. (Beta-238312). A bone fragment recovered from 145 cm within zone 6 yielded an age of **2940 ± 40** years B.P. (Beta-238313) but this conflicts with other, stratigraphically consistent ages from this deposit (which is Early Holocene) and therefore this second age is considered erroneous and is rejected as accurate for the age of this deposit.

Comments:

Zone	Horizon	Depth (cm)	Description
1	A	0-55	Very dark grayish brown (10YR 3/2) sandy loam, very friable, weak medium subangular blocky structure, clear smooth boundary, violently effervescent, many krotovina, <1% coarse fragments; Unit E.
2	AB	55-75	Dark brown (10YR 3/3) loam, friable, moderate very coarse subangular blocky structure, clear smooth boundary, violently effervescent, 1% coarse fragments, few pieces of scattered burned rock were observed within this zone, and vestiges of a possible hearth was observed out of context on the bench within this trench, a radiocarbon sample from this occupation debris yielded an age of 2640 ± 40 years B.P. (Beta-238312); Unit E.
3	2Bw	75-95	Brown (7.5YR 4/4) loam, friable to firm, strong coarse prismatic structure, clear smooth boundary, violently effervescent, few (1-3%) calcium carbonate filaments, few very faint discontinuous white calcium carbonate coats on ped faces; Unit B.
4	3Akb	95-117	Brown (7.5YR 4/3) silty clay loam, friable to firm, strong medium prismatic structure, gradual smooth boundary, violently effervescent, common to many (5-7%) calcium carbonate filaments, possibly a few very small incipient calcium carbonate nodules, Unit B.
5	3Bk	117-144	Brown (7.5YR 5/4) loam to silty clay loam, firm, strong coarse to medium subangular blocky structure, clear smooth boundary, violently effervescent, common to many (5-7%) calcium carbonate filaments, few to common (3-5%) 5-7 mm diameter irregular shaped white calcium carbonate nodules, Unit B.
6	4Akb	144-160	Brown (7.5YR 4/3) loam, friable, moderate medium subangular blocky structure, clear smooth boundary, violently effervescent, few (3%) calcium carbonate filaments, faint A horizon; Unit B. A bone fragment recovered from 145 cm within zone 6 yielded an age of 2940 ± 40 years B.P. (Beta-238313).
7	4ACkb	160-185	Brown (7.5YR 4/3) loam, friable, moderate medium subangular blocky structure, gradual smooth boundary, violently effervescent, few (3%) calcium carbonate filaments; Unit B.
8	4Bk	185-210	Brown (7.5YR 4/4) sandy loam, very friable, moderate to strong coarse subangular blocky structure, clear smooth boundary, violently effervescent, common to many (5-7%) calcium carbonate filaments; Unit B.
9	4Bk	210-260	Light brown (7.5YR 6/4) loamy sand, very friable, moderate medium subangular blocky structure, violently effervescent, many (7-15%) calcium carbonate filaments, common (5-7%) large (1-1.5 cm) irregular shaped white calcium carbonate nodules, abundant diffuse calcium carbonate; Unit A?.

TRENCH 28

Location: 0230566E 3901142N
 Geologic Units: Unit E, although it is possible the bottom 3 zones of this trench may be Unit C, based upon the yellow mottling that was observed in only a few places in the valley, most notably in Trench 40 within the base of Unit C.
 Cultural material: Bones that occur in zone
 Comments: Sands at the base of this trench are part of a channel that begins to crop out within the trench about 2 m east of the place this vertical profile was described.

Zone	Horizon	Depth (cm)	Description
1	A1	0-23	Black (10YR 2/1) sandy loam, very friable, massive, abrupt smooth boundary, violently effervescent, 3-5% coarse fragments, many krotovina; Unit E.
2	A2	23-32	Very dark grayish brown (10YR 3/2) sandy loam, loose, single grin, abrupt smooth boundary, violently effervescent, several bison bone fragments were observed within this zone; bed gradually thickens towards the modern channel (to the west), 7-15% coarse fragments; Unit E.
3	2Ab	32-60	Very dark brown (10YR 2/2) sandy loam, very friable, weak coarse subangular blocky structure, clear smooth boundary, violently effervescent, 3-5% coarse fragments, numerous krotovina; Unit E.
4	2AC	60-110	Very dark grayish brown (10YR 3/2) clay loam, friable, moderate coarse subangular blocky structure, clear smooth boundary, violently effervescent, few (2-3%) calcium carbonate filaments, 7-10% coarse fragments most of which are dispersed throughout but there is one fairly clear stringer around 80 cm; Unit E.
5	2AC	110-125	Very dark grayish brown (10YR 3/2) slightly gravelly sandy clay, friable, moderate very coarse prismatic structure, abrupt smooth boundary, violently effervescent, common (3-5%) calcium carbonate filaments, 20-30% coarse fragments most of which are reworked caliche nodules but there are a few green sandstone slabs; Unit E.
6	2ACg	125-155	Brown (10YR 4/3) sandy clay loam to clay, friable, moderate coarse subangular blocky structure, diffuse smooth boundary, violently effervescent, few to common (3-5%) calcium carbonate filaments, few medium faint brownish yellow(10YR 6/6) mottles; Unit E.
7	2Cg	155-190	Yellowish brown (10YR 5/6) loam to sandy clay loam, friable, moderate coarse subangular blocky structure, diffuse smooth boundary, violently effervescent, few (3%) calcium carbonate filaments, <1 % coarse fragments, zone looks yellow in the field; Unit E or Unit C.
8	3ACg	190-215	Very dark grayish brown-dark grayish brown (10YR 3.5/2) loam, friable, moderate to strong coarse subangular blocky structure, clear smooth boundary, violently effervescent, 7-15% coarse fragments, common medium distinct gray to light brownish gray (2.5Y 6/1 to 6/2) redox depletions; Unit E or Unit C.
9	3Cg	215-240	Light gray (2.5Y 7/2) loamy sand, very friable, weak to moderate coarse subangular blocky structure, violently effervescent, few fine faint yellowish brown (10YR 5/8) mottles lining pores; Unit E or Unit C.

TRENCH 29

Location: 0230546E 3901158N
 Geologic Units: Unit E
 Cultural material: One possible occupation around 45 cm which contained numerous bison bones. No clear cultural material observed.
 Comments: Like Trench 25, the lowest deposits in this trench respect a channel situated east of the modern channel, just east of this trench, which suggests that the position of the channel of West Amarillo Creek has shifted slightly during the period of Unit E deposition.

Zone	Horizon	Depth (cm)	Description
1	A	0-35	Very dark gray (10YR 3/1) loam, very friable, moderate coarse to fine subangular blocky structure, clear smooth boundary, violently effervescent, 5% coarse fragments; Unit E
2	C	35-58	Brown (10YR 4/3) sandy loam, very friable, weak coarse subangular blocky structure, abrupt smooth boundary, violently effervescent, 5-15% coarse fragments; Unit E.
3	C	50-54	Brown (10YR 4/3) gravelly loamy sand, very friable to loose, single grain, abrupt discontinuous boundary, violently effervescent, 40-70% coarse fragments, comprises one clear thin gravelly bed which pinches out within the trench and clearly originated from the modern channel, but there is at least one other, more diffuse gravelly bed within zone 2; Unit E.
4	2Ab	58-77	Very dark grayish brown (10YR 3/2) loam to sandy clay loam, friable, moderate very coarse prismatic structure, clear smooth boundary, violently effervescent, 7-10% coarse fragments; Unit E.
5	2C	77-110	Brown (10YR 4/3) gravelly sandy loam, friable, massive, gradual smooth boundary, violently effervescent, 45-60% coarse fragments; Unit E.
6	2C	110-148	Brown (10YR 4/3) slightly gravelly sandy loam, friable, massive, abrupt smooth boundary, violently effervescent, 30% coarse fragments; Unit E.
7	2C	148-200	Brown (10YR 4/3) sandy loam, very friable, weak coarse subangular blocky structure, abrupt smooth boundary, violently effervescent, few (1%) calcium carbonate filaments, 5% coarse fragments, mostly < 1 cm in diameter and dispersed throughout zone; Unit E.
8	2C	200-270	Brown (10YR 5/3) sandy loam, very friable, massive to weak very coarse subangular blocky structure, abrupt smooth boundary, violently effervescent, 1-3% calcium carbonate filaments, zone 9 and 10 are alternately bedded in this interval and represent near channel overbank sediments; Unit E.
9	2C	200-270	Pale brown (10YR 6/3) sand to loamy sand, very friable, massive, abrupt smooth boundary, violently effervescent, 1-3% calcium carbonate filaments, zone 9 and 10 are alternately bedded in this interval; Unit E.

TRENCH 30

Location: 0230572E 3901113N
 Geologic Units: Unit E resting upon Unit B.
 Cultural material: Two apparent occupations within the sandy veneer on top of Unit B, one at 49-57 cm, and a second between 70 and 73 cm.
 Comments:

Zone	Horizon	Depth (cm)	Description
1	A	0-60	Very dark gray (10YR 3/2) loam, friable to very friable, moderate medium to fine subangular blocky structure, clear smooth boundary, violently effervescent, 1-3% coarse fragments, one possible occupation around 49-59 cm represented by a few burned rock and debitage fragments; Unit E.
2	AB	60-74	Dark brown (10YR 3/3) loam to sandy clay loam, friable, moderate medium subangular blocky structure, clear smooth boundary, violently effervescent, few (1-7%) calcium carbonate filaments which occur in conspicuous small patches, 1-5% coarse fragments, scatter of burned rock and debitage suggest the presence of an occupation around 70-73 cm; Unit E (but transitional to Unit B).
3	2Bw	74-101	Brown (7.5YR 4/4) sandy clay loam, friable, moderate to strong coarse prismatic structure, abrupt smooth boundary, violently effervescent; Unit B.
4	3Ab	101-116	Brown (7.5YR 4/4 to 4/3) sandy clay, friable to firm, strong medium to coarse prismatic structure, clear smooth boundary, violently effervescent, appears visibly darker in field and may be a faint, weakly developed A horizon; Unit B.
5	3Bk	116-140	Yellowish brown (7.5YR 5/4) sandy clay to sandy clay loam, firm, strong coarse subangular blocky structure, abrupt smooth boundary, violently effervescent, few to common (3-5%) calcium carbonate filaments, few (1-3%) small to medium (3-7mm) irregular shaped white calcium carbonate nodules; Unit B.
6	4Akb	140-170	Brown (7.5YR 4/3) loam to sandy clay loam, friable, moderate coarse subangular blocky structure, gradual smooth boundary, violently effervescent, common (5-7% calcium carbonate filaments, few (1-3%) small to medium (3-7mm) irregular shaped white calcium carbonate nodules in the top 10 cm of this zone; Unit B.
7	4Bk	170-190	Yellowish brown (7.5YR 5/4) loam, friable, weak coarse subangular blocky structure, violently effervescent, 5% calcium carbonate filaments and appears to have more diffuse carbonate; Unit B.

TRENCH 31

Location: 0230598E 3901167N
 Geologic Units: Unit E resting upon Unit B.
 Cultural material: Numerous prehistoric artifacts were observed within the top 50 cm of this trench.
 Comments: This trench was not described.

TRENCH 32

Location: 0230571E 3901073N
 Geologic Units: Unit E resting unconformably upon Unit D.
 Cultural material: A quartzite cobble and a sandstone slab were observed at the base of zone 2, but no definite cultural material was observed.
 Comments: Trench was placed into the T_{0a} surface that forms the core of a tortuous meander in this location.

Zone	Horizon	Depth (cm)	Description
1	A1	0-30	Black (10YR 2/1) sandy loam, very friable, weak coarse subangular blocky structure, diffuse smooth boundary, violently effervescent, few krotovina; Unit E.
2	A2	30-85	Very dark brown (10YR 2/2) loamy sand, very friable, massive, abrupt smooth boundary, violently effervescent, extremely bioturbated, a quartzite pebble and sandstone slab were observed near the base of this zone around 82 cm and may be a prehistoric occupation surface; Unit E.
3	2Ab1	85-135	Very dark gray (10YR 3/1) slightly gravelly silty clay, friable, moderate to strong medium subangular blocky structure, clear smooth boundary, violently effervescent, 5-15% coarse fragments, most of which were matrix supported small reworked caliche fragments and mudballs of reworked Triassic, generally 0.5-3 cm in diameter, a few aquatic snails and bivalves throughout; Unit D.
4	2Ab2	135-165	Very dark grayish brown (10YR 3/2) silty clay, friable, moderate to strong medium to coarse prismatic structure, clear smooth boundary, violently effervescent, common (5-7%) calcium carbonate filaments, few (1%) coarse fragments, few aquatic snails and bivalves; Unit D.
5	2Ab3	165-230	Very dark gray (10YR 3/1) slightly gravelly clay to silty clay, friable, strong medium subangular blocky structure, violently effervescent, few to common (3-5%) calcium carbonate filaments, 5-10% coarse fragments throughout, most of which are fine gravel to granule size bits of reworked Ogallala caliche, traces of charcoal. few aquatic snails and bivalves; Unit D.

TRENCH 33

Location: 0230546E 3901062N
 Geologic Units: Three different depositional units are present within this trench. The top 0.9 m is a veneer of Unit E, which rests upon a 55 cm thick drape of Unit D, which in turns rest unconformably upon a truncated core of Unit B.
 Cultural material: Prehistoric cultural material was observed within Unit D, zone 3 and 4.
 Comments: None.

Zone	Horizon	Depth (cm)	Description
1	A1	0-30	Black (10YR 2/1) to very dark brown (10YR 2/2) sandy loam, very friable, weak coarse to medium subangular blocky structure, diffuse smooth boundary, violently effervescent, numerous krotovina; Unit E.
2	A2	30-90	Very dark brown to very dark grayish brown (10YR 2.5/2) sandy loam to loamy sand, very friable, weak to moderate medium subangular blocky structure, clear smooth boundary, violently effervescent, numerous large krotovina.
3	2Ab1	90-145	Very dark grayish brown (10YR 3/2) loam to silty clay loam, friable, strong extremely coarse prismatic structure, clear smooth boundary, violently effervescent, few (1-3%) calcium carbonate filaments, 1-3% coarse fragments; Unit D.
4	3Akb	145-163	Brown (7.5YR 4/2) to dark brown (7.5YR 3/2) loam, firm, strong medium prismatic structure, clear smooth boundary, violently effervescent, few (1-3%) calcium carbonate filaments, 1% coarse fragments, a prehistoric occupation was observed at the interface of this zone with zone 5 around 138 cm; Unit D or Unit B.
5	3Bk	163-194	Brown (7.5YR 5/4) loam, friable, strong extremely coarse prismatic structure, clear smooth boundary, violently effervescent, common (3-5%) calcium carbonate filaments, 1% coarse fragments, a burned rock was observed at approximately 155 cm; Unit D.
6	4Akb	194-230	Brown (7.5YR 4/3) sandy clay loam, friable, strong medium to coarse subangular blocky structure, violently effervescent, common (5-7%) calcium carbonate filaments, 1% coarse fragments, appears to be a weak A horizon; Unit B.

TRENCH 34

Location: 0230552E 3901031 N
 Geologic Units: A thin drape of Units E/D on top of Unit B.
 Cultural material: One prominent prehistoric occupation around 70 cm below surface.
 Comments: This trench is one of the few places where a channel deposit associated with Unit B has been observed. Many of the upper strata dip slightly to the east, toward the modern stream channel.

Zone	Horizon	Depth (cm)	Description
1	A1	0-40	Very dark brown (10YR 2/2) sandy loam, very friable, weak to moderate subangular blocky structure, diffuse smooth boundary, violently effervescent; Unit E.
2	A2	40-70	Dark brown (10YR 3/2) loam to sandy loam, friable, moderate to strong coarse subangular blocky structure, clear smooth boundary, violently effervescent, numerous krotovina 1-3% coarse fragments; Unit E.
3	2Bw	70-100	Brown (7.5YR 4/4) loam, very friable, moderate coarse subangular blocky structure, abrupt irregular boundary, violently effervescent, 1-3% coarse fragments, a prehistoric occupation is present at the very top of this zone, and consists primarily of a burned rock scatter, although at least three features were present within the wall of this trench; Unit B
4	2C	100-120	Brown (7.5YR 4/4) gravelly sandy loam, very friable, weak coarse subangular blocky structure, abrupt smooth boundary, violently effervescent, 40-60% coarse fragments, mostly 1-5mm gravels, few slightly larger, all caliche; Unit B.
5	2C	120-160	White (~10YR 8/1) gravel, loose, single grain, abrupt smooth boundary, violently effervescent, open framework gravel, fining upward, ranging from 3-5 cm diameter clasts at base and grading upwards to mostly 1-3 mm diameter clasts at top, also contains a few reworked burned rock and quartzite pebbles; Unit B.
6	2C	160-165	Strong brown (7.5YR 4/6) slightly gravelly to gravelly sand, very friable to loose, moderate to strong coarse prismatic structure, abrupt smooth boundary, violently effervescent, 30-70% coarse fragments, most of which are 1-5mm reworked caliche nodules, common (5-7%) calcium carbonate filaments; Unit B.
7	2C	165-185	Strong brown (7.5YR 4/6) slightly gravelly sand, very friable, weak coarse prismatic structure, abrupt smooth boundary, violently effervescent, ~30% coarse fragments mostly fine gravel sized reworked caliche, common (5-7%) calcium carbonate filaments; Unit B
8	3Akb	185-200	Brown (7.5YR 4/3 to 4/2) sandy loam, friable, moderate to strong coarse prismatic structure, violently effervescent, common (5-7%) calcium carbonate filaments, weakly expressed A horizon; Unit B

TRENCH 35

TRENCH DATA LOST

TRENCH 36

Location: 0230567E 3900999N
 Geologic Units: Unit E inset into Unit D.
 Cultural material: None observed.
 Comments: This was the longest continuous section of Unit D observed during fieldwork, and was more than 4 m thick, where beveled and overlain by Unit E. The trench also exposed a continuous and superimposed suite of Unit D channel complexes which were sampled by a series of monoliths. Depths are associated with two measured sections, one through Unit E at east end of the trench, and a second through the thickest part of Unit D, which starts at ~160 cmbs. A bison skeleton was observed within the deposits in approximately the position of zones 18-21, although it was not present in the wall where this measured section was made. The codes in the depth column below the depth for zones 10 to 44 are the stratigraphic designations for those strata in the monoliths.

Zone	Horizon	Depth (cm)	Description
1	A	0-30	Very dark grayish brown (10YR 3/2, sandy loam, very friable to loose, massive to weak medium to fine subangular blocky structure, gradual smooth boundary, violently effervescent; Unit E.
2	AC	30-60	Dark brown to brown (10YR 3.5/3) loamy sand, very friable, weak very coarse subangular blocky structure, clear smooth boundary, violently effervescent, 1-3% coarse fragments; Unit E.
3	C	60-72	Yellowish brown (10YR 5/4) loamy sand, very friable, weak to moderate fine subangular blocky structure, abrupt smooth boundary, violently effervescent, 3-5% coarse fragments; Unit E.
4	2Ab	72-95	Very dark grayish brown (10YR 3/2) loam, very friable, weak to moderate coarse subangular blocky structure, clear smooth boundary, violently effervescent, few (1-3%) calcium carbonate filaments, 7-15% coarse fragments, one prominent but discontinuous stringer of gravel near 75 cm; Unit E.
5	2C	95-117	Dark brown to brown (10YR 3.5/3) sandy loam, very friable, weak coarse subangular blocky structure, clear smooth boundary, violently effervescent, few (1-3%) calcium carbonate filaments, 5-7% coarse fragments; Unit E.
6	2C	117-130	White (~10YR 8/1) to very pale brown (10YR 7/3) sandy gravel, loose, single grain, abrupt discontinuous boundary, violently effervescent, 90% coarse fragments; Unit E.
7	2Bk	130-180	Brown (10YR 4/3) loam to sandy loam, very friable, moderate coarse subangular blocky structure, gradual smooth boundary, violently effervescent, many (7%) calcium carbonate filaments, 5-7% coarse fragments, two bison bones were observed around 145-150 cm; Unit E.
8	2Bk	180-220	Brown (10YR 4/3) loam, very friable, weak to moderate coarse subangular blocky structure, abrupt smooth boundary, violently effervescent, violently effervescent, 2-5% calcium carbonate filaments; Unit E.
9	2Cg	220-270	Very pale brown (10YR 7/3) sand, loose, single grain, abrupt smooth boundary, violently effervescent, prominently laminated; Unit E.
10	3C	160-167 M6-1	Pale brown (10YR 6/3) sandy gravel, abrupt smooth boundary, violently effervescent; Unit D.
11	3C	167-192 M6-2	Dark gray (10YR 4/1) silt loam to loam, clear smooth boundary, violently effervescent, 1-3% calcium carbonate filaments, few scattered gravels, few aquatic snails; Unit D.

Zone	Horizon	Depth (cm)	Description
12	3C	192-201 M6-3	Pale brown (10YR 6/3) sandy loam, abrupt smooth boundary, violently effervescent, subtle horizontal laminations; Unit D.
13	3C	201-205 M6-4	Very dark gray (10YR 3/1) silty clay, abrupt smooth boundary, violently effervescent; Unit D.
14	3C	205-209 M6-5	Light gray (2.5Y 7/1) loam (marl?), abrupt wavy boundary, many tiny aquatic snails, possibly some diatomaceous laminae; Unit D.
15	3C	209-220 M6-6 M5-1	Dark gray (10YR 4/1) to very dark gray (10YR 3/1) loam to clay loam, abrupt smooth boundary, violently effervescent, common aquatic snails and mussels; Unit D.
16	3C	220-221 M5-2	Pale brown (10YR 6/3) sand, abrupt smooth boundary, violently effervescent, laminated; Unit D.
17	3C	221-232 M5-3	Very dark gray (10YR 3/1) clay, clear smooth boundary, violently effervescent, common charcoal fragments within this zone, one of which (at 224 cm) was radiocarbon dated and yielded an age of 860±40 years BP (Beta-239635); Unit D
18	3C	232-237 M5-4	Gray (10YR 5/1) sandy loam, clear smooth boundary, violently effervescent; Unit D.
19	3C	237-288 M5-5 M4-1	Very dark gray (10YR 3/1) clay to clay loam, moderate to strong coarse subangular blocky structure, abrupt smooth boundary, common (5-7%) calcium carbonate filaments, numerous tiny (<1mm) snails, a piece of charcoal from 277 cm was submitted for radiocarbon dating and yielded an age of 750 ± 40 years B.P. (Beta-239652); Unit D.
20	3C	288-294 M4-2	Dark gray to gray (10YR 4/1 to 5/1) loam, massive, abrupt wavy boundary, violently effervescent, 1-3% coarse fragments, few (reworked?) small clams; Unit D.
21	3C	294-302 M4-3	Black to very dark gray (10YR 2/1 to 3/1) clay, strong medium to coarse angular blocky structure, abrupt smooth boundary, violently effervescent, 1% calcium carbonate filaments; Unit D.
22	3C	302-303 M4-4	Gray (10YR 5/1) sand parting, abrupt smooth, violently effervescent, prominent break in clay bed; Unit D.
23	3C	303-319 M4-5 M3-1	Dark gray (10YR 4/1) clay loam, abrupt smooth boundary, violently effervescent; Unit D.
24	3C	319-320 M3-2	Light brownish gray (10YR 6/2) fine sand, abrupt smooth boundary, violently effervescent, prominent parting in thicker clay bed; Unit D.
25	3C	320-329 M3-3	Very dark gray (10YR 3/1) clay, strong coarse angular blocky structure, abrupt smooth boundary, violently effervescent, massive clay with prominent tendency to crack, a bulk sediment sample from this zone was radiocarbon dated and yielded an age of 1430 ± 40 years B.P. (Beta-239651); Unit D
26	3C	329-330	Light brownish gray (10YR 6/2) fine sand, abrupt smooth boundary, violently effervescent, prominent parting in thicker clay bed; Unit D.
27	3C	330-339 M3-4	White (10YR 7/1) sandy gravel, abrupt smooth boundary, violently effervescent, gravels are mostly 0.5-3 mm; Unit D.
28	3C	339-350 M3-5	Very dark gray (10YR 3/1) clay, strong coarse angular blocky structure, clear smooth boundary, violently effervescent, possibly laminated; Unit D
29	3Cg	350-360 M3-6	Gray (10YR 5/1) sandy loam, abrupt smooth boundary, violently effervescent, common fine (1-3mm) distinct reddish yellow (7.5YR 6/6) mottles around pores; Unit D
30	3Cg	360-408 z.12 column	Olive gray (5Y 5/2) sand, interdigitated with zone 31, part of a channel body, very friable, abrupt smooth boundary, violently effervescent; Unit D.
31	3Cg	360-408 z.13 column	Dark gray (5Y 4/1) sandy loam, very friable, abrupt smooth boundary, violently effervescent, occasional charcoal fragments, common aquatic mollusks; Unit
32	3Cg	408-413 M2-1	Light brownish gray (10YR 6/2), clear wavy boundary, violently effervescent, common fine (1-3mm) distinct reddish yellow (7.5YR 6/6) mottles around pores; Unit D.

Zone	Horizon	Depth (cm)	Description
33	3Cg	413-447 M2-2a	Light brownish gray (10YR 6/2) sand, abrupt irregular boundary, violently effervescent, intimately interbedded with zone 33, both of which exhibit contorted bedding and appear disturbed; Unit D.
34	3Cg	413-447 M2-2b	Gray (10YR 5/1) loam to silty clay loam, clear smooth boundary, violently effervescent, common fine (1-3 mm) distinct reddish yellow (7.5YR 6/6) mottles around pores, common small pieces of charcoal throughout; Unit D.
35	3Cg	447-450 M2-3	Dark gray (10YR 4/1) silty clay to clay, strong very fine subangular blocky structure, abrupt irregular boundary, violently effervescent, appears to contain some wood fragments; Unit D.
36	3Cg	450-460 M2-4 M1-1	Light brownish gray (10YR 6/2) to pale brown (10YR 6/3) sand to sandy loam, clear smooth boundary, violently effervescent; Unit D.
37	3Cg	460-472 M1-2	Dark gray (10YR 4/1) loam, clear smooth boundary, violently effervescent; Unit D.
38	3Cg	472-484 M1-3	Grayish brown (10YR 5/2) slightly gravelly sandy loam, abrupt smooth boundary, violently effervescent, bottom half of zone is laminated and includes small bivalves; Unit D.
39	3Cg	484-486 M1-4	Dark gray (10YR 4/1) clay, friable, abrupt smooth boundary, violently effervescent; Unit D.
40	3Cg	486-487 M1-5	Light brownish gray (10YR 6/2) sand, loose, abrupt smooth boundary, violently effervescent; Unit D.
41	3Cg	487-490 M1-6	Dark gray (10YR 4/1) silty clay, friable, abrupt smooth boundary, violently effervescent, horizontally laminated; Unit D.
42	3Cg	490-494 M1-7	Light brownish gray (2.5Y 6/2) loam, weak fine platy structure, clear smooth boundary, violently effervescent, seems carbonate rich and possibly is a marl, prominent horizontal laminations; Unit D.
43	3Cg	494-498 M1-8	Dark gray (10YR 4/1) silty clay, friable, abrupt smooth boundary, violently effervescent, horizontally laminated, few white laminations (either marl or diatomite), a bulk sediment sample collected from this zone was submitted for radiocarbon dating but the results are not yet available; Unit D.
44	3Cg	498-506 M1-9	White (10YR 8/1) sand, loose, violently effervescent, few fine (1-3 mm) distinct reddish yellow (7.5YR 6/6) mottles around pores, Unit D

TRENCH 37

Location: 0230474E 3900957N
 Geologic Units: Holocene colluvium (Qc; undifferentiated) resting upon Unit B.
 Cultural material: None observed.
 Comments: Trench is located on a colluvial slope near the margin of the alluvial valley.

Zone	Horizon	Depth (cm)	Description
1	A	0-30	Brown (7.5YR 5/3) slightly gravelly to gravelly loam, very friable, weak medium subangular blocky structure, clear smooth boundary, violently effervescent, 15-35% coarse fragments which are mostly 1-3 cm diameter reworked Ogallala caliche fragments, and a few (5-10%) quartzite pebbles (composition is similar for all Qc deposits in this trench); Qc.
2	C	30-67	Brown (7.5YR 5/4) slightly gravelly to gravelly loam, very friable, weak medium subangular blocky structure, abrupt smooth boundary, violently effervescent, few to common (1-5%) calcium carbonate filaments, 15-35% coarse fragments; Qc
3	2Ab	67-72	Brown (7.5YR 4/3) slightly gravelly to gravelly loam, very friable, weak medium subangular blocky structure, abrupt smooth boundary, violently effervescent, few to common (1-5%) calcium carbonate filaments, 15-35% coarse fragments; Qc
4	2C	72-110	Brown (7.5YR 5/4) slightly gravelly to gravelly loam, very friable, weak medium subangular blocky structure, clear smooth boundary, violently effervescent, few to common (1-5%) calcium carbonate filaments, 15-35% coarse fragments; Qc
5	3Ab	110-118	Brown (7.5YR 4/3) slightly gravelly to gravelly loam, very friable, weak medium subangular blocky structure, clear smooth boundary, violently effervescent, few to common (1-5%) calcium carbonate filaments, 15-35% coarse fragments; Qc.
6	3C	118-155	Brown (7.5YR 4/3) slightly gravelly to gravelly loam, very friable, weak medium subangular blocky structure, gradual smooth boundary, violently effervescent, few to common (1-5%) calcium carbonate filaments, 15-35% coarse fragments; Qc.
7	4AC	155-190	Brown (7.5YR 4/2) slightly gravelly loam, very friable, weak coarse subangular blocky structure, gradual smooth boundary, violently effervescent, 7-25% coarse fragments; Qc/Unit B transition.
8	5Akb	190-240	Dark brown (7.5YR 3/2) sandy clay, very friable, moderate medium to coarse subangular blocky structure, gradual smooth boundary, violently effervescent, common (3-5%) calcium carbonate filaments, few thin discontinuous coats of calcium carbonate on ped faces; Unit B.
9	5Bk	240-300+	Yellowish red (5YR 4.5/6) sandy clay loam, friable, moderate to strong medium to coarse subangular blocky structure, violently effervescent, common to many (5-7%) calcium carbonate filaments; Unit B.

TRENCH 38

Location: 0230425E 3900964N
 Geologic Units: Pliocene Ogallala Formation resting unconformably upon the Triassic Trujillo Formation.
 Cultural material: None.
 Comments: Trench was excavated to examine the geologic context of the quartzite gravel that crops out in mid-slope positions in various areas of the valley. The trench revealed that these quartzite gravels are basal Ogallala Formation, and rest directly upon the Trujillo Formation mudstones.

Zone	Horizon	Depth (cm)	Description
1	A	0-10	Yellowish brown (10YR 5/4) loamy sand, very friable, massive to weak medium subangular blocky structure, clear smooth boundary, violently effervescent; soil formed on Ogallala Formation.
2	Bk	10-70	Light reddish brown-reddish yellow (5YR 6/5) slightly gravelly to gravelly loamy sand, loose, single grain, abrupt smooth boundary, violently effervescent, common 0.5-2 cm irregular shaped calcium carbonate nodules (possibly dissolving), 15-60% coarse fragments; this is the fill of a karstic solution pit formed into the calcrete developed within the Ogallala Formation.
3	K1	5-20	White (N 8/1) massive calcrete sandy gravel conglomerate, extremely hard, massive structure, abrupt smooth boundary, violently effervescent, >70% calcium carbonate; Ogallala Formation.
4	K2	20-70	White (N 8/1) massive calcrete sandy gravel conglomerate, extremely hard, massive, abrupt wavy boundary, violently effervescent, 60-90% coarse fragments, some of the gravel clasts appear to be imbricated toward the southeast, gravel is mostly siliceous (quartzitic) well-rounded and mostly 2-3 cm in diameter although a few are upwards of 15 cm; Ogallala Formation.
5	K3	70-90	Very dark gray (N 3/0) massive calcrete, sandy fine gravel conglomerate, extremely hard, weak very thin, platy structure in places, abrupt smooth boundary, violently effervescent, nearly all gravels are completely coated with manganese oxide, gravels are siliceous (like zone 4 and 6); Ogallala Formation.
6	K4	90-135	White (N 8/1) massive calcrete sandy gravel conglomerate, extremely hard, massive, abrupt wavy boundary, violently effervescent, 60-90% coarse fragments, some of the gravel clasts appear to be imbricated toward the southeast, gravel is mostly siliceous (quartzitic) well-rounded and mostly 2-3 cm in diameter although a few are upwards of 15 cm, very thin laminar calcrete in the top few mm of this zone; Ogallala Formation.
7	K5	135-142	White (N 8/1) laminar calcrete, nearly completely calcium carbonate, extremely hard, strong thin to very thin platy structure, abrupt wavy boundary, violently effervescent; occurs at the interface between the Ogallala and Trujillo Formations.
8	2Bkssg	142-240	Reddish brown (5YR 4/4) clay, extremely hard, strong extremely coarse wedge structure parting to strong fine wedge structure, violently effervescent, many thick (1-2 mm) continuous white coats of calcium carbonate on ped faces in top 50 cm of zone, few coarse prominent light greenish gray (5GY 7/1) mottles on ped faces, common prominent black (N 2/0) coats on ped faces, few 0.5-1.5 cm calcium carbonate nodules in the top 20 cm of this zone; Trujillo Formation.

TRENCH 39

Location: 0230468E 3900900N
 Geologic Units: Unit E resting unconformably upon Unit D.
 Cultural material: None observed.
 Comments: none

Zone	Horizon	Depth (cm)	Description
1	AC	0-50	Brown (10YR 4/3) sandy loam, very friable, weak medium subangular blocky structure, clear smooth boundary, violently effervescent, 3-5% coarse fragments; Unit E.
2	2Ab	50-65	Very dark grayish brown (10YR 3/2) loam, very friable, moderate medium subangular blocky structure, clear smooth boundary, violently effervescent; Unit E.
3	2AC	65-135	Dark grayish brown (10YR 4/2) sandy loam, friable, weak to moderate coarse subangular blocky structure, abrupt smooth boundary, violently effervescent; Unit E.
4	3Ab	135-195	Dark gray (10YR 4/1) silty clay, friable, moderate fine to medium subangular blocky structure, clear smooth boundary, violently effervescent, 5% calcium carbonate filaments, 2-3% coarse fragments; Unit D.
5	3AC	195-210	Brown (10YR 4/3) loam to sandy loam, friable, weak to moderate coarse subangular blocky structure, abrupt smooth boundary, violently effervescent, 1-3% calcium carbonate filaments, 1-3% coarse fragments; Unit D.
6	4Ab	210-260	Black (10YR 2/1) to very dark gray (10YR 3/1) sandy clay, friable, strong very coarse subangular blocky structure, violently effervescent, 1-2% calcium carbonate filaments, hints of bedding, few faintly visible 1-2 cm thick sandier beds; Unit D.

TRENCH 40

Location: 0230484E 3900851N
 Geologic Units: Thin drape of Unit E and possibly Unit D on top of Unit C
 Cultural material: None observed
 Comments: This is the most complete section of Unit C observed in the valley. Zones 5, 6, 7 and 8 appear to be freshwater marl, or at least have significantly elevated amounts of diffuse calcium carbonate.

Zone	Horizon	Depth (cm)	Description
1	A	0-40	Very dark grayish brown (10YR 3/2) sandy loam, very friable, weak medium subangular block structure, clear smooth boundary, violently effervescent; Unit E.
2	AC	40-85	Dark grayish brown (10YR 4/2) loamy sand, very friable, weak very coarse subangular blocky structure, abrupt smooth boundary, violently effervescent; Unit E.
3	2Ab	85-150	Very dark grayish brown (10YR 3/2) loam, friable, moderate medium subangular blocky structure, diffuse smooth boundary, violently effervescent, 3% calcium carbonate filaments; Unit D?
4	2AB	150-180	Very dark grayish brown-dark grayish brown (10YR 3.5/2) loam to silt loam, friable, moderate medium subangular blocky structure, clear smooth boundary, violently effervescent, few (1-3%) calcium carbonate filaments, Unit D?
5	3Ck	180-210	Brown (10YR 5/3) loam (marl?), friable, weak medium subangular blocky structure, gradual smooth boundary, violently effervescent, abundant diffuse calcium carbonate, many (15-25%) calcium carbonate filaments, <1% coarse fragments; Unit C.
6	4Ak	210-245	Dark grayish brown (10YR 4/2) loam, friable, moderate to strong subangular blocky structure, clear smooth boundary, violently effervescent, many (10-15%) calcium carbonate filaments, abundant diffuse calcium carbonate, few fine faint light brownish gray (10YR 6/2) redox depletions, weak A horizon, a bulk sample of which collected from the top of the zone at 210-215 cm yielded an age of 2250 ± 40 years B.P. (Beta-238310); Unit C.
7	4Bk	245-280	Brown (7.5YR 5/4) loam, friable, weak to moderate very coarse subangular blocky structure, gradual smooth boundary, violently effervescent, many (15-25%) calcium carbonate filaments, abundant diffuse calcium carbonate, few articulated bivalves; Unit C.
8	4Bk	280-330	Dark grayish brown (10YR 4/2) sandy loam to loam, friable, weak medium subangular blocky structure, clear smooth boundary, violently effervescent, many (7-10%) calcium carbonate filaments, 3-10% coarse fragments, few articulated bivalves; Unit C.
9	4Cg	330-342	Brown (7.5YR 5/3) slightly gravelly loam, very friable, weak coarse subangular blocky structure, abrupt smooth boundary, violently effervescent, 30-50% coarse fragments most of which are fine gravel size reworked caliche clasts, common medium to coarse light olive gray (5Y 6/2) cylindrical redox depletions; Unit C.
10	4Cg	342-363	Yellowish brown (10YR 5/8) sandy loam, friable, weak very coarse subangular blocky structure, abrupt smooth boundary, violently effervescent, looks yellow in the field, few fine faint light brownish gray (10YR 6/2) cylindrical redox depletions; Unit C.
11	4C	363-371	Brown (7.5YR 5/3) slightly gravelly loam, very friable, weak coarse subangular blocky structure, abrupt smooth boundary, violently effervescent, 30-50% coarse fragments most of which are fine gravel size reworked caliche clasts; Unit C.

Zone	Horizon	Depth (cm)	Description
12	4C	371-420	Brown (7.5YR 5/4) loam, friable, moderate to strong coarse subangular blocky structure, clear smooth boundary, violently effervescent, few (1-3%) calcium carbonate filaments, few fine faint light brownish gray (10YR 6/2) cylindrical redox depletions; Unit C.
13	4C	420-445	Very pale brown (10YR 7/3) sand, loose, single grain, abrupt smooth boundary, violently effervescent; Unit C.
14	5AC	445-458	Brown (10YR 5/3) sandy loam, friable, weak very coarse prismatic structure, abrupt smooth boundary, violently effervescent, possibly a weak A horizon, a bulk sample of which was radiocarbon dated and yielded an age of 4330 ± 40 years B.P. (Beta-238311); Unit C.
15	5C	458-470	Very pale brown (10YR 7/3) slightly gravelly sand, loose, single grain, abrupt smooth boundary, violently effervescent, 20-40% coarse fragments; Unit C.
16	6AC	470-480+	Brown (10YR 5/3) loam, very friable, weak coarse prismatic structure, violently effervescent; Unit C.

TRENCH 41

Location: 0230482E 3900810N
Geologic Units:
Cultural material: None observed.
Comments: Not described.

TRENCH 42

Location: 0230494E 3900771N
 Geologic Units: Thin veneer (0.5 m) of Unit E on top of Unit B
 Cultural material: None observed.
 Comments: This trench was excavated to the maximum reach of the backhoe in an attempt to reach the base of Unit B, but this was unsuccessful, and the trench was terminated at 4.5 m.

Zone	Horizon	Depth (cm)	Description
1	A	0-44	Very dark grayish brown (10YR 3/2) sandy loam, very friable, weak medium subangular blocky structure, abrupt smooth boundary, violently effervescent, 3-5% coarse fragments; Unit E.
2	2Ab	44-85	Black (7.5YR 2.5/1) sandy clay to clay loam, very hard, strong very coarse prismatic structure parting to strong coarse angular blocky structure, clear smooth boundary, violently effervescent, 1-3% coarse fragments; Unit B.
3	2Bw	85-110	Brown (7.5YR 4/3) clay, very hard, strong very coarse prismatic structure parting to strong coarse angular blocky structure, gradual smooth boundary, violently effervescent, 1-3% coarse fragments; Unit B.
4	2Bk	110-170	Brown (7.5YR 4/3) clay, very hard, strong very coarse prismatic structure parting to strong coarse angular blocky structure, clear smooth boundary, violently effervescent, few (1-3%) calcium carbonate filaments; Unit B.
5	3Ab1	170-185	Dark brown (7.5YR 3/3) clay, firm, strong very coarse prismatic structure parting to strong coarse angular blocky structure, clear smooth boundary, violently effervescent, few (1-3%) calcium carbonate filaments (quite coarse ones), 3-5% coarse fragments; Unit B.
6	3Ab2	185-200	Brown (7.5YR 4/4 to 4/3) silty clay, friable, moderate coarse prismatic structure, clear smooth boundary, violently effervescent, common to many (7-10%) calcium carbonate filaments, possibly a few small calcium carbonate nodules but hard to tell owing to the gravel component, 5-20% coarse fragments most of which were 1-5 mm in diameter; Unit B.
7	3Bk	200-280	Brown (7.5YR 4/4) loam to sandy clay, friable, weak to moderate medium to coarse subangular blocky structure parting to weak to moderate coarse prismatic structure, clear smooth boundary, violently effervescent, common (5-7%) calcium carbonate filaments; Unit B.
8	4Ab	280-294	Strong brown (7.5YR 4/6) silty clay, firm, moderate medium subangular blocky structure, clear smooth boundary, violently effervescent, common (5-7%) calcium carbonate filaments, common faint white discontinuous calcium carbonate coats on ped faces; Unit B.
9	4C	294-315	Strong brown (7.5YR 4/6) loam, very friable, moderate medium subangular blocky structure, clear smooth boundary, violently effervescent, common (3-5%) calcium carbonate filaments; Unit B.
10	4C	315-375	Brown (7.5YR 5/4 to 7.5YR 4/4) loam, friable, moderate medium subangular blocky structure, clear smooth boundary, violently effervescent, common (3-5%) calcium carbonate filaments, has a mottled appearance, possible due to presence of small discontinuous manganese coats on grains; Unit B.
11	4C	375-410	Brown-strong brown (7.5YR 5/5) sandy loam, very friable, weak to moderate medium subangular blocky structure, clear smooth boundary, violently effervescent, few (3%) calcium carbonate filaments; Unit B.
12	4C	410-450	Strong brown (7.5YR 5/6) sandy loam, very friable, weak medium subangular blocky structure, violently effervescent, few (1-3%) calcium carbonate filaments, few prominent black (N2/0) thick (3-5 mm) hypocoats of manganese lining a few channels and pores; Unit B.

TRENCH 43

Location: 0230502E 3900765N
 Geologic Units: Unit E
 Cultural material: None observed
 Comments: This appears to be all Unit E deposited in a near channel overbank setting.

Zone	Horizon	Depth (cm)	Description
1	A	0-34	Very dark grayish brown (10YR 3/2) sandy loam, very friable, weak medium subangular blocky structure, abrupt wavy boundary, violently effervescent, <10% coarse fragments; Unit E.
2	C	34-38	Yellowish brown (~10YR 5/4) gravelly sand, very friable, single grain, abrupt wavy boundary, violently effervescent, 40-70% coarse fragments; Unit E.
3	C	38-70	Brown (10YR 4/3) loamy sand, very friable, weak medium subangular blocky structure, abrupt smooth boundary, violently effervescent, 1% coarse fragments; Unit E.
4	2Ab	70-90	Very dark grayish brown (10YR 3/2) loam, very friable to friable, moderate medium subangular blocky structure, clear smooth boundary, violently effervescent, 5-10% coarse fragments; Unit E.
5	2C	90-120	Dark brown (10YR 3/2) slightly gravelly sandy loam, very friable, weak medium subangular blocky structure, clear smooth boundary, violently effervescent, 10-25% coarse fragments mostly 1-3 cm in diameter scattered throughout; Unit E.
6	2C	120-130	Brown (10YR 4/3) slightly gravelly to gravelly sandy loam, very friable, weak medium to coarse subangular blocky structure, abrupt smooth boundary, violently effervescent, 30-60% coarse fragments; Unit E.
7	2C	130-142	Dark yellowish brown (10YR 4/4) loam to slightly gravelly loam, friable, moderate medium subangular blocky structure; abrupt smooth boundary, violently effervescent, few (1-3%) calcium carbonate filaments, 10-25% coarse fragments; Unit E.
8	2C	142-175	Brown (10YR 4/3) loam, very friable, moderate medium subangular blocky structure; abrupt smooth boundary, violently effervescent, few (1-3%) calcium carbonate filaments, <1% coarse fragments; Unit E.
9	2C	175-180	Yellowish brown (~10YR 5/4) extremely gravelly sand, loose, single grain, abrupt smooth boundary, violently effervescent, 60-90% coarse fragments; Unit E.
10	2C	180-200	Yellowish brown (10YR 5/4) sand to loamy sand, loose to very friable, single grain, abrupt smooth boundary, violently effervescent; Unit E.
11	2C	200-217	Brown (10YR 4/3) loam, very friable, weak to moderate medium subangular blocky structure, abrupt smooth boundary, violently effervescent, few (1-3%) calcium carbonate filaments; Unit E.
12	3Akb	217-235	Dark grayish brown (10YR 4/2) loam to sandy clay, very friable, weak to moderate medium subangular blocky structure, clear smooth boundary, violently effervescent, common (5%) calcium carbonate filaments; Unit E.
13	3C	235-245	Light yellowish brown (10YR 6/4) loamy sand, very friable, massive, abrupt smooth boundary, violently effervescent; Unit E.
14	3C	245-250	Very pale brown (10YR 7/4) sand, loose, single grain, abrupt smooth boundary, violently effervescent, <3% coarse fragments; Unit E.
15	3C	250-258	Brown (10YR 4/3) sandy loam, very friable, massive, abrupt smooth boundary, violently effervescent; Unit E.
16	3C	258-280	Yellowish brown (10YR 5/4) loamy sand, very friable, massive, violently effervescent; Unit E.

TRENCH 44

Location: 0230471E 3899821N
 Geologic Units: Holocene colluvium (Qc) overlying Unit A, which in turn rests upon the Ogallala Formation.
 Cultural material: None observed
 Comments: Trench was placed behind and upslope of one of two outcrop exposures of Unit A observed on the Landis Property, and, unfortunately revealed the upslope end of this deposit.

Zone	Horizon	Depth (cm)	Description
1	AC	0-30	Brown (10YR 4/3) slightly gravelly sandy loam, loose to very friable, massive to weak medium subangular blocky structure, abrupt smooth boundary, violently effervescent, 10-20% coarse fragments; Qc.
2	2Ab	30-50	Dark grayish brown (10YR 4/2) slightly gravelly sandy loam, very friable, weak to moderate medium to coarse subangular blocky structure, gradual smooth boundary, violently effervescent, 15% coarse fragments, few worm casts; Qc.
3	2Bk	50-100	Yellowish brown (10YR 5/4) slightly gravelly sandy loam, very friable, weak to moderate coarse subangular blocky structure, abrupt smooth boundary, violently effervescent, 15% coarse fragments, few worm casts; Qc.
4	3Akb1	35-80	Very dark brown (10YR 2/2) loam, very friable, moderate extremely coarse prismatic structure, clear smooth boundary, strongly effervescent, common (5-7%) calcium carbonate filaments, common thin patchy calcium carbonate coats on ped faces; Unit A.
5	3Akb2	80-140	Black (10YR 2/1) loam, very friable, strong extremely coarse prismatic structure, clear smooth boundary, strongly effervescent, many (7-15%) calcium carbonate filaments, many thin prominent white calcium carbonate coats on ped faces, 3% coarse fragments; Unit A.
6	4Bkm	140-150	White (10YR 8/1) sandstone, extremely firm, massive, gradual irregular boundary, violently effervescent, petrocalcic horizon formed in sand; Ogallala Formation.
7	4Bk	150-180	Light brown (7.5YR 6/4) sand, loose to very friable, massive, abrupt irregular boundary, violently effervescent, common (5-7%) calcium carbonate nodules, an un lithified section of the Ogallala Formation.

TRENCH 45

Location: 0230478E 3900071N
 Geologic Units: Mostly Unit B
 Cultural material: None observed.
 Comments: This was a long trench excavated between two trenches on this surface that appeared to contain possible cultural material around 2.5 m below the surface.

Zone	Horizon	Depth (cm)	Description
1	A	0-40	Very dark grayish brown (10YR 3/2) loam to sandy loam, very friable, weak to moderate medium subangular blocky structure, clear smooth boundary, violently effervescent, 1% coarse fragments; Unit E and/or Unit B.
2	Bw	40-70	Brown (7.5YR 4/4) sandy loam, very friable, moderate medium subangular blocky structure, abrupt smooth boundary, violently effervescent, 1% coarse fragments; Unit B.
3	2Ab	70-160	Brown (7.5YR 4/3) loam to silt loam, friable, strong medium prismatic structure, diffuse smooth boundary, violently effervescent, 1-3% coarse fragments, few (1%) calcium carbonate filaments; Unit B.
4	2Bk	160-210	Brown (7.5YR 4/4) loam to silt loam, friable, moderate medium subangular blocky structure, abrupt smooth boundary, violently effervescent, common (5%) calcium carbonate filaments, few faint discontinuous calcium carbonate coats on ped faces; Unit B.
5	2Bk3	210-300	Brown (7.5YR 4/4) loam to silty clay loam, friable, moderate to strong fine prismatic structure parting to moderate medium subangular blocky structure, abrupt smooth boundary, violently effervescent, common (5%) calcium carbonate filaments, few faint discontinuous calcium carbonate coats on ped faces, 5-20 % coarse fragments; Unit B.
6	C	300-320	Brown (7.5YR 4/4) silt loam, very friable, moderate medium subangular blocky structure, clear smooth boundary, violently effervescent, few (1-3%) calcium carbonate filaments, 1% coarse fragments; Unit B.
7	C	320-380	Strong brown (7.5YR 4.5/6) sandy loam, very friable, massive, violently effervescent, few (1%) calcium carbonate filaments; Unit B.

TRENCH 46

Location: Immediately east of BT 40, cutting across the creek channel.
 Geologic Units: Modern alluvium (Unit F)
 Cultural material: A little glass was observed in one deposit. No prehistoric material was observed.
 Comments: Only drew cross-section, did not describe in detail.

This page intentionally left blank.

APPENDIX B
ARTIFACT DISTRIBUTIONS

This page intentionally left blank.

Artifact Frequency Distribution
Site # 41PT185 Locus A

For each test unit, tabulate artifact frequency (from field catalog) by artifact class (columns) and depth (rows). Use '+' for artifacts present (per level notes) but not counted. Note counts which include a temporal diagnostic with '*'. Note bottom of each unit with a heavy horizontal line at end of bottom level. Shade levels in each unit if a feature is present.

cmbs	Test Unit 7								Test Unit 8								Test Unit 9							
	L	B	C	S	Ch	BR	T	GS	L	B	C	S	Ch	BR	T	GS	L	B	C	S	Ch	BR	T	GS
0-10	1																3					3		
10-20																	3					2		
20-30	5																1					1	1	
30-40	1	1															4							
40-50		1				4											11	4				1	1*	
50-60	1					1			3								1	1				4		
60-70									1	1				1			1					7		
70-80									27	4				123		2	3							
80-90									9	1				41										
TOTAL	8	2				5			40	6				165			26	8				18	1	

cmbs	Test Unit 10								Test Unit 11								Test Unit 12							
	L	B	C	S	Ch	BR	T	GS	L	B	C	S	Ch	BR	T	GS	L	B	C	S	Ch	BR	T	GS
0-10	2																							
10-20	2					1																		
20-30	1																1							
30-40	3	1															1	3						
40-50									5				1				1							
50-60																								
60-70		3															1							
70-80																								
80-90		7																						
90-100									1															
100-110																								
110-120																1								
120-130																1	1							
130-140																								
TOTAL	8	11				1			1	5			1				3	7						

L = Lithic, B = Bone, C = Ceramic, S = Shell, Ch = Charcoal, BR = Burned Rock, T = Tool, GS = Ground Stone

Artifact Frequency Distribution
Site # 41PT185 Locus C

For each test unit, tabulate artifact frequency (from field catalog) by artifact class (columns) and depth (rows). Use '+' for artifacts present (per level notes) but not counted. Note counts which include a temporal diagnostic with '*'. Note bottom of each unit with a heavy horizontal line at end of bottom level. Shade levels in each unit if a feature is present.

cmbs	Test Unit 18								Test Unit 19								Test Unit 20							
	L	B	C	S	Ch	BR	T	GS	L	B	C	S	Ch	BR	T	GS	L	B	C	S	Ch	BR	T	GS
0-10	1								1															
10-20																	3					1	1	
20-30	1								1								1					1		
30-40																	2							
40-50									1								1						1	
50-60									1													1		
60-70									1	1				2			2							
70-80		1							4								2							
80-90									1								1					28		
90-100																	2	9				2	1	
100-110																	4					3		
TOTAL	2	1							2	9				2			14	13				36	3	

cmbs	Test Unit 21								Test Unit 22								Test Unit 23							
	L	B	C	S	Ch	BR	T	GS	L	B	C	S	Ch	BR	T	GS	L	B	C	S	Ch	BR	T	GS
0-10																								
10-20									3					1	1*									
20-30									5					4	1									
30-40									5	1				5	1									
40-50									6					5										
50-60									4					6	1									
60-70									1	3				3	1									
70-80	2								5	5				7	1									
80-90									2	5				3			1	1				5		
90-100	2	3							5					6			8					39		
100-110																	2	3				25		
110-120																								
TOTAL	4	3							31	19				40	6		3	12				69		

L = Lithic, B = Bone, C = Ceramic, S = Shell, Ch = Charcoal, BR = Burned Rock, T = Tool, GS = Ground Stone

**Artifact Frequency Distribution
Site # 41PT185 Locus C**

For each test unit, tabulate artifact frequency (from field catalog) by artifact class (columns) and depth (rows). Use '+' for artifacts present (per level notes) but not counted. Note counts which include a temporal diagnostic with '*'. Note bottom of each unit with a heavy horizontal line at end of bottom level. Shade levels in each unit if a feature is present.

cmbs	Test Unit 24								Test Unit 25								Test Unit 26							
	L	B	C	S	Ch	BR	T	GS	L	B	C	S	Ch	BR	T	GS	L	B	C	S	Ch	BR	T	GS
0-10						1																		
10-20																	1							
20-30	1					1			2								2							
30-40	2					1			1								2							
40-50	1	3															2							
50-60	2	3				7	1										4							
60-70	3	6				8																		
70-80	5	1							1															
80-90		11				3			1	1														
90-100																1	3							
100-110									2	3						1								
110-120																								
120-130																								
130-140									1															
140-150																								
TOTAL	14	24				21	1		3	9							1	15						

cmbs	Test Unit 27								Test Unit 28								Test Unit 29							
	L	B	C	S	Ch	BR	T	GS	L	B	C	S	Ch	BR	T	GS	L	B	C	S	Ch	BR	T	GS
0-10																								
10-20						1											1							
20-30		1																						
30-40						1											2					1		
40-50									2								1							
50-60	1																							
60-70	1						1																	
70-80															1*		1							
80-90																	2	2						
90-100																								
TOTAL	2	1				2	1		2						1		7	2				1		

L = Lithic, B = Bone, C = Ceramic, S = Shell, Ch = Charcoal, BR = Burned Rock, T = Tool, GS = Ground Stone

Artifact Frequency Distribution
Site # 41PT185 Locus C

For each test unit, tabulate artifact frequency (from field catalog) by artifact class (columns) and depth (rows). Use '+' for artifacts present (per level notes) but not counted. Note counts which include a temporal diagnostic with '*'. Note bottom of each unit with a heavy horizontal line at end of bottom level. Shade levels in each unit if a feature is present.

cmbs	Test Unit 30							
	L	B	C	S	Ch	BR	T	GS
0-10	1							
10-20	0					1		
20-30								
30-40						2		
40-50								
50-60	1							
60-70		1				3		
70-80								
80-90								
90-100								
TOTAL	2	1				6		

L = Lithic, B = Bone, C = Ceramic, S = Shell, Ch = Charcoal, BR = Burned Rock, T = Tool, GS = Ground Stone

**Artifact Frequency Distribution
Site # 41PT186**

For each test unit, tabulate artifact frequency (from field catalog) by artifact class (columns) and depth (rows). Use '+' for artifacts present (per level notes) but not counted. Note counts which include a temporal diagnostic with '*'. Note bottom of each unit with a heavy horizontal line at end of bottom level. Shade levels in each unit if a feature is present.

cmbs	Test Unit 2								Test Unit 3								Test Unit 4							
	L	B	C	S	Ch	BR	T	GS	L	B	C	S	Ch	BR	T	GS	L	B	C	S	Ch	BR	T	GS
0-10																								
10-20																								
20-30																								
30-40																								
40-50																								
50-60		12																				1	1	
60-70																						2	1	
70-80																								
80-90																								
90-100	3				1					2								5	3			12		8
100-110																		4						
110-120											9							2	1					
120-130																		1						
130-140											1													
140-150																								
TOTAL	3	12			1					12							29	9				15	2	8

L = Lithic, B = Bone, C = Ceramic, S = Shell, Ch = Charcoal, BR = Burned Rock, T = Tool, GS = Ground Stone

Artifact Frequency Distribution
Site # 41PT186

For each test unit, tabulate artifact frequency (from field catalog) by artifact class (columns) and depth (rows). Use '+' for artifacts present (per level notes) but not counted. Note counts which include a temporal diagnostic with '*'. Note bottom of each unit with a heavy horizontal line at end of bottom level. Shade levels in each unit if a feature is present.

cmbs	Test Unit 5								Test Unit 6								Test Unit 7								
	L	B	C	S	Ch	BR	T	GS	L	B	C	S	Ch	BR	T	GS	L	B	C	S	Ch	BR	T	GS	
0-10		2							1	4					1										
10-20	6	9						1	6	7				1											
20-30	4	8							5	10				1	2		3								
30-40	7	7							5	5				3				3							
40-50	5	33							8	12							1	2					1		
50-60	4	14							9	32					1		5								
60-70	1	6						1	3	11					1			2							
70-80	1	8						2	4	32				2			3	4							
80-90	1								6	26							1	6							
90-100	1	3						4 1	5	19				1			1	3							
100-110	4	26							1	9															
110-120	1							1		4															
120-130									2																
130-140																									
140-150									2					1											
150-160									1						1										
160-170									2						2										
170-180															1	1									
180-190									1	1					1										
190-200									1	1					3										
									62	173				1	16	6									
									Test Unit 6B																
100-110									1	12					1										
110-120										13					1										
TOTAL									35	116					6	4		1	25				2		14

L = Lithic, B = Bone, C = Ceramic, S = Shell, Ch = Charcoal, BR = Burned Rock, T = Tool, GS = Ground Stone

**Artifact Frequency Distribution
Site # 41PT186**

For each test unit, tabulate artifact frequency (from field catalog) by artifact class (columns) and depth (rows). Use '+' for artifacts present (per level notes) but not counted. Note counts which include a temporal diagnostic with '*'. Note bottom of each unit with a heavy horizontal line at end of bottom level. Shade levels in each unit if a feature is present.

cmbs	Test Unit 7B								Test Unit 8								Test Unit 9								
	L	B	C	S	Ch	BR	T	GS	L	B	C	S	Ch	BR	T	GS	L	B	C	S	Ch	BR	T	GS	
0-10																									
10-20																		8							
20-30																	8								
30-40																	21								
40-50																	1	3					1		
50-60																	13								
60-70																	110								
70-80																	18								
80-90																	3								
90-100	3	1														31									
100-110	1	17	1													29			1				1		
110-120	1	4														24									
120-130	1	4														11									
130-140		5														2									
140-150	1															1									
150-160		1														1									
160-170	2	8																							
170-180	1	6																							
180-190		4																							
190-200		3																							
TOTAL	10	53	1													1							1		
	1	98											1			1									
	1	184																							

L = Lithic, B = Bone, C = Ceramic, S = Shell, Ch = Charcoal, BR = Burned Rock, T = Tool, GS = Ground Stone

**Artifact Frequency Distribution
 Site # 41PT245**

For each test unit, tabulate artifact frequency (from field catalog) by artifact class (columns) and depth (rows). Use '+' for artifacts present (per level notes) but not counted. Note counts which include a temporal diagnostic with '*'. Note bottom of each unit with a heavy horizontal line at end of bottom level. Shade levels in each unit if a feature is present.

cmbs	Test Unit 3								Test Unit 4								Test Unit 5										
	L	B	C	S	Ch	BR	T	GS	L	B	C	S	Ch	BR	T	GS	L	B	C	S	Ch	BR	T	GS			
0-10	4		6																								
10-20	8		6																								
20-30	6					1																					
30-40	2																										
40-50								2																			
50-60																			1								
60-70																		1									
70-80																											
80-90																		2									
90-100																	8										
100-110																6											
110-120																											
120-130										1	2			1													
130-140										2	39				3	1											
140-150										2					2						1						
150-160										1																	
160-170																											
170-180										7	46			1	8	1											
*120-140										Test Unit 4B																	
										17				4	17												
TOTAL	20		12			1	2			17				4	17						19						

L = Lithic, B = Bone, C = Ceramic, S = Shell, Ch = Charcoal, BR = Burned Rock, T = Tool, GS = Ground Stone

**Artifact Frequency Distribution
Site # 41PT245**

For each test unit, tabulate artifact frequency (from field catalog) by artifact class (columns) and depth (rows). Use '+' for artifacts present (per level notes) but not counted. Note counts which include a temporal diagnostic with '*'. Note bottom of each unit with a heavy horizontal line at end of bottom level. Shade levels in each unit if a feature is present.

cmbs	Test Unit 6								Test Unit 7								Test Unit 8							
	L	B	C	S	Ch	BR	T	GS	L	B	C	S	Ch	BR	T	GS	L	B	C	S	Ch	BR	T	GS
0-10													1											
10-20													3											
20-30																								
30-40									1				2											
40-50																								
50-60																								
60-70																								
70-80																								
80-90		2																						
90-100													1											
100-110	1	2											2											
110-120		2					2	1	1				1											
120-130		2						16																
130-140		3						28																
140-150	1																							
150-160																								
160-170																								
170-180																								
180-190																								
190-200																								
200-210																								
210-220																								
220-230																								
230-240																								
TOTAL																	2	11					46	1
																	1							
																	11							
																	6							

L = Lithic, B = Bone, C = Ceramic, S = Shell, Ch = Charcoal, BR = Burned Rock, T = Tool, GS = Ground Stone

**Artifact Frequency Distribution
Site # 41PT245**

For each test unit, tabulate artifact frequency (from field catalog) by artifact class (columns) and depth (rows). Use '+' for artifacts present (per level notes) but not counted. Note counts which include a temporal diagnostic with '*'. Note bottom of each unit with a heavy horizontal line at end of bottom level. Shade levels in each unit if a feature is present.

cmbs	Test Unit 9									Test Unit 9B								Test Unit 9C							
	L	B	C	S	Ch	BR	T	GS	L	B	C	S	Ch	BR	T	GS	L	B	C	S	Ch	BR	T	GS	
0-10																									
10-20																									
20-30																									
30-40																									
40-50																									
50-60	2	4			1																				
60-70	1	4	1		1																				
70-80																									
80-90																									
90-100																									
100-110																									
110-120																									
120-130		1					1																		
130-140		1					2																		
140-150																									
150-160										1				2	16							3	4		
160-170															1							5	20		
170-180															1							3	11		
180-190														2	2										
190-200																									
TOTAL	3	10	1		2	3				1				4	20							11	35		

L = Lithic, B = Bone, C = Ceramic, S = Shell, Ch = Charcoal, BR = Burned Rock, T = Tool, GS = Ground Stone

**Artifact Frequency Distribution
Site # 41PT245**

For each test unit, tabulate artifact frequency (from field catalog) by artifact class (columns) and depth (rows). Use '+' for artifacts present (per level notes) but not counted. Note counts which include a temporal diagnostic with '*'. Note bottom of each unit with a heavy horizontal line at end of bottom level. Shade levels in each unit if a feature is present.

cmbs	Test Unit 10								Test Unit 11							
	L	B	C	S	Ch	BR	T	GS	L	B	C	S	Ch	BR	T	GS
0-10	1	6	2		1											
10-20	1	2														
20-30	1	3														
30-40	1															
40-50									1							
50-60		2														
60-70	1															
70-80		10														
80-90		2														
90-100		4														
100-110		3														
110-120		7														
120-130		17														
130-140		10														
TOTAL	5	66	2		1				1							

L = Lithic, B = Bone, C = Ceramic, S = Shell, Ch = Charcoal, BR = Burned Rock, T = Tool, GS = Ground Stone

APPENDIX C
OBSIDIAN SOURCE ANALYSIS

This page intentionally left blank.

OBSIDIAN SOURCE ANALYSIS

Prepared for:



**TRC Environmental Corporation
505 East Huntland Drive, Suite 250
Austin, Texas 78752**

Prepared by:

**M. Steven Shackley, Ph.D.
Professor and Director
Berkeley Archaeological XRF Lab.
University of California
Berkeley, CA 94720-3710
<http://www.swxrflab.net>**

This page intentionally left blank.

C.1 INTRODUCTION

The vast majority of the source provenance for the 16 artifacts is from one of the sources in the Jemez Mountains from northern New Mexico. One sample with very high strontium does not match any known source in North or Central America, and one sample appears to be modern or perhaps 19th century glass. The one piece of metal “tinker cone” is indeed a copper alloy dominated by copper and zinc.

C.2 ANALYSIS AND INSTRUMENTATION

All archaeological samples are analyzed whole. The results presented here are quantitative in that they are derived from “filtered” intensity values ratioed to the appropriate x-ray continuum regions through a least squares fitting formula rather than plotting the proportions of the net intensities in a ternary system (McCarthy and Schamber 1981; Schamber 1977). Or more essentially, these data through the analysis of international rock standards, allow for inter-instrument comparison with a predictable degree of certainty (Hampel 1984).

All analyses for this study were conducted on a ThermoScientific Quant’X EDXRF spectrometer, located in the Department of Anthropology, University of California, Berkeley. It is equipped with a thermoelectrically Peltier cooled solid-state Si(Li) X-ray detector, with a 50 kV, 50 W, ultra-high-flux end window bremsstrahlung, Rh target X-ray tube and a 76 µm (3 mil) beryllium (Be) window (air cooled), that runs on a power supply operating 4-50 kV/0.02-1.0 mA at 0.02 mA increments. The spectrometer is equipped with a 200 l min⁻¹ Edwards vacuum pump, allowing for the analysis of lower-atomic-weight elements between sodium (Na) and titanium (Ti). Data acquisition is accomplished with a pulse processor and an analogue-to-digital

converter. Elemental composition is identified with digital filter background removal, least squares empirical peak deconvolution, gross peak intensities and net peak intensities above background.

The analysis for mid Zb condition elements Ti through Nb, Pb, Th, the x-ray tube is operated at 30 kV, using a 0.05 mm (medium) Pd primary beam filter in an air path at 200 seconds livetime to generate x-ray intensity Ka-line data for elements titanium (Ti), manganese (Mn), iron (as Fe₂O₃T), cobalt (Co), nickel (Ni), copper, (Cu), zinc, (Zn), gallium (Ga), rubidium (Rb), strontium (Sr), yttrium (Y), zirconium (Zr), niobium (Nb), lead (Pb), and thorium (Th). Not all these elements are reported since their values in many volcanic rocks are very low. Trace element intensities were converted to concentration estimates by employing a least-squares calibration line ratioed to the Compton scatter established for each element from the analysis of international rock standards certified by the National Institute of Standards and Technology (NIST), the U.S. Geological Survey (USGS), Canadian Centre for Mineral and Energy Technology, and the Centre de Recherches Pétrographiques et Géochimiques in France (Govindaraju 1994). Line fitting is linear (XML) for all elements but Fe where a derivative fitting is used to improve the fit for iron and thus for all the other elements. When barium (Ba) is analyzed in the High Zb condition, the Rh tube is operated at 50 kV and 1.0 mA, ratioed to the bremsstrahlung region (see Davis et al. 1998). Further details concerning the petrological choice of these elements in Southwest obsidians are available in Shackley (1988, 1990, 1992, 1995, 2005; also Mahood and Stimac 1991; and Hughes and Smith 1993). Specific standards used for the best fit regression calibration for elements Ti through Nb, Pb, Th, and Ba, include G-2 (basalt), AGV-2 (andesite), GSP-1 (granodiorite), SY-2 (syenite), BHVO-2 (hawaiite), STM-1 (syenite), QLO-1 (quartz latite), RGM-1

(obsidian), W-2 (diabase), BIR-1 (basalt), SDC-1 (mica schist), TLM-1 (tonalite), SCO-1 (shale), all U.S. Geological Survey standards, BR-1 (basalt) from the Centre de Recherches Pétrographiques et Géochimiques in France, and JR-1 and JR-2 (rhyolite) from the Geological Survey of Japan (Govindaraju 1994).

The data from the WinTrace software were translated directly into Excel for Windows software for manipulation and on into SPSS for Windows for statistical analyses when necessary. In order to evaluate these quantitative determinations, machine data were compared to measurements of known standards during each run. RGM-1 is analyzed during each sample run for obsidian artifacts to check machine calibration.

Trace element data exhibited in Tables C-1 and C-2 and Figure C-1 are reported in parts per million (ppm), a quantitative measure by weight. Source nomenclature is from Baugh and Nelson (1987, and unpublished), Glascock et al. (1999), and Shackley (2005; see also <http://www.swxrflab.net/swobsrsrcs.htm>).

C.3 DISCUSSION

While the vast majority of obsidian used to produce these artifacts was originally procured from northern New Mexico sources, one “unknown” (186-20.1) exhibits chemistry more similar to a mafic or intermediate volcanic rock (Table C-1). It does not resemble any known source north or south of the international border. The analysis in 2009 does not change the mix of obsidian source provenance in any significant way.

The one piece of metal, called a “tinkler cone” is definitely produced from a copper/zinc alloy (Table C-2). The other elements detected appear to be trace elements that are likely part of the original

ore. With this analysis it is impossible to determine whether where or when it was produced. Copper-zinc alloys are commonly made today and presumably in the 19th century.

C.4 REFERENCES CITED

- Baugh, T. G. and F. W. Nelson, Jr.
1987 New Mexico Obsidian Sources and Exchange on the Southern Plains. *Journal of Field Archaeology* 14:313-329.
- Davis, M. K., T. L. Jackson, M. S. Shackley, T. Teague, and J. H. Hampel
1998 Factors Affecting the Energy-Dispersive X-Ray Fluorescence (EDXRF) Analysis of Archaeological Obsidian. In *Archaeological Obsidian Studies: Method and Theory*, edited by M. S. Shackley, pp. 159-180. *Advances in Archaeological and Museum Science* 3. Springer/Plenum Press, New York.
- Glascock, M. D., R. Kunselman, and D. Wolfman
1999 Intrasource Chemical Differentiation of Obsidian in the Jemez Mountains and Taos Plateau, New Mexico. *Journal of Archaeological Science* 26:861-868.
- Govindaraju, K.
1994 Compilation of Working Values and Sample Description for 383 Geostandards. *Geostandards Newsletter* 18 (special issue).
- Hampel, J. H.
1984 Technical Considerations in X-ray Fluorescence Analysis of Obsidian. In *Obsidian Studies in the Great Basin*, edited by R. E. Hughes, pp. 21-25. Contributions of the University of California

- Archaeological Research Facility
45. Berkeley.
- Hughes, R. E., and R. L. Smith
1993 Archaeology, Geology, and Geochemistry in Obsidian Provenance Studies. In *Scale on Archaeological and Geoscientific Perspectives*, edited by J. K. Stein and A. R. Linse, pp. 79-91. Geological Society of America Special Paper 283.
- Mahood, G. A., and J. A. Stimac
1990 Trace-Element Partitioning in Pantellerites and Trachytes. *Geochemica et Cosmochimica Acta* 54:2257-2276.
- McCarthy, J. J., and F. H. Schamber
1981 Least-Squares Fit with Digital Filter: A Status Report. In *Energy Dispersive X-ray Spectrometry*, edited by K. F. J. Heinrich, D. E. Newbury, R. L. Myklebust, and C. E. Fiori, pp. 273-296. National Bureau of Standards Special Publication 604, Washington, D.C.
- Schamber, F. H.
1977 A Modification of the Linear Least-Squares Fitting Method which Provides Continuum Suppression. In *X-ray Fluorescence Analysis of Environmental Samples*, edited by T. G. Dzubay, pp. 241-257. Ann Arbor Science Publishers.
- Shackley, M. S.
1988 Sources of Archaeological Obsidian in the Southwest: An Archaeological, Petrological, and Geochemical Study. *American Antiquity* 53(4):752-772.
- 1992 The Upper Gila River Gravels as an Archaeological Obsidian Source Region: Implications for Models of Exchange and Interaction. *Geoarchaeology* 7(4):315-326.
- 1995 Sources of Archaeological Obsidian in the Greater American Southwest: An Update and Quantitative Analysis. *American Antiquity* 60(3):531-551.
- 1998 Geochemical Differentiation and Prehistoric Procurement of Obsidian in the Mount Taylor Volcanic Field, Northwest New Mexico. *Journal of Archaeological Science* 25:1073-1082.
- 2005 *Obsidian: Geology and Archaeology in the North American Southwest*. University of Arizona Press, Tucson.

Table C-1. Elemental Concentrations for Archeological Rock Samples and RGM-1.
(Note: All Measurements in Parts Per Million [ppm].)

SITE/SAMPLE NO.	Ti	Mn	Fe	Zn	Rb	Sr	Y	Zr	Nb	Ba	Source
185/A-156-001-1	1100	498	11430	108	156	8	39	168	51	80	Valles Rhy
185/A-167-001-1	981	527	12043	98	175	9	47	183	57	61	Valles Rhy
185/C-221-001-1	1206	499	8772	114	147	9	19	75	43	38	El Rechuelos
185/C-221-001-2	984	470	7328	113	157	9	26	71	44	23	El Rechuelos
185/C-264-001	901	533	11214	96	196	7	64	180	98	8	Cerro Toledo Rhy
186-344-001-1	1111	451	10778	85	147	12	44	161	44	24	Valles Rhy
186-20.1	2327	1849	6990	95	50	789	45	108	3	1172	unknown
245-403-001	965	546	11057	133	190	5	62	170	87	7	Cerro Toledo Rhy
186-305-001-1	916	587	11492	103	208	6	59	177	93	7	Cerro Toledo Rhy
185/C-326-001-1	827	579	10561	151	229	5	68	185	97	0	Cerro Toledo Rhy
185/C-312-001-1	1053	530	9932	213	204	8	57	163	83	0	Cerro Toledo Rhy
185/C-310-001-1	872	452	9833	91	173	8	46	178	54	33	Valles Rhy
185/C-480-001-1	906	488	10671	127	186	10	48	171	55	24	Valles Rhy
185/C-480-001-2	983	406	9157	150	159	7	39	157	48	48	Valles Rhy
185/C-642-001-1	869	513	9975	162	215	6	64	180	92	0	Cerro Toledo Rhy
185/C-857-001-1	546	149	2895	46	1	9	2	16	1	19	modern glass?
RGM1-S4	1522	299	12871	36	147	107	25	219	7	835	standard
RGM1-S4	1506	399	14053	35	148	100	24	220	16	824	standard

Table C-2. Elemental Concentrations for the Metal Sample.
(Note: All Measurements in Parts Per Million [ppm].)

Site/Sample	Ti	Mn	Fe	Ni	Cu	Zn	Rb	Sr	Y	Zr	Nb	Ba	Pb	Th
186-506-009-1	2757	145	48323	1065	2080315	140982	15	5	2	25	118	0	9502	120

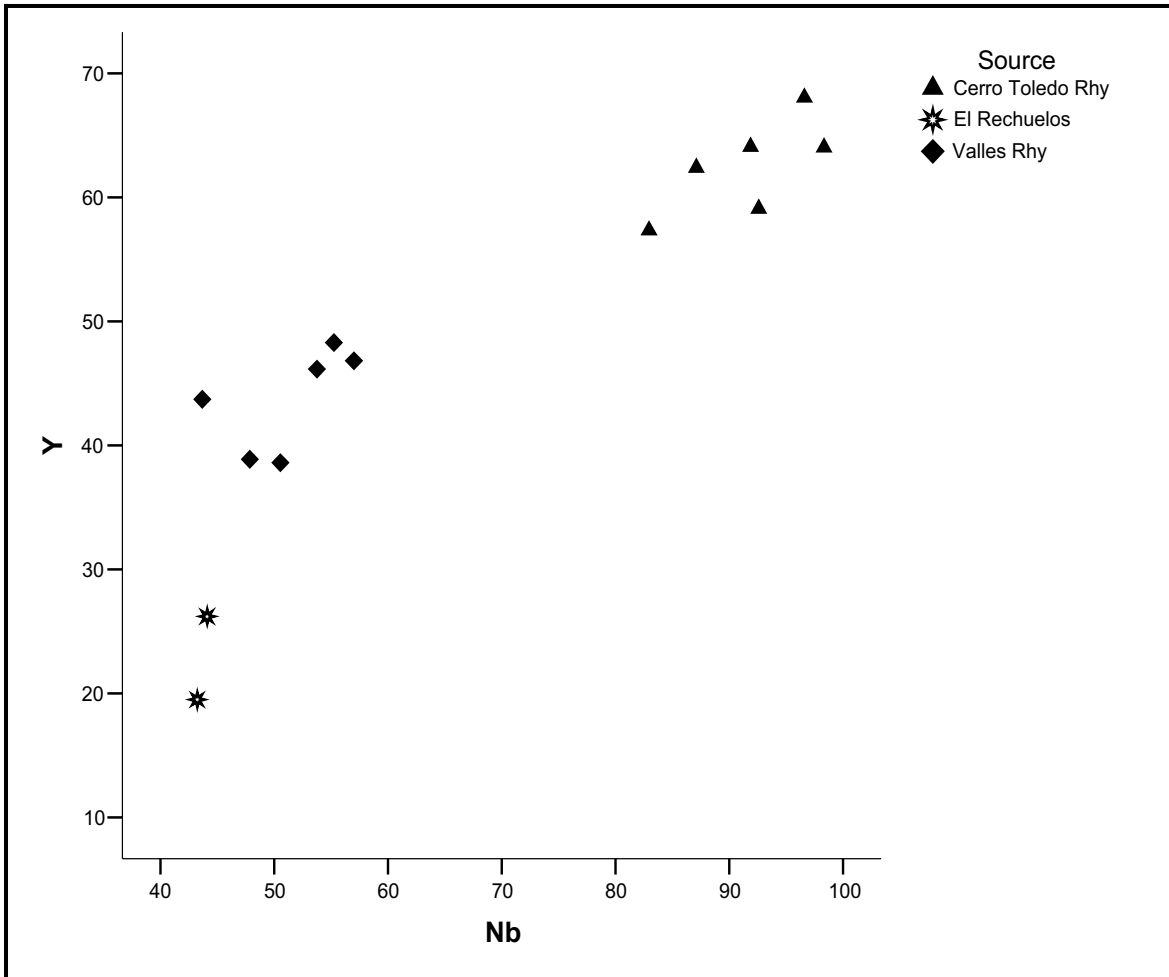


Figure C-1. Y versus Nb Biplot of Archeological Data.

(Note: The one "unknown" sample removed.)

This page intentionally left blank.

APPENDIX D

BIOSILICATE ANALYSIS AND PALYNOLOGY

This page intentionally left blank.

**PALEOENVIRONMENTAL RECONSTRUCTION AT WEST AMARILLO
CREEK, POTTER COUNTY, TEXAS, BASED ON
BIOSILICATE ANALYSIS AND PALYNOLOGY**

Prepared for:



**TRC Environmental Corporation
505 East Huntland Drive, Suite 250
Austin, Texas 78752**

Prepared by:

**Steven Bozarth, Ph.D. and Terri Woodburn
University of Kansas Palynology Laboratory
Department of Geography
July 3, 2009**

This page intentionally left blank.

D.1 INTRODUCTION

D.1.1 PROJECT GOAL

The goal of this study was to reconstruct vegetative histories at 41PT185/C, 41PT186 and 41PT245 based on phytolith analysis and at 41PT185/C based on palynology. Differences in vegetation were then used to reconstruct paleoenvironments. Other biosilicates (diatoms, algal statospores, and sponge spicules) were analyzed to glean as much paleoenvironmental information as possible.

D.1.2 PHYTOLITH FORMATION

Growing plants typically absorb water containing dissolved silica through their roots. Microscopic silica bodies are subsequently produced by the precipitation of hydrated silicon dioxide ($\text{SiO}_2 \cdot n\text{H}_2\text{O}$) within the plant's cells, cell walls, and intercellular spaces. Silica bodies which have characteristic shapes and sizes are called *opal phytoliths* (Wilding and Drees 1971). The term phytolith is derived from the Greek words *phyton*, meaning plant, and *lithos*, meaning stone. Opal is the common name for amorphous, hydrated silica dioxide. Opaline bodies formed in plants without specific shapes are simply plant opal.

Phytoliths form in most plants and are produced in a multitude of shapes and sizes. Many phytolith types are specific to particular groups of plants. A phytolith type is considered "characteristic" if it is common in one specific taxon but also produced in very limited amounts in one or more other taxa. A phytolith type is "diagnostic" if its shape and/or size are specific to a particular taxon. Fortunately, many phytoliths are resistant to weathering and are preserved in most soils for long periods of time. Because phytoliths are formed primarily in the vegetative parts of plants and are released on soil surfaces when the plant decays, a large

proportion of the phytolith record represents localized deposition (Piperno 1988).

D.1.3 PHYTOLITH STABILITY

The dissolution and stability of phytoliths in soils and sediments is not fully understood. Laboratory experiments demonstrate, however, that the solubility of silica is a function of temperature, particle size, pH, and the presence of a disrupted surface layer. Studies show that the solubility of amorphous silica increases linearly with temperature from 0°C. Particle size is another factor affecting stability as opal dissolution is greater with a decrease in size (Wilding et al. 1977, 1979). Pease (1967) experimentally determined that there appears to be a slight increase in phytolith solubility in the range of 5.0 to 8.5, an added increase between pH 8.5 and pH 9.0, and a large increase beginning at pH 9.0. Opal stability is also a function of the presence of certain metallic ions and sesquioxides. The adsorption of Al and Fe ions onto the surface of opal will decrease silica dissolution due to the formation of relatively insoluble silicate coatings. The presence of sesquioxides may increase dissolution of phytoliths due to the adsorption of monosilicic acid (Wilding et al. 1977).

D.1.4 MORPHOLOGY AND TAXONOMY

Monocotyledons, particularly the Poaceae, produce a wide variety of morphologically distinctive phytolith forms. The most taxonomically useful types of grass phytoliths are silicified short cells that range in size from 10 to 35 μm long. Several types of trapezoidal circular, rectangular, and elliptical short cells are diagnostic of the Pooideae (Brown 1984; Twiss 1987; Bozarth 1992b), a grass subfamily adapted to cool temperatures and high available soil moisture (Twiss 1987).

Saddle-shaped bodies occur most commonly in the Chloridoideae (Brown 1984; Twiss 1987; Mulholland and Rapp 1992), a grass

subfamily that flourishes in areas with warm temperatures and low available soil moisture. Saddle-shaped phytoliths are similar in appearance to double-edged battle axes formed by two opposite convex edges and two opposite concave edges. However, a few saddle-shaped phytoliths have only one concave side (Brown 1984).

Bilobate and cross-shaped phytoliths are formed in the Panicoideae (Brown 1984; Twiss 1987; Mulholland and Rapp 1992), a grass subfamily that thrives in warm temperatures and high available soil moisture (Twiss 1987). Bilobates with indented, concave, or pointed lobes are formed only in the Panicoid subfamily. Bilobates with raised lobes edges and round or flat ends which are symmetrical in side view are also formed only in the Panicoids (Bozarth 1992b). Maize (*Zea mays*) cobs produce another type of phytolith that is diagnostic of the species (Bozarth 1993b).

Bilobate phytoliths with raised lobe edges and round ends are also formed in three-awn grasses (*Aristida* species), a genus in the Chloridoid subfamily (Gould and Shaw 1968). However, bilobates formed in *Aristida* differ from Panicoid bilobates in that the raised edges on the top (the longer part) slope down at the ends. In addition, they are asymmetrical in side view as the top is more concave than the bottom (Bozarth 1992b). Needlegrass, a genus (*Stipa*) in the Poid subfamily (Gould and Shaw 1968), also produces bilobates (Bozarth 1992b). These bilobates differ from those produced in Panicoids and *Aristida* by not having raised lobe edges. Many have a small lobe on one side in the middle. Unlike most Poids, *Stipa* species grow in dry areas (Pohl 1968).

There are several other types of phytoliths in addition to short cells produced in grass. Long cells are relatively large (30 to 150 μm long) elongate bodies with smooth or wavy edges (Twiss 1987). Bulliform cells are large keystone shaped-cells. Trichomes are

silicified prickly-hairs composed of two parts, an outer sheath and an inner core. The outer sheath dissolves soon after being deposited on the soil, while the inner core remains well preserved. Silicified tracheids are also formed in grasses, albeit rarely. Silicified stomata are taxonomically useful at various levels, but are typically not well preserved.

Grass floral bracts produce at least three distinctive types of phytoliths not formed in other parts of the plant. Dendriforms are cylindrical rods of varying length with protrusions or spines radiating from a central core. Asteriforms consist of platy bodies with peg like protrusions. Scutiform phytoliths are saucer-shaped bodies that have a unique, slanted apex (Piperno 1988). Scutiforms appear to be diagnostic of Pooideae, whereas dendriforms are formed in most, if not all, native grasses. These three types of phytoliths can be used to identify areas/artifacts used to process native grass seeds as they occur only rarely in natural environments (Bozarth 1998a).

Non-grass monocots also produce numerous taxonomically valuable phytoliths. Sedge (*Cyperus*) produces distinctive phytoliths in the form of cone shaped-bodies with round wavy margins. These phytoliths occur both singly and in multiples. Truncated cones with multiple peaks and round wavy bases are formed in bulrush (*Scripus pallidus*). Both of these phytolith types appear to be diagnostic of the genera that produce them (Bozarth 1995). Sedge phytoliths with angular and verrucate bases and knobby apices may be restricted to inflorescences (Ollendorf 1992).

Several types of phytoliths are formed in woody dicotyledons (deciduous shrubs and trees) and herbaceous dicotyledons (forbs and weeds). The two most common types of diagnostic dicot phytoliths are flat or cupped polyhedrons with 5-8 sides and anticlinal cells (Rovner 1971; Wilding and Drees 1971; Geis 1973; Wilding et al. 1977;

Bozarth 1992a). Anticlinal cells have wavy, undulating walls with the appearance of jigsaw-puzzle pieces. Most of these polyhedral and anticlinal phytoliths consist only of silicified cell walls and are not well preserved in sediment (Wilding and Drees 1974; Bozarth 1992a). Other phytolith types formed only in dicots include branched elements with spiral thickened rings and honeycomb-shaped assemblages (Geis 1973; Wilding and Drees 1973, 1974; Bozarth 1992a).

Several species of arboreal dicots produce opal spheres that range in size from 1 to 50 μm (Wilding and Drees 1973, 1974). Opal spheres are also produced in conifers (Klein and Geis 1978), but are much smaller (3 to 8 μm). Opaque opal spheres have been extracted from the A horizon of several forested soils in Ohio demonstrating that they are well-preserved (Wilding and Drees 1973, 1974). Wilding and Drees (1973) also reported opaque bladed forms (which appear to be opaque platelets), in white oak (*Quercus alba*). Similar particles were observed in isolates from a soil formed under deciduous forest.

Distinctive spinulose spheres are produced, although only rarely, in the leaves of chinkapin oak (*Q. muehlenbergii*), red oak (*Q. rubra*) and red oak (*Q. rubra*), as well as the endocarp of black walnut (*Juglans nigra*). Spinulose spheres have been identified with other deciduous tree phytoliths in late-Pleistocene and Holocene loessal sites in Nebraska (Bozarth 1998a, 1998b, 1998c, 2000, 2008).

Phytolith analysis of 14 dicots and one cactus native to the Central Great Plains shows that diagnostic phytoliths are only rarely formed in edible fruits and nuts. Most of the fruits and nuts studied were from trees and shrubs, including shagbark hickory (*Carya ovata*), hackberry (*Celtis occidentalis*), persimmon (*Diospyros virginiana*), black walnut (*Juglans nigra*), sandhill plum (*Prunus angustifolia*), wild

plum (*P. americana*), choke cherry (*P. virginiana*), currants (*Ribes odoratum*), elderberry (*Sambucus canadensis*), white oak (*Quercus alba*), and burr oak (*Q. macrocarpa*). Other reference species include two forbs, devil's claw (*Proboscidea louisianica*) and groundcherry (*Physalis virginiana*), a wild grape (*Vitis riparia*), and a cactus prickly pear (*Opuntia macrorhiza*). Of these 15 species, diagnostic phytoliths were formed only in hackberry fruits. These phytoliths, produced in the fruit stone, are in the form of platelets with irregular edges and short echinate (spiny) sculpturing on one side (Bozarth 1987b).

Subsequent to this study, four additional samples from economic species were analyzed: nuts and bracts from hazelnut (*Corylus americana*), achenes from marsh elder (*Iva annua*), and achenes with bracts from Pennsylvania smartweed (*Polygonum pensylvanicum*). No taxonomically useful phytoliths were found. Furthermore, previous unpublished studies indicate that Palmer's pigweed (*Amaranthus palmeri*), rough pigweed (*A. retroflexus*), and lamb's quarters (*Chenopodium album*) do not produce diagnostic phytoliths.

Other dicots produce phytoliths diagnostic at various taxonomic levels. Opaque platelets with systematic perforations and certain types of segmented hairs are diagnostic of Asteraceae (the Sunflower family). Flat polyhedrons with 5-8 sides that are filled with coarse verrucae (bumps) appear to be unique to Ulmaceae (the Elm family) (Bozarth 1985a, 1992a). Silicified, multicelled hair bases are formed in the disks of common sunflower (*Helianthus annuus*) and domesticated sunflowers (*H. annuus* var. *macrocarpa*) (Bozarth 1986b). Certain types of stalked verrucate phytoliths are specific to hackberry, mulberry (*Morus*), false nettle (*Boehmeria*), or nettle (*Urtica*). Elongate verrucate phytoliths with one or both ends tapering to a point are unique to clearweed (*Pilea*) (Bozarth 1992a). Phytoliths with deeply scalloped surfaces of

contiguous concavities are diagnostic of squash and wild buffalo gourd (*Cucurbita* species) (Bozarth 1987a). Common beans (*Phaseolus vulgaris*) also produce diagnostic phytoliths (Bozarth 1990b).

Several types of phytoliths are produced in the pine family (Pinaceae). Silicified, irregularly-shaped, polyhedral cells are the most common taxonomically useful Pinaceae phytolith. This type of phytolith is produced in red spruce (*Picea rubens*), black spruce (*P. mariana*), white spruce (*P. glauca*), Engelmann spruce (*P. engelmannii*), and jack pine (*Pinus banksiana*) (Norgren 1973; Klein and Geis 1978; Bozarth 1988, 1993a). Blocky polyhedra with smooth surfaces and at least eight non-parallel sides are characteristic but not diagnostic of Pinaceae, because they are also produced, although relatively infrequently, in grasses (Bozarth 1993a).

In contrast to smooth polyhedrons, polyhedrons with bordered pit impressions on the surface are unique to the Pinaceae. This type of phytolith is abundant in pine (*Pinus*), spruce (*Picea*), Douglas-fir (*Pseudotsuga menziesii*), and less commonly in larch (*Larix*), hemlock (*Tsuga*), and fir (*Abies*) (Klein and Geis 1978). Douglas-fir needles produce distinctive, branched, silicified particles (Brydon et al. 1963). This same type of phytolith was also reported in Douglas-fir by Garber (1966) as irregular shapes with spiny processes and by Norgren (1973) as amoeboid bodies with tapering, conical protrusions. Thin plates with wavy margins on all four sides are formed in needles of white spruce and appear to be unique to that species. Phytoliths with spiny irregular bodies are commonly formed in needles of jack pine and appear to be diagnostic of that species (Bozarth 1993a).

D.1.5 APPLIED PHYTOLITH RESEARCH IN THE GREAT PLAINS

Phytoliths are largely a "decay in place" fossil (Rovner 1975) and represent the vegetation of a site at the time of deposition (Piperno 1988). Opal phytoliths can be isolated from buried sediment samples and analyzed to reconstruct the paleoenvironment for a particular area. This has been successful on a number of sediment types, including loessal sites in Nebraska (Fredlund et al. 1985; Bozarth 1992b, 2008; Johnson 1993), Kansas (Bozarth 1984a; Johnson and Bozarth 1996), and Texas (Bozarth 1995), as well as alluvium in Kansas (Bozarth 1986a, 1990a) and Texas (Bozarth 1995). Regional fossil phytoliths were first recognized by Twiss et al. (1969) in buried soils in north-central Kansas, but the paleoenvironments were not reconstructed.

Phytolith analysis has also been used to identify cultigens and other economic species in prehistoric archaeological sites. Phytolith analysis was first applied to Great Plains paleoethnobotanical studies by Bozarth (1984b) who identified sunflower-like phytoliths in sediment samples collected in features at Site 23DX3, a Central Plains Tradition village in northeast Nebraska. These silicified, multi-celled hair bases are commonly formed in the disks of common sunflower (*Helianthus annuus*) and domesticated sunflower (*Helianthus annuus* var. *macrocarpa*) (Bozarth 1986b).

Additional taxonomic classification demonstrated that diagnostic phytoliths are formed in the rinds of selected varieties of squash (*Cucurbita* species) (Bozarth 1985b, 1986b, 1987a) and in the pods of common beans (*Phaseolus vulgaris*) (Bozarth 1986b, 1990b). Squash phytoliths (scalloped spheroids) were recovered at Site 23DX3 (described above) (Bozarth 1986b) and Site 3CT50, a Late Woodland site in northeast Arkansas (Bozarth 1985b, 1987a). Bean phytoliths (silicified hooked hairs) were

identified in an isolate from Site 14MN328, a Great Bend Aspect village located in central Kansas (Bozarth 1989a, 1990b).

Mulholland (1986, 1987) reported two types of phytoliths characteristic of maize, one in chaff and the other in leaves and husks, which could be used as indicators of maize in archaeological sites in North Dakota. Extensive taxonomic research by Bozarth (1989a, 1989b, 1993b) demonstrated that maize cobs produce diagnostic phytoliths. Based on these studies, maize was identified in two features at Site 14MN328 (described above).

As previously reported, most archaeological phytolith analyses reconstruct paleoenvironments or plant subsistence strategies. However, other types of studies can be done with phytoliths. For example, at the Hatcher Site (14DO19), a Plains Village period habitation structure located in northeastern Kansas, a study of phytoliths from a daub concentration demonstrates that Panicoids (tall-grasses) and Poooids (cool-moist season grasses) were the most common grasses used in construction at the site (Bozarth 1987c). A phytolith analysis of prehistoric bison tooth calculus and impacta from sites in Kansas and Oklahoma demonstrates that this type of study can be used to reconstruct the diet of prehistoric bison in the central Great Plains (Bozarth 1993c).

D.2 PREVIOUS WORK IN STUDY AREA

Palynological results indicate climatic change over time at IO 8 (isolated occurrence of a fossilized bone and a mammoth tooth) but the data were problematic. Paleobotanical analyses at 41PT185 and 41PT186 indicate vegetation continuity but the results were again problematic. No evidence of prehistoric plant use was found (Gish 2000).

D.3 METHODOLOGY

D.3.1 DATA RECOVERY PHASE I (2007)

Phytoliths and other biosilicates (diatoms, algal statospores, and sponge spicules) were analyzed from 13 radiocarbon dated sediment samples collected at 41PT185/C, 41PT186, and 41PT245. Pollen was also analyzed from four dated samples from BT 36 at 41PT185/C (#M-1-1, #M-3-4, #M-5-9, and #M-4-6). The 13 dated samples were collected across the study area to gain an understanding of the overall Holocene environment in West Amarillo Creek.

D.3.2 DATA RECOVERY PHASE II (2008)

Biosilicates and pollen were analyzed from 20 samples collected from a dated column in BT 36 at 41PT185/C, the stratigraphy of which is shown in Figure D-1. Biosilicates were also analyzed from three samples (#471-004-1a, #1129-004-1a, and #3801-004-1a) collected from three cultural features (Features 8, 18, and 10) at archaeological site 41PT185/C. The phytolith classification system reported by Fredlund (Fredlund and Tieszen 1994) was utilized to determine if the prehistoric short cell assemblages at 41PT185/C match any of the modern analogs from various sites in North America.

D.4 BIOSILICATES

Biosilicates were isolated from 2 to 5 gram sediment samples using a procedure based on heavy-liquid (zinc bromide) flotation and centrifugation. This procedure consists of five basic steps: 1) removal of carbonates with dilute hydrochloric acid; 2) removal of colloidal organics, clays, and very fine silts by deflocculation with sodium pyrophosphate, centrifugation, and decantation through a 7- μ m filter; 3) oxidation of sample to remove organics; 4) heavy-liquid flotation of phytoliths from the heavier clastic mineral fraction using zinc bromide concentrated to a specific gravity of

2.3; 5) washing and dehydration of phytoliths with butanol; and 6) dry storage in 1-dram glass vials.

Representative portions of the isolates were mounted on microscope slides in immersion oil under 22 x 40 mm cover glasses and sealed with clear nail lacquer. A minimum of 200 phytoliths were taxonomically classified in each slide. Phytoliths were analyzed at a magnification of 625X with a petrographic Zeiss microscope. Biosilicate data were reported with *TG View*. Phytolith concentrations were calculated using an indirect method reported by Piperno (1988). A known number of exotic spores (in this case *Lycopodium*) were added to each sample after the oxidation stage. The concentration of phytoliths (per gram) was computed as follows:

Phytolith conc. = no. of phytoliths counted x (total no. exotics added / no. exotics counted) / sample wt.

Concentration permits an evaluation of the phytolith production, preservation, and sedimentation rate for a given sample interval.

Phytoliths were classified according to a convention that has been developed and used in other reports and publications. An extensive reference collection of plants native to the Great Plains has been developed in the palynology laboratory through field collection, research plots, solicited samples, and specimens supplied by the University of Kansas Herbarium. The phytolith reference collection consists of phytoliths extracted from complete or representative aerial portions of the following: 1) 25 species of 20 genera of 11 tribes of 6 subfamilies of the Poaceae (grass); 2) 11 species of 4 genera of 4 non-grass monocot families; 3) 65 species of 62 genera of 11 families of herbaceous dicots; 4) 20 species of 18 genera of 13 families of woody (mostly arboreal) dicots; 5) 14 species of 7 genera of 5 families of

gymnosperms; and 6) 2 species of Equisetum.

D.5 POLLEN

A number of pollen extraction procedures exist, but heavy-liquid flotation and centrifugation was selected because of the vulnerability of pollen from the study area to degradation by chemical digestion techniques. The heavy-liquid flotation and centrifugation procedure has been refined in the University of Kansas Palynology Laboratory and has proven to be highly effective in the isolation of pollen from a variety of sediment matrices.

Pollen was extracted from 3-50 gram sediment samples, depending on the amount available. This procedure is similar to that for phytoliths and consists of six steps; 1) introduction of "spike" spores; 2) removal of carbonates with dilute hydrochloric acid; 3) removal of colloidal organics, clays, and very fine silts by deflocculation with sodium pyrophosphate, centrifugation, and decantation through a 7- m filter; 4) heavy-liquid flotation of phytoliths from the heavier clastic mineral fraction using zinc bromide concentrated to a specific gravity of 1.95; 5) washing and dehydration of isolate with butanol; and 6) storage in a 1-dram glass vial with several times as much silicone fluid (1000-centistoke viscosity) as isolate. After thorough mixing, aliquots of the mixture were mounted on two microscope slides under 22 x 40 mm cover glasses and sealed with paraffin.

A minimum of 200 pollen grains were taxonomically classified in each slide with adequate concentrations. Otherwise, one complete slide was analyzed. Classification of pollen was based largely on analysis of the University of Kansas Palynology Laboratory reference collection in addition to standard reference keys (Kapp 1969; Lewis et al. 1983; McAndrews et al. 1973; Moore and Webb 1978). Palynology is

especially useful for identifying non-grass plants, including forbs, shrubs, and trees. Pollen data were reported with *TG View*.

Pollen concentration studies can be useful for determining the amount of pollen that may have been destroyed during the post-depositional period of a deposit. Post-depositional processes, such as pedogenesis, mechanical destruction, chemical oxidation, rapid changes in atmospheric-moisture levels, high pH levels, and microbial activity, may greatly reduce the amount of pollen in a deposit. The pollen recovered from archaeological site sediments represent the sum total of the originally deposited pollen minus the pollen lost to the various processes of deterioration. Pollen concentrations from open air sites which do not contain at least 1,000 pollen grains per gram have undergone severe pollen loss through post depositional alteration and may not provide reliable information. Low numbers of identified plant taxa and high percentages of indeterminate grains also suggest that the pollen data may be suspect because of poor preservation (Bryant and Hall 1993).

As mentioned above, "spike" tablets containing *Lycopodium* spores were introduced into the soil/sediment sample prior to the flotation in order to verify pollen extractions and for quantitative evaluation of microfossil concentrations. The pollen concentration per gram was calculated as follows: $Pollen\ conc. = no.\ of\ pollen\ grains\ counted \times (total\ no.\ exotics\ added / no.\ exotics\ counted) / sample\ wt.$

D.6 MICROFOSILL DATA PRESENTATION

D.6.1 DATA RECOVERY PHASE I

Interpretation of microfossil spectra is based on sample chronology. Biosilicate frequencies are shown in Table D-1 and phytolith frequency data for short cells and trees and shrubs in Table D-2. Pollen data

are presented in Table D-3. Pollen data without vesiculate grains (pine and spruce) are shown in Table D-4.

D.6.2 DATA RECOVERY PHASE II

Figure D-2 consists of biosilicate frequencies and concentrations. Figure D-3 consists of total phytolith data and Figure D-4 of only short cells data. A temperature index (Pooids/Pooids + Chloridoids + Panicoids) and an aridity index (Chloridoids/Chloridoids + Panicoids + Pooids) reported by Twiss (1987) and are presented in Figure D-5. Pollen frequencies and concentrations are presented in Figure D-6. A separate pollen frequency table was created, but without vesiculate grains (pine and spruce) which can be blown long distance from the source, to better understand local vegetation (Figure D-7). A diagram of pine pollen frequencies is presented in Figure D-8. Tables D-5, D-6, and D-7 consist of biosilicate, phytolith, and short cell frequency data, respectively, for the three archaeological samples.

D.7 RECONSTRUCTION OF HOLOCENE ENVIRONMENT – PHASE I

Biosilicates were well-preserved in all 13 dated samples from 41PT185/C, 41PT186, and 41PT245. Pollen was also preserved in four stratified samples from BT 36 at 41PT185/C. These samples were collected across the study area to understand the Holocene environment. Interpretation of microfossil spectra is based on sample chronology (Table D-1).

At 10,850 B.P. the study area was relatively cold based on the highest frequency of Pooids found in any of the samples. The vegetation consisted of grassland with a limited number of deciduous trees/shrubs as revealed by the presence of 0.5 percent spinulose spheres. The high phytolith concentration (498,839) is the result of relatively stable surface at this time.

At 9610 B.P. conditions were warmer based on a decrease of Pooids and drier given a decrease in Panicoids and an increase of Chloridoids. As in the first sample, deciduous trees/shrubs were present based on the low frequency (0.5 percent) of spinulose spheres.

At 8280 B.P. the vegetation consisted of many more deciduous shrubs/trees based on a much higher frequency of spinulose arboreal phytoliths (6.9 percent). The relatively low phytolith concentration is explained by the fact that arboreal species produce very few phytoliths compared to grasses. The predominance of Pooid grasses, within the native grass component of the overall assemblage, indicates that the area had cooled almost to the temperature at 10,850 B.P. No evidence of an increase in deciduous shrubs/trees for this time period was found in studies by Bryant and Holloway (1985) and Hall (1985).

At 4330 B.P. conditions were much warmer based on a lower frequency of Pooids and drier given a higher frequency of Chloridoids. The vegetation was largely grassland with far fewer deciduous shrubs/trees given the low frequency of spinulose spheres (0.5 percent). This assemblage is very similar to that for 9610 B.P. except that it formed on a more rapidly aggrading surface based on the lower phytolith concentration (70,510 versus 241,182).

At 2250 B.P. vegetation consisted of slightly more humid grassland based on an increase in Panicoids. The surface was much more stable given the much higher phytolith concentration (204,280). Deciduous shrubs/trees were present in low numbers based on the same frequency of spinulose spheres (0.5 percent).

At 1890 B.P. conditions were much warmer and more arid based on an increase in Chloridoids and a decrease in Pooids. No more spinulose spheres were identified from

this time on but a low frequency of flat polyhedral phytoliths (0.3 percent) indicates that another type of woody dicot was present. Pollen was well-preserved at this level, but is difficult to interpret as it is the lowest pollen sample in the column. However, it is clear that pine (*Pinus ponderosa* and *P. edulis*) pollen blew in from some distance as pine phytoliths were not found in any of the samples.

At 1840 B.P. cooler conditions are indicated based on an increase in Pooids. There was no evidence of trees or shrubs at this time.

At 1430 B.P. conditions were warmer and drier based on an increase in Chloridoids and a decrease in Pooids. This interpretation is supported by the pollen data in that the frequency of pine (*Pinus edulis*) increased considerable at this level compared to the 1890 B.P. assemblage. The decrease in willow (*Salix*) pollen from 4 to 0.4 percent provides additional evidence of increasing aridity. The surface was very stable at this time given the very high phytolith concentration (622,797).

At 1390 B.P. conditions may have cooled based on a higher frequency of Pooids. However, comparison to the previous sample, which is from pond sediment, may not be reliable. The 1390 B.P. assemblage is very similar to assemblage dated to 1840 B.P. except that an increase in Chloridoids and a decrease in Pooids show that conditions were slightly warmer and drier.

At 860 B.P. the study area was warmer and drier based on a lower frequency of Pooids and a higher frequency of Chloridoids. A decrease in frequency of algal statospores and diatoms at this level compared to the 1430 B.P. sample provides additional evidence of drier local conditions. An increase in pine pollen, with *P. edulis* remaining the dominant type, may reflect a more arid regional environment when compared to the 1430 B.P. sample. The absence of oak (*Quercus*) and willow (*Salix*)

pollen provide evidence of increasing local aridity as well. However, the composition of native grass in the study area was not much different given the similarity of short cell assemblages between this sample and the one dated at 1430 B.P.

There is a clear increase in pollen aggregates at this level. Aggregates that consist of over six grains were found for sage (*Artemisia*), low-spine Asteraceae and Brassicaceae. These are especially interesting since aggregates of six or more grains usually do not occur naturally (Bohrer 1984). These aggregates may have been “created”, i.e., knocked off the inflorescences, by grazing animals. This interpretation is supported by the presence of a dung fungus spore (*Sporomiella*) found only at this level.

At 750 B.P. vegetation and climate were largely unchanged given the overall similarity in the phytolith and pollen data compared to the previous sample. However, the surface was more stable based on the higher phytolith and pollen concentrations. The pollen aggregate data for high-spine Asteraceae may indicate disturbance from grazing as in the previous sample.

At 600 B.P. conditions were much cooler based on a higher frequency of Pooids. The phytolith concentration (180,700) shows that the surface was aggrading relatively rapidly at this time.

At 300 B.P. conditions were more arid based on an increase in frequency of Chloridoid grasses. It was also considerably warmer given a lower percentage of Pooid grasses compared to the previous sample. The phytolith data from this sample are a close match to those of a surface sample collected at Lubbock, Texas (Fredlund and Tieszen 1994).

In summary, analysis of phytoliths and pollen show a dynamic vegetation history and paleoenvironment for West Amarillo Creek, Potter County, Texas from 10,850

B.P. until 300 B.P. The overall trend was from relatively cool and humid savannas with scattered deciduous trees/shrubs to warmer and drier grasslands. The sample dated to 8280 B.P. was especially interesting in that the phytolith data show an unexpected increase of deciduous trees/shrubs.

D.8 PALEOENVIRONMENTAL RECONSTRUCTION OF COLUMN SAMPLES IN BT 36 AT 41PT185/C – PHASE II

Twenty one sediment samples were collected in a column for a precise reconstruction of approximately the last 2,000 years (Figure D-1). Biosilicates and pollen were generally well-preserved. Twenty four types of phytoliths were identified, in addition to diatoms, algal statospores and sponge spicules. Twenty eight plant taxa were classified in the pollen record, as well as two types of non-fungal spores. Zones were created based on similarity of microfossil data to trace changes in vegetation and thus paleoenvironments.

Zone A: Study area warm and dry; stable site surface.

Sample #1 (482-486 cmbs): At 1890 B.P. the study area was clearly arid based on the dominance of Chloridoids (83.1 percent). However, the frequency of diatoms (19.5 percent) and the presence of cattail (*Typha*) and willow (*Salix*) pollen, and to a lesser extent the sedge family (Cyperaceae) pollen, show that the site was ponded. The site surface was relatively stable based on a phytolith concentration of 3,282,358. Zone A is largely defined by the relative high concentration of non-vesiculate pollen. The source area of vesiculate pollen was relatively dry based on the low percentage of pine pollen (7.1 percent).

Zone B: Study area cooler and moister;
aggrading site surface.

Sample #2 (475-479 cmbs): The study area was slightly cooler and moister based on the climate indices (Figure D-5). The site was more ponded given an increase cattail and Cyperaceae pollen. Willow pollen decreased slightly but remained relatively high. There was also a slight increase in diatoms. The site surface was aggrading more rapidly based on a phytolith concentration of 2,480,342. The source area for the vesiculate pollen was also moister given the increase in pine and spruce pollen from 7.1 to 30.5 percent.

Sample #3 (458-462 cmbs): The study area became warmer and drier based on the climate indices. However, the site was more ponded based on an increase in cattail and willow pollen, as well as the presence of a fern spore. Moreover, the percentage of diatoms remained high. The surface was aggrading more rapidly. The source of the vesiculate pollen was moister based on an increase in pine and spruce pollen to 41.2 percent.

Sample #4 (429-432 cmbs): The study area became considerably cooler given an increase in frequency of Pooids from 7.3 to 26.4 percent. It was also moister (Figure D-5). A decrease in diatoms indicates that the site was less ponded. An increase of willow pollen from 8.7 to 16.4 percent may be the result of willows colonizing the “disturbed” marsh margin. This interpretation is supported by the as the highest percentage (3.0 percent) of *Lycopodium* (moss) spores found in the study and the continued presence of cattail pollen. The source of the vesiculate pollen was drier based on a decrease in pine pollen to 25.1 percent.

Sample #6 (387-391 cmbs): The study area became cooler and moister at this level based on the climate indices. An increase in diatoms (14.8 percent) shows that the site returned to a marsh. However, the decline

of cattail pollen to only 0.5 percent and the absence of willow pollen indicate that ponded area was relatively small. The source of the vesiculate pollen may have been more mesic based on an increase in pine pollen to 34.5 percent.

Zone C: Study area warm and dry; stable
site surface.

Sample #7 (367-370 cmbs): The study area was warmer at this level based on a decrease in Pooids and drier based on an increase in Chloridoids and a decrease in Panicoids. The site was generally drier given the absence of cattail pollen and the paucity of willow pollen. However, an increase in frequency of diatoms (36.4 percent) shows that the site was still ponded. An increase in native grass pollen may be the result of more arid conditions that favored drought tolerant grasses. Cottonwood (*Populus*) and oak (*Quercus*) become the principal woody species at the site. An increase in phytolith concentration (8,027,856) reflects an increase in site stability. The regional environment was also drier based on a decrease in vesiculate pollen to 24 percent.

Sample #8 (350-354 cmbs): The study area was warmer and drier based on the climate indices. A decrease in diatoms indicates that marsh had shrunk. Sedge and moss may have been growing on the disturbed damp area around the marsh based on the presence of moss spores and sedge pollen. Cottonwood is the dominant arboreal species in the area. The high frequency of pine pollen (50.2 percent) shows that the source area was more mesic.

Sample #9 (336-340 cmbs): At 1430 B.P. the study area was cooler and slightly moister based on the climate indices. The site was still ponded based on the diatom frequency. Cattail and sedge were present. The non-vesiculate pollen and phytolith concentrations are the highest at this level reflecting a very stable site surface. The source of the vesiculate pollen was

considerably drier based on a pine frequency of only 18.1 percent.

Sample #10 (318-321 cmbs): The study area was warmer and drier based on an increase in Chloridoids and a decrease in Pooids. The site was drier, but still ponded, based on a decrease in diatoms. Pollen from water loving plants such as cattail and willow is absent at this level. However, cottonwood is still relatively common. The surface was very stable given the high phytolith and pollen concentrations. The source area of the pine pollen was more mesic based on a higher frequency of pine pollen (30.3 percent).

Sample #11 (305-309 cmbs): The study area was slightly warmer and drier based on the climate indices. The ponded area was slightly larger based on an increase in diatoms. This is the only sample with a sponge spicule. The absence of cattail and willow pollen may be due to the absence of these plants from the site due to increased aridity. This was evidently the most stable surface as it had the highest phytolith concentration (12,787,513). However, the pollen concentration decreased. Thus, relatively more phytoliths were being deposited than pollen as compared to the previous samples. These differences in concentrations can be explained by less vegetation around the marsh which evidently was producing much of the pollen. The source area of the pine pollen was drier.

Sample #12 (290-293 cmbs): The study area is slightly cooler and drier based on relative differences in short cells. The frequency of diatoms (11.4 percent) show the site was still ponded. The presence of sedge pollen and fern spores shows that these plants were growing nearby, probably on the wet margin. Cottonwood and oak are still present. The surface was less stable at this level based on a lower phytolith concentration (7,497,837) but still relatively stable. The source of the pine pollen was more mesic.

Sample #13 (275-278 cmbs): At ca. 800 B.P. the study area was slightly warmer and drier based on the climate indices. However, the ponded area was slightly larger given an increase in diatoms to 15.7 percent. Sedge pollen and fern spores are present at the same frequencies as the previous sample. Surface stability was about the same. The source of the pine pollen was slightly drier.

Zone D: Study area warmer and drier; more rapid site aggradation.

Sample #14 (260-264 cmbs): The study area was cooler and moister (Figure D-5). The marsh was smaller based on a decrease in diatoms. Moreover, the absence of cottonwood pollen indicates more arid local conditions. Surface stability decreased based on both the phytolith and pollen concentrations. The source of the pine pollen was slightly moister.

Sample #15 (247-251 cmbs): The study area was slightly warmer and drier (Figure D-5). The marsh was larger given an increase in diatoms which may relate to an increase in Ambrosia pollen. The site was less stable based on a decrease in phytolith and pollen concentrations. The source of the pine pollen was moister.

Sample #16 (188-192 cmbs): The trend towards warmer and drier conditions continued in the study area based on the climate indices. However, the site itself was more ponded given the very high frequency of diatoms (72.4 percent) at a level. The presence of moss spores supports this interpretation. The site was also aggrading more rapidly. The source of the pine pollen was significantly drier.

Zone E: Study area moister; more rapid site aggradation.

Sample #17 (194-199 cmbs): The study area was slightly warmer and drier (Figure D-5). The site was much drier than the

previous level given the dramatic drop in the frequency of diatoms. Sage (*Artemisia*) pollen is absent from this level to the top of the sequence. Site stability was about the same. The source of the vesiculate pollen was more mesic.

Sample #18 (188-192 cmbs): The study area was cooler and moister based on an increase in Pooids and Panicoids with a concomitant decrease in Chloridoids. A significant decrease in diatoms reflects a significantly smaller marsh. Grass pollen increases at this level. The site was aggrading more rapidly based on an increase in pollen and phytolith concentrations. The source of the pine pollen was slightly drier.

Sample #19 (185-178 cmbs): The study area was slightly warmer and drier (Figure D-5). The site continued to be dry based low diatom frequency. Surface stability was about the same. The source of the pine pollen was slightly moister.

Sample #20 (163-167 cmbs): At 500 B.P. (projected date) the study area was slightly warmer and moister (Figure D-5). The site continued to be dry. Surface stability at the site did not change significantly. The source of the pine pollen was drier.

Sample #21 (146-151 cmbs): The study area was somewhat cooler and moister (Figure D-5). The site continued to be relatively dry as in the as in the three previous samples. The site was aggrading somewhat more rapidly at this level. The source of the pine pollen was drier.

D.8.1 SUMMARY OF BT 36 COLUMN SAMPLES

Analysis of phytoliths, diatoms, and pollen show a dynamic vegetational history and paleoenvironment for the site, study area, and the source of vesiculate (pine and spruce) pollen. Five paleoenvironmental zones were identified.

Zone A (482-486 cmbs): At 1890 B.P the study area was warm and dry. The site was ponded with a stable surface.

Zone B (475-391 cmbs): The study area was cooler and moister. The site surface was more rapidly aggrading and was ponded except at 429-432 cmbs when the marsh nearly dried up.

Zone C (367-278 cmbs): The study area was warmer and drier. The site had a stable surface and was ponded to varying degrees.

Zone D (260-192 cmbs): The study area was warmer and drier. The site was the most ponded at (188-192 cmbs) and experienced more rapid aggradation.

Zone E (194-151 cmbs): The study area was slightly moister. The site was much drier and aggraded more rapidly.

The vesiculate pollen, mostly pine, evidently blew in from some distance (probably to the southwest in New Mexico) as it does not occur in the study area today (<http://plants.usda.gov>). Moreover, pine phytoliths were not found in any of the samples. Fluctuations in pine pollen frequencies show that the climate varied considerably in the source area. However, there were no clear correlations with the site or study area data.

There were no close matches between the phytolith data from this study and modern phytolith assemblages analyzed by Fredlund (Fredlund and Tieszen 1994). Grass phytoliths, other than short cells, were not sensitive to paleoenvironmental changes.

Pollen concentrations low in Zones B, D, and E due to rapid aggradation not poor preservation.

D.9 ARCHAEOLOGICAL SITE 41PT185/C

The terrace on which the archaeological site was situated was covered by a short grass prairie dominated by Chloridoids grasses typical of the study area today. No evidence of plant use was found in these three feature (Features 8, 18, and 10) samples. The charred phytoliths (produced when plant materials burn) in these samples do not reflect cultural activities given that similar numbers of burned phytoliths were found in the non-archaeological samples. This suggests short-term occupation. Phytolith concentrations are typical of what was found in BT 36 and thus do not indicate cultural activities. The algal statospores and diatoms may have blown in from the adjacent marsh. No evidence of plant subsistence was found, including maize phytoliths.

D.10 REFERENCES CITED

- Bohrer, Vorsila L.
1984 Domesticated and Wild Crops in the Caep Study Area. In *Prehistoric Cultural Development in Central Arizona: Archaeology of the Upper New River Region*, edited by Patricia M. Spoerl and George J. Gumerman, pp. 183-379. Occasional Paper 5, Center for Archaeological Investigations, Southern Illinois University, Carbondale, Illinois.
- Bozarth, Steven R.
1984a Pollen and Opal Phytolith Analysis, the Jetmore Mammoth Site, 14HO1. In *Kansas Preservation Plan for the Conservation of Archaeological Resources*, edited by K. L. Brown and A. H. Simmons, pp. 4-56 to 4-67. Ms. on file, Office of Archaeological Research, Museum of Anthropology, University of Kansas, Lawrence.
- 1984b Cultigen Phytolith Analysis at 23DX3. Ms. on file, Department of Anthropology, Wichita State University, Kansas, and the Nebraska State Historical Society.
- 1985a Distinctive Phytoliths from Various Dicot Species. Paper presented at the 2nd Phytolith Conference, University of Minnesota, Duluth.
- 1985b *An Analysis of Opal Phytoliths from Rinds of Selected Cucurbitaceae Species*. M. A. thesis, Department of Anthropology, University of Kansas, Lawrence, Kansas.
- 1986a Phytoliths. In *Along the Pawnee Trail, Cultural Resources at Wilson Lake*, by Donald Blakeslee, Robert Blasing, and Hector Garcia, pp. 86-101. U.S. Army Corps of Engineers (Kansas City District), Contract DACW41-85-C-0135.
- 1986b Morphological Distinctive *Phaseolus*, *Cucurbita*, and *Helianthus annuus* Phytoliths. In *Plant Opal Phytolith Analysis in Archeology and Paleoecology; Proceedings of the 1984 Phytolith Research Workshop*, edited by Irwin Rover, pp. 56-66. *Occasional Papers No. 1 THE PHYTOLITHARIEN*, North Carolina State University, Raleigh.
- 1987a Diagnostic Opal Phytoliths from Rinds of Selected *Cucurbita* Species. *American Antiquity* 52: 607-615.
- 1987b Opal Phytolith Analysis of Edible Fruits and Nuts Native to the Central Plains. *Phytolitharien Newsletter* 4(3): 9-10.
- 1987c Opal Phytolith Analysis of Daub Samples from the Hatcher Site. In *Archaeological Investigations of the*

- Clinton Reservoir Area in Northeastern Kansas - National Register Evaluation of 27 Prehistoric Sites*, edited by Brad Logan, pp. 237-244. Kaw Valley Engineering and Development, Inc., Junction City, Kansas. Submitted to the U. S. Army Corps of Engineers, Kansas City District, Contract DACW41-86-C-0072.
- 1988 Preliminary Opal Phytolith Analysis of Modern Analogs from Parklands, Mixed Forest, and Selected Conifer Stands in Prince Albert National Park, Saskatchewan. *Current Research in the Pleistocene* 5: 45-46.
- 1989a Opal Phytoliths. In *Final Summary Report, 1986 Archaeological Investigations at 14MN328, a Great Bend Aspect Site Along U. S. Highway 56, Marion, Kansas*, by William B; Lees, John D. Reynolds, Terrance J. Martin, Mary Adair, and Steven Bozarth, pp. 85-90. Archaeology Department, Kansas State Historical Society. Submitted to the Kansas Department of Transportation.
- 1989b Evidence for *Zea Mays* at 14MN328 Based on Opal Phytolith Analysis. Paper presented at the 11th Annual Flint Hills Archaeological Conference.
- 1990a Results of Preliminary Biosilicate Analysis of 14LT351. In *The Archaeology of the Stigenwalt Site, 14LT351*, by Randall Thies, pp. 149-156. Contract Archaeological Series, Publication Number 7, Kansas State Historical Society.
- 1990b Diagnostic Opal Phytoliths from Pods of Selected Varieties of Common Beans (*Phaseolus vulgaris*). *American Antiquity* 55:98-104.
- 1991 Paleoenvironmental Reconstruction of the La Sena Site Based on Opal Phytolith Analysis. In *The La Sena Mammoth Site, 25FT177 - Medicine Creek Reservoir, Frontier County*, edited by Steven Holen, pp. 129-142. Technical Report 2008-09, Denver Museum of Nature and Science.
- 1992a Classification of Opal Phytoliths Formed in Selected Dicotyledons Native to the Great Plains. In *Phytolith Systematics-Emerging Issues*, edited by George Rapp, Jr. and Susan Mulholland, pp. 193-214. Plenum Press, New York.
- 1992b Paleoenvironmental Reconstruction of the Sargent Site, a Fossil Biosilicate Analysis. Ms. on file, Department of Geology, University of Kansas, Lawrence, Kansas, 22 p.
- 1993a Biosilicate Assemblages of Boreal Forests and Aspen Parklands. In *Current Research in Phytolith Analysis: Applications in Archaeology and Paleoecology*, edited by Deborah Pearsall and Dolores Piperno, pp. 95-105. MASCA (Museum Applied Science Center for Archaeology) Series, University of Pennsylvania, Vol. 10.
- 1993b Maize (*Zea mays*) Cob Phytoliths from a Central Kansas Great Bend Aspect Archaeological Site. *Plains Anthropologist* 38(146):279-286.
- 1993c Phytolith Analysis of Bison Teeth Calculus and Impacta from Sites in Kansas and Oklahoma. In *Investigations of Seasonality, Herd Structure, Taphonomy, and Paleoecology at Folsom Bison Kill*

- Sites on the Great Plains: 10,500 B. P.*, edited by Jack Hoffman, Department of Anthropology, University of Kansas, Lawrence.
- 1995 Analysis of Fossil Biosilicates from the Valley Fill. In *Stratigraphy and Paleoenvironments of Late Quaternary Valley Fills on the Southern High Plains*, edited by Vance Holliday, pp. 161-171. Geological Society of America Memoir 186.
- 1998a Opal Phytolith Analysis at 14LV1071. In *Prehistoric Settlement of the Lower Missouri Uplands, the View from DB Ridge, Fort Leavenworth, Kansas*, edited by Brad Logan, pp. 74-85. Museum of Anthropology, University of Kansas, Project Report Series 98.
- 1998b Paleoenvironmental Reconstruction of the Great Plains Based on Biosilicate Analysis. *Abstracts – Annual Meetings of the Great Plains/Rocky Mountain Division of the Association of the American Geographers*.
- 1998c Paleoenvironmental Reconstruction of the Sargent Site, Southwestern Nebraska – a Fossil Biosilicate Analysis. *Abstracts – Institute for Tertiary-Quaternary Studies*.
- 2000 Reconstruction of Vegetative Histories and Paleoenvironments in Northeastern Kansas Based on Opal Phytolith Analysis. *Current Research in the Pleistocene* 15:95-96.
- 2008 Paleoenvironmental Reconstruction of the La Sena Site Based on Biosilicate Analysis. In *The La Sena Mammoth Site, 25FT177 – Medicine Creek Reservoir, Frontier County, Nebraska – Volume 1: History of Investigations, Paleoecology and Stratigraphy*, edited by Steven Holen, pp. 129-142. Technical Report 2008-09, Denver Museum of Nature and Science.
- Brown, Dwight A.
1984 Prospects and Limits of a Phytolith Key for Grasses in the Central United States. *Journal of Archaeological Science* 11:345-368.
- Bryant, Vaughn M. Jr. and Richard G. Holloway
1985 *A Late-Quaternary Paleoenvironmental Record of Texas: An Overview of the Pollen Evidence*, edited by Vaughn M. Bryant, Jr. and Richard G. Holloway, pp. 95-123. American Association of Stratigraphic Palynologists Foundation.
- Bryant, Vaughn M. Jr., and Stephen A. Hall
1993 Archaeological Palynology in the United States: a Critique. *American Antiquity* 58:277-286.
- Brydon, James E., William G. Dore, and John S. Clark
1963 Silicified Plant Asterosclereids Preserved in Soil. *Proceedings of the Soil Science Society of America* 27:476-477.
- Fredlund, Glen, W.C. Johnson, and W. Dort, Jr.
1985 A preliminary analysis of opal phytoliths from the Eustis ash pit, Frontier County, Nebraska: Nebraska Academy of Sciences, Institute for Tertiary-Quaternary Studies, TER-QUA Symposium Series 1:147-162.
- Fredlund, Glen and Larry Tieszen
1994 Modern phytolith assemblages from the North American Great Plains.

- Journal of Biogeography* 21:321-335.
- Garber, Lowell W.
1966 *Influence of Volcanic Ash on the Genesis and Classification of Two Spodosols in Idaho*. Master's thesis, Department of Soil Science, University of Idaho, Moscow.
- Geis, James W.
1973 Biogenic Silica in Selected Species of Deciduous Angiosperms. *Soil Science* 116:113-130.
- Gish, Jannifer W.
2000 Paleobotanical Results from IO 8, 41PT185, and 41PT186, Texas. Appendix F – Paleobotanical Analysis. In *Phase II Archeological Testing: Landis Property, Potter County, Texas*, by G. M. Haecker. National Park Service, Intermountain Support Office, Anthropology Program, Santa Fe, New Mexico for the Bureau of Land Management, Helium Operations Unit, Amarillo, Texas.
- Gould, F. W., and R. B Shaw
1968 *Grass Systematics*, 2nd edition. Texas A & M University Press, College Station.
- Hall, Stephen A.
1985 Quaternary Pollen Analysis and Vegetational History of the Southwest. In *Pollen Records of Late-Quaternary North American Sediments*, edited by Vaughn M. Bryant, Jr. and Richard G. Holloway, pp. 95-123. American Association of Stratigraphic Palynologists Foundation.
- Johnson, William C. (editor)
1993 Second International Paleopedology Symposium Field Excursion: Kansas Geological Survey Open-File Report No. 93-30.
- Johnson, William C., and Steven R. Bozarth
1996 *Variation in Opal Phytolith Assemblages as an Indicator of Late Quaternary Environmental Change on Fort Riley, Kansas*, review draft. Prepared under contract No. DACA88-95-M-0422, for the U.S. Army Construction Engineering Research Laboratory (USACERL).
- Kapp, Ronald O.
1969 *Pollen and Spores*. Wm. C. Brown Company, Dubuque, Iowa.
- Klein, Robert L., and James W. Geis
1978 Biogenic Silica in the Pinaceae. *Soil Science* 126:145-155.
- Lewis, Walter H., Prathibha Vinay, and Vincent E. Zenger
1983 *Airborne and Allergenic Pollen of North America*. The John Hopkins University Press, Baltimore.
- McAndrews, John H., Albert A. Berti, and Geoffrey Norris
1973 *Key to the Quaternary Pollen and Spores of the Great Lakes Region*. Life Sciences Miscellaneous Publication, Royal Ontario Museum, Canada.
- Moore, P. D., and J. A. Webb
1978 *An Illustrated Guide to Pollen Analysis*. Halstead Press, John Wiley and Sons, New York.
- Mulholland, Susan C.
1986 Phytolith Studies at Big Hidatsa, North Dakota: Preliminary Results. In *The Prairie: Past, Present and Future. Proceedings of the Ninth North American Prairie Conference, July 29 to August 1, 1984, Moorhead, Minnesota*, edited by Gary K. Clambey and Richard H. Pemble, pp. 21-24. Tri-College University Center for Environmental Studies.

- 1987 Phytolith Studies at Big Hidatsa. Unpublished Ph. D. dissertation, University of Minnesota.
- Mulholland, Susan C., and George Rapp, Jr.
1992 A Morphological Classification of Grass Silica-Bodies. In *Phytolith Systematics*, edited by George Rapp, Jr. and Susan C. Mulholland, pp. 65-89. Plenum Press, New York.
- Norgren, J.
1973 Distribution, Form and Significance of Plant Opal in Oregon Soils. Unpublished Ph.D. dissertation, Department of Soil Science, Oregon State University, Corvallis, 176 p.
- Ollendorf, Amy L.
1992 A Morphological Classification of Grass Silica-Bodies. In *Phytolith Systematics*, edited by George Rapp, Jr. and Susan C. Mulholland, pp. 65-89. Plenum Press, New York.
- Pease, D. S.
1967 *Opal Phytoliths as Indicators of Paleosols*. Unpublished Master's thesis, New Mexico State University, University Park.
- Piperno, Dolores R.
1988 *Phytolith Analysis - An Archaeological and Geological Perspective*. Academic Press, Inc. New York.
- Pohl, R. W.
1968 *How to Know the Grasses*, 3rd edition. The Pictured Key Nature Series, Wm. C. Brown Company Publishers, Dubuque, Iowa.
- Rovner, Irwin
1971 Potential of Opal Phytoliths for Use in Paleoecological Reconstruction. *Quaternary Research* 1:343-359.
1975 Plant Opal Phytolith Analysis in Midwestern Archaeology. *Michigan Academician* 8:591.
- Twiss, P. C.
1987 Grass Opal Phytoliths as Climatic Indicators of the Great Plains Pleistocene. In *Quaternary Environments of Kansas*, edited by W. C. Johnson, pp. 179-188. Kansas Geological Guide Book, Series 5, Lawrence, Kansas.
- Twiss, P. C., E. Suess, and R. M. Smith
1969 Morphological Classification of Grass Phytoliths. *Soil Science Society of America, Proceedings*, Vol. 33, p. 109-115
- Wilding, L. P., and L. R. Drees
1971 Biogenic Opal in Ohio Soils. *Proceedings of the Soil Science Society of America* 35:1004-1010.
1973 Scanning Electron Microscopy of Opaque Opaline Forms Isolated from Forest Soils in Ohio. *Proceedings of the Soil Science Society of America* 37:647-650.
1974 Contributions of Forest Opal and Associated Crystalline Phases of Fine Clay Fractions of Soils. *Clays and Clay Minerals* 22:295-306.
- Wilding, L. P., C. T. Hallmark, and N. E. Smeck
1979 Dissolution and Stability of Biogenic Opal. *Journal of Soil Science Society of America* 43:800-802.
- Wilding, L. P., N. E. Smeck, and L. R. Drees
1977 Silica in Soils: Quartz, Cristobalite, Tridymite, and Opal. In *Minerals in Soils Environment*, edited by J. B. Dixon and S. B. Weed, pp. 471-552. Soil Science Society of America, Madison, Wisconsin.

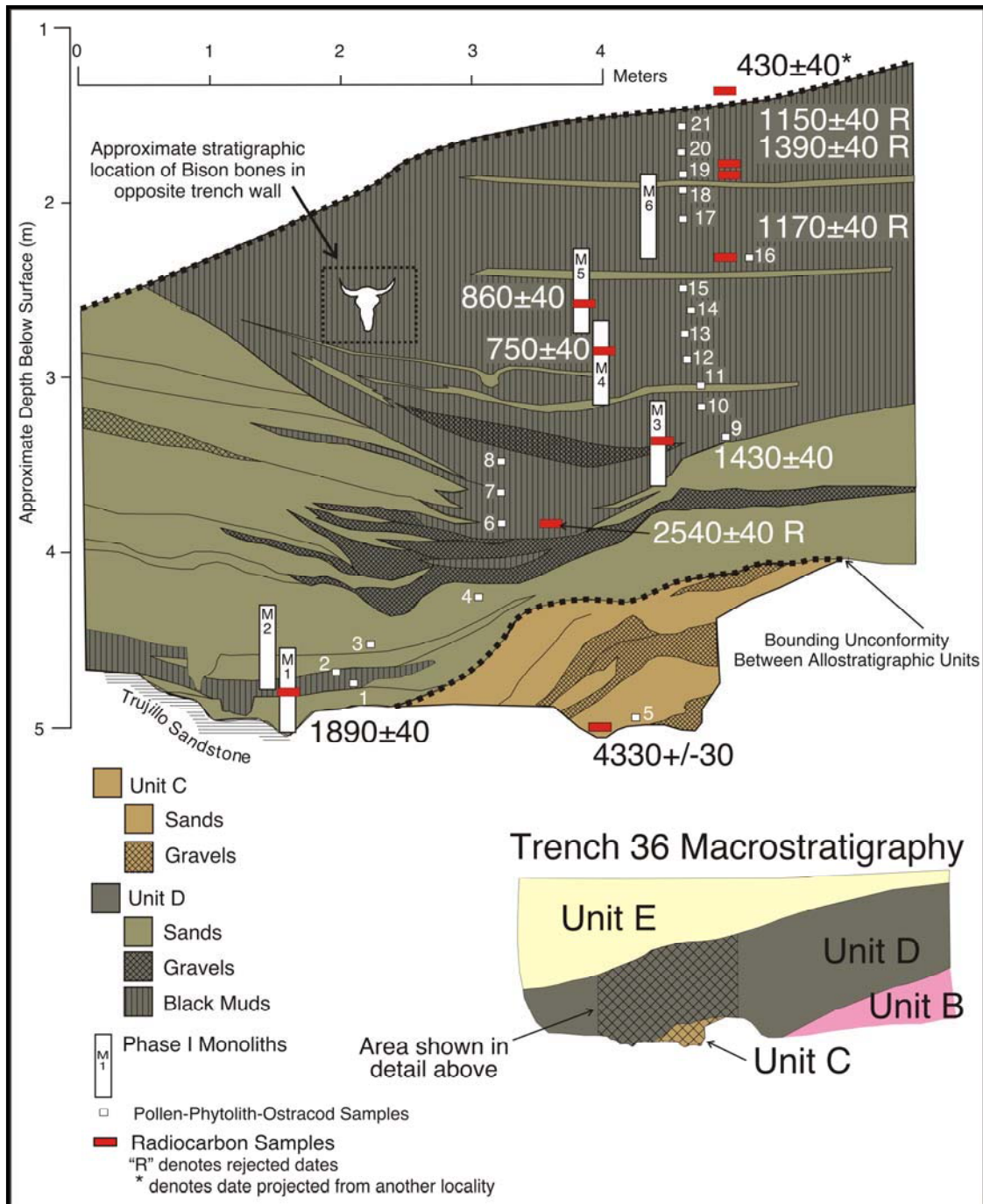


Figure D-1. Profile of Backhoe Trench 36 Showing Sample and Radiocarbon Locations.

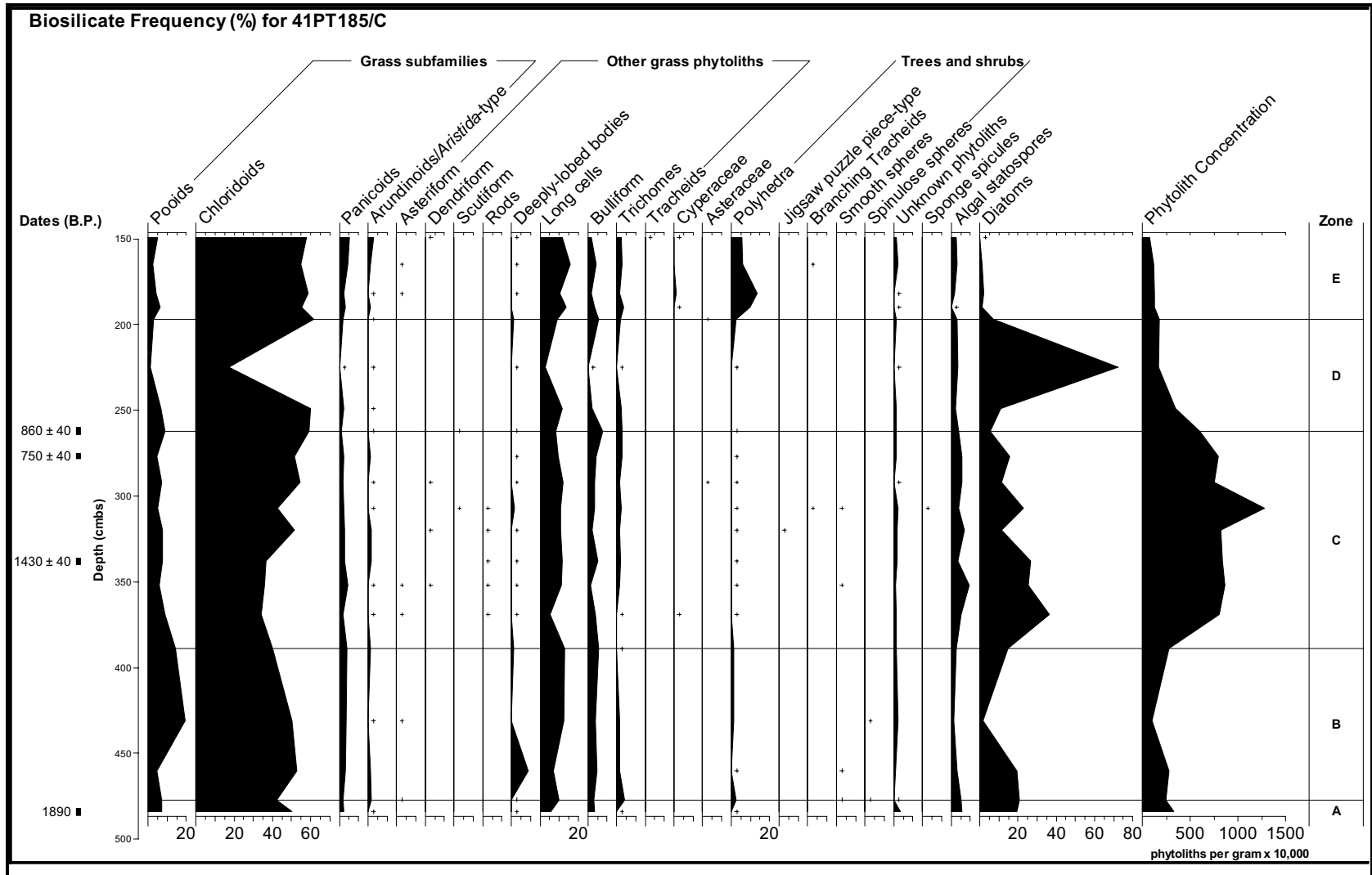


Figure D-2. Biosilicate Frequency (percentages for 21 Column Samples from BT 36 at 41PT185/C Showing Interpreted Paleoenvironmental Zones at Right Side

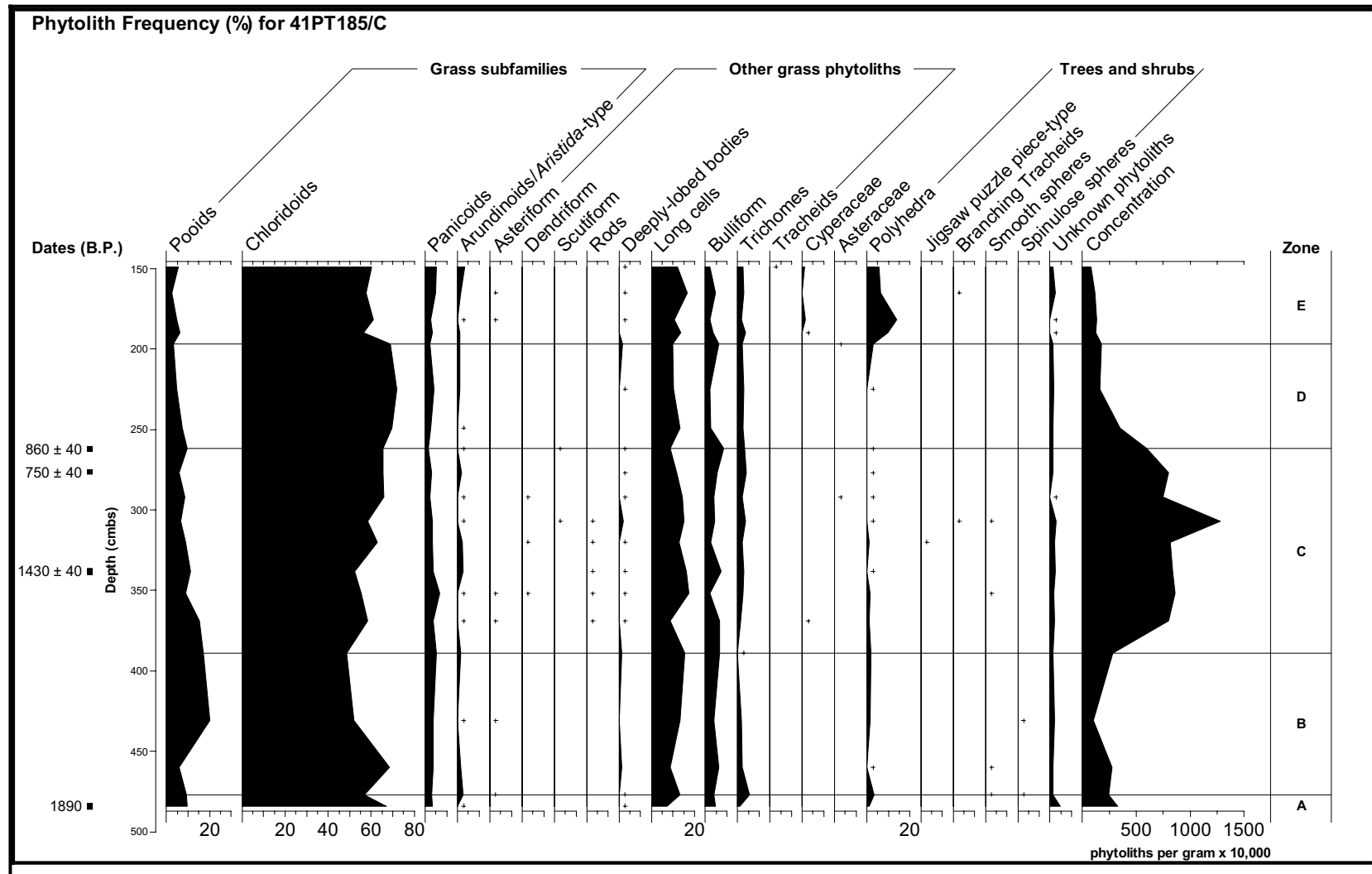


Figure D-3. Phytolith Frequency (percentages) for 21 Column Samples from BT 36 at 41PT185/C Showing Interpreted Paleoenvironmental Zones at Right Side.

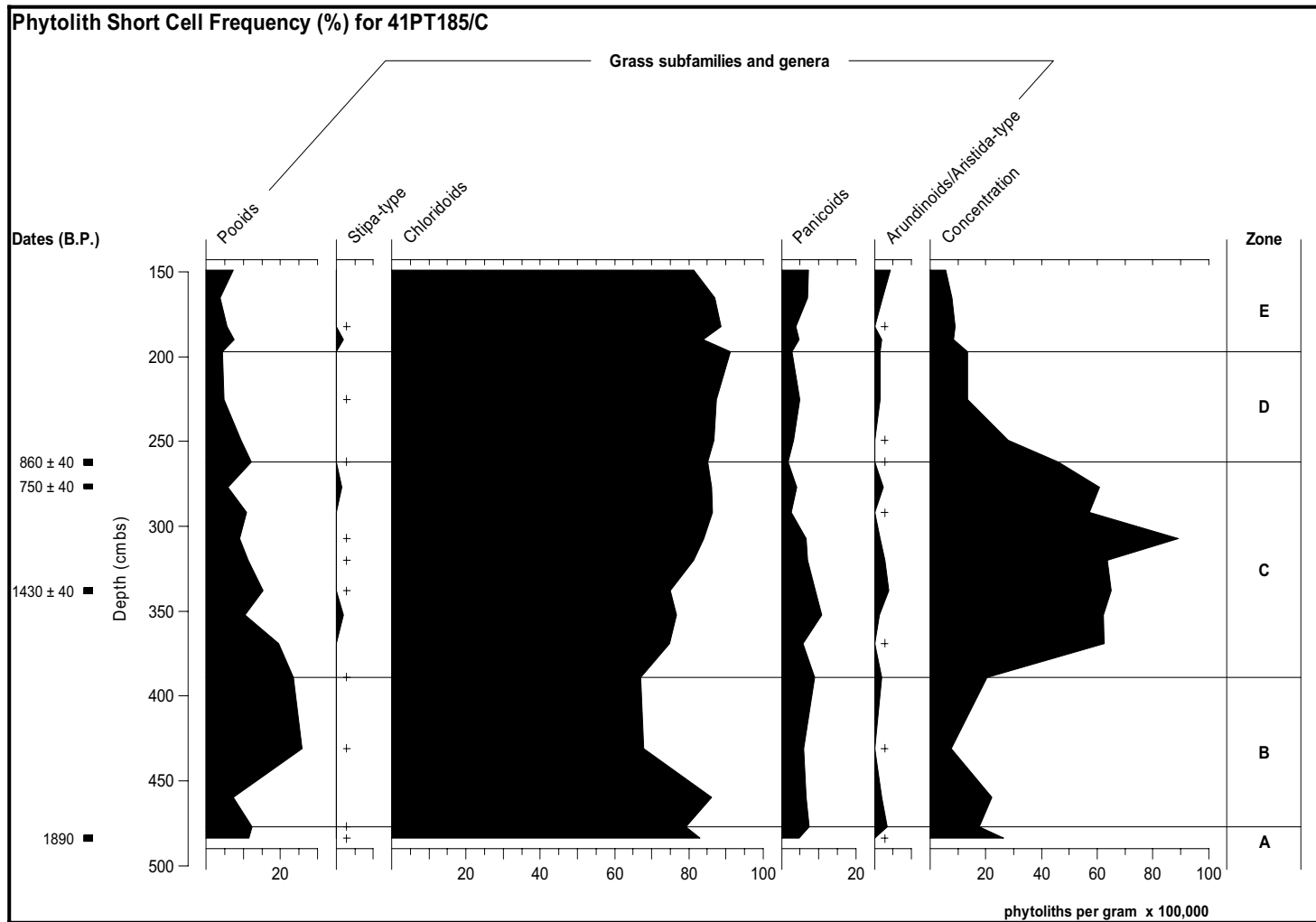


Figure D-4. Phytolith Short Cell Frequency (percentages) for 21 Column Samples from BT 36 at 41PT185/C Showing Interpreted Paleoenvironmental Zones at Right Side.

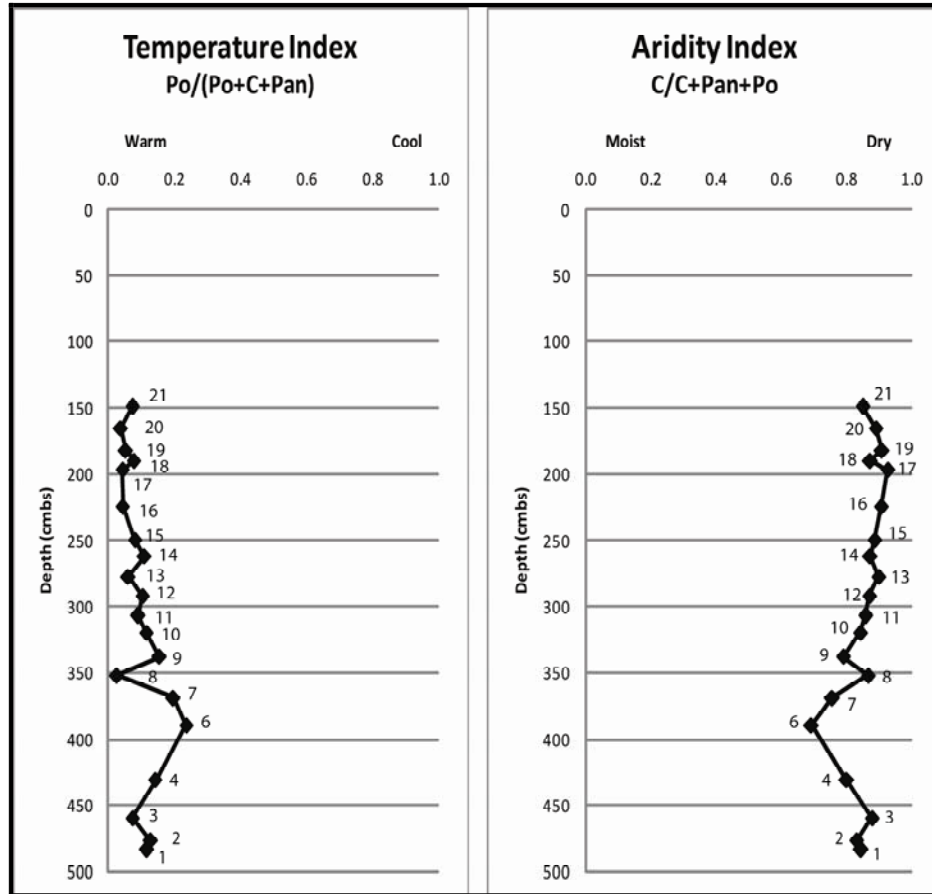


Figure D-5. Climate Indices Calculated from Phytolith Frequencies of Poides (Po), Chloridoids (C), and Panicoids (Pan), Indicating Relative Temperature and Moisture Changes Through Time from the 321 Column Samples out of BT 36, 41PT185/C.

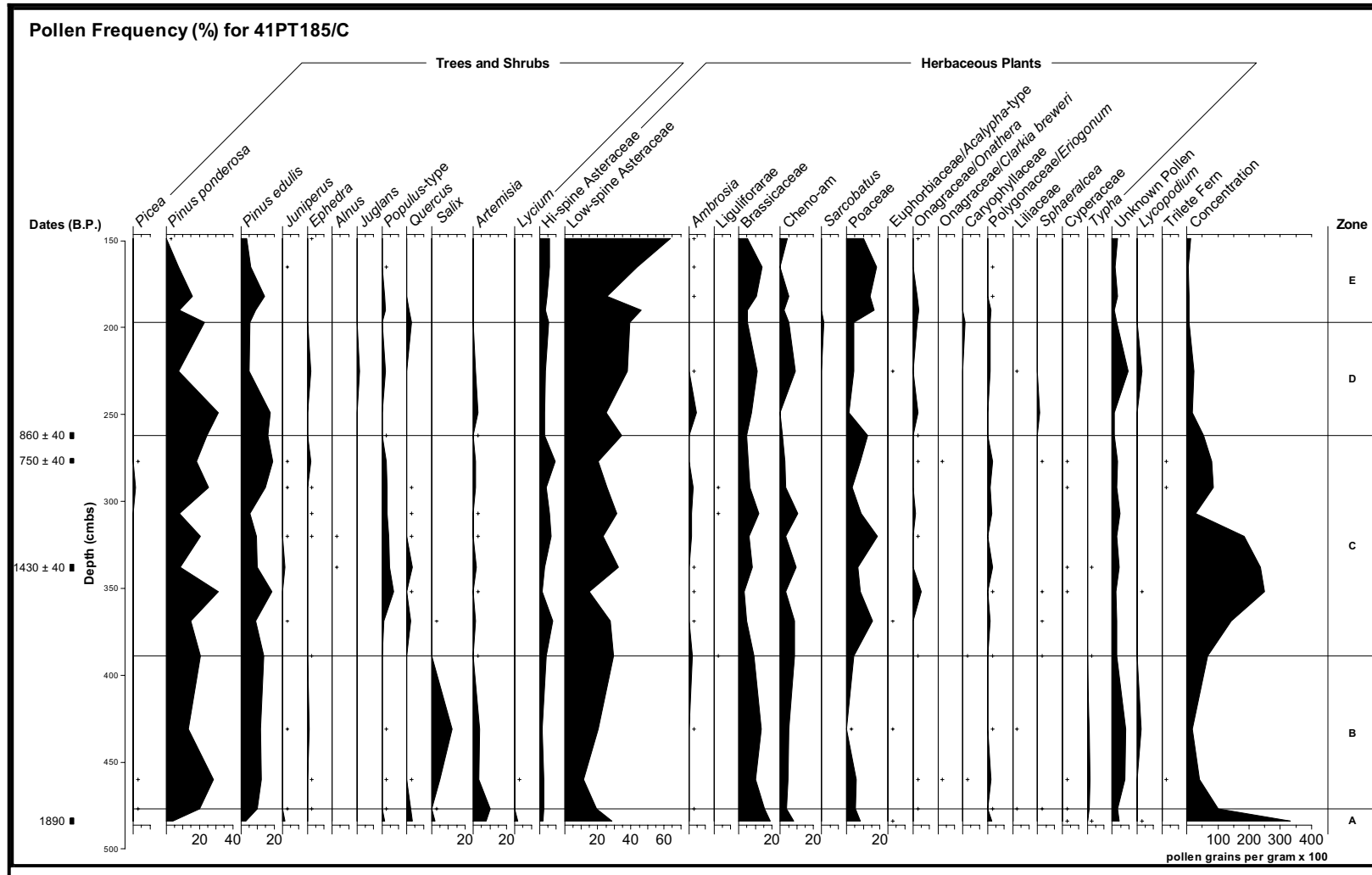


Figure D-6. Pollen Frequency (percentages) for 21 Column Samples from BT 36 at 41PT185/C Showing Interpreted Paleoenvironmental Zones at Right Side.

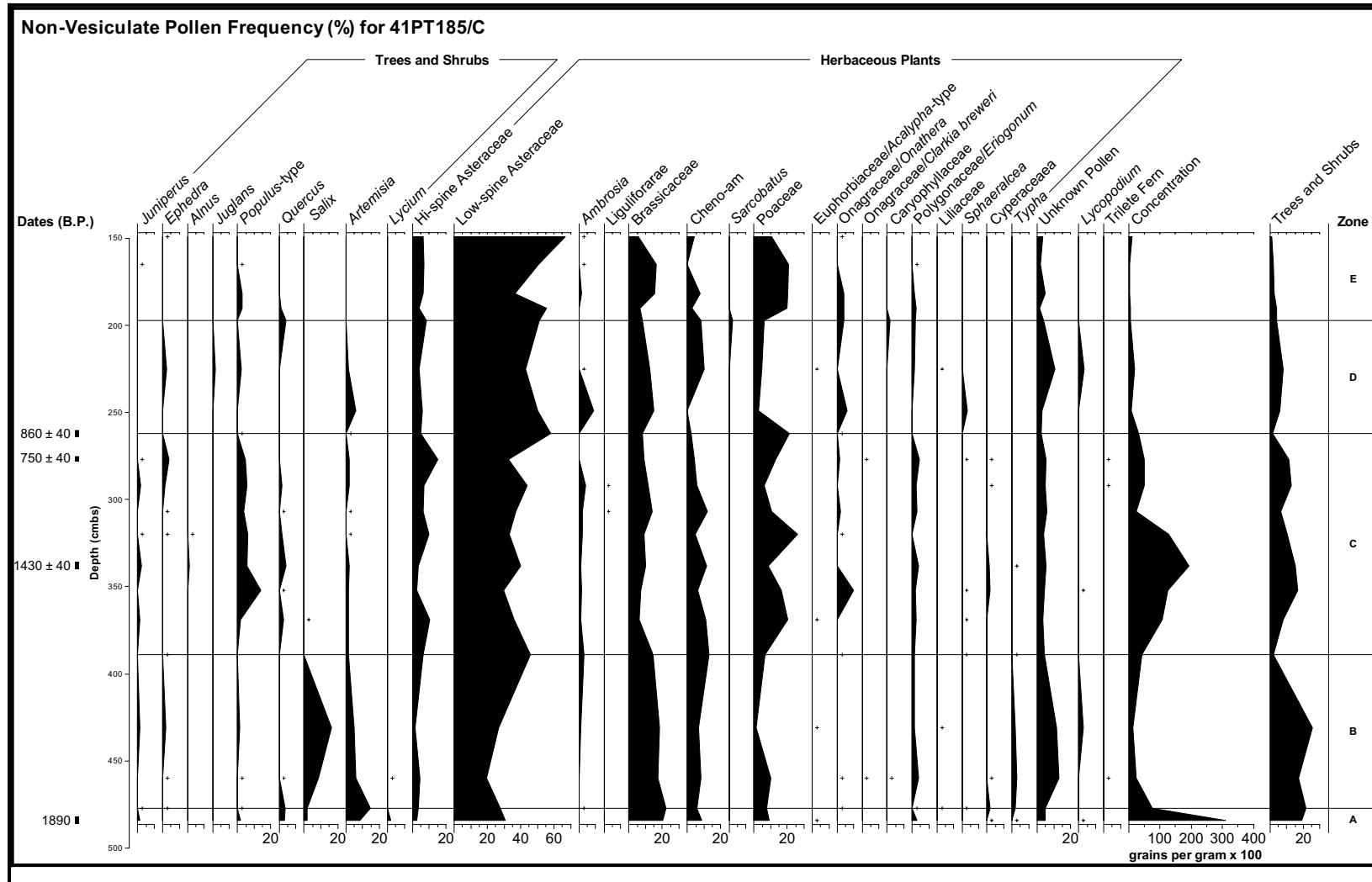


Figure D-7. Non-Vesiculate Pollen Frequency (percentages) for 21 Column Samples from BT 36 at 41PT185/C Showing Interpreted Paleoenvironmental Zones at Right Side.

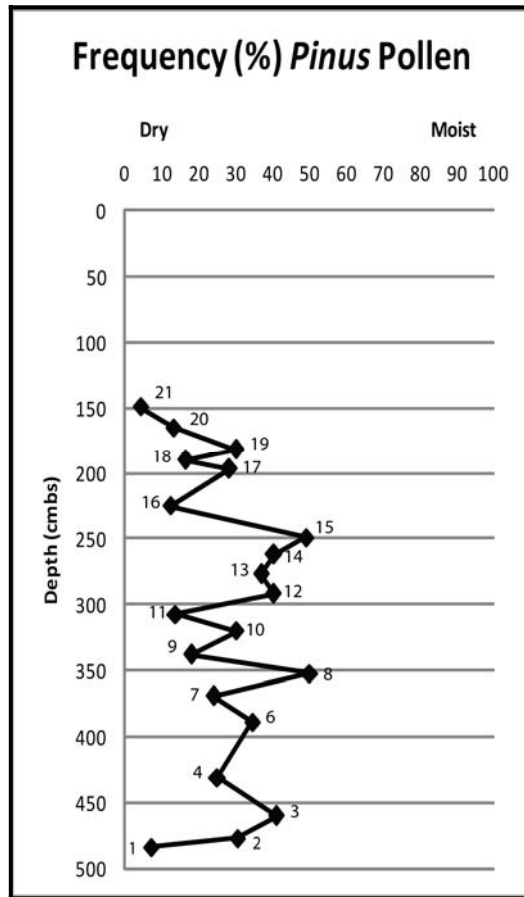


Figure D-8. Aridity Index Based on *Pinus* Pollen Frequency, Indicating Relative Moisture Shifts through Time for 21 Column Samples from BT 36 at 41PT185/C.

Table D-1. Biosilicate Frequency Data for West Amarillo Creek, Potter County, Texas

Age B.P.													
	10850	9610	8280	4330	2250	1890	1840	1430	1390	860	750	600	300
Site	41PT245	41PT186	41PT186	41PT186	41PT186	41PT185/C	41PT245	41PT185/C	41PT245	41PT185/C	41PT185/C	41PT186	41PT186
Trench/Unit	BT 21	BT 6-2a	BT 6-1a	BT 40	BT 40	BT 36	BT 20-2	BT 36	TU 4 bulk	BT 36	BT 36	BT 9-1	BT 5-5
Depth (cmbs)	271-274	264-268	136-139	445-448	210-215	480	240	346-348	120-130	265-268	282-285	125	A horizon
Catalog number	418-004- 1a	341-004- 2a	341-004- 1a	10-004- 2a	10-004- 1b	263-004-5	417-004- 1a	263-004- 4a	353-004- 1a	263-004- 1a	263-004- 2a	343-004- 1a	340-004- 1a
Phytolith Sum	215	213	200	211	212	216	203	200	217	213	220	221	221
Phytolith Concentration	498,839	241,182	61,943	70,510	204,280	311,073	376,271	622,797	222,731	718,933	931,561	180,700	394,063
Biosilicate Sum/counts	216	214	202	217	222	321	205	308	218	229	286	223	227
Grass Subfamilies													
Arundinoids; Aristida	0.5	3.3	1.0	0.9	0.5	-	1.0	-	0.9	-	0.3	0.4	0.4
Chloridooids	28.7	40.7	6.4	41.5	37.4	48.3	44.9	41.6	51.4	60.3	52.8	12.1	51.1
Panicoids	5.1	0.5	0.5	1.8	4.1	3.4	1.5	2.6	1.4	1.7	1.7	0.4	4.4
Pooids	31.9	24.3	12.9	27.6	24.3	7.8	22	4.2	19.7	8.3	7	7.6	16.3
Pooids; Stipa	1.6	-	0.5	0.9	0.5	-	0.5	-	0.5	-	0.7	0.4	0.9
Grass Inflorescence/ seeds													
Asteriform	-	-	-	-	-	-	0.5	-	-	-	-	-	-
Dendriform	0.9	-	-	-	0.9	-	-	-	-	-	-	-	-
Scutiform	-	-	-	-	-	-	-	-	-	-	-	0.4	-
Rods	-	-	-	-	-	-	-	-	-	-	-	-	-
Deeply-lobed bodies	0.5	-	-	0.5	1.8	-	1.5	0.3	0.5	0.4	-	-	0.9
Other Grass Phytoliths													
Long cells	17.6	13.1	24.3	8.3	12.2	5.2	13.7	10.4	11.9	10	8.4	33.2	12.8
Bulliform	8.3	10.7	38.6	10.1	7.7	-	5.9	3.9	8.9	4.8	3.1	36.8	2.6
Trichomes	1.4	3.7	5.4	2.8	3.2	2.2	6.3	1.6	3.2	7	2.1	7.6	4.4
Tracheids	0.5	-	-	-	-	-	-	-	-	-	-	-	-
Stomata	-	-	-	-	0.5	-	-	-	-	-	-	-	-

Cyperaceae plant	-	-	-	-	-	-	-	-	-	-	-	-	-
Cyperaceae inflorescence	-	-	-	-	-	-	-	-	-	-	-	-	-
Dicotyledons													
Trees, Shrubs and Herbs													
Flat Polyhedra	-	-	-	-	-	0.3	-	-	0.5	-	0.3	-	-
Trees and shrubs													
Spinulose spheres	0.5	0.5	6.9	0.5	0.5	-	-	-	-	-	-	-	-
Unknown phytoliths	1.6	2.8	2.5	2.3	2.3	-	1.5	0.3	0.9	0.4	0.3	-	3.5
Sponge spicules	-	-	0.5	-	-	-	-	0.3	-	-	-	-	-
Algal statospores	0.5	0.5	-	1.8	4.5	6.8	0.5	4.2	0.5	2.2	5.6	0.9	1.3
Diatoms	-	-	0.5	0.9	-	25.9	0.5	30.5	-	4.8	17.5	-	1.3

Table D-2. Phytolith Frequency Data for Short Cells and Trees and Shrubs at West Amarillo Creek, Potter County, Texas

Age B P.													
	10850	9610	8280	4330	2250	1890	1840	1430	1390	860	750	600	300
Site	41PT245	41PT186	41PT186	41PT186	41PT186	41PT185/C	41PT245	41PT185/C	41PT245	41PT185/C	41PT185/C	41PT186	41PT186
Provenience	BT 21	BT 6-2a	BT 6-1a	BT 40	BT 40	BT-36	BT 20-2	BT-36	TU 4 bulk	BT-36	BT-36	BT-9-1	BT 5-5
Depth (cmbs)	271-274	264-268	136-139	445-448	210-215	480	240	346-348	120-130	265-268	282-285	125	A horizon
Catalog number	418-004-1a	341-004-2a	341-004-1a	10-004-2a	10-004-1a	263-004-5	417-004-1a	263-004-4a	353-004-1a	263-004-1a	263-004-2a	343-004-1a	340-004-1a
Phytolith Sum	148	147	57	159	149	192	143	149	162	161	180	47	166
Grass subfamilies													
Arundinoids; Aristida	0.7	4.8	3.5	1.3	0.7		1.4	-	1.2	-	0.6	2.1	0.6
Chloridoids	41.9	58.5	22.8	56.6	55.7	80.7	64.3	85.9	69.1	85.7	83.9	57.4	69.9
Panicoids	7.4	0.7	1.8	2.5	6	5.7	2.1	5.4	1.9	2.5	2.8	2.1	6
Pooids	46.6	35.3	45.6	37.7	36.2	13.1	31.5	8.7	26.5	11.8	11.1	36.2	22.3
Pooids; Stipa	2.7	-	1.8	1.3	0.7	-	0.7	-	0.6	-	1.1	2.1	1.2
Dicotyledons													
Trees, shrubs and herbs													
Flat Polyhedra	-	-	-	-	-	0.5	-	-	0.6	-	0.6	-	-
Trees and shrubs													
Spinulose spheres	0.7	0.7	24.6	0.6	0.7	-	-	-	-	-	-	-	-

Table D-3. Pollen Data for 41PT185/C				
Age (B.P.)				
	1890 ± 40	1430 ± 40	860 ± 40	750 ± 40
Depth (cmbs)	480	334-336	265-268	282-285
Provenience	BT 36, M-1-1	BT 36, M-3-4	BT 36, M-5-9	BT 36, M-4-6
Catalog No.	263-004-5	263-004-3a	263-004-1a	263-004-2a
Pollen Sum	227	276	225	228
Pollen Concentration	24,912	25,670	3,566	11,005
Trees and Shrubs				
Abies	-	0.4	0.4	0.4
Pinus	-	0.4	0.9	1.3
Pinus ponderosa-type	11.9	3.6	15.1	15.4
Pinus edulis-type	5.7	14.6	24.4	20.6
Juniperus	1.3	1.1	0.4	-
Ephedra	1.3	1.4	-	2.2
Alnus	-	0.4	-	-
Juglans	-	-	0.4	-
Populus-type	0.9	-	0.4	1.3
Quercus	2.2	2.5	-	-
Salix	4	0.4	-	-
Artemisia	9.7	4.7	4	1.8
Herbaceous Plants				
Acalypha-type	1.3			
Long-spine ASTERACEAE	-	0.7	-	-
Hi-spine ASTERACEAE	4.4	6.5	5.3	20.6
Low-spine ASTERACEAE	21.6	36.6	20	14.4
Ambrosia	0.4	2.2	6.2	1.8
BRASSICACEAE	4	5.1	3.1	1.8
Cheno-am	4.8	6.5	2.2	4.4
Eriogonum-type	2.6	0.4	-	-
FABACEAE	1.3			
MALVACEAE	2.2			
ONAGRACEAE	-	0.4	0.9	1.3
POACEAE	5.3	4.7	12.9	7.4
Polygonum	2.6	2.2	0.9	1.8
CYPERACEAE	1.3	2.5	0.9	0.9
Unknown pollen	11	2.5	0.9	2.6
Sporomiella	-		0.4	
Aggregates				
Artemisia		-	4, 5.5, 9	-
High-spine Asteraceae	1, 2, 2	-	1, 2, 2	18, 2.7, 8
Low-spine Asteraceae	2, 2.5, 3	4, 2.3, 3	17, 4.1, 12	-
Cheno-am		-	1, 3, 3	-
BRASSICACEAE		-	4, 14.3, 30	1, 3, 3
Ephdra		-	-	2, 2, 2
POACEAE		-	-	4, 3.5, 5
*Aggregate notation shows total number, mean size, and largest aggregate (Texas pollen 2)				

Table D-4. Pollen Data (without vesiculate grains) on Four Samples from 41PT185/C

Age (B.P.)	1890 ± 40	1430 ± 40	860 ± 40	750 ± 40
Depth (cmbs)	480	334-336	265-268	282-285
Provenience	BT 36, M-1-1	BT 36, M-3-4	BT 36, M-5-9	BT 36, M-4-6
Catalog No.	263-004-5	263-004-3a	263-004-1a	263-004-2a
Pollen Sum	187	223	135	140
Pollen Concentration	20,522	20,741	2,140	6,757
Trees and shrubs				
Juniperus	1.6	1.3	0.7	-
Ephedra	1.6	1.8	-	3.6
Alnus	-	0.5	-	-
Juglans	-	-	0.7	-
Populus-type	1.1	-	1.5	2.1
Quercus	2.7	3.1	-	-
Salix	4.8	0.5	-	-
Artemisia	11.8	5.8	6.7	2.9
Herbaceous plants				
Acalypha-type	1.6	-	-	-
Long-spine ASTERACEAE	-	0.9	-	-
Hi-spine ASTERACEAE	5.3	8.1	8.9	33.6
Low-spine ASTERACEAE	26.2	45.3	33.3	23.6
Ambrosia	0.5	2.7	10.4	2.9
BRASSICACEAE	4.8	6.3	5.2	2.9
Cheno-am	5.9	8.1	3.7	7.1
Eriogonum-type	3.2	0.5	-	-
FABACEAE	1.6	-	-	-
MALVACEAE	2.7	-	-	-
ONAGRACEAE	-	0.5	1.5	2.1
POACEAE	6.4	5.8	21.5	12.1
Polygonum	3.2	2.7	1.5	2.9
CYPERACEAE	1.6	3.1	1.5	1.4
Unknown pollen	13.4	3.1	2.2	2.9
Sporomiella	-	-	0.7	-
Aggregates				
Artemisia		-	4, 5.5, 9	-
High-spine Asteraceae	1, 2, 2	-	1, 2, 2	18, 2.7, 8
Low-spine Asteraceae	2, 2.5, 3	4, 2.3, 3	17, 4.1, 12	-
Cheno-am		-	1, 3, 3	-
BRASSICACEAE		-	4, 14.3, 30	1, 3, 3
Ephedra		-	-	2, 2, 2
POACEAE		-	-	4, 3.5, 5
*Aggregate notation shows total number, mean size, and largest aggregate (Texas pollen 3)				

Table D-5. Biosilicate Frequency Data for 41PT185/C			
Provenience	N104 E105	N118 E105	N112 E105
Catalog number	471-004-1a	1129-004-1a	801-004-1a
Depth (cmbs)	50-60	50-60	62-65
Feature	8	18	10
Phytolith Sum	285	283	358
Phytolith Concentration	3,259,172	2,404,109	2,289,106
Biosilicate Sum	288	285	362
Grass subfamilies			
Pooids (total) =	6.9	7.8	9.4
Keeled	1	3.2 {2}	1.4
Conical	2.4	0.4	3
Pyramidal	-	-	0.3
Crenate	3.5	3.5	3.3
Disks w/ peg like sculpturing	-	0.7	1.4
Stipa-type	-	-	-
Chloridoids (total) =	66.3 {1}	60	50.8 {1}
Panicoids (total) =	1.3	0.7	1.2
Simple lobate	0.7	0.7	-
Panicoid type	0.3	-	0.6
Cross	0.3	-	0.6
Arundinoids	-	-	-
Aristida-type	0.3	2.1	1.1
Grass inflorescence/seeds			
Asteriform	-	-	-
Dendriform	-	-	.3
Scutiform	-	-	-
Rods	-	-	-
Deeply-lobed bodies	0.7	-	1.1
Other grass phytoliths			
Long cells	14.9	16.1	21.5 {1}
Bulliform	4.5	6.7 {1}	6.9
Trichomes	2.8	3.9	5
Tracheids	-	-	-
Cyperaceae	-	-	-
Asteraceae	-	-	-
Trees and shrubs			
Polyhedra	0.7	-	0.6
Spinulose spheres	-	0.4	-
Unknown phytoliths	0.3	1.8	1.1
Sponge spicules	-	-	-
Algal statospores	1	0.4	0.3
Diatoms	-	0.4	0.8
*(41PT185/C biosilicates features) {number of charred phytoliths}			

Table D-6. Phytolith Frequency Data for 41PT185/C			
Provenience	N104 E105	N118 E105	N112 E105
Catalog Number	471-004-1a	1129-004-1a	801-004-1a
Depth (cmbs)	50-60	50-60	62-65
Feature	8	18	10
Phytolith Sum	285	283	358
Phytolith Concentration	3,259,172	2,404,109	2,289,106
Grass subfamilies			
Pooids (total) =	<u>7</u>	<u>7.8</u>	<u>9.6</u>
Keeled	1	3.2 {2}	1.4
Conical	2.5	0.4	3.1
Pyramidal	-	-	0.3
Crenate	3.5	3.5	3.4
Disks w/ peg like sculpturing	-	0.7	1.4
Stipa-type	-	-	-
Chloridoids (total) =	<u>67.0 {1}</u>	<u>60.4</u>	<u>51.4 {1}</u>
Panicoids (total) =	<u>1.3</u>	<u>0.7</u>	<u>1.2</u>
Simple lobate	0.7	0.7	-
Panicoid type	0.3	-	0.6
Cross	0.3	-	0.6
Arundinoids	-	-	-
Aristida-type	<u>0.3</u>	<u>2.1</u>	<u>1.1</u>
Grass inflorescence/seeds			
Asteriform	-	-	-
Dendriform	-	-	.3
Scutiform	-	-	-
Rods	-	-	-
Deeply-lobed bodies	0.7	-	1.1
Other grass phytoliths			
Long cells	15.1	16.3	21.8
Bulliform	4.6	6.7 {1}	7
Trichomes	2.8	3.9	5
Tracheids	-	-	-
Cyperaceae	-	-	-
Asteraceae	-	-	-
Trees and shrubs			
Polyhedra	0.7	-	0.6
Spinulose spheres	-	0.4	-
Unknown phytoliths	0.3	1.8	1.1
*(41PT185/C phytoliths features) {number of charred phytoliths}			

Table D-7. Grass Short-Cell Frequency Data for 41PT185/C

Provenience	N104 E105	N118 E105	N112 E105
Catalog Number	471-004-1a	1129-004-1a	801-004-1a
Depth (cmbs)	50-60	50-60	62-65
Feature	8	18	10
Short-Cell Sum	216	201	227
Short-Cell Concentration	2,470,110	1,707,512	1,451,472
Grass subfamilies			
Pooids (total) =	9.2	11	14.9
Keeled	1.4	4.5 {2}	2.2
Conical	3.2	0.5	4.8
Pyramidal	-	-	0.4
Crenate	4.6	5	5.3
Disks w/ peg like sculpturing	-	1	2.2
Stipa-type	-	-	-
Chloridoids (total) =	88.4 {1}	85.1	81.1 {1}
Panicoids (total) =	1.9	1	1.8
Simple lobate	0.9	1	-
Panicoid type	0.5	-	0.9
Cross	0.5	-	0.9
Arundinoids	-	-	-
Aristida-type	0.5	3	1.8
*(41PT185/C short cell features) {number of charred phytoliths}			

This page intentionally left blank.

APPENDIX E

**CHERT SOURCING IN THE TEXAS PANHANDLE:
COMPOSITIONAL ANALYSES OF CHERT AND JASPER
SOURCES AND ARTIFACTS, LANDIS PROPERTY PROJECT**

This page intentionally left blank.

**CHERT SOURCING IN THE TEXAS PANHANDLE: COMPOSITIONAL
ANALYSES OF CHERT AND JASPER SOURCES AND ARTIFACTS,
LANDIS PROPERTY PROJECT**

Prepared for:



**TRC Environmental Corporation
505 East Huntland Drive, Suite 250
Austin, Texas 78752**

Prepared by:

**Matthew T. Boulanger and Michael D. Glascock
Archaeometry Laboratory,
University of Missouri Research Reactor
Columbia, MO 65211**

July 5, 2009

This page intentionally left blank.

E.1 INTRODUCTION

One-hundred and twenty-nine chert samples from Texas and New Mexico were submitted for compositional analysis by neutron activation. Analyses were conducted at the Archaeometry Laboratory at the University of Missouri Research Reactor (MURR). Samples analyzed in this study represent materials collected from chert and jasper sources in the Texas Panhandle and northeastern New Mexico (Table E-1 and Figure E-1) as well as chert and jasper artifacts from three archaeological sites in Potter County, Texas (Table E-2, Figures E-2). Samples were submitted by Mike Quigg, of TRC, Austin, Texas, as part of the Landis Property project (TRC Project 150832) in the Texas Panhandle.

Instrumental Neutron Activation Analyses (INAA) of Texas cherts, here used as a catch-all term for cryptocrystalline silicates such as flint, jasper, agate, etc., have been undertaken at MURR by multiple researchers since 1994 (Table E-3). In some instances (e.g., Frederick et al. 1994) these studies have resulted in meaningful discrimination among geological sources. Other studies have demonstrated that chemical variation within individual sources is too great to allow confident identification by INAA (e.g., Boulanger and Glascock 2008).

The primary goals of the current study are to determine whether sufficient chemical variation exists among different chert sources in the Texas Panhandle to allow confident association of artifacts with a particular geological source. Specifically, chert (more-properly an agatized dolomite) from the Quartermaster Formation and chert (colloquially referred to as a jasper) from the Tecovas Formation are compared. The two lithic materials have highly variable characteristics, some of which confound efforts to distinguish either material based solely on visual criteria. Chemical analysis

may be one means of confidently identifying the stone from which a particular artifact is made. This analysis also seeks to determine whether unique chemical “fingerprints” can be identified for specific prehistoric quarries or geological sources of these lithic materials, thereby allowing archaeologists to address questions relating to the procurement and distribution of lithic resources.

E.2 SAMPLE PREPARATION

Upon arrival at MURR, the source samples were washed in deionized water to remove all possible dirt and loose material from their surfaces. Samples for INAA were prepared by placing source specimens between two tool-steel plates and crushing them with a Carver Press. Several small 50–100 mg fragments were obtained from the crushed specimens. Fragments were examined under low-power magnification, and fragments with metallic streaks or crush fractures were eliminated from consideration. Several grams of the remaining fragments were obtained from each sample and temporarily stored in plastic bags.

Two analytical samples were prepared from each source specimen. Portions of approximately 200 mg of rock fragments were weighed into clean high-density polyethylene vials used for short irradiations at MURR. At the same time, 800 mg aliquots from each sample were weighed into clean high-purity quartz vials used for long irradiations. Individual sample weights were recorded to the nearest 0.01 mg using an analytical balance. Both vials were sealed prior to irradiation. Along with the unknown samples, standards made from National Institute of Standards and Technology (NIST) certified standard reference materials of SRM-1633a (Coal Fly Ash), SRM-278 (Obsidian Rock), and SRM-688 (Basalt Rock) were similarly prepared.

E.3 IRRADIATION AND GAMMA-RAY SPECTROSCOPY

Neutron activation analysis (NAA) of most archaeological samples at MURR, which consists of two irradiations and a total of three gamma counts, constitutes a superset of the procedures used at most other NAA laboratories (Glascock 1992; Glascock and Neff 2003; Neff 2000). As discussed in detail by Glascock (1992), a short irradiation is carried out through the pneumatic tube irradiation system. Samples in the polyvials are sequentially irradiated, two at a time, for five seconds by a neutron flux of $8 \times 10^{13} \text{ n cm}^{-2} \text{ s}^{-1}$. The 720-second count yields gamma spectra containing peaks for nine short-lived elements aluminum (Al), barium (Ba), calcium (Ca), dysprosium (Dy), potassium (K), manganese (Mn), sodium (Na), titanium (Ti), and vanadium (V).

The long-irradiation samples are encapsulated in quartz vials and are subjected to a 70-hour irradiation at a neutron flux of $5 \times 10^{13} \text{ n cm}^{-2} \text{ s}^{-1}$. This long irradiation is analogous to the single irradiation utilized at most other laboratories. After the long irradiation, samples decay for seven days, and then are counted for 1800 seconds (the "middle count") on a high-resolution germanium detector coupled to an automatic sample changer. The middle count yields determinations of seven medium half-life elements, namely arsenic (As), lanthanum (La), lutetium (Lu), neodymium (Nd), samarium (Sm), uranium (U), and ytterbium (Yb). After an additional three- or four-week decay, a final count of 8500 seconds is carried out on each sample. The latter measurement yields the following 17 long half-life elements: cerium (Ce), cobalt (Co), chromium (Cr), cesium (Cs), europium (Eu), iron (Fe), hafnium (Hf), nickel (Ni), rubidium (Rb), antimony (Sb), scandium (Sc), strontium (Sr), tantalum (Ta), terbium (Tb), thorium (Th), zinc (Zn), and zirconium (Zr).

The element concentration data from the three measurements are tabulated in parts per million using Microsoft® Office Excel. Descriptive data for archaeological samples are appended to the concentration spreadsheet. These data are also stored in a dBase/FoxPro database file useful for organizing, sorting, and extracting sample information. The combined descriptive, contextual, and compositional database for samples analyzed as part of this study is available upon request to the Archaeometry Laboratory.

E.4 INTERPRETING CHEMICAL DATA

Analyses at MURR described previously produce elemental concentration values for 32 elements in most analyzed samples. However, cryptocrystalline silicates do not always have sufficient quantities of these 32 elements to be detectable using the above procedures. Compositional data for the 129 samples were divided into subgroups reflecting each geological source location. Each of these subgroups was then assessed for missing elemental values. Any element missing in greater than 50% of the samples within each particular subgroup was eliminated from consideration in the statistical evaluation of these data. This process eliminated 14 elements from the database (Table E-4).

All subgroups were then re-combined, and statistical analyses were subsequently carried out on base-10 logarithms of concentrations on the remaining 18 elements. Use of log concentrations rather than raw data compensates for differences in magnitude between the major elements, such as sodium, and trace elements, such as the rare earth or lanthanide elements (REEs). Transformation to base-10 logarithms also yields a more normal distribution for many trace elements.

The interpretation of compositional data obtained from the analysis of archaeological materials is discussed in detail elsewhere (e.g., Baxter and Buck 2000; Bieber, et al. 1976; Bishop and Neff 1989; Glascock 1992; Harbottle 1976; Neff 2000) and will only be summarized here. The main goal of data analysis is to identify distinct homogeneous groups within the analytical database. Based on the provenance postulate of Weigand et al. (1977), different chemical groups may be assumed to represent geographically restricted sources. For lithic materials such as obsidian, basalt, and cryptocrystalline silicates (e.g., chert, flint, or jasper), raw material samples are frequently collected from known outcrops or secondary deposits and the compositional data obtained on the samples is used to define the source localities or boundaries. The locations of sources can also be inferred by comparing unknown specimens (i.e., ceramic artifacts) to knowns (i.e., clay samples) or by indirect methods such as the “criterion of abundance” (Bishop, et al. 1982) or by arguments based on geological and sedimentological characteristics (e.g., Steponaitis, et al. 1996). The ubiquity of ceramic raw materials usually makes it impossible to sample all potential “sources” intensively enough to create groups of knowns to which unknowns can be compared. Lithic sources tend to be more localized and compositionally homogeneous in the case of obsidian or compositionally heterogeneous as is the case for most cherts.

Compositional groups can be viewed as “centers of mass” in the compositional hyperspace described by the measured elemental data. Groups are characterized by the locations of their centroids and the unique relationships (i.e., correlations) between the elements. Decisions about whether to assign a specimen to a particular compositional group are based on the overall probability that the measured concentrations for the specimen could have been obtained from that group.

Initial hypotheses about source-related subgroups in the compositional data can be derived from non-compositional information (e.g., archaeological context, decorative attributes, etc.) or from application of various pattern-recognition techniques to the multivariate chemical data. Some of the pattern recognition techniques that have been used to investigate archaeological data sets are cluster analysis (CA), principal components analysis (PCA), and discriminant analysis (DA). Each of the techniques has its own advantages and disadvantages which may depend upon the types and quantity of data available for interpretation.

The variables (measured elements) in archaeological and geological data sets are often correlated and frequently large in number. This makes handling and interpreting patterns within the data difficult. Therefore, it is often useful to transform the original variables into a smaller set of uncorrelated variables in order to make data interpretation easier. Of the above-mentioned pattern recognition techniques, PCA is a technique that transforms from the data from the original correlated variables into uncorrelated variables most easily.

Principal components analysis creates a new set of reference axes arranged in decreasing order of variance subsumed. The individual PCs are linear combinations of the original variables. The data can be displayed on combinations of the new axes, just as they can be displayed on the original elemental concentration axes. PCA can be used in a pure pattern-recognition mode, i.e., to search for subgroups in an undifferentiated data set, or in a more evaluative mode, i.e., to assess the coherence of hypothetical groups suggested by other criteria. Generally, compositional differences between specimens can be expected to be larger for specimens in different groups than for specimens in the same group, and this implies that groups should be detectable as

distinct areas of high point density on plots of the first few components.

Principal components analysis of chemical data is scale dependent, and analyses tend to be dominated by those elements or isotopes for which the concentrations are relatively large. As a result, standardization methods are common to most statistical packages. A common approach is to transform the data into logarithms (e.g., base 10). As an initial step in the PCA of most chemical data at MURR, the data are transformed into log concentrations to equalize the differences in variance between the major elements such as Al, Ca and Fe, on one hand and trace elements, such as the rare-earth elements (REEs), on the other hand. An additional advantage of the transformation is that it appears to produce more nearly normal distributions for the trace elements.

One frequently exploited strength of PCA, discussed by Baxter (1992), Baxter and Buck (2000), and Neff (1994; 2002), is that it can be applied as a simultaneous R- and Q-mode technique, with both variables (elements) and objects (individual analyzed samples) displayed on the same set of principal component reference axes. A plot using the first two principal components as axes is usually the best possible two-dimensional representation of the correlation or variance-covariance structure within the data set. Small angles between the vectors from the origin to variable coordinates indicate strong positive correlation; angles at 90 degrees indicate no correlation; and angles close to 180 degrees indicate strong negative correlation. Likewise, a plot of sample coordinates on these same axes will be the best two-dimensional representation of Euclidean relations among the samples in log-concentration space (if the PCA was based on the variance-covariance matrix) or standardized log-concentration space (if the PCA was based on the correlation matrix). Displaying both objects and variables on the same plot makes it possible to observe the contributions of specific elements to group

separation and to the distinctive shapes of the various groups. Such a plot is commonly referred to as a “biplot” in reference to the simultaneous plotting of objects and variables. The variable interrelationships inferred from a biplot can be verified directly by inspecting bivariate elemental concentration plots.

Whether a group can be discriminated easily from other groups can be evaluated visually in two dimensions or statistically in multiple dimensions. A metric known as the Mahalanobis distance (or generalized distance) makes it possible to describe the separation between groups or between individual samples and groups on multiple dimensions. The Mahalanobis distance of a specimen from a group centroid (Bieber, et al. 1976; Bishop and Neff 1989) is defined by:

$$D_{y,x}^2 = [y - \bar{X}]' I_x [y - \bar{X}]$$

where y is the $1 \times m$ array of logged elemental concentrations for the specimen of interest, X is the $n \times m$ data matrix of logged concentrations for the group to which the point is being compared with \bar{X} being it $1 \times m$ centroid, and I_x is the inverse of the $m \times m$ variance-covariance matrix of group X . Because Mahalanobis distance takes into account variances and covariances in the multivariate group it is analogous to expressing distance from a univariate mean in standard deviation units. Like standard deviation units, Mahalanobis distances can be converted into probabilities of group membership for individual specimens. For relatively small sample sizes, it is appropriate to base probabilities on Hotelling's T^2 , which is the multivariate extension of the univariate Student's t .

When group sizes are small, Mahalanobis distance-based probabilities can fluctuate dramatically depending upon whether or not each specimen is assumed to be a member of the group to which it is being compared.

Harbottle (1976) calls this phenomenon “stretchability” in reference to the tendency of an included specimen to stretch the group in the direction of its own location in elemental concentration space. This problem can be circumvented by cross-validation, that is, by removing each specimen from its presumed group before calculating its own probability of membership (Baxter 1994; Leese and Main 1994). This is a conservative approach to group evaluation that may sometimes exclude true group members.

Small sample and group sizes place further constraints on the use of Mahalanobis distance: with more elements than samples, the group variance-covariance matrix is singular thus rendering calculation of I_x (and D^2 itself) impossible. Therefore, the dimensionality of the groups must somehow be reduced. One approach would be to eliminate elements considered irrelevant or redundant. The problem with this approach is that the investigator’s preconceptions about which elements should be discriminate may not be valid. It also squanders the main advantage of multielement analysis, namely the capability to measure a large number of elements. An alternative approach is to calculate Mahalanobis distances with the scores on principal components extracted from the variance-covariance or correlation matrix for the complete data set. This approach entails only the assumption, entirely reasonable in light of the above discussion of PCA, that most group-separating differences should be visible on the first several PCs. Unless a data set is extremely complex, containing numerous distinct groups, using enough components to subsume at least 90 percent of the total variance in the data can be generally assumed to yield Mahalanobis distances that approximate Mahalanobis distances in full elemental concentration space.

Lastly, Mahalanobis distance calculations are also quite useful for handling missing

data (Sayre 1975). When many specimens are analyzed for a large number of elements, it is almost certain that a few element concentrations will be missed for some of the specimens. This occurs most frequently when the concentration for an element is near the detection limit. Rather than eliminate the specimen or the element from consideration, it is possible to substitute a missing value by replacing it with a value that minimizes the Mahalanobis distance for the specimen from the group centroid. Thus, those few specimens which are missing a single concentration value can still be used in group calculations.

E.5 RESULTS AND DISCUSSION

As stated above, the NAA results were entered into a spreadsheet and combined with the provided descriptive data to create a database for sorting and extraction of quarry subgroups. These data are provided in Appendix E-1.

An RQ-mode principal components analysis (PCA) with variance-covariance matrix reveals that greater than 90% of the cumulative variance in the dataset is explained by 10 principal components (Table E-5). The first three eigenvectors are most-heavily loaded by transition metals—specifically Mn and Fe. Biplots of PC scores show a high degree of overlap between all of the chert sources in the Texas Panhandle database (Figures E-3 and E-4). Failure to separate individual sources or specific geological formations in PC space reflects general compositional similarities among all of the sources. However, the relatively large number of elements excluded from this analysis ($N = 14$) and the relatively small number of samples representing individual sources (min. = 1; max. = 13) are factors that likely bias these results.

It is not surprising that most of the Quartermaster cherts are chemically similar,

particularly when it is considered that most of the samples are derived from two geographically close sources in Potter County. What is surprising is that the various sources of Tecovas jasper appear to have highly variable compositions, despite some of them being separated by distances of more than 60 miles. Despite general chemical similarities of the jasper samples, samples from Randall County are enriched in Mn such that they can be easily distinguished from other jasper sources. Similarly, the two chert samples from the Dockum Group of northeastern New Mexico are distinguished from chert/dolomite of the Quartermaster Formation.

Given that only slight differences in chemistry exist among specific sources, canonical discriminant analysis (CDA) was conducted on the source samples grouped according to geological formation of origin. Scores from the resulting CDA matrix produce clear separation between the Quartermaster chert/dolomite samples and the Tecovas jasper sources. Elements La, Sb, Ce, Na, and Co are responsible for the greatest differences between these two source materials in CDA space (Figure E-5). When artifact samples are projected in a biplot of CD scores for the Tecovas jasper and Quartermaster chert/dolomite, most artifacts visually classified as chert/dolomite from the Quartermaster Formation appear to be compositionally similar to source samples from that formation (Figure E-6). There is less agreement between the visual and chemical classifications of suspected Tecovas jasper artifacts (Figure E-7). Figure E-8 shows artifacts that were not visually classified.

A second CDA on individual quarries represented in the database met with mixed success. Based on the highly similar compositions of samples from 41PT1 and the unnamed Potter County source, and the geographical proximity of these two sources, we opted to consolidate them into a single Potter County source group. Biplots of the

resulting CD scores fail to fully distinguish most of the sources from each other, with the exceptions of the Randall County jasper source and the chert source in Baldy Hill, NM. Randall County jaspers appear to be enriched in Na, whereas Baldy Hill cherts appear enriched in Th and Sm. As with the previous CDA, there appears to be some separation between Quartermaster chert and Tecovas jasper. Quartermaster cherts, in general, are La, Co, and U. Tecovas jaspers are enriched in Sb, Na, Ce, Ba, and Eu. However, samples from Roberts County appear to split into both the chert and jasper portions of the biplots (Figure E-9). Given the overlap of most individual sources in CD space, resolving artifact “source” appears restricted to designating a general provenance to Potter County Alibates, Tecovas Jasper, Baldy Hill, and Randall County jasper. As with the previous CDA, visual characterization is in general agreement with chemical characterization (Figures E-10, E-11, and E-12).

The overall low number of samples representing each quarry prevents us from calculating artifact probabilities of membership within specific quarry compositional groups. Further, given the current sample database, we do not believe that sufficient elemental variation exists among specific quarries to result in meaningful artifact assignments. However, we are able to demonstrate that Quartermaster chert/dolomite is chemically distinct from Tecovas formation jasper. As such, when source samples are grouped according to geological formation and canonical discriminant scores are used as the distance metric, probabilities of membership in these compositional groups may be calculated for artifacts (Table E-6). Care should be taken in interpreting these results given the chemical heterogeneity of individual sources. We recommend that as a general rule, samples with greater than 5 percent probability of belonging to a certain group be considered members of that group. Importantly, this is statistical argument.

Although decreasing the probability level necessary for considering a sample a valid group member would increase the number of assignments, but it would also increase the chances of incorrectly classifying individual specimens.

E.6 CONCLUSIONS

Analysis of a large sample of chert and jasper samples from the Texas Panhandle has demonstrated that meaningful chemical differences may exist among different geological formations. Jasper source samples obtained from Randall County, and chert samples obtained from Baldy Hill appear to be distinct from all other sources sampled in this study. Admittedly, only a handful of samples have been analyzed from these sources, so these findings must be considered preliminary. Importantly, we have demonstrated that source samples of the Alibates agatized dolomite/chert from the Quartermaster Formation can be distinguished from source samples of the Tecovas jasper using CDA. Projecting artifact samples into the CD space for the database suggests that visual classification of Quartermaster materials is in good agreement with chemical characterization. Visual classification of Tecovas jasper is in less agreement.

Given the chemical heterogeneity of source samples analyzed here and the number of elements that had to be eliminated because of low or no concentrations, sourcing studies may also be well served by comparative petrographic analyses of source samples. Our inability to refine these results to produce quarry-specific compositional groups is hampered by the relatively few samples analyzed from each source. Future studies of these sources should focus on obtaining at least 10 to 5 representative samples from each individual source. Enlarging the number of samples per quarry should allow refinement of these results, as well as a better understanding of the

compositional variability in these lithic materials.

E.7 ACKNOWLEDGEMENTS

Corinne Rosania and Chris Oswald were responsible for sample preparation and analysis of the chert samples by INAA, and we gratefully acknowledge their contributions to the completion of this project. Any errors in interpretation and text are the responsibility of the authors.

E.8 REFERENCES

- Baxter, M. J.
1992 Archaeological Uses of the Biplot—A Neglected Technique? In *Computer Applications and Quantitative Methods in Archaeology, 1991*, edited by G. Lock and J. Moffett, pp. 141-148. BAR International Series. Vol. S577. Tempvs Reparavm, Oxford.
- 1994 *Exploratory Multivariate Analysis in Archaeology*. Edinburgh University Press, Edinburgh.
- Baxter, M. J. and C. E. Buck
2000 Data Handling and Statistical Analysis. In *Modern Analytical Methods in Art and Archaeology*, edited by E. Ciliberto and G. Spoto, pp. 681-746. John Wiley and Sons, New York.
- Bieber, A. M. J., D. W. Brooks, G. Harbottle and E. V. Sayre
1976 Application of Multivariate Techniques to Analytical Data on Aegean Ceramics. *Archaeometry* 18:59-74.
- Bishop, R. L. and H. Neff
1989 Compositional Data Analysis in Archaeology. In *Archaeological Chemistry IV*, edited by R. O. Allen, pp. 576-586. Advances in

- Chemistry. vol. 220. American Chemical Society, Washington, D.C.
- Bishop, R. L., R. L. Rands and G. R. Holley
1982 Ceramic Compositional Analysis in Archaeological Perspective. *Advances in Archaeological Method and Theory* 5:275-330.
- Boulanger, M. T. and M. D. Glascock
2007 *Neutron Activation Analysis of Chert Artifacts from 41MS69 and of Geological Chert Samples from the Llano River Gravel, the Gorman Formation, and the Marble Falls Formation.* Archaeometry Laboratory, Missouri University Research Reactor. Submitted to Mike Quigg, TRC, Austin, TX.
- 2008 *Neutron Activation Analysis of Geological and Archaeological Chert Source Samples from the Callahan Divide, Jones, Nolan, and Taylor Counties, Texas.* Archaeometry Laboratory, Missouri University Research Reactor. Submitted to Karen Caffrey, Department of Anthropology, University of Texas at Austin.
- Frederick, C. D., M. D. Glascock, H. Neff and C. M. Stevenson
1994 *Evaluation of Chert Patination as a Dating Technique: A Case Study from Fort Hood, Texas.* Research Report No. 32, Archaeological Resource Management Series. United States Army, Fort Hood.
- Glascock, M. D.
1992 Characterization of Archaeological Ceramics at MURR by Neutron Activation Analysis and Multivariate Statistics. In *Chemical Characterization of Ceramic Pastes in Archaeology*, edited by H. Neff, pp. 11-26. Prehistory Press, Madison, WI.
- 2001 *Letter report dated May 10, 2001, summarizing INAA of 30 chert samples from Leon Creek, Bluff, Texas.* Archaeometry Laboratory, University of Missouri Research Reactor. Submitted to Dale Hudler, Texas Archaeological Research Laboratory.
- Glascock, M. D. and H. Neff
2003 Neutron Activation Analysis and Provenance Research in Archaeology. *Measurement Science and Technology* 14:1516-1526.
- Glascock, M. D. and R. J. Speakman
2006a *Instrumental Neutron Activation Analysis of Natural Chert from Gillespie County in Central Texas -- TRC Project 46843/0020.* Archaeometry Laboratory, University of Missouri Research Reactor. Submitted to Mike Quigg, TRC Companies, Inc., Austin, TX.
- 2006b *Instrumental Neutron Activation Analysis of Natural Chert from the Callahan Divide Area of North Central Texas -- TRC Project 49150.* Archaeometry Laboratory, University of Missouri Research Reactor. Submitted to Mike Quigg, TRC Companies, Inc., Austin, TX. In *Reconnaissance In Phase II East and Chert Collection Across Phase I and II East for FPL Energy's Horse Hollow Project, Taylor County, Texas*, by J. M. Quigg, M. Glascock, and R. J. Speakman. Technical Report No. 49150.
- 2008 Instrumental Neutron Activation Analysis of Chert from the Varga Site (41ED28) in Southwest Texas. In *The Varga Site: A Multicomponent, Stratified Campsite in the Canyonlands of Edwards County, Texas*, by J. M. Quigg, J. D. Owens, P. M. Matchen,

- G. D. Smith, R. A. Ricklis, M. C. Cody, and C. D. Frederick, Volume II:885-950. Texas Department of Transportation, Environmental Affairs Division, Archeological Studies Program Report No. 110 and TRC Technical Report No. 35319, Austin.
- Harbottle, G.
1976 Activation Analysis in Archaeology. *Radiochemistry* 3(1):33-72.
- Leese, M. N. and P. L. Main
1994 The Efficient Computation of Unbiased Mahalanobis Distances and their Interpretation in Archaeometry. *Archaeometry* 36:307-316.
- Neff, H.
1994 RQ-mode Principal Component Analysis of Ceramic Compositional Data. *Archaeometry* 36:115-130.
- 2000 Neutron Activation Analysis for Provenance Determination in Archaeology. In *Modern Analytical Methods in Art and Archaeology*, edited by E. Ciliberto and G. Spoto, pp. 81-134. John Wiley and Sons, New York.
- 2002 Quantitative Techniques for Analyzing Ceramic Compositional Data. In *Ceramic Source Determination in the Greater Southwest*, edited by D. M. Glowacki and H. Neff. Monograph 44. Cotsen Institute of Archaeology, Los Angeles.
- Sayre, E. V.
1975 *Brookhaven Procedures for Statistical Analyses of Multivariate Archaeometric Data*. Brookhaven National Laboratory Report BNL-23128.
- Steponaitis, V., M. J. Blackman and H. Neff
1996 Large-scale Compositional Patterns in the Chemical Composition of Mississippian Pottery. *American Antiquity* 61(3):555-572.
- Turnbow, C. A. and D. P. Staley
1995 *Cultural Resource Investigations of Three Lithic Procurement Sites (4IRG39, 4IRG40, and 41HW52) in Howard and Reagan Counties, Texas*. For Cap Rock Electric Cooperative, Inc., Stanton, Texas. MAI Project 1089, Mariah Associates, Inc., Albuquerque. Confidential.
- Weigand, P. C., G. Harbottle and E. V. Sayre
1977 Turquoise Sources and Source Analysis: Mesoamerica and the Southwestern U.S.A. In *Exchange Systems in Prehistory*, edited by T. K. Earle and J. E. Ericson, pp. 15-34. Academic Press, New York.

Table E-1. Analytical IDs (ANIDs), Provenience, Type, and Number of Chert and Jasper Source samples Analyzed in this study.

All assessments of the geological nature of material are made by M. Quigg

Quartermaster Formation Chert/Dolomite						
ANIDs	Site	Material	Formation	Location	Sample Type	No. Samples
TRC407–411, 448, 520–526	41PT1	Agatized Dolomite	Quartermaster	Potter Co., TX	Source	13
TRC438	Greenbelt	Day Creek Chert ?	Quartermaster	Donley Co., TX	Source	1
TRC390–393		Agatized Dolomite	Quartermaster	Roberts Co., TX	Source	4
TRC399–404, 441–442		Agatized Dolomite	Quartermaster	Potter Co., TX	Source	8
Tecovas Formation Jasper						
ANIDs	Site	Material	Formation	Location	Sample Type	No. Samples
TRC439–440	Blue Creek 1 & 3	Jasper	Tecovas	Moore Co., TX	Source	2
TRC510–514	41PT434	Jasper	Tecovas	Potter Co., TX	Source	5
TRC515–519	41OL284	Jasper	Tecovas	Oldham Co., TX	Source	5
TRC384–389, 487–490	41PT276	Jasper	Tecovas	Potter, Co., TX	Source	9
TRC394–398		Jasper	Tecovas	Briscoe Co., TX	Source	5
TRC444–447		Jasper	Tecovas	Randall Co., TX	Source	4
Other Chert Sources						
ANIDs	Site	Material	Formation	Location	Sample Type	No. Samples
TRC405–406	Baldy Hill	Chert	Dockum	Union Co., NM	Source	2

Table E-2. Analytical IDs (ANIDs), Provenience, Type, and Number of Chert and Jasper Artifacts Analyzed in this Study.

ANIDs	Site No.	Site Name	Location	No. Samples
TRC412–418, 449–471, 491–509	41PT185/C	Pipeline	Potter Co., TX	49
TRC419–423, 472–483	41PT186	Corral	Potter Co., TX	17
TRC424–428	41PT245	Pavilion	Potter Co., TX	5

Table E-3. Prior Studies of Texas Cherts Conducted by NAA at MURR.

Note that published reports for projects by Hudler (1998) could not be located at the time of this writing.

Investigator	Year	Formation or Chert Name	Location	Reference
C. Frederick	1994	Edwards	Fort Hood, TX	(Frederick, et al. 1994)
C. Turnbull	1994	Edwards/ Segovia	Howard County, TX	Turnbow and Staley 1995
D. Hudler	1998	Willis Gravels	De Witt County, TX	
D. Hudler	2001	Leon Creek	Bluff, TX	(Glascock 2001)
M. Quigg	2004	Edwards Fmt.	Southwest TX (multiple)	(Glascock and Speakman 2008)
M. Quigg	2006	Glen Rose	Gillespie County, TX	(Glascock and Speakman 2006a)
M. Quigg	2006	Edwards Fmt.	Taylor County, TX	(Glascock and Speakman 2006b)
M. Quigg	2007	Llano Riv. Gravel, Gorman Fmt., & Marble Falls Fmt.	Mason County, TX	(Boulanger and Glascock 2007)
K. Caffrey	2008	Edwards Fmt.	Callahan Divide, TX (multiple)	(Boulanger and Glascock 2008)

Table E-4. List of Elements in Chert Samples from the Texas Panhandle Found to be at or Below the Minimum Detectable Limits using Standard MURR Procedures.

These elements were removed from consideration

Quartermaster Chert/Dolomite														
	As	Lu	Yb	Cs	Ni	Rb	Ta	Zn	Al	Ca	Dy	K	Ti	V
41PT1		X			X							X	X	
Roberts Co.		X			X								X	
Potter Co.		X			X								X	
Greenbelt	X	X			X		X		X		X	X	X	
Tecovas Jasper														
	As	Lu	Yb	Cs	Ni	Rb	Ta	Zn	Al	Ca	Dy	K	Ti	V
41OL284		X		X	X	X						X	X	
41PT276		X			X								X	
41PT434					X								X	
Briscoe Co.					X									
Blue Creek		X		X	X		X				X		X	
Randall Co.		X			X		X		X	X	X	X	X	X
Other														
	As	Lu	Yb	Cs	Ni	Rb	Ta	Zn	Al	Ca	Dy	K	Ti	V
Baldy Hill		X	X		X			X			X		X	

Table E-5. RQ-Mode Principal Component Analysis with Variance-Covariance Matrix.

The first eight principal components are shown, representing greater than 90% cumulative variance within the dataset. Strong elemental loading scores on eigenvectors are shown in bold.

Principal Components								
	PC1	PC2	PC3	PC4	PC5	PC6	PC7	PC8
% Variance	34.63461	20.18220	13.55667	7.00662	5.99693	4.97551	3.53998	2.50200
Cum. % Var.	34.63461	54.81681	68.37348	75.38010	81.37703	86.35254	89.89251	92.39451
Eigenvectors								
Mn	0.48263	0.61678	0.10174	-0.06124	0.21039	-0.12939	0.39232	0.14787
Cr	0.30444	-0.31126	-0.15430	-0.02140	0.74736	-0.17515	-0.35016	-0.18661
Co	0.28206	0.16631	-0.07789	-0.23831	-0.07122	-0.42179	-0.09487	0.14838
Sb	0.25534	-0.04137	-0.43423	0.02125	-0.14448	0.04533	0.27647	-0.43832
Ce	0.24784	-0.00204	0.09863	0.25670	-0.05871	0.10014	-0.02223	0.01477
Fe	0.24570	-0.14924	-0.65560	-0.08341	-0.38195	-0.07345	-0.10227	0.15656
Sm	0.22868	0.03140	0.05127	0.31094	-0.07447	0.15469	-0.18032	-0.04145
U	0.22750	0.11009	-0.03171	0.37138	-0.02102	0.25915	-0.19727	-0.05318
Nd	0.21297	0.02381	0.09319	0.26264	-0.08068	0.16322	-0.17081	-0.00946
Ba	0.21007	0.05873	0.13239	-0.38016	-0.17693	0.46644	-0.19392	-0.17006
La	0.19483	-0.01944	0.15499	0.20833	-0.06206	0.08725	-0.13112	0.21104
Sr	0.19140	-0.04668	0.19360	-0.59085	-0.01765	0.25627	-0.12312	-0.13520
Tb	0.18034	-0.20945	0.33703	0.00932	-0.30359	-0.38714	-0.09489	-0.15285
Eu	0.17748	-0.21795	0.32414	0.01703	-0.25332	-0.37136	-0.06382	-0.11003
Hf	0.16591	-0.40334	0.13688	0.09710	0.06052	0.11019	0.63694	-0.25549
Th	0.15614	-0.35475	0.03891	-0.06605	0.02627	0.19538	0.17927	0.58869
Sc	0.12911	-0.25027	-0.01587	-0.05964	0.03257	0.01263	0.05028	0.39873
Na	0.08427	-0.09400	0.03426	-0.08584	0.11041	0.10179	0.05555	0.04206

Table E-6. Mahalanobis-Distance-Based Probabilities of Group Membership within the Quartermaster Formation or Tecovas Formation Compositional Groups.

Probabilities are derived from canonical discriminant scores calculated from a matrix derived from the Quartermaster, Tecovas, Day Creek, and Baldy Hill samples. Visual classification of the samples is also provided. Best group designation is made by evaluating both probability values, and using a cut-off of 1%.

Catalog	ANID	Quartermaster Formation	Tecovas Formation	Best Group	Visual Classification
195-001a	TRC412	74.26	0.07	Quartermaster	n/a
199-001a	TRC413	58.38	0	Quartermaster	n/a
209-001a	TRC414	12.96	0	Quartermaster	n/a
210-001-1a	TRC415	3.92	0.13	Quartermaster	n/a
214-001-1a	TRC416	2.06	0.16	Quartermaster	Tecovas
226-001a	TRC417	68.75	0.01	Quartermaster	n/a
255-001a	TRC418	80.97	0.01	Quartermaster	n/a
265-010a	TRC419	30.44	0.01	Quartermaster	n/a
*265-001a	TRC420	0.02	10.54	Tecovas	Tecovas
*284-001a	TRC421	10.82	5.72	Quartermaster	Tecovas
*288-001a	TRC422	0.22	38.51	Tecovas	n/a
*307-001a	TRC423	0	0.96	n/a	Tecovas
**347-001a	TRC424	1.13	1.83	n/a	Tecovas
**351-001	TRC425	0.13	10.42	Tecovas	n/a
**362-001a	TRC426	0.49	0	n/a	Tecovas
**363-010a	TRC427	0	0.54	n/a	n/a
**366-001a	TRC428	3.34	0	Quartermaster	Tecovas
346-010a	TRC449	32.69	0.29	Quartermaster	Quartermaster
347-010a	TRC450	95.22	0.03	Quartermaster	Quartermaster
962-010a	TRC451	0.07	27.51	Tecovas	Tecovas
522-010a	TRC452	69.95	0.12	Quartermaster	Quartermaster
545-001-1a	TRC453	90.49	0.01	Quartermaster	n/a
596-010a	TRC454	93.14	0	Quartermaster	Quartermaster
621-010a	TRC455	16.54	0.01	Quartermaster	Quartermaster
785-010a	TRC456	19.8	0.01	Quartermaster	Quartermaster
800-010a	TRC457	76.15	0.03	Quartermaster	Tecovas
802-010a	TRC458	89.1	0.01	Quartermaster	Tecovas
836-010a	TRC459	1.75	1.76	n/a	Quartermaster
916-010a	TRC460	3.26	39.28	Tecovas	Tecovas
928-010a	TRC461	33.42	0.02	Quartermaster	Quartermaster
942-010a	TRC462	0.17	5.76	Tecovas	n/a
1022-010a	TRC463	70.24	0.2	Quartermaster	Tecovas
1038-010a	TRC464	0	0.01	n/a	Tecovas
1085-011a	TRC465	91.78	0.06	Quartermaster	Quartermaster

Catalog	ANID	Quartermaster Formation	Tecovas Formation	Best Group	Visual Classification
1091-010a	TRC466	38.41	0.09	Quartermaster	Quartermaster
1132-010a	TRC467	95.85	0.01	Quartermaster	Quartermaster
1155-010a	TRC468	62.2	0.23	Quartermaster	Quartermaster
1206-010a	TRC469	0.02	24.08	Tecovas	Tecovas
1221-010a	TRC470	0.01	26.19	Tecovas	Tecovas
1269-010a	TRC471	65.85	0	Quartermaster	Quartermaster
461-001-1	TRC472	81.18	0	Quartermaster	Quartermaster
473-001-1a	TRC473	0.2	44.57	Tecovas	n/a
482-001-1	TRC474	83.02	0	Quartermaster	Quartermaster
498-001-1	TRC475	5.95	0.84	Quartermaster	Quartermaster
446-014a	TRC476	42.07	0.16	Quartermaster	Quartermaster
446-015a	TRC477	97.38	0	Quartermaster	Tecovas
446-016a	TRC478	84.66	0.05	Quartermaster	Quartermaster
446-017a	TRC479	80.67	0.12	Quartermaster	Tecovas
503-001a	TRC480	97.42	0.03	Quartermaster	Quartermaster
528-001	TRC481	12.12	1.11	Quartermaster	Quartermaster
533-001	TRC482	79.46	0.03	Quartermaster	Quartermaster
537-001-1	TRC483	88.29	0.02	Quartermaster	Tecovas
268-001-1a	TRC491	0	1.02	Tecovas	Tecovas
374-001-1a	TRC492	0.92	63.77	Tecovas	Quartermaster
400-001-1	TRC493	8.6	0.01	Quartermaster	n/a
533-001-1a	TRC494	82.95	0.02	Quartermaster	Quartermaster
593-001-1	TRC495	10.85	19.77	Tecovas	Quartermaster
781-001-1	TRC496	0	0.7	n/a	Tecovas
805-001-1	TRC497	1.39	12.63	Tecovas	n/a
802-001-1a	TRC498	6.49	0.07	Quartermaster	Tecovas
867-001-1a	TRC499	15.11	0	Quartermaster	Tecovas
878-001-1a	TRC500	0.02	0.95	n/a	n/a
953-001-1a	TRC501	91.15	0	Quartermaster	Tecovas
963-001-1	TRC502	15.25	0	Quartermaster	Tecovas
989-001-1a	TRC503	0	4.08	Tecovas	Tecovas
992-001-1a	TRC504	13.48	7.02	Quartermaster	Tecovas
1094-001-1	TRC505	0.02	47.58	Tecovas	Tecovas
1125-001-1a	TRC506	26.44	0	Quartermaster	Quartermaster
1193-001-1a	TRC507	0.2	0	n/a	n/a
1213-001-1a	TRC508	0	9.24	Tecovas	Tecovas
1321-001-1a	TRC509	0.08	17.28	Tecovas	Tecovas

* = site 41PT186; ** = 41PT245

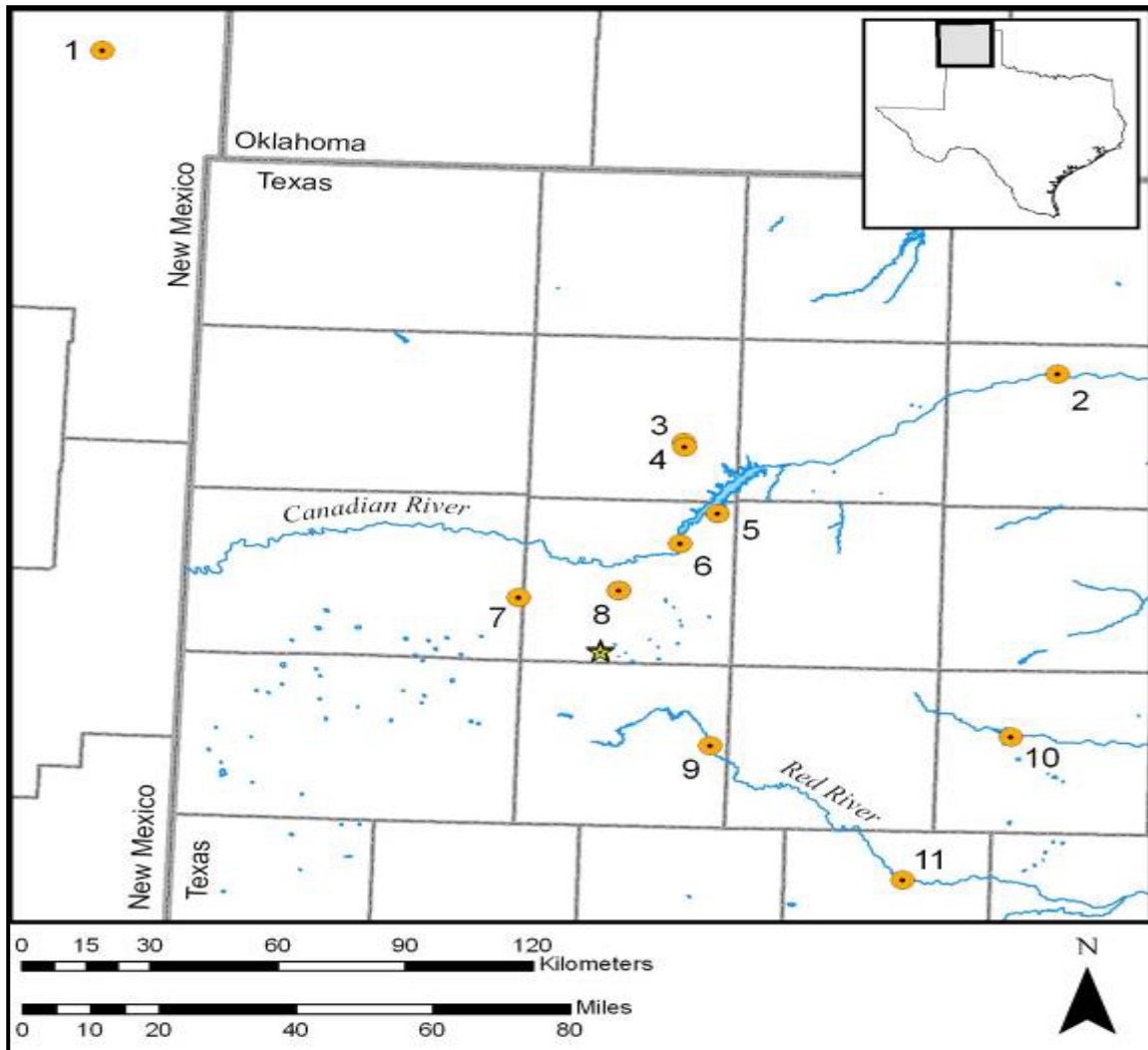


Figure E-1. Locations from which Archaeological and Geological Samples were Obtained for this Study.

Circles indicate geological (both primary and secondary depositional contexts) sources of chert and jasper. Star indicates location of three archaeological sites from which artifacts were sampled (see Figure 2). 1: Baldy Hill, NM; 2: Roberts Co., TX; 3: Blue Creek #1, Moore Co., TX; 4: Blue Creek #3, Moore Co., TX; 5: 41PT1 (Alibates Flint Quarry National Monument) and unnamed Potter Co. source; 6: 41PT434 (Coetas Creek Quarry); 7: 41OL284 (South Basin Quarry); 8: 41PT276; 9: Randall Co., TX; 10: Greenbelt, Donley Co., TX; 11: Briscoe Co., TX. Unnamed Tecovas Jasper source in Potter Co. is not shown. Sample locations provided by M. Quigg. Basemap data obtained from the Texas Natural Resources Information System (TNRIS).

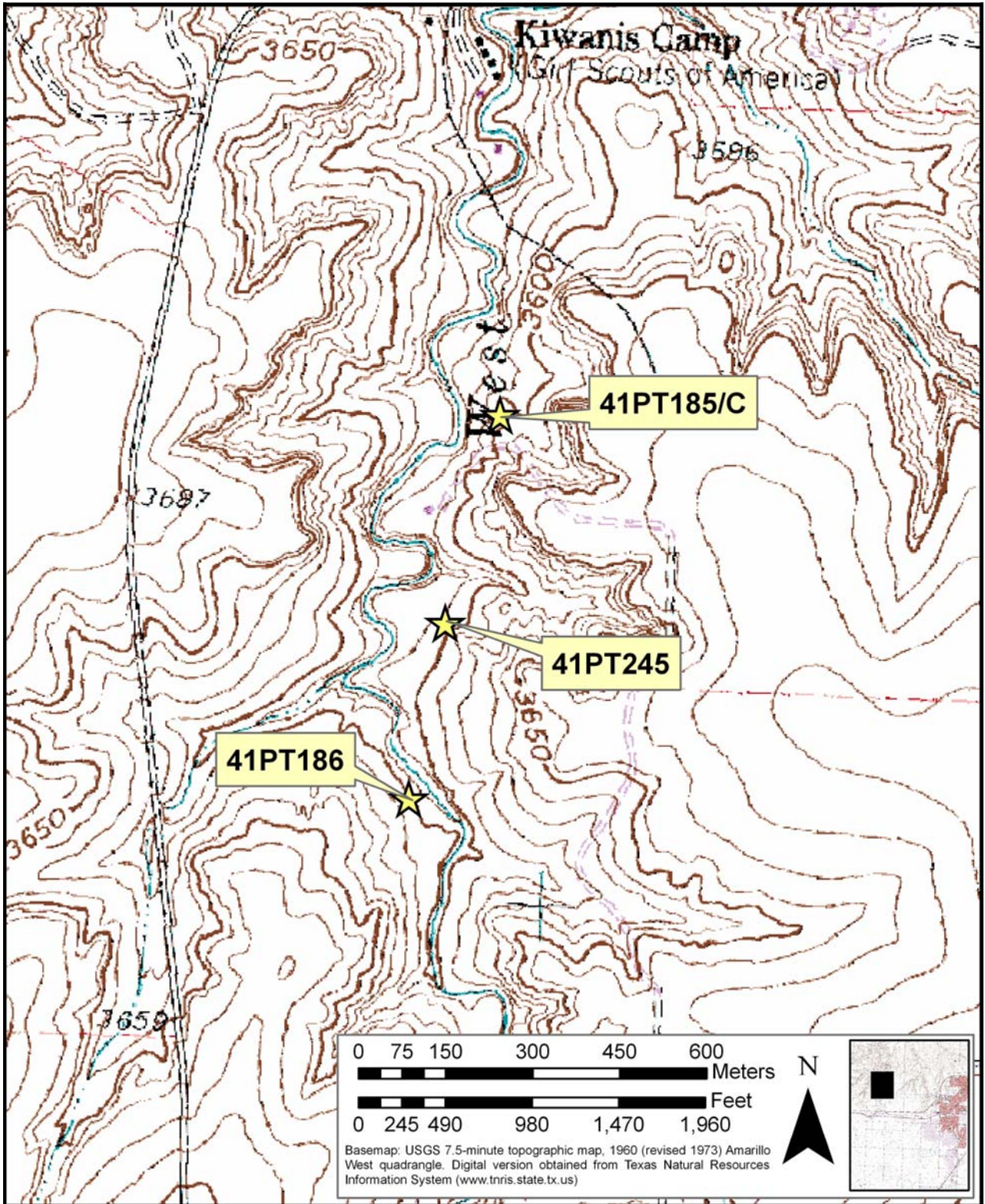


Figure E-2. Locations of Archeological Sites from which Chert and Jasper Samples were Obtained.

All sites are located in Potter County, Texas. Site locations provided by M. Quigg.

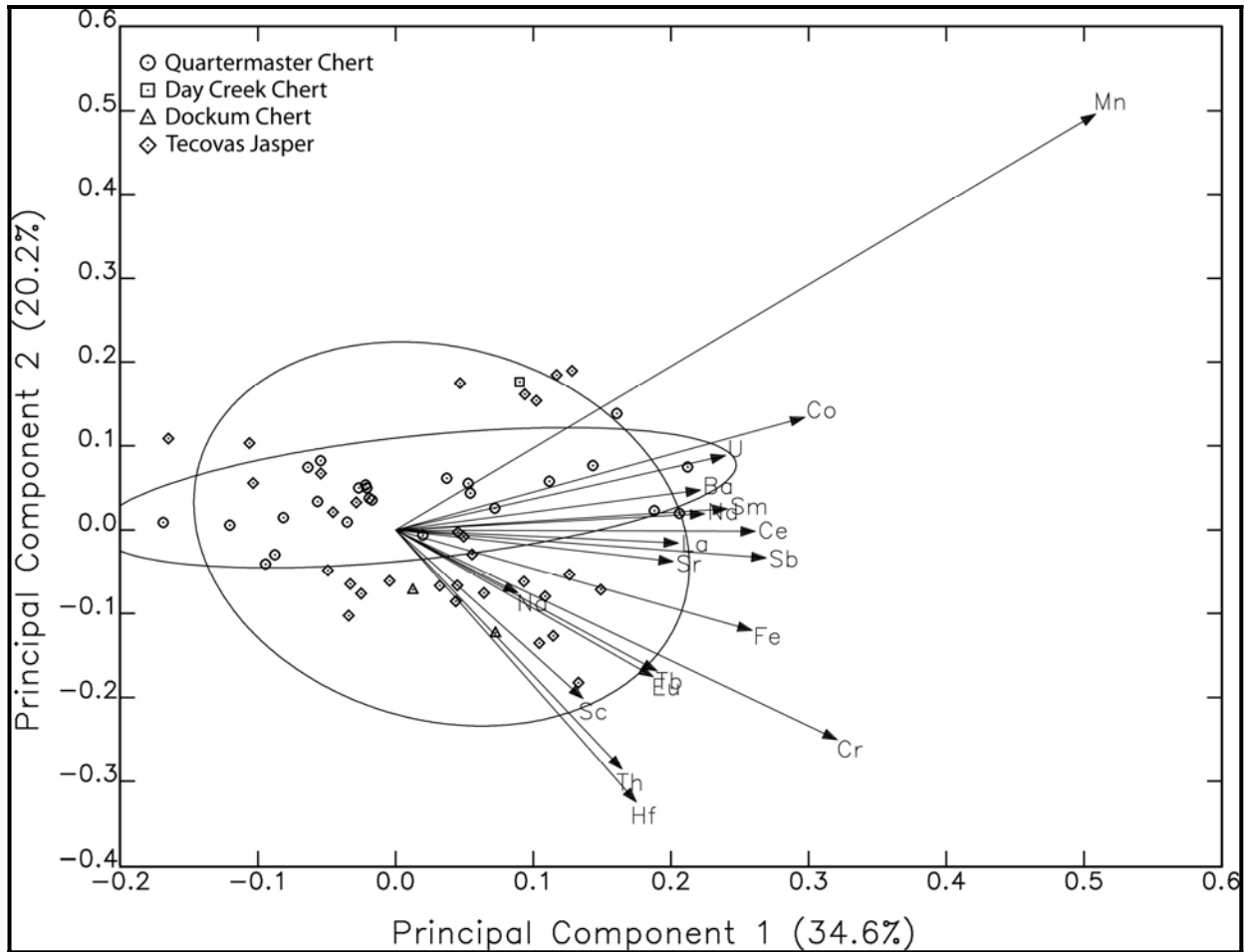


Figure E-3. Biplot of the First Two Principal Components for the Texas Panhandle Chert Dataset.

Source samples of Quartermaster chert/dolomite and Tecovas jasper are shown.
Ellipses represent 90% confidence interval of group membership.
Elemental-loading axes are shown and labeled.

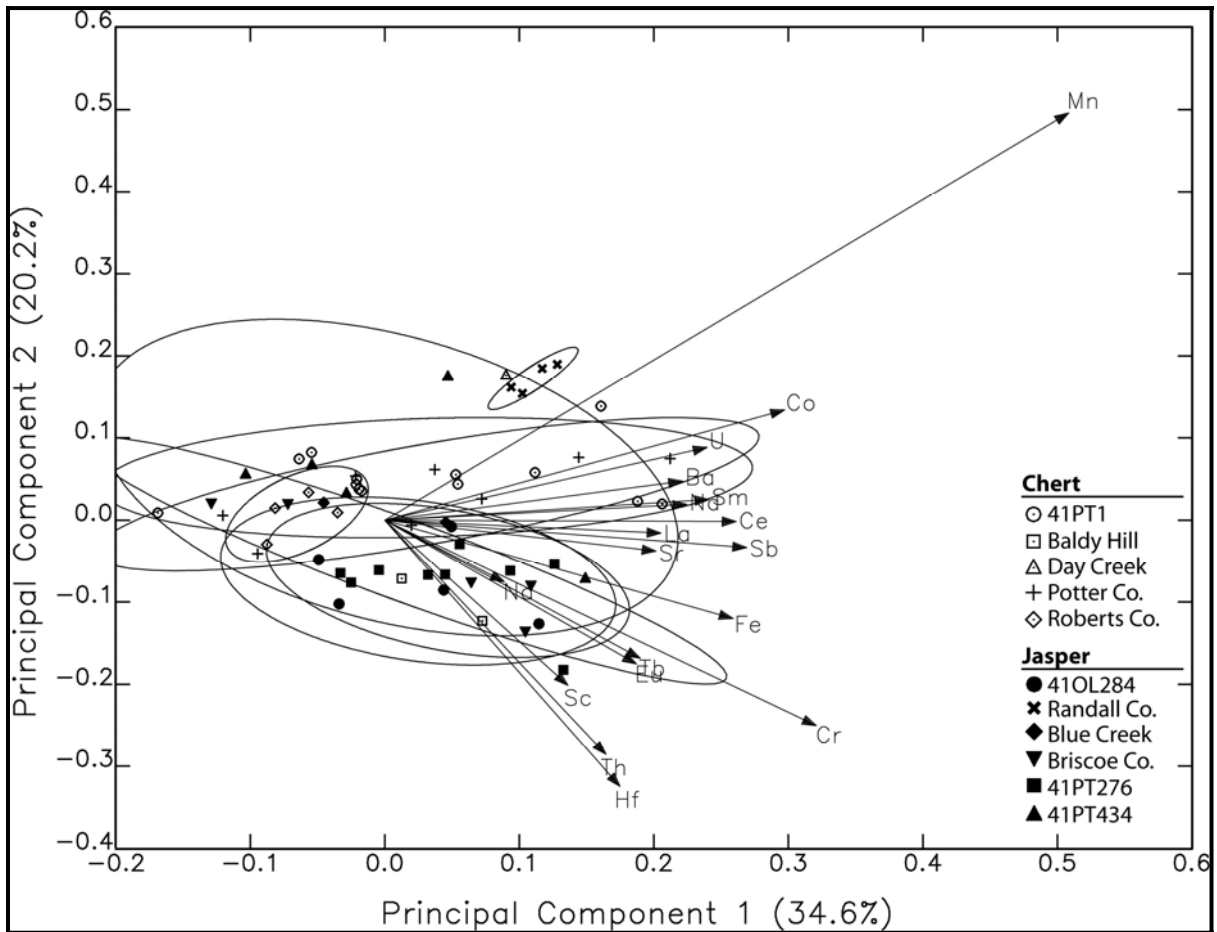


Figure E-4. Biplot of the First Two Principal Components for the Texas Panhandle Chert Dataset.

Source samples of Quartermaster chert/dolomite and Tecovas jasper are shown.
Ellipses represent 90% confidence interval of group membership.
Elemental-loading axes are shown and labeled.

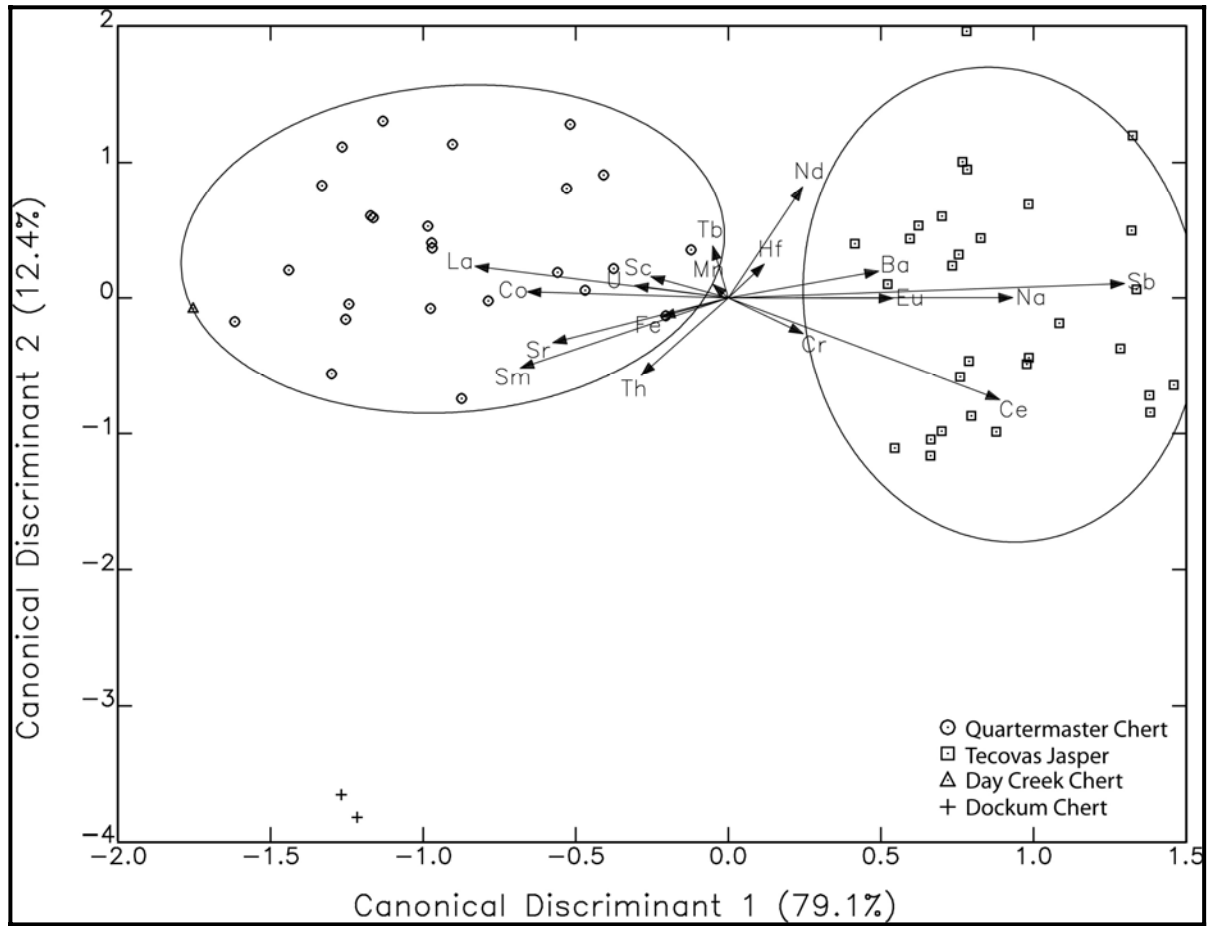


Figure E-5. Biplot of the First Canonical Discriminant Functions for the Texas Panhandle Chert Dataset.

Source samples of Quartermaster chert/dolomite and Tecovas jasper are shown.
Ellipses represent 90% confidence interval of group membership.
Elemental-loading axes are shown and labeled.

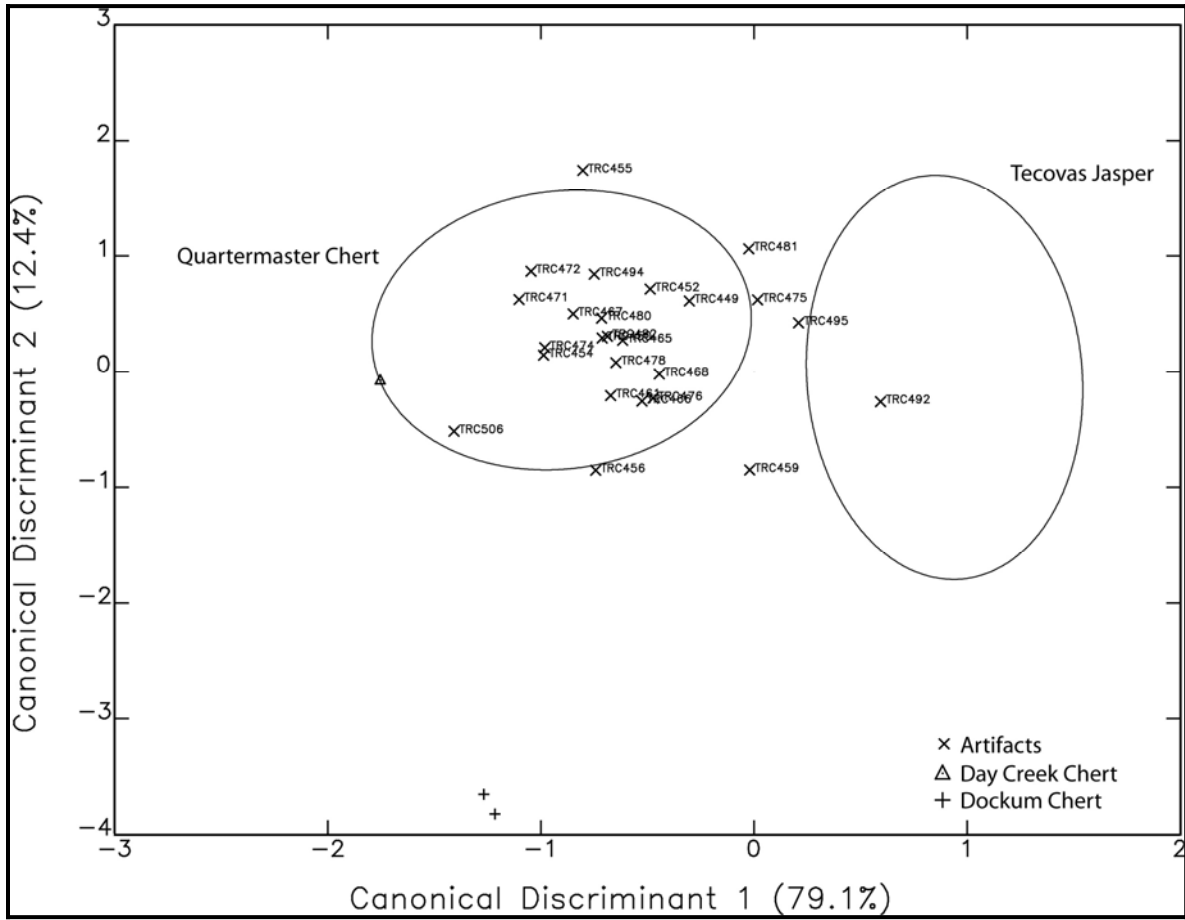


Figure E-6. Biplot of the first Canonical Discriminant Functions for the Texas Panhandle Chert Dataset.

Artifacts classified visually as Quartermaster chert/dolomite are projected against the 90% confidence ellipses of group membership for the Tecovas jasper and Quartermaster chert/dolomite source samples.

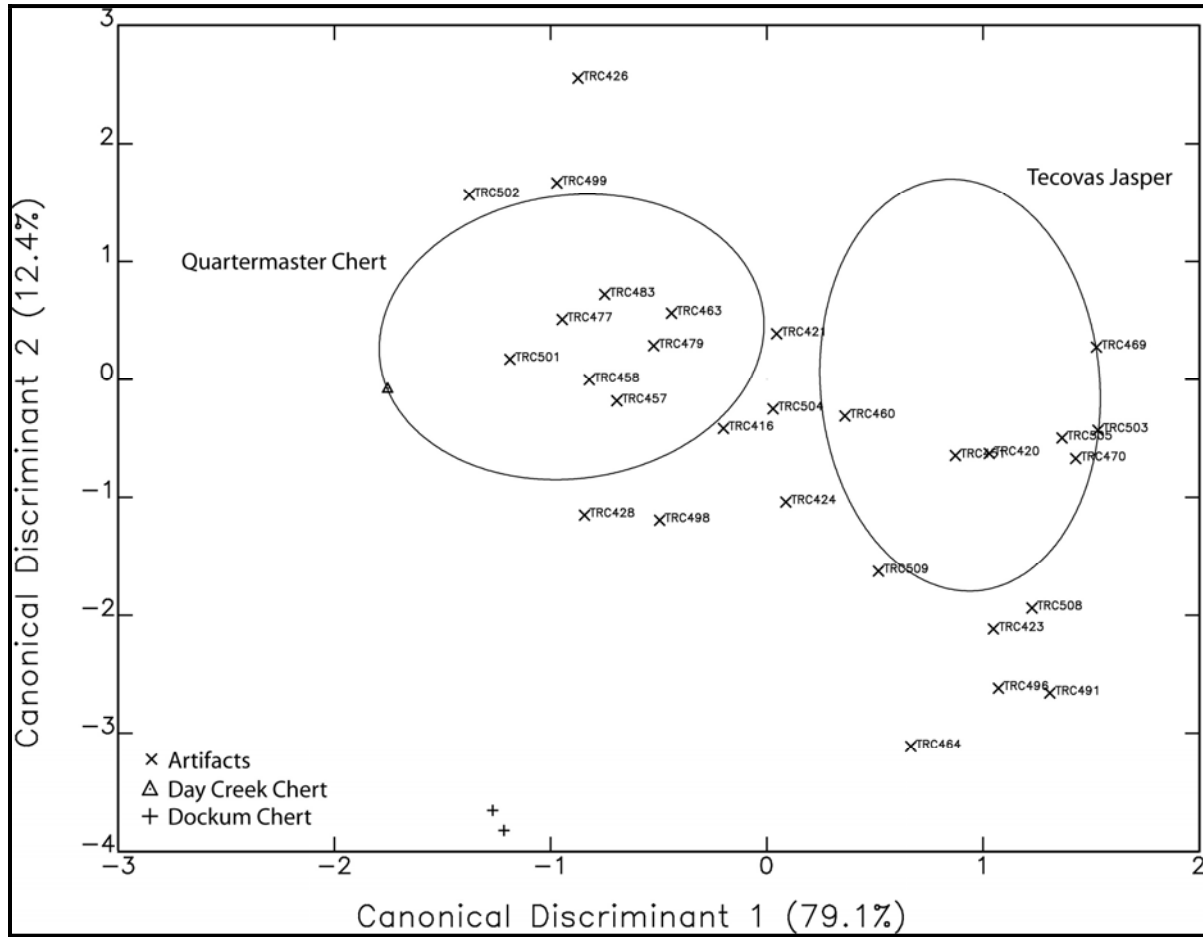


Figure E-7. Biplot of the First Canonical Discriminant Functions for the Texas Panhandle Chert Dataset.

Artifacts classified visually as Tecovas jasper are projected against the 90% confidence ellipses of group membership for the Tecovas jasper and Quartermaster chert/dolomite source samples.

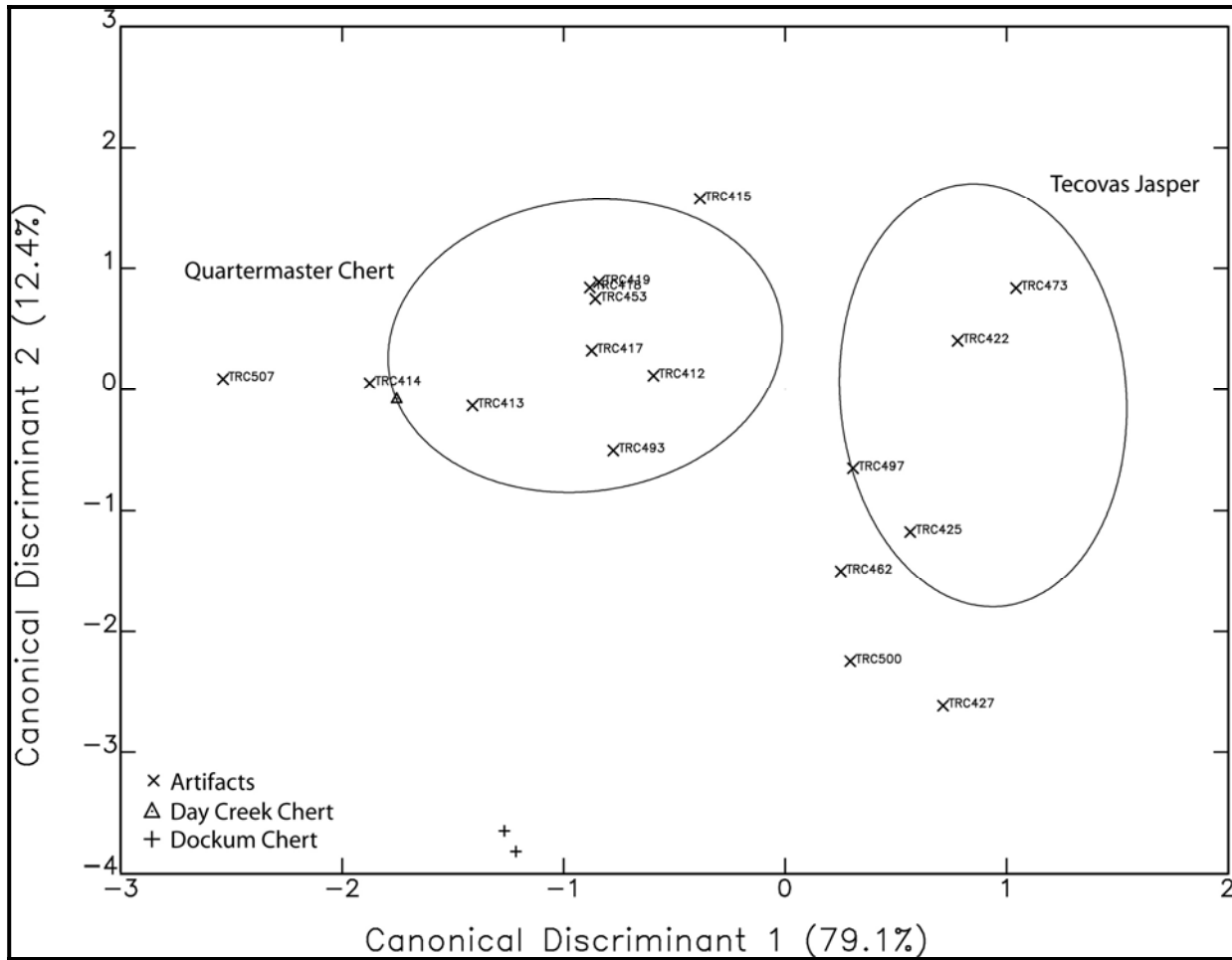


Figure E-8. Biplot of the first Canonical Discriminant Functions for the Texas Panhandle Chert Dataset.

Artifacts not given a visual classification are projected against the 90% confidence ellipses of group membership for the Tecovas jasper and Quartermaster chert/dolomite source samples.

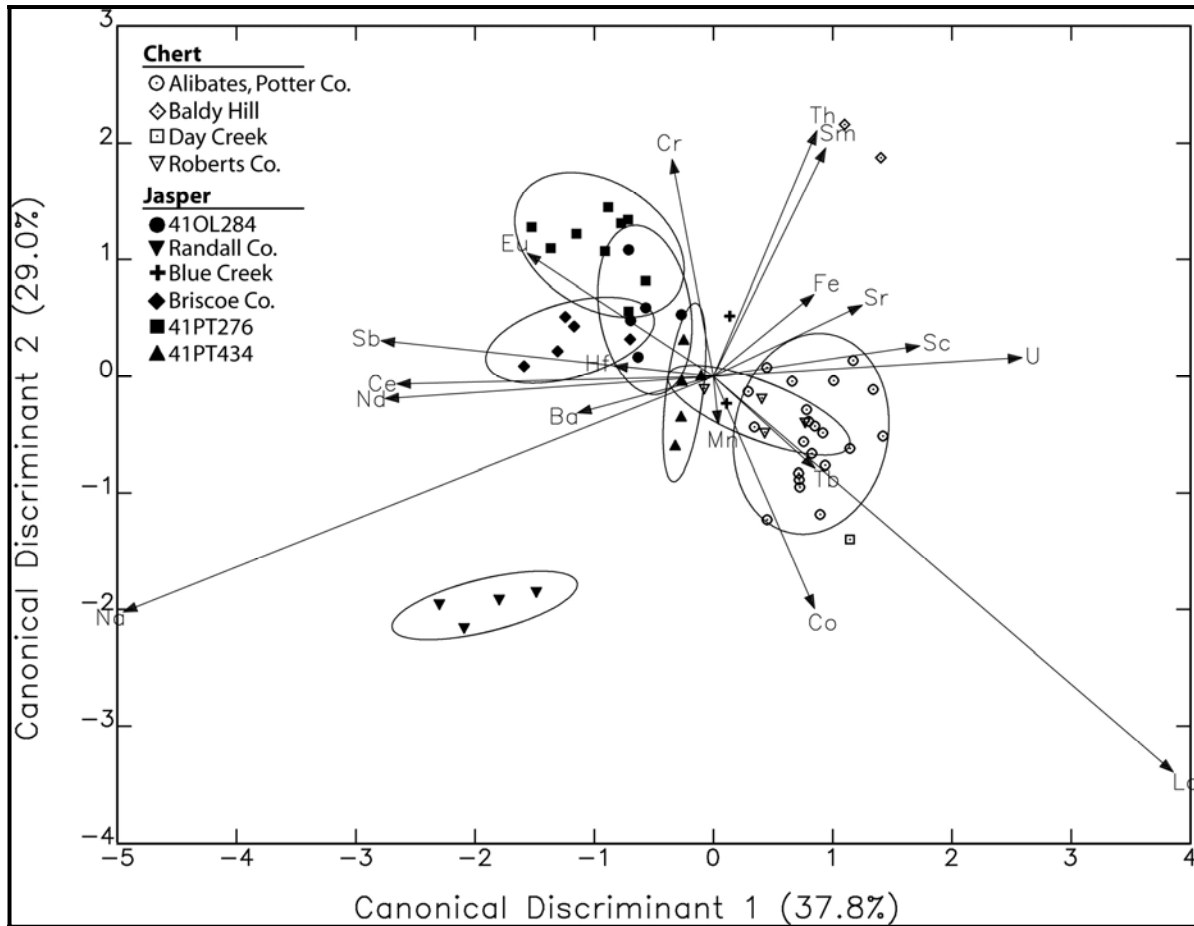


Figure E-9. Biplot of the First Two Canonical Discriminant Functions for the Texas Panhandle Chert Dataset.

All samples sources are shown with 90% confidence ellipses for membership. Elemental-loading axes are shown and labeled. Note that samples from 41PT1 and the unnamed Potter Co. chert source are combined to represent an Alibates source group. Also note that samples from Randall Co. and Baldy Hill are clearly separated from all other source samples.

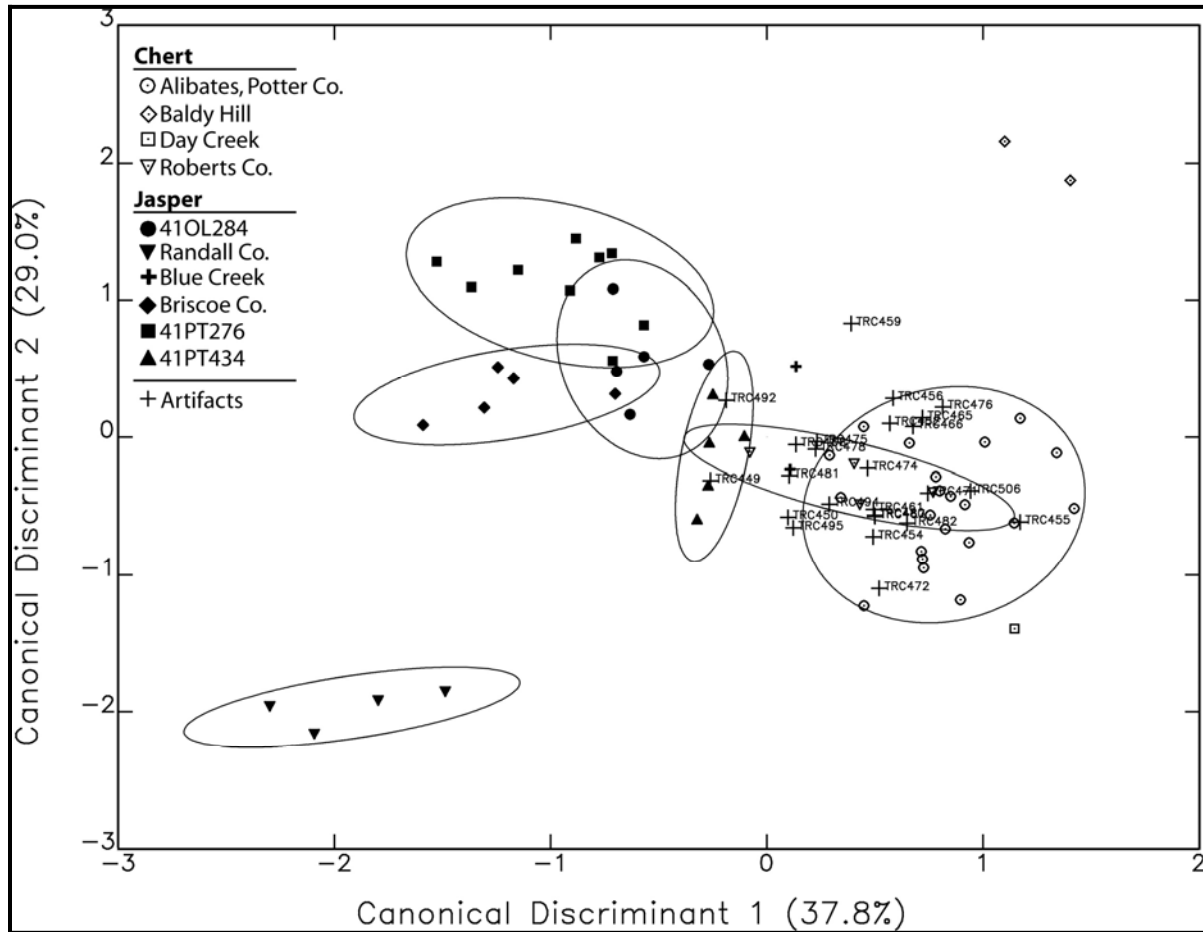


Figure E-10. Biplot of the First Two Canonical Discriminant Functions for the Texas Panhandle Chert Dataset.

Sources are shown with 90% confidence ellipses for membership. Artifacts classified visually as Quartermaster formation chert/dolomite are shown and labeled with ANIDs. Note that most samples cluster within or near the 90% confidence ellipse for the Alibates source group comprised of Potter Co. source samples.

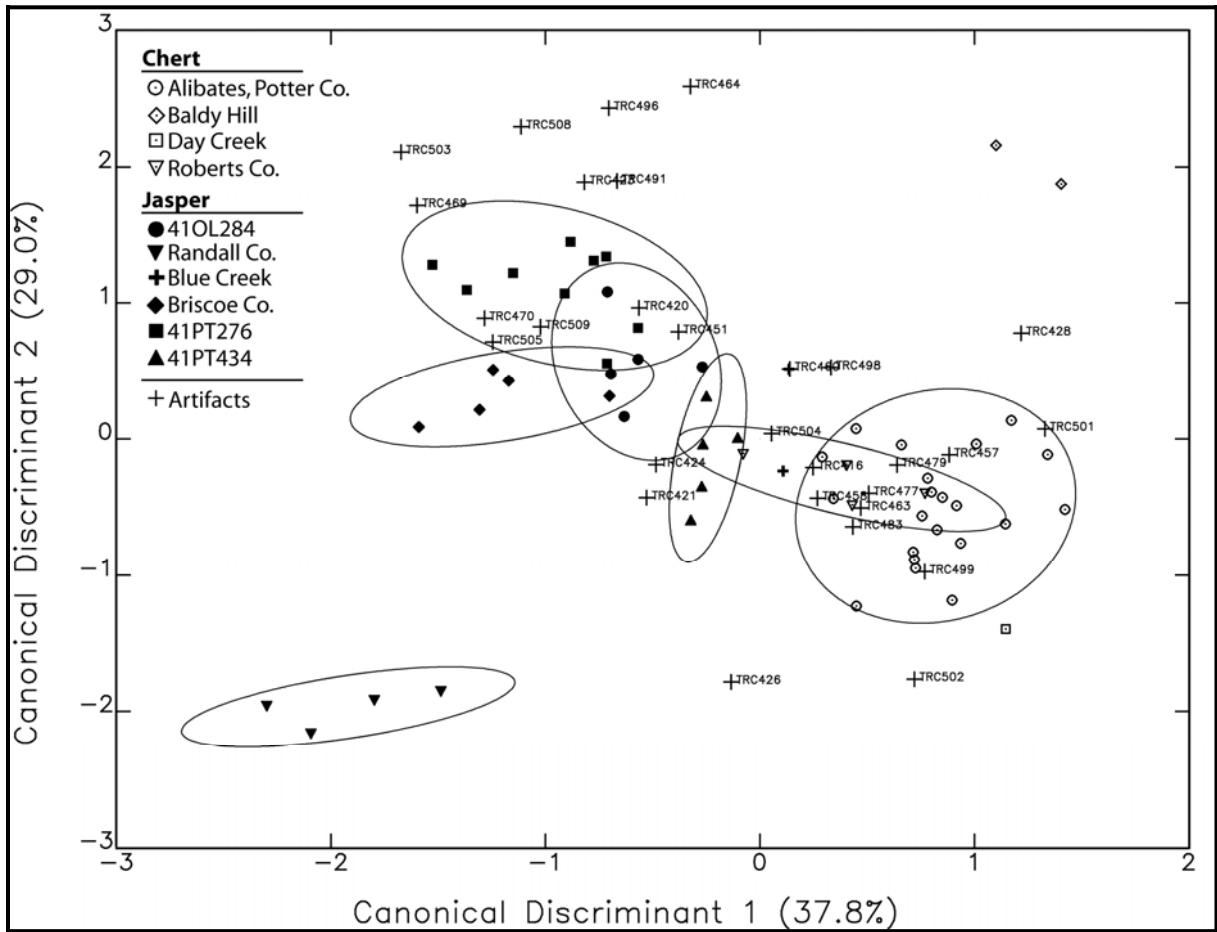


Figure E-11. Biplot of the First Two Canonical Discriminant Functions for the Texas Panhandle Chert Dataset.

Sources are shown with 90% confidence ellipses for membership. Artifacts classified visually as Tecovas jasper are shown and labeled with ANIDs. Note that most samples appear to either 41PT276 or to the Potter Co. Alibates sources.

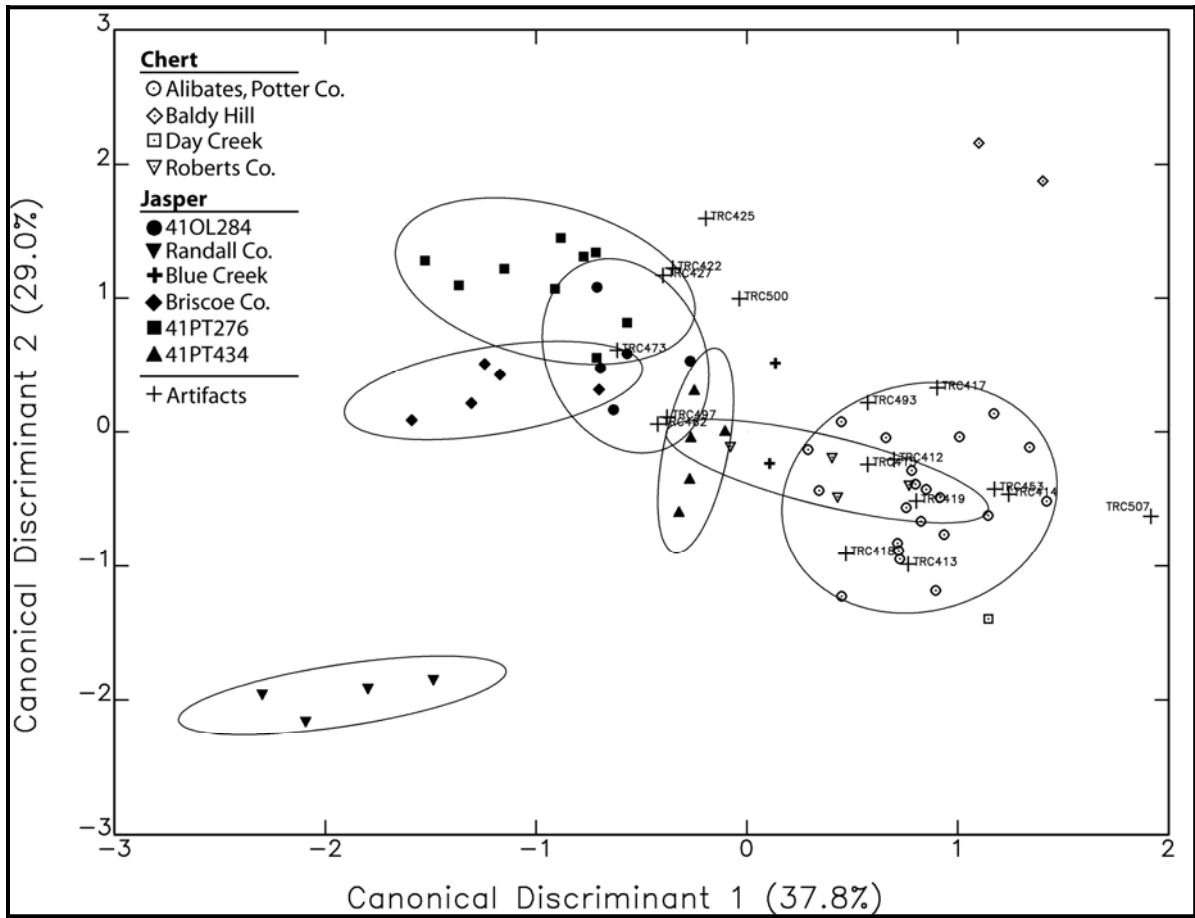


Figure E-12. Biplot of the First Two Canonical Discriminant Functions for the Texas Panhandle Chert Dataset.

Sources are shown with 90% confidence ellipses for membership. Artifacts not classified visually are shown and labeled with ANIDs. Note that most samples cluster within or near the 90% confidence ellipse for the Alibates source group comprised of Potter Co. source samples.

Attachment E-1
Compositional Data for Chert and Jasper Samples from the Texas
Panhandle

This page intentionally left blank.

APPENDIX F

STARCH ANALYSES FROM THE BLM LANDIS PROPERTY

This page intentionally left blank.

STARCH ANALYSES FROM THE BLM LANDIS PROPERTY

Prepared for:



**TRC Environmental Corporation
505 East Huntland Drive, Suite 250
Austin, Texas 78752**

Prepared by:

**Linda Perry, Ph.D.
Research Collaborator
Archaeobiology Program
Smithsonian National Museum of Natural History**

16 May 2009

This page intentionally left blank.

F.1 INTRODUCTION TO STARCH GRAIN ANALYSES

Archeobotanical investigators are constantly seeking new methods by which previously unobtainable data can be recovered. Among archeologists who work in regions characterized by the poor preservation of organic remains, the analyses of starch granules have proven particularly useful in accessing the residues of starchy root and tuber crops that have previously been invisible in the archeological record (Bryant 2003; Coil et al. 2003; Fullagar et al. 1998; Hall et al. 1989; Iriarté et al. 2004; Loy et al. 1992; Pearsall et al. 2004; Perry 2001, 2002a, 2004, 2005, 2007; Perry et al. 2006, 2007; Piperno and Holst 1998; Piperno et al. 2000). These residues have proven to be tenacious survivors in harsh climates, and their preservation on the surfaces of lithic tools that were used in the processing of starch-bearing plants occurs consistently in archeobotanical investigations (Iriarté et al. 2004; Pearsall et al. 2004; Perry 2001, 2002a, 2004, 2005, 2007; Perry et al. 2006, 2007; Piperno and Holst 1998; Piperno et al. 2000).

Investigations of the starchy remains of plant foods on the surfaces of archeological lithic tools began with simple analyses using chemical reagents that identified the residues in question as plant-derived storage starch (Bruier 1976) rather than animal tissue. Within the last fifteen years, however, archeologists have been successfully employing morphological criteria to identify plant taxa. The methods are almost identical to those used in the analysis of phytolith microfossils.

Just as different plants produce characteristically shaped leaves, flowers, and seeds, different genera and species make starch grains that are distinctive to and diagnostic for each taxon. The anatomical features that distinguish the starch of one species of plant from another have been noted by botanists (e.g., Denniston 1904;

MacMasters 1964; Reichert 1913), and their methods have been expanded by archeobotanists who are now able even to distinguish wild from domesticated species in some plant families (Iriarté et al. 2004; Pearsall et al. 2004; Perry 2001, 2002a, 2004; Piperno et al. 2000). Basic physical features that are comparable between modern reference specimens and archeological samples can be viewed using a light microscope and include gross morphological features such as shape and faceting, the location of and appearance of the hilum, and presence and patterning of lamellae (Iriarté et al. 2004; Loy 1994; Pearsall 2004; Perry 2004; Piperno and Holst 1998; Piperno et al. 2000). Fissuring and other internal patterning have also proven to be useful criteria for identification. The successful identification of starch granules relies upon the viewing of each granule in three dimensions to gain an accurate assessment of its morphological features.

Because starch granules differ morphologically between plants, their distinctive characteristics can often allow identification to the level of genus or species in archeological samples (e.g., Iriarté et al. 2004; Pearsall et al. 2004; Perry 2001, 2002a, 2004, 2005, 2006, 2007a, 2007b; Piperno and Holst 1998; Piperno et al. 2000). The method has proven particularly useful in identifying the remains of plant tissues that would not usually be preserved as macroremains, such as the remnants of root and tuber crops (Bryant 2003; Coil et al. 2003; Fullagar et al. 1998; Hall et al. 1989; Iriarté et al. 2004; Loy et al. 1992; Pearsall et al. 2004; Perry 2001, 2002a, 2004, 2005; Piperno and Holst 1998; Piperno et al. 2000). This role of starch analysis as a tool for revealing the significance of plant foods in the archeobotanical record also adds to our understanding of the pre-contact significance of starchy seed crops like maize (*Zea mays*).

In a citation of preliminary results from an ongoing study, the archeological remains of maize starch have been extracted from 2000 year old obsidian artifacts from the Honduran site of Copán (Haslam 2003, 2004). The starchy residues of maize were also successfully recovered and identified from a migmatite milling stone from Cueva de los Corrales 1 in Argentina (Babot and Apella 2003). In this case, the grinding stone was found to have multiple purposes, including the grinding of burnt bone, presumable for a non-food purpose. Starch analyses of ground stone artifacts from Real Alto have supported previously published phytolith studies that indicate the great antiquity of maize in Ecuador, and its role in subsistence during the Formative period (Pearsall et al. 2004). Seventeen examined artifacts from Real Alto yielded concentrations of maize starch granules ranging from one to more than ten granules per sampled tool. Other Neotropical studies have resulted in the recovery of more complex assemblages of starches.

Archeologists have recovered starch granules from maize, beans (*Phaseolus* sp.), and Canna from the Los Ajos mound complex in Uruguay (Iriarté et al. 2004). Maize starch granules were reported from three ground stone tools including one mano and two milling stone bases. Concentrations of maize starches ranged from two to eleven granules on tools from contexts dating from 3600 years before present (B.P.) to about 500 years B.P. (Iriarté et al. 2004: supplementary information). The starch data were combined with phytolith evidence and, together, these results introduce compelling evidence for the early development of a mixed subsistence economy in this region of South America. In other regions of the Neotropics, starch analysis has been an essential tool in defining similar subsistence patterns that included the exploitation of root and tuberous food plants.

Starch granules of maize, manioc (*Manihot esculenta*), both wild type and domesticated yams (*Dioscorea* spp.), and arrowroot (*Maranta arundinacea*) have been recovered from edge-ground cobbles and grinding stone bases collected from the Aguadulce rock shelter as well as the sites of Monagrillo, La Mula, and Cerro Juan Diaz in Panama (Piperno and Holst 1998; Piperno et al. 2000). Edge-ground cobbles are characterized by faceting that is hypothesized to have resulted from the processing of root crops against larger grinding stone bases (Ranere 1975), and the analyses of the residual remains of plant tissues supports this hypothesis. However, the use of the milling stones does appear to have been more complex than previously believed. Maize remains were recovered from all twelve artifacts that bore starch (Piperno et al. 2000). The numbers of starch granules of maize per artifact ranged from one to twenty-five per artifact. Two starch granules of arrowroot occurred on a single artifact, manioc starch granules were recovered from three artifacts (one, five, and eight granules), and yam starch granules were found on the surfaces of three of the artifacts (two, three, and sixteen granules) (Piperno et al. 2000). These investigations resulted in the recovery of the oldest evidence for root and tuber crop cultivation in the Neotropics, with radiocarbon dates spanning from 5000 to 7000 years B.P.

Starch granules of maize, yams, and arrowroot have also been recovered from twelve flake and three ground stone tools collected from Pozo Azul Norte 1 and Los Mangos del Parguaza in Venezuela (Perry 2001, 2002a, 2004, 2005). These sites date from the middle first century A.D. to contact. As in the above-cited set of studies, maize remains were recovered from every examined artifact and ranged in number from two to fifty-one per artifact. Additionally, four granules of yam starch were recovered from two flake tools, four flake tools yielded four granules of guapo (*Myrosma* sp.) starch, and seven starch

granules from arrowroot were collected from five tools, one of which was a ground stone artifact. These findings were significant in that five of the examined artifacts were chosen for study due to their hypothetical function as microlithic grater flakes from a manioc specific grater board. The evidence indicated a more complex function of these tools that did not include the processing of manioc.

More recent investigations have led to the recovery of direct evidence for contact between the highland Peruvian Andes and the lowland tropical forest to the east (Perry et al. 2006). This contact and interaction had been a significant component of Andean theory for decades, but direct evidence had been elusive until starch microfossils of arrowroot were collected from both sediment samples and lithic tools at the mid-elevation site of Waynuna (Perry et al. 2006). Further, the discovery and cataloging of a microfossil will allow for the recovery and understanding of the origins and subsequent dispersals of chili peppers (Perry et al. 2007), plants whose histories are poorly understood due to the lack of preservation of macroremains in the archeobotanical record. Remains of these plants have been successfully recovered throughout the Americas from ceramic sherds, lithic tools, and sediment samples dating from 6250 B.P. to European contact.

F.2 UNDERSTANDING THE RELATIONSHIP BETWEEN RESIDUES AND ARTIFACTS

Early work on starch remains from Panamanian sites used stepwise analysis to support the direct association between starchy residues on tools and the tools' use (Piperno et al. 2000). These studies demonstrated that starch grains were not present in sediments adhering to stone tools or on unused parts of the lithic tools, but they did occur in the cracks and crevices of the tools on used surfaces, thus indicating

that the residues were the result of the tools' use and not environmental contamination. Similar experiments have been undertaken independently by other researchers, and the results were equivalent.

In a study of obsidian artifacts recovered from an open air site in Papua New Guinea, the frequency of starch granules recovered from stone artifacts was compared to that present in the soil matrix immediate to the tool (Barton et al. 1998). The frequency of starch granules was found to be much higher on used artifacts than in the surrounding soil. Thus, the conclusion was drawn that the tools were not contaminated by environmental starch sources. Further, use-wear analyses were used in combination with the soil and starch analyses to assess the degree of association of starchy residues with the used surfaces of tools (Barton et al. 1998). The researchers found that, indeed, the occurrence of starch granules was highly correlated with obsidian tools that bore use-wear and was not correlated with unused tools.

In a study of starch residues occurring on stone pounding tools from the Jimmium site in north central Australia, the starch forms in soil samples were compared to those extracted from the artifacts (Atchison and Fullagar 1998). It was found that, although starch granules did occur in the soil matrices surrounding the tools, they were of different size and shape than those present on the pounding stones, and, therefore, are probably not from the same plant source. This result was interpreted as evidence that the tools had not been contaminated by soil-borne starches.

Another method for assessing whether or not starch residues are culturally deposited involves the analysis of control samples from non-cultural contexts surrounding a site. If different types of starches, or different concentrations of starches, or no plant residue whatsoever are recovered from the control samples than are recovered from

the artifacts undergoing testing, then one can be more secure that the residues are the remains of prehistoric food processing (Brieur 1976).

In addition to the study of association of microfossils with tool use, experimentation with processing methods has also been undertaken. In Argentina, a researcher replicated ancient Andean methods of food processing and found that each different process resulted in diagnostic damage to starch granules in plant tissues including potato tubers (*Solanum tuberosum*) and quinoa seeds (*Chenopodium* spp.) (Babot 2003). Modern plant materials were subjected to freeze-drying, dehydration, roasting, charring, desaponification (a process particular to the preparation of quinoa), and grinding. It was found that fragments of starches that would probably otherwise be identified as unknowns or non-starches are actually damaged starches. Further, with careful analysis, researchers can link damage patterns with processing techniques (Babot 2003). Experimentation with various cooking techniques has resulted in similar conclusions: cooked starches are identifiable as such, and different cooking techniques yield different patterns of damage (Henry et al. 2009).

Archeobotanists have focused their energies upon honing their methods toward the effective recovery of and identification of residual starch granules to understand plant use and processing. Studies have resulted in an impressive assemblage of various suites of starchy food plants, both wild and domesticated, raw and cooked. At this juncture in time, more studies are being undertaken and starch remains are being successfully recovered. What we now lack are baseline data as to how and why different plant materials may or may not adhere to stone tools. Thus, we are not yet able to understand issues such as intensity of use based upon numbers of recovered grains, or the history of a tool based upon the numbers of species of plants recovered

from its surface. Funding has been sought for experimentation to address these issues, but it has not yet been obtained.

F.3 STARCH ANALYSES AND TEXAS ARCHEOLOGY

Archeological investigations that include starch analyses allow researchers to access data that is otherwise unavailable to them, and to determine if models of subsistence ranging from simple artifact function to staple crop reliance are well founded. In the harsh climate of Texas where organic remains often preserve poorly, these techniques will prove invaluable to archeologists interested in understanding plant exploitation and subsistence strategies. Because every journey must begin with a first step, we have applied the techniques of starch analysis to burned rocks, both ground stone and flaked lithic tools, sediment samples, and ceramic sherds from the BLM Landis project.

The Landis Property lies in the Texas Panhandle just outside Amarillo, Texas. The region is part of the Southern Plains at the very northern end of the Llano Estacado in what is often referred to as the Canadian Breaks. The project area is centered on a 1.6 km long section of the upper reaches of West Amarillo Creek. This creek drains northward through the middle of this property into the Canadian River.

The data recovery occurred at three known archeological sites 41PT185 (Pipeline), 41PT186 (Corral), and 41PT245 (Pavilion). Site 41PT185 was divided into three Loci labeled A, B, and C with the data recovery only at Locus C, abbreviated as 41PT185/C.

The data recovery excavations at the Pipeline site (41PT185/C) targeted a Late Archaic component. Hand excavations in a large block yielded a diverse cultural assemblage that included 15 recognized cultural features (3 through 19), chipped

stone tools, ground stone tools, a faunal assemblage dominated by bison remains, a few bone tools, limited lithic debitage, sparse charcoal, and large quantities of burned rocks. These diverse classes indicate a broad range of daily tasks, which indicate generalized hunter-gatherer camp activities. Over a dozen radiocarbon dates document a period of occupation between ca. 1600 and 2400 B.P.

The data recovery at the Corral site (41PT186) targeted a deeply buried Protohistoric event in low alluvial terrace on the southern edge of the larger site through a large block investigation that totaled 144 m². This Protohistoric occupation, radiocarbon dated to ca. 200 to 300 B.P., represents a single, short-term camp with horizontally discrete activity areas and a sparse cultural assemblage. This event included two *in situ* hearths, an ash dump, a cluster of butchered bison bones, and a small cache of chipped stone tools. The horizontal pattern reflects the clear distribution of various tasks that included animal butchering/processing, stone tool resharpening, and cooking, and indicates a highly intact occupation surface. This assemblage reflects a very short-term camp (a few days at most) in which the Native American occupants resharpened a few chipped stone tools, cached a few important scrapers and flakes for the future, killed and butchered at least one deer and one bison, and employed at least two heating elements.

Data recovery at the Pavilion site (41PT245) targeted a ca. 1200 to 1400 B.P. occupation. Initial investigations across multiple terraces indicated multiple events of different ages, mostly less than 2000 years old. The planned block excavation was terminated early on as the occupation was not sufficiently well-defined to justify continued excavations. Notably, all three sites contained heating elements characterized by burned rock artifacts.

The role of burned rocks in archeological sites has been studied and debated for decades, and many scholars believe that these artifacts were used in food preparation (for a review, see Thomas 2009). It is hypothesized that rocks were heated in an open fire after which they were placed into containers filled with food in an aqueous medium. The heated rocks would then heat the food and cook it directly in the container. As in the cases discussed above, microfossil analysis, and starch grain analysis in particular, will allow us to examine microscopic residues from these artifacts. In theory, plant remains from the food being cooked in containers will adhere to the hot rocks, and these residues should be recoverable. Three main questions can be addressed using these analyses.

First, the presence of starchy residues on the burned rocks will allow us to determine if they have come into contact with starchy plant foods. With large enough assemblages of microfossils, taxa may be identifiable so that it can be determined which plants were being cooked. Second, the presence of damage in starch remains will provide a positive indicator of the cooking of starchy plant foods in an aqueous solution. Third, the patterning of starch remains from artifacts derived from different features will allow for an assessment of the type of feature being studied and its role in food processing at the site. These studies may also result in the definition of typical patterns of residues that can be associated with different feature types. Thus, starch grain analysis will allow us to test the hypothesis that these artifacts were used as cooking tools, they can reveal what plants were being cooked, and they will provide data that will delineate cooking features from those used for other purposes. Finally, the inclusion of other categories of artifacts such as ground stone tools will allow for comparison between starch assemblages.

F.4 METHODS:

The methods of starch grain analysis can be distilled down into a few simple tasks. These tasks include removing the archeological material from the artifact, placing it on a glass slide, and observing the residue using a light microscope. The analysis amounts to a careful cleaning of each artifact and examination of the material that was collected during cleaning. If the cleaning results in a relatively large quantity of sediment, the microfossils must be separated from the matrix so that they can be clearly viewed via microscopy. This step is completed with a heavy liquid flotation. Detailed methods are as follows.

Seventy-two (72) artifacts and sediment samples were chosen for analysis. Included in the sample were six lithic tools, three ceramic sherds, ten ground stone artifacts, forty-eight burned rocks from various types of features, three sediment samples, one burned rock collected from a non-cooking feature, and a modern experimental rock that was used in a cooking experiment (see Table F-1). In this experiment, the limestone rock was heated in an open fire and then used to boil cattail roots in water. All artifacts were collected and bagged separately without washing. Washing is a traditional step in the collection and curation of artifacts, but it will remove some of the residues that are of interest to archeologists.

All burned rocks were placed in clean glass beakers with the unbroken “used” side pointed toward the base of the vessel. Reverse-osmosis filtered water was added to the beaker just to cover the used surface leaving the broken surfaces exposed and, thus, not subject to extraction procedures. The rocks and beakers were then set aside for five minutes to soak in the hope that this step would loosen the microfossils and allow for a better extraction. At this point, the beakers were placed in a sonic bath for ten minutes to shake the microfossils loose from the artifacts. The rocks were removed from

the beakers and the surfaces that were cleaned were rinsed again with reverse-osmosis filtered water that was collected in the same effluent vessel.

Ground stone artifacts and flaked tools were treated in a slightly different manner. The ground stone artifacts were immersed completely, as were the flaked tools with no clear concentrations of starches. The exception was the corner tang knife, which had what appeared to be small groupings of starches on different edges. This tool was placed in a beaker with the edge of interest against the base of the vessel. The water was then added until only this edge was immersed, and then the procedure continued as described above. In this manner, a section of a tool, or multiple areas, can be sampled separately from the remainder of the artifact.

The effluent from the cleaning was allowed to settle overnight, then the settled material was centrifuged for ten minutes at 1000 RPM to pellet out the solids. The solid materials were then subject to a heavy liquid flotation using Cesium chloride (CsCl) at a density of 1.8 g/cm³ to separate the starch grains from the sediment matrix.

The material collected from the flotation was rinsed and centrifuged three times with reverse-osmosis filtered water to ensure that the CsCl was completely removed from the solution. At this point, the pellet from the final centrifugation was placed on a clean glass slide with a small amount of water/glycerin solution. Slides were scanned with a Zeiss Axio Imager A1 compound light microscope at 200x using cross polarized light microscopy, and identifications were made at 400x using standard methods. The designation “cf.” indicates that the microfossils are probably derived from this taxon, but a secure identification cannot be made at this time. Intact starch grains were counted singly unless they occurred in a cluster that was

clearly derived from a single source (see Table F-1).

In the case of the Landis Property study, artifacts that were hypothesized to be both grinding tools and cooking tools were sampled. Experiments performed by M. Quigg included various methods of heating the starchy seeds of wildrye (*Elymus canadensis*), the probable source of most of the starch remains recovered in this study. “Cooking” was performed both in the presence and absence of water, and seeds were ground with a porcelain mortar and pestle to simulate ground stone damage. The types of damage were noted and compared with that seen in the archeological residues observed in the samples (Table F-1).

During scanning of both archeological and modern starch samples, digital images were captured at 400x magnification using Zeiss Axiovision software version 4.6. Images were processed and scale bars were added using this software that is integrated into and included with the microscope package.

F.5 RESULTS

The remains of plant tissues in the form of 276 starch grains or granules were recovered from the analyzed samples (Table F-1). Types of plant remains include intact starch grains that have or have not been identified, damaged or degraded starch grains, and starches that are clearly gelatinized (Figure F-1, Figure F-2). Specific results will be discussed by archeological feature.

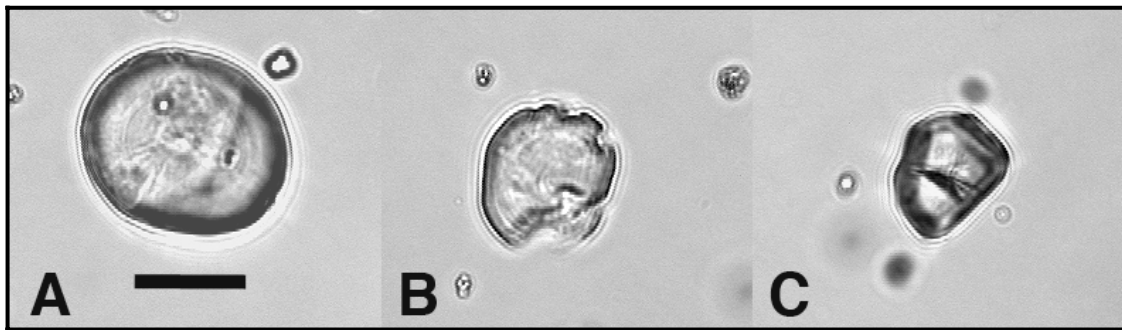


Figure F-1. Starch Remains.

(Note: The scale bar indicates 20 microns, and all images are at equivalent magnification. A. A lenticular starch granule from a Late Archaic metate fragment (41PT185/C, 1070-010). B. A lenticular starch granule from a mano (41PT185/C, 1175-010) showing damage from grinding. C. A polygonal starch grain with morphological features consistent with those of maize. This starch was recovered from a Late Archaic burned rock (41PT185/C, #899-003-5b, Feature 12)

A note on classes of plant remains

During analysis, I made notes when I encountered plant fibers in samples. Because of the presence of plant fibers in the sediment samples, I believe that the vast majority of these plant fragments are part of the background assemblage of soil constituents – noise – that also included various phytoliths and charcoal flecks. In the future, however, it may prove useful to count fibers, as my notes indicate that the

burned rocks had “many” or “abundant” fibers compared to “some” or “few” on the ground stone tools and in the sediment samples. Presumably, this larger quantity of fibers from the burned rocks is due to the contact with fuel in the fire, and the remains of this tissue, wood or other plant fibers, adhered to the rocks. Experimentation would be helpful to aid in the understanding of, if and how the numbers of fibers relate to the use of these artifacts, and will also yield data that indicate whether numbers of fibers

may differ statistically from one category of artifact to the next. In any case, I do believe this category of plant remains may prove useful in future studies.

Damaged starches as noted in the table are those that have been processed in some way, e.g., cooking, or grinding, but the type of damage is no longer identifiable due to the degraded nature of the residue. When the damage to a starch grain or group of grains could be clearly categorized, it is noted both in the data table and in the text.

The categorization of damage was assessed using one-on-one comparisons with modern

experimental starches of wildrye (*Elymus canadensis*) grains that had been subjected to several processes including parching, grinding, and boiling. These samples were provided by M. Quigg. Two main patterns of damage that relate to this study were identified. First, gelatinization of starches was noted only in the samples of wildrye that were boiled, not in those that were cooked with dry heat (Figure F-2). Second, samples that were “cooked” then ground showed clumps of distorted starches that do not occur in any examined sample from this study.

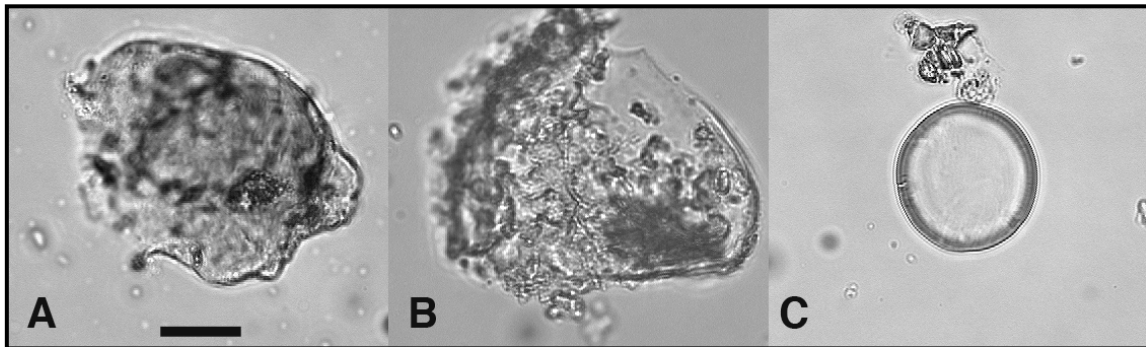


Figure F-2. Damaged Starch Granules.

(Note: The scale bar indicates 20 microns, and all images are of equivalent magnification. A. Gelatinized starch from a Late Archaic burned rock [41PT185/C, #361-003-1b, F11]. B. Experimental gelatinized starch from boiled wildrye. C. In contrast, a distorted experimental starch granule from parched [dry roasted] wildrye.)

41PT185/C Lithic Tools:

Four lithic tools were sampled, and, of those, two yielded starch remains. The chopper (#467-010) contained nineteen lenticular granules and damaged starches. One of the side scrapers, a flaked tool (#1221-011), yielded two lenticular starches, while the other had none (#452-010). The corner-tang knife yielded no starch grains.

41PT186 Lithic Tools:

Two lithic tools were sampled, and starch remains were recovered from both. The scraper yielded seven lenticular granules, and five were recovered from the flake.

41PT186 Ceramic Sherd:

No identifiable starch was extracted from the ceramic sherd (#443-008).

41PT245 Ceramic Sherds:

Sherd #401-008-1b yielded a single, lenticular starch granule. The other sherd did not have identifiable starchy residues.

41PT185/C Sediment Samples:

No identifiable, fragmentary, or damaged starches were recovered from the sediment samples collected in Features 8, 10, and 18.

41PT185/C Ground Stone Artifacts:

Of the ten ground stone artifacts that were studied, six were not associated with any feature (#405-010, #514-010, #966-010, #1089-010, #1070-010, #1175-010), and two were derived from Feature 18 (#1129-011, #1129-010). All ground stone tools yielded lenticular starch granules and six of the eight tools yielded starch grains from grasses that produce either polygonal or globular starch grains. Additionally, artifact #1089-10 yielded a clump of very small starch granules from an unknown source that may be a wild grass.

The largest numbers of starches were derived from the ground stone mano (#1175-010) which also yielded one starch grain that had been gelatinized, either by heating in the presence of water, or by intensive grinding. Damage consistent with that produced by mechanical grinding of modern starches in the laboratory was observed on two artifacts, #1070-010 and #1129-010. Damage consistent with heating in the presence of water was also observed in the residues derived from artifact #514-010, and these gelatinized fragments were observed in large numbers that were not seen on the other ground stone artifacts.

The two samples from Feature 13, a fragmented metate, yielded no identifiable starch remains.

41PT186 Burned Rock Artifacts:

Two burned rocks, neither of which was associated with a feature, were sampled

from site 41PT186. Sample #535-003-1b did not contain any identifiable plant remains. Sample #470-003-1b, in contrast, yielded damaged starch as well as starch that was clearly gelatinized.

41PT185 Burned Rock Artifacts:

Samples from Feature 13, a fragmented metate, Features 15a, 15c, and 19, burned rock discard piles, and 15b, an intact basin shaped heating element, yielded no identifiable starch remains.

Feature 2: Two burned rocks from Feature 2, an intact, burned rock heating element, were sampled for starches, and both yielded single intact grains. Sample #112-003-1b contained a single unidentified grain, and #112-003-2b contained an unidentified grass grain as well as clearly gelatinized starch.

Feature 3: Four burned rocks from Feature 3, a cluster of smaller burned rocks, were examined. Two of the rocks, #198-003-2b and #198-003-4b, yielded no identifiable remains. Sample #198-003-1b contained clearly gelatinized starch while one unidentified and one lenticular starch granule were recovered from #198-003-3b.

Feature 4: Four burned rocks from Feature 4, a large, intact heating element, were studied. Rocks #214-003-1b and #214-003-2b both yielded gelatinized starches. Rock #214-003-3b contained two lenticular starches, and no identifiable remains were recovered from rock #214-003-4b.

Feature 5: Two burned rocks, #1348-003-1b and #1348-003-2b from Feature 5, a discard pile of used rocks and other debris, were examined for starch remains. The former yielded gelatinized starch, while the latter had five lenticular starch granules adhering to it.

Feature 6: Two burned rocks, #854-003-1b and #854-003-2b were sampled from Feature 6, another discard pile of rocks. The

former rock had gelatinized starches on it, and the latter yielded a single lenticular granule.

Feature 8: Four burned rocks were sampled from Feature 8, an *in-situ*, circular, rock-filled heating element. Rocks #1341-003-2b and #474-003-1b yielded no identifiable remains. A single lenticular granule and damaged starch that may be gelatinized were recovered from #1341-003-3b. #464-003-1b yielded damaged starch, two lenticular granules, and a single starch grain from an unknown grass.

Feature 9: Six burned rocks from Feature 9 were analyzed. Part of this feature consists of discard piles of rocks (9b and c) presumably derived from a circular heating element (9d). Rock #1332-003-1b yielded no identifiable remains. Sample #1340-003-2b yielded clearly gelatinized starch, damaged starch and a single grass starch were recovered from #502-003-2b, and rocks #1337-003-1b and #1337-003-2c yielded single lenticular granules. The latter also contained damaged starch. Rock #1337-003-2b, unlike any other artifact analyzed from any site included in the study yielded a single starch grain that is derived from an unidentified root. Three starch grains from grasses, an unidentified starch grain, and damaged starch were also recovered from the same artifact.

Feature 11: Two burned rocks were sampled from Feature 11, a burned rock discard pile, and gelatinized starch was recovered from both samples. Damaged starch and a grass starch were also found on rock #361-003-2b.

Feature 12: Four burned rocks were sampled from this circular *in-situ* heating element, and, notably, the largest numbers of starch grains recovered from burned rocks were from this feature. Two rocks (#899-003-5b and #901-003-2b) contained clearly gelatinized starch, unidentified starch, lenticular starch, and starches from

unidentified grasses. Rock #901-003-4b yielded the same three types of starch, but had damaged starch that was not clearly gelatinized. Rock #901-003-1b yielded a single lenticular starch granule.

Notably, two of the starch grains from rock #899-003-5b have morphological characteristics that fall within the realm of those observed in maize (Figure F-1). Because of the presence of other unidentified grasses, both within this sample and throughout the assemblage from the site, at this time I am not comfortable making a secure identification. These two starches could very well be derived from another grass that has not yet been identified. Nonetheless, the possibility of the presence of maize at this date and location should be noted for future research in the region.

Feature 16: Two burned rocks from Feature 16, a burned rock discard pile, were sampled. Sample #875-003-1b yielded one lenticular granule and one grain derived from an unknown grass. Ten lenticular granules and damaged starch were recovered from #875-003-2b.

Feature 18: One burned rock sampled from Feature 18, a small, square heating element, yielded gelatinized starch as well as a single starch grain derived from an unknown grass. A single lenticular granule and damaged starch were recovered from the second sampled rock.

41PT245 Burned Rock Artifacts:

Feature 2: Three burned rocks from Feature 2, a burned rock hearth/heating element, were sampled and #353-003-2b yielded gelatinized starch, two lenticular starch granules and an unidentified grain, while #353-003-3b contained a single degraded lenticular granule. Sample #353-003-1b contained a single unidentified starch grain.

Feature 4/5: Three rocks from this feature, a discard pile, were sampled. One, #389-003-1b, yielded a single unidentified grain.

41PT186 “Control” Rock:

The “control” rock was excavated from a context directly under a Late Prehistoric bison skull that had a hole smashed into its skull to remove the brains and the skull was turned upside down on the rock.

The control rock yielded fragments of starches that have been gelatinized.

Experimental Rock:

The experimental rock was a piece of fresh limestone that was heated in a fire and was used to boil cattail roots in water. Once the cooking was complete, the rock was allowed to air dry and then was stored unwashed at room temperature.

This experimental rock was sampled in the same manner as the others. The plant remains included flecks of charcoal, fibers, fragments of plant tissues including sheets of entire cells, and high numbers of small fragments of starch grains, some of which bore signs of distortion through gelatinization. No intact, identifiable starches were recovered.

F.6 DISCUSSION

F.6.1 THE PRESENCE AND ABSENCE OF STARCH REMAINS

Beginning with the features that did not yield any identifiable starches, Feature 10 consisted of two large manuports, sandstone slabs, and the lack of identifiable starches from this feature indicate that the stones probably had no use as plant processing implements. This sample also fills the role of a control, indicating that the starches associated with the other classes of artifacts, those from features believed to have been used for food processing, are related to the use of those features. The absence of

identifiable starch remains from Features 15 and 19 are less easily explained because these features do not differ morphologically from other food processing features that did yield plant remains. It is possible that these features were used for animal, rather than plant processing.

Starch of any sort was also absent from the sediment samples collected from the soil matrices of Features 8, 10, and 18 at 41PT185/C. This absence strengthens the argument that the starches recovered from the lithic artifacts are associated with their use and are not the result of contamination from surrounding sediments.

Interestingly, the control rock #331-003-1b from Feature 3 at 41PT186, a buried bison skull, yielded gelatinized starches. While this rock did not derive from a cooking feature, it appears that it may have been used previously in a cooking event and was then repurposed for burial with the bison skull.

F.6.2 PREDICTING PATTERNS

In terms of both assessing and predicting the likelihood of starch recovery based upon classes of artifacts, generally speaking, the ground stone artifacts yielded more intact, identifiable starch grains than the ceramic sherds, burned rocks, or sediment samples did. The notable exceptions are the burned rocks from Feature 12, an intact heating element.

When the pilot study of this project was completed, it appeared that there would be fairly clear patterns of starch recovery from burned rocks based upon the type of feature under study. Intact features appeared to be more likely to contain identifiable starch. As more data accumulate, however, it becomes more difficult to assess whether or not burned rocks collected from an intact heating element will reliably yield more starch remains than discarded rocks. Of the four features from which all studied artifacts

yielded intact starch (Features 9d, 12, 16, and 18), two of the four are intact heating elements. However, rocks collected from Feature 15, an intact heating element, yielded no starch. While intact features appear to have yielded more starch grains overall, one of the larger counts (10) was recovered from a burned rock from a discard pile (Feature 16).

F.6.3 IDENTIFICATION OF THE STARCH REMAINS

The presence of starchy residues on the artifacts indicates that they have come into contact with starchy plant foods. The most commonly identified group of starches were those with a lenticular shape that is characteristic of the grass subfamily Pooidae, and more specifically, the tribes Bromeae and Triticeae. Wildrye is classified within the Triticeae. Only the genus *Bromus* occurs in the Bromeae, and the starches of this genus are smaller in size than those recovered at the BLM Landis Property (see Messner 2008).

Identification of wildrye, members of the genus *Elymus*, in the starch record is both easier and more reliable when there is a fairly large assemblage of grains (Messner 2008). At this point in time, the intensive comparative work necessary to define one member of the New World Triticeae from another has not been completed. However, Messner's study on the North American grasses in the Triticeae indicates that size comparisons can be quite useful in determining if wildrye is presented in an assemblage.

The starch assemblage from this study includes 223 lenticular starch grains, 164 of which were measured (Table F-2). The sizes of the intact starch grains measured between 12.9 and 43.3 microns, with a mean of 26.5 microns. According to work completed by Messner, (2008 Figure 11.4), the range of sizes of starch grains (extending a single standard deviation from the mean)

from several species of the genus *Elymus* is between about 11 and 31 microns. While there is significant overlap with the sizes of starch grains from other genera at the lower end of the range, no other starches studied from the New World Triticeae had sizes consistently over about 20 microns. The measurements of lenticular starch granules from the BLM Landis Property are consistently over 20 microns, and the overall mean of the sample is 26.5 microns, higher than the mean of modern *Elymus canadensis*, the grass with the largest starch grains of all Triticeae measured in the study. In addition to the evidence provided by the sizes of the grains, the morphological features and characteristics of many of the lenticular grains are equivalent to those of modern *Elymus* observed by the author in comparative work completed for this study.

The genus *Elymus* ranges from Canada to Mexico and occurs throughout Texas (for excellent range maps, see <http://plants.usda.gov/>). The seeds of this genus are large and have been commonly identified in the macrobotanical assemblages from northeast archeological contexts in both northeast coastal and northern mixed economy sites where they represent a potential food source (Crawford and Smith 2003). Stands of modern wildrye have also been observed growing outside of cave sites in Montana, even in areas outside the natural distribution of the grass (Loendorf 1985). Human activity, specifically deliberate planting, is implicated in those sites. Perhaps the most significant citation in the literature is an archeobotanical report from the Blood Run site in Iowa (Green and Tolmie 2004). Here, the researchers report a macrobotanical grass seed assemblage dominated by wildrye with a few other grasses, including several that remain unidentified. This pattern seems to be identical to that of the BLM Landis Property where the vast majority of grass starches are derived from wildrye, but a few other types occur as well.

Identification of the non-lenticular grass starches is not complete at this time in large part due to the fact that nearly all the types observed in the assemblage occur in small numbers, and most occur as single grains from single contexts. While most of the best known grasses from the region have been studied, given the great diversity of grasses in the Texas Panhandle, it would be premature to assign any of these grains to a taxon without further comparative studies. Continuing accumulation of data from the region, however, could enlarge the data set, thus making identification of some of the more distinct types more likely. In terms of interpretation of these data, it appears that, as was mentioned above, these various grasses make up a small component of the larger wildrye-dominated assemblage.

Notably, several starch grains in the “other grass” category, and two in particular from Feature 12, bear similar morphological features and have general characteristics that are consistent with those of some maize samples (*Zea mays*) in the author’s comparative collection. Because the phytolith record does not document the presence of maize at these three sites, and because the numbers of these grains are small, at this time I am comfortable mentioning the identification as a possibility, albeit a very exciting one, that may help guide future research.

F.6.4 ASSESSING TOOL FUNCTION

The ground stone tools yielded starch remains consistent with their hypothesized function as implements used for the processing of grass seeds. Starch grains from grasses, including those that bear recognizable grinding damage, were recovered from these artifacts. Due to the larger numbers of damaged, gelatinized, and fragmentary starches present on artifact #514-010, I believe that this artifact was likely used as a cooking implement, either instead of, or in addition to use as a grinding tool. Another possibility is that it was used

in the processing of previously cooked plant foods. In contrast to the presence of gelatinized starch on a single ground stone tool, starches bearing damage from cooking occur throughout the assemblage of burned rocks.

Gelatinized starches typically result from heating in the presence of water, and the damage is characterized by both morphological distortion and changes in the extinction cross (Henry et al. 2009). The starches identified as gelatinized in this study bear those characteristics, and were, therefore, exposed to heat in the presence of water, conditions associated with cooking processes. It has been noted that the interpretation of the specific type of cooking, e.g., boiling or baking, should be based upon experiments that are performed with starch derived from the plant in question (Henry et al. 2009). Such experiments were performed by M. Quigg using seeds of wildrye, and the resulting processed grains were sent to me for analysis. The gelatinized grains in this study bear damage consistent with boiling (Figure F-2).

To further understand what residues might result from hot rock cooking, an experiment was undertaken in which a rock was heated in an open fire, then was used to boil roots in a pot. This experimental rock was sampled in the same manner as the others. The plant remains included flecks of charcoal, fibers, fragments of plant tissues including sheets of entire cells, and high numbers of small fragments of starch grains, some of which bore signs of distortion through gelatinization. This pattern of residue is equivalent to that recovered from the burned rocks, with the exception that there were no intact, identifiable starch grains recovered from this rock. The results from both experiments indicate that the initial hypothesis, that these rocks were used for cooking in exactly this manner, is supported by the microfossil evidence recovered from the artifacts.

F.6.5 COMPARISONS BETWEEN SITES

When the three sites are compared, a single, major pattern occurs in the starch data. Starches from grasses other than wildrye occur only in the Late Archaic component of the study, and were not found in the Late Prehistoric and Protohistoric sites. It is unclear why this absence occurs, and I am fully aware that the absence of evidence does not necessarily reflect evidence of absence. With that disclaimer in mind, the following discussion should be considered speculative. It is possible that the smaller number of samples from the later sites resulted in a bias that simply missed the presence of other plant remains. It is also possible, however, that the change in the starch data reflects a shift in the stands of grasses from which the people collected their food. Weeding of these stands to encourage the proliferation of the preferred wildrye may have occurred over time, thus resulting in nearly pure stands of wildrye from which later groups collected.

This same absence of a variety of starches was noted in the six lithic tools sampled. It is more likely that this pattern is the result of a small sample size, particularly because only four of the six artifacts yielded any starch, and this subsample represents two artifacts from each of two different sites.

F.6.6 CONCLUSIONS

In addition to recovering the remains of what is very likely wildrye, a plant that has been documented in many other sites as macroremains, the patterns of residue on the burned rocks studied in this pilot project are solid indicators that they are very likely the remnants of food preparation processes. Charcoal flecks indicate exposure to open fire, starch grains and other plant tissues indicate contact with food plants, and gelatinized materials indicate that the heated rocks were used for cooking plant foods by boiling them. The experimental rock that was used in a boiling experiment yielded an

identical assemblage of plant remains including charcoal flecks, plant tissues, and both fragmentary and gelatinized starches, but no intact, identifiable starch grains. Control specimens support the contention that the plant materials recovered from the burned rocks are associated with their use.

A small number of starch grains from the Late Archaic site may have been derived from maize. At this time, identification cannot be made with certainty due to the number of grasses that have not yet been identified and studied. The possibility, however, should be noted for future research.

General patterns seem to be emerging in regard to the predictability of starch recovery from a site. Intact features and ground stone tools may be more likely to yield entire, identifiable starch grains.

In summary, the starch analyses from the BLM Landis project have provided rare and important data on the use of wildrye and other plants for food at the site and have supported the hypothesis that the burned rocks were used as cooking tools.

F.7 REFERENCES CITED

- Atchison, J. and R. Fullagar,
1998 Starch Residues on Pounding Implements from Jinmium Rock-Shelter. In *A Closer Look: Recent Studies of Australian Stone Tools*, edited by R. Fullagar. Sydney University Archaeological Methods Series 6, Archaeological Computing Laboratory, School of Archaeology, University of Sydney, Sydney.
- Babot, M. del Pilar
2003 Starch Grain Damage as an Indicator of Food Processing. In *Phytolith and Starch Research in the Australian-Pacific-Asian Regions: The State of the Art*, edited

- by D. M. Hart and L. A. Wallis, pp. 69-81. Papers from a conference held at the ANU, August 2001, Canberra, Australia. Pandanus Books.
- Babot, M. del Pilar and M. C. Apella
2004 Maize and Bone: Residues of Grinding in Northwestern Argentina. *Archaeometry* 45:121-132.
- Briuer, F. L.
1976 New Clues to Stone Tool Function: Plant and Animal Residues. *American Antiquity*: 41(4):478-484.
- Bryant, V. M.
2003 Invisible Clues to New World Plant Domestication. *Science* 299:1029-1030.
- Coil, J., M. A. Korstanje, S. Archer, and C. A. Hastorf
2003 Laboratory Goals and Considerations for Multiple Microfossil Extraction in Archaeology. *Journal of Archaeological Science* 30:991-1008.
- Crawford, G. W. and D. G. Smith
2003 Paleoethnobotany in the Northeast. In *People and Plants in Ancient Eastern North America*, edited by P. E. Minnis, pp. 172-257. Smithsonian Books, Washington D.C.
- Denniston, R. H.
1904 The Growth and Organization of the Starch Grain. Unpublished Ph.D. dissertation. University of Wisconsin, Madison, Wisconsin.
- Fullagar, R., T. Loy, and S. Cox,
1998 Starch Grains, Sediments and Stone Tool Function: Evidence from Bitokara, Papua New Guinea. In *A Closer Look: Recent Australian Studies of Stone Tools*, edited by R. Fullagar, pp. 49-58. Archaeological Computing Laboratory, University of Sydney.
- Green W. and C. Tolmie
2004 Analysis of Plant Remains from Blood Run. *Plains Anthropologist* 49(192):525-542.
- Hall, J., S. Higgins, and R. Fullagar
1989 Plant Residues on Stone Tools. *Tempus* 1:136-155.
- Haslam, M.
2003 Evidence for Maize Processing on 2000 Year Old Obsidian Artefacts from Copán, Honduras. In *Phytolith and Starch Research in the Australian-Pacific-Asian Regions: The State of the Art*. edited by D. M. Hart and L. A. Wallis, pp. 153-161. Papers from a conference held at the ANU, August.
- 2001 *Canberra, Australia*. Pandanus Books.
- 2004 The Decomposition of Starch Grains in Soils: Implications for Archaeological Residue Analyses. *Journal of Archaeological Science* 31:1715-1734.
- Henry A. G., Hudson H. F. and Piperno D. R.
2009 Changes in Starch Grain Morphologies from Cooking. *Journal of Archaeological Science* 36: 915-922.
- Iriarté, J., I. Holst, O. Marozzi, C. Listopad, E. Alonso, A. Rinderknecht, and J. Montaña
2004 Evidence for Cultivar Adoption and Emerging Complexity During the Mid-Holocene in the La Plata Basin. *Nature* 432:614-617.

- Loendorf, L. L.
1985 A Possible Explanation for the Association between Wildrye Grass (*Elymus* spp.) and Formerly Occupied Cave Sites in the Pryor Mountains, Montana. *Plains Anthropologist* 30(108):137-144.
- Loy, T. H.
1994 Methods in the Analysis of Starch Residues on Prehistoric Stone Tools. In *Tropical Archaeobotany: Applications and New Developments*, edited by J. G. Hather, pp. 86-113. Routledge.
- Loy, T. H., M. Spriggs, and S. Wickler
1992 Direct Evidence for Human Use of Plants 28,000 Years Ago: Starch Residues on Stone Artifacts from the Northern Solomon Islands. *Antiquity* 66:898-912.
- MacMasters, M. M.
1964 Microscopic Techniques for Determining Starch Granule Properties. In *Methods in Carbohydrate Chemistry*, edited by R. L. Whistler, pp. 233-240. Academic Press.
- Messner, T. C.
2008 Woodland Period People and Plant Interactions: New Insights from Starch Grain Analysis. Unpublished Ph.D. dissertation, Department of Anthropology, Temple University.
- Pearsall, D. M., K. Chandler-Ezell, and J. A. Zeidler
2004 Maize in Ancient Ecuador: Results of Residue Analysis of Stone Tools from the Real Alto Site. *Journal of Archaeological Science* 31:423-442.
- Perry, L.
2001 Prehispanic Subsistence in the Middle Orinoco Basin: Starch Analyses Yield New Evidence. Unpublished Ph.D. dissertation, Southern Illinois University Carbondale, Illinois.
- 2002a Starch Analyses Indicate Multiple Functions of Quartz "Manioc" Grater Flakes from the Orinoco Basin, Venezuela. *Interciencia* 27(11):635-639.
- 2002b Starch Granule Size and the Domestication of Manioc (*Manihot esculenta*) and Sweet Potato (*Ipomoea batatas*). *Economic Botany* 56(4):335-349.
- 2004 Starch Analyses Reveal the Relationship Between Tool Type and Function: An Example from the Orinoco Valley of Venezuela. *Journal of Archaeological Science* 31(8):1069-1081.
- 2005 Reassessing the Traditional Interpretation of "Manioc" Artifacts in the Orinoco Valley of Venezuela. *Latin American Antiquity*.
- 2007 Starch Grains, Preservation Biases, and Plant Histories. In *Rethinking Agriculture: Archaeological and Ethnographic Perspectives*, edited by T. Denham, L. Vrydaghs and J. Iriarte. One World Archaeology, Left Coast Press.
- Perry, L., D. Sandweiss, D. Piperno, K. Rademaker, M. Malpass, A. Umire, and P. de la Vera.
2006 Early Maize Agriculture and Interzonal Interaction in Southern Peru. *Nature* 440:76-79.
- Perry, L., R. Dickau, S. Zarrillo, I. Holst, D. Pearsall, D. Piperno, M. Berman, R. Cooke, K. Rademaker, A. Ranere, J. Raymond, D. Sandweiss, F. Scaramelli, K. Tarble, and J. Zeidler.

- 2007 Starch Fossils and the Domestication and Dispersal of Chili Peppers (*Capsicum* spp. L.) in the Americas. *Science* 315:986-988. With accompanying Perspective, by S. Knapp. Some Like it Hot. *Science* 315: 946-947.
- Piperno, D. R. and I. Holst
1998 The Presence of Starch Grains on Prehistoric Stone Tools from the Humid Neotropics: Indications of Early Tuber Use and Agriculture in Panama. *Journal of Archaeological Science* 25:765-776.
- Piperno, D. R., A.J. Ranere, I. Holst, and P. Hansell
2000 Starch Grains Reveal Early Root Crop Horticulture in the Panamanian Tropical Forest. *Nature* 407:894-897.
- Ranere, A. J.
1975 Toolmaking and Tool Use Among the Preceramic Peoples of Panama. In *Lithic Technology*, edited by E. H. Swanson, pp. 173-210. Mouton.
- Reichert, E. T.
1913 *The Differentiation and Specificity of Starches in Relation to Genera, Species, Etc.* In two parts. Carnegie Institution of Washington.
- Thoms, A.
2009 Rocks of Ages: Propagation of Hot-Rock Cookery in Western North America. *Journal of Archaeological Science* 36:573-591.

Table F-1. Starch Remains Recovered from Artifacts.

(Note: Damaged starches have been processed in some way that has clearly altered them from their native, completely intact form. The designation “gd” indicates the damage is characteristic of that due to grinding. Gelatinized starches have been damaged by exposure to heat and water. “UD” indicates unidentified starches. Lenticular starch grains are those of a specific shape common to grasses in the Pooidae, and are identified in this study as derived from the genus *Elymus* [see text]. Grass starches are those that are not lenticular in shape, but exhibit characteristics typical of starches produced by grasses that are classified in other taxa. Root starches bear morphological features typical of grains that form in this plant organ).

Site	Cat# / Feature	Artifact	Damaged	Gel'd	UD	Lenticular	Grass	Root	Total
41PT185/C	#452-010/NA	Side Scraper							
41PT185/C	#-010/NA	Chopper	X			19			19
41PT185/C	#609-010/NA	Corner-Tang Knife							
41PT185/C	#1221-011/NA	Side Scraper				2			2
41PT186	#446-011/6	Scraper				7			7
41PT186	#446-017/6	Flake				5			5
41PT186	#443-008/NA	Ceramic							
41PT245	#401-008-1b/NA	Ceramic				1			1
41PT245	#341-008-1b/NA	Ceramic							
41PT185/C	#405-010/NA	Ground stone	X			14	2		16
41PT185/C	#514-010/NA	Ground stone	X	X		1	1		2
41PT185/C	#966-010/NA	Ground stone	X			3	1		4
41PT185/C	#1089-010/NA	Ground stone			clump	3			3
41PT185/C	#1070-010/NA	Ground stone	X gd			2			2
41PT185/C	#1175-010/NA	Ground stone	X	X		47	5		52
41PT185/C	#1129-011/18	Ground stone				14	1		15
41PT185/C	#1129-010/18	Ground stone	X gd			9	2		11
41PT185/C	#677-010b/13	Metate Frag							
41PT185/C	#712-010b/13	Metate Frag							
41PT185/C	#112-003-1b/2	Burned Rock			1				1
41PT185/C	#112-003-2b/2	Burned Rock		X			1		1
41PT185/C	#198-003-1b/3	Burned Rock		X					

Site	Cat# / Feature	Artifact	Damaged	Gel'd	UD	Lenticular	Grass	Root	Total
41PT185/C	#198-003-2b/3	Burned Rock							
41PT185/C	#198-003-3b/3	Burned Rock			1	1			2
41PT185/C	#198-003-4b/3	Burned Rock							
41PT185/C	#214-003-1b/4	Burned Rock		X					
41PT185/C	#214-003-2b/4	Burned Rock		X					
41PT185/C	#214-003-3b/4	Burned Rock				2			2
41PT185/C	#214-003-4b/4	Burned Rock							
41PT185/C	#1348-003-1b/5	Burned Rock		X					
41PT185/C	#1348-003-2b/5	Burned Rock				5			5
41PT185/C	#854-003-1b/6	Burned Rock		X					
41PT185/C	#854-003-2b/6	Burned Rock				1			1
41PT185/C	#1341-003-2b/8	Burned Rock							
41PT185/C	#1341-003-3a/8	Burned Rock	X	?		1			1
41PT185/C	#464-003-1b/8	Burned Rock	X			2	1		3
41PT185/C	#474-003-1b/8 low	Burned Rock							
41PT185/C	#1340-003-2b/9b	Burned Rock		X					
41PT185/C	#502-003-2b/9c	Burned Rock	X				1		1
41PT185/C	#1332-003-1b/9c	Burned Rock							
41PT185/C	#1337-003-1b/9d	Burned Rock				1			1
41PT185/C	#1337-003-2b/9d	Burned Rock	X		1		3	1	5
41PT185/C	#1337-003-2c/9d	Burned Rock	X			1			1
41PT185/C	#361-003-1b/11	Burned Rock		X					
41PT185/C	#361-003-2b/11	Burned Rock	X	X			1		1
41PT185/C	#899-003-5b/12	Burned Rock		X	1	18	11		30
41PT185/C	#901-003-1b/12	Burned Rock				1			1

Site	Cat# / Feature	Artifact	Damaged	Gel'd	UD	Lenticular	Grass	Root	Total
41PT185/C	#901-003-2b/12	Burned Rock		X	2	3	6		11
41PT185/C	#901-003-4a/12	Burned Rock	X		3	45	2		50
41PT185/C	#1234-003-1b/15a	Burned Rock							
41PT185/C	#1234-003-2b/15a	Burned Rock							
41PT185/C	#1181-003-2b/15b	Burned Rock							
41PT185/C	#1192-003-1b/15c	Burned Rock							
41PT185/C	#1192-003-2b/15c	Burned Rock							
41PT185/C	#875-003-1b/16	Burned Rock				1	1		2
41PT185/C	#875-003-2b/16	Burned Rock	X			10			10
41PT185/C	#1129-003-1b/18	Burned Rock	X			1			1
41PT185/C	#1129-003-2b/18	Burned Rock		X			1		1
41PT185/C	#1070-003-1b/19	Burned Rock							
41PT186	#470-003-1b/NA	Burned Rock	X	X					
41PT186	#535-003-1b/NA	Burned Rock							
41PT245	#353-003-1b/2	Burned Rock			1				1
41PT245	#353-003-2b/2	Burned Rock		X	1	2			3
41PT245	#353-003-3b/2	Burned Rock	X			1			1
41PT245	#389-003-1b/4/5	Burned Rock			1				1
41PT245	#398-003-3b/4/5	Burned Rock							
41PT245	#398-003-4b/4/5	Burned Rock							
41PT186	#345-005-1b/17	Control		X					
None	#MQ CE#14	Exp. Rock		X					
41PT185/C	#1341-004-1b/8	Sediment							
41PT185/C	#801-004-2b/10	Sediment							
41PT185/C	#1129-004-1b/18	Sediment							
	Totals				12 +	223	40	1	276

Table F-2. Measurements of Lenticular Starch Grains from Artifacts.

(Note: All measurements are in microns).

Site	Cat # / Feature	Type	No.	Range	Mean
41PT245	#401-008-1b / NA	Ceramic	1	31	31
41PT185/C	#405-010 / NA	GS	12	15.5 – 37.1	27.1
41PT185/C	#966-010 / NA	GS	3	24.8 – 28.4	27
41PT185/C	#1070-010 / NA	GS	2	27.9 – 39.6	33.8
41PT185/C	#1089-010 / NA	GS	3	18.8 – 25.8	22.9
41PT185/C	#1175-010 / NA	Mano	42	17.5 – 43.3	27.5
41PT185/C	#1129-011 / 18	GS	11	18.5 – 38.2	29.4
41PT185/C	#1129-010 / 18	GS	6	19.8 – 32.5	25.6
41PT185/C	#198-003-3b / 3	BR	1	30.3	30.3
41PT185/C	#214-003-3b / 4	BR	2	28.1 – 42.8	35.5
41PT185/C	#1348-003-2b / 5	BR	5	22.6 – 36.7	29.5
41PT185/C	#854-003-2b / 6	BR	1	23.8	23.8
41PT185/C	#464-003-1b / 8	BR	2	24.8 – 27	25.9
41PT185/C	#1341-003-2b / 8	BR	1	36.4	36.4
41PT185/C	#1337-003-1b / 9d	BR	1	27.4	27.4
41PT185/C	#899-003-5b / 12	BR	16	16.8 – 37	26.2
41PT185/C	#901-003-1b / 12	BR	1	30.4	30.4
41PT185/C	#901-003-2b / 12	BR	3	17 – 29.7	23.1
41PT185/C	#901-003-4a / 12	BR	41	12.9 – 34.5	24
41PT185/C	#875-003-1b / 16	BR	1	35	35
41PT185/C	#875-003-2b / 16	BR	7	16 – 30	23.4
41PT245	#353-003-2b / 2	BR	2	19.1 – 25.1	22.1
	Totals		164	12.9 – 43.3	26.5

GS = Ground Stone, BR = Burned Rock.

This page intentionally left blank.

APPENDIX G

ANALYSIS OF LIPIDS EXTRACTED FROM ARCHAEOLOGICAL BURNED ROCK AND POTTERY RESIDUES FROM SITES IN POTTER COUNTY, TEXAS

This page intentionally left blank.

**ANALYSIS OF LIPIDS EXTRACTED FROM ARCHAEOLOGICAL
BURNED ROCK AND POTTERY RESIDUES FROM SITES IN POTTER
COUNTY, TEXAS**

Prepared for:



**TRC Environmental Corporation
505 East Huntland Drive, Suite 250
Austin, Texas 78752**

Prepared by:

**M. E. Malainey, Ph.D. and Timothy Figol
11 Mager Drive West
Winnipeg, MB
Canada R2M 0R9**

2009

This page intentionally left blank.

G.1 INTRODUCTION

A total of 21 burned rock fragments and two ceramic sherds were submitted for analysis in 2008; 42 samples of burned rock and metate fragments were submitted in 2009. Where necessary, subsamples were taken for analysis from larger pieces of material. Exterior surfaces were ground off to remove any contaminants and samples were crushed. Absorbed lipid residues were extracted with organic solvents. Lipid extracts were analyzed using gas chromatography (GC) and high temperature GC (HT-GC) and high temperature gas chromatography with mass spectrometry (HT-GC/MS). Residues were identified on the basis of fatty acid decomposition patterns of experimental residues, lipid distribution patterns and through the presence of biomarkers. Procedures for the identification of archaeological residues are outlined below; following this, analytical procedures and results are presented.

G.1.1 THE IDENTIFICATION OF ARCHAEOLOGICAL RESIDUES

G.1.1.1 Identification of Fatty Acids

Fatty acids are the major constituents of fats and oils (lipids) and occur in nature as triglycerides, consisting of three fatty acids attached to a glycerol molecule by ester-linkages. The shorthand convention for designating fatty acids, C_x:y ω z, contains three components. The “C_x” refers to a fatty acid with a carbon chain length of x number of atoms. The “y” represents the number of double bonds or points of unsaturation, and the “ ω z” indicates the location of the most distal double bond on the carbon chain, i.e. closest to the methyl end. Thus, the fatty acid expressed as C₁₈:1 ω 9, refers to a mono-unsaturated isomer with a chain length of 18 carbon atoms with a single double bond located nine carbons from the methyl end of the chain. Similarly, the shorthand designation,

C₁₆:0, refers to a saturated fatty acid with a chain length of 16 carbons.

Their insolubility in water and relative abundance compared to other classes of lipids, such as sterols and waxes, make fatty acids suitable for residue analysis. Since employed by Condamin *et al.* (1976), gas chromatography has been used extensively to analyze the fatty acid component of absorbed archaeological residues. The composition of uncooked plants and animals provides important baseline information, but it is not possible to directly compare modern uncooked plants and animals with highly degraded archaeological residues. Unsaturated fatty acids, which are found widely in fish and plants, decompose more readily than saturated fatty acids, sterols or waxes. In the course of decomposition, simple addition reactions might occur at points of unsaturation (Solomons 1980) or peroxidation might lead to the formation of a variety of volatile and non-volatile products which continue to degrade (Frankel 1991). Peroxidation occurs most readily in fatty acids with more than one point of unsaturation.

Attempts have been made to identify archaeological residues using criteria that discriminate uncooked foods (Marchbanks 1989; Skibo 1992; Loy 1994). The major drawback of the distinguishing ratios proposed by Marchbanks (1989), Skibo (1992) and Loy (1994) is they have never been empirically tested. The proposed ratios are based on criteria that discriminate food classes on the basis of their original fatty acid composition. The resistance of these criteria to the effects of decompositional changes has not been demonstrated. Rather, Skibo (1992) found his fatty acid ratio criteria could not be used to identify highly decomposed archaeological samples.

In order to identify a fatty acid ratio unaffected by degradation processes, Patrick *et al.* (1985) simulated the long-term decomposition of one sample and monitored

the resulting changes. An experimental cooking residue of seal was prepared and degraded in order to identify a stable fatty acid ratio. Patrick *et al.* (1985) found that the ratio of two C18:1 isomers, oleic and vaccenic, did not change with decomposition; this fatty acid ratio was then used to identify an archaeological vessel residue as seal. While the fatty acid composition of uncooked foods must be known, Patrick *et al.* (1985) showed that the effects of cooking and decomposition over long periods of time on the fatty acids must also be understood.

G.1.1.2 Development of the Identification Criteria

As the first stage in developing the identification criteria used herein, the fatty acid compositions of more than 130 uncooked Native food plants and animals from Western Canada were determined using gas chromatography (Malainey 1997; Malainey *et al.* 1999a). When the fatty acid compositions of modern food plants and animals were subject to cluster and principal component analyses, the resultant groupings generally corresponded to divisions that exist in nature (Table G-1). Clear differences in the fatty acid composition of large mammal fat, large herbivore meat, fish, plant roots, greens and berries/seeds/nuts were detected, but the fatty acid composition of meat from medium-sized mammals resembles berries/seeds/nuts.

Samples in cluster A, the large mammal and fish cluster had elevated levels of C16:0 and C18:1 (Table G-1). Divisions within this cluster stemmed from the very high level of C18:1 isomers in fat, high levels of C18:0 in bison and deer meat and high levels of very long chain unsaturated fatty acids (VLCU) in fish. Differences in the fatty acid composition of plant roots, greens and berries/seeds/nuts reflect the amounts of C18:2 and C18:3 ω 3 present. The berry, seed, nut and small mammal meat samples

appearing in cluster B have very high levels of C18:2, ranging from 35% to 64% (Table G-1). Samples in subclusters V, VI and VII have levels of C18:1 isomers from 29% to 51%, as well. Plant roots, plant greens and some berries appear in cluster C. All cluster C samples have moderately high levels of C18:2; except for the berries in subcluster XII, levels of C16:0 are also elevated. Higher levels of C18:3 ω 3 and/or very long chain saturated fatty acids (VLCS) are also common except in the roots which form subcluster XV.

Secondly, the effects of cooking and degradation over time on fatty acid compositions were examined. Originally, 19 modern residues of plants and animals from the plains, parkland and forests of Western Canada were prepared by cooking samples of meats, fish and plants, alone or combined, in replica vessels over an open fire (Malainey 1997; Malainey *et al.* 1999b). After four days at room temperature, the vessels were broken and a set of sherds analysed to determine changes after a short term of decomposition. A second set of sherds remained at room temperature for 80 days, then placed in an oven at 75°C for a period of 30 days in order to simulate the processes of long term decomposition. The relative percentages were calculated on the basis of the ten fatty acids (C12:0, C14:0, C15:0, C16:0, C16:1, C17:0, C18:0, C18:1 ω 9, C18:1 ω 11, C18:2) that regularly appeared in Precontact Period vessel residues from Western Canada. Observed changes in fatty acid composition of the experimental cooking residues enabled the development of a method for identifying the archaeological residues (Table G-2).

It was determined that levels of medium chain fatty acids (C12:0, C14:0 and C15:0), C18:0 and C18:1 isomers in the sample could be used to distinguish degraded experimental cooking residues (Malainey 1997; Malainey *et al.* 1999b). Higher levels of medium chain fatty acids, combined with low levels of C18:0 and C18:1 isomers,

were detected in the decomposed experimental residues of plants, such as roots, greens and most berries. High levels of C18:0 indicated the presence of large herbivores. Moderate levels of C18:1 isomers, with low levels of C18:0, indicated the presence of either fish or foods similar in composition to corn. High levels of C18:1 isomers with low levels of C18:0, were found in residues of beaver or foods of similar fatty acid composition. The criteria for identifying six types of residues were established experimentally; the seventh type, plant with large herbivore, was inferred (Table G-2). These criteria were applied to residues extracted from more than 200 pottery cooking vessels from 18 Western Canadian sites (Malainey 1997; Malainey *et al.* 1999c; 2001b). The identifications were found to be consistent with the evidence from faunal and tool assemblages for each site.

Work has continued to understand the decomposition patterns of various foods and food combinations (Malainey *et al.* 2000a, 2000b, 2000c, 2001a; Quigg *et al.* 2001). The collection of modern foods has expanded to include plants from the Southern Plains. The fatty acid compositions of mesquite beans (*Prosopis glandulosa*), Texas ebony seeds (*Pithecellobium ebano Berlandier*), tasajillo berry (*Opuntia leptocaulis*), prickly pear fruit and pads (*Opuntia engelmannii*), Spanish dagger pods (*Yucca treculeana*), cooked sotol (*Dasyilirion wheeler*), agave (*Agave lechuguilla*), cholla (*Opuntia imbricata*), piñon (*Pinus edulis*) and Texas mountain laurel (or mescal) seed (*Sophora secundiflora*) have been determined. Experimental residues of many of these plants, alone or in combination with deer meat, have been prepared by boiling foods in clay cylinders or using sandstone for either stone boiling (Quigg *et al.* 2000) or as a griddle. In order to accelerate the processes of oxidative degradation that naturally occur at a slow rate with the passage of time, the rock or clay tile

containing the experimental residue was placed in an oven at 75°C. After either 30 or 68 days, residues were extracted and analysed using gas chromatography. The results of these decomposition studies enabled refinement of the identification criteria (Malainey 2007).

G.1.1.3 Using Lipid Distribution and Biomarkers to Identify Archaeological Residues

Archaeological scientists working in the United Kingdom have had tremendous success using high temperature-gas chromatography (HT-GC) and gas chromatography with mass spectrometry (HT-GC/MS) to identify biomarkers. High temperature gas chromatography is used to separate and assess a wide range of lipid components, including fatty acids, long chain alcohols and hydrocarbons, sterols, waxes, terpenoids and triacylglycerols (Evershed *et al.* 2001). The molecular structure of separated components is elucidated by mass spectrometry (Evershed 2000).

Triacylglycerols, diacylglycerols and sterols can be used to distinguish animal-derived residues, which contain cholesterol and significant levels of both triacylglycerols, from plant-derived residues, indicated by plant sterols, such as β -sitosterol, stigmasterol and campesterol, and only traces of triacylglycerols (Evershed 1993; Evershed *et al.* 1997a; Dudd and Evershed 1998). Barnard *et al.* (2007), however, have recently suggested that micro-organisms living off residues can introduce β -sitosterol into residues resulting from the preparation of animal products. Waxes, which are long-chain fatty acids and long-chain alcohols that form protective coatings on skin, fur, feathers, leaves and fruit, also resist decay. Evershed *et al.* (1991) found epicuticular leaf waxes from plants of the genus *Brassica* in vessel residues from a Late Saxon/Medieval settlement. Cooking experiments later confirmed the utility of

nonacosane, nonacosan-15-one and nonacosan-15-ol to indicate the preparation of leafy vegetables, such as turnip or cabbage (Charters *et al.* 1997). Reber *et al.* (2004) recently suggested *n*-dotriacontanol could serve as an effective biomarker for maize in vessel residues from sites located in Midwestern and Eastern North America. Beeswax can be identified by the presence and distribution of *n*-alkanes with carbon chains 23 to 33 atoms in length and palmitic acid wax esters with chains between 40 and 52 carbons in length (Heron *et al.* 1994; Evershed *et al.* 1997b).

Terpenoid compounds, or terpenes, are long chain alkenes that occur in the tars and pitches of higher plants. The use of GC and GC/MS to detect the diterpenoid, dehydroabietic acid, from conifer products in archaeological residues extends over a span of 25 years (Shackley 1982; Heron and Pollard 1988). Lupeol, α - and β -amyrin and their derivatives indicate the presence of plant materials (Regert 2007). Eerkens (2002) used the predominance of the diterpenoid, Δ -8(9)-isopimaric acid, in a vessel residue from the western Great Basin to argue it contained piñon resins. Other analytical techniques have also been used to identify terpenoid compounds. Sauter *et al.* (1987) detected the triterpenoid, betulin, in Iron Age tar using both ^1H and ^{13}C nuclear magnetic resonance spectroscopy (NMR), confirming the tar was produced from birch.

G.2 METHODOLOGY

Descriptions of the samples are presented in Tables G-3 and G-4. Possible contaminants were removed by grinding off the exterior surfaces with a Dremel® tool fitted with a silicon carbide bit. Immediately thereafter, the sample was crushed with a hammer mortar and pestle and the powder transferred to an Erlenmeyer flask. Lipids were extracted using a variation of the method developed by Folch *et al.* (1957). The powdered sample was mixed with a 2:1

mixture, by volume, of chloroform and methanol (2 X 25 mL) using ultrasonication (2 X 10 min). Solids were removed by filtering the solvent mixture into a separatory funnel. The lipid/solvent filtrate was washed with 13.3 mL of ultrapure water. Once separation into two phases was complete, the lower chloroform-lipid phase was transferred to a round-bottomed flask and the chloroform removed by rotary evaporation. Any remaining water was removed by evaporation with benzene (1.5 mL); 1.5 mL of chloroform-methanol (2:1, v/v) was used to transfer the dry total lipid extract to a screw-top glass vial with a Teflon®-lined cap. The sample was flushed with nitrogen and stored in a -20°C freezer.

G.2.1 PREPARATION OF FAMES

A 400 μL aliquot of the total lipid extract solution was placed in a screw-top test tube and dried in a heating block under nitrogen. Fatty acid methyl esters (FAMES) were prepared by treating the dry lipid with 5 mL of 0.5 N anhydrous hydrochloric acid in methanol (68°C; 60 min). Fatty acids that occur in the sample as di- or triglycerides are detached from the glycerol molecule and converted to methyl esters. After cooling to room temperature, 3.4 mL of ultrapure water was added. FAMES were recovered with petroleum ether (2.5 mL) and transferred to a vial. The solvent was removed by heat under a gentle stream of nitrogen; the FAMES were dissolved in 75 μL of *iso*-octane then transferred to a GC vial with a conical glass insert.

G.2.2 PREPARATION OF TMS DERIVATIVES

A 100 μL aliquot of the total lipid extract solution was placed in a screw-top vial and dried in a heating block under nitrogen. Trimethylsilyl (TMS) derivatives were prepared by treating the dry lipid with 70 μL of *N,O*-bis(trimethylsilyl)trifluoroacetamide (BSTFA) containing 1% trimethylchlorosilane, by volume (70°C; 30

min.). In 2008, the derivatives were injected directly; in 2009, they were dried under nitrogen and then redissolved in 80 μ L hexane.

Solvents and chemicals were checked for purity by running a sample blank. The entire lipid extraction was performed; FAMES and TMS derivatives were prepared and analyzed. Traces of contamination were subtracted from sample chromatograms. The relative percentage composition was calculated by dividing the integrated peak area of each fatty acid by the total area of fatty acids present in the sample.

The step in the extraction procedure where the chloroform, methanol and lipid mixture is washed with water is standard procedure for the extraction of lipids from modern samples. Following Evershed *et al.* (1990), who reported that this step was unnecessary for the analysis of archaeological residues, previously the solvent-lipid mixture was not washed. This step was adopted to remove impurities so that clearer chromatograms could be obtained in the region where very long chain fatty acids (C20:0, C20:1, C22:0 and C24:0) occur. It was anticipated that the detection and accurate assessment of these fatty acids could be instrumental in separating residues of animal origin from those of plant (Malainey *et al.* 2000a, 2000b, 2000c, 2001a).

In order to identify the residue on the basis of fatty acid composition, the relative percentage composition was determined first with respect to all fatty acids present in the sample (including very long chain fatty acids) (see Table G-4) and secondly with respect to the ten fatty acids utilized in the development of the identification criteria (C12:0, C14:0, C15:0, C16:0, C16:1, C17:0, C18:0, C18:1w9, C18:1w11 and C18:2) (not shown). The second step is necessary for the application of the identification criteria presented in Table G-2. It must be understood that the identifications given do not necessarily mean that those particular

foods were actually prepared because different foods of similar fatty acid composition and lipid content would produce similar residues. It is possible only to say that the material of origin for the residue was similar in composition to the food(s) indicated. High temperature gas chromatography and high temperature gas chromatography is used to further clarify the identifications.

G.2.3 GAS CHROMATOGRAPHY ANALYSIS PARAMETERS

The GC analysis was performed on a Varian 3800 gas chromatograph fitted with a flame ionization detector connected to a personal computer. Samples were separated using a DB-23 fused silica capillary column (30 m X 0.25 mm I.D.; J&W Scientific; Folsom, CA). An autosampler injected a 3 μ L sample using a split/splitless injection system. Hydrogen was used as the carrier gas with a column flow of 1.0 mL/min. Column temperature was held at 80°C for one minute then increased to 140°C at a rate of 20°C per minute. It was then programmed from 140 to 230°C at 4°C per minute. The upper temperature was held for 17 minutes. Chromatogram peaks were integrated using Varian Microsoft Workstation® software and identified through comparisons with external qualitative standards (NuCheck Prep; Elysian, MN).

G.2.4 HIGH TEMPERATURE GAS CHROMATOGRAPHY AND GAS CHROMATOGRAPHY WITH MASS SPECTROMETRY

Both HT-GC and HT GC-MS analyses were performed on a Varian 3800 gas chromatograph fitted with both a flame ionization detector and Varian 4000 mass spectrometer connected to a personal computer. For HT-GC analysis, the sample was injected onto a DB-1ht fused silica capillary column (15 m X 0.32 mm I.D.; Agilent J&W; Santa Clara, CA) connected

to the flame ionization detector, using hydrogen as the carrier gas. For HT-GC/MS analysis, samples were injected onto a VF-5ht fused silica capillary column (30 m X 0.25 mm I.D.; Varian; Palo Alto, CA) connected to the mass spectrometer, using helium as the carrier gas. For both analyses, the column temperature were held at 50°C for two minutes then increased to 350°C at a rate of 10°C per minute. The Varian 400 mass spectrometer was operated in electron-impact ionization mode scanning from m/z 50-700. Chromatogram peaks and Microsoft spectra were processed using Varian Microsoft Workstation® software and identified through comparisons with external qualitative standards (Sigma Aldrich; St. Louis, MO and NuCheck Prep; Elysian, MN), reference samples and the NIST database.

G.3 RESULTS OF ARCHEOLOGICAL DATA ANALYSIS

The compositions of residues extracted from eight samples analyzed in 2008 are presented in Table G-5; the 2009 analysis results are presented in Tables G-6 and G-7. The term, Area, represents the area under the chromatographic peak of a given fatty acid, as calculated by the Varian Microsoft Workstation® software minus the solvent blank. The term, Rel%, represents the relative percentage of the fatty acid with respect to the total fatty acids in the sample. Insufficient lipids were recovered from 15 samples submitted in 2008 to attempt identification: residues 8MQ 6 (112-3-2a), 8MQ 7 (112-3-3a), 8MQ 8 (112-3-4a), 8MQ 10 (214-3-2a), 8MQ 11 (214-3-3a), 8MQ 13 (198-3-1a), 8MQ 14 (198-3-2a), 8MQ 15 (198-3-3a), 8MQ 16 (198-3-4a), 8MQ 17 (389-3-1a), 8MQ 18 (398-3-2a), 8MQ 19 (398-3-3a), 8MQ 20 (398-3-4a), 8MQ 21 (341-8-1a) and 8MQ 21 (345-5-1a). The identifications of the fatty acids were verified through high temperature GC/MS, in addition, lipid biomarkers were detected.

Two samples submitted in 2009 contained insufficient fatty acids to attempt identification and no lipid biomarkers were detected: 9MQ 10 (502-3-1a) and 9MQ 26 (1234-3-1a).

G.3.1 RESIDUES CONTAINING LARGE HERBIVORE PRODUCTS

Of the eight residues with sufficient lipids analyzed in 2008, large herbivore products appear to be present in five: 8MQ 1 (353-3-1a), 8MQ 2 (353-3-2a), 8MQ 3 (353-3-3a), 8MQ 4 (353-3-4a) and 8MQ 5 (112-3-1a). These identifications are made on the basis of: 1) levels of C18:0 in the residues, 2) significant levels of cholesterol and 3) the presence of triacylglycerols. The sample from which residue 8MQ 3 was extracted differs from the other Site 41PT245, feature 2 burned rocks in that significantly less lipid was extracted; amounts of fatty acids ranged between 6% and 10% the amounts recovered from the other samples. Levels of the plant sterol, β -sitosterol, also appear to be quite high. With further analysis it may be possible to determine the relative amounts of the cholesterol and β -sitosterol in the sample; both emerge from the column at the same time as other components (co-elute), so accurate peak integration is not possible. Levels of triacylglycerols in this residue are very low compared to the other residues from this feature. The HT-GC chromatogram of residue 8MQ 5 is similar to residue 8MQ 3 with respect to high levels of β -sitosterol and low levels of triacylglycerols. Levels of medium chain fatty acids are both slightly elevated in these residues, as well. For these reasons, residues 8MQ 3 and 8MQ 5 are identified as large herbivore residues with traces of plant material present. Large herbivore residues result from the preparation of bison, deer, moose, fat elk meat or other bovines or cervids; but javelina meat also produce residues high in C18:0 and must be considered as a potential source where available.

High levels of C18:0 in seven residues analyzed in 2009 indicated the presence of large herbivore products. Four of the residues are similar in that the level of C18:0 ranges between about 29% and 34% and either moderate-high 9MQ 28 (1181-3-1a) and 9MQ 39 (514-10) or high levels 9MQ 17 (1337-3-1a) and 9MQ 25 (712-3-1a), levels of C18:1 isomers. Residue 9 MQ 28 has highly significant levels of triacylglycerols; cholesterol is present and levels of C18:2 are low, suggesting it consists of only large herbivore products, perhaps a combination of meat and marrow. Triacylglycerols were present in 9MQ 25 but only traces were detected in residue 9MQ 17 and 9MQ 39. Slightly elevated levels of C18:2 could indicate the presence of plant material in the last two residues. The lipid biomarkers dehydroabietic acid was detected in residue 9MQ39, which confirms the presence of conifer products. The source of the conifer products is not known; they may have been introduced from firewood, resins or other conifer products.

One residue, 9MQ 19 (355-3-1a) has similarly high levels of C18:0 but a medium level of C18:1 isomers, 21.61%. This residue appears to represent a combination of large herbivore products and medium or moderate-high fat content plants. Traces of triacylglycerols were detected but three lipid biomarkers appeared in this residue: the plant sterol β -sitosterol, the animal sterol cholesterol and dehydroabietic acid, which indicates conifer products.

Two of these residues, 9MQ 16 (1332-3-1a) and 9MQ 24 (901-3-3a), are characterized by slightly lower levels of C18:0, 25.50 to 26.26%, and moderate-high levels of C18:1 isomers. This combination is known to occur in the decomposed residues of large herbivore bone marrow and large herbivore meat prepared with moderate-high or high fat content seeds or nuts. The levels of C18:2 are quite high in these residues, 5% to 6%, which is consistent with the presence of seeds or nuts. Significant levels of

triacylglycerols were preserved in residue 9MQ 16, which further confirms the presence of animal products; however, no lipid biomarkers were present in this residue. Highly significant levels of triacylglycerols appear in residue 9MQ 24 and the animal sterol cholesterol was detected. Dehydroabietic acid was also detected, which confirms the presence of conifer products. The source of the conifer products is not known; they may have been introduced from firewood, resins or other conifer products.

G.3.2 VERY HIGH FAT CONTENT RESIDUES

The levels of C18:1 isomers in one residue analyzed in 2008, 8MQ 12 (214-3-4a) is very high, 63.38%. Very high levels of C18:1 isomers are observed in the decomposed residues of foods of very high fat content seeds or nuts, such as piñon. The elevated levels of C18:2 in this residue are also typical of plant material. The presence of the plant sterol, β -sitosterol, in the residue was confirmed with HT-GC/MS; the animal sterol, cholesterol is absent. This further supports a seed or nut origin for this residue.

Eleven of the residues analyzed in 2009 had levels of C18:1 isomers in excess of 50%; all also have elevated levels of C18:2, ranging between 7.5 and 15.23%, which is consistent with the preparation of seeds or nuts. These very high fat content residues can be divided into three groups based on C18:0 levels. Five residues, 9MQ 2 (1348-3-2a), 9MQ 3 (854-3-1a), 9MQ 4 (854-3-2a), 9MQ 15 (1340-3-2a) and 9MQ 23 (901-3-2a), have C18:0 levels that are less than 5%. Triacylglycerols were present in low levels in the first three of these residues, which is consistent with plant materials. Azelaic acid is present in residue 9MQ 2, which is a short chain dicarboxylic acid associated with the oxidation of unsaturated fatty acids (Regert et al. 1998). Unsaturated fatty acids are most abundant in seed oils, which suggest that plant seeds or nuts were

prepared. Dehydroabietic acid indicates the presence of conifer products in residue 9MQ 4. Levels of triacylglycerols are somewhat higher in the 9MQ 15 and much higher in residue 9MQ 23, which suggests the presence of animal products. Cholesterol was detected in both of these residues and β -sitosterol was detected in only the latter residue.

The second group consists of four residues with C18:0 levels between 7 and 10%: 9MQ 14 (1340-3-1a), 9MQ 27 (1234-3-2a), 9MQ 30 (1181-3-3a) and 9MQ 31 (1192-3-1a). Triacylglycerol levels were either present in trace amount or were not detected in these residues, which is consistent with plant materials. Even so, cholesterol was detected in 9MQ 14 and 9MQ 30, which confirms the presence of animal products; β -sitosterol was present in 9MQ 30. Dehydroabietic acid, an indicator of conifer products, was detected in residues 9MQ 30 and 9MQ 31.

The third group consists of two residues, 9MQ 5 (464-3-1a) and 9MQ 9 (1341-3-2a), that have C18:0 levels of between 13% and 16%. Only traces of triacylglycerols are present in these residues, which is consistent with plant products. The higher levels of C18:0 in these residues, however, may indicate the presence of plant materials and cholesterol is present in residue 9MQ 9. Azelaic acid and dehydroabietic acid appear in residue 9MQ 5, so only plant materials seem to be present.

G.3.3 HIGH FAT CONTENT RESIDUES

One residue analyzed in 2008, 8MQ 9 (214-3-1a) is high, 42.98%, was characterized as high fat content. The amount of lipid recovered was very low, which added a dimension of uncertainty to the identification process. Similarly high levels of C18:1 isomers are observed in the decomposed residues of high fat content seeds or nuts and the rendered fats of certain mammals (other than large herbivores). The HT-GC chromatogram of this residue is very

similar to that of residue 8MQ 12, except residue 8MQ 9 has lower levels of C18:1 isomers and a higher level of C18:0, over 10%. The presence of the plant sterol, β -sitosterol, and the animal sterol, cholesterol, was confirmed with HT-GC/MS. This residue appears to represent that of a plant material with traces of animal products present.

A total of 13 residues analyzed in 2009 were characterized as high fat content. Three of the residues are similar in that the levels of C18:0 are less than 8%: 9MQ 7 (474-3-1a), 9MQ 20 (361-3-1a) and 9MQ 21 (361-3-2a). Triacylglycerols are present in low levels in these residues. Azelaic acid is present in residue 9MQ 7; dehydroabietic acid was detected in all three. Both β -sitosterol and cholesterol are present in residue 9MQ 21, but the latter is the only evidence of animal products.

Six other residues have levels of C18:0 that range between about 10% and 12% and C18:2 levels occur between 4 and 7%: 9MQ 11 (502-3-2a), 9MQ 13 (504-3-4a), 9MQ 18 (1337-3-2a), 9MQ 22(901-3-1a), 9MQ 34 (875-3-2a) and 9MQ 40 (1127-11). Triacylglycerols are present but occur in all residues at fairly low or trace levels. Lipid biomarkers are present in all residues. β -sitosterol and cholesterol both appear in residues 9MQ 11, 9MQ 18 and 9MQ 40. β -sitosterol and dehydroabietic acid both appear in residue 9MQ 40. Cholesterol is present in residue 9MQ 13; dehydroabietic acid is present in 9MQ 34.

Four other residues are similar in the levels of C18:0 are higher, between about 14 and 21%: 9MQ 32 (1192-3-2a), 9MQ 36 (1129-3-2a), 9MQ 37 (1070-3-1a) and 9MQ 42 (406-3-1a). Levels of C18:2 range between 4.23 and 6.38% in most residues and triacylglycerols are present in low or trace amounts. The exception is residue 9MQ 36 which has a high level of C18:2, 10.26%, indicating plant products, and significant levels of triacylglycerols, indicating animal

products. Three biomarkers were detected in this residue, β -sitosterol, dehydroabietic acid and azelaic acid, which all indicate plant products. Both cholesterol and azelaic acid occur in residue 9MQ 37, suggesting animal products are present with the plant material. Dehydroabietic acid occurs in residue 9MQ 32. No lipid biomarkers were detected in residue 9MQ 42, but its elevated C18:0 level suggests animal products could be present.

Two residues were on the border between high and very high fat content, 9MQ 12 (504-3-3a) and 9MQ 29 (1181-3-2a). Levels of C18:2 in these residues are 5.45 and 7.19%, respectively, which suggests plant products are present. Only traces of triacylglycerols appear in these residues; levels of C18:0 are variable, 6.50% and 11.24%, respectively. Somewhat contrary to expectations, cholesterol and dehydroabietic acid appear in residue 9MQ 12; only β -sitosterol was detected in residue 9MQ 29.

G.3.4 MODERATE-HIGH FAT CONTENT RESIDUES

One residue analyzed in 2008, 8MQ 22 (401-8-1a), had a moderately-high level of C18:1 isomers, 30.76% and levels of medium chain fatty acids of over 20%. Foods known to produce similar levels of C18:1 isomers include Texas ebony seeds and the fatty meat of medium-sized mammals, such as beaver. High levels of medium chain fatty acids are associated with plant residues and the HT-GC/MS chromatogram is consistent with that of plant material. The presence of the plant sterol, β -sitosterol, and the animal sterol, cholesterol, was confirmed with HT-GC/MS, however. This residue appears to primarily result from the preparation of plant material, but animal products are also present.

Two residues analyzed in 2009 were characterized by moderate-high levels of C18:1 isomers, 9MQ 38 (1070-3-2a) and

9MQ 41 (1089-10). Level of C18:0 is somewhat elevated in 9MQ 38, 17.06%, but the level of C18:2 is also elevated, 5.78%. Two biomarkers appear in the residue, azelaic acid and dehydroabietic acid, suggesting only plant products are present. The level of C18:0 is higher in 9MQ 41, 23.01%, and levels of C18:2 are fairly low, 2.36%. Significant levels of triacylglycerols occur in this residue, indicating animal products; but no lipid biomarkers were detected.

G.3.5 MEDIUM FAT CONTENT RESIDUES

Two residues analyzed in 2009 were characterized as medium fat content, 9MQ 33 (875-3-1a) and 9MQ 35 (1129-3-1a). Examples of medium fat content plant foods include mesquite, corn and cholla. Freshwater fish, terrapin, *Rabdotus* snail and late winter, fat-depleted elk are examples of medium fat content animal foods. The source of residue 9MQ 33 is ambiguous because levels of C18:0, C18:2 and medium chain fatty acids are all low; triacylglycerols are present in low amounts but no lipid biomarkers were detected. Levels of C18:0, C18:2 and medium chain fatty acids are higher in 9MQ 35, suggesting a possible plant and animal combination. This is supported by the detection of cholesterol, azelaic acid and dehydroabietic acid in the residue but no triacylglycerols were detected.

G.3.6 RESIDUES WITH LOW FATTY ACID RECOVERIES

Although three residues contained insufficient fatty acids to attempt identification, lipid biomarkers were detected using HT-GC/MS (Table G-7). Azelaic acid was detected in residue 9MQ 1 (1348-3-1a), 9MQ 6 (464-3-2a) and 9MQ 8 (1341-3-1a). As noted above, this short chain dicarboxylic acid is associated with the oxidation of unsaturated fatty acids (Regert et al. 1998). Unsaturated fatty acids are most abundant in seed oils, which

suggests that plant seeds or nuts were prepared. Dehydroabietic acid appears to be present 9MQ 1 and 9MQ 6, which confirms the presence of conifer products. The source of the conifer products is not known; they may have been introduced from firewood, resins or other conifer products. Cholesterol appears to be present in residue 9MQ 6, indicating an animal origin for the residue.

G.3.7 CONCLUDING REMARKS

Cholesterol, the lipid biomarker of animal products, occasionally appears in residues with all the characteristics of high fat content plant residues. Plant seed or nut residues typically have high levels of C18:1 isomers, elevated levels of C18:2, low levels of C18:0, trace amounts of triacylglycerols and the presence of azelaic acid. It is possible that the animal sterol was retained from a previous use.

G.4 REFERENCES CITED

- Barnard, H., A. N. Dooley and K. F. Faull
2007 Chapter 5: An Introduction to Archaeological Lipid Analysis by GC/MS. In *Theory and Practice of Archaeological Residue Analysis*, edited by H. Barnard and J. W. Eerkens, pp.42-60. British Archaeological Reports International Series 1650. Oxford, UK.
- Charters, S., R. P. Evershed, A. Quye, P. W. Blinkhorn and V. Denham
1997 Simulation Experiments for Determining the Use of Ancient Pottery Vessels: The Behaviour of Epicuticular Leaf Wax during Boiling of a Leafy Vegetable. *Journal of Archaeological Science* 24: 1-7.
- Collins M. B., B. Ellis and C. Dodt-Ellis
1990 *Excavations at the Camp Pearl Wheat Site (41KR243): An Early Archaic Campsite on Town Creek, Kerr County, Texas*. Studies in Archaeology 6. Texas Archaeological Research Laboratory, The University of Texas at Austin.
- Condamine, J., F. Formenti, M. O. Metais, M. Michel, and P. Blond
1976 The Application of Gas Chromatography to the Tracing of Oil in Ancient Amphorae. *Archaeometry* 18(2):195-201.
- Dudd, S. N. and R. P. Evershed
1998 Direct demonstration of milk as an element of archaeological economies. *Science* 282: 1478-1481.
- Eerkens, J. W.
2002 The Preservation and Identification of Pinon Resins by GC-MS in Pottery from the Western Great Basin. *Archaeometry* 44(1):95-105.
- Evershed, R.P.
1993 Biomolecular Archaeology and Lipids. *World Archaeology* 25(1):74-93.
- Evershed, R. P.
2000 Biomolecular Analysis by Organic Mass Spectrometry. In *Modern Analytical Methods in Art and Archaeology*, edited by E. Ciliberto and G. Spoto, pp. 177-239. Volume 155, Chemical Analysis. John Wiley & Sons, New York.
- Evershed, R. P., C. Heron and L. J. Goad
1990 Analysis of Organic Residues of Archaeological Origin by High Temperature Gas Chromatography and Gas Chromatography-Mass Spectroscopy. *Analyst* 115:1339-1342.
- Evershed, R.P., C. Heron and L.J. Goad
1991 Epicuticular Wax Components Preserved in Potsherds as Chemical

- Indicators of Leafy Vegetables in Ancient Diets. *Antiquity* 65:540-544.
- Evershed, R. P., H. R. Mottram, S. N. Dudd, S. Charters, A. W. Stott, G. J. Lawrence, A. M. Gibson, A. Conner, P. W. Blinkhorn and V. Reeves
1997a New Criteria for the Identification of Animal Fats in Archaeological Pottery. *Naturwissenschaften* 84: 402-406.
- Evershed, R. P., S. J. Vaughn, S. N. Dudd and J. S. Soles
1997b Fuel for Thought? Beeswax in Lamps and Conical Cups from Late Minoan Crete. *Antiquity* 71: 979-985.
- Evershed, R. P., S. N. Dudd, M. J. Lockheart and S. Jim
2001 Lipids in Archaeology. In *Handbook of Archaeological Sciences*, edited by D. R. Brothwell and A. M. Pollard, pp. 331-349. John Wiley & Sons, New York.
- Folch, J., M. Lees and G. H. Sloane-Stanley
1957 A simple method for the isolation and purification of lipid extracts from brain tissue. *Journal of Biological Chemistry* 191:833.
- Frankel, E. N.
1991 Recent Advances in Lipid Oxidation. *Journal of the Science of Food and Agriculture* 54:465-511.
- Heron, C., and A.M. Pollard
1988 The Analysis of Natural Resinous Materials from Roman Amphoras. In *Science and Archaeology Glasgow 1987. Proceedings of a Conference on the Application of Scientific Techniques to Archaeology, Glasgow, 1987*, edited by E. A. Slater and J. O. Tate, pp. 429-447. BAR British Series 196 (ii), Oxford.
- Heron, C., N. Nemcek, K. M. Bonfield, J. Dixon and B. S. Ottaway
1994 The Chemistry of Neolithic Beeswax. *Naturwissenschaften* 81: 266-269.
- Loy, T.
1994 Residue Analysis of Artifacts and Burned Rock from the Mustang Branch and Barton Sites (41HY209 and 41HY202). In: *Archaic and Late Prehistoric Human Ecology in the Middle Onion Creek Valley, Hays County, Texas. Volume 2: Topical Studies*, by R. A. Ricklis and M. B. Collins, pp. 607- 627. Studies in Archeology 19, Texas Archaeological Research Laboratory, The University of Texas at Austin.
- Malainey, M. E.
1997 The Reconstruction and Testing of Subsistence and Settlement Strategies for the Plains, Parkland and Southern boreal forest. Unpublished Ph.D. thesis, University of Manitoba.
- Malainey, M. E.
2007 Chapter 7: Fatty Acid Analysis of Archaeological Residues: Procedures and Possibilities. In *Theory and Practice of Archaeological Residue Analysis*, edited by H. Barnard and J. W. Eerkens, pp. 77-89. British Archaeological Reports International Series 1650. Oxford, UK.
- Malainey, M. E., K. L. Malisza, R. Przybylski and G. Monks
2001a The Key to Identifying Archaeological Fatty Acid Residues. Paper presented at the 34th Annual Meeting of the Canadian

- Archaeological Association, Banff, Alberta, May 2001.*
- Malainey, M. E., R. Przybylski and B. L. Sherriff
1999a The Fatty Acid Composition of Native Food Plants and Animals of Western Canada. *Journal of Archaeological Science* 26:83-94.
- Malainey, M. E., R. Przybylski and B. L. Sherriff
1999b The Effects of Thermal and Oxidative Decomposition on the Fatty Acid Composition of Food Plants and Animals of Western Canada: Implications for the Identification of archaeological vessel residues. *Journal of Archaeological Science* 26:95-103.
- 1999c Identifying the former contents of Late Precontact Period pottery vessels from Western Canada using gas chromatography. *Journal of Archaeological Science* 26(4):425-438.
- 2001b One Person's Food: How and Why Fish Avoidance May Affect the Settlement and Subsistence Patterns of Hunter-Gatherers. *American Antiquity* 66(1):141-161.
- Malainey, M.E., R. Przybylski and G. Monks
2000a The identification of archaeological residues using gas chromatography and applications to archaeological problems in Canada, United States and Africa. Papers presented at *The 11th Annual Workshops in Archaeometry*, State University of New York at Buffalo, February 2000.
- 2000b Refining and testing the criteria for identifying archaeological lipid residues using gas chromatography. Paper presented at the *33rd Annual Meeting of the Canadian Archaeological Association, Ottawa, May 2000.*
- 2000c Developing a General Method for Identifying Archaeological Lipid Residues on the Basis of Fatty Acid Composition. Paper presented at the *Joint Midwest Archaeological & Plains Anthropological Conference*, Minneapolis, Minnesota, November 2000.
- Marchbanks, M. L.
1989 Lipid Analysis in Archaeology: An Initial Study of Ceramics and Subsistence at the George C. Davis Site. Unpublished M.A. thesis, The University of Texas at Austin.
- Marchbanks, M. L. and J. M. Quigg
1990 Appendix G: Organic Residue and Phytolith Analysis. In: *Phase II Investigations at Prehistoric and Rock Art Sites, Justiceburg Reservoir, Garza and Kent Counties, Texas, Volume II*, by D. K. Boyd, J. T. Abbott, W. A. Bryan, C. M. Garvey, S. A. Tomka and R. C. Fields. pp. 496-519. Reports of Investigations No. 71. Prewitt and Associates, Inc., Austin.
- Patrick, M., A. J. de Konig and A. B. Smith
1985 Gas Liquid Chromatographic Analysis of Fatty Acids in Food Residues from Ceramics Found in the Southwestern Cape, South Africa. *Archaeometry* 27(2):231-236.
- Quigg, J. M., C. Lintz, S. Smith and S. Wilcox
2000 *The Lino Site: A Stratified Late Archaic Campsite in a Terrace of the San Idelfonso Creek, Webb County, Southern Texas*. Technical Report No. 23765, TRC Mariah Associates Inc., Austin. Texas Department of Transportation, Environmental Affairs Division,

- Archaeological Studies Program
Report 20, Austin.
- Quigg, J. M., M. E. Malainey, R. Przybylski
and G. Monks
2001 No bones about it: using lipid
analysis of burned rock and
groundstone residues to examine
Late Archaic subsistence practices
in South Texas. *Plains
Anthropologist* 46(177): 283-303.
- Reber, E. A., S. N. Dudd, N. J. van der
Merwe and R. P. Evershed
2004 Direct detection of maize in pottery
residue via compound specific
stable carbon isotope analysis.
Antiquity 78: 682-691.
- Regert, M., H. A. Bland, S. N. Dudd, P. F.
van Bergen and R. P. Evershed
1998 Free and Bound Fatty Acid
Oxidation Products in
Archaeological Ceramic Vessels.
*Philosophical Transactions of the
Royal Society of London, B* 265
(1409):2027-2032.
- Regert, M.
2007 Chapter 6: Elucidating Pottery
Function using a Multi-step
Analytical Methodology combining
Infrared Spectroscopy,
Chromatographic Procedures and
Mass Spectrometry. In *Theory and
Practice of Archaeological Residue
Analysis*, edited by H. Barnard and
J. W. Eerkens, pp. 61-76. British
Archaeological Reports
International Series 1650. Oxford,
UK.
- Sauter, F., E.W.H. Hayek, W. Moche and U.
Jordis
1987 Betulin aus archäologischem
Schwelteer. *Z. für Naturforsch* 42c
(11-12):1151-1152.
- Shackley, M.
1982 Gas Chromatographic Identification
of a Resinous Deposit from a 6th
Century Storage Jar and Its Possible
Identification. *Journal of
Archaeological Science* 9:305-306.
- Skibo, J. M.
1992 *Pottery Function: A Use-Alteration
Perspective*. Plenum Press, New
York.
- Solomons, T. W. G.
1980 *Organic Chemistry*. John Wiley &
Sons, Toronto.

Table G-1. Summary of average fatty acid compositions of modern food groups generated by hierarchical cluster analysis.

Cluster	A				B						C				
Subcluster	I	II	III	IV	V	VI	VII	VIII	IX	X	XI	XII	XIII	XIV	XV
Type	Mammal Fat and Marrow	Large Herbivore Meat	Fish	Fish	Berries and Nuts	Mixed	Seeds and Berries	Roots	Seeds	Mixed	Greens	Berries	Roots	Greens	Roots
C16:0	19.90	19.39	16.07	14.10	3.75	12.06	7.48	19.98	7.52	10.33	18.71	3.47	22.68	24.19	18.71
C18:0	7.06	20.35	3.87	2.78	1.47	2.36	2.58	2.59	3.55	2.43	2.48	1.34	3.15	3.66	5.94
C18:1	56.77	35.79	18.28	31.96	51.14	35.29	29.12	6.55	10.02	15.62	5.03	14.95	12.12	4.05	3.34
C18:2	7.01	8.93	2.91	4.04	41.44	35.83	54.69	48.74	64.14	39.24	18.82	29.08	26.24	16.15	15.61
C18:3	0.68	2.61	4.39	3.83	1.05	3.66	1.51	7.24	5.49	19.77	35.08	39.75	9.64	17.88	3.42
VLCS	0.16	0.32	0.23	0.15	0.76	4.46	2.98	8.50	5.19	3.73	6.77	9.10	15.32	18.68	43.36
VLCU	0.77	4.29	39.92	24.11	0.25	2.70	1.00	2.23	0.99	2.65	1.13	0.95	2.06	0.72	1.10

VLCS- Very Long Chain (C20, C22 and C24) Saturated Fatty Acids

VLCU - Very Long Chain (C20, C22 and C24) Unsaturated Fatty Acids

Table G-2. Criteria for the Identification of Archaeological Residues Based on the Decomposition Patterns of Experimental Cooking Residues Prepared in Pottery Vessels.

Identification	Medium Chain	C18:0	C18:1 isomers
Large herbivore	≤ 15%	≥ 27.5%	≤ 15%
Large herbivore with plant or Bone marrow	low	≥ 25%	15% ≤ X ≤ 25%
Plant with large herbivore	≥ 15%	≥ 25%	no data
Beaver	low	Low	≥ 25%
Fish or Corn	low	≤ 25%	15% ≤ X ≤ 27.5%
Fish or Corn with Plant	≥ 15%	≤ 25%	15% ≤ X ≤ 27.5%
Plant (except corn)	≥ 10%	≤ 27.5%	≤ 15%

Table G-3. List of Burned Rock and Pottery Samples Analyzed in 2008.

Lab No.	Site	Catalogue Number	Feature	Provenience	Description	Sample Size (g)
8MQ 1	41PT245	353-003-1a	2	TU4, bulk, 130-136 cmbs	Burned rock	46.135
8MQ 2	41PT245	353-003-2a	2	TU4, bulk, 130-136 cmbs	Burned rock	26.429
8MQ 3	41PT245	353-003-3a	2	TU4, bulk, 130-136 cmbs	Burned rock	34.229
8MQ 4	41PT245	353-003-4a	2	TU4, bulk, 130-136 cmbs	Burned rock	32.456
8MQ 5	41PT185/A	112-003-1a	2	TU 8, 80-90 cmbs	Burned rock	39.695
8MQ 6	41PT185/A	112-003-2a	2	TU 8, 80-90 cmbs	Burned rock	22.988
8MQ 7	41PT185/A	112-003-3a	2	TU 8, 80-90 cmbs	Burned rock	16.753
8MQ 8	41PT185/A	112-003-4a	2	TU 8, 80-90 cmbs	Burned rock	22.994
8MQ 9	41PT185/C	214-003-1a	4	TU 23, 90-102 cmbs	Burned rock	33.665
8MQ 10	41PT185/C	214-003-2a	4	TU 23, 90-102 cmbs	Burned rock	35.271
8MQ 11	41PT185/C	214-003-3a	4	TU 23, 90-102 cmbs	Burned rock	30.959
8MQ 12	41PT185/C	214-003-4a	4	TU 23, 90-102 cmbs	Burned rock	31.578
8MQ 13	41PT185/C	198-003-1a	3	TU 20, 85-93 cmbs	Burned rock	31.574
8MQ 14	41PT185/C	198-003-2a	3	TU 20, 85-93 cmbs	Burned rock	33.123
8MQ 15	41PT185/C	198-003-3a	3	TU 20, 85-93 cmbs	Burned rock	28.167
8MQ 16	41PT185/C	198-003-4a	3	TU 20, 85-93 cmbs	Burned rock	32.483
8MQ 17	41PT245	389-003-1a	4/5	TU 9c, 160-170 cmbs	Burned rock	38.406
8MQ 18	41PT245	398-003-2a	4/5	TU 9b, 160-170 cmbs	Burned rock	31.359
8MQ 19	41PT245	398-003-3a	4/5	TU 9c, 160-170 cmbs	Burned rock	25.932
8MQ 20	41PT245	398-003-4a	4/5	TU 9c, 160-170 cmbs	Burned rock	21.371
8MQ 21	41PT245	341-008-1a		TU 3, 10-20 cmbs	Ceramic	1.222
8MQ 22	41PT245	401-008-1a		TU 10, 0-10 cmbs	Ceramic	2.474
8MQ 23	41PT186	345-003-1a		TU 8, 155 cmbs	Burned rock	21.208

Table G-4. List of Samples from Site 41PT185/C Analyzed in 2009.

Lab No.	Catalogue Number	Feature	Provenience	Description	Sample Size (g)
9MQ 1	1348-003-1a	5	N110 E105, 50-60	Burned Rock	21.923
9MQ 2	1348-003-2a	5	N110 E105, 50-60	Burned Rock	27.465
9MQ 3	854-003-1a	6	N113 E106, 40-50	Burned Rock	25.904
9MQ 4	854-003-2a	6	N113 E106, 40-50	Burned Rock	15.140
9MQ 5	464-003-1a	8	N104 E104, 50-60	Burned Rock	16.032
9MQ 6	464-003-2a	8	N104 E104, 50-60	Burned Rock	20.241
9MQ 7	474-003-1a	8	N104 E105, 60-70	Burned Rock	26.002
9MQ 8	1341-003-1a	8	N104 E105, 50-60	Burned Rock	20.639
9MQ 9	1341-003-2a	8	N104 E105, 50-60	Burned Rock	24.257
9MQ 10	502-003-1a	9c	N104 E117, 40-50	Burned Rock	20.487
9MQ 11	502-003-2a	9c	N104 E117, 40-50	Burned Rock	23.016
9MQ 12	504-003-3a	9b	N104 E117	Burned Rock	17.440
9MQ 13	504-003-4a	9b	N104 E117	Burned Rock	23.527
9MQ 14	1340-003-1a	9b	N105 E117, 50-60	Burned Rock	17.982
9MQ 15	1340-003-2a	9b	N105 E117, 50-60	Burned Rock	23.919
9MQ 16	1332-003-1a	9c	N103 E117, 50-60	Burned Rock	23.995
9MQ 17	1337-003-1a	9b	N104 E116, 40-50	Burned Rock	19.669
9MQ 18	1337-003-2a	9b	N104 E116, 40-50	Burned Rock	14.174
9MQ 19	355-003-1a	11	N102 E104, 55-60	Burned Rock	28.812
9MQ 20	361-003-1a	11	N102 E105, 50-60	Burned Rock	14.143
9MQ 21	361-003-2a	11	N102 E105, 50-60	Burned Rock	23.899
9MQ 22	901-003-1a	12	N114 E106, 40-50	Burned Rock	17.249
9MQ 23	901-003-2a	12	N114 E106, 40-50	Burned Rock	29.909
9MQ 24	901-003-3a	12	N114 E106, 40-50	Burned Rock	18.197
9MQ 25	712-010-1a	13	N110 E106, 40-50	Metate frag.	18.613
9MQ 26	1234-003-1a	15a	N120 E103, 40-50	Burned Rock	19.796
9MQ 27	1234-003-2a	15a	N120 E103, 40-50	Burned Rock	23.662
9MQ 28	1181-003-1a	15b	N119 E104, 40-50	Burned Rock	25.277
9MQ 29	1181-003-2a	15b	N119 E104, 40-50	Burned Rock	27.379

Table G-4. Continued. List of Samples from Site 41PT185/C Analyzed in 2009

Lab No.	Catalogue Number	Feature	Provenience	Description	Sample Size (g)
9MQ 30	1181-003-3a	15b	N119 E104, 40-50	Burned Rock	22.070
9MQ 31	1192-003-1a	15c	N119 E106, 40-50	Burned Rock	16.441
9MQ 32	1192-003-2a	15c	N119 E106, 40-50	Burned Rock	20.695
9MQ 33	875-003-1a	16	N114 E98, 70-80	Burned Rock	28.818
9MQ 34	875-003-2a	16	N114 E98, 70-80	Burned Rock	29.610
9MQ 35	1129-003-1a	18	N118 E105, 50-60	Burned Rock	27.599
9MQ 36	1129-003-2a	18	N118 E105, 50-60	Burned Rock	21.036
9MQ 37	1070-003-1a	19	N117 E107, 60-70	Burned Rock	28.078
9MQ 38	1070-003-2a	19	N117 E107, 60-70	Burned Rock	17.081
9MQ 39	514-010-1	N/A	N105 E98, 72 cm bs	Metate frag.	22.948
9MQ 40	1129-010	18	N118 E105	Metate frag.	36.061
9MQ 41	1089-010	N/A	N118 E97, 58 cm bs	Metate frag.	31.661
9MQ 42	406-003-1a	11	N103 E104	Burned Rock	25.661

Table G-5. Lipid Composition and Identification of Residues Analyzed in 2008.

Fatty acid	8MQ 1		8MQ 2		8MQ 3		8MQ 4	
	Area	Rel%	Area	Rel%	Area	Rel%	Area	Rel%
C12:0	12894	0.16	6365	0.09	12091	2.26	9985	0.18
C14:0	244556	2.99	194522	2.63	14547	2.72	118314	2.17
C14:1	0	0.00	0	0.00	0	0.00	0	0.00
C15:0	116656	1.43	67494	0.91	4930	0.92	58312	1.07
C16:0	2737630	33.51	2378175	32.19	145087	27.16	1919479	35.16
C16:1	5251	0.06	1374	0.02	1374	0.26	1374	0.03
C17:0	282938	3.46	228074	3.09	20914	3.91	199288	3.65
C18:0	4093125	50.10	3311584	44.82	288798	54.06	2916976	53.43
C18:1s	639953	7.83	1170559	15.84	39127	7.32	209185	3.83
C18:2	0	0.00	0	0.00	3113	0.58	0	0.00
C18:3w3	0	0.00	0	0.00	0	0.00	0	0.00
C20:0	32850	0.40	23726	0.32	4277	0.80	22967	0.42
C20:1	0	0.00	3700	0.05	0	0.00	0	0.00
C24:0	3371	0.04	2583	0.03	0	0.00	3488	0.06
Total	8169224	100.00	7388156	100.00	534258	100.00	5459368	100.00
Triacyl-glycerols	Present		Present		Trace		Present	
Sterols	Cholesterol		Cholesterol		Cholesterol and β -sitosterol		Cholesterol	
Identification	Large Herbivore		Large Herbivore		Large Herbivore and Plant		Large Herbivore	
Catalogue No.	353-003-1a		353-003-2a		353-003-3a		353-003-4a	

Table G-5 continued. Lipid Composition and Identification of Residues Analyzed in 2008.

Fatty acid	8MQ 5		8MQ 9		8MQ 12		8MQ 22	
	Area	Rel%	Area	Rel%	Area	Rel%	Area	Rel%
C12:0	12037	1.25	7905	2.44	3315	0.66	39570	3.69
C14:0	26606	2.77	11137	3.44	3556	0.70	113467	10.57
C14:1	0	0.00	0	0.00	0	0.00	10474	0.98
C15:0	8222	0.86	2145	0.66	0	0.00	63416	5.91
C16:0	358973	37.33	75852	23.42	89497	17.71	360220	33.56
C16:1	108	0.01	40748	12.58	4013	0.79	8255	0.77
C17:0	27410	2.85	3722	1.15	0	0.00	14075	1.31
C18:0	383047	39.83	32937	10.17	16763	3.32	78660	7.33
C18:1s	133402	13.87	139178	42.98	320257	63.38	330147	30.76
C18:2	11795	1.23	10208	3.15	65444	12.95	46989	4.38
C18:3w3	0	0.00	0	0.00	0	0.00	3280	0.31
C20:0	0	0.00	0	0.00	52	0.01	1106	0.10
C20:1	0	0.00	0	0.00	2415	0.48	0	0.00
C24:0	0	0.00	0	0.00	0	0.00	3663	0.34
Total	961600	100.00	323832	100.00	505312	100.00	1073322	100.00
Triacyl-glycerols	Trace		Trace/Absent		Trace		Trace/Absent	
Sterols	Cholesterol and β -sitosterol		β -sitosterol and Cholesterol		β -sitosterol		β -sitosterol and Cholesterol	
Identification	Large Herbivore and Plant		High Fat Content Plant with trace of animal products		Nuts or Seeds, Very High Fat Content Plant		Moderately-high fat content Residue containing Plant and Animal products	
Catalogue No.	112-003-1a		214-003-1a		214-003-4a		401-003-1a	

Table G-6. Lipid Composition and Identification of Residues Analyzed in 2009.

Fatty acid	9MQ 2		9MQ 3		9MQ 4		9MQ 5	
	Area	Rel%	Area	Rel%	Area	Rel%	Area	Rel%
C12:0	11385	2.60	2979	0.36	0	0.00	7564	1.91
C14:0	11775	2.69	10261	1.26	4986	0.93	9347	2.37
C14:1	0	0.00	3781	0.46	0	0.00	0	0.00
C15:0	5549	1.27	5096	0.62	4641	0.86	4067	1.03
C16:0	24451	5.59	121470	14.87	48600	9.02	45907	11.62
C16:1	10187	2.33	13943	1.71	21880	4.06	5108	1.29
C17:0	1229	0.28	1385	0.17	763	0.14	1596	0.40
C17:1	3304	0.76	3022	0.37	2484	0.46	3070	0.78
C18:0	0	0.00	12970	1.59	7291	1.35	61762	15.63
C18:1s	301375	68.89	507906	62.18	380244	70.56	211534	53.55
C18:2	61794	14.12	117329	14.36	49303	9.15	36888	9.34
C18:3s	0	0.00	1247	0.15	3436	0.64	0	0.00
C20:0	1582	0.36	2791	0.34	2946	0.55	2873	0.73
C20:1	3823	0.87	6712	0.82	7903	1.47	2311	0.59
C24:0	1030	0.24	1418	0.17	1895	0.35	3007	0.76
C24:1	0	0.00	4482	0.55	2556	0.47	0	0.00
Total	437484	100.00	816792	100.00	538928	100.00	395034	100.00
Triacyl-glycerols	Trace		Trace/Present		Trace/Present		Trace	
Lipid Biomarkers	Azelaic acid		None Detected		Dehydroabietic acid		Azelaic acid; Dehydroabietic acid	
Identification	Very High Fat Content Plant (Seeds/Nuts)		Very High Fat Content Plant (Seeds/Nuts)		Very High Fat Content Plant (Seeds/Nuts); conifer products present		Very High Fat Content Plant (Seeds/Nuts); conifer products present	
Catalogue No.	1348-003-2a		854-003-1a		854-003-2a		464-003-1a	

Table G-6. continued. Lipid Composition and Identification of Residues Analyzed in 2009.

Fatty acid	9MQ 7		9MQ 9		9MQ 11		9MQ 12	
	Area	Rel%	Area	Rel%	Area	Rel%	Area	Rel%
C12:0	8720	1.36	7166	2.24	5371	0.76	2979	0.67
C14:0	13236	2.06	11269	3.52	17083	2.41	11823	2.66
C14:1	0	0.00	0	0.00	0	0.00	2407	0.54
C15:0	9079	1.41	6740	2.11	7634	1.08	8066	1.82
C16:0	125988	19.59	27137	8.48	213281	30.12	113516	25.55
C16:1	18908	2.94	8110	2.54	10467	1.48	11575	2.60
C17:0	3855	0.60	2496	0.78	3691	0.52	2644	0.60
C17:1	3481	0.54	3783	1.18	5348	0.76	2937	0.66
C18:0	40094	6.23	42223	13.20	87369	12.34	28901	6.50
C18:1s	307373	47.79	171097	53.49	289322	40.86	220991	49.73
C18:2	53632	8.34	27902	8.72	47652	6.73	24201	5.45
C18:3s	29078	4.52	0	0.00	452	0.06	0	0.00
C20:0	4583	0.71	2887	0.90	6882	0.97	4216	0.95
C20:1	18496	2.88	4372	1.37	5644	0.80	3725	0.84
C24:0	3160	0.49	2426	0.76	4553	0.64	3821	0.86
C24:1	3444	0.54	2289	0.72	3398	0.48	2566	0.58
Total	643127	100.00	319897	100.00	708147	100.00	444368	100.00
Triacyl-glycerols	Trace		Trace		Present		Trace	
Lipid Biomarkers	Azelaic acid; Dehydroabietic acid		Cholesterol		Cholesterol; β-sitosterol		Cholesterol; Dehydroabietic acid	
Identification	High Fat Content Plant (Seeds/Nuts); conifer products present		Very High Fat Content Plant (Seeds/Nuts) with trace of animal products		High Fat Content Plant (Seeds/Nuts) with trace of animal products		Borderline High and Very High Fat Content Plant (Seeds/Nuts) with trace of animal products; conifer products present	
Catalogue No.	474-003-1a		1341-003-2a		502-003-2a		504-005-3a	

Table G-6. continued. Lipid Composition and Identification of Residues Analyzed in 2009.

Fatty acid	9MQ 13		9MQ 14		9MQ 15		9MQ 16	
	Area	Rel%	Area	Rel%	Area	Rel%	Area	Rel%
C12:0	3976	1.19	3184	0.61	3824	0.46	4481	0.62
C14:0	11829	3.55	7217	1.39	6432	0.77	14011	1.93
C14:1	0	0.00	0	0.00	0	0.00	0	0.00
C15:0	5796	1.74	6125	1.18	4825	0.58	6530	0.90
C16:0	110722	33.21	114488	22.03	80445	9.67	186040	25.60
C16:1	9152	2.75	13550	2.61	18765	2.25	11484	1.58
C17:0	4174	1.25	3229	0.62	2605	0.31	6350	0.87
C17:1	3364	1.01	0	0.00	4547	0.55	4314	0.59
C18:0	36533	10.96	36560	7.03	11316	1.36	185332	25.50
C18:1s	129323	38.79	268296	51.62	567672	68.20	244662	33.66
C18:2	18485	5.55	64465	12.40	126730	15.23	44221	6.08
C18:3s	0	0.00	0	0.00	0	0.00	5790	0.80
C20:0	0	0.00	0	0.00	0	0.00	6948	0.96
C20:1	0	0.00	0	0.00	2975	0.36	3396	0.47
C24:0	0	0.00	0	0.00	0	0.00	0	0.00
C24:1	0	0.00	2595	0.50	2181	0.26	3298	0.45
Total	333354	100.00	519709	100.00	832317	100.00	726857	100.00
Triacyl-glycerols	Trace		Trace		Present		Significant	
Lipid Biomarkers	Cholesterol		Cholesterol		Cholesterol		None Detected	
Identification	High Fat Content Plant (Seeds/Nuts) with trace of animal products		Very High Fat Content Plant (Seeds/Nuts) with trace of animal products		Very High Fat Content Plant (Seeds/Nuts) with trace of animal products		Large Herbivore Bone Marrow or Flesh with Moderate-High Fat Plant	
Catalogue No.	504-003-4a		1340-003-1a		1340-003-2a		1332-003-1a	

Table G-6. continued. Lipid Composition and Identification of Residues Analyzed in 2009.

Fatty acid	9MQ 17		9MQ 18		9MQ 19		9MQ 20	
	Area	Rel%	Area	Rel%	Area	Rel%	Area	Rel%
C12:0	9287	1.64	6399	2.15	3805	0.22	0	0.00
C14:0	16756	2.96	8738	2.94	51264	3.03	5975	1.31
C14:1	2898	0.51	0	0.00	0	0.00	0	0.00
C15:0	6421	1.13	4420	1.49	19806	1.17	4023	0.88
C16:0	110968	19.61	93411	31.45	559347	33.06	134915	29.68
C16:1	9561	1.69	8620	2.90	22200	1.31	13543	2.98
C17:0	4770	0.84	2465	0.83	44066	2.60	1824	0.40
C17:1	4278	0.76	3695	1.24	6171	0.36	2274	0.50
C18:0	172720	30.52	30239	10.18	530793	31.37	33275	7.32
C18:1s	202271	35.74	114574	38.57	365639	21.61	211865	46.61
C18:2	16469	2.91	11620	3.91	57386	3.39	19163	4.22
C18:3s	0	0.00	0	0.00	0	0.00	0	0.00
C20:0	5143	0.91	4343	1.46	17924	1.06	5672	1.25
C20:1	2286	0.40	4412	1.49	10154	0.60	13644	3.00
C24:0	0	0.00	4092	1.38	0	0.00	4075	0.90
C24:1	2107	0.37	0	0.00	3221	0.19	4338	0.95
Total	565935	100.00	297028	100.00	1691776	100.00	454586	100.00
Triacyl-glycerols	Trace		Trace		Trace		Trace/Present	
Lipid Biomarkers	None Detected		Cholesterol; β-sitosterol		Dehydroabietic acid; Cholesterol; β-sitosterol		Dehydroabietic acid	
Identification	Large Herbivore-Fatty Meat or with Moderate-High Fat Content Plants		High Fat Content Plant (Seeds/Nuts) with trace of animal products		Large Herbivore and Medium Fat Content Plants; conifer products present		High Fat Content Plant (Seeds/Nuts); conifer products present	
Catalogue No.	1337-003-1a		1337-003-2a		355-003-1a		361-003-1a	

Table G-6. continued. Lipid Composition and Identification of Residues Analyzed in 2009.

Fatty acid	9MQ 21		9MQ 22		9MQ 23		9MQ 24	
	Area	Rel%	Area	Rel%	Area	Rel%	Area	Rel%
C12:0	2811	0.62	8278	2.15	4408	0.55	9574	1.05
C14:0	10614	2.33	11542	3.00	9469	1.18	14923	1.64
C14:1	3397	0.75	0	0.00	3931	0.49	2714	0.30
C15:0	6241	1.37	5647	1.47	4652	0.58	6887	0.76
C16:0	146105	32.11	88797	23.09	206397	25.79	199851	21.92
C16:1	12329	2.71	12405	3.23	23066	2.88	6405	0.70
C17:0	5275	1.16	4270	1.11	3016	0.38	5826	0.64
C17:1	7368	1.62	4894	1.27	3132	0.39	3287	0.36
C18:0	35595	7.82	47332	12.31	35827	4.48	239469	26.26
C18:1s	192880	42.39	165020	42.91	429816	53.70	376415	41.28
C18:2	22123	4.86	19011	4.94	76706	9.58	46576	5.11
C18:3s	1418	0.31	0	0.00	0	0.00	0	0.00
C20:0	0	0.00	5553	1.44	0	0.00	0	0.00
C20:1	5277	1.16	4581	1.19	0	0.00	0	0.00
C24:0	0	0.00	4589	1.19	0	0.00	0	0.00
C24:1	3575	0.79	2661	0.69	0	0.00	0	0.00
Total	455008	100.00	384580	100.00	800420	100.00	911927	100.00
Triacyl-glycerols	Trace		Trace		Significant		Highly Significant	
Lipid Biomarkers	Cholesterol; β-sitosterol; Dehydroabietic acid		Cholesterol; β-sitosterol		Cholesterol; β-sitosterol		Cholesterol; Dehydroabietic acid	
Identification	High Fat Content Plant (Seeds/Nuts) with trace of animal products; conifer products present		High Fat Content Plant (Seeds/Nuts) with trace of animal products		Very High Fat Content Plant and Animal Combination		Large Herbivore Bone Marrow or Flesh with High Fat Plant; conifer products present	
Catalogue No.	361-003-2a		901-003-1a		901-003-2a		901-003-3a	

Table G-6. continued. Lipid Composition and Identification of Residues Analyzed in 2009.

Fatty acid	9MQ 25		9MQ 27		9MQ 28		9MQ 29	
	Area	Rel%	Area	Rel%	Area	Rel%	Area	Rel%
C12:0	17766	0.96	3885	0.73	9176	1.01	8201	1.50
C14:0	28024	1.51	5847	1.10	24109	2.65	8574	1.57
C14:1	2072	0.11	0	0.00	0	0.00	2400	0.44
C15:0	11008	0.59	4061	0.77	12688	1.39	4989	0.92
C16:0	391090	21.05	105895	20.01	264515	29.07	122295	22.43
C16:1	23398	1.26	12792	2.42	4553	0.50	13353	2.45
C17:0	10448	0.56	0	0.00	32403	3.56	1857	0.34
C17:1	5051	0.27	3522	0.67	2757	0.30	3106	0.57
C18:0	543757	29.27	38412	7.26	307005	33.74	61268	11.24
C18:1s	769965	41.45	314896	59.49	238800	26.25	272047	49.90
C18:2	49264	2.65	39424	7.45	11442	1.26	39184	7.19
C18:3s	5759	0.31	598	0.11	0	0.00	1708	0.31
C20:0	0	0.00	0	0.00	0	0.00	0	0.00
C20:1	0	0.00	0	0.00	2438	0.27	6211	1.14
C24:0	0	0.00	0	0.00	0	0.00	0	0.00
C24:1	0	0.00	0	0.00	0	0.00	0	0.00
Total	1857602	100.00	529332	100.00	909886	100.00	545193	100.00
Triacyl-glycerols	Present		None Detected		Highly Significant		Trace	
Lipid Biomarkers	None Detected		None Detected		Cholesterol		β-sitosterol	
Identification	Large Herbivore-Fatty Meat or with High Fat Content Plants		Very High Fat Content Plant (Seeds/Nuts)		Large Herbivore-Fatty Meat or with Moderate-High Fat Content Plants		Borderline High and Very High Fat Content Plant (Seeds/Nuts)	
Catalogue No.	712-010-1a, metate		1234-003-2a		1181-003-1a		1181-003-2a	

Table G-6. continued. Lipid Composition and Identification of Residues Analyzed in 2009.

Fatty acid	9MQ 30		9MQ 31		9MQ 32		9MQ 33	
	Area	Rel%	Area	Rel%	Area	Rel%	Area	Rel%
C12:0	8538	0.82	8950	2.40	3139	0.77	14073	0.17
C14:0	12841	1.24	8389	2.25	8468	2.09	212612	2.57
C14:1	2375	0.23	0	0.00	2612	0.64	0	0.00
C15:0	6919	0.67	3986	1.07	4073	1.00	90761	1.10
C16:0	152480	14.69	56519	15.14	81978	20.19	5576682	67.35
C16:1	26195	2.52	7353	1.97	0	0.00	0	0.00
C17:0	6204	0.60	252	0.07	0	0.00	179578	2.17
C17:1	5901	0.57	0	0.00	4081	1.01	12400	0.15
C18:0	96049	9.25	31883	8.54	81845	20.16	714497	8.63
C18:1s	601662	57.97	219447	58.80	192057	47.31	1415668	17.10
C18:2	107517	10.36	29633	7.94	24824	6.12	38462	0.46
C18:3s	2757	0.27	0	0.00	2866	0.71	0	0.00
C20:0	0	0.00	0	0.00	0	0.00	0	0.00
C20:1	5098	0.49	4436	1.19	0	0.00	25422	0.31
C24:0	0	0.00	0	0.00	0	0.00	0	0.00
C24:1	3357	0.32	2362	0.63	0	0.00	0	0.00
Total	1037893	100.00	373210	100.00	405943	100.00	8280155	100.00
Triacyl-glycerols	Trace		None Detected		Trace		Present	
Lipid Biomarkers	Cholesterol; β-sitosterol; Dehydroabietic acid		Dehydroabietic acid		Dehydroabietic acid		None Detected	
Identification	Very High Fat Content Plant (Seeds/Nuts) with trace of animal products; conifer products present		Very High Fat Content Plant (Seeds/Nuts); conifer products present		High Fat Content Plant (Seeds/Nuts), with plant with elevated C18:0 levels or animal products; conifer products present		Medium Fat Content (ambiguous)	
Catalogue No.	1181-003-3a		1192-003-1a		1192-003-2a		875-003-1a	

Table G-6. continued. Lipid Composition and Identification of Residues Analyzed in 2009.

Fatty acid	9MQ 34		9MQ 35		9MQ 36		9MQ 37	
	Area	Rel%	Area	Rel%	Area	Rel%	Area	Rel%
C12:0	12565	3.16	12657	2.14	2754	0.33	4469	0.56
C14:0	13060	3.28	16432	2.78	6654	0.81	12877	1.60
C14:1	0	0.00	0	0.00	0	0.00	0	0.00
C15:0	5634	1.41	8731	1.48	4461	0.54	6912	0.86
C16:0	101986	25.61	210243	35.62	172680	20.92	218769	27.18
C16:1	11041	2.77	3631	0.62	13120	1.59	10222	1.27
C17:0	4083	1.03	6016	1.02	2736	0.33	3692	0.46
C17:1	6447	1.62	13398	2.27	7207	0.87	9005	1.12
C18:0	44031	11.06	118449	20.07	139358	16.88	115783	14.39
C18:1s	178978	44.94	134426	22.77	370199	44.85	327705	40.72
C18:2	18952	4.76	21277	3.60	84734	10.26	51335	6.38
C18:3s	1479	0.37	9944	1.68	153	0.02	13512	1.68
C20:0	0	0.00	6487	1.10	5082	0.62	6945	0.86
C20:1	0	0.00	16163	2.74	14272	1.73	18008	2.24
C24:0	0	0.00	6030	1.02	0	0.00	0	0.00
C24:1	0	0.00	6391	1.08	2081	0.25	5593	0.69
Total	398256	100.00	590275	100.00	825491	100.00	804827	100.00
Triacyl-glycerols	Trace/Present		None Detected		Significant		Present	
Lipid Biomarkers	Dehydroabietic acid		Cholesterol; Azelaic acid; Dehydroabietic acid		β-sitosterol; Azelaic acid; Dehydroabietic acid		Cholesterol; Azelaic acid	
Identification	High Fat Content Plants (Seeds/Nuts); conifer products present		Medium Fat Content Plant and Animal Combination; conifer products present		High Fat Content Plants (Seeds/Nuts) and Animal Products; conifer products present		High Fat Content Plants (Seeds/Nuts) with Animal Products	
Catalogue No.	875-003-2a		1129-003-1a		1129-003-2a		1070-003-1a	

Table G-6. continued. Lipid Composition and Identification of Residues Analyzed in 2009.

Fatty acid	9MQ 38		9MQ 39		9MQ 40	
	Area	Rel%	Area	Rel%	Area	Rel%
C12:0	7401	1.55	5174	0.40	5513	0.57
C14:0	9732	2.04	19177	1.49	17806	1.83
C14:1	0	0.00	4194	0.32	3075	0.32
C15:0	5321	1.12	6830	0.53	8458	0.87
C16:0	138044	29.00	392378	30.40	304902	31.36
C16:1	8717	1.83	7138	0.55	18159	1.87
C17:0	4480	0.94	9072	0.70	5429	0.56
C17:1	7331	1.54	6892	0.53	6542	0.67
C18:0	81186	17.06	439263	34.03	109482	11.26
C18:1s	167187	35.13	345975	26.80	422813	43.49
C18:2	27527	5.78	46306	3.59	68023	7.00
C18:3s	3303	0.69	0	0.00	1953	0.20
C20:0	5641	1.19	0	0.00	0	0.00
C20:1	10087	2.12	4653	0.36	0	0.00
C24:0	0	0.00	331	0.03	0	0.00
C24:1	0	0.00	3343	0.26	0	0.00
Total	475957	100.00	1290726	100.00	972155	100.00
Triacyl-glycerols	Trace		Trace		Present	
Lipid Biomarkers	Azelaic acid; Dehydroabietic acid		Dehydroabietic acid		β-sitosterol; Dehydroabietic acid	
Identification	Moderate-High Fat Content Plant (Seeds); conifer products present		Large Herbivore – Fatty Meat or with Moderate-High Fat Content Plant; conifer products present		High Fat Content Plant (Seeds/Nuts); conifer products present	
Catalogue No.	1070-003-2a		514-010-1, metate		1129-010, metate	

Table G-6. continued. Lipid Composition and Identification of Residues Analyzed in 2009.

Fatty acid	9MQ 41		9MQ 42	
	Area	Rel%	Area	Rel%
C12:0	6309	0.53	4595	0.81
C14:0	21174	1.77	9929	1.75
C14:1	0	0.00	0	0.00
C15:0	9023	0.76	4593	0.81
C16:0	371175	31.10	126891	22.41
C16:1	17490	1.47	13501	2.38
C17:0	9137	0.77	3346	0.59
C17:1	0	0.00	5236	0.92
C18:0	274655	23.01	117850	20.81
C18:1s	425628	35.66	238508	42.12
C18:2	28167	2.36	23972	4.23
C18:3s	3019	0.25	0	0.00
C20:0	8574	0.72	5138	0.91
C20:1	10077	0.84	10444	1.84
C24:0	6412	0.54	0	0.00
C24:1	2688	0.23	2192	0.39
Total	1193528	100.00	566195	100.00
Triacyl-glycerols	Significant		Trace	
Lipid Biomarkers	None Detected		None Detected	
Identification	Moderate-High Fat Content, animal or possible animal and plant combination		High Fat Content Plant (Seeds/Nuts), with plant with elevated C18:0 levels or animal products	
Catalogue No.	1089-010, metate		406-3-1a	

Table G-7. Results from Residues with Low Levels of Fatty Acids.

Lab No.	Catalogue No.	Biomarker	Identification
9MQ 1	1348-003-1a	Azelaic acid; Dehydroabietic acid	Possibly plant seeds or nuts; Conifer products present
9MQ 6	464-003-2a	Cholesterol derivative; Dehydroabietic acid; Azelaic acid	Animal products confirmed; Possibly plant seeds or nuts; Conifer products present
9MQ 8	1341-003-1a	Azelaic acid	Possibly plant seeds or nuts

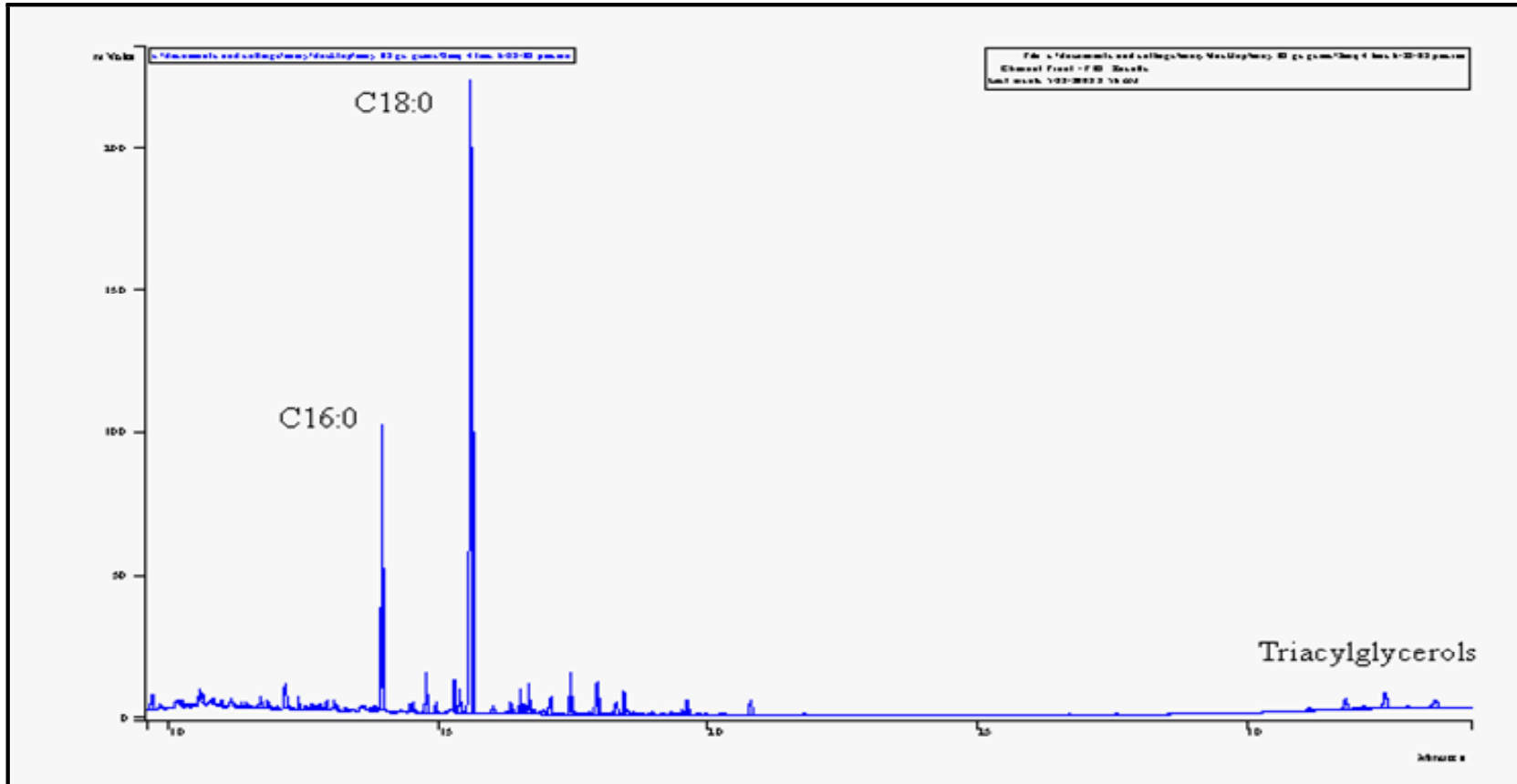


Figure G-1. Chromatogram of Residue 8MQ4 using High Temperature Gas Chromatography.

APPENDIX H

STABLE ISOTOPE ANALYSIS ON BISON BONES

This page intentionally left blank.

STABLE ISOTOPE ANALYSIS ON BISON BONES

Prepared for:



**TRC Environmental Corporation
505 East Huntland Drive, Suite 250
Austin, Texas 78752**

Prepared by:

**Geochron Laboratories:
A Division of Krueger Enterprises, Inc.
Billerica, Massachusetts 01821**

This page intentionally left blank.

Table H-1. Stable Isotope Analyses on Bison Bone Elements by Time Period.

Age Groups, Catalog No.	Bone Element	Submitted Bone Wt. (g)	Geochron Lab. No. CNR-	$\delta^{13}\text{C}$ (‰)	$\delta^{15}\text{N}$ (‰)
Protohistoric (<300 B.P.) (o)					
41PT186 #260-002-1a	long bone	10	115897	-8.4	5.9
41PT186 #261-002-1b**	immature bison radius	8	115898	-8.4	5.7
41PT186 #261-002-2a	proximal tibia	6	115899	-10.6, -10.0	3.7
41PT186 #261-002-3a	distal metacarpal	12	115900	-9.2	3.2
41PT245 #357-002-1b	long bone	13	115901	-8.1	5.1
Average				-8.8	4.72
Plains Village (500 - 800 B.P.) (●)					
41PT185 #263-002-1a	rib fragment	11	115902	-9.9	4.3
41PT186 #325-002-1a	distal tibia	19	115903	-8.4	5.6
41PT186 #326-002-1a	long bone	9	115904	-8.6	3.1
41PT186 #343-002-2a	mature rib head	23	115905	-9.5	3.6
41PT186 #345-002-1a	skull fragment	25	115906	-10.3	3.2
Average				-9.34	4.6
Palo Duro/Woodland (1200 - 1500 B.P.) (Δ)					
41PT245 #353-002-1a	rib fragment	13	115907	-8.2	6.7
41PT245 #353-002-2a	immature mandible	3	115908	-8.3	6.8
41PT245 #364-002-1a	long bone	6	115909	-10.3	4.9
41PT245 #416-002-1c	long bone	8	115910	-15.6*	6.5
41PT245 #417-002-1b**	long bone	17	115911	-9.2	3.5
Average				-8.95	5.84
Late Archaic (2200 - 2750 B.P.) (■)					
41PT185/A #157-002-1b	distal tibia	7	115912	-9.2	3.5
41PT185/C #210-002-1b**	metacarpal	9	115913	-10.7	4.9
41PT185/C #221-002-1a	distal metapodial	10	115914	-9.8	5.0
41PT185/C #236-002-1b**	radius	20	115915	-9.3	6.9
41PT185/C #261-002-1b	immature radius	12	115916	-9.1	-7.6*
Average				-9.62	5.07
* questionable value from lab and value dropped from average.					
** bone was also radiocarbon dated					

This page intentionally left blank.

APPENDIX I

**PETROGRAPHIC ANALYSIS OF ABORIGINAL CERAMICS FROM
THE BLM LANDIS PROPERTY, TEXAS PANHANDLE**

This page intentionally left blank.

**PETROGRAPHIC ANALYSIS OF ABORIGINAL CERAMICS FROM THE
BLM LANDIS PROPERTY, TEXAS PANHANDLE**

Prepared for:



**TRC Environmental Corporation
505 East Huntland Drive, Suite 250
Austin, Texas 78752**

Prepared by:

**David G. Robinson, Ph.D.
Austin, Texas**

This page intentionally left blank.

I.1 INTRODUCTION

A petrographic analysis was performed on the aboriginal ceramics from three sites in Potter County, the Texas Panhandle (41PT185, 41PT186 and 41PT245). The principal work of the analysis was performed in April and May 2008, with follow-on work performed in February 2009. The work had three branches: (1) thin-section analysis of ceramic sherds, (2) thin-section analysis of sediment samples, and (3) wet mount analysis of sherd fragments too small to be made into thin-sections. The ceramic thin-section analysis was conducted on six sections prepared from the pottery. Three small sherd fragments were studied by wet mount analysis. The first point of interest in the ceramics lay in their typological variance from Borger Cordmarked pottery, the Woodland-based pottery that dominates Panhandle Antelope Creek focus assemblages. The ceramics were all very small sherds, and beyond their distinction from Borger Cordmarked little typological information is known about them. Further, the block excavation at site 41PT186 dates to the Protohistoric period (ca. 200 to 300 B.P.), thus the artifacts from this block may belong to the Tierra Blanca complex. As well, the thin-sectioned sherd from the site, #343-008-1b, had a corrugated exterior, giving it a very strong likelihood of being imported from the Southwest, either by trade or direct transport. One wet mount analysis sherd fragment, #443-008-1, also came from the site. Although very small, it lacked evidence of the corrugated surface treatment.

Eleven sediment samples formed into thin-sections were studied for comparisons with the ceramic sections. The sediment samples came from sites 41PT185 and 41PT186 in Potter County and from seven other collection localities spread throughout the Texas Panhandle region.

I.1.1 RESEARCH QUESTIONS

The first major research question is, if the pottery is other than Borger Cordmarked, what then are its typological affinities? A second related question is, is this an aberrant type or types locally manufactured or transported into the sites? And, if the ceramics were transported, do they also offer clues to the mechanism of transport, such as trade? Also, could these ceramics hail regionally from a mobile hunter-gatherer culture rather than from the village farming societies that produced Borger Cordmarked pottery? Lastly, is the typologically Southwestern corrugated sherd from 41PT186 distinct from the other analyzed sherds and samples in its paste and other physical traits?

I.1.2 PASTE GROUPS

The best way to examine or address the research questions is first to determine through petrographic analysis the ceramic composition of the sections and then to define groupings of the ceramics according to similarities of paste materials and structures. These paste groups can be compared to paste groups in published ceramic petrographic studies.

I.1.3 SEDIMENT SAMPLES

The study of nonceramic sediments in thin-sections can give direct optical identification of minerals and other particles that may have been used as resources in the ceramic pastes. Such identifications may give fairly close identifications of the locales of manufacture of the ceramics, thus information on the principal research questions. The eleven sediment samples were a combination of soil samples collected from trenches and clay samples from clay deposits and stream sediments.

I.1.4 WET MOUNT ANALYSIS OF SHERD FRAGMENTS

Wet mount analysis allows stereoscopic microscope examination of ceramic sherd fragments too small to be formed into thin-

sections. Three sherds from two sites presented this dilemma to the analysis. The sherds came from 41PT185 (#850-008-1 and #915-008-1) and 41PT186 (#443-008-1). The goal of the wet mount analysis was to gain paste temper identifications that would allow comparisons to the paste groups defined by the thin-section analysis. Paste texture, sherd thickness, exterior surface finish, paste color, and interior and exterior colors were recorded also to gain additional comparative and descriptive data on the sherd fragments.

I.2 METHODOLOGY

I.2.1 PETROGRAPHIC THIN-SECTION ANALYSIS

I.2.1.1 Microscopy and Point Counting

The principal method of the analysis was identification and point-counting of minerals and ceramic structures following the method of Chayes (1949) and the approach to petrographic analysis pioneered in archeology by Shepard (1942, 1954). The thin-sections were prepared by National Petrographic Service, Inc. in Houston. The microscopic analysis was performed at the Texas Archeological Research Laboratory, microscopy lab, on an Olympus stereographic microscope.

Point counting is a standard procedure that offers replicable results; it amounts to counting a set number (200 in this case) of ceramic attributes observed in the viewing field during systematic microscopic traverses of each thin-section. Counting the same number of ceramic attributes in each thin-section allows reliable statistical comparisons. As a practical matter, however, some of the ceramics failed to offer sufficient area in the section to achieve the 200 count. In no case did the total count fall below 100. Proportional comparisons of the section materials remain valid at this level. If counts had fallen below 100, the section would have

been removed from the analysis. Counted attributes included the ceramic fabric “matrix”, pore space, and discrete inclusions such as crushed minerals and sand. Additional information such as grain size and shape was recorded on the counting sheet for potential future reference. The color and isotropy of the ceramic matrix was determined and recorded. Any mineral species that was observed in the viewing field but did not fall into the count was recorded as “tr” for trace, so as not to lose information on rare but potentially significant bodies.

I.2.2 SEDIMENT SAMPLE ANALYSIS

The eleven sediment samples were analyzed more qualitatively. As their unconsolidated material was mixed and stirred into setting resin, the validity of a point count was thought potentially to be compromised. Instead, a particle density measurement of each section was made by comparison with visual percentage estimation charts developed and published by Folk (1951) and Terry and Chilingar (1955). As with the ceramic sections, matrix color and isotropy were recorded as well as mineral particle sizes and shapes.

I.2.3 WET MOUNT ANALYSIS

Also known as watch-glass analysis, a wet mount analysis submerges in water material crushed or broken from a specimen. A watch glass or microscope slide contains the wet mixture for convenient microscopy. One of the specimens, 41PT186 #443-008-1, was designated for Instrumental Neutron Activation Analysis (INAA), and so was manipulated only by cleaned steel instruments and mounted using distilled water on a sterile microscope slide. After analysis, the mount and sherd dried under a covering of cellophane in order to avoid dust contamination. After drying, the crushed material and remnant sherd were sealed in a container. The wet mount analysis was performed with a Nikon

stereoscopic microscope in the TRC laboratory in Austin.

I.2.4 OBSERVATIONAL CONVENTIONS

Rock fragments were common components of the sections. The rock minerals commonly comprise granite (quartz, feldspars and biotite), but as rocks are commonly determined on textural relations, the rocks were designated Rock A and Rock B, their petrology termed granitic. The rock fragments in the sections are reduced in size as part of the ceramic manufacturing process, so it was thought better to avoid unsupportable assumptions about petrogenesis.

Another convention was the variable treatment of biotite. This was so as the mineral occurred in the sections in two forms; the first very fine to medium lathes and strips of the mineral; and the second medium to coarse masses of mineral, frequently integrated into rock fragments. It is likely that these two forms of the same mineral had different origins in the material, one in the original clay and the other in the crushed rock temper. It is more informative therefore to track these bodies separately through the collection although they are the same mineral.

I.3 OBSERVATIONS AND FINDINGS

I.3.1 THIN-SECTION ANALYSIS

The point-count analysis of the six ceramic thin-sections showed them all to have clay pastes with volcanic-derived inclusions and crushed granitic rock tempering agents. The results are reported in Table I-1. The matrixes of all the sherds were isotropic; therefore that variable was left off the table. The implications of isotropic matrixes are that the ceramics were formed in low earthenware firings with heating insufficient to reform the clay minerals into more homogeneous structures that pattern the behavior of light

transmitted through them, or in other words, to render them anisotropic.

Within this overall suite of ceramic materials, three paste groups can be discerned. The groups are classified on the basis of significant material variations, and are described below.

I.3.2 PASTE GROUP CLASSIFICATION AND DESCRIPTIONS

Paste Group 1

Thin-sections:

41PT245 #340-008-2, thin, gray plain exterior

41PT245 #340-008-3, thin, gray plain exterior

41PT245 #341-008-1b, thin, gray plain exterior

The matrix is dark and of moderate density, containing pore spaces in jagged strips (Figure I-1). The tempering agent is Rock A, a crushed granitic rock formed of quartz, microcline feldspar and biotite. Fine-sized subrounded and subangular quartz grains and fine-sized lathes of biotite may have been resident in the original clay material. Orthoclase feldspar and pyroxene are incidental members of the group.

Paste Group 2

Thin-sections:

41PT245 #378-008-1, thin, dark gray to black exterior

41PT245 #401-008-1e, polished red plain exterior

The group has a moderately dense, dark matrix with jagged pore strips (Figures I-2 and I-4). Crushed granitic rock tempered the clay paste and contributed additional grains of quartz, feldspar and biotite to the mass. The group distinguishes itself from Paste Group 1 in

having ferric hematite particles in the matrix. These may have been clay residents; their presence may mark the use of a clay source different from that of Paste Group 1. Similar proportions of all the group's minerals indicate that the two sections may have come from the same ceramic vessel.

Paste Group 3

Thin-section:

41PT186 #343-008-1b, dark grayish to brown corrugated exterior

The group claims a single section. The ceramic material showed enough differences in its composition to give it distinction from the other two groups (Figure I-3). The section shows a moderately dense reddish-black matrix interrupted by jagged pore strips. Its primary distinction is its tempering with a crushed rock (Rock B) of quartz and biotite masses. The rock seems aberrant in its lack of feldspar, which is also lacking elsewhere in the section. This situation appears to be a rarity, as feldspar is nearly ubiquitous in the collection and common but variable in its distribution in the igneous rocks of the Panhandle and other regions.

I.3.3 SEDIMENT SAMPLE SECTIONS

Eleven samples of sediments were studied in thin-section as the second branch of the study. The samples were of soils and clays consolidated with setting resin and ground to produce thin-sections. The samples came from three sites on the BLM Landis Property, three additional locales in Potter County, and one sample each from Briscoe, Roberts, Donley, and Hall counties. The results are reported in Table I-2.

The BLM Landis Property trench samples have high particle densities, and the particles are mostly quartz. Two samples with clay-resident biotite lathes have fairly strong similarities with the study sections, in

particular the sample from 41PT186 and Paste Group 3. The remaining samples show only general resemblances to the ceramic matrixes from the same sites; of course, these resemblances would heighten with the addition of granitic rock tempering in the preparation of materials for a ceramic matrix. The Potter County clay (#20-004-1b) sample from Blue Creek north of Lake Meredith is highly distinctive in having lighter color, very low particle density and ferrous iron (hematite) particles. The sample is also anisotropic, perhaps signaling that it is a nearly unitary clay mineral apart from its resident particles.

The samples from the other counties comprise what may be thought of as a typical collection of natural clay sediments that may have been available to ancient potters. Three of the four samples have significant amounts of biotite lathes and masses, and two contain particles of hematite. The Roberts County Ogallala clay sample, #MQ-GC-RB, in particular, appears very similar to the ceramic matrixes in the BLM Landis Property sherds. The sample came from a locale in Government Canyon, more than fifty km from Potter County.

I.3.4 WET MOUNT ANALYSIS

Wet mount analysis is the third branch of this study. Table I-3 presents the results of this branch of the work. Additional aspects of the paste particles are discussed in the text. Descriptive colors are the correlates of the Munsell® readings.

41PT186 #443-008-1. Quartz dominates the paste and clearly comprises the tempering agent of the ceramic (Figure I-6). The mineral entered the paste in coarse and medium sizes and subangular shapes. Comparative examination of the natural gray sandstone from West Amarillo Creek valley floor showed it to have fine and very fine quartz sand particles in subrounded and rounded shapes; therefore it was not a contributor to the paste. The ceramic quartz was likely crushed and ground

from selected mineral and rock sources and added to the raw ceramic clay. The sherd has a minor fraction of very fine biotite particles distributed through the paste. The biotite appears as small black specks. The sherd is designated for INAA study.

The ceramic specimen is strikingly similar to Paste Group 3, which was defined on a single sherd from the same site, 41PT186. The wet mount specimen lacks Rock B, composed of quartz and biotite. It is thought that Rock B would be hard to distinguish from the rough paste texture or would be misidentified as quartz. Again, the lack of feldspar is signal in this paste group, in a region where feldspar is common but variable in its distribution.

41PT185/C #850-008-1. The tempering agent is medium to fine sized quartz, and a secondary particle is fine sized, opaque white feldspar (Figure I-7). A few of the feldspar particles are medium, but all are subrounded in shape. The sherd has a finely striated interior surface. The paste is of a dense texture, as would be expected in a matrix having relatively few tempering particles.

41PT185/C #915-008-1. The tempering agent is coarse to medium feldspar in small quantities (Figure I-8). Quartz was observed in lesser amounts. Particle C is carbonate strands, probable caliche, which may have formed post-depositionally along the joint planes of the platy layers of the paste matrix. The platy layers are pronounced, and the white strands of carbonate accentuate them. Particles of temper interrupt the plates and their lines, suggesting that the plate like layers formed during firing. This platy matrix structure is uncommon among earthenware ceramics and currently lacks a satisfying technical explanation.

Both of the sherd fragments from 41PT185/C fail to fall easily into any defined paste group as they are tempered with quartz and feldspar in varying proportions. Their pastes would

compare potentially with several regional pastes, but they lack any distinctive marker such as hematite or biotite that would permit a more affirmative attribution.

I.4 COMPARISONS AND DISCUSSION

The ceramic pastes and their crushed rock tempering materials, of a generally igneous stamp, may have connections with similarly formed clay bodies in the region and outside of it. Previous petrographic studies, summarized below, show that crushed volcanic rock-tempered pastes are fairly common in the Panhandle. This technology is commonly accepted as having been centered in the Southwestern region, but does not imply that any particular group of vessels or wares were manufactured in the Southwest. Regional comparisons may help relate the Landis Property ceramics to points of origin and show local affinities by their contrasts and dissimilarities. In the Panhandle itself, Reese Taylor (1991) studied a collection from the Palo Duro Creek in Hansford County in the very northern reaches of the Texas Panhandle. Lintz and Reese-Taylor (1997) also conducted a large petrographic study on a set of decorated ceramic types and extended their work to make wide extraregional comparisons (Nebraska). Outlying regions with available comparable ceramic studies lay southward (Turpin and Robinson 1998), just east of Lubbock below the caprock (Robinson 1992, 1994), far southeastward on the Edwards Plateau (Robinson 2008), and westward in eastern and northeastern New Mexico (Garrett 1988a, 1988b).

Reese-Taylor (1991:Appendix H) conducted petrological analysis on six Panhandle specimens from sites in the Palo Duro Reservoir in Hansford County. She defined four paste groups in the collection, which included Borger Cordmarked and plainwares. The paste groups included one bone-tempered paste group, two sand-tempered, and one sand

and basalt-tempered paste group (Reese-Taylor 1991:H-9 to H-11). The two sand-tempered pastes had dense matrixes, quartz, feldspar and carbonates (dolomite), and particle shapes varied from subrounded to angular. The pastes contained a small amount of hematite, but were entirely lacking in biotite. Although the paste groups contained varying amounts of feldspar, the groups altogether bear little resemblance to the Potter County paste groups.

Interestingly, Reese-Taylor (1991:H-2) conducted petrological analysis of two surface sediment samples collected from two nearby localities. The aplastic inclusions ranged in size from fine sand to coarse sand and were rounded to subrounded in shape. The principal mineral component was quartz sand, from 78 per cent to 86 per cent of the totals. The samples also contained minor amounts of feldspar, carbonate (calcite), clinopyroxene and a trace of woody organic matter (Reese-Taylor 1991:H-2). These sediments are very dissimilar to the Potter County specimens.

Lintz and Reese-Taylor (1997) conducted a largely petrographic study of decorated ceramics from Plain village sites along the Canadian River drainage in Potter and Hutchinson counties and northward to Plains village sites along Wolf Creek, a tributary of the North Canadian River in Ochiltree County. They made comparisons with ceramics from Nebraska, well outside the region. The relevant findings are that ceramic sources with naturally resident biotite, quartz, alkali feldspars and occasionally occurring pyroxene, hematite, carbonates and volcanic rock fragments are widespread through the region. Ceramic pastes made with these materials and the addition of crushed granitic rock temper are similarly common (Lintz and Reese-Taylor 1997:288-295; Table 3). The BLM Landis Property ceramic pastes compare closely with these ceramics, although they are typologically distinct.

Turpin and Robinson (1998) analyzed a thin-section of one plainware sherd recovered from the Floydada Country Club (41FL1) in Floyd County, as part of a larger study. The sherd was strongly bone-tempered, which gave it affinities with Late Prehistoric plainwares of central Texas and the Edwards Plateau (Turpin and Robinson 1998:94).

Southward, and southeast of Lubbock below the caprock (but along streams draining it), at Lake Alan Henry in Garza and Kent counties, twelve specimens of non-local plainwares were studied in thin-section by Robinson (1992:221-227). As in Potter County, many of the plainwares have dense matrixes reflected in high point-count proportions and crushed minerals and rock fragments. Typological identifications were made in that collection and the closest comparisons of the BLM Landis Property sherds from Potter County with the Lake Alan Henry materials are with five sherds of Middle Pecos Micaceous brownware and one section of Jornada Brown. The regional origins of these wares are the Middle Pecos River region and southern New Mexico/Trans Pecos Texas, respectively. The comparative elements are higher proportions of biotite and iron in addition to crushed mineral temper and dense matrix. These comparisons are closest with the BLM Landis Property Paste Group 2. The Middle Pecos region is directly west of the Lake Alan Henry region across the major physiographic divide formed by the Southern High Plains, or Llano Estacado.

An additional five thin-sections were analyzed from a single site in the Lake Alan Henry region (Robinson 1994:355-361). The site is 41GR291, the Sam Wahl site and represents a late variant of the Palo Duro complex. Two paste groups were identified, both having crushed mineral tempers and dense matrixes. Group 1 contained much crushed granitic rock as tempering material. Group 2 was comprised of two thin-sections, one of which had biotite but no iron, the other having iron but no

biotite. The ceramics of the Sam Wahl site altogether were grouped typologically as belonging to a Southwestern crushed mineral ceramic tradition without finer typological breakdown (Robinson 1994: 360).

In his study of Edwards Plateau aboriginal ceramics, Robinson (2008) identified two minor paste groups with crushed granitic rock tempering and additional feldspars and hematite. One of the paste groups belonged entirely to the Historic period (Mission San Lorenzo, some occupants were Apaches), and the other paste group was defined on a single sherd from the Varga site, 41ED28, in Edwards County on the southern margin of the Edwards Plateau just north of Uvalde Texas. This specimen, however, bears a close resemblance to Paste Group 2.

Garrett (1988a: Appendix H) conducted petrological analysis on nine potsherds from the Melrose Air Force Base, west of Portales in east-central New Mexico. Three of the examined sections were brownwares, all of which were tempered with crushed volcanic rocks. Two of these also contained hematite and magnetite. One held biotite. The minerals' proportions were not broken down individually in the thin-sections.

Garrett (1988b: Appendix G) also analyzed thin-sections from ceramics recovered from the Conchas Lake Reservoir in northeast New Mexico. The latter reservoir is in the Canadian River drainage upstream, and due west of Potter County and the Landis Property. Six of the seven examined sherds were tempered with quartz mica schist, a metamorphic rock. The remaining specimen was a sherd of Chupadero Black-on-White tempered with a basaltic rock. Garrett (1988b:G-4, G-5) argued that all these sherds were non-local; metamorphic rocks outcrop in the Sangre de Cristo Mountains farther west from the Conchas Reservoir region. Basaltic rocks outcrop no closer than 30 kilometers from the locality. The local rocks are shales and sandstones. The Conchas

Reservoir assemblage is distinct from the Potter County BLM Landis Property study sherds.

I.4.1 THE PRESENCE AND ABSENCE OF FELDSPAR IN PANHANDLE CERAMIC PASTES

Feldspar is a common constituent of igneous rocks, the sediments eroded from them, and the metamorphic rocks formed from them (Figure I-1). Feldspars have various sources in the Panhandle and its ceramics, yet this study has shown that they are not ubiquitous. They are present in most paste groups but entirely lacking in others. Paste Group 3 is one such feldspar-deficient paste. Other paste groups lack feldspar, and its absence from them may indicate source connections.

Paste Group 3 is defined on one corrugated sherd thin-section from 41PT186, and the sherd may have a Late Prehistoric association. In the natural sediment samples, five have no feldspar; these are 41PT185 #18-004-1b, 41PT186 #341-004-1d (same site), #20-004-1b, #13-004-1b, and #MQ-ML-B1. All these samples contain quartz, and all but #MQ-ML-B1 and #20-004-1b show small quantities of biotite. Here is a minimal level of distinction for pottery resource clays and paste groups. Simple logic would suggest that Paste Group 3 was manufactured on the site.

Farther a field, Reese-Taylor and Lintz (1997:293-294) studied three sherds without feldspars, one (#542) from the Roper site (41HC6) in the North Canadian River Basin, and two (#188 and #064) from the Kit Courson site (41OC43) in the Wolf Creek valley that drains into the North Canadian of the northeastern Panhandle. The Roper site sherd has quartz and abundant granite in place of feldspar, and the Kit Courson feldspar-free sherds both contain quartz and abundant mica (probably muscovite), carbonates, and generally lighter colored pastes. These are examples of feldspar-free paste groups that

have regional distinctiveness. As described above, the Palo Duro Reservoir paste groups all show varying amounts of feldspars, and otherwise contrast with the Landis Property sites paste groups and those mentioned (Reese-Taylor 1991).

I.5 SUMMARY AND IMPLICATIONS

Four general research questions were outlined at the beginning of this study:

1. What are the typological affinities of the ceramics?
2. Were the ceramics locally manufactured or transported to the sites?
 - 2a. If transported, can a transport mechanism such as trade be identified or suggested?
3. Could the ceramics be produced by a hunter-gatherer society distinct from the village farming society that produced Borger Cordmarked ceramics?
4. Is the Southwestern corrugated sherd distinct from the local ceramics and clay resources?

The six ceramic thin-sections, eleven sediment sections, and three wet mount analysis sherd fragments were studied to answer these questions, and the results apply to all the questions in varying degrees of confidence and accuracy.

Regarding the first question, typological affinities, and the study collection belongs to the crushed mineral tempering tradition of aboriginal ceramics. This is a very general result, but it is an interesting finding in that it gives the ware or wares of the Landis Property ceramics affinities with the Southwestern pottery making tradition rather than the grog, shell, and bone-tempered Woodland (Eastern) tradition. This is an important distinction in the Panhandle region as the cordmarked wares

and types of the Antelope Creek village farming culture are commonly accepted as having Woodland origins ultimately. Despite this, the decorated wares in the Texas Panhandle were also commonly tempered with crushed minerals (Lintz and Reese-Taylor 1997). To be more specific regarding the Landis plainwares, they have significant biotite paste components, an important trait shared with Middle Pecos micaceous brownwares (Jelinek 1967), but the common occurrence of biotite and other micas in the clays and rocks of the Texas Panhandle region prevents separating the ceramics of the two regions typologically.

On the question of local manufacture or transport, Paste Group 1 and Paste Group 3 could have been manufactured from various clay resources within Potter County, based on the broad similarities with the studied sediment samples. In fact, Paste Group 3 is closely similar to a sediment sample from the same site, 41PT186, but this fact presents problems to interpretation because it is defined on a typologically Southwestern corrugated sherd. The problem will receive further consideration below. At this point, it is important to note that any clay source in the county likely would lie within a one-day round trip for an aboriginal potter living and working in a site within the geographic boundaries of what is now Potter County. Complicating this picture, however, is Paste Group 2 and its significant proportions of hematite. Within the county, only studied sediment sample #20-004-1b, the very interesting clay from Blue Creek, contains hematite, and that is in a trace amount insufficient to serve as one of the clay residents in the Landis Property Paste Group 2 sherds. A fair conclusion is that the Paste Group 2 clays were non-local, perhaps outside a one-day round trip distance.

On the topic of Question 2a, mechanisms of transport, the evidence from the thin-sections can provide only vague indications. Paste Group 1, since its clays were effectively local,

may have been manufactured on or near the sites. Paste Group 2 may have been manufactured elsewhere and the finished pot transported to 41PT245. Beyond this, a mechanism of transport cannot be surmised at this time.

Perhaps a more interesting question at this juncture is why a local and a nonlocal paste group exist at the same site. This situation may be the evidence for ceramic trade in the aboriginal economies of the Potter County prehistoric people. The evidence shows that pottery was not kept on sites for utilitarian purposes only, but that it circulated among sites. This basic circumstance finds support in other modes of archeological analysis. Initial findings of INAA of Borger Cordmarked pottery in the Canadian River valley and neighboring regions have given an emerging picture of local manufacturing zones and vessel transport during the Antelope Creek phase (Meier 2007). Meier's results in the bivariate plots of the principal components suggest manufacturing sites centered on the hamlets and manufacturing zones shared among hamlets in the Canadian drainage (Meier 2007:58-59). She attributed these findings to local exchange of ceramics and potential sharing of clay source beds (Meier 2007:59, 62-63). Returning to petrographic methods, Lintz and Reese-Taylor (1997:288-295) defined resource subgroups, equivalent to this study's paste groups. Of the eight defined subgroups, six contained sherds from two or more sites, and all of the subject Antelope Creek hamlets had pots of more than one subgroup. Clearly, pot sharing had an economic basis in the Texas Panhandle region, either in commodities transported in ceramic vessels or in the vessels themselves.

The evidence from this study cannot support the hypothesis (Question 3) that the apparently plainware ceramics in the region may have been produced by a mobile hunting and gathering society, as in the Late Prehistoric period of central Texas. The patterns in this

study's data on paste groups and implied manufacturing and transport models compare favorably with those being developed on the decorated ceramics of the village farming Antelope Creek phase. Research design would anticipate variant patterns of hunter-gatherer ceramics along the dimensions of technology, distribution, form, decoration, materials and perhaps others. No such variant, or contrastive, patterns have been observed at this incipient stage of the work.

On the question of the distinction of the Southwestern corrugated sherd, #343-008-1b, there are more questions than answers. The sherd displays its own paste group, distinct from the other two defined in this study. This fact by itself would suggest an extraregional source, but the paste group, Group 3, is similar in composition to the sediment sample from the same site, 41PT186. The difference between the two is largely the presence in the sherd of Rock B, of a size and quantity in the paste to be one of the tempering agents of the ceramic; Rock B is lacking in the sediment sample. Further, the wet mount ceramic fragment, #443-008-1, resembles Paste Group 3 although Rock B was not identified in it. This lack, of course, gives it a fairly close correspondence to the on-site sediment sample. Thus all three items appear outwardly to originate on the site. Corrugated pottery is rare in the Texas Panhandle; all of it is identified as Southwestern imported ceramic. In the Southwest, however, corrugated wares technologically and typologically comprise a longstanding and widespread tradition. Explanations for this contradictory situation are more suggestive than certain at this time. There are four possibilities that may apply:

1. The sherd is clearly Southwestern in origin, and Rock B is the only necessary determinant of nonlocal status. Rock B is absent from the sediment sample and unidentified in the wet mount sample; this is the sole significant difference, and it is a world of difference.

2. Ethnohistorically, Apache groups in northern New Mexico procured ceramic clay from a source eighteen miles southeast of Taos. The locality was a sacred site, but open to all to gain their needed raw material (Opler 1971). As an outside possibility, the sherds #343-008-1b and #443-008-1 were manufactured each from the same New Mexican source (either the one cited or perhaps others) and then deposited in the same site at different times. The probability of this being the case increases the longer the period of time the source locality was used by many groups. Further, if the production from the clay resource locality moved over the same transport routes, eventually some of the ceramics would be deposited in the same sites or locales of deposition. This could be a marker of regular trading relations, but the probability of this being the case in this instance cannot currently be assessed, and it does not account for similarities with the sediment sample. Other features of site 41PT186's artifact assemblage and physiographic setting may help assess this model.

3. Again as an outside possibility, the sherds #343-008-1b and #443-008-1, the only ceramic pieces from a small site, may originate in the same vessel. Sherd fragment #443-008-1 has a smooth exterior, but most if not all corrugated types have smooth surfaces on their vessels, especially toward their bases, and is not fully corrugated as a surface modification.

4. It may also be the case here that petrological and mineralogical analyses cannot approach the level of discernment needed to decide the issues of locality and transport. The sediment sample is defined on common minerals (quartz and biotite), and the other bodies in it, calcitic lithoclasts and organic opaques, are also common in soils. This common composition may or may not provide any distinctive keys for interpretation. Further still, the data set here is comprised of one ceramic thin-section, one wet mount sherd, and

one sediment sample. Accurate and robust characterizations require multiple examples to form statistically representative data sets available for balanced comparisons. The lack of such is a critique leveled at other regional studies, described below, and the critique is one to which Question 4 is subject here. The best common sense assessment available now is that the implications of typology are to be preferred to the imponderables of technology/petrology, and that the corrugated sherd in question was imported from New Mexico. The elemental analysis technique of INAA (Instrumental Neutron Activation Analysis) may sidestep the limitations of the current analysis. The technique is capable of discerning varying key elements in samples that have the same or similar mineral suites (Bennyhoff and Heizer 1965). The sherd fragment #443-008-1 is designated for INAA. A finding that the sample hails from nonlocal source beds would provide satisfying explanations.

I.5.1 PROTOHISTORIC IMPLICATIONS

The current radiocarbon dating of charcoal and bone to ca. 200 to 300 B.P. associated with plain sherd 41PT186 #443-008-1 places it within the Protohistoric period, and this location is on the northern margin of the Tierra Blanca complex, implicitly the manifestation of a late bison-hunting culture. The ceramics of the Tierra Blanca complex have figured prominently in current interpretations of Plains/Southwestern U.S. economic and sociopolitical interactions (Habicht-Mauche 1987, 1991, 1992). The two sherds from 41PT186 #343-008-1 and #443-008-1, compare to Tierra Blanca ceramics, but note that #343-008-1 is Southwestern. More specific aspects of the ceramics place them at variance with the characterizations published on highly selected data sets. The single dimension of color suffices as one example of several. Habicht-Mauche (1991:62) reports a range of paste colors of Tierra Blanca ceramics: black, very dark gray, dark gray,

gray, gray-brown, brown and miscellaneous. By contrast, the paste color of sherd 41PT186 #443-008-1 is pinkish gray, 7.5YR6/2. Habicht-Mauche (1991) doesn't report the application of the Munsell® color system or any other published scale. Perhaps the most significant implication of this study is that there is more variation in the region in Protohistoric times than thought hitherto, and that patterns within this variety can be assessed with formalized (statistical) comparisons of balanced data sets. The most parsimonious interpretation from this small study with a comparative survey of regional studies is that crushed mineral pastes were applied to local and regional ceramics in Antelope Creek times, and they persisted into Protohistoric times as a ceramic legacy. The degree and nature of Southwestern influence on the ceramic technology cannot be determined affirmatively at this time with this information.

I.6 CONCLUSION

The findings of this study support models of local manufacture, regional trade and transport, and sharing of resource localities. The potential of interregional trade with the Middle Pecos region in Antelope Creek times cannot be assessed currently due to the obscuring effects of similar minerals occurring in the clays and rocks of both regions, these being abundant micas. Complex ceramic models regarding Protohistoric Plains/Southwest interactions require comparisons of much larger data sets. The development of interpretive models will be helped by further petrographic analysis of regional wares and INAA as well, which is capable of identifying varying elements in sherds when minerals are the same in two or more groups (Bennyhoff and Heizer 1965).

I.7 REFERENCES CITED

Bennyhoff, J. A. and R. F. Heizer

1965 Neutron Activation Analysis of Some Cuicuilco and Teotihuacan Pottery: Archaeological Interpretation of Results. *American Antiquity*, 30(3):348-349.

Chayes, F.

1949 A Simple Point-Counter for Thin-section Analysis. *American Mineralogist* 34:1- 11.

Folk, R. L.

1951 A comparison chart for visual perception estimates. *Journal of Sedimentary Petrology*. 21:32-33.

Garrett, B.

1988a Petrographic Analysis of Prehistoric Ceramics from the Melrose Range Project, ACOE, 1987. Appendix H in: *Class II Survey and Testing of Cultural Resources at the Melrose Air Force Range, Curry and Roosevelt Counties, New Mexico*, by C. Lintz, K. Kramer, A. Earls, W. N. Trierweiler, T. Del Bene, J. Acklen, F. Nials, and J. Bertram. Mariah Associates, Inc., Albuquerque.

1988b Petrographic Analysis of Selected Conchas River Ceramics. Appendix G in *Report of the 1986 and 1987 Class II Surveys and Testing of Cultural Resources at Conchas Lake, New Mexico*, by K. Kramer, C. Lintz, W. N. Trierweiler, S. Lent, J. Frizell, M. Stiner, J.C. Acklen, and S. Kuhn. Mariah Associates, Inc., Albuquerque.

Habicht-Mauche, J. A.

1987 Southwestern-Style Culinary Ceramics on the Southern Plains: A Case Study of Technological Innovation and Cross-Cultural Interaction. *Plains Anthropologist* 32 (115):175-189.

1991 Evidence for the Manufacture of Southwestern-Style Culinary Ceramics

- on the Southern Plains. In *Farmers, Hunters and Colonists. Interaction between the Southwest and the Southern Plains*, edited by Katherine A. Spielman. The University of Arizona Press. Tucson.
- 1992 Coronado's Querechos and Teyas in the Archaeological Record of the Texas Panhandle. *Plains Anthropologist* 37(140):247-259.
- Jelinek, A. J.
1967 *A Prehistoric Sequence in the Middle Pecos Valley, New Mexico*. Anthropological Papers 31. Museum of Anthropology, University of Michigan. Ann Arbor.
- Lintz, C. and K. Reese-Taylor
1997 Migrations, Trade, or Replicated Ceramics: Petrographic Study of Collared Rim Sherds from the Texas Panhandle. *Bulletin of the Texas Archeological Society* 68:273-300.
- Meier, H. A.
2007 An Evaluation of Antelope Creek Phase Interaction Using INAA. Unpublished Master's thesis. Department of Anthropology. Texas State University. San Marcos.
- Opler, M. E.
1971 Pots, Apache, and the Dismal River Culture Aspect. In *Apachean Cultural History and Ethnology*, edited by K. H. Basso and M. E. Opler, pp. 29-33. Anthropological Papers of the University of Arizona Number 21, The University of Arizona Press, Tucson.
- Reese-Taylor, K.
1991 Petrographic analysis. Appendix H in *Historic and Prehistoric Data Recovery at Palo Duro Reservoir, Hansford County, Texas*, by J. M. Quigg, C. Lintz, F. M. Oglesby, A. C. Earls, C. D. Frederick, W. N. Trierweiler, D. Owsley and K. W. Kibler. Technical Report #485. Mariah Associates, Inc. Austin.
- Robinson, D. G.
1992 Petrographic Analysis of Nonlocal Plainwares. Appendix F in *Data Recovery at Justiceburg Reservoir (Lake Alan Henry), Garza and Kent Counties, Texas: Phase III, Season 1*, by D. K. Boyd, S. A. Tomka, C. B. Bousman, K. M. Gardner, and M. D. Freeman, pp. 221-227. Reports of Investigations No. 84. Prewitt and Associates, Inc., Austin.
- 1994 Petrographic Analysis of Plainwares from 41GR291. Appendix G in *Data Recovery at Lake Alan Henry (Justiceburg Reservoir), Garza and Kent Counties, Texas: Phase III, Season 3*, by D. K. Boyd, J. Peck, S. A. Tomka, K. W. Kibler and M. D. Freeman, pp. 357-361. Reports of Investigations No. 93, Prewitt and Associates, Inc., Austin.
- 1999 Petrographic Analysis of Plainware Pottery from 41VV444. Appendix C in "Val Verde on the Sunny Rio Grande". Geoarcheological and Historical Investigations at San Felipe Springs, Val Verde County, Texas, by G. Mehalchick, T. Myers, K. W. Kibler, and D. K. Boyd. Reports of Investigations 122. Prewitt and Associates, Inc. Austin.
- 2008 Petrographic Analysis of Toyah Ceramics from the Varga Site, 41ED28, and Comparative Sites. Appendix D in *The Varga Site: A multicomponent, Stratified Campsite in the Canyonlands of Edwards County, Texas*, by J. M. Quigg, J. D. Owens, P. M. Matchen, G. D. Smith, R. A. Ricklis, M. C. Cody, and C. D.

- Frederick pp. 872-889. Texas Department of Transportation, Environmental Affairs Division, Archeological Studies Program, and TRC Technical Report No. 35319. TRC Environmental Corp., Austin.
- Shepard, A. O.
1942 Rio Grande Glaze Paint Ware: A Study Illustrating the Place of Ceramic Technological Analysis in Archeological Research. *Contributions to American Anthropology and History* 7(39): entire volume. Carnegie Institution of Washington, Washington, D.C.
- 1954 *Ceramics for the Archaeologist*. Publication 609. Carnegie Institution of Washington, Washington, D.C.
- Terry, D. and G. V. Chilingar
1955 Summary of "Concerning some additional aids in studying sedimentary formations," by M. S. Shvetsov. *Journal of Sedimentary Petrology* 25:229-234.
- Turpin, S. A. and D. G. Robinson
1998 Infierno Phase Pottery of the Lower Pecos River Region. *Bulletin of the Texas Archeological Society* 69:89-97.

Table I-1. BLM Landis Property Petrographic Analysis on Six Ceramic Sherds. Point Count Data Percentages and Observations.

	Paste Group 1			Paste Group 2		Paste Group 3
Catalog No. (point count)	41PT245- #340-008-2 (103)	41PT245- #340-008-3 (143)	41PT245- #341-008-1c (134)	41PT245- #378-008-1 (125)	41PT245- #401-008- 1e (200)	41PT186- #343-008- 1b (200)
matrix plain	black	black	reddish brown	brown to gray transition	reddish-brown to dark grey transition	reddish black
matrix cross-n	black	black	black	dark gray	dark gray	reddish black
matrix percent	49.5	47.5	44.0	52.8	47.5	48.5
pore space	14.6	16.1	3.7	12.8	15.0	20.0
Quartz	24.3	22.4	29.1	21.6	25.0	22.5
Rock A		2.8	9.7	2.4	4.0	
Rock B						4.5
microcline feldspar	3.9	3.5	3.0	1.6	1.5	
orthoclase feldspar		0.7				
biotite mass	3.0	3.5	5.2	4.8	3.5	2.0
biotite lathe	5.0	3.5	5.2			2.5
pyroxene (ortho)			tr	tr		
hematite				4.0	3.5	
Percent Total	100.3	100	99.9	100	100	100
Number in parentheses is point count						
cross-n is cross-nichols						
tr is trace						
Rock A contains quartz, microcline feldspar and biotite masses						
Rock B contains quartz and biotite (lacks feldspar).						

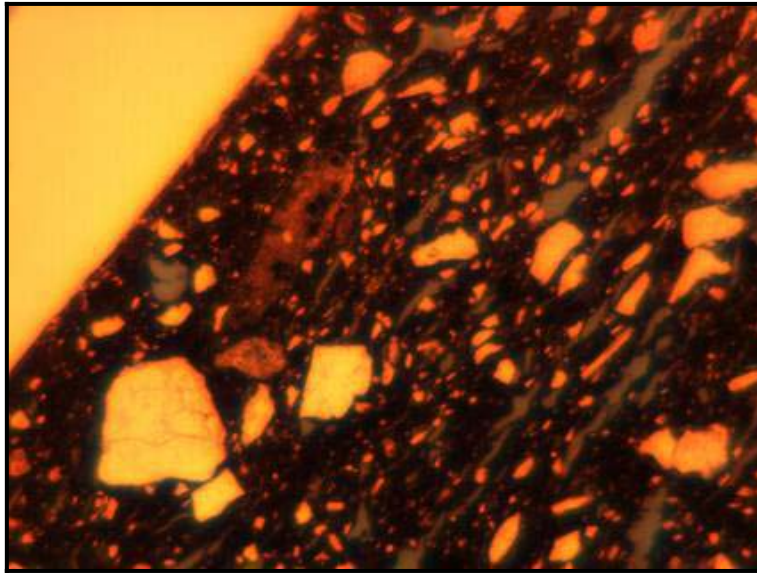


Figure I-1. Thin-Section 41PT245-#340-008-3.

(Note: Ceramic fabric is typical of Paste Group 1. A large feldspar grain lies in left center near the section edge. Two large, subrounded grains of biotite (biotite masses) lie above and to the right of the feldspar grain. Biotite lathes are thin, bright bodies elsewhere in the paste. Voids are medium gray irregular and jagged strips oriented in parallel with the section edge.)

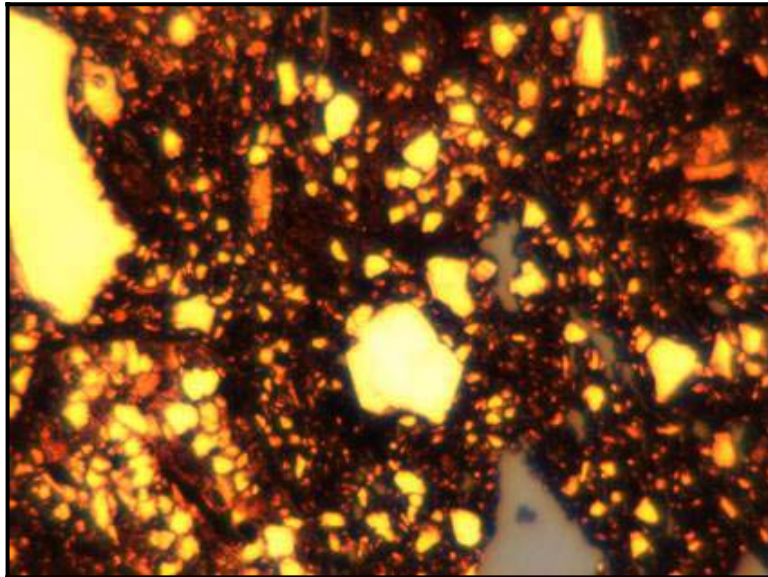


Figure I-2. Thin-Section 41PT245-#378-008-1.

(Note: Ceramic fabric is typical of Paste Group 2. Large angular grain of quartz dominates the field. Fine, rounded, opaque grains of ferrous hematite lie on either side of the quartz grain.)

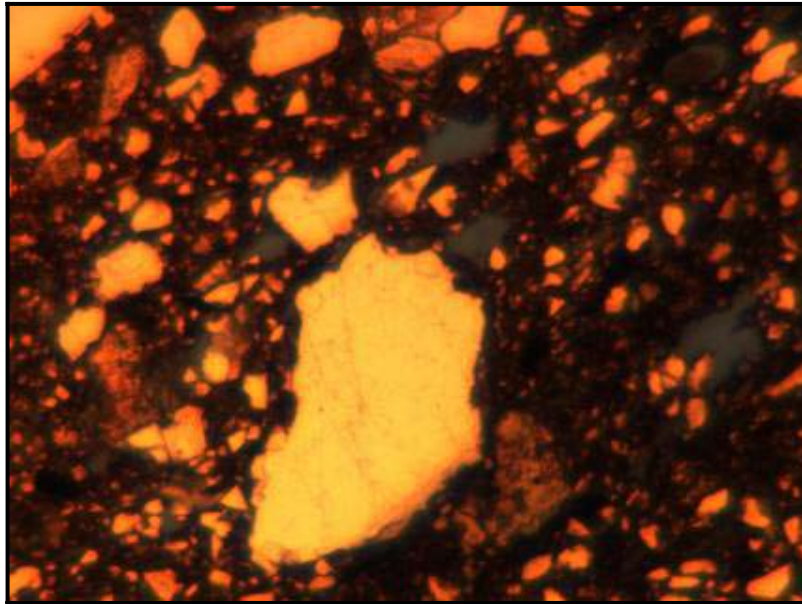


Figure I-3. Thin-Section 41PT186-#343-008-1b.

(Note: Ceramic fabric is typical of Paste Group 3. Large subangular quartz grains lie near center and extreme upper left. Coarse subrounded grains of Rock B lie beneath the quartz grain on the left and at the extreme right of the view.)

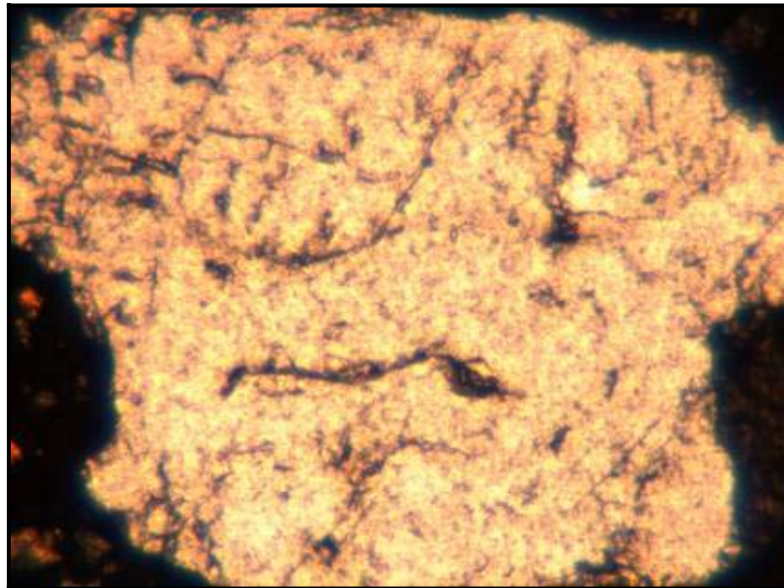


Figure I-4. Thin-Section 41PT245-#401-008-1e.

(Note: Paste Group 2 ceramic fabric with medium, rounded grains of ferrous hematite near center of field. Grains appear slightly reddish.)

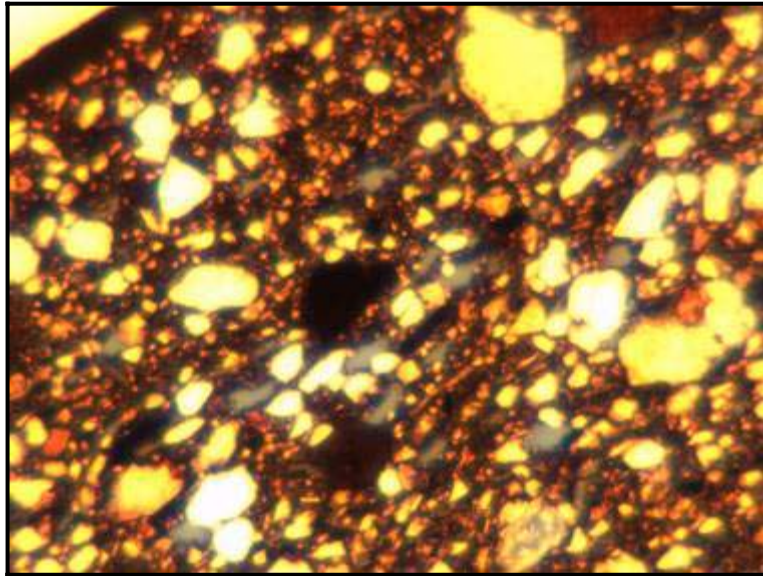


Figure I-5. Large Grain of Feldspar in Plain Polarized Light.

(Note: Erosion patterns, particularly along the cleavage boundaries. Thin-section unrecorded.)

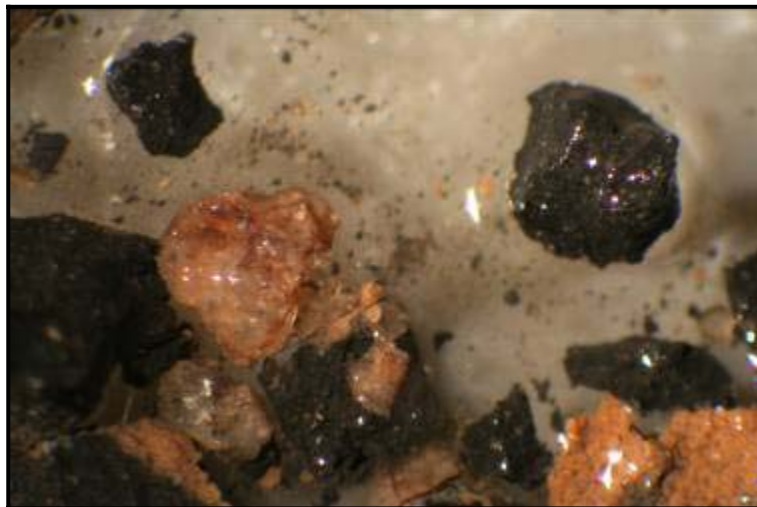


Figure I-5. Microscopic View of Wet Mount of 41PT186-#443-008-1.

(Note: Shows quartz with biotite as small black specks. The quartz temper was coarse to medium and subrounded.)

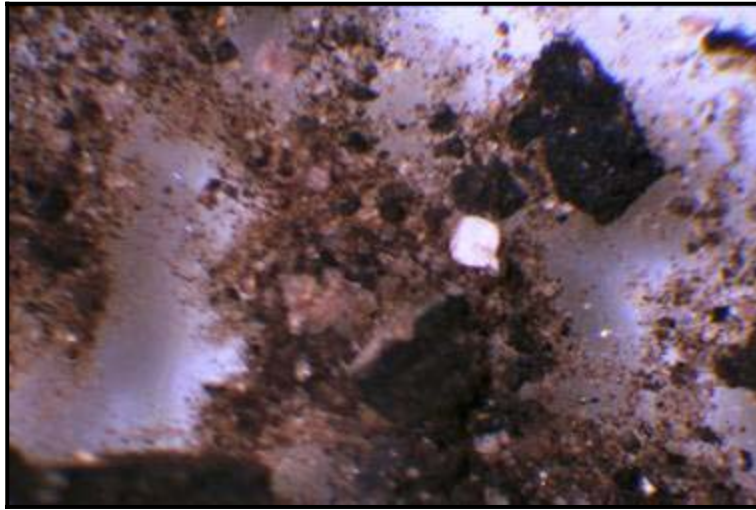


Figure I-7. View Shows Wet Mount of 41PT185/C-#850-008-1.

(Note: The temper is medium to fine sized quartz, and a secondary particle is fine sized, opaque white feldspar are subrounded in shape.)



Figure I-7. View of Wet Mount of Sherds #915-008-1 from 41PT185/C.

(Note: Shows tempering agent of coarse to medium feldspar in small quantities.)

Table I-2. BLM Landis Property Natural Sediment Sample Characteristics.

Catalogue No.	Location	Material Type	Particle Density	Matrix Color	Matrix Cross-nichols	Isotropy	Materials Observed							
							quartz	biotite	organic opaques	plagioclase feldspar	Lithoclasts (poss. Calcitic)	biotite (tr. spicules)	Organic opaques	lithoclasts (poss. biotite)
41PT185-18-004-1b	Potter County, 41PT185, Triassic clay, upper bed	clay	50-55 %	Light reddish tan	medium brown	isotropic	quartz	biotite	organic opaques	microcline feldspar	lithoclasts (poss. biotite)			
41PT185-263-004-4b	Potter County 41PT185, Backhoe Trench 36, M-3-3, 1430 B.P.	soil	40-45 %	medium brownish gray	Medium gray	isotropic	quartz	organic opaques	plagioclase feldspar	Organic opaques	lithoclasts (poss. biotite)			
41PT185-263-004-6a	Potter County, 41PT185 Backhoe Trench 36, M-4-7, 860 B.P.	soil	35-40 %	medium brownish gray	medium greenish gray	isotropic	quartz	organic opaques	plagioclase feldspar	Lithoclasts (poss. Calcitic)	biotite (tr. spicules)			
41PT186-341-004-1d	Potter Co. 41PT186, Backhoe Trench 6-1a 136-139 cmbs.	soil	40%	Light Tannish brown	medium grayish brown	isotropic	quartz	organic opaques	Organic opaques	Lithoclasts (tr. ferrous iron)	Organic opaques			
20-004-1b	Potter Co. Blue Creek	Alluvial clay	5-7 %	yellow-brown	golden-brown	anisotropic	quartz	Organic opaques	Organic opaques					
13-004-1b	Potter Co. Wildcat Bluff Nature Center	Triassic clay	50-55 %	white	Dark gray	isotropic	quartz	Organic opaques	Organic opaques					
5-004-1b	Potter County BT-11 153-158 cmbs.	Alluvial clay	50-55 %	Light grayish brown	mottled, red, gold and grayish brown	isotropic	quartz	microcline feldspar	microcline feldspar	Biotite (lathes)	organic opaques			
MQ-ML-B1	Briscoe County, Mackenzie Lake	white clay sample	20%	mottled, greenish, gray and orange	Greenish gray and brown	isotropic	quartz	organic opaques	organic opaques (particles and patches)	ferrous iron stain				
MQ-GC-RB	Roberts County Government Canyon	Ogallala clay	30-35 %	greenish gold brown	Reddish gold brown	anisotropic	quartz	Biotite (lathes)	Biotite (lathes)	Biotite (masses)	microcline feldspar	Plagioclase feldspar	clino-pyroxene	
MQ-SF70-DY	Donley County, Salt Fork of Red River at US 70,	Alluvial clay	30%	Reddish brown	Reddish brown	isotropic	quartz	Biotite (lathes)	Biotite (lathes)	Biotite (masses)	orthoclase feldspar	Organic opaques	Sandstone (tr)	volcanic Tuff (tr)
MQ-PDT 70-HL	Hall County, Prairie Dog Town of Red River at US 70	Alluvial clay	20-25 %	medium reddish brown	mottled gold and reddish brown	anisotropic	quartz	Biotite (lathes)	Biotite (lathes)	Biotite (masses)	calcite (1-2 % of field)	ferric and ferrous iron opaques		

Table I-3. Ceramic Wet Mount Analysis, BLM Landis Property

Catalogue No.	Munsell Paste Color	Exterior Surface Color	Interior Surface Color	Paste Texture	Thickness (mm)	Exterior Surface Finish	Particle A ¹	Particle B	Particle C
41PT186- #443-008-1	7.5YR6/2 pinkish gray	7.5YR5/2 brown	7.5YR4/2 dark brown	coarse	5	smooth	coarse/ medium subangular quartz	minor very fine biotite mica	
41PT185/C- #850-008-1	5YR3/1 very dark gray	5YR5/1 gray	5YR4/1 dark gray	medium	4	grainy	medium to fine angular and subangular quartz	medium to fine feldspar	
41PT185/C- #915-008-1	2.5YR4/4 reddish brown	5YR6/3 light reddish brown	5YR6/2 pinkish gray	platy, or medium	3	smooth	coarse to medium feldspar	coarse to medium subangular quartz	flaky strands of carbonate ²

¹ Particles presented in order of abundance

² Probably caliche formed along plates of matrix. See text.

APPENDIX J

**INSTRUMENTAL NEUTRON ACTIVATION ANALYSIS OF CLAYS
AND CERAMICS FROM THE TEXAS PANHANDLE**

This page intentionally left blank.

INSTRUMENTAL NEUTRON ACTIVATION ANALYSIS OF CLAYS AND CERAMICS FROM THE TEXAS PANHANDLE

Prepared for:



**TRC Environmental Corporation
505 East Huntland Drive, Suite 250
Austin, Texas 78752**

Prepared by:

**Jeffrey R. Ferguson, Ph.D. and Michael D. Glascock, Ph.D.
Archaeometry Laboratory, Research Reactor Center
University of Missouri
Columbia, MO 65211**

This page intentionally left blank.

J.1 INTRODUCTION

This report describes the preparation, analysis, and interpretation of six pottery samples and nine clay samples from the Texas panhandle. Five of the pottery samples and all of the clay samples were submitted for analysis in 2008. An additional pottery sample (#443-008-1 [TRC527]) was submitted for analysis in 2009. Consequently, this report first discusses those samples submitted in 2008. Discussion of the single sample submitted in 2009 follows. The primary goal of this research is to determine if the pottery might have been made using any of the local clay sources included in this analysis. The samples are also compared to a recent study of ceramics from the Antelope Creek area (Meier 2007).

J.1.1 SAMPLE PREPARATION

Pottery samples were prepared for Instrumental Neutron Activation Analysis (INAA) using procedures standard at University of Missouri Research Reactor (MURR). Fragments of about 1 cm² were removed from each sample and abraded using a silicon carbide burr in order to remove glaze, slip, paint, and adhering soil, thereby reducing the risk of measuring contamination. The samples were washed in deionized water and allowed to dry in the laboratory. Once dry, the individual sherds were ground to powder in an agate mortar to homogenize the samples. Archival samples were retained from each sherd (when possible) for future research. Clay samples were prepared in a similar manner, except the samples were fired in a ceramic kiln to approximately 700 degrees centigrade and were not burred or washed prior to grinding.

Two analytical samples were prepared from each specimen. Portions of approximately 150 mg of powder were weighed into clean high-density polyethylene vials used for short irradiations at MURR. At the same time, 200 mg of each sample was weighed into clean high-purity quartz vials used for

long irradiations. Individual sample weights were recorded to the nearest 0.01 mg using an analytical balance. Both vials were sealed prior to irradiation. Along with the unknown samples, Standards made from National Institute of Standards and Technology (NIST) certified standard reference materials of SRM-1633a (coal fly ash) and SRM-688 (basalt rock) were similarly prepared, as were quality control samples (e.g., standards treated as unknowns) of SRM-278 (obsidian rock) and Ohio Red Clay (a standard developed for in-house applications).

J.1.2 IRRADIATION AND GAMMA-RAY SPECTROSCOPY

Neutron activation analysis of ceramics at MURR, which consists of two irradiations and a total of three gamma counts, constitutes a superset of the procedures used at most other INAA laboratories (Glascok 1992; Neff 1992, 2000). As discussed in detail by Glascok (1992), a short irradiation is carried out through the pneumatic tube irradiation system. Samples in the polyvials are sequentially irradiated, two at a time, for five seconds by a neutron flux of $8 \times 10^{13} \text{ n cm}^{-2} \text{ s}^{-1}$. The 720-second count yields gamma spectra containing peaks for nine short-lived elements aluminum (Al), barium (Ba), calcium (Ca), dysprosium (Dy), potassium (K), manganese (Mn), sodium (Na), titanium (Ti), and vanadium (V). The samples are encapsulated in quartz vials and are subjected to a 24-hour irradiation at a neutron flux of $5 \times 10^{13} \text{ n cm}^{-2} \text{ s}^{-1}$. This long irradiation is analogous to the single irradiation utilized at most other laboratories. After the long irradiation, samples decay for seven days, and then are counted for 1,800 seconds (the "middle count") on a high-resolution germanium detector coupled to an automatic sample changer. The middle count yields determinations of seven medium half-life elements, namely arsenic (As), lanthanum (La), lutetium (Lu), neodymium (Nd), samarium (Sm), uranium (U), and ytterbium (Yb). After an additional three- or four-

week decay, a final count of 8,500 seconds is carried out on each sample. The latter measurement yields the following 17 long half-life elements: cerium (Ce), cobalt (Co), chromium (Cr), cesium (Cs), europium (Eu), iron (Fe), hafnium (Hf), nickel (Ni), rubidium (Rb), antimony (Sb), scandium (Sc), strontium (Sr), tantalum (Ta), terbium (Tb), thorium (Th), zinc (Zn), and zirconium (Zr).

The element concentration data from the three measurements are tabulated in parts per million using the Microsoft® Office Excel spreadsheet program. Descriptive data for the archaeological samples were appended to the concentration spreadsheet. The data are also stored in a dBase/FoxPro database file useful for organizing, sorting, and extracting sample information. The elemental concentrations are included as Appendix J-1.

J.2 INTERPRETING CHEMICAL DATA

The analyses at MURR described previously produced elemental concentration values for 33 elements in most of the analyzed samples. Nickel (Ni) was below detection limits in half of the samples and was thus dropped from the analysis. Calcium (Ca) levels were generally between 1 and 12 percent, thus requiring a mathematical adjustment to account for the high calcium levels. The comparative data (Meier 2007) also used a calcium adjustment. Further information on calcium correction can be found here: Cogswell et al. 1998:64; Steponaitis et al. 1988.

Statistical analysis was carried out on base-10 logarithms of concentrations of the 31 elements, following the deletion of Ni and Ca. Use of log concentrations rather than raw data compensates for differences in magnitude between the major elements, such as iron, on one hand and trace elements, such as the rare earth or lanthanide elements (REEs). Transformation to base-10

logarithms also yields a more normal distribution for many trace elements.

The interpretation of compositional data obtained from the analysis of archaeological materials is discussed in detail elsewhere (e.g., Baxter and Buck 2000; Bieber et al. 1976; Bishop and Neff 1989; Glascock 1992; Harbottle 1976; Neff 2000) and will only be summarized here. The main goal of data analysis is usually to identify distinct homogeneous groups within the analytical database. Based on the provenance postulate of Weigand et al. (1977), different chemical groups may be assumed to represent geographically restricted sources. For lithic materials such as obsidian, basalt, and cryptocrystalline silicates (e.g., chert, flint, or jasper), raw material samples are frequently collected from known outcrops or secondary deposits and the compositional data obtained on the samples is used to define the source localities or boundaries. The locations of sources can also be inferred by comparing unknown specimens (i.e., ceramic artifacts) to knowns (i.e., clay samples) or by indirect methods such as the “criterion of abundance” (Bishop et al. 1992) or by arguments based on geological and sedimentological characteristics (e.g., Steponaitis et al. 1996). The ubiquity of ceramic raw materials usually makes it impossible to sample all potential “sources” intensively enough to create groups of knowns to which unknowns can be compared. Lithic sources tend to be more localized and compositionally homogeneous in the case of obsidian or compositionally heterogeneous as is the case for most cherts.

Compositional groups can be viewed as “centers of mass” in the compositional hyperspace described by the measured elemental data. Groups are characterized by the locations of their centroids and the unique relationships (i.e., correlations) between the elements. Decisions about whether to assign a specimen to a particular compositional group are based on the overall probability that the measured concentrations

for the specimen could have been obtained from that group.

Initial hypotheses about source-related subgroups in the compositional data can be derived from non-compositional information (e.g., archaeological context, decorative attributes, etc.) or from application of various pattern-recognition techniques to the multivariate chemical data. Some of the pattern recognition techniques that have been used to investigate archaeological data sets are cluster analysis (CA), principal components analysis (PCA), and discriminant analysis (DA). Each of the techniques has its own advantages and disadvantages which may depend upon the types and quantity of data available for interpretation.

The variables (measured elements) in archaeological and geological data sets are often correlated and frequently large in number. This makes handling and interpreting patterns within the data difficult. Therefore, it is often useful to transform the original variables into a smaller set of uncorrelated variables in order to make data interpretation easier. Of the above-mentioned pattern recognition techniques, PCA is a technique that transforms the data from the original correlated variables into uncorrelated variables most easily.

PCA creates a new set of reference axes arranged in decreasing order of variance subsumed. The individual PCs are linear combinations of the original variables. The data can be displayed on combinations of the new axes, just as they can be displayed on the original elemental concentration axes. PCA can be used in a pure pattern-recognition mode, i.e., to search for subgroups in an undifferentiated data set, or in a more evaluative mode, i.e., to assess the coherence of hypothetical groups suggested by other criteria. Generally, compositional differences between specimens can be expected to be larger for specimens in different groups than for specimens in the same group, and this implies that groups

should be detectable as distinct areas of high point density on plots of the first few components.

It is well known that PCA of chemical data is scale dependent (Mardia et al. 1979), and analyses tend to be dominated by those elements or isotopes for which the concentrations are relatively large. As a result, standardization methods are common to most statistical packages. A common approach is to transform the data into logarithms (e.g., base 10). As an initial step in the PCA of most chemical data at MURR, the data are transformed into log concentrations to equalize the differences in variance between the major elements such as Al, Ca and Fe, on one hand and trace elements, such as the rare-earth elements (REEs), on the other hand. An additional advantage of the transformation is that it appears to produce more nearly normal distributions for the trace elements.

One frequently exploited strength of PCA, discussed by Baxter (1992), Baxter and Buck (2000z), and Neff (1994, 2002), is that it can be applied as a simultaneous R- and Q-mode technique, with both variables (elements) and objects (individual analyzed samples) displayed on the same set of principal component reference axes. A plot using the first two principal components as axes is usually the best possible two-dimensional representation of the correlation or variance-covariance structure within the data set. Small angles between the vectors from the origin to variable coordinates indicate strong positive correlation; angles at 90 degrees indicate no correlation; and angles close to 180 degrees indicate strong negative correlation. Likewise, a plot of sample coordinates on these same axes will be the best two-dimensional representation of Euclidean relations among the samples in log-concentration space (if the PCA was based on the variance-covariance matrix) or standardized log-concentration space (if the PCA was based on the correlation matrix). Displaying both objects and variables on the same plot makes it possible to observe the

contributions of specific elements to group separation and to the distinctive shapes of the various groups. Such a plot is commonly referred to as a “biplot” in reference to the simultaneous plotting of objects and variables. The variable inter-relationships inferred from a biplot can be verified directly by inspecting bivariate elemental concentration plots. [Note that a bivariate plot of elemental concentrations is not a biplot.]

Whether a group can be discriminated easily from other groups can be evaluated visually in two dimensions or statistically in multiple dimensions. A metric known as the Mahalanobis distance (or generalized distance) makes it possible to describe the separation between groups or between individual samples and groups on multiple dimensions. The Mahalanobis distance of a specimen from a group centroid (Bieber et al. 1976, Bishop and Neff 1989) is defined by:

$$D_{y,x}^2 = [y - \bar{X}]' I_x [y - \bar{X}]$$

where y is the $1 \times m$ array of logged elemental concentrations for the specimen of interest, X is the $n \times m$ data matrix of logged concentrations for the group to which the point is being compared with \bar{X} being its $1 \times m$ centroid, and I_x is the inverse of the $m \times m$ variance-covariance matrix of group X . Because Mahalanobis distance takes into account variances and covariances in the multivariate group it is analogous to expressing distance from a univariate mean in standard deviation units. Like standard deviation units, Mahalanobis distances can be converted into probabilities of group membership for individual specimens. For relatively small sample sizes, it is appropriate to base probabilities on Hotelling's T^2 , which is the multivariate extension of the univariate Student's t .

When group sizes are small, Mahalanobis distance-based probabilities can fluctuate

dramatically depending upon whether or not each specimen is assumed to be a member of the group to which it is being compared. Harbottle (1976) calls this phenomenon “stretchability” in reference to the tendency of an included specimen to stretch the group in the direction of its own location in elemental concentration space. This problem can be circumvented by cross-validation, that is, by removing each specimen from its presumed group before calculating its own probability of membership (Baxter 1994; Leese and Main 1994). This is a conservative approach to group evaluation that may sometimes exclude true group members.

Small sample and group sizes place further constraints on the use of Mahalanobis distance: with more elements than samples, the group variance-covariance matrix is singular thus rendering calculation of I_x (and D^2 itself) impossible. Therefore, the dimensionality of the groups must somehow be reduced. One approach would be to eliminate elements considered irrelevant or redundant. The problem with this approach is that the investigator's preconceptions about which elements should be discriminate may not be valid. It also squanders the main advantage of multielement analysis, namely the capability to measure a large number of elements. An alternative approach is to calculate Mahalanobis distances with the scores on principal components extracted from the variance-covariance or correlation matrix for the complete data set. This approach entails only the assumption, entirely reasonable in light of the above discussion of PCA, that most group-separating differences should be visible on the first several PCs. Unless a data set is extremely complex, containing numerous distinct groups, using enough components to subsume at least 90% of the total variance in the data can be generally assumed to yield Mahalanobis distances that approximate Mahalanobis distances in full elemental concentration space.

Lastly, Mahalanobis distance calculations are also quite useful for handling missing data (Sayre 1975). When many specimens are analyzed for a large number of elements, it is almost certain that a few element concentrations will be missed for some of the specimens. This occurs most frequently when the concentration for an element is near the detection limit. Rather than eliminate the specimen or the element from consideration, it is possible to substitute a missing value by replacing it with a value that minimizes the Mahalanobis distance for the specimen from the group centroid. Thus, those few specimens which are missing a single concentration value can still be used in group calculations.

containing 14 samples (5 pottery and 9 clay) received in 2008, and one containing a single sample received in 2009. Results for the two separate analyses are presented in this order.

2008 Analysis

The primary questions addressed here are: 1) How similar are the ceramics, and do they match any of the clay samples? 2) Are there any matches with other samples in the MURR database? 3) Are there similarities between the samples in this study and those analyzed by Meier (2007)? Table J-1 lists the descriptive data for the samples. Table J-2 provides the eigenvalues and variances for the first ten principal components.

J.3 RESULTS AND CONCLUSIONS

As discussed earlier, the samples in this analysis were submitted in two batches: one

Table J-1. Descriptive Information.

Analytical No.	Alternate ID No.	Material Type	Site Name	Site #
TRC379	#18-004-1a	Clay	Pipeline	41PT185
TRC 380	#20-004-1a	Clay	Big Blue Creek	N/A
TRC 381	#263-004-2c	Clay	Pipeline	41PT185/C
TRC382	#13-004-1a	Clay	Wildcat Bluff N.C.	N/A
TRC383	#1-a	Clay and sand	Big Blue Creek Pot	N/A
TRC429	#401-008-1	Redware sherd	Pavilion	41PT245
TRC430	#340-008-1	Plain sherd	Pavilion	41PT245
TRC431	#343-008-1a	Corrugated sherd	Corral	41PT186
TRC432	#FS 68.1	Cordmarked sherd	Corral	41PT186
TRC433	#341-008-3	Plain sherd	Pavilion	41PT245
TRC434	#341-004-1b	Silty clay	Corral	41PT186
TRC435	#5-004-1	Sandy loam	Off-site	—
TRC436	#419-004-2c	Clay	Pavilion	41PT245
TRC437	#12-004-1	Clay	Off-site	—
TRC527	#443-8-1	Sherd		41PT186

Table J-2. Eigenvalues and Variances for the First Ten Principal Components.

Simultaneous R-Q Factor Analysis Based on Variance-Covariance Matrix

Eigenvalues and Percentage of Variance Explained:

	Eigenvalue	%Variance	Cum. %Var.
1	0.2470	41.4723	41.4723
2	0.0884	14.8494	56.3216
3	0.0610	10.2405	66.5622
4	0.0436	7.3208	73.8830
5	0.0389	6.5274	80.4104
6	0.0322	5.4046	85.8150
7	0.0253	4.2434	90.0583
8	0.0141	2.3633	92.4216
9	0.0111	1.8559	94.2776
10	0.0063	1.0509	95.3285

Eigenvectors (largest to smallest):

As	0.0791	0.1699	0.2739	0.2563	0.1378	0.5640	0.0197	0.4238	-0.3170	0.3746
La	0.1650	0.0061	-0.0185	0.0603	-0.0371	-0.0434	-0.1631	-0.0388	-0.0669	0.1083
Lu	0.1818	-0.0293	0.0195	0.0495	-0.0523	-0.1547	-0.1532	0.1143	-0.0427	-0.0555
Nd	0.1755	0.0424	-0.0016	0.0855	-0.0006	-0.0607	-0.1580	-0.0799	0.0246	0.2283
Sm	0.1822	-0.0238	-0.0081	0.0811	-0.0336	-0.0767	-0.1876	-0.0163	0.0799	0.0854
U	0.1098	-0.0899	0.3207	0.3141	-0.4405	0.2540	0.0089	0.0337	0.4257	-0.2806
Yb	0.1890	-0.0453	0.0153	0.0566	0.0099	-0.1690	-0.1813	0.0956	-0.0709	-0.0584
Ce	0.1886	-0.0163	-0.0286	0.0481	0.0188	-0.0614	-0.1643	0.0044	-0.0643	0.0798
Co	0.2127	-0.0006	0.1288	-0.2649	0.1325	0.2031	0.1771	-0.0802	0.4184	0.3582
Cr	0.2298	0.0543	-0.1077	-0.2307	0.0351	0.1477	0.0575	-0.0637	0.2095	-0.0134
Cs	0.2777	0.0166	-0.0680	-0.1742	-0.0029	0.1848	0.2002	-0.0906	-0.1589	-0.4031
Eu	0.1474	-0.0008	-0.0443	0.0569	-0.0202	-0.0621	-0.1601	-0.0994	0.0629	0.1240
Fe	0.2161	0.1255	-0.0294	-0.1528	0.0971	0.0273	0.0160	-0.1227	0.0611	0.0839
Hf	0.0816	-0.0797	0.0905	0.1346	0.1502	-0.0535	-0.1943	0.1217	0.1974	-0.0830
Rb	0.2275	-0.0759	0.1045	-0.1500	-0.0013	-0.1349	0.2635	-0.0136	-0.0730	-0.0611
Sb	0.2239	0.3417	-0.3418	0.6275	0.2154	-0.1398	0.4685	-0.0893	0.0832	-0.0453
Sc	0.2444	0.0520	-0.0899	-0.1885	-0.0046	0.0763	0.0363	-0.0871	0.0937	0.0806
Sr	-0.0582	0.2790	0.1531	0.1112	-0.4733	0.1075	-0.0530	-0.6058	-0.1348	0.1660
Ta	0.2269	-0.0193	-0.0489	-0.0245	0.0271	0.0378	-0.1459	0.1225	-0.0499	-0.1175
Tb	0.1908	-0.0411	-0.0047	0.1090	0.0019	-0.1772	-0.2205	-0.0255	-0.0338	0.1306
Th	0.1954	0.0169	-0.0335	-0.0320	-0.0164	0.0186	-0.0649	0.0329	-0.1065	-0.0667
Zn	0.1866	0.0548	-0.0646	0.0624	-0.1914	-0.0192	-0.1491	-0.0661	-0.2050	0.0310
Zr	0.0612	-0.0615	0.1178	0.1768	0.0381	0.0411	-0.1363	0.0721	0.3653	-0.1231
Al	0.1902	0.0039	-0.0251	-0.1085	-0.0405	0.0315	0.0287	0.0349	-0.1132	-0.0352
Ba	-0.0565	0.7700	0.3498	-0.2212	-0.0345	-0.3320	-0.0359	0.2634	0.1093	-0.1181
Dy	0.1933	-0.0173	-0.0359	0.0385	-0.0726	-0.1415	-0.1992	0.1293	-0.0255	-0.0588
K	0.1911	-0.0882	0.1606	-0.0718	-0.0916	-0.2324	0.1808	-0.0146	-0.0728	0.3369
Mn	0.0452	0.0576	0.3882	0.0576	0.6064	0.1196	-0.2398	-0.4712	-0.1031	-0.2458
Na	0.1505	-0.3204	0.5365	0.0827	-0.0300	-0.2849	0.3877	0.0084	-0.1850	-0.0404
Ti	0.1718	0.0335	-0.0612	-0.1113	-0.0294	0.0987	0.0261	0.0666	0.1571	-0.0169
V	0.1970	0.1087	-0.0573	-0.0950	-0.1860	0.2532	0.0034	0.0857	-0.2739	-0.3016

J.3.1 COMPARISON OF POTTERY AND CLAY SAMPLES:

The small number of ceramic samples ($N = 5$) makes the determination of internal compositional groups impractical and the comparison to local clays difficult. The clays are generally similar to the sherds.

The only element consistently different between the clays and the sherds is barium, in which the clays are slightly lower in barium concentration. Figure J-1 is a typical bivariate plot of these data showing the general similarity between the clays and the sherds. The clays tend to be more variable, but not excessively so.

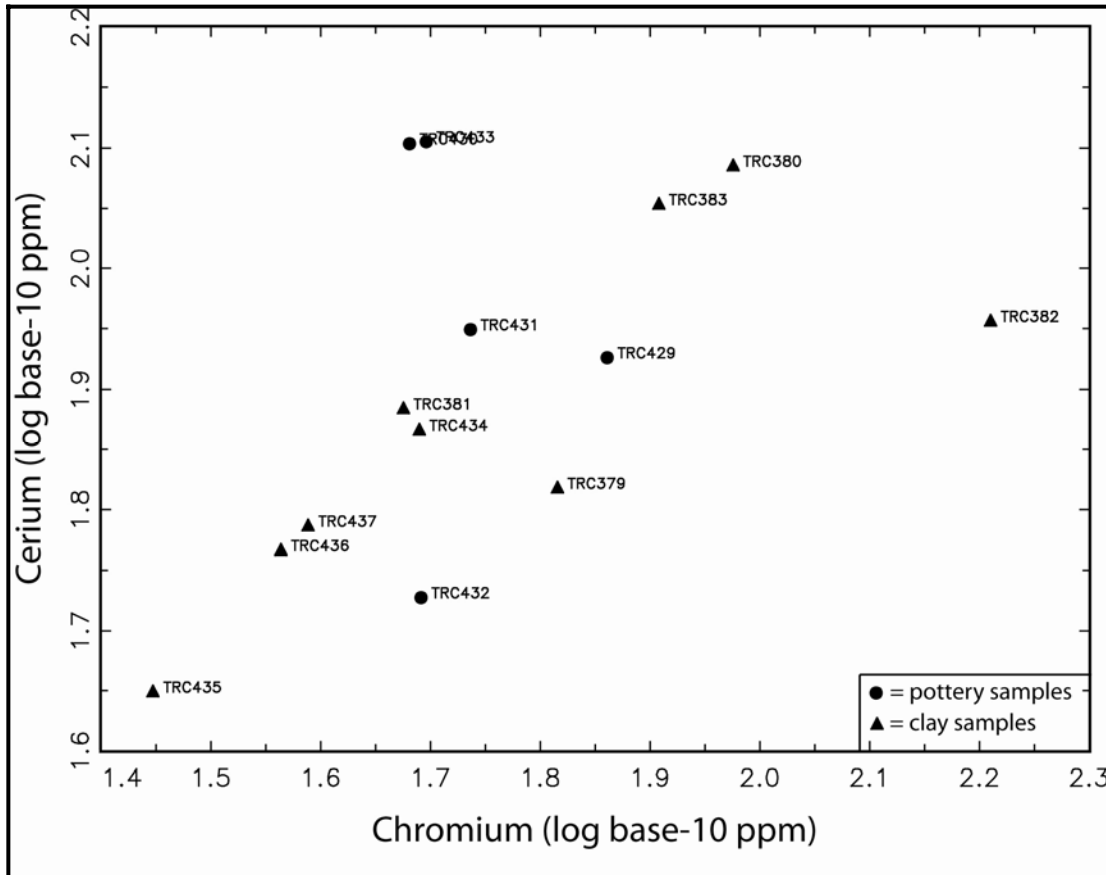


Figure J-1. Bivariate of Log Base-10 Concentrations of Chromium and Cerium Showing the Similarity Between the Pottery and Clay Samples.

A hierarchical cluster diagram (Figure J-2) divides the samples into three main groups. One of the groups consists of only two samples: both of the plain sherds from the Pavilion site. The other two groups consist of both pottery and clay samples. A hierarchical cluster analysis of such a small number of samples is not a particularly robust technique, thus we refrain from developing compositional groups based on this analysis, but the separation of the two

plainware sherds may suggest that these vessels were not manufactured from the local clays included in this analysis. There is a distinct possibility that the clays may have been tempered with aplastics that are limiting the ability to link specific clay deposits with particular sherds. The two Triassic clays may be slightly different (both at the bottom of the cluster diagram), but the differences are slight.

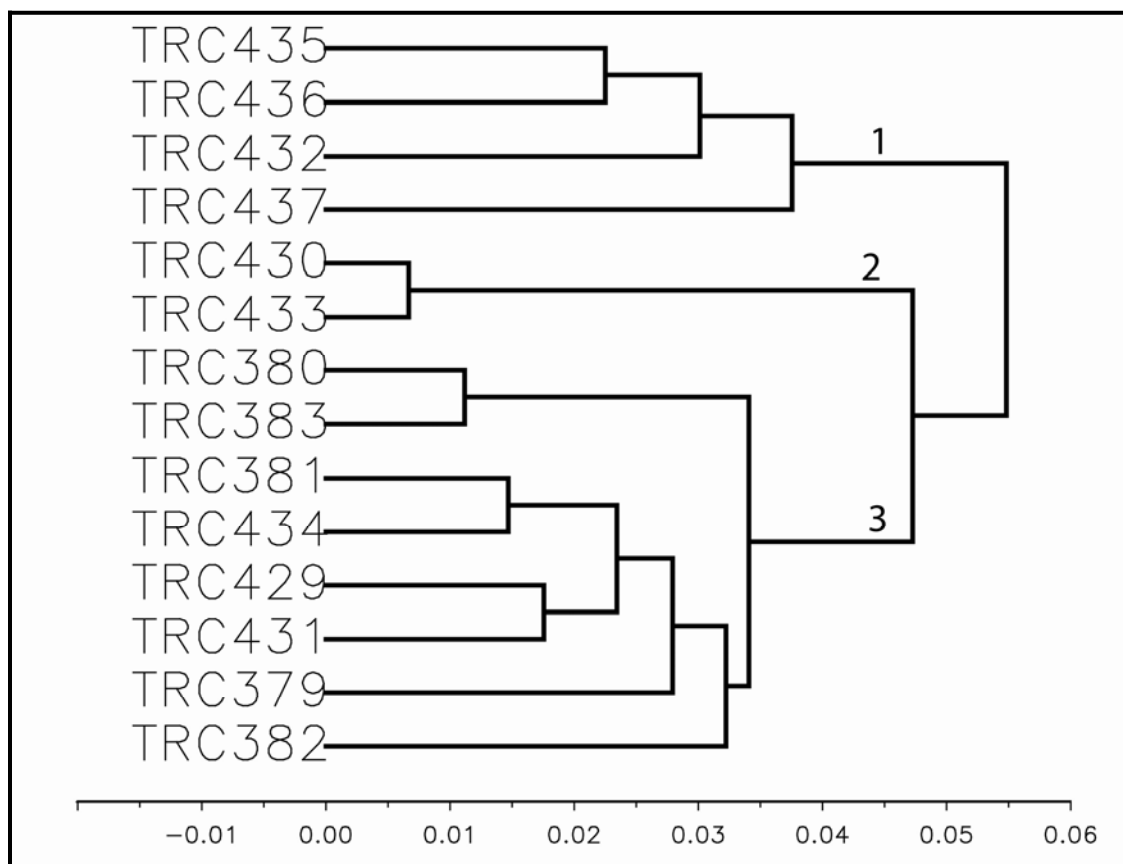


Figure J-2. Hierarchical Cluster Diagram of the TRC Samples. The Major Groups are Noted by the Numbers 1-3, but These do not Represent True Compositional Groups.

J.3.2 COMPARISON WITH THE MURR DATABASE:

A Euclidian distance search of the entire MURR ceramic database turned up only one possible match with the samples in this study. The only potentially similar samples were those analyzed for Holly Meier in 2007 and reported in her Master's thesis from Texas State University, San Marcos (Meier 2007) and are discussed below.

J.3.3 COMPARISON WITH MEIER DATA:

Meier conducted her own interpretation of the data, following initial training at MURR, and her compositional groups are similar to those initially developed while working directly with MURR staff. The samples did not easily separate into compositional

groups using bivariate plots, and are still overlapping when using principal components. Figure J-3 is a bivariate elemental plot of Meier's samples and the TRC samples. None of the TRC samples consistently plot within the ellipse for any of the compositional groups.

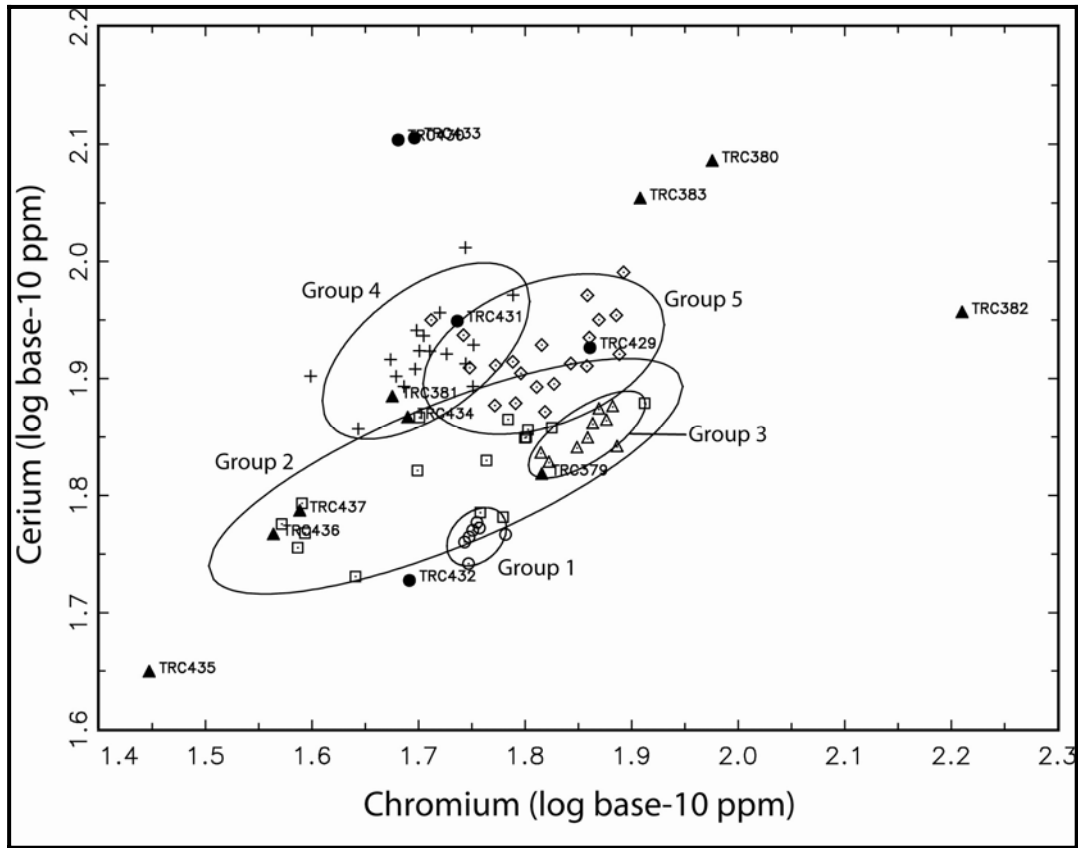


Figure J-3. Bivariate of Log Base-10 Concentrations of Chromium and Cerium showing the General Similarity Between the TRC Samples and those Analyzed by Holly Meier. Ellipses Represent 90% Confidence Intervals for Group Membership.

Ideally we would like to project the new samples against the groups developed by Meier. One of the best measures of group membership is the Mahalanobis distance calculation, but this requires a minimum sample size of one more than the number of elements measured (in this project we included 31 elements in the analysis). The best way to calculate Mahalanobis distances in cases where the sample sizes are small is to use as large of a subset of the principal components as possible (again, one less than the samples size). Unfortunately, principal components were not helpful in discriminating the groups developed by Meier, and instead we use canonical

discriminant analysis (CDA). CDA is similar to PCA in that it creates a new set of variables to maximize variance, but while PCA maximizes the total variance in the entire dataset, CDA creates variables that maximize the distance between established groups. This is entirely dependent upon the integrity of the initial grouping. CDA creates a number of variables equal to one less than the number of groups, in this case there are 4 variables. Each of the groups contains enough samples to use all of the CDA variables in the Mahalanobis distance calculations. Figure J-4 is a plot of the Meier groups and the TRC samples according to the first two CD functions.

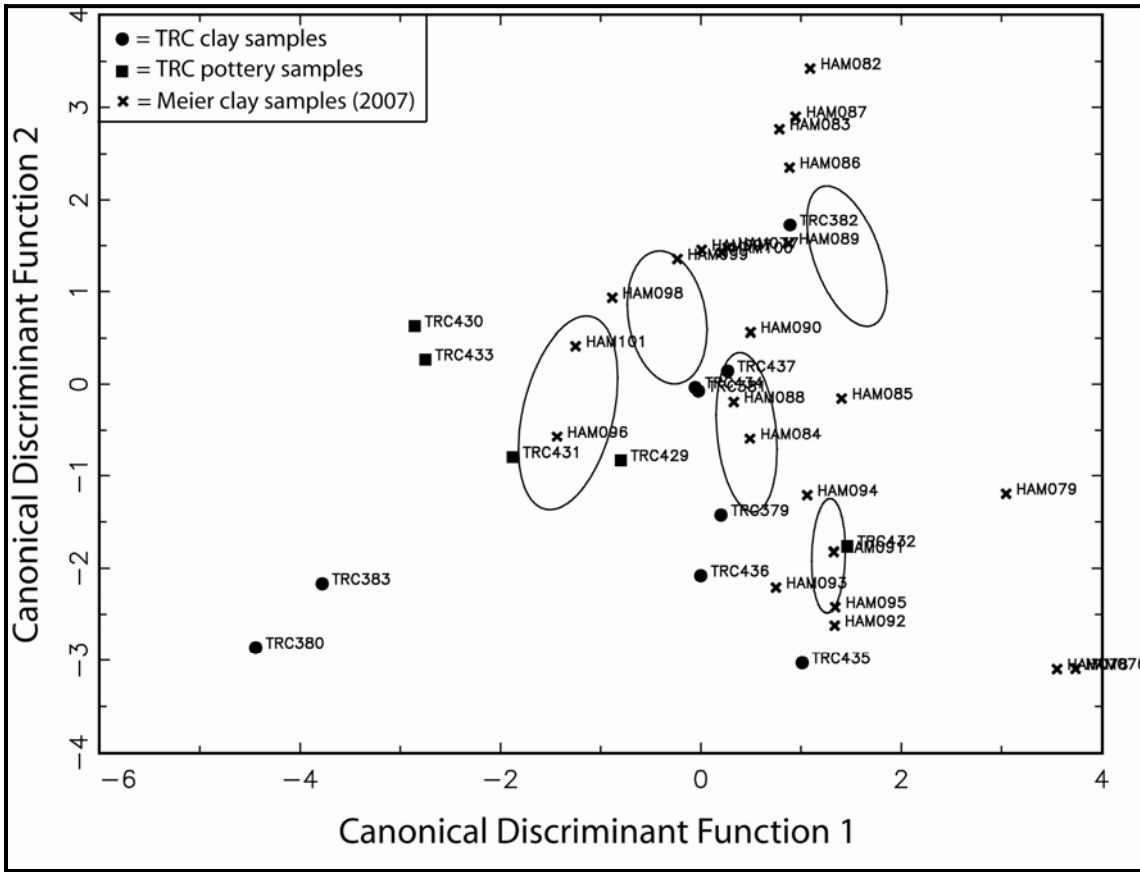


Figure J-4. Bivariate of Canonical Discriminant Functions 1 and 2 Showing the General Similarity between the TRC Samples and those Analyzed by Holly Meier. Ellipses Represent 90% Confidence Intervals for Group Membership.

Assuming that the groups developed by Meier are sound, it is possible to calculate the probability of group membership using a Mahalanobis distance calculation based on the four CDA variables. Table J-3 is a list of these probabilities for each of the assigned samples in Meier’s database.

Table J-3 shows that CDA successfully isolated the compositional groups, and thus it is possible to project the TRC samples against these groups to determine any possible matches. Table J-4 is a list of the probabilities of group membership for each of the TRC samples.

Table J-3. Probability of Group Membership Based on a Mahalanobis Distance Calculation using the Four CDA Functions.

MAHALANOBIS DISTANCE CALCULATION AND POSTERIOR CLASSIFICATION FOR TWO OR MORE GROUPS.

Groups are:

1	CDG1
2	CDG2
3	CDG3
4	CDG4
5	CDG5

Variables used:

CD01 CD02 CD03 CD04

Probabilities are jackknifed for specimens included in each group.

The following specimens are in the file CDG1

Probabilities:

ID. NO.	CDG1	CDG2	CDG3	CDG4	CDG5	From:	Into:
HAM001	33.546	0.037	0.028	0.000	0.000	1	1
HAM015	5.479	0.109	0.141	0.000	0.000	1	1
HAM022	12.721	0.767	0.206	0.000	0.000	1	1
HAM023	97.922	0.060	0.077	0.000	0.000	1	1
HAM024	95.854	0.061	0.226	0.000	0.000	1	1
HAM025	50.295	0.033	0.173	0.000	0.000	1	1
HAM062	20.394	0.024	0.216	0.000	0.000	1	1

The following specimens are in the file CDG2

Probabilities:

ID. NO.	CDG1	CDG2	CDG3	CDG4	CDG5	From:	Into:
HAM002	1.265	69.888	0.318	0.000	0.210	2	2
HAM003	1.097	85.664	0.456	0.001	0.468	2	2
HAM006	1.374	65.829	0.253	0.000	0.501	2	2
HAM008	1.335	94.407	0.225	0.000	0.191	2	2
HAM010	3.141	11.239	0.140	0.000	0.026	2	2
HAM012	1.430	55.382	0.291	0.000	0.183	2	2
HAM016	1.159	34.774	0.265	0.000	0.900	2	2
HAM019	1.356	43.548	0.270	0.000	0.074	2	2
HAM035	2.436	12.328	0.322	0.000	0.019	2	2
HAM039	0.742	3.464	1.094	0.008	3.022	2	2
HAM058	2.224	73.961	0.618	0.000	0.213	2	2
HAM060	1.217	99.549	0.276	0.000	0.365	2	2
HAM065	1.173	56.963	0.160	0.000	0.105	2	2
HAM066	3.388	69.030	0.403	0.000	0.062	2	2
HAM067	1.454	62.662	0.173	0.000	0.106	2	2
HAM074	0.387	0.872	0.198	0.019	7.007	2	5

The following specimens are in the file CDG3

Probabilities:

ID. NO.	CDG1	CDG2	CDG3	CDG4	CDG5	From:	Into:
HAM029	1.914	0.002	3.402	0.000	0.000	3	3
HAM031	1.518	0.002	84.332	0.000	0.000	3	3
HAM032	1.892	0.002	70.485	0.000	0.000	3	3
HAM036	1.056	0.002	1.720	0.000	0.000	3	3

HAM037	1.027	0.000	15.975	0.000	0.000	3	3
HAM038	1.865	0.003	93.792	0.000	0.000	3	3
HAM040	1.585	0.007	74.141	0.000	0.001	3	3
HAM044	1.818	0.004	90.294	0.000	0.000	3	3
HAM046	2.900	0.009	27.611	0.000	0.000	3	3

The following specimens are in the file CDG4
 Probabilities:

ID. NO.	CDG1	CDG2	CDG3	CDG4	CDG5	From:	Into:
HAM004	0.032	0.000	0.005	4.013	0.000	4	4
HAM007	0.039	0.000	0.010	87.275	0.000	4	4
HAM009	0.058	0.000	0.013	42.993	0.000	4	4
HAM017	0.041	0.000	0.014	95.865	0.000	4	4
HAM026	0.039	0.000	0.010	15.604	0.000	4	4
HAM028	0.045	0.000	0.008	64.203	0.000	4	4
HAM042	0.036	0.000	0.017	27.874	0.000	4	4
HAM051	0.034	0.000	0.005	29.014	0.000	4	4
HAM052	0.045	0.000	0.012	96.839	0.000	4	4
HAM053	0.064	0.001	0.024	7.532	0.001	4	4
HAM054	0.056	0.001	0.038	63.285	0.007	4	4
HAM056	0.044	0.000	0.030	35.343	0.001	4	4
HAM063	0.049	0.000	0.020	86.505	0.001	4	4
HAM064	0.051	0.001	0.023	47.703	0.003	4	4
HAM068	0.049	0.000	0.020	73.928	0.000	4	4
HAM070	0.027	0.000	0.008	15.623	0.000	4	4
HAM071	0.053	0.001	0.027	50.950	0.015	4	4

The following specimens are in the file CDG5
 Probabilities:

ID. NO.	CDG1	CDG2	CDG3	CDG4	CDG5	From:	Into:
HAM005	0.096	0.022	0.093	0.200	27.599	5	5
HAM013	0.080	0.020	0.077	1.577	78.763	5	5
HAM018	0.206	0.751	0.462	0.210	10.593	5	5
HAM020	0.266	5.926	0.307	0.203	34.388	5	5
HAM021	0.162	0.640	0.079	0.165	28.371	5	5
HAM027	0.108	0.073	0.065	0.605	24.224	5	5
HAM030	0.094	0.041	0.066	0.488	34.998	5	5
HAM033	0.114	0.112	0.226	0.548	76.475	5	5
HAM034	0.107	0.104	0.079	1.828	32.096	5	5
HAM041	0.113	0.073	0.381	0.284	0.681	5	5
HAM043	0.124	0.229	0.098	1.518	78.777	5	5
HAM045	0.066	0.005	0.077	0.135	21.828	5	5
HAM047	0.086	0.028	0.109	1.683	50.533	5	5
HAM048	0.126	0.214	0.116	1.531	96.687	5	5
HAM049	0.085	0.021	0.108	0.151	70.769	5	5
HAM050	0.164	0.651	0.221	1.372	66.312	5	5
HAM057	0.093	0.056	0.102	3.590	68.190	5	5
HAM061	0.180	1.225	0.172	0.844	60.585	5	5
HAM069	0.226	3.446	0.265	0.297	62.024	5	5
HAM073	0.101	0.066	0.088	3.946	74.823	5	5

Summary of Classification Success:
Into:

From:	CDG1	CDG2	CDG3	CDG4	CDG5	Total
CDG1	7	0	0	0	0	7
CDG2	0	15	0	0	1	16
CDG3	0	0	9	0	0	9
CDG4	0	0	0	17	0	17
CDG5	0	0	0	0	20	20
Total	7	15	9	17	21	69

Table J-4. Probability of Group Membership for Each of the TRC Samples Based on a Mahalanobis Distance Projection using the Four CDA Functions. Possible Matches are Shown in Bold Font.

MAHALANOBIS DISTANCE CALCULATION FOR MISCELLANEOUS SPECIMENS
PROJECTED AGAINST TWO OR MORE GROUPS.

Reference groups and numbers of specimens:		
1	CDG1	7
2	CDG2	16
3	CDG3	9
4	CDG4	17
5	CDG5	20

Variables used:
CD01 CD02 CD03 CD04

The following specimens are in the file CDTRC
Probabilities:

ID. NO.	CDG1	CDG2	CDG3	CDG4	CDG5
TRC379	0.484	0.001	0.002	0.000	0.000
TRC380	0.004	0.000	0.000	0.000	0.000
TRC381	0.334	8.125	0.095	0.002	5.279
TRC382	0.929	0.013	24.827	0.001	0.006
TRC383	0.005	0.000	0.001	0.000	0.000
TRC429	0.126	0.000	0.005	0.003	0.000
TRC430	0.015	0.000	0.001	0.000	0.000
TRC431	0.026	0.000	0.003	4.682	0.000
TRC432	9.875	0.049	0.117	0.000	0.000
TRC433	0.016	0.000	0.001	0.001	0.000
TRC434	0.321	8.435	0.156	0.007	14.303
TRC435	3.932	0.096	0.046	0.000	0.000
TRC436	0.496	0.208	0.027	0.000	0.002
TRC437	0.662	0.937	0.025	0.000	0.007

J.4 2009 ANALYSIS

We have compared the compositional data for the single ceramic sherd (TRC527) to the MURR database using a Euclidian distance calculation and, as expected, the only close matches were other samples from Potter County including those submitted by Holly Meier (2007). As with the previous analysis

the data are calcium corrected and compared to the groups developed by Meier. Meier's groups separate well using a canonical discriminant analysis, and a plot of discriminant variables 1 and 2 (Figure J-5) along with a Mahalanobis distance projection (Table J-5) show that

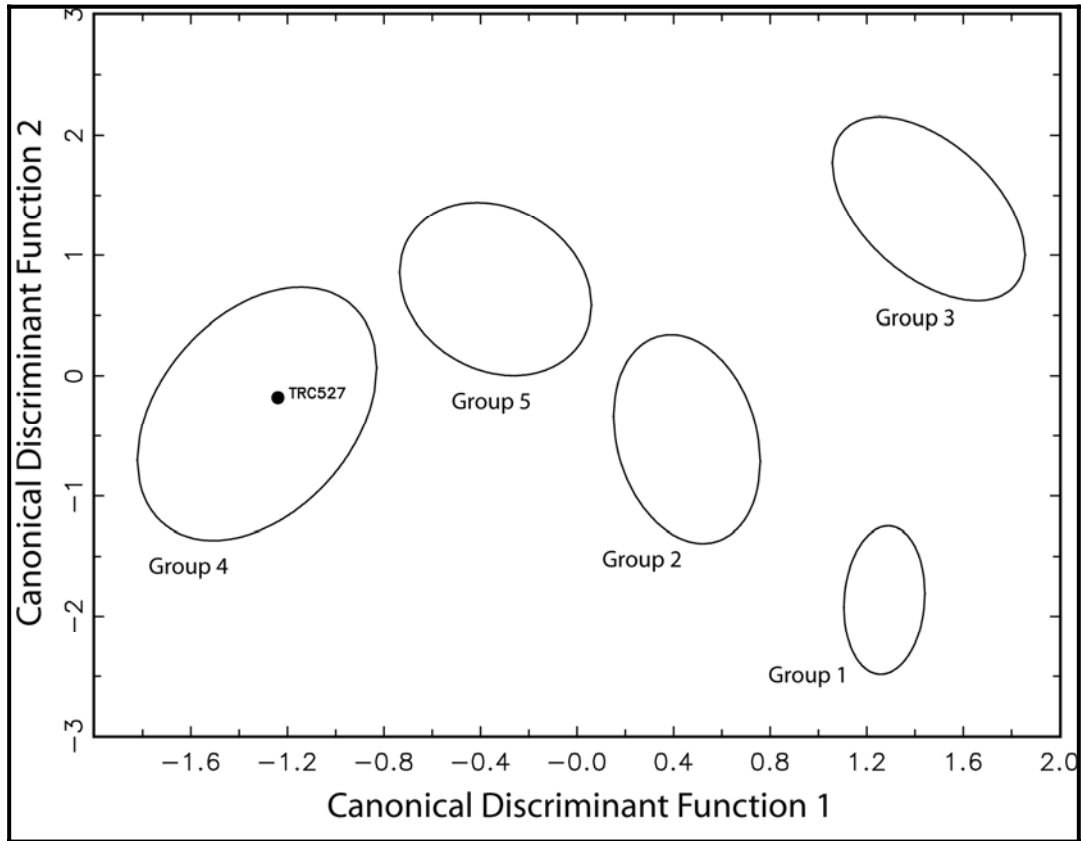


Figure J-5. Bivariate Plot of Canonical Discriminant Functions 1 and 2 Showing the Similarity TRC527 and the Groups Developed by Holly Meier (2007). Ellipses Represent 90% Confidence Intervals for Group Membership.

Table J-5. Probability of Group Membership for TRC527 Based on a Mahalanobis Distance Projection using the Four CDA Functions. The Possible Match is Shown in Bold Font.

ID. NO.	Probabilities:				
	Group 1	Group 2	Group 3	Group 4	Group 5
TRC527	0.058	0.000	0.009	1.421	0.000

this single sample is similar to Meier's Group 4. Of the previously analyzed TRC samples, the only one compositionally similar to TRC527 is TRC431, assigned to Meier's Group 4.

We have used elemental bivariate plots to compare TCR to Meier's Group 4, and

found that the sample falls within the 90% confidence interval for group membership for all elements except hafnium and zirconium. The elevated levels of these two elements suggest a presence or increased amounts of zircons, likely contained in sand temper.

J.5 CONCLUSION

While there are some possible matches between a few of the TRC samples and the groups developed by Meier, we are hesitant to emphasize this connection. The groups created by Meier are not very distinct - except in CDA plots - and may not represent significant differences in production recipes. Rather than link the TRC samples to specific groups, it is more prudent to simply note the similarity of the TRC samples with those analyzed by Meier. A hierarchical cluster diagram of the combined datasets shows no distinct separation or grouping of the TRC samples within the Meier dataset. Perhaps a larger number of ceramic samples would help to demonstrate internal compositional groups, particularly the separation of the two plainware sherds. A larger sample of sherds would also help to determine which ceramics are likely locally made, an impossible task with only five samples.

Linking sherds to clay sources is typically a difficult task, particularly when the temper is not analyzed (and thus cannot be mathematically combined with the clay for comparison) and the number of sherds is small. The general similarity of the clays and the sherds does not rule out the possibility that some of the clay sources sampled for analysis could have been used to produce the sherds.

J.6 ACKNOWLEDGMENTS

We acknowledge Mark Beary and Corinne Rosania for their role in preparing the samples for irradiation.

J.7 REFERENCES CITED

Baxter, Michael J.
1992 Archaeological uses of the biplot—a neglected technique? In *Computer Applications and Quantitative Methods in Archaeology, 1991*, edited by G. Lock and J. Moffett.

BAR International Series S577, 141–148. Tempvs Reparavm, Archaeological and Historical Associates, Oxford.

1994 *Exploratory Multivariate Analysis in Archaeology*. Edinburgh University Press, Edinburgh.

Baxter, M. J. and C. E. Buck
2000 Data Handling and Statistical Analysis. In *Modern Analytical Methods in Art and Archaeology*, edited by E. Ciliberto and G. Spoto, pp. 681-746. John Wiley and Sons,

Bieber, Alan M. Jr., Dorothea W. Brooks, Garman Harbottle, and Edward V. Sayre

1976 Application of multivariate techniques to analytical data on Aegean ceramics. *Archaeometry* 18:59–74.

Bishop, Ronald L. and Hector Neff
1989 Compositional data analysis in archaeology. In *Archaeological Chemistry IV*, edited by R. O. Allen, pp. 576–586. Advances in Chemistry Series 220, American Chemical Society, Washington, D.C.

Bishop, Ronald L., Robert L. Rands, and George R. Holley

1992 Ceramic compositional analysis in archaeological perspective. In *Advances in Archaeological Method and Theory*, vol. 5, pp. 275–330. Academic Press, New York.

Glascocock, Michael D.
1992 Characterization of archaeological ceramics at MURR by neutron activation analysis and multivariate statistics. In *Chemical Characterization of Ceramic Pastes in Archaeology*, edited by H. Neff, pp. 11–26. Prehistory Press, Madison, WI.

Harbottle, Garman

1976 Activation analysis in archaeology. *Radiochemistry* 3:33–72. The Chemical Society, London.

Leese, Morven N. and Peter L. Main

1994 The efficient computation of unbiased Mahalanobis distances and their interpretation in archaeometry. *Archaeometry* 36:307–316.

Lynott, Mark J., Hector Neff, James E. Price, James W. Cogswell, and Michael D. Glascock

2000 Inferences about prehistoric ceramics and people in Southeast Missouri: Results of ceramic compositional analysis. *American Antiquity* 65(1):103–126.

Meier, Holly A.

2007 An Evaluation of Antelope Creek Phase Interaction using INAA. Master's thesis, Department of Anthropology, Texas State University-San Marcos.

Neff, Hector

1992 Introduction. In *Chemical Characterization of Ceramic Pastes in Archaeology*, edited by H. Neff, pp. 1–10. Prehistory Press, Madison, WI.

1994 RQ-mode principal components analysis of ceramic compositional data. *Archaeometry* 36:115–130.

2000 Neutron activation analysis for provenance determination in archaeology. In *Modern Analytical Methods in Art and Archaeology*, edited by E. Ciliberto and G. Spoto, pp. 81–134. John Wiley and Sons, Inc., New York.

2002 Quantitative techniques for analyzing ceramic compositional data. In *Ceramic Source Determination in the Greater Southwest*, edited by D. M. Glowacki and H. Neff. Monograph 44, Cotsen Institute of Archaeology, UCLA, Los Angeles.

Neff, Hector, Ronald L. Bishop, and Edward V. Sayre

1988 A simulation approach to the problem of tempering in compositional studies of archaeological ceramics. *Journal of Archaeological Science* 15:159–172.

Sayre, Edward V.

1975 *Brookhaven Procedures for Statistical Analyses of Multivariate Archaeometric Data*. Brookhaven National Laboratory Report BNL-23128. New York.

Steponaitis, Vincas, M. James Blackman, and Hector Neff

1996 Large-scale compositional patterns in the chemical composition of Mississippian pottery. *American Antiquity* 61:555–572.

Weigand, Phil C., Garman Harbottle, and Edward V. Sayre

1977 Turquoise sources and source analysis: Mesoamerica and the southwestern U.S.A. In *Exchange Systems in Prehistory*, edited by T. K. Earle and J. E. Ericson, pp. 15–34. Academic Press, New York.

Attachment J-1. Elemental Concentration Listed in Parts Per Million (ppm).

anid	As	La	Lu	Nd	Sm	U	Yb	Ce	Co	Cr	Cs
TRC379	2.828	31.884	0.411	25.490	6.206	2.036	2.808	63.433	11.543	63.103	4.869
TRC380	2.993	54.432	0.580	37.691	9.103	4.178	4.620	116.759	8.106	90.690	4.207
TRC381	2.923	25.311	0.336	21.881	4.610	3.734	2.073	54.164	5.647	33.487	3.566
TRC382	7.361	37.892	0.414	32.776	7.368	2.219	2.979	77.604	15.036	139.285	6.908
TRC383	4.453	52.215	0.579	37.810	8.744	3.824	4.258	105.351	7.558	75.380	4.954
TRC429	4.320	38.532	0.529	32.890	7.458	3.571	3.588	78.244	10.205	67.317	7.547
TRC430	5.012	56.958	0.522	49.435	10.769	3.849	3.670	123.279	13.416	46.570	11.388
TRC431	4.694	41.881	0.489	33.408	7.562	4.815	3.218	88.907	11.432	54.482	3.998
TRC432	3.885	22.607	0.291	19.111	4.262	1.504	2.072	50.658	7.923	46.632	3.036
TRC433	4.119	60.347	0.526	49.654	11.289	3.498	4.205	127.415	15.695	49.661	12.526
TRC434	6.744	31.645	0.441	26.049	5.673	3.513	2.960	67.671	8.171	45.074	4.302
TRC435	3.635	20.928	0.254	19.061	3.590	2.034	1.753	42.371	4.953	26.644	2.659
TRC436	1.936	25.778	0.306	23.330	4.500	2.760	2.357	51.723	5.024	32.439	3.237
TRC437	12.024	23.938	0.421	22.842	4.826	7.356	2.158	51.988	5.402	32.968	3.142
TRC527	4.8945	36.9434	0.5221	36.8778	7.3893	4.2608	3.6354	69.6279	9.8144	50.7065	3.7633

anid	Eu	Fe	Hf	Ni	Rb	Sb	Sc	Sr	Ta	Tb	Th
TRC379	1.242	41627.1	8.080	0.000	103.479	1.200	12.188	118.865	1.039	0.860	11.140
TRC380	0.927	32604.4	7.371	0.000	100.635	0.591	9.812	340.138	2.796	1.474	21.005
TRC381	0.857	16332.5	6.425	0.000	66.852	0.541	6.113	341.884	0.812	0.601	7.958
TRC382	1.470	44416.1	5.778	43.642	129.729	0.794	14.093	159.549	1.151	1.062	11.599
TRC383	0.956	29121.4	7.372	32.670	98.226	0.649	9.606	346.600	2.570	1.340	19.733
TRC429	1.500	34066.1	7.602	46.025	90.414	0.699	14.062	177.238	1.405	1.110	11.851
TRC430	2.604	47000.2	7.673	28.750	105.048	0.535	16.692	111.946	1.697	1.560	11.883
TRC431	1.401	37173.2	7.413	43.779	88.141	0.671	13.669	177.322	1.269	0.922	12.406
TRC432	0.794	23086.7	6.237	2.306	75.184	0.737	7.632	127.988	0.779	0.593	7.897
TRC433	2.728	49039.1	8.750	0.000	114.007	0.561	17.550	101.636	1.567	1.583	12.457
TRC434	1.042	22298.3	11.148	28.951	85.972	0.696	7.278	231.144	1.017	0.776	10.258
TRC435	0.683	13478.4	7.286	0.000	66.633	0.442	4.346	0.000	0.726	0.590	6.396
TRC436	0.861	15817.2	7.417	0.000	64.027	0.478	5.374	177.773	0.689	0.605	7.417
TRC437	0.814	17841.9	8.541	0.000	67.620	0.630	5.726	192.162	0.782	0.587	7.881
TRC527	1.3895	29416.7	8.8968	22.38	102.27	0.5203	9.8983	211.76	0.9519	0.8992	10.7639

anid	Zn	Zr	Al	Ba	Ca	Dy	K	Mn	Na	Ti	V
TRC379	82.475	198.087	75178.5	365.6	13944.0	5.478	23411.6	211.416	8219.6	4347.6	99.037
TRC380	70.083	155.586	95669.2	325.9	16213.8	8.758	19649.5	279.753	13504.2	2781.3	66.454
TRC381	49.519	179.903	43393.9	600.3	117053.3	3.204	13278.0	188.215	4779.3	2448.2	47.914
TRC382	86.324	147.016	74503.5	466.8	56482.1	6.085	26988.6	561.086	7777.7	4341.2	96.303
TRC383	70.416	166.816	91185.9	461.3	27249.1	7.589	19025.3	248.674	10109.0	3325.7	85.428
TRC429	50.229	198.687	84489.8	795.2	29075.3	6.675	17941.1	379.693	9062.7	4294.7	84.103
TRC430	107.774	198.596	92901.9	4656.9	11510.7	8.691	24663.3	535.534	8802.7	4489.7	88.562
TRC431	82.117	193.226	88470.8	1272.2	9786.8	6.432	20914.3	446.536	6271.1	3567.7	88.379
TRC432	40.098	130.047	53694.4	2322.2	20417.8	3.432	18223.0	288.366	3723.7	2742.7	56.616
TRC433	114.829	227.814	97711.4	5234.3	9326.3	8.936	21345.6	605.764	7826.5	4459.8	92.470
TRC434	62.939	289.392	54825.0	649.1	31622.1	4.382	17265.1	409.308	7882.5	3167.9	61.798
TRC435	32.939	180.602	35431.1	486.1	19421.9	2.950	14619.7	268.104	4797.4	1742.7	40.061
TRC436	46.989	197.014	38723.3	789.2	45555.8	2.909	13976.2	118.592	4459.5	2256.4	39.373
TRC437	47.238	251.547	39745.1	569.1	59877.3	3.145	14742.0	177.417	4627.8	2583.3	52.022
TRC527	73.34	222.80	63732.1	1305.9	36908.4	5.7253	23574.0	268.45	8523.8	3357.6	74.71

APPENDIX K
RADIOCARBON ASSAYS

This page intentionally left blank.

RADIOCARBON ASSAYS

Prepared for:



**TRC Environmental Corporation
505 East Huntland Drive, Suite 250
Austin, Texas 78752**

Prepared by:

**Darden Hood
Beta Analytic
4985 SW74 Court
Miami, Florida 33155**

September 25, 2009

This page intentionally left blank.



Consistent Accuracy
Delivered On Time

Beta Analytic Inc
4985 SW 74 Court
Miami, Florida 33155
Tel: 305-667-5167
Fax: 305-663-0964
beta@radiocarbon.com
www.radiocarbon.com

The Radiocarbon Laboratory Accredited to ISO-17025 Testing Standards (PJLA Accreditation #59423)

Mr. Darden Hood
President

Mr. Ronald Hatfield
Mr. Christopher Patrick
Deputy Directors

Final Report

The final report package includes the final date report, a statement outlining our analytical procedures, a glossary of pretreatment terms, calendar calibration information, billing documents (containing balance/credit information and the number of samples submitted within the yearly discount period), and peripheral items to use with future submittals. The final report includes the individual analysis method, the delivery basis, the material type and the individual pretreatments applied. The final report has been sent by mail and e-mail (where available).

Pretreatment

Pretreatment methods are reported along with each result. All necessary chemical and mechanical pretreatments of the submitted material were applied at the laboratory to isolate the carbon, which may best represent the time event of interest. When interpreting the results, it is important to consider the pretreatments. Some samples cannot be fully pretreated, making their ^{14}C ages more subjective than samples, which can be fully pretreated. Some materials receive no pretreatments. Please look at the pretreatment indicated for each sample and read the pretreatment glossary to understand the implications.

Analysis

Materials measured by the radiometric technique were analyzed by synthesizing sample carbon to benzene (92% C), measuring for ^{14}C content in one of 53 scintillation spectrometers, and then calculating for radiocarbon age. If the Extended Counting Service was used, the ^{14}C content was measured for a greatly extended period of time. AMS results were derived from reduction of sample carbon to graphite (100 %C), along with standards and backgrounds. The graphite was then detected for ^{14}C content in one of 9 accelerator-mass-spectrometers (AMS).

The Radiocarbon Age and Calendar Calibration

The "Conventional ^{14}C Age (*)" is the result after applying $^{13}\text{C}/^{12}\text{C}$ corrections to the measured age and is the most appropriate radiocarbon age. If an "*" is attached to this date, it means the $^{13}\text{C}/^{12}\text{C}$ was estimated rather than measured (The ratio is an option for radiometric analysis, but included on all AMS analyses.) Ages are reported with the units "BP" (Before Present). "Present" is defined as AD 1950 for the purposes of radiocarbon dating.

Results for samples containing more ^{14}C than the modern reference standard are reported as "percent modern carbon" (pMC). These results indicate the material was respiring carbon after the advent of thermo-nuclear weapons testing and is less than ~ 50 years old.

Applicable calendar calibrations are included for materials between about 100 and 19,000 BP. If calibrations are not included with a report, those results were too young, too old, or inappropriate for calibration. Please read the enclosed page discussing calibration.

PRETREATMENT GLOSSARY
Standard Pretreatment Protocols at Beta Analytic

Unless otherwise requested by a submitter or discussed in a final date report, the following procedures apply to pretreatment of samples submitted for analysis. This glossary defines the pretreatment methods applied to each result listed on the date report form (e.g. you will see the designation "acid/alkali/acid" listed along with the result for a charcoal sample receiving such pretreatment).

Pretreatment of submitted materials is required to eliminate secondary carbon components. These components, if not eliminated, could result in a radiocarbon date, which is too young or too old. Pretreatment does not ensure that the radiocarbon date will represent the time event of interest. This is determined by the sample integrity. Effects such as the old wood effect, burned intrusive roots, bioturbation, secondary deposition, secondary biogenic activity incorporating recent carbon (bacteria) and the analysis of multiple components of differing age are just some examples of potential problems. The pretreatment philosophy is to reduce the sample to a single component, where possible, to minimize the added subjectivity associated with these types of problems. If you suspect your sample requires special pretreatment considerations be sure to tell the laboratory prior to analysis.

"acid/alkali/acid"

The sample was first gently crushed/dispersed in deionized water. It was then given hot HCl acid washes to eliminate carbonates and alkali washes (NaOH) to remove secondary organic acids. The alkali washes were followed by a final acid rinse to neutralize the solution prior to drying. Chemical concentrations, temperatures, exposure times, and number of repetitions, were applied accordingly with the uniqueness of the sample. Each chemical solution was neutralized prior to application of the next. During these serial rinses, mechanical contaminants such as associated sediments and rootlets were eliminated. This type of pretreatment is considered a "full pretreatment". On occasion the report will list the pretreatment as "acid/alkali/acid - insolubles" to specify which fraction of the sample was analyzed. This is done on occasion with sediments (See "acid/alkali/acid - solubles")

Typically applied to: charcoal, wood, some peats, some sediments, and textiles "acid/alkali/acid - solubles"

On occasion the alkali soluble fraction will be analyzed. This is a special case where soil conditions imply that the soluble fraction will provide a more accurate date. It is also used on some occasions to verify the present/absence or degree of contamination present from secondary organic acids. The sample was first pretreated with acid to remove any carbonates and to weaken organic bonds. After the alkali washes (as discussed above) are used, the solution containing the alkali soluble fraction is isolated/filtered and combined with acid. The soluble fraction, which precipitates, is rinsed and dried prior to combustion.

"acid/alkali/acid/cellulose extraction"

Following full acid/alkali/acid pretreatments, the sample is bathed in (sodium chlorite) NaClO₂ under very controlled conditions (Ph = 3, temperature = 70 degrees C). This eliminates all components except wood cellulose. It is useful for woods that are either very old or highly contaminated.

Applied to: wood

"acid washes"

Surface area was increased as much as possible. Solid chunks were crushed, fibrous materials were shredded, and sediments were dispersed. Acid (HCl) was applied repeatedly to ensure the absence of carbonates. Chemical concentrations, temperatures, exposure times, and number of repetitions, were applied accordingly with the uniqueness of each sample. The sample was not be subjected to alkali washes to ensure the absence of secondary organic acids for intentional reasons. The most common reason is that the primary carbon is soluble in the alkali. Dating results reflect the total organic content of the analyzed material. Their accuracy depends on the researcher's ability to subjectively eliminate potential contaminants based on contextual facts.

Typically applied to: organic sediments, some peats, small wood or charcoal, special cases

BETA ANALYTIC INC. - 4985 SW 74 Court, Miami, Florida 33155 USA - Tel: 305-667-5167 - Fax 305-663-0964 - beta@radiocarbon.com

PRETREATMENT GLOSSARY
Standard Pretreatment Protocols at Beta Analytic
(Continued)

"collagen extraction: with alkali or collagen extraction: without alkali"

The material was first tested for friability ("softness"). Very soft bone material is an indication of the potential absence of the collagen fraction (basal bone protein acting as a "reinforcing agent" within the crystalline apatite structure). It was then washed in de-ionized water, the surface scraped free of the outer most layers and then gently crushed. Dilute, cold HCl acid was repeatedly applied and replenished until the mineral fraction (bone apatite) was eliminated. The collagen was then dissected and inspected for rootlets. Any rootlets present were also removed when replenishing the acid solutions. "With alkali" refers to additional pretreatment with sodium hydroxide (NaOH) to ensure the absence of secondary organic acids. "Without alkali" refers to the NaOH step being skipped due to poor preservation conditions, which could result in removal of all available organics if performed.

Typically applied to: bones

"acid etch"

The calcareous material was first washed in de-ionized water, removing associated organic sediments and debris (where present). The material was then crushed/dispersed and repeatedly subjected to HCl etches to eliminate secondary carbonate components. In the case of thick shells, the surfaces were physically abraded prior to etching down to a hard, primary core remained. In the case of porous carbonate nodules and caliches, very long exposure times were applied to allow infiltration of the acid. Acid exposure times, concentrations, and number of repetitions, were applied accordingly with the uniqueness of the sample.

Typically applied to: shells, caliches, and calcareous nodules

"neutralized"

Carbonates precipitated from ground water are usually submitted in an alkaline condition (ammonium Hydroxide or sodium hydroxide solution). Typically this solution is neutralized in the original sample container, using deionized water. If larger volume dilution was required, the precipitate and solution were transferred to a sealed separatory flask and rinsed to neutrality. Exposure to atmosphere was minimal.

Typically applied to: Strontium carbonate, Barium carbonate
(i.e. precipitated ground water samples)

"carbonate precipitation"

Dissolved carbon dioxide and carbonate species are precipitated from submitted water by complexing them as ammonium carbonate. Strontium chloride is added to the ammonium carbonate solution and strontium carbonate is precipitated for the analysis. The result is representative of the dissolved inorganic carbon within the water. Results are reported as "water DIC".

Applied to: water

"solvent extraction"

The sample was subjected to a series of solvent baths typically consisting of benzene, toluene, hexane, pentane, and/or acetone. This is usually performed prior to acid/alkali/acid pretreatments.

Applied to: textiles, prevalent or suspected cases of pitch/tar contamination, conserved materials.

"none"

No laboratory pretreatments were applied. Special requests and pre-laboratory pretreatment usually accounts for this.



Consistent Accuracy
Delivered On Time

Beta Analytic Inc

4985 SW 74 Court
Miami, Florida 33155
Tel: 305-667-5167
Fax: 305-663-0964
beta@radiocarbon.com
www.radiocarbon.com

The Radiocarbon Laboratory Accredited to ISO-17025 Testing Standards (PJLA Accreditation #59423)

Mr. Darden Hood
President

Mr. Ronald Hatfield
Mr. Christopher Patrick
Deputy Directors

Calendar Calibration at Beta Analytic

Calibrations of radiocarbon age determinations are applied to convert BP results to calendar years. The short-term difference between the two is caused by fluctuations in the heliomagnetic modulation of the galactic cosmic radiation and, recently, large scale burning of fossil fuels and nuclear devices testing. Geomagnetic variations are the probable cause of longer-term differences.

The parameters used for the corrections have been obtained through precise analyses of hundreds of samples taken from known-age tree rings of oak, sequoia, and fir up to about 10,000 BP. Calibration using tree-rings to about 12,000 BP is still being researched and provides somewhat less precise correlation. Beyond that, up to about 20,000 BP, correlation using a modeled curve determined from U/Th measurements on corals is used. This data is still highly subjective. Calibrations are provided up to about 19,000 years BP using the most recent calibration data available.

The Pretoria Calibration Procedure (Radiocarbon, Vol 35, No.1, 1993, pg 317) program has been chosen for these calendar calibrations. It uses splines through the tree-ring data as calibration curves, which eliminates a large part of the statistical scatter of the actual data points. The spline calibration allows adjustment of the average curve by a quantified closeness-of-fit parameter to the measured data points. A single spline is used for the precise correlation data available back to 9900 BP for terrestrial samples and about 6900 BP for marine samples. Beyond that, splines are taken on the error limits of the correlation curve to account for the lack of precision in the data points.

In describing our calibration curves, the solid bars represent one sigma statistics (68% probability) and the hollow bars represent two sigma statistics (95% probability). Marine carbonate samples that have been corrected for $^{13}\text{C}/^{12}\text{C}$, have also been corrected for both global and local geographic reservoir effects (as published in Radiocarbon, Volume 35, Number 1, 1993) prior to the calibration. Marine carbonates that have not been corrected for $^{13}\text{C}/^{12}\text{C}$ are adjusted by an assumed value of 0 ‰ in addition to the reservoir corrections. Reservoir corrections for fresh water carbonates are usually unknown and are generally not accounted for in those calibrations. In the absence of measured $^{13}\text{C}/^{12}\text{C}$ ratios, a typical value of -5 ‰ is assumed for freshwater carbonates.

(Caveat: the correlation curve for organic materials assume that the material dated was living for exactly ten years (e.g. a collection of 10 individual tree rings taken from the outer portion of a tree that was cut down to produce the sample in the feature dated). For other materials, the maximum and minimum calibrated age ranges given by the computer program are uncertain. The possibility of an "old wood effect" must also be considered, as well as the potential inclusion of younger or older material in matrix samples. Since these factors are in determinant error in most cases, these calendar calibration results should be used only for illustrative purposes. In the case of carbonates, reservoir correction is theoretical and the local variations are real, highly variable and dependent on provenience. Since imprecision in the correlation data beyond 10,000 years is high, calibrations in this range are likely to change in the future with refinement in the correlation curve. The age ranges and especially the intercept ages generated by the program must be considered as approximations.)

CALIBRATION OF RADIOCARBON AGE TO CALENDAR YEARS

Variables used in the calculation of age calibration (Variables: est. C13/C12=-25;lab. mult=1)

Laboratory number: **Beta-123456**

Conventional radiocarbon age: **2400±60 BP** ← The uncalibrated Conventional Radiocarbon Age (± 1 sigma)

The calendar age range in both calendar years (AD or BC) and in Radiocarbon Years (BP)

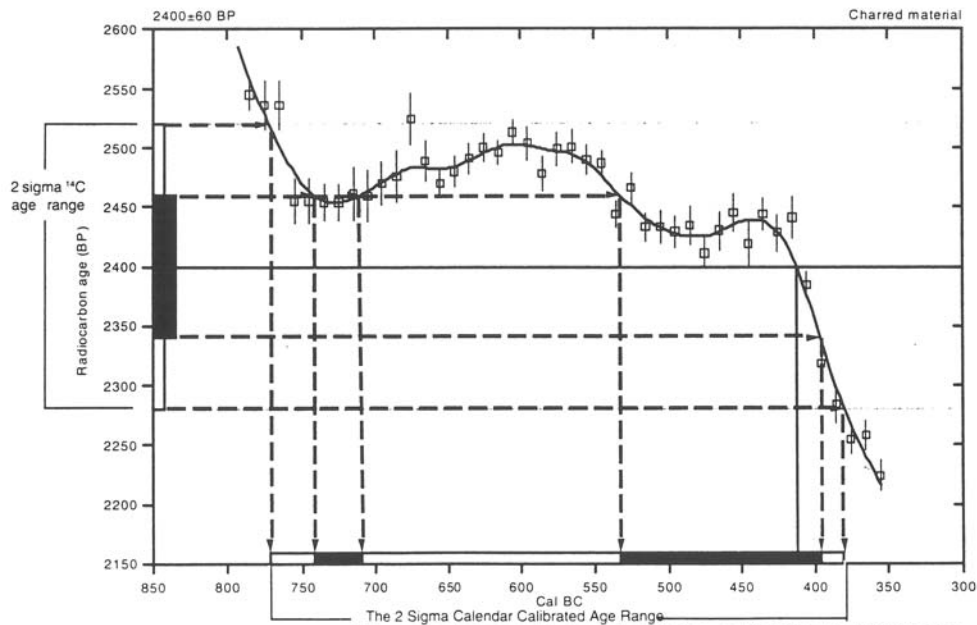
2 Sigma calibrated result: Cal BC 770 to 380 (Cal BP 2720 to 2330)
 (95% probability)

1 Sigma calibrated result: Cal BC 740 to 710 (Cal BP 2690 to 2660) and Cal BC 535 to 395 (Cal BP 2485 to 2345)
 (68% probability)

Intercept data: Intercept of radiocarbon age with calibration curve: **Cal BC 410 (Cal BP 2360)**

13C/12C ratio estimated

The intercept between the average radiocarbon age and the calibrated curve time scale. This value is illustrative and should not be used by itself.



References:

- Database used*
Intcal 98
- Calibration Database*
Editorial Comment
- Stuiver, M., van der Plicht, H., 1998, Radiocarbon 40(3), pxii-xiii
- INTCAL98 Radiocarbon Age Calibration
- Stuiver, M., et al., 1998, Radiocarbon 40(3), p1041-1083
- Mathematics*
A Simplified Approach to Calibrating C14 Dates
- Talma, A. S., Vogel, J. C., 1993, Radiocarbon 35(2), p317-322

References for the calibration data and the mathematics applied to the data. These references, as well as the Conventional Radiocarbon Age and the 13C/12C ratio used should be included in your papers.

Beta Analytic Radiocarbon Dating Laboratory

4985 S.W. 74th Court, Miami, Florida 33155 • Tel: (305)667-5167 • Fax: (305)663-0964 • E-mail: beta@radiocarbon.com



Consistent Accuracy
Delivered On Time.

Beta Analytic Inc.
4985 SW 74 Court
Miami, Florida 33155 USA
Tel: 305 667 5167
Fax: 305 663 0964
beta@radiocarbon.com
www.radiocarbon.com

DR. MURRY TAMERS
MR. DARDEN HOOD
Co-directors

Mr. Ronald Hatfield
Laboratory Manager

Mr. Christopher Patrick
Ms. Teresa Zilko-Miller
Associate Managers

December 3, 1999

Mr. Charles M. Haecker
National Park Service
P.O. Box 728
Santa Fe, NM 87504

Dear Mr. Haecker:

Please find enclosed the radiocarbon dating result for three samples which were received on October 22. They each provided plenty of carbon for accurate AMS analysis and all analytical steps went normally.

Printouts of the calendar calibrations are enclosed. The two sigma results are as follows:

Beta-135417: Cal BC 350 to 300 (Cal BP 2300 to 2250) and --41PT185
Cal BC 220 to 50 (Cal BP 2170 to 2000)
Beta-135418: Cal AD 1680 to 1745 (Cal BP 270 to 205) and --41PT186
Cal AD 1805 to 1935 (Cal BP 145 to 15) and
Cal AD 1945 to 1955 (Cal BP 5 to 5)
Beta-135419: Cal AD 30 to 135 (Cal BP 1920 to 1815) --41PT187

Our invoice is enclosed. Please forward it to the appropriate office or send VISA charge authorization. Thank you. As always, if you have any questions or would like to discuss the results, don't hesitate to contact me.

Sincerely,



BETA ANALYTIC INC.

DR. M.A. TAMERS and MR. D.G. HOOD

UNIVERSITY BRANCH
 4985 S.W. 74 COURT
 MIAMI, FLORIDA, USA 33155
 PH: 305/667-5167 FAX: 305/663-0964
 E-MAIL: beta@radiocarbon.com

REPORT OF RADIOCARBON DATING ANALYSES

Mr. Charles M. Haecker

Report Date: December 3, 1999

National Park Service

Material Received: October 22, 1999

Sample Data	Measured Radiocarbon Age	¹³ C / ¹² C Ratio	Conventional Radiocarbon Age (±)
Beta-135417 SAMPLE #: FS16.1 TU1 FEA 1 0-10 cm ANALYSIS: Standard-AMS MATERIAL/PRETREATMENT:(bone collagen): collagen extraction with alkali	1890 ± 40 BP	-10.1 ‰	2130 ± 40 BP
Beta-135418 SAMPLE #: FS24.1 TU1 47 cm ANALYSIS: Standard-AMS MATERIAL/PRETREATMENT:(charred material): acid/alkali/acid	80 ± 40 BP	-24.7 ‰	80 ± 40 BP
Beta-135419 SAMPLE #: FS43.2 TU2 0-5 cm ANALYSIS: Standard-AMS MATERIAL/PRETREATMENT:(shell): acid etch	1620 ± 30 BP	-6.5 ‰	1920 ± 30 BP

NOTE: It is important to read the calendar calibration information and to use the calendar calibrated results (reported separately) when interpreting these results in AD/BC terms.

NOTE: Sample "FS11.1 TU1 10-20 cm" was canceled (as instructed).

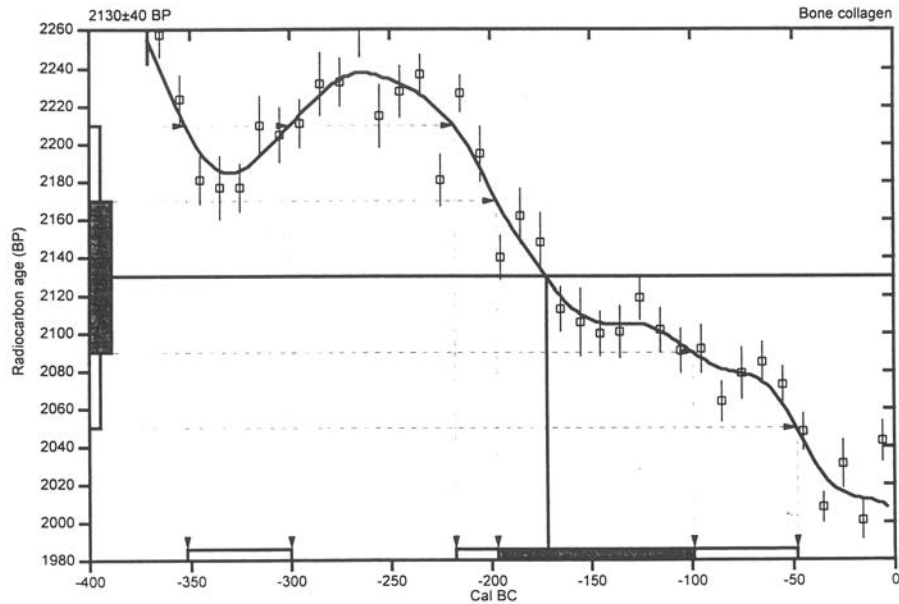
Dates are reported as RCYBP (radiocarbon years before present, "present" = 1950 A.D.). By International convention, the modern reference standard was 95% of the C14 content of the National Bureau of Standards' Oxalic Acid & calculated using the Libby C14 half life (5568 years). Quoted errors represent 1 standard deviation statistics (68% probability) & are based on combined measurements of the sample, background, and modern reference standards.

Measured C13/C12 ratios were calculated relative to the PDB-1 international standard and the RCYBP ages were normalized to -25 per mil. If the ratio and age are accompanied by an (‰), then the C13/C12 value was estimated, based on values typical of the material type. The quoted results are NOT calibrated to calendar years. Calibration to calendar years should be calculated using the Conventional C14 age.

CALIBRATION OF RADIOCARBON AGE TO CALENDAR YEARS

(Variables: C13/C12=-10.1:lab. mult=1)

Laboratory number: **Beta-135417** **41PT185**
Conventional radiocarbon age: **2130±40 BP**
2 Sigma calibrated results: **Cal BC 350 to 300 (Cal BP 2300 to 2250) and**
(95% probability) Cal BC 220 to 50 (Cal BP 2170 to 2000)
Intercept data
Intercept of radiocarbon age
with calibration curve: **Cal BC 170 (Cal BP 2120)**
1 Sigma calibrated result: **Cal BC 195 to 100 (Cal BP 2145 to 2050)**
(68% probability)



References:

- Database used
INTCAL98
Calibration Database
Editorial Comment
Stuiver, M., van der Plicht, H., 1998, *Radiocarbon* 40(3), pxii-xiii
- INTCAL98 Radiocarbon Age Calibration
Stuiver, M., et. al., 1998, *Radiocarbon* 40(3), p1041-1083
- Mathematics
A Simplified Approach to Calibrating C14 Dates
Talma, A. S., Vogel, J. C., 1993, *Radiocarbon* 35(2), p317-322

Beta Analytic Radiocarbon Dating Laboratory

4985 S.W. 74th Court, Miami, Florida 33155 • Tel: (305)667-5167 • Fax: (305)663-0964 • E-mail: beta@radiocarbon.com

CALIBRATION OF RADIOCARBON AGE TO CALENDAR YEARS

(Variables: C13/C12=-24.7;lab. mult=1)

Laboratory number: Beta-135418 41PT186

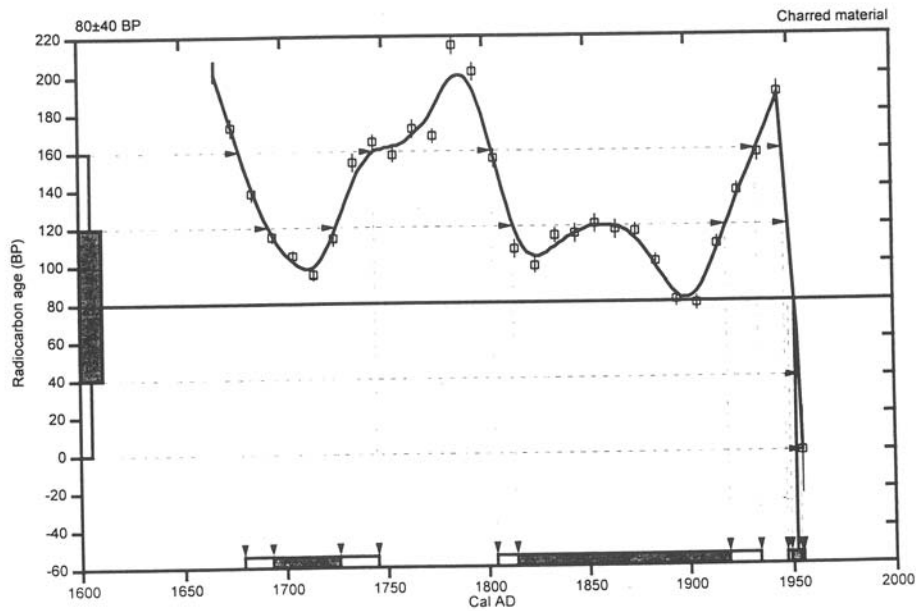
Conventional radiocarbon age: 80±40 BP

2 Sigma calibrated results: Cal AD 1680 to 1745 (Cal BP 270 to 205) and
Cal AD 1805 to 1935 (Cal BP 145 to 15) and
Cal AD 1945 to 1955 (Cal BP 5 to 5)

Intercept data

Intercept of radiocarbon age
with calibration curve: Cal AD 1950 (Cal BP 0)

1 Sigma calibrated results: Cal AD 1695 to 1725 (Cal BP 255 to 225) and
Cal AD 1815 to 1920 (Cal BP 135 to 30) and
Cal AD 1950 to 1955 (Cal BP 0 to 5)



References:

- Database used
INTCAL98
- Calibration Database
Editorial Comment
Stuiver, M., van der Plicht, H., 1998, Radiocarbon 40(3), pxi-xiii
- INTCAL98 Radiocarbon Age Calibration
Stuiver, M., et al., 1998, Radiocarbon 40(3), p1041-1083
- Mathematics
A Simplified Approach to Calibrating C14 Dates
Talma, A. S., Vogel, J. C., 1993, Radiocarbon 35(2), p317-322

Beta Analytic Radiocarbon Dating Laboratory

1985 S.W. 74th Court, Miami, Florida 33155 • Tel: (305)667-5167 • Fax: (305)663-0964 • E-mail: beta@radiocarbon.com

CALIBRATION OF RADIOCARBON AGE TO CALENDAR YEARS

(Variables: C13/C12=-6.5;lab. mult=1)

Laboratory number: Beta-135419 41PT187

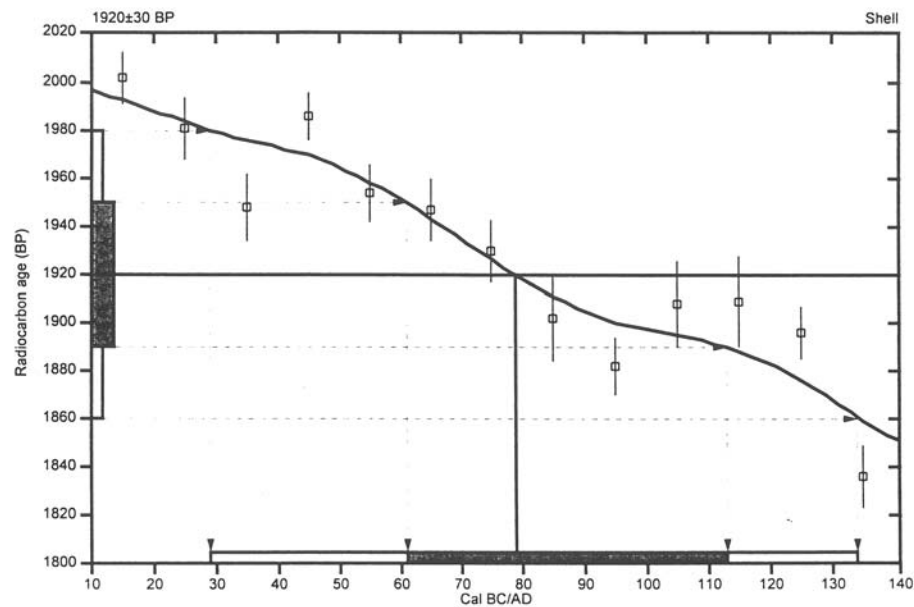
Conventional radiocarbon age: 1920±30 BP

2 Sigma calibrated result: Cal AD 30 to 135 (Cal BP 1920 to 1815)
(95% probability)

Intercept data

Intercept of radiocarbon age
with calibration curve: Cal AD 80 (Cal BP 1870)

1 Sigma calibrated result: Cal AD 60 to 115 (Cal BP 1890 to 1835)
(68% probability)



References:

Database used

INTCAL98

Calibration Database

Editorial Comment

Stuiver, M., van der Plicht, H., 1998, *Radiocarbon* 40(3), pxii-xiii

INTCAL98 Radiocarbon Age Calibration

Stuiver, M., et al., 1998, *Radiocarbon* 40(3), p1041-1083

Mathematics

A Simplified Approach to Calibrating C14 Dates

Talma, A. S., Vogel, J. C., 1993, *Radiocarbon* 35(2), p317-322

Beta Analytic Radiocarbon Dating Laboratory

4985 S.W. 74th Court, Miami, Florida 33155 • Tel: (305)667-5167 • Fax: (305)663-0964 • E-mail: beta@radiocarbon.com



Consistent Accuracy
Delivered On Time.

Beta Analytic Inc.
4985 SW 74 Court
Miami, Florida 33155 USA
Tel: 305 667 5167
Fax: 305 663 0964
beta@radiocarbon.com
www.radiocarbon.com

DR. MURRY TAMERS
MR. DARDEN HOOD
Co-directors

Mr. Ronald Hatfield
Laboratory Manager

Mr. Christopher Patrick
Ms. Teresa Zilko-Miller
Associate Managers

February 10, 2000

Mr. Charles M. Haecker
National Park Service
P.O. Box 728
Santa Fe, NM 87504

Dear Mr. Haecker:

Please find enclosed the radiocarbon dating result for two bone samples (PAVILION and 41PT186) which were received on January 3. They each provided plenty of carbon for accurate AMS analysis and all analytical steps went normally. Note that the $^{13}C/^{12}C$ ratios of both are typical of individuals eating either corn, fresh water fish/shellfish or marine fish/shellfish.

Printouts of the calendar calibrations are enclosed (also available in digital format via email). The two sigma results are as follows:

Beta-138512: Cal AD 1310 to 1360 (Cal BP 640 to 590) and --41PT245
Cal AD 1385 to 1435 (Cal BP 565 to 515)
Beta-138513: Cal AD 1450 to 1650 (Cal BP 500 to 300) --41PT186

Our invoice is enclosed. Please, forward it to the appropriate office or send VISA charge authorization. Thank you. As always, if you have any questions or would like to discuss the results, don't hesitate to contact me.

Sincerely,

BETA	BETA ANALYTIC INC.	UNIVERSITY BRANCH
	DR. M.A. TAMERS and MR. D.G. HOOD	4985 S.W. 74 COURT MIAMI, FLORIDA, USA 33155 PH: 305/667-5167 FAX: 305/663-0964 E-MAIL: beta@radiocarbon.com

REPORT OF RADIOCARBON DATING ANALYSES

Mr. Charles M. Haecker
National Park Service

Report Date: February 10, 2000
Material Received: January 3, 2000

Sample Data	Measured Radiocarbon Age	¹³ C / ¹² C Ratio	Conventional Radiocarbon Age (*)
Beta-138512 SAMPLE #: PAVILION ANALYSIS: Standard-AMS MATERIAL/PRETREATMENT:(bone collagen): collagen extraction with alkali	300 +/- 40 BP	-10.3 o/oo	540 +/- 40 BP
Beta-138513 SAMPLE #: 41PT186 ANALYSIS: Standard-AMS MATERIAL/PRETREATMENT:(bone collagen): collagen extraction with alkali	100 +/- 40 BP	-10.0 o/oo	340 +/- 40 BP

NOTE: It is important to read the calendar calibration information and to use the calendar calibrated results (reported separately) when interpreting these results in AD/BC terms.

Dates are reported as RCYBP (radiocarbon years before present, "present" = 1950A.D.). By International convention, the modern reference standard was 95% of the C14 content of the National Bureau of Standards' Oxalic Acid & calculated using the Libby C14 half life (5568 years). Quoted errors represent 1 standard deviation statistics (68% probability) & are based on combined measurements of the sample, background, and modern reference standards.

Measured C13/C12 ratios were calculated relative to the PDB-1 international standard and the RCYBP ages were normalized to -25 per mil. If the ratio and age are accompanied by an (*), then the C13/C12 value was estimated, based on values typical of the material type. The quoted results are NOT calibrated to calendar years. Calibration to calendar years should be calculated using the Conventional C14 age.

CALIBRATION OF RADIOCARBON AGE TO CALENDAR YEARS

(Variables: C13/C12=-10:lab. mult=1)

Laboratory number: Beta-138513

41PT186

Conventional radiocarbon age: 340±40 BP

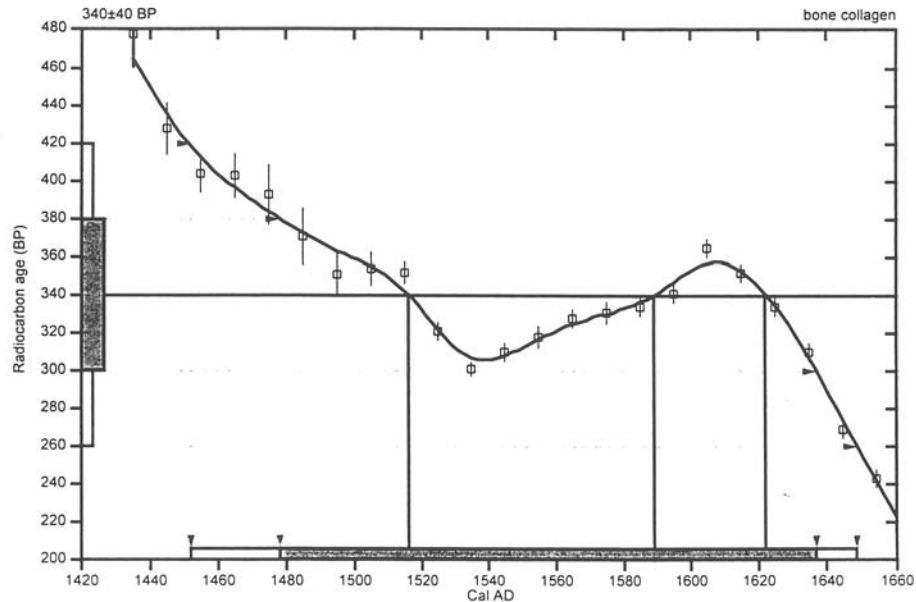
2 Sigma calibrated result: Cal AD 1450 to 1650 (Cal BP 500 to 300)
(95% probability)

Intercept data

Intercepts of radiocarbon age
with calibration curve:

Cal AD 1515 (Cal BP 435) and
Cal AD 1590 (Cal BP 360) and
Cal AD 1620 (Cal BP 330)

1 Sigma calibrated result: Cal AD 1480 to 1635 (Cal BP 470 to 315)
(68% probability)



References:

Database used

INTCAL98

Calibration Database

Editorial Comment

Stuiver, M., van der Plicht, H., 1998, *Radiocarbon* 40(3), pxi-xiii

INTCAL98 Radiocarbon Age Calibration

Stuiver, M., et. al., 1998, *Radiocarbon* 40(3), p1041-1083

Mathematics

A Simplified Approach to Calibrating C14 Dates

Talma, A. S., Vogel, J. C., 1993, *Radiocarbon* 35(2), p317-322

Beta Analytic Radiocarbon Dating Laboratory

4985 S.W. 74th Court, Miami, Florida 33155 • Tel: (305)667-5167 • Fax: (305)663-0964 • E-mail: beta@radiocarbon.com

CALIBRATION OF RADIOCARBON AGE TO CALENDAR YEARS

(Variables: C13/C12=-10.3;lab. mult=1)

Laboratory number: **Beta-138512** **41PT245**

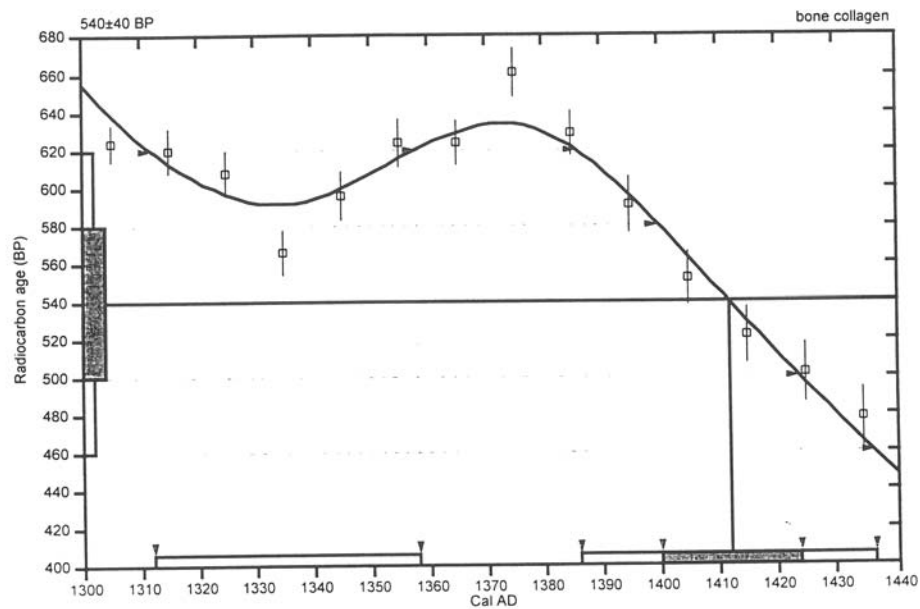
Conventional radiocarbon age: **540±40 BP**

2 Sigma calibrated results: Cal AD 1310 to 1360 (Cal BP 640 to 590) and
(95% probability) Cal AD 1385 to 1435 (Cal BP 565 to 515)

Intercept data

Intercept of radiocarbon age
with calibration curve: Cal AD 1410 (Cal BP 540)

1 Sigma calibrated result: Cal AD 1400 to 1425 (Cal BP 550 to 525)
(68% probability)



References:

Database used

INTCAL98

Calibration Database

Editorial Comment

Stuiver, M., van der Plicht, H., 1998, *Radiocarbon* 40(3), pxii-xiii

INTCAL98 Radiocarbon Age Calibration

Stuiver, M., et al., 1998, *Radiocarbon* 40(3), p1041-1083

Mathematics

A Simplified Approach to Calibrating C14 Dates

Talma, A. S., Vogel, J. C., 1993, *Radiocarbon* 35(2), p317-322

Beta Analytic Radiocarbon Dating Laboratory

4985 S.W. 74th Court, Miami, Florida 33155 • Tel: (305)667-5167 • Fax: (305)663-0964 • E-mail: beta@radiocarbon.com



Consistent Accuracy
Delivered On Time.

Beta Analytic Inc.

4985 SW 74 Court
Miami, Florida 33155 USA
Tel: 305 667 5167
Fax: 305 663 0964
beta@radiocarbon.com
www.radiocarbon.com

MR. DARDEN HOOD
Director

Mr. Ronald Hatfield
Mr. Christopher Patrick
Deputy Directors

November 5, 2007

Mr. J. Mike Quigg
TRC Mariah Associates, Incorporated
505 East Huntland Drive
Suite 250
Austin, TX 78752
USA

RE: Radiocarbon Dating Results For Samples PT186/BT5-1, PT186/BT6-1, PT186/BT6-2, PT186/BT9-1, PT186/BT9-2

Dear Mr. Quigg:

Enclosed are the radiocarbon dating results for five samples recently sent to us. They each provided plenty of carbon for accurate measurements and all the analyses proceeded normally. As usual, the method of analysis is listed on the report with the results and calibration data is provided where applicable.

As always, no students or intern researchers who would necessarily be distracted with other obligations and priorities were used in the analyses. We analyzed them with the combined attention of our entire professional staff.

If you have specific questions about the analyses, please contact us. We are always available to answer your questions.

The cost of the analysis was charged to the VISA card provided. A receipt is enclosed. Thank you. As always, if you have any questions or would like to discuss the results, don't hesitate to contact me.

Sincerely,

A handwritten signature in blue ink that reads "Darden Hood".

	BETA ANALYTIC INC.	UNIVERSITY BRANCH 4985 S.W. 74 COURT MIAMI, FLORIDA, USA 33155 PH: 305/667-5167 FAX: 305/663-0964 E-MAIL: beta@radiocarbon.com
	DR. M.A. TAMERS and MR. D.G. HOOD	

REPORT OF RADIOCARBON DATING ANALYSES

Mr. J. Mike Quigg

Report Date: 11/5/2007

TRC Mariah Associates, Incorporated

Material Received: 10/4/2007

Sample Data	Measured Radiocarbon Age	13C/12C Ratio	Conventional Radiocarbon Age(*)
Beta - 235482 SAMPLE : PT186/BT5-1 ANALYSIS : AMS-Standard delivery MATERIAL/PRETREATMENT : (charred material): acid/alkali/acid 2 SIGMA CALIBRATION : Cal AD 1540 to 1540 (Cal BP 420 to 400) AND Cal AD 1630 to 1680 (Cal BP 320 to 270) Cal AD 1740 to 1810 (Cal BP 210 to 140) AND Cal AD 1930 to 1950 (Cal BP 20 to 0)	220 +/- 40 BP	-24.5 o/oo	230 +/- 40 BP
Beta - 235483 SAMPLE : PT186/BT6-1 ANALYSIS : AMS-Standard delivery MATERIAL/PRETREATMENT : (organic sediment): acid washes 2 SIGMA CALIBRATION : Cal BC 7480 to 7170 (Cal BP 9440 to 9120)	8240 +/- 50 BP	-22.7 o/oo	8280 +/- 50 BP
Beta - 235484 SAMPLE : PT186/BT6-2 ANALYSIS : AMS-Standard delivery MATERIAL/PRETREATMENT : (organic sediment): acid washes 2 SIGMA CALIBRATION : Cal BC 9230 to 8800 (Cal BP 11180 to 10740)	9560 +/- 50 BP	-22.0 o/oo	9610 +/- 50 BP
Beta - 235485 SAMPLE : PT186/BT9-1 ANALYSIS : AMS-Standard delivery MATERIAL/PRETREATMENT : (organic sediment): acid washes 2 SIGMA CALIBRATION : Cal BC 170 to Cal AD 50 (Cal BP 2120 to 1900)	1940 +/- 40 BP	-19.2 o/oo	2040 +/- 40 BP
Beta - 235486 SAMPLE : PT186/BT9-2 ANALYSIS : AMS-Standard delivery MATERIAL/PRETREATMENT : (charred material): acid/alkali/acid 2 SIGMA CALIBRATION : Cal BC 360 to 280 (Cal BP 2310 to 2230) AND Cal BC 260 to 60 (Cal BP 2200 to 2010)	2160 +/- 40 BP	-25.5 o/oo	2150 +/- 40 BP

Dates are reported as RCYBP (radiocarbon years before present, "present" = 1950 A.D.). By International convention, the modern reference standard was 95% of the C14 content of the National Bureau of Standards' Oxalic Acid & calculated using the Libby C14 half life (5568 years). Quoted errors represent 1 standard deviation statistics (68% probability) & are based on combined measurements of the sample, background, and modern reference standards.

Measured C13/C12 ratios were calculated relative to the PDB-1 international standard and the RCYBP ages were normalized to -25 per mil. If the ratio and age are accompanied by an (*), then the C13/C12 value was estimated, based on values typical of the material type. The quoted results are NOT calibrated to calendar years. Calibration to calendar years should be calculated using the Conventional C14 age.

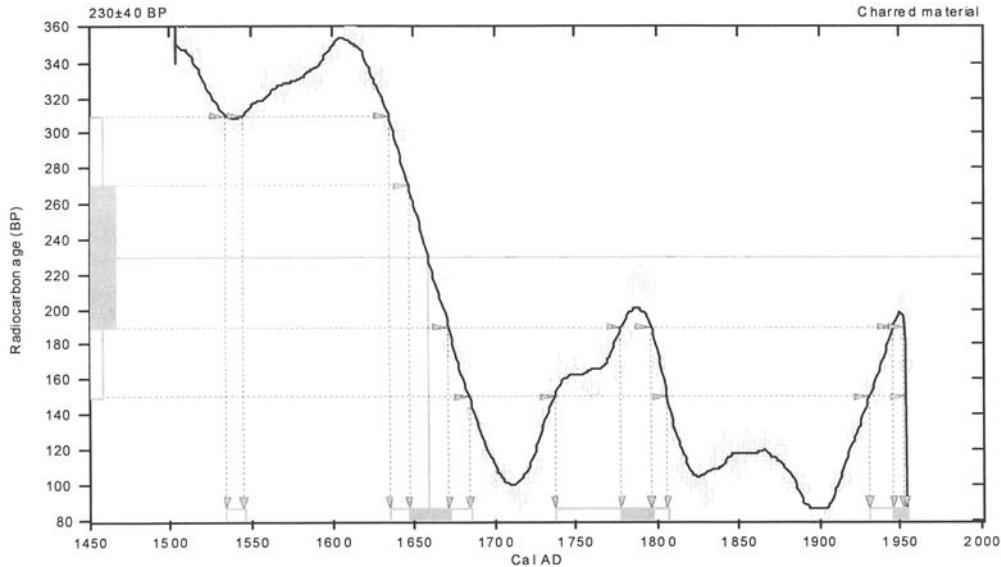
CALIBRATION OF RADIOCARBON AGE TO CALENDAR YEARS

(Variables: C13/C12=-24.5;lab. mult=1)

Laboratory number: **Beta-235482**
Conventional radiocarbon age: **230±40 BP**
2 Sigma calibrated results: **Cal AD 1540 to 1540 (Cal BP 420 to 400) and
(95% probability) Cal AD 1630 to 1680 (Cal BP 320 to 270) and
Cal AD 1740 to 1810 (Cal BP 210 to 140) and
Cal AD 1930 to 1950 (Cal BP 20 to 0)**

Intercept data

Intercept of radiocarbon age
with calibration curve: **Cal AD 1660 (Cal BP 290)**
1 Sigma calibrated results: **Cal AD 1650 to 1670 (Cal BP 300 to 280) and
(68% probability) Cal AD 1780 to 1800 (Cal BP 170 to 150) and
Cal AD 1950 to 1950 (Cal BP 0 to 0)**



References:

- Data base used*
INTCAL04
Calibration Data base
INTCAL04 Radiocarbon Age Calibration
IntCal04: Calibration Issue of Radiocarbon (Volume 46, nr 3, 2004).
- Mathematics*
A Simplified Approach to Calibrating C14 Dates
Talma, A. S., Vogel, J. C., 1993, Radiocarbon 35(2), p317-322

Beta Analytic Radiocarbon Dating Laboratory

4985 S.W. 74th Court, Miami, Florida 33155 • Tel: (305)667-5167 • Fax: (305)663-0964 • E-Mail: beta@radiocarbon.com

CALIBRATION OF RADIOCARBON AGE TO CALENDAR YEARS

(Variables: C13/C12=-22.7:lab. mult=1)

Laboratory number: Beta-235483

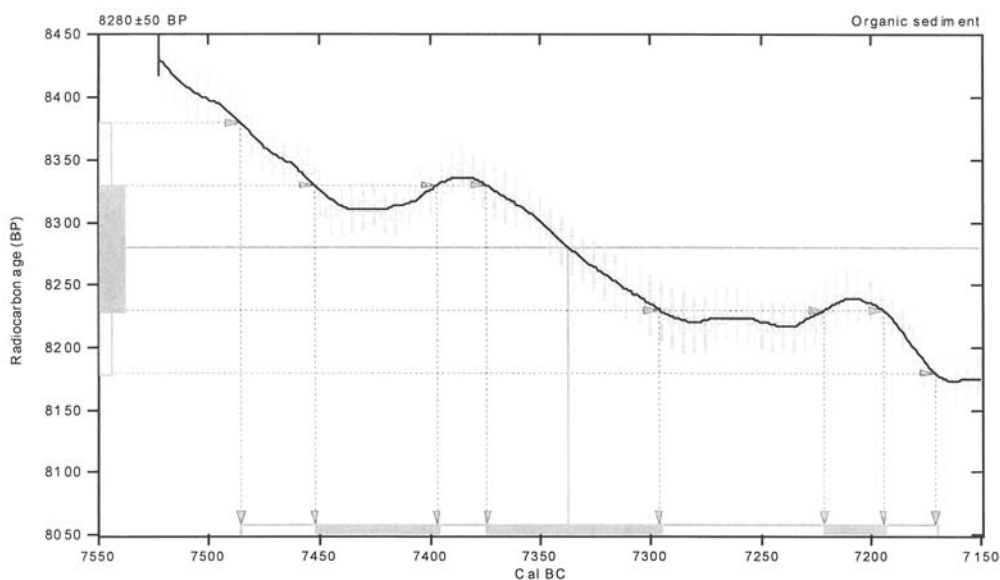
Conventional radiocarbon age: 8280±50 BP

2 Sigma calibrated result: Cal BC 7480 to 7170 (Cal BP 9440 to 9120)
(95% probability)

Intercept data

Intercept of radiocarbon age
with calibration curve: Cal BC 7340 (Cal BP 9290)

1 Sigma calibrated results: Cal BC 7450 to 7400 (Cal BP 9400 to 9350) and
(68% probability) Cal BC 7370 to 7300 (Cal BP 9320 to 9250) and
Cal BC 7220 to 7190 (Cal BP 9170 to 9140)



References:

Database used

INTCAL04

Calibration Database

INTCAL04 Radiocarbon Age Calibration

IntCal04: Calibration Issue of Radiocarbon (Volume 46, nr 3, 2004).

Mathematics

A Simplified Approach to Calibrating C14 Dates

Talma, A. S., Vogel, J. C., 1993, Radiocarbon 35(2), p317-322

Beta Analytic Radiocarbon Dating Laboratory

4985 S.W. 74th Court, Miami, Florida 33155 • Tel: (305)667-5167 • Fax: (305)663-0964 • E-Mail: beta@radiocarbon.com

CALIBRATION OF RADIOCARBON AGE TO CALENDAR YEARS

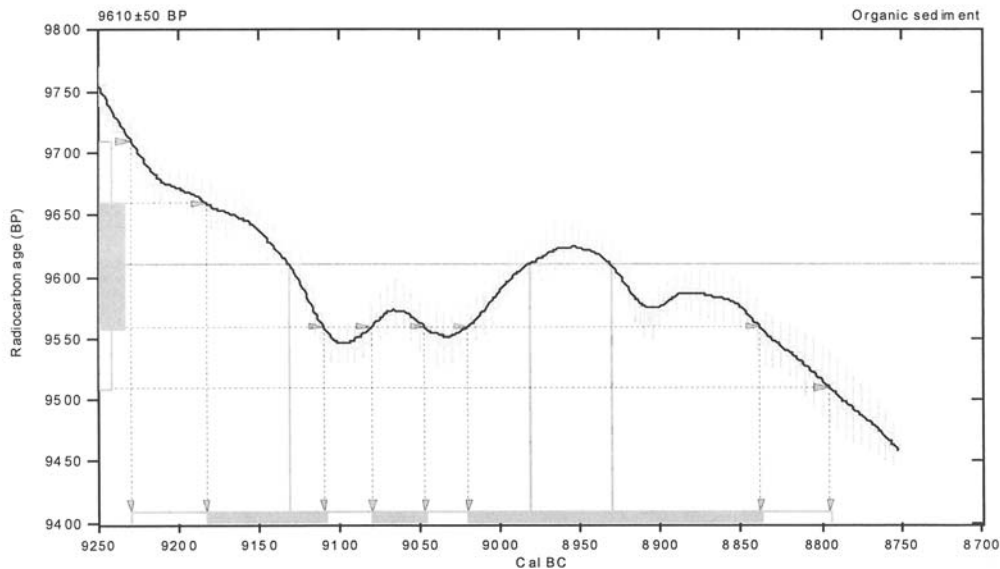
(Variables: C13/C12=-22;lab. mult=1)

Laboratory number: **Beta-235484**
Conventional radiocarbon age: **9610±50 BP**
2 Sigma calibrated result: **Cal BC 9230 to 8800 (Cal BP 11180 to 10740)**
(95% probability)

Intercept data

Intercepts of radiocarbon age
with calibration curve: Cal BC 9130 (Cal BP 11080) and
Cal BC 8980 (Cal BP 10930) and
Cal BC 8930 (Cal BP 10880)

1 Sigma calibrated results: Cal BC 9180 to 9110 (Cal BP 11130 to 11060) and
(68% probability) Cal BC 9080 to 9050 (Cal BP 11030 to 11000) and
Cal BC 9020 to 8840 (Cal BP 10970 to 10790)



References:

Database used
INTCAL04
Calibration Database
INTCAL04 Radiocarbon Age Calibration
IntCal04: Calibration Issue of Radiocarbon (Volume 46, nr 3, 2004).
Mathematics
A Simplified Approach to Calibrating C14 Dates
Talma, A. S., Vogel, J. C., 1993, Radiocarbon 35(2), p317-322

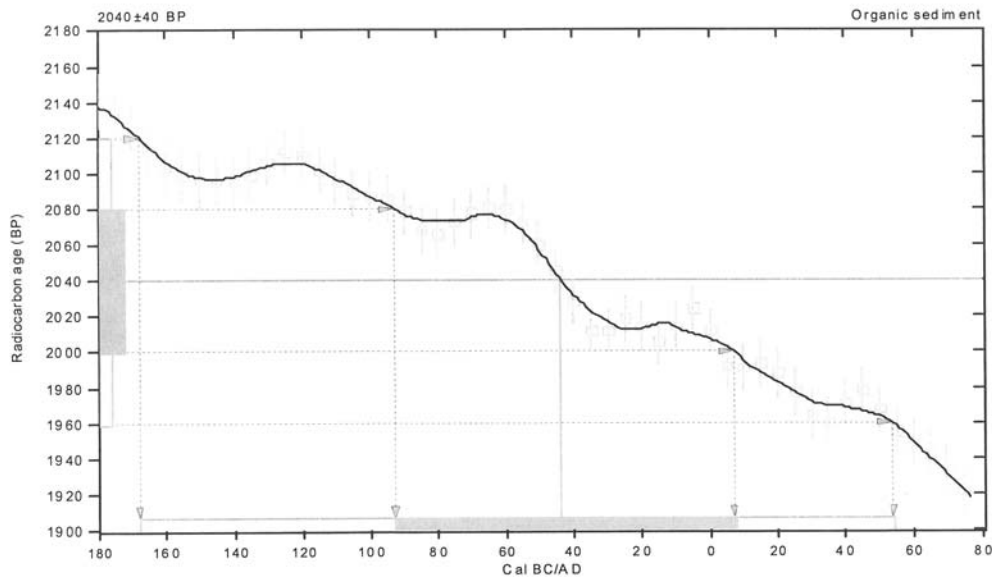
Beta Analytic Radiocarbon Dating Laboratory

4985 S.W. 74th Court, Miami, Florida 33155 • Tel: (305)667-5167 • Fax: (305)663-0964 • E-Mail: beta@radiocarbon.com

CALIBRATION OF RADIOCARBON AGE TO CALENDAR YEARS

(Variables: C13/C12=-19.2:lab. mult=1)

Laboratory number: Beta-235485
Conventional radiocarbon age: 2040±40 BP
2 Sigma calibrated result: Cal BC 170 to Cal AD 50 (Cal BP 2120 to 1900)
(95% probability)
Intercept data
Intercept of radiocarbon age
with calibration curve: Cal BC 40 (Cal BP 1990)
1 Sigma calibrated result: Cal BC 90 to Cal AD 10 (Cal BP 2040 to 1940)
(68% probability)



References:

- Database used*
INTCAL04
Calibration Database
INTCAL04 Radiocarbon Age Calibration
IntCal04: Calibration Issue of Radiocarbon (Volume 46, nr 3, 2004).
- Mathematics*
A Simplified Approach to Calibrating C14 Dates
Talma, A. S., Vogel, J. C., 1993, Radiocarbon 35(2), p317-322

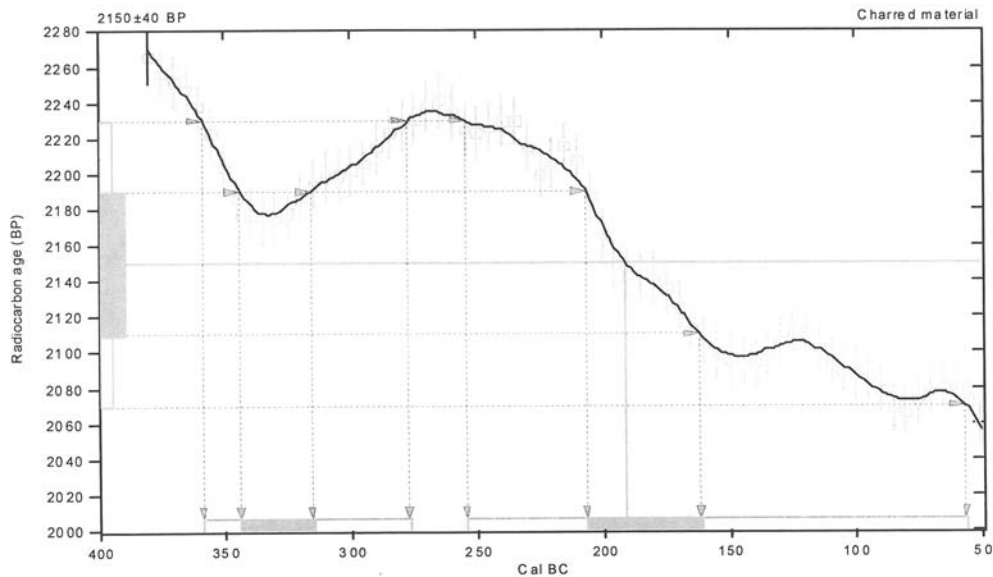
Beta Analytic Radiocarbon Dating Laboratory

4985 S.W. 74th Court, Miami, Florida 33155 • Tel: (305)667-5167 • Fax: (305)663-0964 • E-Mail: beta@radiocarbon.com

CALIBRATION OF RADIOCARBON AGE TO CALENDAR YEARS

(Variables: C13/C12=-25.5:lab. mult=1)

Laboratory number: **Beta-235486**
Conventional radiocarbon age: **2150±40 BP**
2 Sigma calibrated results: **Cal BC 360 to 280 (Cal BP 2310 to 2230) and**
(95% probability) Cal BC 260 to 60 (Cal BP 2200 to 2010)
Intercept data
Intercept of radiocarbon age
with calibration curve: **Cal BC 190 (Cal BP 2140)**
1 Sigma calibrated results: **Cal BC 340 to 320 (Cal BP 2290 to 2270) and**
(68% probability) Cal BC 210 to 160 (Cal BP 2160 to 2110)



References:

- Data base used*
INTCAL04
Calibration Data base
INTCAL04 Radiocarbon Age Calibration
IntCal04: Calibration Issue of Radiocarbon (Volume 46, nr 3, 2004).
- Mathematics*
A Simplified Approach to Calibrating C14 Dates
Talma, A. S., Vogel, J. C., 1993, Radiocarbon 35(2), p317-322

Beta Analytic Radiocarbon Dating Laboratory

4985 S.W. 74th Court, Miami, Florida 33155 • Tel: (305)667-5167 • Fax: (305)663-0964 • E-Mail: beta@radiocarbon.com



*Consistent Accuracy
Delivered On Time.*

Beta Analytic Inc.

4985 SW 74 Court
Miami, Florida 33155 USA
Tel: 305 667 5167
Fax: 305 663 0964
beta@radiocarbon.com
www.radiocarbon.com

MR. DARDEN HOOD
Director

Mr. Ronald Hatfield
Mr. Christopher Patrick
Deputy Directors

December 7, 2007

Mr. J. Mike Quigg
TRC Mariah Associates, Incorporated
505 East Huntland Drive
Suite 250
Austin, TX 78752
USA

RE: Radiocarbon Dating Result For Sample PT185-BT35-1

Dear Mr. Quigg:

Enclosed is the radiocarbon dating result for one sample recently sent to us. It provided plenty of carbon for an accurate measurement and the analysis proceeded normally. As usual, the method of analysis is listed on the report sheet and calibration data is provided where applicable.

As always, no students or intern researchers who would necessarily be distracted with other obligations and priorities were used in the analysis. It was analyzed with the combined attention of our entire professional staff.

If you have specific questions about the analyses, please contact us. We are always available to answer your questions.

The cost of the analysis was charged to the VISA card provided. A receipt is enclosed. Thank you. As always, if you have any questions or would like to discuss the results, don't hesitate to contact me.

Sincerely,

	BETA ANALYTIC INC. DR. M.A. TAMERS and MR. D.G. HOOD	UNIVERSITY BRANCH 4985 S.W. 74 COURT MIAMI, FLORIDA, USA 33155 PH: 305/667-5167 FAX: 305/663-0964 E-MAIL: beta@radiocarbon.com
---	--	---

REPORT OF RADIOCARBON DATING ANALYSES

Mr. J. Mike Quigg

Report Date: 12/7/2007

TRC Mariah Associates, Incorporated

Material Received: 11/7/2007

Sample Data	Measured Radiocarbon Age	¹³ C/ ¹² C Ratio	Conventional Radiocarbon Age(*)
Beta - 237024 SAMPLE : PT185-BT35-1 ANALYSIS : AMS-Standard delivery MATERIAL/PRETREATMENT : (bone collagen): collagen extraction: with alkali 2 SIGMA CALIBRATION : Cal BC 400 to 340 (Cal BP 2350 to 2290) AND Cal BC 320 to 210 (Cal BP 2270 to 2160)	2000 +/- 40 BP	-8.7 ‰	2270 +/- 40 BP

Dates are reported as RYBP (radiocarbon years before present, "present" = 1950 A.D.). By International convention, the modern reference standard was 95% of the C14 content of the National Bureau of Standards' Oxalic Acid & calculated using the Libby C14 half life (5568 years). Quoted errors represent 1 standard deviation statistics (68% probability) & are based on combined measurements of the sample, background, and modern reference standards.

Measured C13/C12 ratios were calculated relative to the PDB-1 international standard and the RYBP ages were normalized to -25 per mil. If the ratio and age are accompanied by an (*), then the C13/C12 value was estimated, based on values typical of the material type. The quoted results are NOT calibrated to calendar years. Calibration to calendar years should be calculated using the Conventional C14 age.

CALIBRATION OF RADIOCARBON AGE TO CALENDAR YEARS

(Variables: C13/C12=-8.7:lab. mult=1)

Laboratory number: Beta-237024

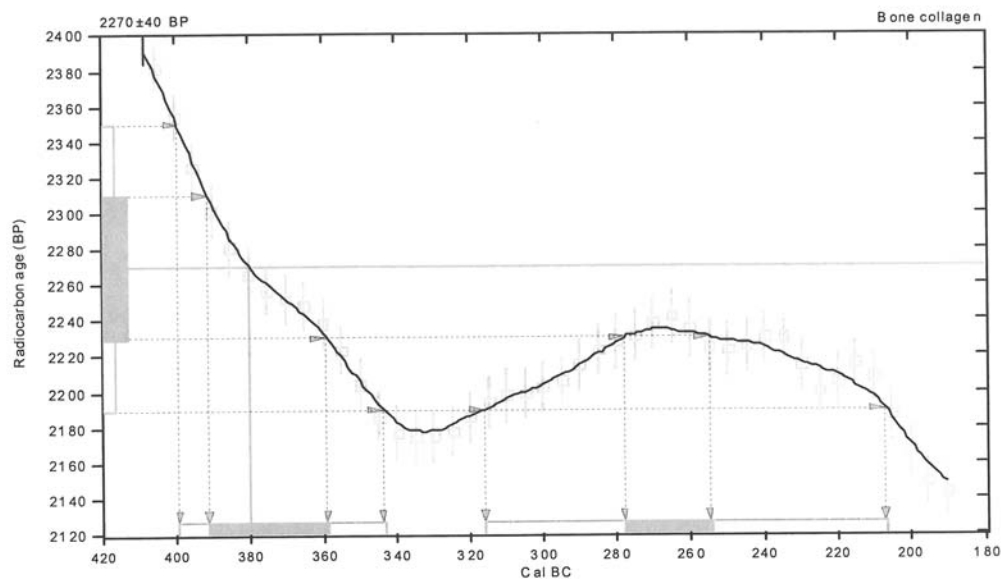
Conventional radiocarbon age: 2270±40 BP

2 Sigma calibrated results: Cal BC 400 to 340 (Cal BP 2350 to 2290) and
(95% probability) Cal BC 320 to 210 (Cal BP 2270 to 2160)

Intercept data

Intercept of radiocarbon age
with calibration curve: Cal BC 380 (Cal BP 2330)

1 Sigma calibrated results: Cal BC 390 to 360 (Cal BP 2340 to 2310) and
(68% probability) Cal BC 280 to 260 (Cal BP 2230 to 2200)



References:

Database used

INTCAL04

Calibration Database

INTCAL04 Radiocarbon Age Calibration

IntCal04: Calibration Issue of Radiocarbon (Volume 46, nr 3, 2004).

Mathematics

A Simplified Approach to Calibrating C14 Dates

Talma, A. S., Vogel, J. C., 1993, Radiocarbon 35(2), p317-322

Beta Analytic Radiocarbon Dating Laboratory

4985 S.W. 74th Court, Miami, Florida 33155 • Tel: (305)667-5167 • Fax: (305)663-0964 • E-Mail: beta@radiocarbon.com



Consistent Accuracy
Delivered On Time.

Beta Analytic Inc.
4985 SW 74 Court
Miami, Florida 33155 USA
Tel: 305 667 5167
Fax: 305 663 0964
beta@radiocarbon.com
www.radiocarbon.com

MR. DARDEN HOOD
Director

Mr. Ronald Hatfield
Mr. Christopher Patrick
Deputy Directors

December 11, 2007

Mr. J. Mike Quigg
TRC Mariah Associates, Incorporated
505 East Huntland Drive
Suite 250
Austin, TX 78752
USA

RE: Radiocarbon Dating Results For Samples PT186-BT9-1, PT186-FS170, PT245-BT20-1, PT245-BT20-2, PT245-FS23, PT245-FS84-1

Dear Mr. Quigg:

Enclosed are the radiocarbon dating results for six samples recently sent to us. They each provided plenty of carbon for accurate measurements and all the analyses proceeded normally. As usual, the method of analysis is listed on the report with the results and calibration data is provided where applicable.

Note that one of the samples (PT186-FS170, Beta-237021) does not have a Measured Radiocarbon Age and $^{13}\text{C}/^{12}\text{C}$ Ratio reported. This is because the sample was too small to do a separate $^{13}\text{C}/^{12}\text{C}$ ratio and AMS analysis. The only available $^{13}\text{C}/^{12}\text{C}$ ratio available to calculate a Conventional Radiocarbon Age was that determined on a small aliquot of graphite. Although this ratio corrects to the appropriate Conventional Radiocarbon Age, it is not reported since it includes laboratory chemical and detector induced fractionation.

As always, no students or intern researchers who would necessarily be distracted with other obligations and priorities were used in the analyses. We analyzed them with the combined attention of our entire professional staff.

If you have specific questions about the analyses, please contact us. We are always available to answer your questions.

The cost of the analysis was charged to the VISA card provided. A receipt is enclosed. Thank you. As always, if you have any questions or would like to discuss the results, don't hesitate to contact me.

Sincerely,

A handwritten signature in black ink that reads "Darden Hood". The signature is written in a cursive style with a large, prominent "D" and "H".

BETA	BETA ANALYTIC INC. DR. M.A. TAMERS and MR. D.G. HOOD	UNIVERSITY BRANCH 4985 S.W. 74 COURT MIAMI, FLORIDA, USA 33155 PH: 305/667-5167 FAX: 305/663-0964 E-MAIL: beta@radiocarbon.com
-------------	--	--

REPORT OF RADIOCARBON DATING ANALYSES

Mr. J. Mike Quigg

Report Date: 12/11/2007

TRC Mariah Associates, Incorporated

Material Received: 11/7/2007

Sample Data	Measured Radiocarbon Age	13C/12C Ratio	Conventional Radiocarbon Age(*)
Beta - 237020 SAMPLE : PT186-BT9-1 ANALYSIS : AMS-Standard delivery MATERIAL/PRETREATMENT : (bone collagen): collagen extraction: with alkali 2 SIGMA CALIBRATION : Cal AD 1290 to 1420 (Cal BP 660 to 530)	350 +/- 40 BP	-9.9 o/oo	600 +/- 40 BP
Beta - 237021 SAMPLE : PT186-FS170 ANALYSIS : AMS-Standard delivery MATERIAL/PRETREATMENT : (charred material): acid/alkali/acid 2 SIGMA CALIBRATION : Cal BC 780 to 410 (Cal BP 2740 to 2360) COMMENT: the original sample was too small for a 13C/12C ratio measurement. However, a ratio including both natural and laboratory effects was measured during the 14C detection to derive a Conventional Radiocarbon Age, suitable for applicable calendar calibration.	NA	NA	2490 +/- 40 BP
Beta - 237022 SAMPLE : PT245-BT20-1 ANALYSIS : AMS-Standard delivery MATERIAL/PRETREATMENT : (bone collagen): collagen extraction: with alkali 2 SIGMA CALIBRATION : Cal AD 690 to 900 (Cal BP 1260 to 1050)	970 +/- 40 BP	-10.2 o/oo	1210 +/- 40 BP
Beta - 237023 SAMPLE : PT245-BT20-2 ANALYSIS : AMS-Standard delivery MATERIAL/PRETREATMENT : (organic sediment): acid washes 2 SIGMA CALIBRATION : Cal AD 80 to 250 (Cal BP 1870 to 1700)	1750 +/- 40 BP	-19.7 o/oo	1840 +/- 40 BP
Beta - 237025 SAMPLE : PT245-FS23 ANALYSIS : AMS-Standard delivery MATERIAL/PRETREATMENT : (bone collagen): collagen extraction: with alkali 2 SIGMA CALIBRATION : Cal AD 1660 to 1960 (Cal BP 290 to 0)	101.6 +/- 0.5 pMC	-7.5 o/oo	160 +/- 40 BP

Dates are reported as RCYBP (radiocarbon years before present, "present" = 1950A.D.). By International convention, the modern reference standard was 95% of the C14 content of the National Bureau of Standards' Oxalic Acid & calculated using the Libby C14 half life (5568 years). Quoted errors represent 1 standard deviation statistics (68% probability) & are based on combined measurements of the sample, background, and modern reference standards.

Measured C13/C12 ratios were calculated relative to the PDB-1 international standard and the RCYBP ages were normalized to -25 per mil. If the ratio and age are accompanied by an (*), then the C13/C12 value was estimated, based on values typical of the material type. The quoted results are NOT calibrated to calendar years. Calibration to calendar years should be calculated using the Conventional C14 age.



BETA ANALYTIC INC.

DR. M.A. TAMERS and MR. D.G. HOOD

UNIVERSITY BRANCH
4985 S.W. 74 COURT
MIAMI, FLORIDA, USA 33155
PH: 305/667-5167 FAX: 305/663-0964
E-MAIL: beta@radiocarbon.com

REPORT OF RADIOCARBON DATING ANALYSES

Mr. J. Mike Quigg

Report Date: 12/11/2007

Sample Data	Measured Radiocarbon Age	¹³ C/ ¹² C Ratio	Conventional Radiocarbon Age(*)
Beta - 237026 SAMPLE : PT245-FS84-1 ANALYSIS : AMS-Standard delivery MATERIAL/PRETREATMENT : (organic sediment): acid washes 2 SIGMA CALIBRATION : Cal AD 600 to 680 (Cal BP 1350 to 1270)	1310 +/- 40 BP	-19.9 o/oo	1390 +/- 40 BP

Dates are reported as RCYBP (radiocarbon years before present, "present" = 1950 A.D.). By International convention, the modern reference standard was 95% of the C14 content of the National Bureau of Standards' Oxalic Acid & calculated using the Libby C14 half life (5568 years). Quoted errors represent 1 standard deviation statistics (68% probability) & are based on combined measurements of the sample, background, and modern reference standards.

Measured C13/C12 ratios were calculated relative to the PDB-1 international standard and the RCYBP ages were normalized to -25 per mil. If the ratio and age are accompanied by an (*), then the C13/C12 value was estimated, based on values typical of the material type. The quoted results are NOT calibrated to calendar years. Calibration to calendar years should be calculated using the Conventional C14 age.

CALIBRATION OF RADIOCARBON AGE TO CALENDAR YEARS

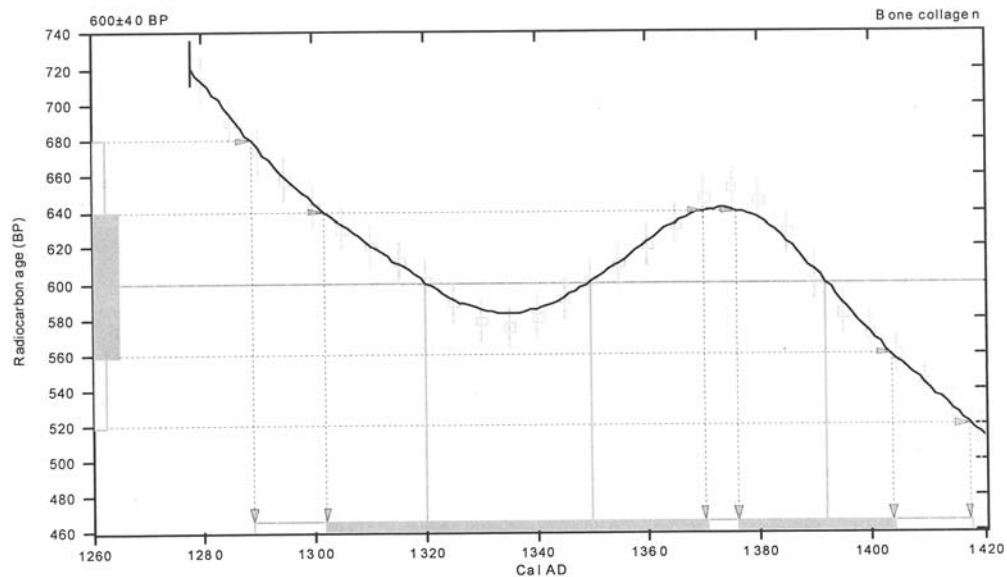
(Variables: C13/C12=-9.9;lab. mult=1)

Laboratory number: **Beta-237020**
Conventional radiocarbon age: **600±40 BP**
2 Sigma calibrated result: **Cal AD 1290 to 1420 (Cal BP 660 to 530)**
(95% probability)

Intercept data

Intercepts of radiocarbon age
with calibration curve: Cal AD 1320 (Cal BP 630) and
Cal AD 1350 (Cal BP 600) and
Cal AD 1390 (Cal BP 560)

1 Sigma calibrated results: Cal AD 1300 to 1370 (Cal BP 650 to 580) and
(68% probability) Cal AD 1380 to 1400 (Cal BP 570 to 550)



References:

Database used
INTCAL04
Calibration Database
INTCAL04 Radiocarbon Age Calibration
In Cal04: Calibration Issue of Radiocarbon (Volume 46, nr 3, 2004).
Mathematics
A Simplified Approach to Calibrating C14 Dates
Talma, A. S., Vogel, J. C., 1993, Radiocarbon 35(2), p317-322

Beta Analytic Radiocarbon Dating Laboratory

4985 S.W. 74th Court, Miami, Florida 33155 • Tel: (305)667-5167 • Fax: (305)663-0964 • E-Mail: beta@radiocarbon.com

CALIBRATION OF RADIOCARBON AGE TO CALENDAR YEARS

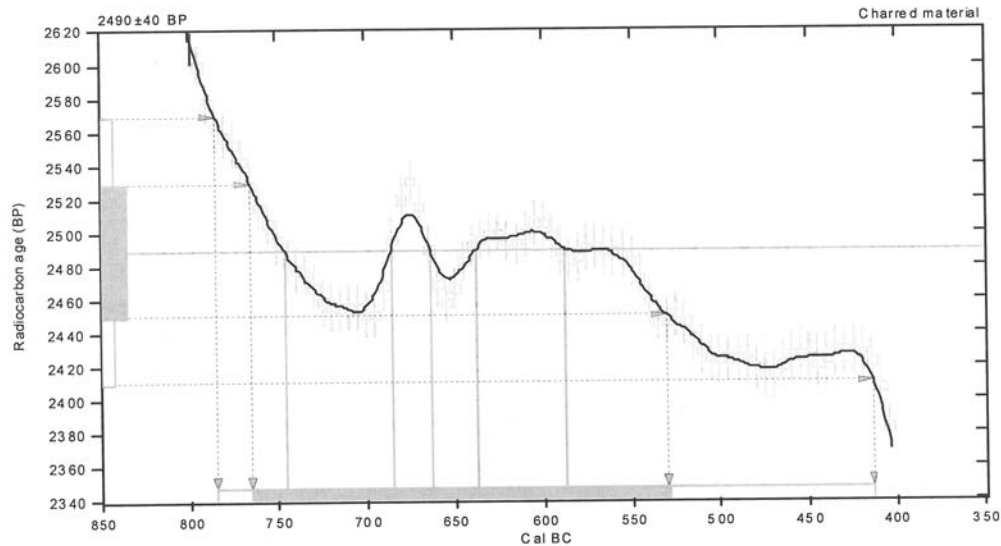
(Variables: C13/C12=-1.4:lab. mult=1)

Laboratory number: **Beta-237021**
Conventional radiocarbon age: **2490±40 BP**
2 Sigma calibrated result: **Cal BC 780 to 410 (Cal BP 2740 to 2360)**
(95% probability)

Intercept data

Intercepts of radiocarbon age
with calibration curve: Cal BC 750 (Cal BP 2700) and
Cal BC 690 (Cal BP 2640) and
Cal BC 660 (Cal BP 2610) and
Cal BC 640 (Cal BP 2590) and
Cal BC 590 (Cal BP 2540)

1 Sigma calibrated result: **Cal BC 760 to 530 (Cal BP 2720 to 2480)**
(68% probability)



References:

- Database used*
INTCAL04
- Calibration Database*
INTCAL04 Radiocarbon Age Calibration
IntCal04: Calibration Issue of Radiocarbon (Volume 46, nr 3, 2004).
- Mathematics*
A Simplified Approach to Calibrating C14 Dates
Talma, A. S., Vogel, J. C., 1993, *Radiocarbon* 35(2), p317-322

Beta Analytic Radiocarbon Dating Laboratory

4985 S.W. 74th Court, Miami, Florida 33155 • Tel: (305)667-5167 • Fax: (305)663-0964 • E-Mail: beta@radiocarbon.com

CALIBRATION OF RADIOCARBON AGE TO CALENDAR YEARS

(Variables: C13/C12=-10.2:lab. mult=1)

Laboratory number: Beta-237022

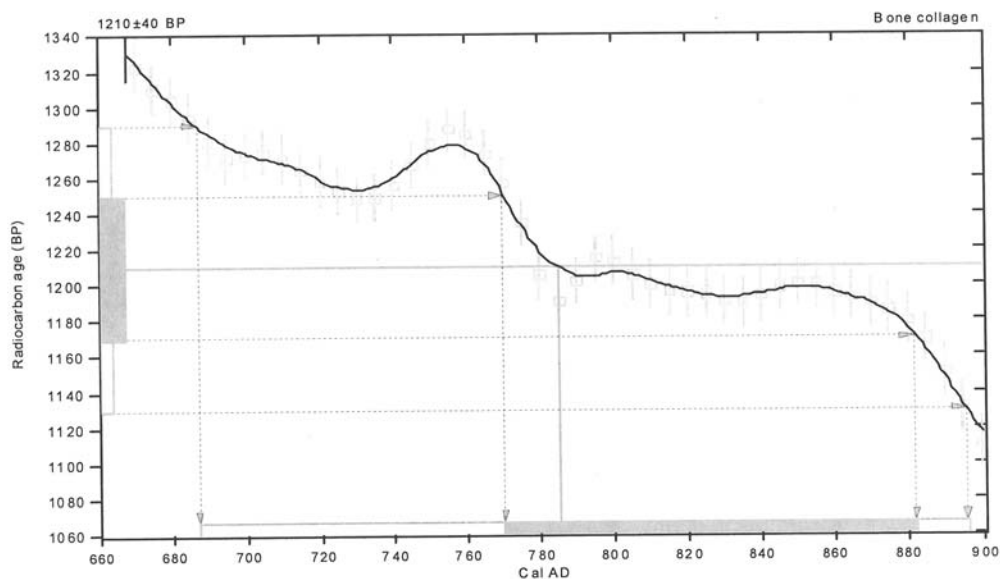
Conventional radiocarbon age: 1210±40 BP

2 Sigma calibrated result: Cal AD 690 to 900 (Cal BP 1260 to 1050)
(95% probability)

Intercept data

Intercept of radiocarbon age
with calibration curve: Cal AD 780 (Cal BP 1160)

1 Sigma calibrated result: Cal AD 770 to 880 (Cal BP 1180 to 1070)
(68% probability)



References:

Database used

INTCAL04

Calibration Database

INTCAL04 Radiocarbon Age Calibration

IntCal04: Calibration Issue of Radiocarbon (Volume 46, nr 3, 2004).

Mathematics

A Simplified Approach to Calibrating C14 Dates

Talma, A. S., Vogel, J. C., 1993, *Radiocarbon* 35(2), p317-322

Beta Analytic Radiocarbon Dating Laboratory

4985 S.W. 74th Court, Miami, Florida 33155 • Tel: (305)667-5167 • Fax: (305)663-0964 • E-Mail: beta@radiocarbon.com

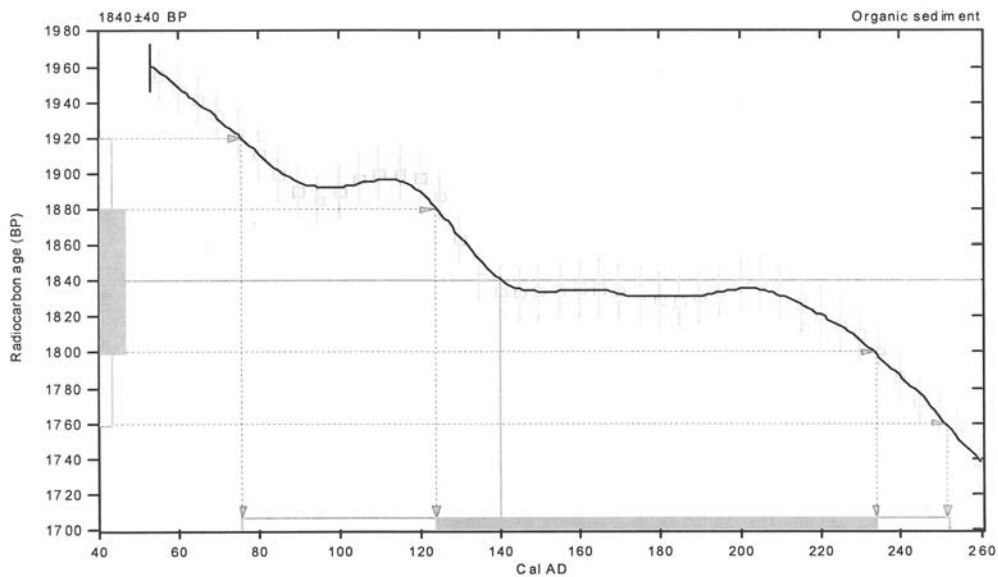
CALIBRATION OF RADIOCARBON AGE TO CALENDAR YEARS

(Variables: C13/C12=-19.7:lab. mult=1)

Laboratory number: Beta-237023
Conventional radiocarbon age: 1840±40 BP
2 Sigma calibrated result: Cal AD 80 to 250 (Cal BP 1870 to 1700)
(95% probability)

Intercept data

Intercept of radiocarbon age
with calibration curve: Cal AD 140 (Cal BP 1810)
1 Sigma calibrated result: Cal AD 120 to 230 (Cal BP 1830 to 1720)
(68% probability)



References:

- Data base used*
INTCAL04
Calibration Data base
INTCAL04 Radiocarbon Age Calibration
IntCal04: Calibration Issue of Radiocarbon (Volume 46, nr 3, 2004).
- Mathematics*
A Simplified Approach to Calibrating C14 Dates
Talma, A. S., Vogel, J. C., 1993, Radiocarbon 35(2), p317-322

Beta Analytic Radiocarbon Dating Laboratory

4985 S.W. 74th Court, Miami, Florida 33155 • Tel: (305)667-5167 • Fax: (305)663-0964 • E-Mail: beta@radiocarbon.com

CALIBRATION OF RADIOCARBON AGE TO CALENDAR YEARS

(Variables: C13/C12=-7.5:lab. mult=1)

Laboratory number: Beta-237025

Conventional radiocarbon age: 160 ± 40 BP

2 Sigma calibrated result: Cal AD 1660 to 1960 (Cal BP 290 to 0)
(95% probability)

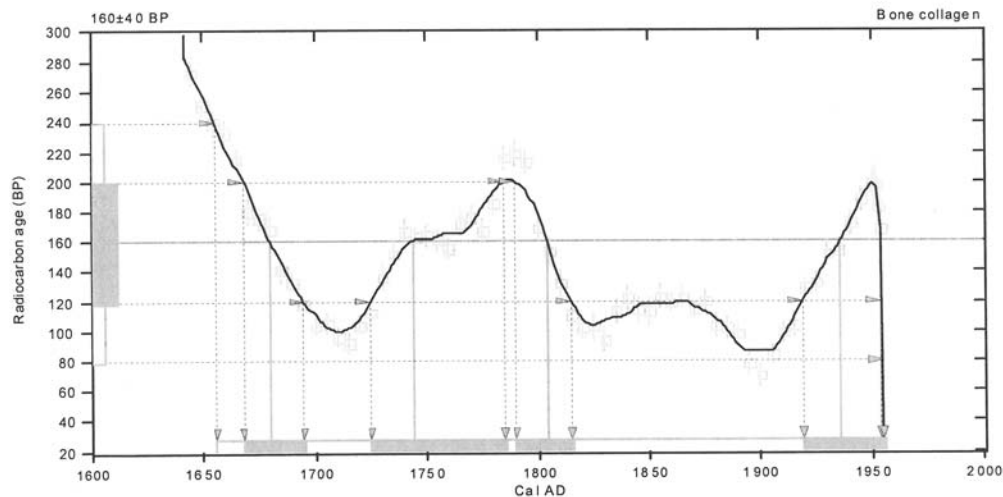
Intercept data

Intercepts of radiocarbon age
with calibration curve:

Cal AD 1680 (Cal BP 270) and
Cal AD 1740 (Cal BP 210) and
Cal AD 1800 (Cal BP 150) and
Cal AD 1940 (Cal BP 20) and
Cal AD 1950 (Cal BP 0)

1 Sigma calibrated results:
(68% probability)

Cal AD 1670 to 1700 (Cal BP 280 to 260) and
Cal AD 1720 to 1780 (Cal BP 220 to 160) and
Cal AD 1790 to 1820 (Cal BP 160 to 140) and
Cal AD 1920 to 1950 (Cal BP 30 to 0)



References:

Data base used

INTCAL04

Calibration Data base

INTCAL04 Radiocarbon Age Calibration

IntCal04: Calibration Issue of Radiocarbon (Volume 46, nr 3, 2004).

Mathematics

A Simplified Approach to Calibrating C14 Dates

Talma, A. S., Vogel, J. C., 1993, Radiocarbon 35(2), p317-322

Beta Analytic Radiocarbon Dating Laboratory

4985 S.W. 74th Court, Miami, Florida 33155 • Tel: (305)667-5167 • Fax: (305)663-0964 • E-Mail: beta@radiocarbon.com

CALIBRATION OF RADIOCARBON AGE TO CALENDAR YEARS

(Variables: C13/C12=-19.9:lab. mult=1)

Laboratory number: Beta-237026

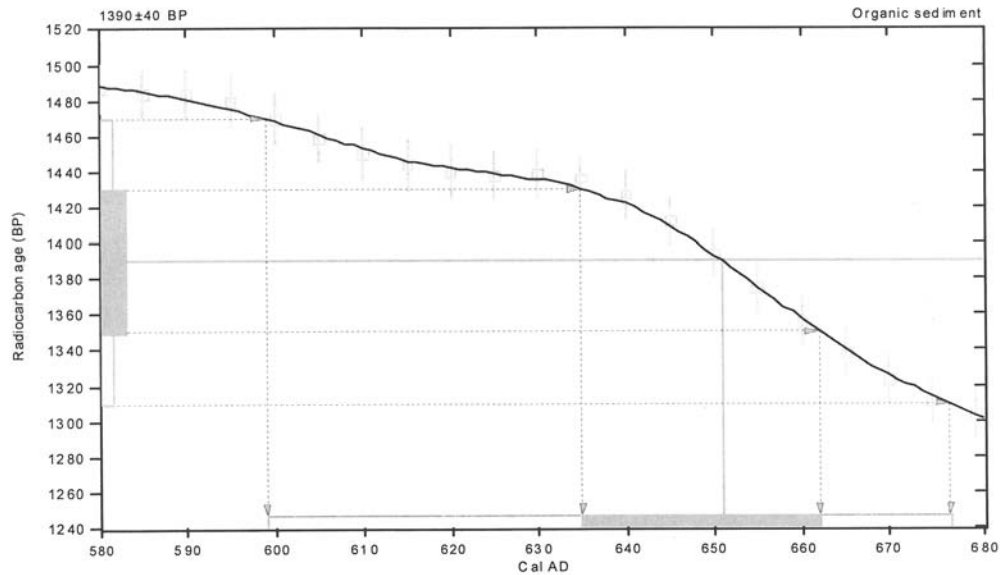
Conventional radiocarbon age: 1390±40 BP

2 Sigma calibrated result: Cal AD 600 to 680 (Cal BP 1350 to 1270)
(95% probability)

Intercept data

Intercept of radiocarbon age
with calibration curve: Cal AD 650 (Cal BP 1300)

1 Sigma calibrated result: Cal AD 640 to 660 (Cal BP 1320 to 1290)
(68% probability)



References:

- Data base used*
INTCAL04
- Calibration Data base*
INTCAL04 Radiocarbon Age Calibration
IntCal04: Calibration Issue of Radiocarbon (Volume 46, nr 3, 2004).
- Mathematics*
A Simplified Approach to Calibrating C14 Dates
Talma, A. S., Vogel, J. C., 1993, Radiocarbon 35(2), p317-322

Beta Analytic Radiocarbon Dating Laboratory

4985 S.W. 74th Court, Miami, Florida 33155 • Tel: (305)667-5167 • Fax: (305)663-0964 • E-Mail: beta@radiocarbon.com



Consistent Accuracy
Delivered On Time.

Beta Analytic Inc.

4985 SW 74 Court
Miami, Florida 33155 USA
Tel: 305 667 5167
Fax: 305 663 0964
beta@radiocarbon.com
www.radiocarbon.com

MR. DARDEN HOOD
Director

Mr. Ronald Hatfield
Mr. Christopher Patrick
Deputy Directors

January 7, 2008

Mr. J. Mike Quigg
TRC Mariah Associates, Incorporated
505 East Huntland Drive
Suite 250
Austin, TX 78752
USA

RE: Radiocarbon Dating Results For Samples BT1-FS3, BT11-FS27, BT40-FS46, BT40-FS47, PT185-FS248, PT185-FS250, PT185-FS278, PT185-FS348, PT185-FS355, PT186-FS99, PT245-FS167, PT245-FS168, PT245-FS169

Dear Mr. Quigg:

Enclosed are the radiocarbon dating results for 13 samples recently sent to us. They each provided plenty of carbon for accurate measurements and all the analyses proceeded normally. As usual, the method of analysis is listed on the report with the results and calibration data is provided where applicable.

As always, no students or intern researchers who would necessarily be distracted with other obligations and priorities were used in the analyses. We analyzed them with the combined attention of our entire professional staff.

If you have specific questions about the analyses, please contact us. We are always available to answer your questions.

The cost of the analysis was charged to the VISA card provided. A receipt is enclosed. Thank you. As always, if you have any questions or would like to discuss the results, don't hesitate to contact me.

Sincerely,

	BETA ANALYTIC INC. DR. M.A. TAMERS and MR. D.G. HOOD	UNIVERSITY BRANCH 4985 S.W. 74 COURT MIAMI, FLORIDA, USA 33155 PH: 305/667-5167 FAX: 305/663-0964 E-MAIL: beta@radiocarbon.com
---	--	--

REPORT OF RADIOCARBON DATING ANALYSES

Mr. J. Mike Quigg

Report Date: 1/7/2008

TRC Mariah Associates, Incorporated

Material Received: 12/3/2007

Sample Data	Measured Radiocarbon Age	13C/12C Ratio	Conventional Radiocarbon Age(*)
Beta - 238307 SAMPLE : BT1-FS3 ANALYSIS : AMS-Standard delivery MATERIAL/PRETREATMENT : (organic sediment): acid washes 2 SIGMA CALIBRATION : Cal BC 370 to 150 (Cal BP 2320 to 2100) AND Cal BC 140 to 110 (Cal BP 2090 to 2060)	2110 +/- 40 BP	-20.8 o/oo	2180 +/- 40 BP
Beta - 238309 SAMPLE : BT11-FS27 ANALYSIS : AMS-Standard delivery MATERIAL/PRETREATMENT : (organic sediment): acid washes 2 SIGMA CALIBRATION : Cal BC 10920 to 10700 (Cal BP 12870 to 12650)	10590 +/- 70 BP	-16.2 o/oo	10730 +/- 70 BP
Beta - 238310 SAMPLE : BT40-FS46 ANALYSIS : AMS-Standard delivery MATERIAL/PRETREATMENT : (organic sediment): acid washes 2 SIGMA CALIBRATION : Cal BC 400 to 200 (Cal BP 2340 to 2150)	2200 +/- 40 BP	-22.0 o/oo	2250 +/- 40 BP
Beta - 238311 SAMPLE : BT40-FS47 ANALYSIS : AMS-Standard delivery MATERIAL/PRETREATMENT : (organic sediment): acid washes 2 SIGMA CALIBRATION : Cal BC 3020 to 2890 (Cal BP 4970 to 4840)	4290 +/- 40 BP	-22.4 o/oo	4330 +/- 40 BP
Beta - 238312 SAMPLE : PT185-FS248 ANALYSIS : AMS-Standard delivery MATERIAL/PRETREATMENT : (bone collagen): collagen extraction: with alkali 2 SIGMA CALIBRATION : Cal BC 840 to 780 (Cal BP 2790 to 2730)	2450 +/- 40 BP	-13.7 o/oo	2640 +/- 40 BP

Dates are reported as RCYBP (radiocarbon years before present, "present" = 1950A.D.). By International convention, the modern reference standard was 95% of the C14 content of the National Bureau of Standards' Oxalic Acid & calculated using the Libby C14 half life (5568 years). Quoted errors represent 1 standard deviation statistics (68% probability) & are based on combined measurements of the sample, background, and modern reference standards.

Measured C13/C12 ratios were calculated relative to the PDB-1 international standard and the RCYBP ages were normalized to -25 per mil. If the ratio and age are accompanied by an (*), then the C13/C12 value was estimated, based on values typical of the material type. The quoted results are NOT calibrated to calendar years. Calibration to calendar years should be calculated using the Conventional C14 age.

BETA	BETA ANALYTIC INC.	UNIVERSITY BRANCH 4985 S.W. 74 COURT MIAMI, FLORIDA, USA 33155 PH: 305/667-5167 FAX: 305/663-0964 E-MAIL: beta@radiocarbon.com
	DR. M.A. TAMERS and MR. D.G. HOOD	

REPORT OF RADIOCARBON DATING ANALYSES

Mr. J. Mike Quigg

Report Date: 1/7/2008

Sample Data	Measured Radiocarbon Age	¹³ C/ ¹² C Ratio	Conventional Radiocarbon Age(*)
Beta - 238313 SAMPLE : PT185-FS250 ANALYSIS : AMS-Standard delivery MATERIAL/PRETREATMENT : (bone collagen): collagen extraction: with alkali 2 SIGMA CALIBRATION : Cal BC 1280 to 1010 (Cal BP 3230 to 2960)	2700 +/- 40 BP	-10.6 o/oo	2940 +/- 40 BP
Beta - 238314 SAMPLE : PT185-FS278 ANALYSIS : AMS-Standard delivery MATERIAL/PRETREATMENT : (bone collagen): collagen extraction: with alkali 2 SIGMA CALIBRATION : Cal BC 930 to 800 (Cal BP 2880 to 2750)	2450 +/- 40 BP	-8.8 o/oo	2720 +/- 40 BP
Beta - 238315 SAMPLE : PT185-FS348 ANALYSIS : AMS-Standard delivery MATERIAL/PRETREATMENT : (bone collagen): collagen extraction: with alkali 2 SIGMA CALIBRATION : Cal BC 520 to 380 (Cal BP 2470 to 2330)	2130 +/- 40 BP	-10.9 o/oo	2360 +/- 40 BP
Beta - 238316 SAMPLE : PT185-FS355 ANALYSIS : AMS-Standard delivery MATERIAL/PRETREATMENT : (bone collagen): collagen extraction: with alkali 2 SIGMA CALIBRATION : Cal BC 750 to 680 (Cal BP 2700 to 2630) AND Cal BC 670 to 610 (Cal BP 2620 to 2560) Cal BC 600 to 400 (Cal BP 2560 to 2350)	2160 +/- 40 BP	-9.2 o/oo	2420 +/- 40 BP
Beta - 238317 SAMPLE : PT186-FS99 ANALYSIS : AMS-Standard delivery MATERIAL/PRETREATMENT : (bone collagen): collagen extraction: with alkali 2 SIGMA CALIBRATION : Cal AD 1640 to 1690 (Cal BP 310 to 260) AND Cal AD 1730 to 1810 (Cal BP 220 to 140) Cal AD 1920 to 1950 (Cal BP 30 to 0)	100.8 +/- 0.5 pMC	-7.8 o/oo	210 +/- 40 BP

Dates are reported as RCYBP (radiocarbon years before present, "present" = 1950A.D.). By International convention, the modern reference standard was 95% of the C14 content of the National Bureau of Standards' Oxalic Acid & calculated using the Libby C14 half life (5568 years). Quoted errors represent 1 standard deviation statistics (68% probability) & are based on combined measurements of the sample, background, and modern reference standards.

Measured C13/C12 ratios were calculated relative to the PDB-1 international standard and the RCYBP ages were normalized to -25 per mil. If the ratio and age are accompanied by an (*), then the C13/C12 value was estimated, based on values typical of the material type. The quoted results are NOT calibrated to calendar years. Calibration to calendar years should be calculated using the Conventional C14 age.



BETA ANALYTIC INC.

DR. M.A. TAMERS and MR. D.G. HOOD

UNIVERSITY BRANCH
4985 S.W. 74 COURT
MIAMI, FLORIDA, USA 33155
PH: 305/667-5167 FAX: 305/663-0964
E-MAIL: beta@radiocarbon.com

REPORT OF RADIOCARBON DATING ANALYSES

Mr. J. Mike Quigg

Report Date: 1/7/2008

Sample Data	Measured Radiocarbon Age	¹³ C/ ¹² C Ratio	Conventional Radiocarbon Age(*)
Beta - 238318 SAMPLE : PT245-FS167 ANALYSIS : AMS-Standard delivery MATERIAL/PRETREATMENT : (charred material): acid/alkali/acid 2 SIGMA CALIBRATION : Cal AD 1420 to 1500 (Cal BP 530 to 440) AND Cal AD 1600 to 1610 (Cal BP 350 to 340)	430 +/- 40 BP	-24.7 o/oo	430 +/- 40 BP
Beta - 238319 SAMPLE : PT245-FS168 ANALYSIS : AMS-Standard delivery MATERIAL/PRETREATMENT : (organic sediment): acid washes 2 SIGMA CALIBRATION : Cal BC 10960 to 10850 (Cal BP 12900 to 12800)	10770 +/- 50 BP	-19.9 o/oo	10850 +/- 50 BP
Beta - 238320 SAMPLE : PT245-FS169 ANALYSIS : AMS-Standard delivery MATERIAL/PRETREATMENT : (organic sediment): acid washes 2 SIGMA CALIBRATION : Cal BC 10840 to 10610 (Cal BP 12790 to 12560) AND Cal BC 10560 to 10450 (Cal BP 12510 to 12400)	10560 +/- 40 BP	-23.1 o/oo	10590 +/- 40 BP

Dates are reported as RCYBP (radiocarbon years before present, "present" = 1950A.D.). By International convention, the modern reference standard was 95% of the C14 content of the National Bureau of Standards' Oxalic Acid & calculated using the Libby C14 half life (5568 years). Quoted errors represent 1 standard deviation statistics (68% probability) & are based on combined measurements of the sample, background, and modern reference standards.

Measured C13/C12 ratios were calculated relative to the PDB-1 international standard and the RCYBP ages were normalized to -25 per mil. If the ratio and age are accompanied by an (*), then the C13/C12 value was estimated, based on values typical of the material type. The quoted results are NOT calibrated to calendar years. Calibration to calendar years should be calculated using the Conventional C14 age.

CALIBRATION OF RADIOCARBON AGE TO CALENDAR YEARS

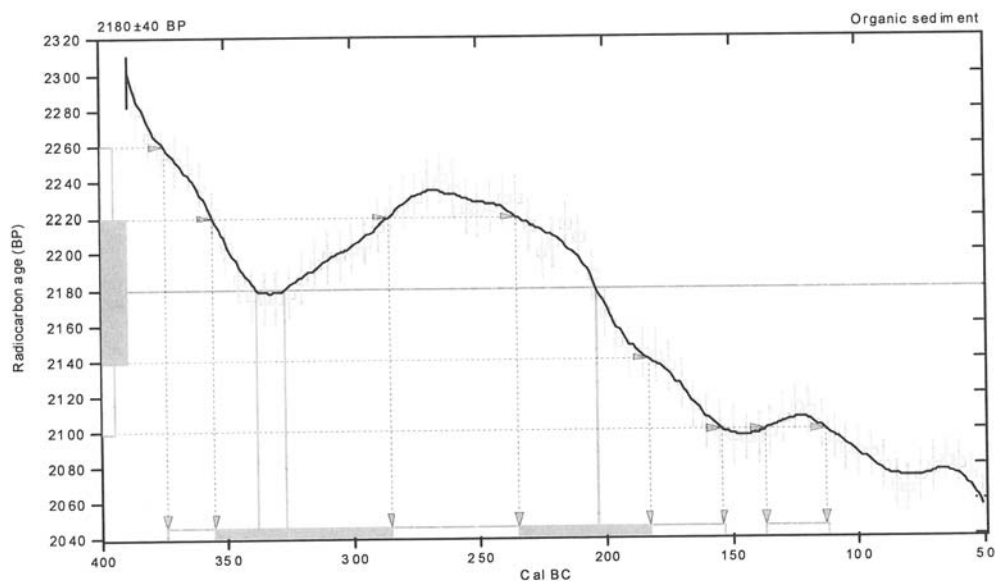
(Variables: C13/C12=-20.8:lab. mult=1)

Laboratory number: **Beta-238307**
Conventional radiocarbon age: **2180±40 BP**
2 Sigma calibrated results: **Cal BC 370 to 150 (Cal BP 2320 to 2100) and**
(95% probability) **Cal BC 140 to 110 (Cal BP 2090 to 2060)**

Intercept data

Intercepts of radiocarbon age
with calibration curve: Cal BC 340 (Cal BP 2290) and
Cal BC 330 (Cal BP 2280) and
Cal BC 200 (Cal BP 2150)

1 Sigma calibrated results: Cal BC 360 to 290 (Cal BP 2300 to 2240) and
(68% probability) Cal BC 240 to 180 (Cal BP 2180 to 2130)



References:

- Database used*
INTCAL04
- Calibration Database*
INTCAL04 Radiocarbon Age Calibration
IntCal04: Calibration Issue of Radiocarbon (Volume 46, nr 3, 2004).
- Mathematics*
A Simplified Approach to Calibrating C14 Dates
Talma, A. S., Vogel, J. C., 1993, Radiocarbon 35(2), p317-322

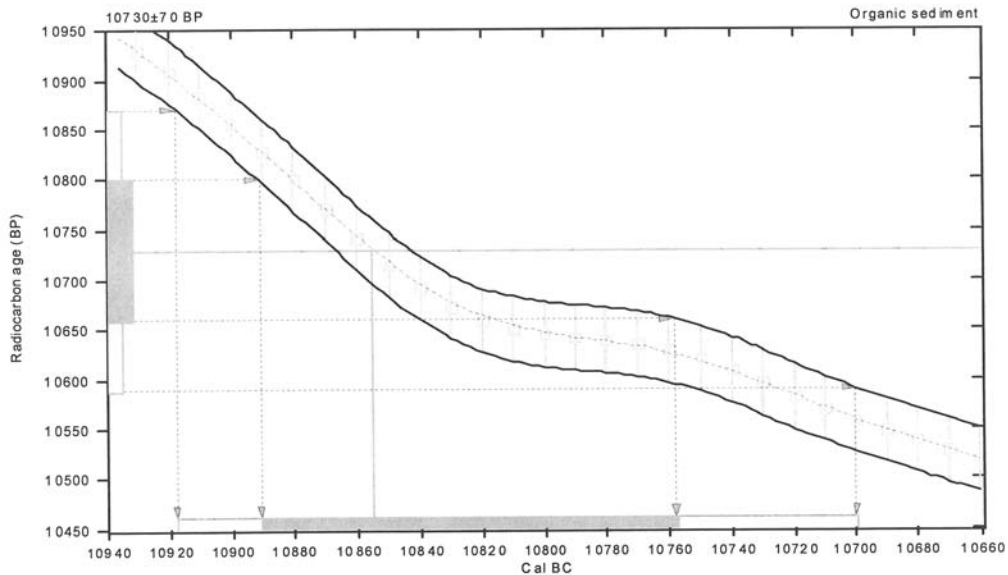
Beta Analytic Radiocarbon Dating Laboratory

4985 S.W. 74th Court, Miami, Florida 33155 • Tel: (305)667-5167 • Fax: (305)663-0964 • E-Mail: beta@radiocarbon.com

CALIBRATION OF RADIOCARBON AGE TO CALENDAR YEARS

(Variables: C13/C12=-16.2:lab. mult=1)

Laboratory number: Beta-238309
Conventional radiocarbon age: 10730±70 BP
2 Sigma calibrated result: Cal BC 10920 to 10700 (Cal BP 12870 to 12650)
(95% probability)
Intercept data
Intercept of radiocarbon age
with calibration curve: Cal BC 10860 (Cal BP 12800)
1 Sigma calibrated result: Cal BC 10890 to 10760 (Cal BP 12840 to 12710)
(68% probability)



References:

- Data base used*
INTCAL04
Calibration Data base
INTCAL04 Radiocarbon Age Calibration
IntCal04: Calibration Issue of Radiocarbon (Volume 46, nr 3, 2004).
- Mathematics*
A Simplified Approach to Calibrating C14 Dates
Talma, A. S., Vogel, J. C., 1993, Radiocarbon 35(2), p317-322

Beta Analytic Radiocarbon Dating Laboratory

4985 S.W. 74th Court, Miami, Florida 33155 • Tel: (305)667-5167 • Fax: (305)663-0964 • E-Mail: beta@radiocarbon.com

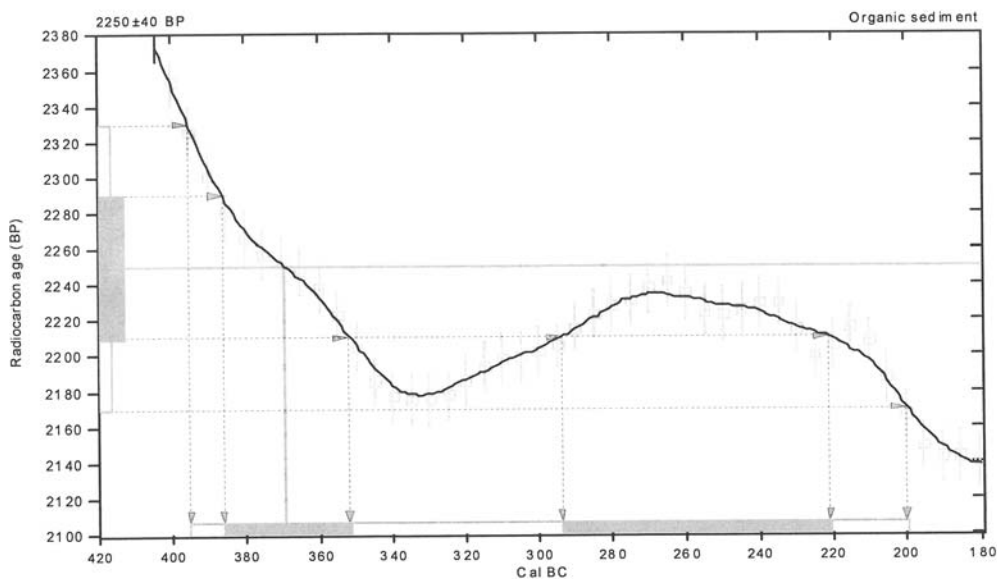
CALIBRATION OF RADIOCARBON AGE TO CALENDAR YEARS

(Variables: C13/C12=-22;lab. mult=1)

Laboratory number: **Beta-238310**
Conventional radiocarbon age: **2250±40 BP**
2 Sigma calibrated result: **Cal BC 400 to 200 (Cal BP 2340 to 2150)**
(95% probability)

Intercept data

Intercept of radiocarbon age
with calibration curve: **Cal BC 370 (Cal BP 2320)**
1 Sigma calibrated results: **Cal BC 390 to 350 (Cal BP 2340 to 2300) and**
Cal BC 290 to 220 (Cal BP 2240 to 2170)



References:

- Data base used*
INTCAL04
Calibration Data base
INTCAL04 Radiocarbon Age Calibration
IntCal04: Calibration Issue of Radiocarbon (Volume 46, nr 3, 2004).
- Mathematics*
A Simplified Approach to Calibrating C14 Dates
Talma, A. S., Vogel, J. C., 1993, Radiocarbon 35(2), p317-322

Beta Analytic Radiocarbon Dating Laboratory

4985 S.W. 74th Court, Miami, Florida 33155 • Tel: (305)667-5167 • Fax: (305)663-0964 • E-Mail: beta@radiocarbon.com

CALIBRATION OF RADIOCARBON AGE TO CALENDAR YEARS

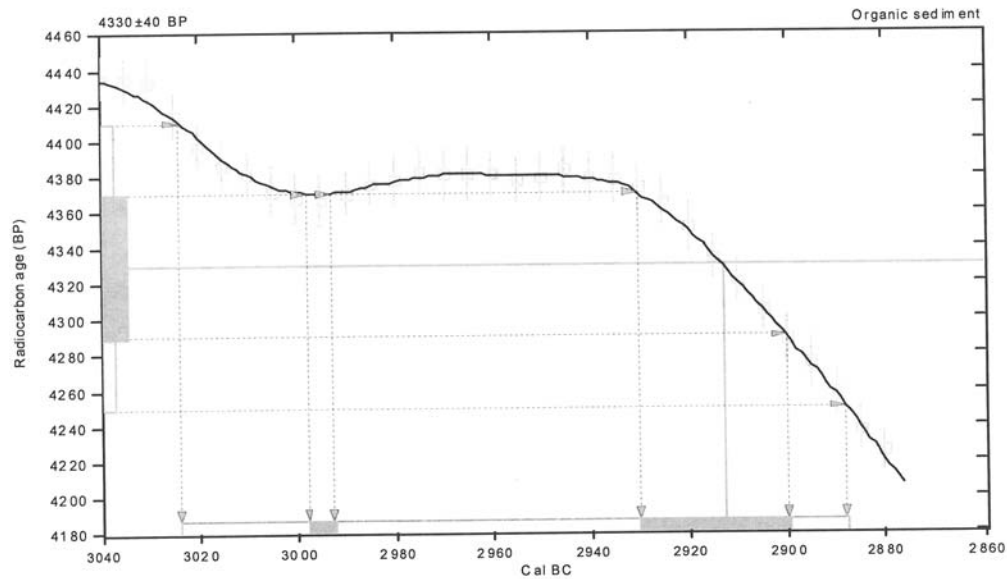
(Variables: C13/C12=-22.4:lab. mult=1)

Laboratory number: **Beta-238311**
Conventional radiocarbon age: **4330±40 BP**
2 Sigma calibrated result: **Cal BC 3020 to 2890 (Cal BP 4970 to 4840)**
(95% probability)

Intercept data

Intercept of radiocarbon age
with calibration curve: **Cal BC 2910 (Cal BP 4860)**

1 Sigma calibrated results: **Cal BC 3000 to 2990 (Cal BP 4950 to 4940) and**
Cal BC 2930 to 2900 (Cal BP 4880 to 4850)



References:

- Database used*
INTCAL04
- Calibration Database*
INTCAL04 Radiocarbon Age Calibration
IntCal04: Calibration Issue of Radiocarbon (Volume 46, nr 3, 2004).
- Mathematics*
A Simplified Approach to Calibrating C14 Dates
Talma, A. S., Vogel, J. C., 1993, Radiocarbon 35(2), p317-322

Beta Analytic Radiocarbon Dating Laboratory

4985 S.W. 74th Court, Miami, Florida 33155 • Tel: (305)667-5167 • Fax: (305)663-0964 • E-Mail: beta@radiocarbon.com

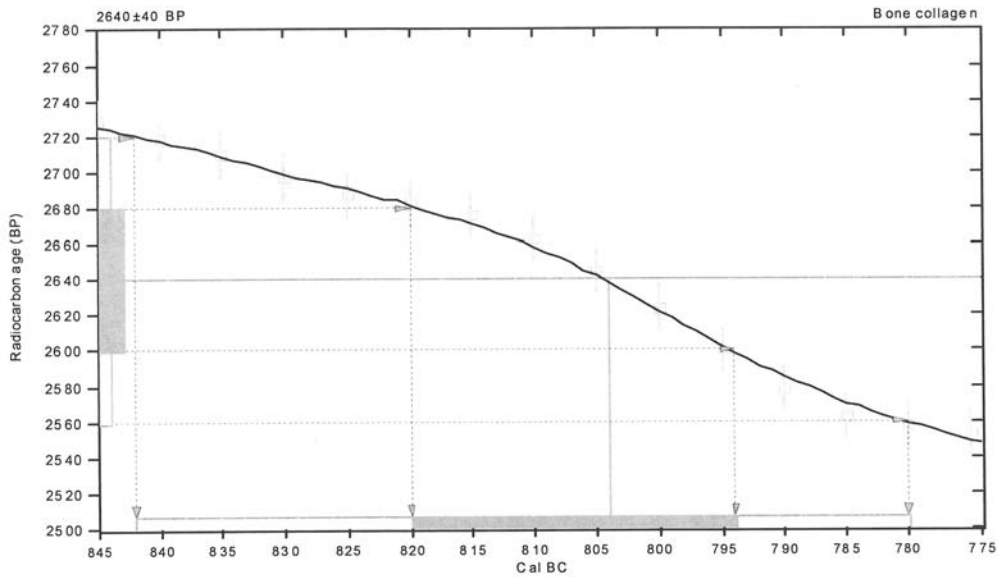
CALIBRATION OF RADIOCARBON AGE TO CALENDAR YEARS

(Variables: C13/C12=-13.7:lab. mult=1)

Laboratory number: **Beta-238312**
Conventional radiocarbon age: **2640±40 BP**
2 Sigma calibrated result: **Cal BC 840 to 780 (Cal BP 2790 to 2730)**
(95% probability)

Intercept data

Intercept of radiocarbon age
with calibration curve: **Cal BC 800 (Cal BP 2750)**
1 Sigma calibrated result: **Cal BC 820 to 790 (Cal BP 2770 to 2740)**
(68% probability)



References:

- Data base used*
INTCAL04
Calibration Data base
INTCAL04 Radiocarbon Age Calibration
IntCal04: Calibration Issue of Radiocarbon (Volume 46, nr 3, 2004).
- Mathematics*
A Simplified Approach to Calibrating C14 Dates
Talma, A. S., Vogel, J. C., 1993, Radiocarbon 35(2), p317-322

Beta Analytic Radiocarbon Dating Laboratory

4985 S.W. 74th Court, Miami, Florida 33155 • Tel: (305)667-5167 • Fax: (305)663-0964 • E-Mail: beta@radiocarbon.com

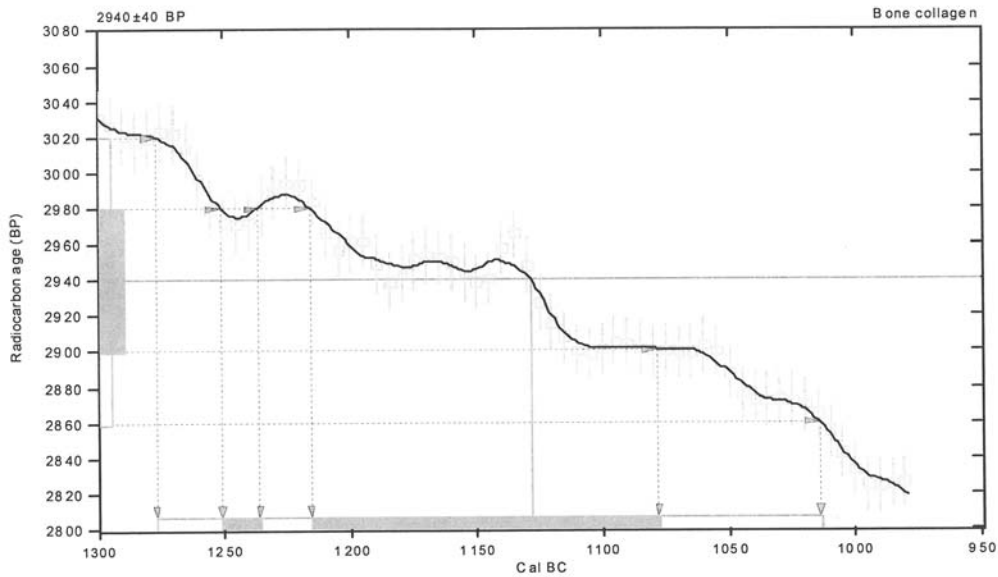
CALIBRATION OF RADIOCARBON AGE TO CALENDAR YEARS

(Variables: C13/C12=-10.6:lab. mult=1)

Laboratory number: **Beta-238313**
Conventional radiocarbon age: **2940±40 BP**
2 Sigma calibrated result: **Cal BC 1280 to 1010 (Cal BP 3230 to 2960)**
(95% probability)

Intercept data

Intercept of radiocarbon age
with calibration curve: **Cal BC 1130 (Cal BP 3080)**
1 Sigma calibrated results: **Cal BC 1250 to 1240 (Cal BP 3200 to 3190)** and
Cal BC 1220 to 1080 (Cal BP 3170 to 3030)



References:

- Data base used*
INTCAL04
Calibration Data base
INTCAL04 Radiocarbon Age Calibration
IntCal04: Calibration Issue of Radiocarbon (Volume 46, nr 3, 2004).
- Mathematics*
A Simplified Approach to Calibrating C14 Dates
Talma, A. S., Vogel, J. C., 1993, Radiocarbon 35(2), p317-322

Beta Analytic Radiocarbon Dating Laboratory

4985 S.W. 74th Court, Miami, Florida 33155 • Tel: (305)667-5167 • Fax: (305)663-0964 • E-Mail: beta@radiocarbon.com

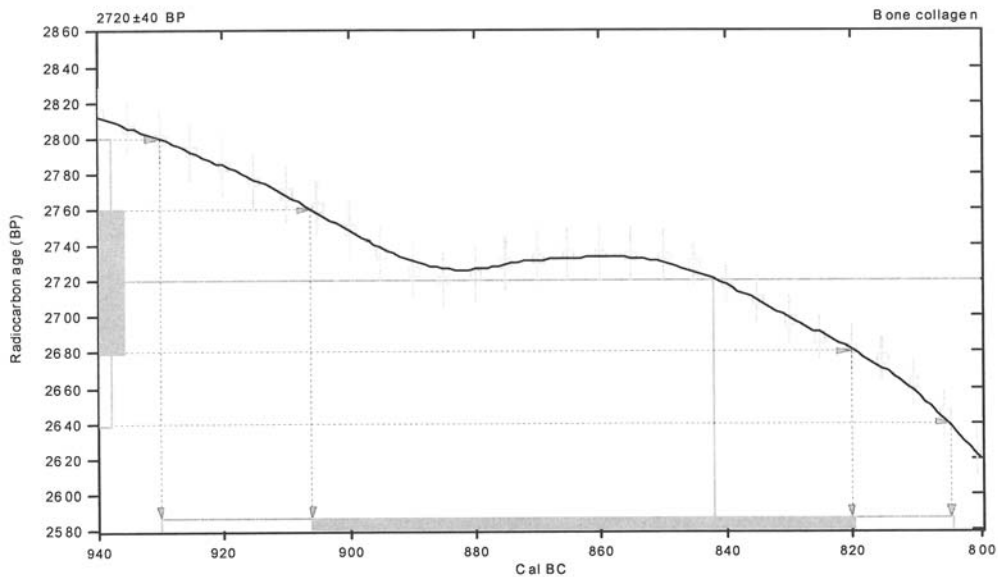
CALIBRATION OF RADIOCARBON AGE TO CALENDAR YEARS

(Variables: C13/C12=-8.8:lab. mult=1)

Laboratory number: **Beta-238314**
Conventional radiocarbon age: **2720±40 BP**
2 Sigma calibrated result: **Cal BC 930 to 800 (Cal BP 2880 to 2750)**
(95% probability)

Intercept data

Intercept of radiocarbon age
with calibration curve: **Cal BC 840 (Cal BP 2790)**
1 Sigma calibrated result: **Cal BC 910 to 820 (Cal BP 2860 to 2770)**
(68% probability)



References:

- Database used*
INTCAL04
Calibration Database
INTCAL04 Radiocarbon Age Calibration
IntCal04: Calibration Issue of Radiocarbon (Volume 46, nr 3, 2004).
- Mathematics*
A Simplified Approach to Calibrating C14 Dates
Talma, A. S., Vogel, J. C., 1993, *Radiocarbon* 35(2), p317-322

Beta Analytic Radiocarbon Dating Laboratory

4983 S.W. 74th Court, Miami, Florida 33155 • Tel: (305)667-5167 • Fax: (305)663-0964 • E-Mail: beta@radiocarbon.com

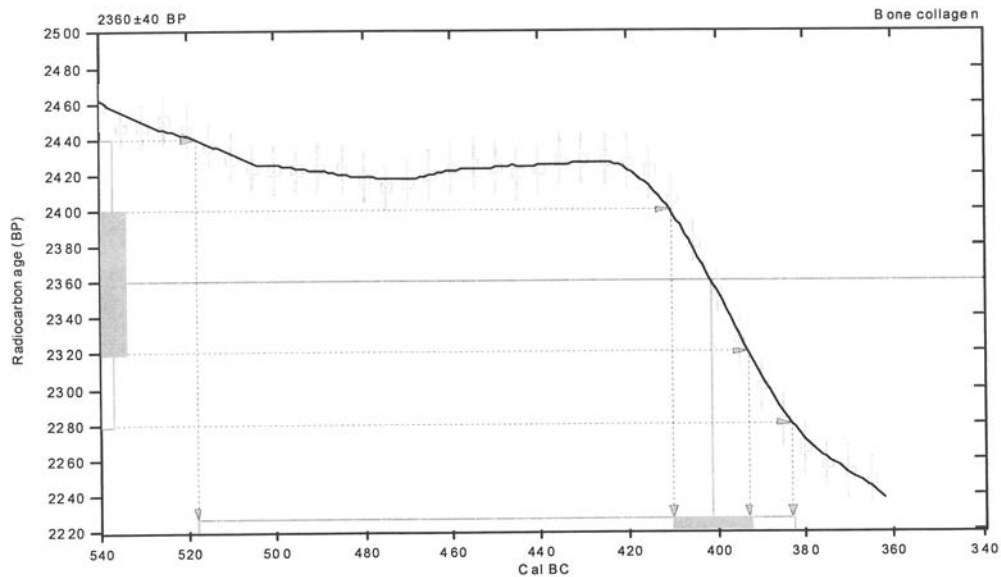
CALIBRATION OF RADIOCARBON AGE TO CALENDAR YEARS

(Variables: C13/C12=-10.9:lab. mult=1)

Laboratory number: Beta-238315
Conventional radiocarbon age: 2360±40 BP
2 Sigma calibrated result: Cal BC 520 to 380 (Cal BP 2470 to 2330)
(95% probability)

Intercept data

Intercept of radiocarbon age
with calibration curve: Cal BC 400 (Cal BP 2350)
1 Sigma calibrated result: Cal BC 410 to 390 (Cal BP 2360 to 2340)
(68% probability)



References:

- Data base used*
INTCAL04
Calibration Data base
INTCAL04 Radiocarbon Age Calibration
In IntCal04: Calibration Issue of Radiocarbon (Volume 46, nr 3, 2004).
- Mathematics*
A Simplified Approach to Calibrating C14 Dates
Talma, A. S., Vogel, J. C., 1993, Radiocarbon 35(2), p317-322

Beta Analytic Radiocarbon Dating Laboratory

4985 S.W. 74th Court, Miami, Florida 33155 • Tel: (305)667-5167 • Fax: (305)663-0964 • E-Mail: beta@radiocarbon.com

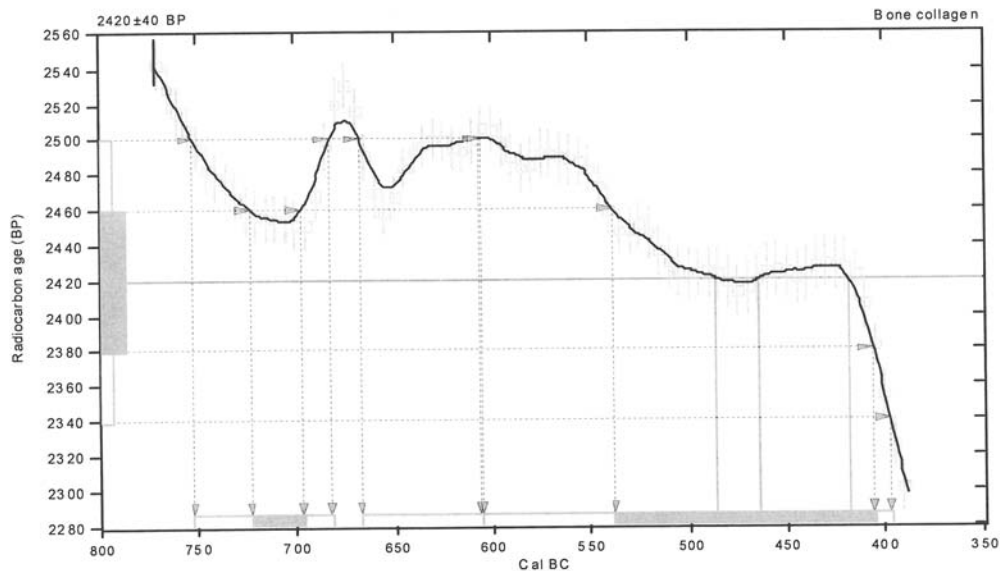
CALIBRATION OF RADIOCARBON AGE TO CALENDAR YEARS

(Variables: C13/C12=-9.2;lab. mult=1)

Laboratory number: **Beta-238316**
Conventional radiocarbon age: **2420±40 BP**
2 Sigma calibrated results: **Cal BC 750 to 680 (Cal BP 2700 to 2630) and**
(95% probability) **Cal BC 670 to 610 (Cal BP 2620 to 2560) and**
Cal BC 600 to 400 (Cal BP 2560 to 2350)

Intercept data

Intercepts of radiocarbon age
with calibration curve: **Cal BC 490 (Cal BP 2440) and**
Cal BC 460 (Cal BP 2410) and
Cal BC 420 (Cal BP 2370)
1 Sigma calibrated results: **Cal BC 720 to 700 (Cal BP 2670 to 2650) and**
(68% probability) **Cal BC 540 to 410 (Cal BP 2490 to 2360)**



References:

Data base used
INTCAL04
Calibration Data base
INTCAL04 Radiocarbon Age Calibration
IntCal04: Calibration Issue of Radiocarbon (Volume 46, nr 3, 2004).
Mathematics
A Simplified Approach to Calibrating C14 Dates
Talma, A. S., Vogel, J. C., 1993, Radiocarbon 35(2), p317-322

Beta Analytic Radiocarbon Dating Laboratory

4985 S.W. 74th Court, Miami, Florida 33155 • Tel: (305) 667-5167 • Fax: (305) 663-0964 • E-Mail: beta@radiocarbon.com

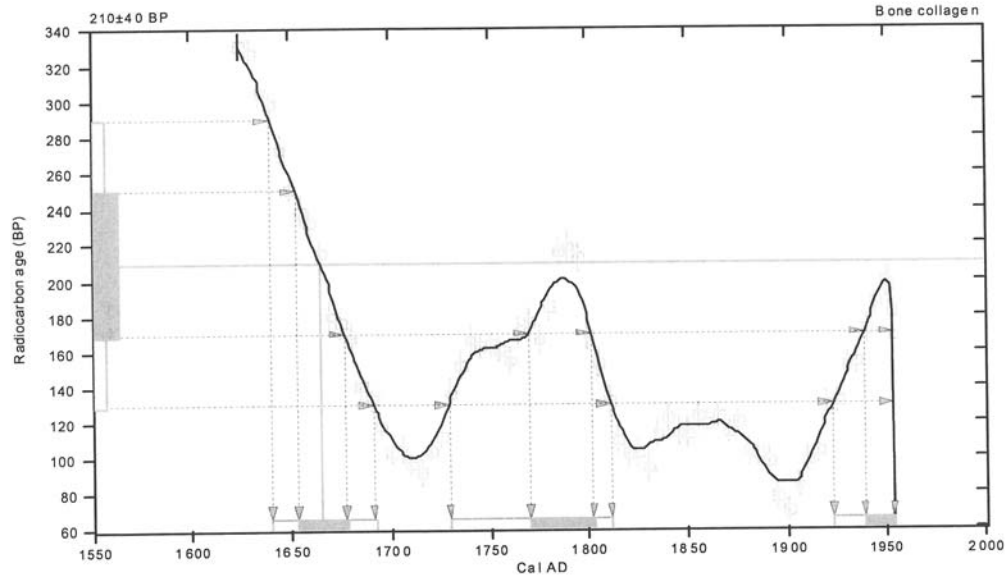
CALIBRATION OF RADIOCARBON AGE TO CALENDAR YEARS

(Variables: C13/C12=-7.8;lab. mult=1)

Laboratory number: **Beta-238317**
Conventional radiocarbon age: **210±40 BP**
2 Sigma calibrated results: **Cal AD 1640 to 1690 (Cal BP 310 to 260) and**
(95% probability) Cal AD 1730 to 1810 (Cal BP 220 to 140) and
Cal AD 1920 to 1950 (Cal BP 30 to 0)

Intercept data

Intercept of radiocarbon age
with calibration curve: **Cal AD 1660 (Cal BP 280)**
1 Sigma calibrated results: **Cal AD 1650 to 1680 (Cal BP 300 to 270) and**
(68% probability) Cal AD 1770 to 1800 (Cal BP 180 to 150) and
Cal AD 1940 to 1950 (Cal BP 10 to 0)



References:

- Data base used*
INTCAL04
- Calibration Database*
INTCAL04 Radiocarbon Age Calibration
IntCal04: Calibration Issue of Radiocarbon (Volume 46, nr 3, 2004).
- Mathematics*
A Simplified Approach to Calibrating C14 Dates
Talma, A. S., Vogel, J. C., 1993, Radiocarbon 35(2), p317-322

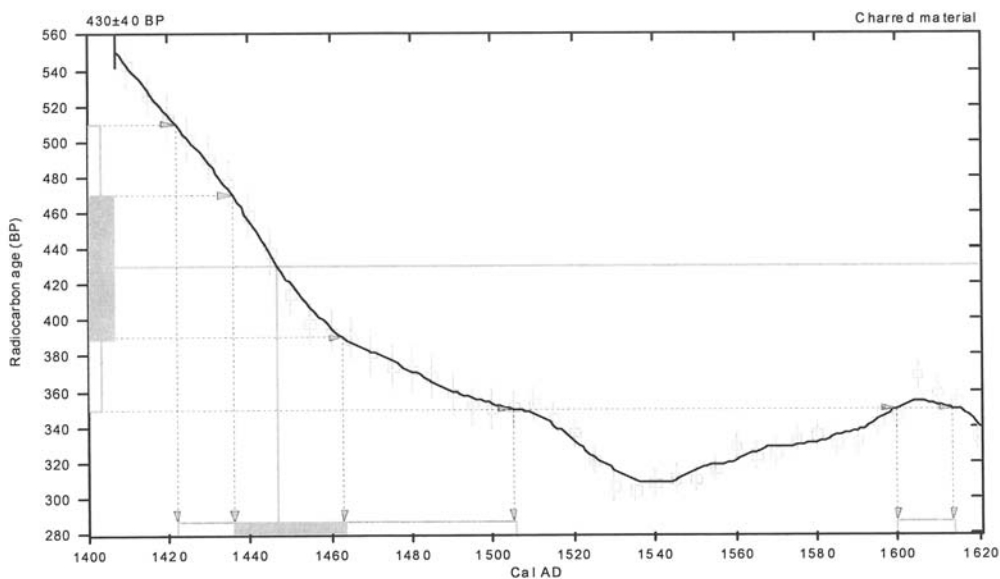
Beta Analytic Radiocarbon Dating Laboratory

4985 S.W. 74th Court, Miami, Florida 33155 • Tel: (305)667-5167 • Fax: (305)663-0964 • E-Mail: beta@radiocarbon.com

CALIBRATION OF RADIOCARBON AGE TO CALENDAR YEARS

(Variables: C13/C12=-24.7:lab. mult=1)

Laboratory number: **Beta-238318**
Conventional radiocarbon age: **430±40 BP**
2 Sigma calibrated results: **Cal AD 1420 to 1500 (Cal BP 530 to 440) and**
(95% probability) Cal AD 1600 to 1610 (Cal BP 350 to 340)
Intercept data
Intercept of radiocarbon age
with calibration curve: **Cal AD 1450 (Cal BP 500)**
1 Sigma calibrated result: **Cal AD 1440 to 1460 (Cal BP 510 to 490)**
(68% probability)



References:

- Data base used*
INTCAL04
Calibration Data base
INTCAL04 Radiocarbon Age Calibration
IntCal04: Calibration Issue of Radiocarbon (Volume 46, nr 3, 2004).
- Mathematics*
A Simplified Approach to Calibrating C14 Dates
Talma, A. S., Vogel, J. C., 1993, Radiocarbon 35(2), p317-322

Beta Analytic Radiocarbon Dating Laboratory

4985 S.W. 74th Court, Miami, Florida 33155 • Tel: (305)667-5167 • Fax: (305)663-0964 • E-Mail: beta@radiocarbon.com

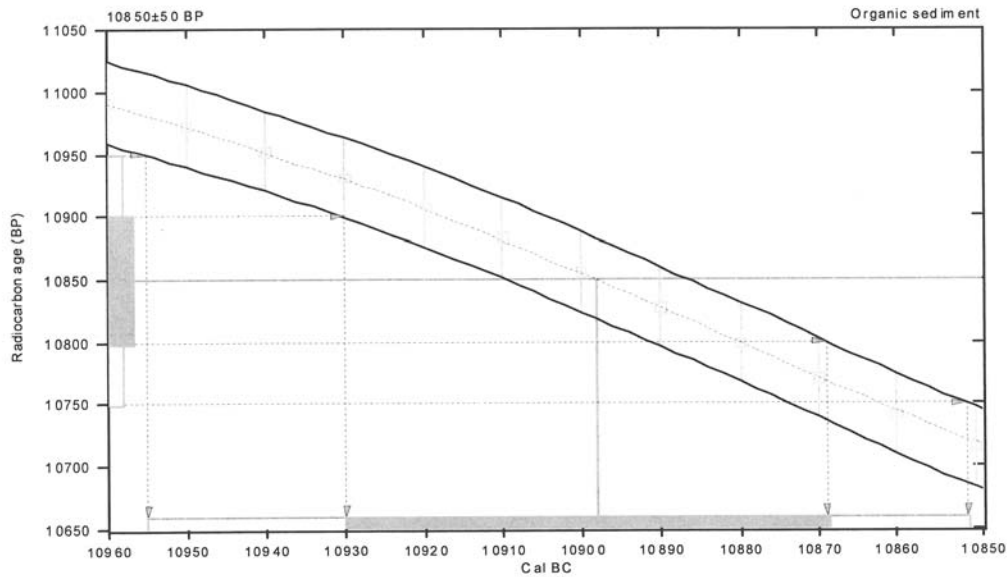
CALIBRATION OF RADIOCARBON AGE TO CALENDAR YEARS

(Variables: C13/C12=-19.9:lab. mult=1)

Laboratory number: **Beta-238319**
Conventional radiocarbon age: **10850±50 BP**
2 Sigma calibrated result: **Cal BC 10960 to 10850 (Cal BP 12900 to 12800)**
(95% probability)

Intercept data

Intercept of radiocarbon age
with calibration curve: **Cal BC 10900 (Cal BP 12850)**
1 Sigma calibrated result: **Cal BC 10930 to 10870 (Cal BP 12880 to 12820)**
(68% probability)



References:

- Data base used*
INTCAL04
Calibration Data base
INTCAL04 Radiocarbon Age Calibration
IntCal04: Calibration Issue of Radiocarbon (Volume 46, nr 3, 2004).
- Mathematics*
A Simplified Approach to Calibrating C14 Dates
Talma, A. S., Vogel, J. C., 1993, Radiocarbon 35(2), p317-322

Beta Analytic Radiocarbon Dating Laboratory

4985 S.W. 74th Court, Miami, Florida 33155 • Tel: (305)667-5167 • Fax: (305)663-0964 • E-Mail: beta@radiocarbon.com

CALIBRATION OF RADIOCARBON AGE TO CALENDAR YEARS

(Variables: C13/C12=-23.1:lab. mult=1)

Laboratory number: **Beta-238320**

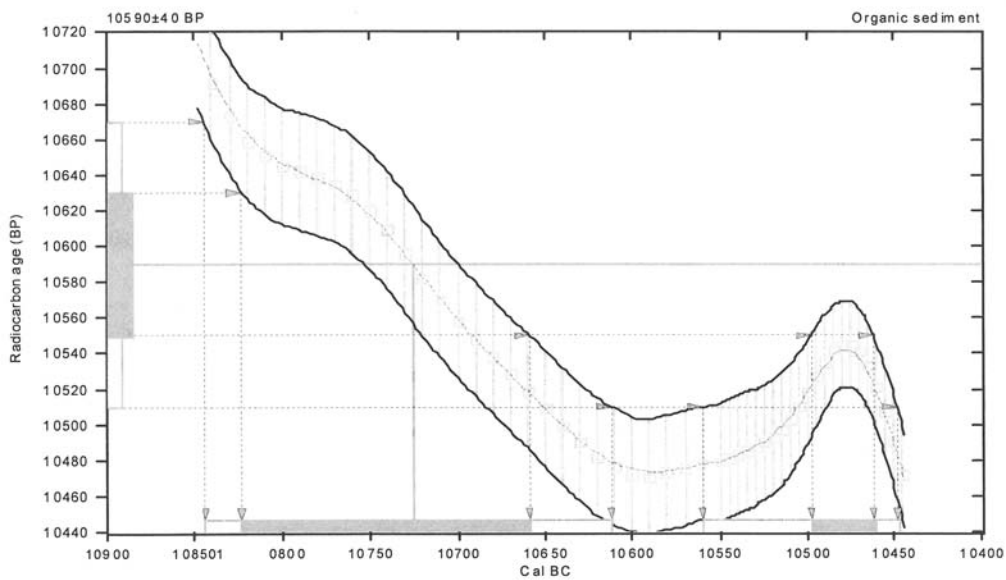
Conventional radiocarbon age: **10590±40 BP**

2 Sigma calibrated results: **Cal BC 10840 to 10610 (Cal BP 12790 to 12560) and
(95% probability) Cal BC 10560 to 10450 (Cal BP 12510 to 12400)**

Intercept data

Intercept of radiocarbon age
with calibration curve: **Cal BC 10730 (Cal BP 12680)**

1 Sigma calibrated results: **Cal BC 10820 to 10660 (Cal BP 12770 to 12610) and
(68% probability) Cal BC 10500 to 10460 (Cal BP 12450 to 12410)**



References:

Data base used

INTCAL04

Calibration Data base

INTCAL04 Radiocarbon Age Calibration

IntCal04: Calibration Issue of Radiocarbon (Volume 46, nr 3, 2004).

Mathematics

A Simplified Approach to Calibrating C14 Dates

Talma, A. S., Vogel, J. C., 1993, Radiocarbon 35(2), p317-322

Beta Analytic Radiocarbon Dating Laboratory

4985 S.W. 74th Court, Miami, Florida 33155 • Tel: (305)667-5167 • Fax: (305)663-0964 • E-Mail: beta@radiocarbon.com



Consistent Accuracy
Delivered On Time.

Beta Analytic Inc.

4985 SW 74 Court
Miami, Florida 33155 USA
Tel: 305 667 5167
Fax: 305 663 0964
beta@radiocarbon.com
www.radiocarbon.com

MR. DARDEN HOOD
Director

Mr. Ronald Hatfield
Mr. Christopher Patrick
Deputy Directors

February 6, 2008

Mr. J. Mike Quigg
TRC Mariah Associates, Incorporated
505 East Huntland Drive
Suite 250
Austin, TX 78752
USA

RE: Radiocarbon Dating Results For Samples BT-36-M-3, BT-36-M-4, BT-36-M-5

Dear Mr. Quigg:

Enclosed are the radiocarbon dating results for three samples recently sent to us. They each provided plenty of carbon for accurate measurements and all the analyses proceeded normally. As usual, the method of analysis is listed on the report with the results and calibration data is provided where applicable.

As always, no students or intern researchers who would necessarily be distracted with other obligations and priorities were used in the analyses. We analyzed them with the combined attention of our entire professional staff.

If you have specific questions about the analyses, please contact us. We are always available to answer your questions.

The cost of the analysis was charged to the VISA card provided. A receipt is enclosed. Thank you. As always, if you have any questions or would like to discuss the results, don't hesitate to contact me.

Sincerely,

A handwritten signature in blue ink that reads "Darden Hood".

	BETA ANALYTIC INC.	UNIVERSITY BRANCH 4985 S.W. 74 COURT MIAMI, FLORIDA, USA 33155 PH: 305/667-5167 FAX: 305/663-0964 E-MAIL: beta@radiocarbon.com
	DR. M.A. TAMERS and MR. D.G. HOOD	

REPORT OF RADIOCARBON DATING ANALYSES

Mr. J. Mike Quigg

Report Date: 2/6/2008

TRC Mariah Associates, Incorporated

Material Received: 1/8/2008

Sample Data	Measured Radiocarbon Age	¹³ C/ ¹² C Ratio	Conventional Radiocarbon Age(*)
Beta - 239651 SAMPLE : BT-36-M-3 ANALYSIS : AMS-Standard delivery MATERIAL/PRETREATMENT : (organic sediment): acid washes 2 SIGMA CALIBRATION : Cal AD 560 to 660 (Cal BP 1390 to 1290)	1320 +/- 40 BP	-18.5 o/oo	1430 +/- 40 BP
Beta - 239652 SAMPLE : BT-36-M-4 ANALYSIS : AMS-Standard delivery MATERIAL/PRETREATMENT : (charred material): acid/alkali/acid 2 SIGMA CALIBRATION : Cal AD 1220 to 1290 (Cal BP 730 to 660)	750 +/- 40 BP	-25.1 o/oo	750 +/- 40 BP
Beta - 239653 SAMPLE : BT-36-M-5 ANALYSIS : AMS-Standard delivery MATERIAL/PRETREATMENT : (charred material): acid/alkali/acid 2 SIGMA CALIBRATION : Cal AD 1040 to 1100 (Cal BP 910 to 850) AND Cal AD 1120 to 1260 (Cal BP 830 to 690)	860 +/- 40 BP	-25.3 o/oo	860 +/- 40 BP

Dates are reported as RCYBP (radiocarbon years before present, "present" = 1950A.D.). By International convention, the modern reference standard was 95% of the C14 content of the National Bureau of Standards' Oxalic Acid & calculated using the Libby C14 half life (5568 years). Quoted errors represent 1 standard deviation statistics (68% probability) & are based on combined measurements of the sample, background, and modern reference standards.

Measured C13/C12 ratios were calculated relative to the PDB-1 international standard and the RCYBP ages were normalized to -25 per mil. If the ratio and age are accompanied by an (*), then the C13/C12 value was estimated, based on values typical of the material type. The quoted results are NOT calibrated to calendar years. Calibration to calendar years should be calculated using the Conventional C14 age.

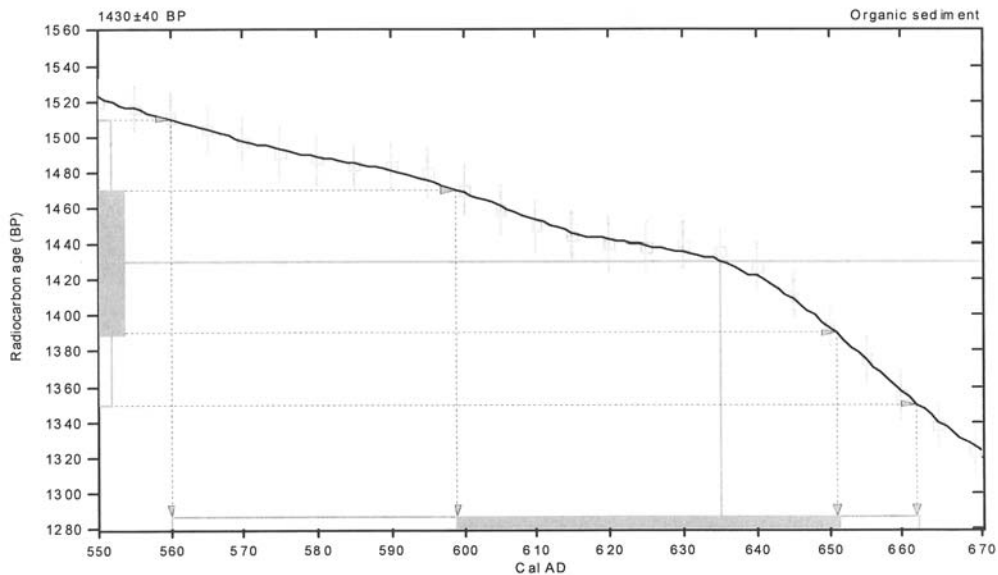
CALIBRATION OF RADIOCARBON AGE TO CALENDAR YEARS

(Variables: C13/C12=-18.5:lab. mult=1)

Laboratory number: **Beta-239651**
Conventional radiocarbon age: **1430±40 BP**
2 Sigma calibrated result: **Cal AD 560 to 660 (Cal BP 1390 to 1290)**
(95% probability)

Intercept data

Intercept of radiocarbon age
with calibration curve: **Cal AD 640 (Cal BP 1320)**
1 Sigma calibrated result: **Cal AD 600 to 650 (Cal BP 1350 to 1300)**
(68% probability)



References:

- Data base used*
INTCAL04
Calibration Data base
INTCAL04 Radiocarbon Age Calibration
IntCal04: Calibration Issue of Radiocarbon (Volume 46, nr 3, 2004).
- Mathematics*
A Simplified Approach to Calibrating C14 Dates
Talma, A. S., Vogel, J. C., 1993, *Radiocarbon* 35(2), p317-322

Beta Analytic Radiocarbon Dating Laboratory

4985 S.W. 74th Court, Miami, Florida 33155 • Tel: (305)667-5167 • Fax: (305)663-0964 • E-Mail: beta@radiocarbon.com

CALIBRATION OF RADIOCARBON AGE TO CALENDAR YEARS

(Variables: C13/C12=-25.1:lab. mult=1)

Laboratory number: Beta-239652

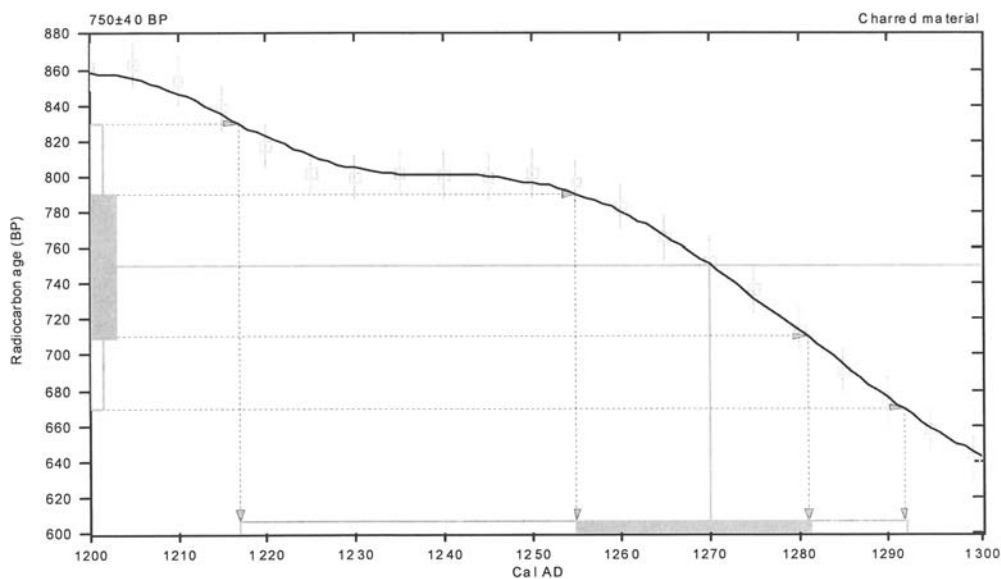
Conventional radiocarbon age: 750±40 BP

2 Sigma calibrated result: Cal AD 1220 to 1290 (Cal BP 730 to 660)
(95% probability)

Intercept data

Intercept of radiocarbon age
with calibration curve: Cal AD 1270 (Cal BP 680)

1 Sigma calibrated result: Cal AD 1260 to 1280 (Cal BP 700 to 670)
(68% probability)



References:

Data base used

INTCAL04

Calibration Data base

INTCAL04 Radiocarbon Age Calibration

IntCal04: Calibration Issue of Radiocarbon (Volume 46, nr 3, 2004).

Mathematics

A Simplified Approach to Calibrating C14 Dates

Talma, A. S., Vogel, J. C., 1993, Radiocarbon 35(2), p317-322

Beta Analytic Radiocarbon Dating Laboratory

4985 S.W. 74th Court, Miami, Florida 33155 • Tel: (305)667-5167 • Fax: (305)663-0964 • E-Mail: beta@radiocarbon.com

CALIBRATION OF RADIOCARBON AGE TO CALENDAR YEARS

(Variables: C13/C12=-25.3:lab. mult=1)

Laboratory number: Beta-239653

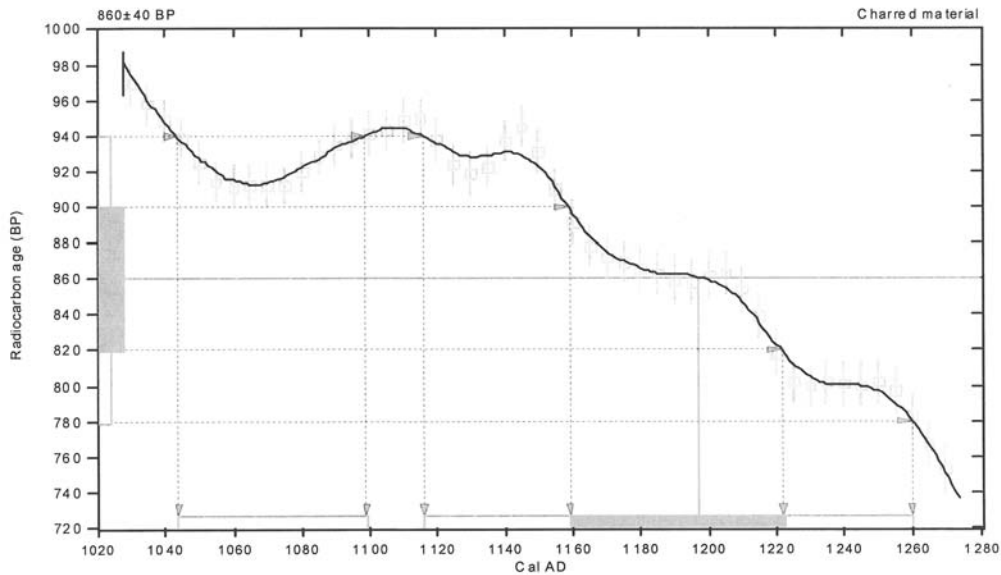
Conventional radiocarbon age: 860 ± 40 BP

2 Sigma calibrated results: Cal AD 1040 to 1100 (Cal BP 910 to 850) and
(95% probability) Cal AD 1120 to 1260 (Cal BP 830 to 690)

Intercept data

Intercept of radiocarbon age
with calibration curve: Cal AD 1200 (Cal BP 750)

1 Sigma calibrated result: Cal AD 1160 to 1220 (Cal BP 790 to 730)
(68% probability)



References:

Data base used

INTCAL04

Calibration Data base

INTCAL04 Radiocarbon Age Calibration

IntCal04: Calibration Issue of Radiocarbon (Volume 46, nr 3, 2004).

Mathematics

A Simplified Approach to Calibrating C14 Dates

Talma, A. S., Vogel, J. C., 1993, Radiocarbon 35(2), p317-322

Beta Analytic Radiocarbon Dating Laboratory

4985 S.W. 74th Court, Miami, Florida 33155 • Tel: (305)667-5167 • Fax: (305)663-0964 • E-Mail: beta@radiocarbon.com



Consistent Accuracy
Delivered On Time.

Beta Analytic Inc.

4985 SW 74 Court
Miami, Florida 33155 USA
Tel: 305 667 5167
Fax: 305 663 0964
beta@radiocarbon.com
www.radiocarbon.com

MR. DARDEN HOOD
Director

Mr. Ronald Hatfield
Mr. Christopher Patrick
Deputy Directors

March 13, 2008

Mr. J. Mike Quigg
TRC Solutions, Incorporated
505 East Huntland Drive
Suite 250
Austin, TX 78752
USA

RE: Radiocarbon Dating Result For Sample BT36-M-1

Dear Mr. Quigg:

Enclosed is the radiocarbon dating result for one sample recently sent to us. It provided plenty of carbon for an accurate measurement and the analysis proceeded normally. As usual, the method of analysis is listed on the report sheet and calibration data is provided where applicable.

As always, no students or intern researchers who would necessarily be distracted with other obligations and priorities were used in the analysis. It was analyzed with the combined attention of our entire professional staff.

If you have specific questions about the analyses, please contact us. We are always available to answer your questions.

Our invoice is enclosed. Please, forward it to the appropriate officer or send VISA charge authorization. Thank you. As always, if you have any questions or would like to discuss the results, don't hesitate to contact me.

Sincerely,

	BETA ANALYTIC INC. DR. M.A. TAMERS and MR. D.G. HOOD	UNIVERSITY BRANCH 4985 S.W. 74 COURT MIAMI, FLORIDA, USA 33155 PH: 305/667-5167 FAX: 305/663-0964 E-MAIL: beta@radiocarbon.com
---	--	--

REPORT OF RADIOCARBON DATING ANALYSES

Mr. J. Mike Quigg

Report Date: 3/13/2008

TRC Solutions, Incorporated

Material Received: 2/8/2008

Sample Data	Measured Radiocarbon Age	¹³ C/ ¹² C Ratio	Conventional Radiocarbon Age(*)
Beta - 241070 SAMPLE : BT36-M-1 ANALYSIS : AMS-Standard delivery MATERIAL/PRETREATMENT : (plant material): acid/alkali/acid 2 SIGMA CALIBRATION : Cal AD 30 to 230 (Cal BP 1920 to 1720)	1930 +/- 40 BP	-27.3 o/oo	1890 +/- 40 BP

Dates are reported as RCYBP (radiocarbon years before present, "present" = 1950A.D.). By International convention, the modern reference standard was 95% of the C14 content of the National Bureau of Standards' Oxalic Acid & calculated using the Libby C14 half life (5568 years). Quoted errors represent 1 standard deviation statistics (68% probability) & are based on combined measurements of the sample, background, and modern reference standards.

Measured C13/C12 ratios were calculated relative to the PDB-1 international standard and the RCYBP ages were normalized to -25 per mil. If the ratio and age are accompanied by an (*), then the C13/C12 value was estimated, based on values typical of the material type. The quoted results are NOT calibrated to calendar years. Calibration to calendar years should be calculated using the Conventional C14 age.

CALIBRATION OF RADIOCARBON AGE TO CALENDAR YEARS

(Variables: C13/C12=-27.3:lab. mult=1)

Laboratory number: Beta-241070

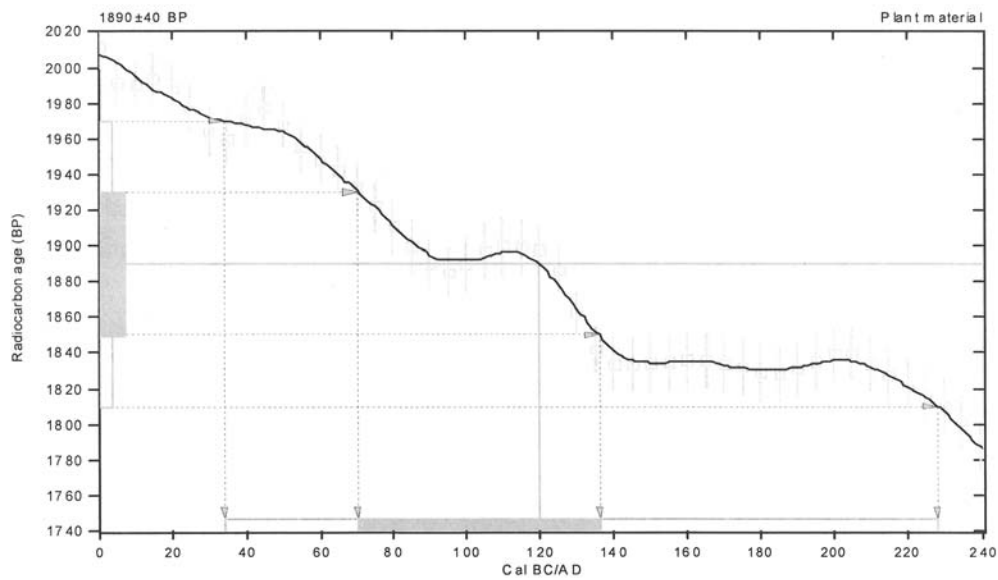
Conventional radiocarbon age: 1890±40 BP

2 Sigma calibrated result: Cal AD 30 to 230 (Cal BP 1920 to 1720)
(95% probability)

Intercept data

Intercept of radiocarbon age
with calibration curve: Cal AD 120 (Cal BP 1830)

1 Sigma calibrated result: Cal AD 70 to 140 (Cal BP 1880 to 1810)
(68% probability)



References:

Data base used

INTCAL04

Calibration Data base

INTCAL04 Radiocarbon Age Calibration

IntCal04: Calibration Issue of Radiocarbon (Volume 46, nr 3, 2004).

Mathematics

A Simplified Approach to Calibrating C14 Dates

Talma, A. S., Vogel, J. C., 1993, Radiocarbon 35(2), p317-322

Beta Analytic Radiocarbon Dating Laboratory

4985 S.W. 74th Court, Miami, Florida 33155 • Tel: (305)667-5167 • Fax: (305)663-0964 • E-Mail: beta@radiocarbon.com



Consistent Accuracy . . .
. . . Delivered On-time

Beta Analytic Inc.
4985 SW 74 Court
Miami, Florida 33155 USA
Tel: 305 667 5167
Fax: 305 663 0964
Beta@radiocarbon.com
www.radiocarbon.com

Darden Hood
President

Ronald Hatfield
Christopher Patrick
Deputy Directors

November 12, 2008

Mr. J. Mike Quigg
TRC Solutions, Incorporated
505 East Huntland Drive
Suite 250
Austin, TX 78752
USA

RE: Radiocarbon Dating Results For Samples PT185C-FSXXX, PT185C-FS630, PT186-FS643

Dear Mr. Quigg:

Enclosed are the radiocarbon dating results for three samples recently sent to us. They each provided plenty of carbon for accurate measurements and all the analyses proceeded normally. As usual, the method of analysis is listed on the report with the results and calibration data is provided where applicable.

As always, no students or intern researchers who would necessarily be distracted with other obligations and priorities were used in the analyses. We analyzed them with the combined attention of our entire professional staff.

If you have specific questions about the analyses, please contact us. We are always available to answer your questions.

The cost of the analysis was charged to the VISA card provided. A receipt has been sent electronically. Thank you. As always, if you have any questions or would like to discuss the results, don't hesitate to contact me.

Sincerely,

Digital signature on file

	BETA ANALYTIC INC.	4985 S.W. 74 COURT MIAMI, FLORIDA, USA 33155 PH: 305-667-5167 FAX: 305-663-0964 beta@radiocarbon.com
	DR. M.A. TAMERS and MR. D.G. HOOD	

REPORT OF RADIOCARBON DATING ANALYSES

Mr. J. Mike Quigg

Report Date: 11/12/2008

TRC Solutions, Incorporated

Material Received: 10/24/2008

Sample Data	Measured Radiocarbon Age	13C/12C Ratio	Conventional Radiocarbon Age(*)
Beta - 250877 SAMPLE : PT185C-FSXXX ANALYSIS : AMS-Standard delivery MATERIAL/PRETREATMENT : (charred material): acid/alkali/acid 2 SIGMA CALIBRATION : Cal AD 340 to 540 (Cal BP 1610 to 1410)	1590 +/- 40 BP	-22.4 o/oo	1630 +/- 40 BP
Beta - 250878 SAMPLE : PT185C-FS630 ANALYSIS : AMS-Standard delivery MATERIAL/PRETREATMENT : (charred material): acid/alkali/acid 2 SIGMA CALIBRATION : Cal BC 1120 to 910 (Cal BP 3070 to 2860)	2820 +/- 40 BP	-23.0 o/oo	2850 +/- 40 BP
Beta - 250879 SAMPLE : PT186-FS643 ANALYSIS : AMS-Standard delivery MATERIAL/PRETREATMENT : (charred material): acid/alkali/acid 2 SIGMA CALIBRATION : Cal AD 1480 to 1660 (Cal BP 470 to 280)	370 +/- 40 BP	-29.6 o/oo	290 +/- 40 BP

Dates are reported as RCYBP (radiocarbon years before present, "present" = AD 1950). By international convention, the modern reference standard was 95% the 14C activity of the National Institute of Standards and Technology (NIST) Oxalic Acid (SRM 4990C) and calculated using the Libby 14C half-life (5568 years). Quoted errors represent 1 relative standard deviation statistics (68% probability) counting errors based on the combined measurements of the sample, background, and modern reference standards. Measured 13C/12C ratios (delta 13C) were calculated relative to the PDB-1 standard.

The Conventional Radiocarbon Age represents the Measured Radiocarbon Age corrected for isotopic fractionation, calculated using the delta 13C. On rare occasion where the Conventional Radiocarbon Age was calculated using an assumed delta 13C, the ratio and the Conventional Radiocarbon Age will be followed by "m". The Conventional Radiocarbon Age is not calendar calibrated. When available, the Calendar Calibrated result is calculated from the Conventional Radiocarbon Age and is listed as the "Two Sigma Calibrated Result" for each sample.

CALIBRATION OF RADIOCARBON AGE TO CALENDAR YEARS

(Variables: C13/C12=-22.4:lab. mult=1)

Laboratory number: **Beta-250877**

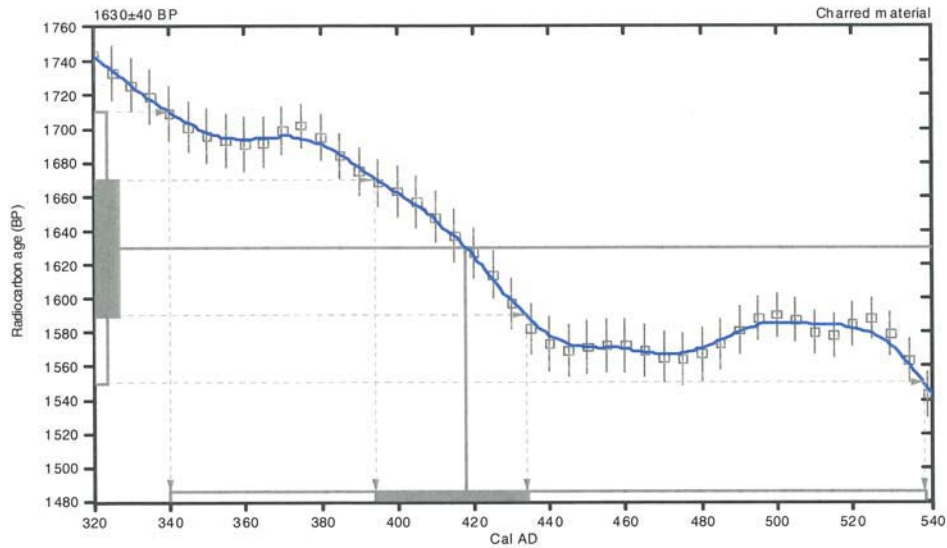
Conventional radiocarbon age: **1630±40 BP**

2 Sigma calibrated result: Cal AD 340 to 540 (Cal BP 1610 to 1410)
(95% probability)

Intercept data

Intercept of radiocarbon age
with calibration curve: **Cal AD 420 (Cal BP 1530)**

1 Sigma calibrated result: Cal AD 390 to 430 (Cal BP 1560 to 1520)
(68% probability)



References:

Database used

INTCAL04

Calibration Database

INTCAL04 Radiocarbon Age Calibration

IntCal04: Calibration Issue of Radiocarbon (Volume 46, nr 3, 2004).

Mathematics

A Simplified Approach to Calibrating C14 Dates

Talma, A. S., Vogel, J. C., 1993, Radiocarbon 35(2), p317-322

Beta Analytic Radiocarbon Dating Laboratory

4985 S.W. 74th Court, Miami, Florida 33155 • Tel: (305)667-5167 • Fax: (305)663-0964 • E-Mail: beta@radiocarbon.com

CALIBRATION OF RADIOCARBON AGE TO CALENDAR YEARS

(Variables: C13/C12=-23:lab. mult=1)

Laboratory number: **Beta-250878**

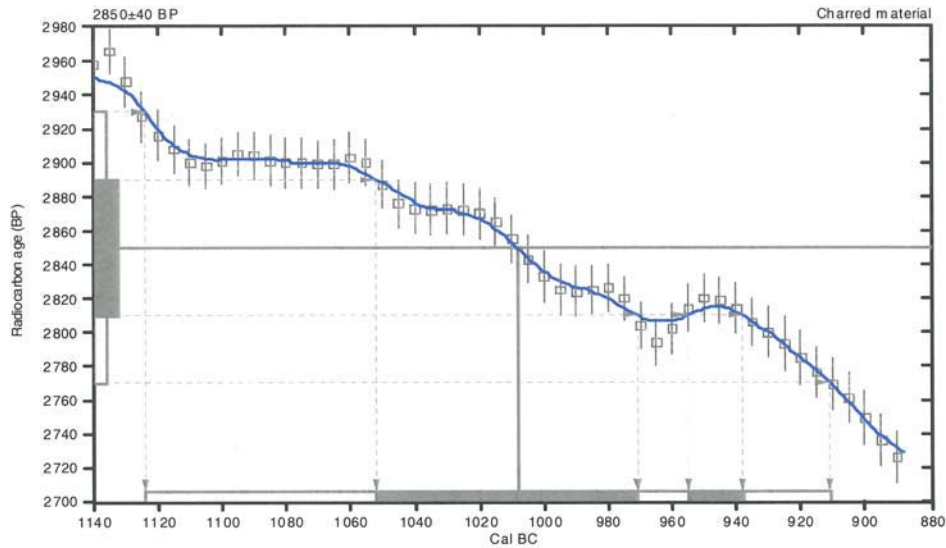
Conventional radiocarbon age: **2850±40 BP**

2 Sigma calibrated result: Cal BC 1120 to 910 (Cal BP 3070 to 2860)
(95% probability)

Intercept data

Intercept of radiocarbon age
with calibration curve: Cal BC 1010 (Cal BP 2960)

1 Sigma calibrated results: Cal BC 1050 to 970 (Cal BP 3000 to 2920) and
(68% probability) **Cal BC 960 to 940 (Cal BP 2900 to 2890)**



References:

Database used

INTCAL04

Calibration Database

INTCAL04 Radiocarbon Age Calibration

IntCal04: Calibration Issue of Radiocarbon (Volume 46, nr 3, 2004).

Mathematics

A Simplified Approach to Calibrating C14 Dates

Talma, A. S., Vogel, J. C., 1993, Radiocarbon 35(2), p317-322

Beta Analytic Radiocarbon Dating Laboratory

4985 S.W. 74th Court, Miami, Florida 33155 • Tel: (305)667-5167 • Fax: (305)663-0964 • E-Mail: beta@radiocarbon.com

CALIBRATION OF RADIOCARBON AGE TO CALENDAR YEARS

(Variables: C13/C12=-29.6;lab. mult=1)

Laboratory number: **Beta-250879**

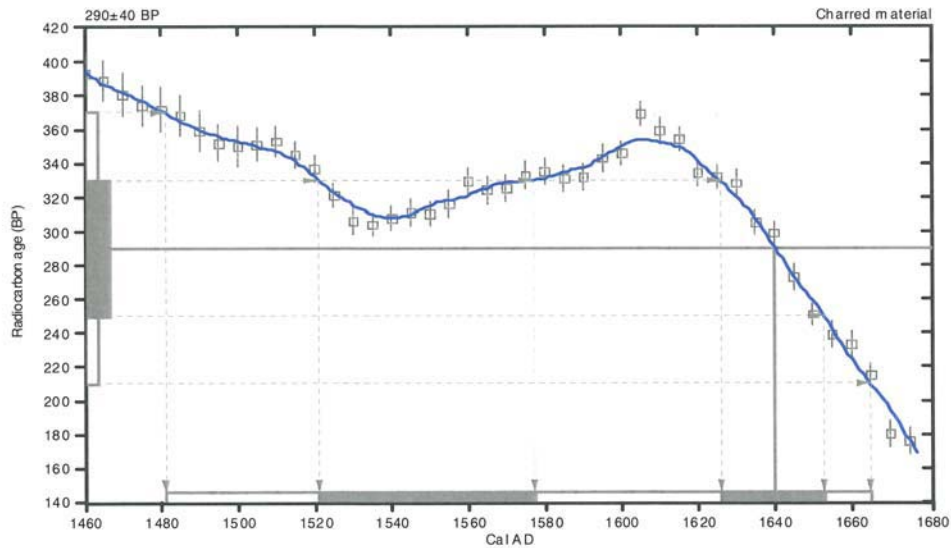
Conventional radiocarbon age: **290±40 BP**

2 Sigma calibrated result: Cal AD 1480 to 1660 (Cal BP 470 to 280)
(95% probability)

Intercept data

Intercept of radiocarbon age
with calibration curve: Cal AD 1640 (Cal BP 310)

1 Sigma calibrated results: Cal AD 1520 to 1580 (Cal BP 430 to 370) and
(68% probability) **Cal AD 1630 to 1650 (Cal BP 320 to 300)**



References:

Database used

INTCAL04

Calibration Database

INTCAL04 Radiocarbon Age Calibration

IntCal04: Calibration Issue of Radiocarbon (Volume 46, nr 3, 2004).

Mathematics

A Simplified Approach to Calibrating C14 Dates

Talma, A. S., Vogel, J. C., 1993, Radiocarbon 35(2), p317-322

Beta Analytic Radiocarbon Dating Laboratory

4985 S.W. 74th Court, Miami, Florida 33155 • Tel: (305)667-5167 • Fax: (305)663-0964 • E-Mail: beta@radiocarbon.com



Consistent Accuracy . . .
... Delivered On-time

Beta Analytic Inc.
4985 SW 74 Court
Miami, Florida 33155 USA
Tel: 305 667 5167
Fax: 305 663 0964
Beta@radiocarbon.com
www.radiocarbon.com

Darden Hood
President

Ronald Hatfield
Christopher Patrick
Deputy Directors

January 15, 2009

Mr. J. Mike Quigg
TRC Solutions, Incorporated
505 East Huntland Drive
Suite 250
Austin, TX 78752
USA

RE: Radiocarbon Dating Results For Samples PT185C-BT36N, PT185C-FS1049, PT185C-FS1322

Dear Mr. Quigg:

Enclosed are the radiocarbon dating results for three samples recently sent to us. They each provided plenty of carbon for accurate measurements and all the analyses proceeded normally. As usual, the method of analysis is listed on the report with the results and calibration data is provided where applicable.


As always, no students or intern researchers who would necessarily be distracted with other obligations and priorities were used in the analyses. We analyzed them with the combined attention of our entire professional staff.

If you have specific questions about the analyses, please contact us. We are always available to answer your questions.

The cost of the analysis was charged to the VISA card provided. A receipt is enclosed with the mailed report copy. Thank you. As always, if you have any questions or would like to discuss the results, don't hesitate to contact me.

Sincerely,

Digital signature on file

	BETA ANALYTIC INC.	4985 S.W. 74 COURT MIAMI, FLORIDA, USA 33155
	DR. M.A. TAMERS and MR. D.G. HOOD	PH: 305-667-5167 FAX:305-663-0964 beta@radiocarbon.com

REPORT OF RADIOCARBON DATING ANALYSES

Mr. J. Mike Quigg

Report Date: 1/15/2009

TRC Solutions, Incorporated

Material Received: 12/12/2008

Sample Data	Measured Radiocarbon Age	13C/12C Ratio	Conventional Radiocarbon Age(*)
Beta - 253238 SAMPLE : PT185C-BT36N ANALYSIS : AMS-Standard delivery MATERIAL/PRETREATMENT : (organic sediment): acid washes 2 SIGMA CALIBRATION : Cal BC 3330 to 3210 (Cal BP 5280 to 5160) AND Cal BC 3180 to 3150 (Cal BP 5130 to 5100) Cal BC 3130 to 2920 (Cal BP 5080 to 4870)	4400 +/- 40 BP	-23.1 o/oo	4430 +/- 40 BP
Beta - 253239 SAMPLE : PT185C-FS1049 ANALYSIS : AMS-Standard delivery MATERIAL/PRETREATMENT : (bone collagen): collagen extraction: with alkali 2 SIGMA CALIBRATION : Cal BC 800 to 720 (Cal BP 2750 to 2670) AND Cal BC 700 to 540 (Cal BP 2650 to 2490)	2270 +/- 40 BP	-8.8 o/oo	2540 +/- 40 BP
Beta - 253240 SAMPLE : PT185C-FS1322 ANALYSIS : AMS-Standard delivery MATERIAL/PRETREATMENT : (bone collagen): collagen extraction: with alkali 2 SIGMA CALIBRATION : Cal AD 220 to 400 (Cal BP 1730 to 1550)	1500 +/- 40 BP	-10.3 o/oo	1740 +/- 40 BP

Dates are reported as RCYBP (radiocarbon years before present, "present" = AD 1950). By international convention, the modern reference standard was 95% the 14C activity of the National Institute of Standards and Technology (NIST) Oxalic Acid (SRM 4990C) and calculated using the Libby 14C half-life (5568 years). Quoted errors represent 1 relative standard deviation statistics (68% probability) counting errors based on the combined measurements of the sample, background, and modern reference standards. Measured 13C/12C ratios (delta 13C) were calculated relative to the PDB-1 standard.

The Conventional Radiocarbon Age represents the Measured Radiocarbon Age corrected for isotopic fractionation, calculated using the delta 13C. On rare occasion where the Conventional Radiocarbon Age was calculated using an assumed delta 13C, the ratio and the Conventional Radiocarbon Age will be followed by "**". The Conventional Radiocarbon Age is not calendar calibrated. When available, the Calendar Calibrated result is calculated from the Conventional Radiocarbon Age and is listed as the "Two Sigma Calibrated Result" for each sample.

CALIBRATION OF RADIOCARBON AGE TO CALENDAR YEARS

(Variables: C13/C12=-23.1:lab. mult=1)

Laboratory number: **Beta-253238**

Conventional radiocarbon age: **4430±40 BP**

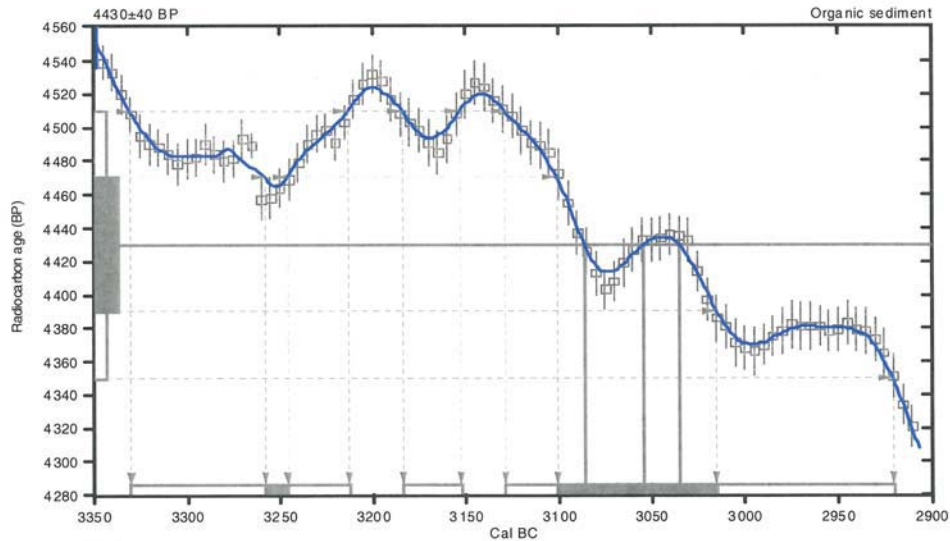
2 Sigma calibrated results: Cal BC 3330 to 3210 (Cal BP 5280 to 5160) and
(95% probability) Cal BC 3180 to 3150 (Cal BP 5130 to 5100) and
Cal BC 3130 to 2920 (Cal BP 5080 to 4870)

Intercept data

Intercepts of radiocarbon age
with calibration curve:

Cal BC 3090 (Cal BP 5040) and
Cal BC 3050 (Cal BP 5000) and
Cal BC 3040 (Cal BP 4980)

1 Sigma calibrated results: Cal BC 3260 to 3250 (Cal BP 5210 to 5200) and
(68% probability) Cal BC 3100 to 3020 (Cal BP 5050 to 4960)



References:

Database used

INTCAL04

Calibration Database

INTCAL04 Radiocarbon Age Calibration

IntCal04: Calibration Issue of Radiocarbon (Volume 46, nr 3, 2004).

Mathematics

A Simplified Approach to Calibrating C14 Dates

Talma, A. S., Vogel, J. C., 1993, Radiocarbon 35(2), p317-322

Beta Analytic Radiocarbon Dating Laboratory

4985 S.W. 74th Court, Miami, Florida 33155 • Tel: (305)667-5167 • Fax: (305)663-0964 • E-Mail: beta@radiocarbon.com

CALIBRATION OF RADIOCARBON AGE TO CALENDAR YEARS

(Variables: C13/C12=-8.8:lab. mult=1)

Laboratory number: **Beta-253239**

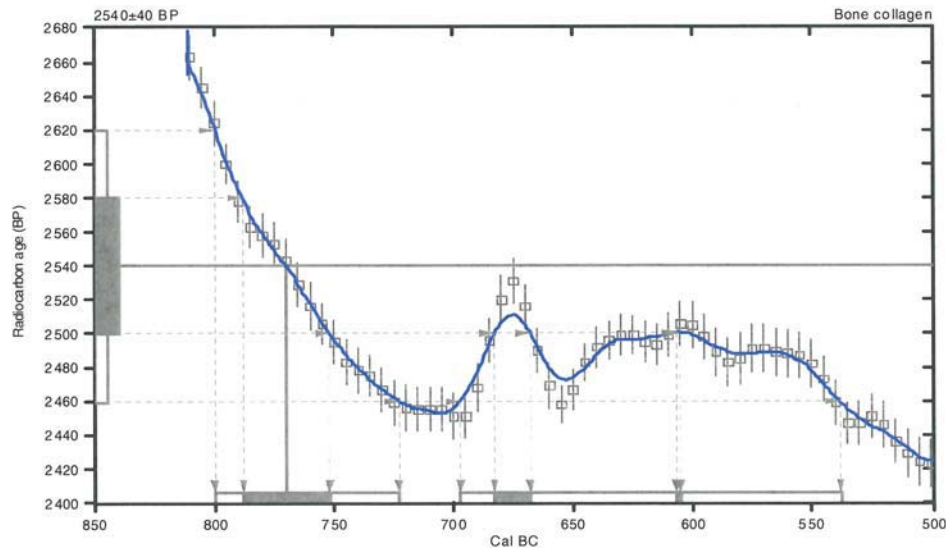
Conventional radiocarbon age: **2540±40 BP**

2 Sigma calibrated results: **Cal BC 800 to 720 (Cal BP 2750 to 2670) and
(95% probability) Cal BC 700 to 540 (Cal BP 2650 to 2490)**

Intercept data

Intercept of radiocarbon age
with calibration curve: **Cal BC 770 (Cal BP 2720)**

1 Sigma calibrated results: **Cal BC 790 to 750 (Cal BP 2740 to 2700) and
(68% probability) Cal BC 680 to 670 (Cal BP 2630 to 2620) and
Cal BC 610 to 600 (Cal BP 2560 to 2560)**



References:

- Database used*
INTCAL04
Calibration Database
INTCAL04 Radiocarbon Age Calibration
IntCal04: Calibration Issue of Radiocarbon (Volume 46, nr 3, 2004).
- Mathematics*
A Simplified Approach to Calibrating C14 Dates
Talma, A. S., Vogel, J. C., 1993, Radiocarbon 35(2), p317-322

Beta Analytic Radiocarbon Dating Laboratory

4985 S.W. 74th Court, Miami, Florida 33155 • Tel: (305)667-5167 • Fax: (305)663-0964 • E-Mail: beta@radiocarbon.com

CALIBRATION OF RADIOCARBON AGE TO CALENDAR YEARS

(Variables: C13/C12=-10.3;lab. mult=1)

Laboratory number: **Beta-253240**

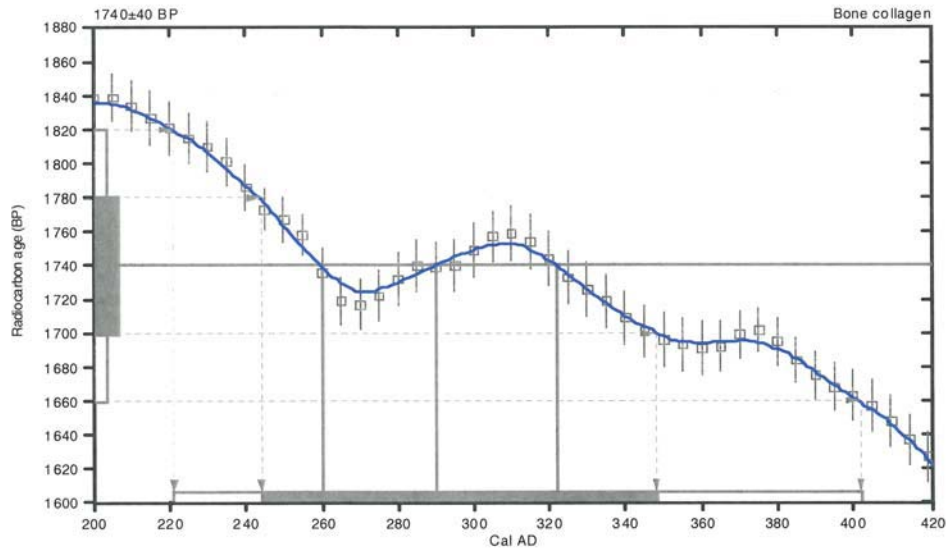
Conventional radiocarbon age: **1740±40 BP**

2 Sigma calibrated result: **Cal AD 220 to 400 (Cal BP 1730 to 1550)**
(95% probability)

Intercept data

Intercepts of radiocarbon age
with calibration curve: Cal AD 260 (Cal BP 1690) and
Cal AD 290 (Cal BP 1660) and
Cal AD 320 (Cal BP 1630)

1 Sigma calibrated result: **Cal AD 240 to 350 (Cal BP 1710 to 1600)**
(68% probability)



References:

- Database used
INTCAL04
Calibration Database
INTCAL04 Radiocarbon Age Calibration
IntCal04: Calibration Issue of Radiocarbon (Volume 46, nr 3, 2004).
- Mathematics
A Simplified Approach to Calibrating C14 Dates
Talma, A. S., Vogel, J. C., 1993, Radiocarbon 35(2), p317-322

Beta Analytic Radiocarbon Dating Laboratory

4985 S.W. 74th Court, Miami, Florida 33155 • Tel: (305)667-5167 • Fax: (305)663-0964 • E-Mail: beta@ndiocarbon.com



Consistent Accuracy . . .
. . . Delivered On-time

Beta Analytic Inc.
4985 SW 74 Court
Miami, Florida 33155 USA
Tel: 305 667 5167
Fax: 305 663 0964
Beta@radiocarbon.com
www.radiocarbon.com

Darden Hood
President

Ronald Hatfield
Christopher Patrick
Deputy Directors

March 11, 2009

Mr. J. Mike Quigg
TRC Solutions, Incorporated
505 East Huntland Drive
Suite 250
Austin, TX 78752
USA

RE: Radiocarbon Dating Results For Samples PT185/C-263-4-109, PT185/C-279-02-1, PT185/C-493-02-1

Dear Mr. Quigg:

Enclosed are the radiocarbon dating results for three samples recently sent to us. They each provided plenty of carbon for accurate measurements and all the analyses proceeded normally. As usual, the method of analysis is listed on the report with the results and calibration data is provided where applicable.

As always, no students or intern researchers who would necessarily be distracted with other obligations and priorities were used in the analyses. We analyzed them with the combined attention of our entire professional staff.


If you have specific questions about the analyses, please contact us. We are always available to answer your questions.

The cost of the analysis was charged to the VISA card provided. A receipt is enclosed with the mailed report copy. Thank you. As always, if you have any questions or would like to discuss the results, don't hesitate to contact me.

Sincerely,

A handwritten signature in black ink that reads "Darden Hood". Below the signature, the text "Digital signature on file" is printed in a small font.

Darden Hood
Digital signature on file



BETA ANALYTIC INC.
DR. M.A. TAMERS and MR. D.G. HOOD

4985 S.W. 74 COURT
MIAMI, FLORIDA, USA 33155
PH: 305-667-5167 FAX:305-663-0964
beta@radiocarbon.com

REPORT OF RADIOCARBON DATING ANALYSES

Mr. J. Mike Quigg

Report Date: 3/11/2009

TRC Solutions, Incorporated

Material Received: 2/12/2009

Sample Data	Measured Radiocarbon Age	13C/12C Ratio	Conventional Radiocarbon Age(*)
Beta - 255835 SAMPLE : PT185/C-263-4-109 ANALYSIS : AMS-Standard delivery MATERIAL/PRETREATMENT : (organic sediment): acid washes 2 SIGMA CALIBRATION : Cal AD 600 to 680 (Cal BP 1350 to 1270)	1320 +/- 40 BP	-20.6 o/oo	1390 +/- 40 BP
Beta - 255836 SAMPLE : PT185/C-279-02-1 ANALYSIS : AMS-Standard delivery MATERIAL/PRETREATMENT : (bone collagen): collagen extraction: with alkali 2 SIGMA CALIBRATION : Cal BC 410 to 360 (Cal BP 2360 to 2310) AND Cal BC 280 to 260 (Cal BP 2230 to 2200)	2020 +/- 40 BP	-7.5 o/oo	2310 +/- 40 BP
Beta - 255837 SAMPLE : PT185/C-493-02-1 ANALYSIS : AMS-Standard delivery MATERIAL/PRETREATMENT : (bone collagen): collagen extraction: with alkali 2 SIGMA CALIBRATION : Cal BC 400 to 200 (Cal BP 2340 to 2150)	2010 +/- 40 BP	-10.3 o/oo	2250 +/- 40 BP

Dates are reported as RCYBP (radiocarbon years before present, "present" = AD 1950). By international convention, the modern reference standard was 95% the 14C activity of the National Institute of Standards and Technology (NIST) Oxalic Acid (SRM 4990C) and calculated using the Libby 14C half-life (5568 years). Quoted errors represent 1 relative standard deviation statistics (68% probability) counting errors based on the combined measurements of the sample, background, and modern reference standards. Measured 13C/12C ratios (delta 13C) were calculated relative to the PDB-1 standard.

The Conventional Radiocarbon Age represents the Measured Radiocarbon Age corrected for isotopic fractionation, calculated using the delta 13C. On rare occasion where the Conventional Radiocarbon Age was calculated using an assumed delta 13C, the ratio and the Conventional Radiocarbon Age will be followed by "m". The Conventional Radiocarbon Age is not calendar calibrated. When available, the Calendar Calibrated result is calculated from the Conventional Radiocarbon Age and is listed as the "Two Sigma Calibrated Result" for each sample.

CALIBRATION OF RADIOCARBON AGE TO CALENDAR YEARS

(Variables: C13/C12=-20.6:lab. mult=1)

Laboratory number: Beta-255835

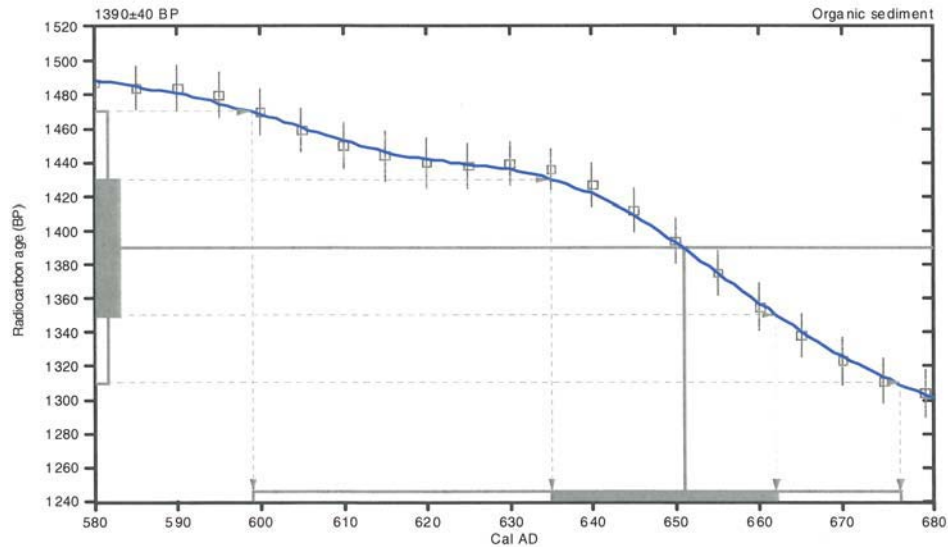
Conventional radiocarbon age: 1390±40 BP

2 Sigma calibrated result: Cal AD 600 to 680 (Cal BP 1350 to 1270)
(95% probability)

Intercept data

Intercept of radiocarbon age
with calibration curve: Cal AD 650 (Cal BP 1300)

1 Sigma calibrated result: Cal AD 640 to 660 (Cal BP 1320 to 1290)
(68% probability)



References:

- Database used
INTCAL04
Calibration Database
INTCAL04 Radiocarbon Age Calibration
IntCal04: Calibration Issue of Radiocarbon (Volume 46, nr 3, 2004).
- Mathematics
A Simplified Approach to Calibrating C14 Dates
Talma, A. S., Vogel, J. C., 1993, *Radiocarbon* 35(2), p317-322

Beta Analytic Radiocarbon Dating Laboratory

4985 S.W. 74th Court, Miami, Florida 33155 • Tel: (305)667-5167 • Fax: (305)663-0964 • E-Mail: beta@radiocarbon.com

CALIBRATION OF RADIOCARBON AGE TO CALENDAR YEARS

(Variables: C13/C12=-7.5;lab. mult=1)

Laboratory number: Beta-255836

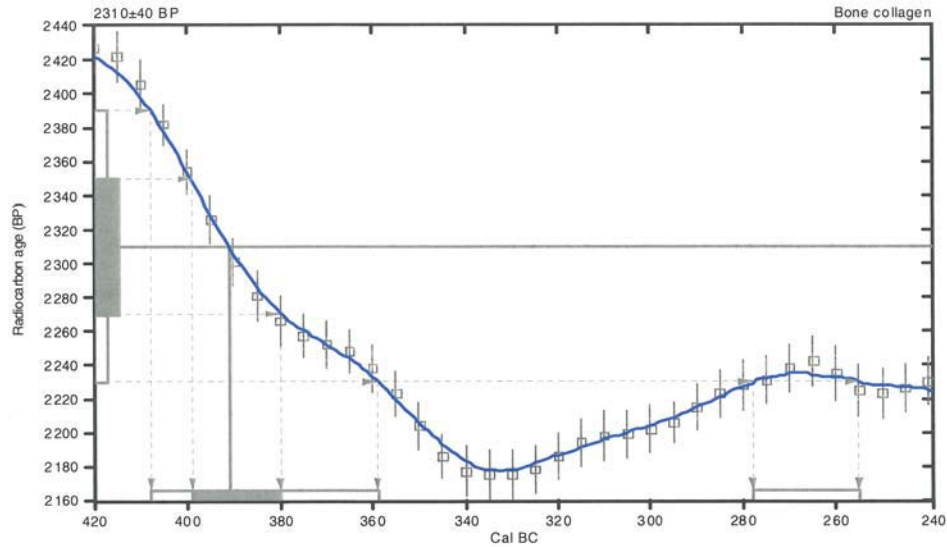
Conventional radiocarbon age: 2310±40 BP

2 Sigma calibrated results: Cal BC 410 to 360 (Cal BP 2360 to 2310) and
(95% probability) Cal BC 280 to 260 (Cal BP 2230 to 2200)

Intercept data

Intercept of radiocarbon age
with calibration curve: Cal BC 390 (Cal BP 2340)

1 Sigma calibrated result: Cal BC 400 to 380 (Cal BP 2350 to 2330)
(68% probability)



References:

Database used

INTCAL04

Calibration Database

INTCAL04 Radiocarbon Age Calibration

IntCal04: Calibration Issue of Radiocarbon (Volume 46, nr 3, 2004).

Mathematics

A Simplified Approach to Calibrating C14 Dates

Talma, A. S., Vogel, J. C., 1993, Radiocarbon 35(2), p317-322

Beta Analytic Radiocarbon Dating Laboratory

4985 S.W. 74th Court, Miami, Florida 33155 • Tel: (305)667-5167 • Fax: (305)663-0964 • E-Mail: beta@radiocarbon.com

CALIBRATION OF RADIOCARBON AGE TO CALENDAR YEARS

(Variables: C13/C12=-10.3:lab. mult=1)

Laboratory number: Beta-255837

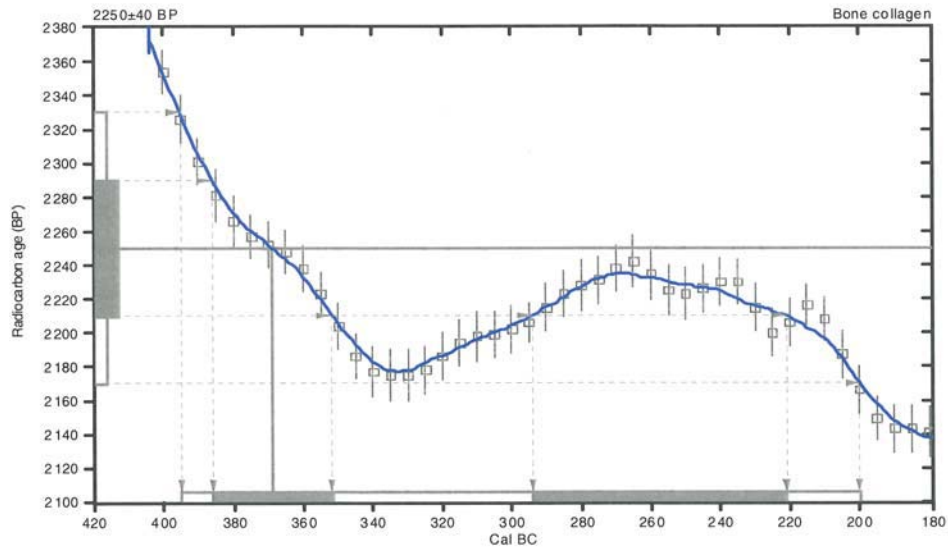
Conventional radiocarbon age: 2250±40 BP

2 Sigma calibrated result: Cal BC 400 to 200 (Cal BP 2340 to 2150)
(95% probability)

Intercept data

Intercept of radiocarbon age
with calibration curve: Cal BC 370 (Cal BP 2320)

1 Sigma calibrated results: Cal BC 390 to 350 (Cal BP 2340 to 2300) and
(68% probability) Cal BC 290 to 220 (Cal BP 2240 to 2170)



References:

Database used

INTCAL04

Calibration Database

INTCAL04 Radiocarbon Age Calibration

IntCal04: Calibration Issue of Radiocarbon (Volume 46, nr 3, 2004).

Mathematics

A Simplified Approach to Calibrating C14 Dates

Talma, A. S., Vogel, J. C., 1993, Radiocarbon 35(2), p317-322

Beta Analytic Radiocarbon Dating Laboratory

4985 S.W. 74th Court, Miami, Florida 33155 • Tel: (305)667-5167 • Fax: (305)663-0964 • E-Mail: beta@radiocarbon.com

FROM: Darden Hood, Director (mailto:<mailto:dhood@radiocarbon.com>)
(This is a copy of the letter being mailed. Invoices/receipts follow only by mail.)

March 13, 2008

Mr. J. Mike Quigg
TRC Solutions, Incorporated
505 East Huntland Drive
Suite 250
Austin, TX 78752
USA

RE: Radiocarbon Dating Result For Sample BT36-M-1

Dear Mr. Quigg:

Enclosed is the radiocarbon dating result for one sample recently sent to us. It provided plenty of carbon for an accurate measurement and the analysis proceeded normally. As usual, the method of analysis is listed on the report sheet and calibration data is provided where applicable.

As always, no students or intern researchers who would necessarily be distracted with other obligations and priorities were used in the analysis. It was analyzed with the combined attention of our entire professional staff.

If you have specific questions about the analyses, please contact us. We are always available to answer your questions.

Our invoice is enclosed. Please, forward it to the appropriate officer or send VISA charge authorization. Thank you. As always, if you have any questions or would like to discuss the results, don't hesitate to contact me.

Sincerely,



Mr. J. Mike Quigg

Report Date: 3/13/2008

TRC Solutions, Incorporated

Material Received: 2/8/2008

Sample Data	Measured Radiocarbon Age	$^{13}\text{C}/^{12}\text{C}$ Ratio	Conventional Radiocarbon Age(*)
Beta - 241070 SAMPLE : BT36-M-1 ANALYSIS : AMS-Standard delivery MATERIAL/PRETREATMENT : (plant material): acid/alkali/acid 2 SIGMA CALIBRATION : Cal AD 30 to 230 (Cal BP 1920 to 1720)	1930 +/- 40 BP	-27.3 ‰	1890 +/- 40 BP

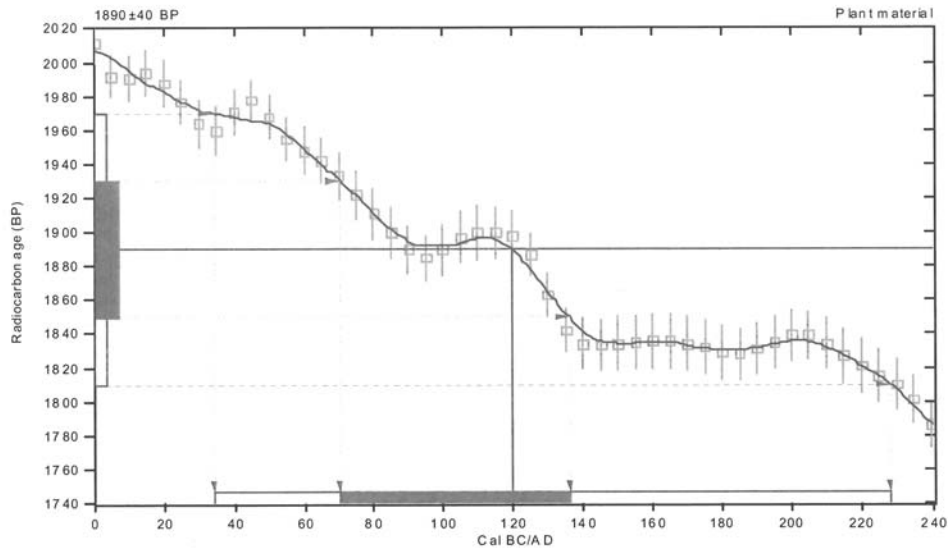
CALIBRATION OF RADIOCARBON AGE TO CALENDAR YEARS

(Variables: C13/C12=-27.3:lab. mult=1)

Laboratory number: **Beta-241070**
Conventional radiocarbon age: **1890±40 BP**
2 Sigma calibrated result: **Cal AD 30 to 230 (Cal BP 1920 to 1720)**
(95% probability)

Intercept data

Intercept of radiocarbon age
with calibration curve: **Cal AD 120 (Cal BP 1830)**
1 Sigma calibrated result: **Cal AD 70 to 140 (Cal BP 1880 to 1810)**
(68% probability)



References:

- Data base used*
INTCAL04
Calibration Data base
INTCAL04 Radiocarbon Age Calibration
IntCal04: Calibration Issue of Radiocarbon (Volume 46, nr 3, 2004).
- Mathematics*
A Simplified Approach to Calibrating C14 Dates
Talma, A. S., Vogel, J. C., 1993, Radiocarbon 35(2), p317-322

Beta Analytic Radiocarbon Dating Laboratory

4985 S.W. 74th Court, Miami, Florida 33155 • Tel: (305)667-5167 • Fax: (305)663-0964 • E-Mail: beta@radiocarbon.com



Consistent Accuracy
Delivered On Time

Beta Analytic Inc

4985 SW 74 Court
Miami, Florida 33155
Tel: 305-667-5167
Fax: 305-663-0964
beta@radiocarbon.com
www.radiocarbon.com

The Radiocarbon Laboratory Accredited to ISO-17025 Testing Standards (PJLA Accreditation #59423)

Mr. Darden Hood
President

Mr. Ronald Hatfield
Mr. Christopher Patrick
Deputy Directors

April 21, 2009

Mr. J. Mike Quigg
TRC Solutions, Incorporated
505 East Huntland Drive
Suite 250
Austin, TX 78752
USA

RE: Radiocarbon Dating Result For Sample PT185C-1174

Dear Mr. Quigg:

Enclosed is the radiocarbon dating result for one sample recently sent to us. It provided plenty of carbon for an accurate measurement and the analysis proceeded normally. As usual, the method of analysis is listed on the report sheet and calibration data is provided where applicable.

As always, no students or intern researchers who would necessarily be distracted with other obligations and priorities were used in the analysis. It was analyzed with the combined attention of our entire professional staff.

If you have specific questions about the analyses, please contact us. We are always available to answer your questions.

The cost of the analysis was charged to the VISA card provided. A receipt is enclosed with the paper report copy. Thank you. As always, if you have any questions or would like to discuss the results, don't hesitate to contact me.

Sincerely,



BETA ANALYTIC INC.

DR. M.A. TAMERS and MR. D.G. HOOD

4985 S.W. 74 COURT
MIAMI, FLORIDA, USA 33155
PH: 305-667-5167 FAX: 305-663-0964
beta@radiocarbon.com

REPORT OF RADIOCARBON DATING ANALYSES

Mr. J. Mike Quigg

Report Date: 4/21/2009

TRC Solutions, Incorporated

Material Received: 4/1/2009

Sample Data	Measured Radiocarbon Age	¹³ C/ ¹² C Ratio	Conventional Radiocarbon Age(*)
Beta - 257845 SAMPLE : PT185C-1174 ANALYSIS : AMS-Standard delivery MATERIAL/PRETREATMENT : (bone collagen): collagen extraction: with alkali 2 SIGMA CALIBRATION : Cal AD 410 to 590 (Cal BP 1540 to 1360)	1290 +/- 40 BP	-8.5 o/oo	1560 +/- 40 BP

Dates are reported as RCYBP (radiocarbon years before present, "present" = AD 1950). By international convention, the modern reference standard was 95% the ¹⁴C activity of the National Institute of Standards and Technology (NIST) Oxalic Acid (SRM 4990C) and calculated using the Libby ¹⁴C half-life (5568 years). Quoted errors represent 1 relative standard deviation statistics (68% probability) counting errors based on the combined measurements of the sample, background, and modern reference standards. Measured ¹³C/¹²C ratios (delta ¹³C) were calculated relative to the PDB-1 standard.

The Conventional Radiocarbon Age represents the Measured Radiocarbon Age corrected for isotopic fractionation, calculated using the delta ¹³C. On rare occasion where the Conventional Radiocarbon Age was calculated using an assumed delta ¹³C, the ratio and the Conventional Radiocarbon Age will be followed by "**". The Conventional Radiocarbon Age is not calendar calibrated. When available, the Calendar Calibrated result is calculated from the Conventional Radiocarbon Age and is listed as the "Two Sigma Calibrated Result" for each sample.

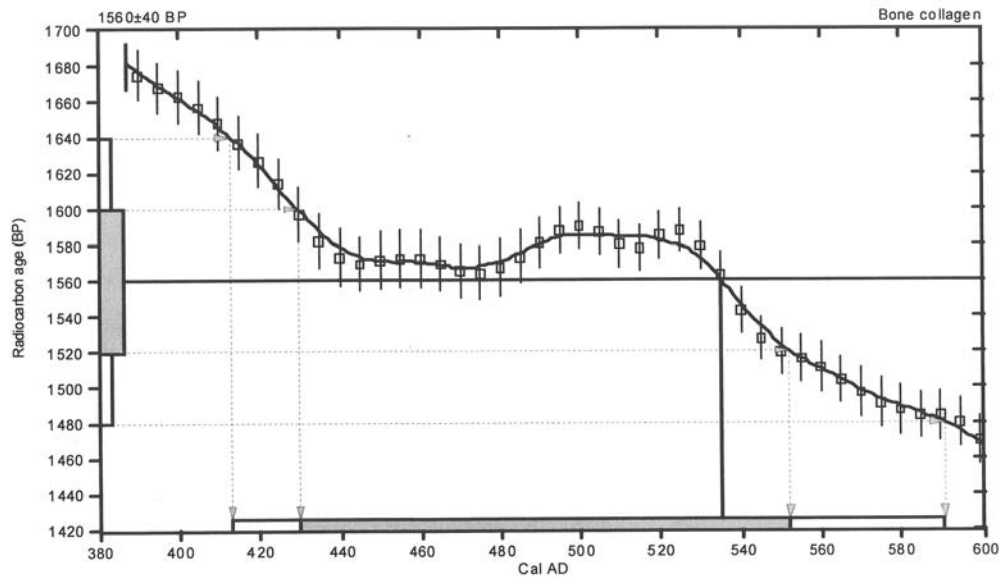
CALIBRATION OF RADIOCARBON AGE TO CALENDAR YEARS

(Variables: C13/C12=-8.5:lab. mult=1)

Laboratory number: **Beta-257845**
Conventional radiocarbon age: **1560±40 BP**
2 Sigma calibrated result: **Cal AD 410 to 590 (Cal BP 1540 to 1360)**
(95% probability)

Intercept data

Intercept of radiocarbon age
with calibration curve: **Cal AD 540 (Cal BP 1420)**
1 Sigma calibrated result: **Cal AD 430 to 550 (Cal BP 1520 to 1400)**
(68% probability)



References:

- Database used*
INTCAL04
Calibration Database
INTCAL04 Radiocarbon Age Calibration
IntCal04: Calibration Issue of Radiocarbon (Volume 46, nr 3, 2004).
- Mathematics*
A Simplified Approach to Calibrating C14 Dates
Talma, A. S., Vogel, J. C., 1993, Radiocarbon 35(2), p317-322

Beta Analytic Radiocarbon Dating Laboratory

4985 S.W. 74th Court, Miami, Florida 33155 • Tel: (305)667-5167 • Fax: (305)663-0964 • E-Mail: beta@radiocarbon.com



Consistent Accuracy . . .
... Delivered On-time

Beta Analytic Inc.
4985 SW 74 Court
Miami, Florida 33155 USA
Tel: 305 667 5167
Fax: 305 663 0964
Beta@radiocarbon.com
www.radiocarbon.com

Darden Hood
President

Ronald Hatfield
Christopher Patrick
Deputy Directors

August 4, 2009

Mr. J. Mike Quigg
TRC Solutions, Incorporated
505 East Huntland Drive
Suite 250
Austin, TX 78752
USA

RE: Radiocarbon Dating Results For Samples PT185C263-86, PT185C263-91, PT185C263-97b

Dear Mr. Quigg:

Enclosed are the radiocarbon dating results for three samples recently sent to us. They each provided plenty of carbon for accurate measurements and all the analyses proceeded normally. As usual, the method of analysis is listed on the report with the results and calibration data is provided where applicable.

As always, no students or intern researchers who would necessarily be distracted with other obligations and priorities were used in the analyses. We analyzed them with the combined attention of our entire professional staff.

If you have specific questions about the analyses, please contact us. We are always available to answer your questions.

The cost of the analysis was charged to the VISA card provided. A receipt is enclosed. Thank you. As always, if you have any questions or would like to discuss the results, don't hesitate to contact me.

Sincerely,

Digital signature on file



BETA ANALYTIC INC.

DR. M.A. TAMERS and MR. D.G. HOOD

4985 S.W. 74 COURT
MIAMI, FLORIDA, USA 33155
PH: 305-667-5167 FAX: 305-663-0964
beta@radiocarbon.com

REPORT OF RADIOCARBON DATING ANALYSES

Mr. J. Mike Quigg

Report Date: 8/4/2009

TRC Solutions, Incorporated

Material Received: 7/13/2009

Sample Data	Measured Radiocarbon Age	13C/12C Ratio	Conventional Radiocarbon Age(*)
Beta - 261753 SAMPLE : PT185C263-86 ANALYSIS : AMS-Standard delivery MATERIAL/PRETREATMENT : (shell): acid etch 2 SIGMA CALIBRATION : Cal AD 780 to 980 (Cal BP 1170 to 960)	820 +/- 40 BP	-5.1 o/oo	1150 +/- 40 BP
Beta - 261754 SAMPLE : PT185C263-91 ANALYSIS : AMS-Standard delivery MATERIAL/PRETREATMENT : (shell): acid etch 2 SIGMA CALIBRATION : Cal AD 770 to 980 (Cal BP 1180 to 970)	890 +/- 40 BP	-8.0 o/oo	1170 +/- 40 BP
Beta - 261755 SAMPLE : PT185C263-97b ANALYSIS : AMS-Standard delivery MATERIAL/PRETREATMENT : (shell): acid etch 2 SIGMA CALIBRATION : Cal BC 800 to 720 (Cal BP 2750 to 2670) AND Cal BC 700 to 540 (Cal BP 2650 to 2490)	2240 +/- 40 BP	-6.8 o/oo	2540 +/- 40 BP

Dates are reported as RCYBP (radiocarbon years before present, "present" = AD 1950). By international convention, the modern reference standard was 95% the ¹⁴C activity of the National Institute of Standards and Technology (NIST) Oxalic Acid (SRM 4990C) and calculated using the Libby ¹⁴C half-life (5568 years). Quoted errors represent 1 relative standard deviation statistics (68% probability) counting errors based on the combined measurements of the sample, background, and modern reference standards. Measured ¹³C/¹²C ratios (delta ¹³C) were calculated relative to the PDB-1 standard.

The Conventional Radiocarbon Age represents the Measured Radiocarbon Age corrected for isotopic fractionation, calculated using the delta ¹³C. On rare occasion where the Conventional Radiocarbon Age was calculated using an assumed delta ¹³C, the ratio and the Conventional Radiocarbon Age will be followed by ***. The Conventional Radiocarbon Age is not calendar calibrated. When available, the Calendar Calibrated result is calculated from the Conventional Radiocarbon Age and is listed as the "Two Sigma Calibrated Result" for each sample.

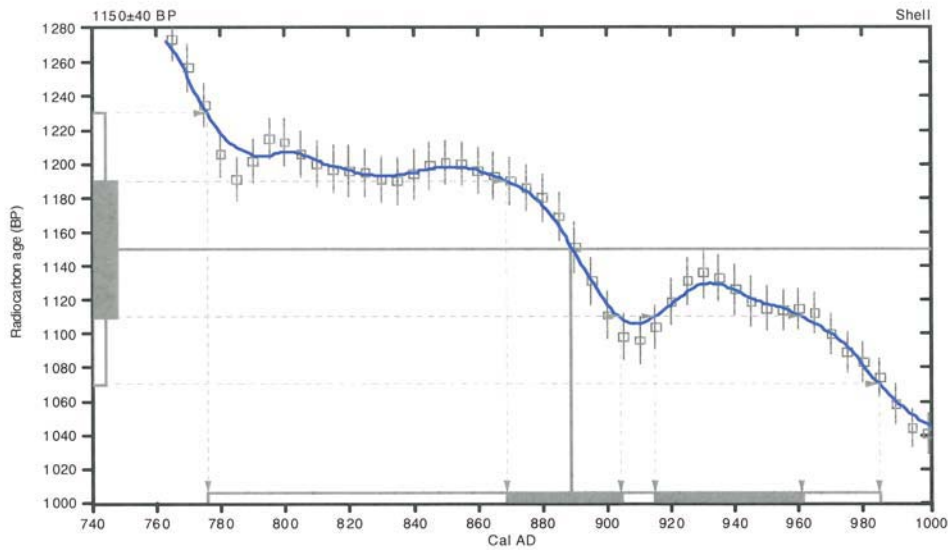
CALIBRATION OF RADIOCARBON AGE TO CALENDAR YEARS

(Variables: C13/C12=-5.1:lab. mult=1)

Laboratory number: **Beta-261753**
Conventional radiocarbon age: **1150±40 BP**
2 Sigma calibrated result: **Cal AD 780 to 980 (Cal BP 1170 to 960)**
(95% probability)

Intercept data

Intercept of radiocarbon age
with calibration curve: **Cal AD 890 (Cal BP 1060)**
1 Sigma calibrated results: **Cal AD 870 to 900 (Cal BP 1080 to 1050) and**
(68% probability) Cal AD 920 to 960 (Cal BP 1040 to 990)



References:

Database used
INTCAL04
Calibration Database
INTCAL04 Radiocarbon Age Calibration
IntCal04: Calibration Issue of Radiocarbon (Volume 46, nr 3, 2004).
Mathematics
A Simplified Approach to Calibrating C14 Dates
Talma, A. S., Vogel, J. C., 1993, Radiocarbon 35(2), p317-322

Beta Analytic Radiocarbon Dating Laboratory

4985 S.W. 74th Court, Miami, Florida 33155 • Tel: (305)667-5167 • Fax: (305)663-0964 • E-Mail: beta@radiocarbon.com

CALIBRATION OF RADIOCARBON AGE TO CALENDAR YEARS

(Variables: C13/C12=-8;lab. mult=1)

Laboratory number: **Beta-261754**

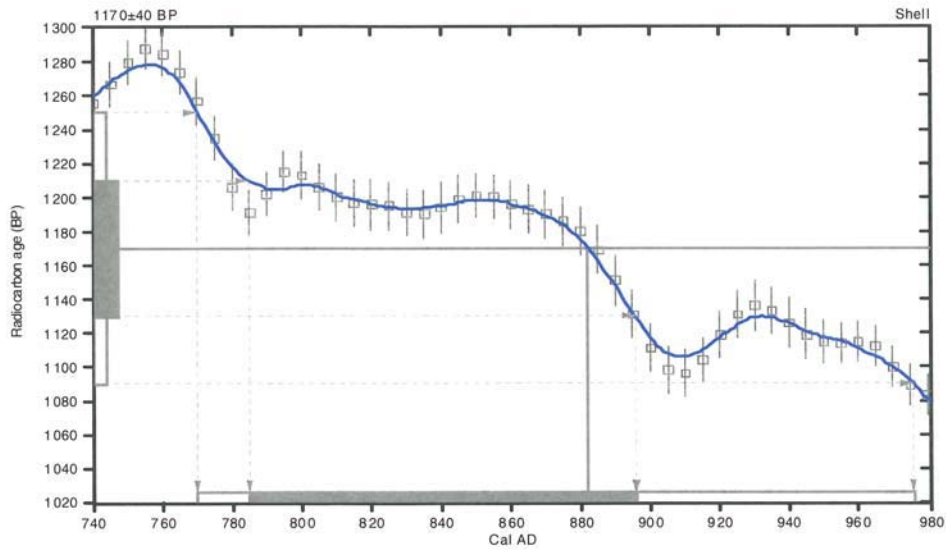
Conventional radiocarbon age: **1170±40 BP**

2 Sigma calibrated result: **Cal AD 770 to 980 (Cal BP 1180 to 970)**
(95% probability)

Intercept data

Intercept of radiocarbon age
with calibration curve: **Cal AD 880 (Cal BP 1070)**

1 Sigma calibrated result: **Cal AD 780 to 900 (Cal BP 1160 to 1050)**
(68% probability)



References:

Database used

INTCAL04

Calibration Database

INTCAL04 Radiocarbon Age Calibration

IntCal04: Calibration Issue of Radiocarbon (Volume 46, nr 3, 2004).

Mathematics

A Simplified Approach to Calibrating C14 Dates

Talma, A. S., Vogel, J. C., 1993, Radiocarbon 35(2), p.317-322

Beta Analytic Radiocarbon Dating Laboratory

4985 S.W. 74th Court, Miami, Florida 33155 • Tel: (305)667-5167 • Fax: (305)663-0964 • E-Mail: beta@radiocarbon.com

CALIBRATION OF RADIOCARBON AGE TO CALENDAR YEARS

(Variables: C13/C12=-6.8;lab. mult=1)

Laboratory number: **Beta-261755**

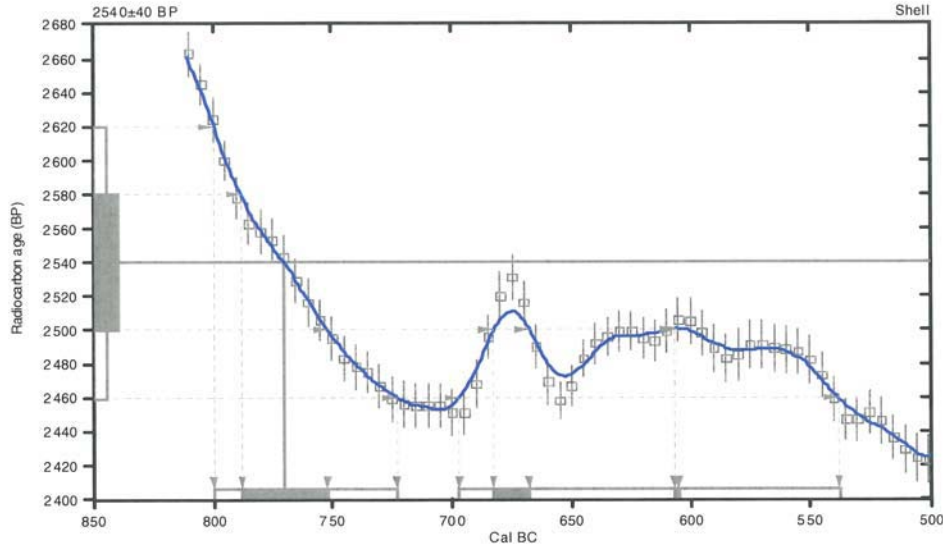
Conventional radiocarbon age: **2540±40 BP**

2 Sigma calibrated results: **Cal BC 800 to 720 (Cal BP 2750 to 2670) and
(95% probability) Cal BC 700 to 540 (Cal BP 2650 to 2490)**

Intercept data

Intercept of radiocarbon age
with calibration curve: **Cal BC 770 (Cal BP 2720)**

1 Sigma calibrated results: **Cal BC 790 to 750 (Cal BP 2740 to 2700) and
(68% probability) Cal BC 680 to 670 (Cal BP 2630 to 2620) and
Cal BC 610 to 600 (Cal BP 2560 to 2560)**



References:

Database used

INTCAL04

Calibration Database

INTCAL04 Radiocarbon Age Calibration

IntCal04: Calibration Issue of Radiocarbon (Volume 46, nr 3, 2004).

Mathematics

A Simplified Approach to Calibrating C14 Dates

Talma, A. S., Vogel, J. C., 1993, Radiocarbon 35(2), p317-322

Beta Analytic Radiocarbon Dating Laboratory

4985 S.W. 74th Court, Miami, Florida 33155 • Tel: (305)667-5167 • Fax: (305)663-0964 • E-Mail: beta@radiocarbon.com



Consistent Accuracy
Delivered On Time

Beta Analytic Inc

4985 SW 74 Court
Miami, Florida 33155
Tel: 305-667-5167
Fax: 305-663-0964
beta@radiocarbon.com
www.radiocarbon.com

The Radiocarbon Laboratory Accredited to ISO-17025 Testing Standards (PJLA Accreditation #59423)

Mr. Darden Hood
President

Mr. Ronald Hatfield
Mr. Christopher Patrick
Deputy Directors

August 4, 2009

Mr. J. Mike Quigg
TRC Solutions, Incorporated
505 East Huntland Drive
Suite 250
Austin, TX 78752
USA

RE: Radiocarbon Dating Results For Samples PT185C263-86, PT185C263-91, PT185C263-97b

Dear Mr. Quigg:

Enclosed are the radiocarbon dating results for three samples recently sent to us. They each provided plenty of carbon for accurate measurements and all the analyses proceeded normally. As usual, the method of analysis is listed on the report with the results and calibration data is provided where applicable.

As always, no students or intern researchers who would necessarily be distracted with other obligations and priorities were used in the analyses. We analyzed them with the combined attention of our entire professional staff.

If you have specific questions about the analyses, please contact us. We are always available to answer your questions.

The cost of the analysis was charged to the VISA card provided. A receipt is enclosed. Thank you. As always, if you have any questions or would like to discuss the results, don't hesitate to contact me.

Sincerely,



BETA ANALYTIC INC.

DR. M.A. TAMERS and MR. D.G. HOOD

4985 S.W. 74 COURT
MIAMI, FLORIDA, USA 33155
PH: 305-667-5167 FAX:305-663-0964
beta@radiocarbon.com

REPORT OF RADIOCARBON DATING ANALYSES

Mr. J. Mike Quigg

Report Date: 8/4/2009

TRC Solutions, Incorporated

Material Received: 7/13/2009

Sample Data	Measured Radiocarbon Age	¹³ C/ ¹² C Ratio	Conventional Radiocarbon Age(*)
Beta - 261753 SAMPLE : PT185C263-86 ANALYSIS : AMS-Standard delivery MATERIAL/PRETREATMENT : (shell): acid etch 2 SIGMA CALIBRATION : Cal AD 780 to 980 (Cal BP 1170 to 960)	820 +/- 40 BP	-5.1 o/oo	1150 +/- 40 BP
Beta - 261754 SAMPLE : PT185C263-91 ANALYSIS : AMS-Standard delivery MATERIAL/PRETREATMENT : (shell): acid etch 2 SIGMA CALIBRATION : Cal AD 770 to 980 (Cal BP 1180 to 970)	890 +/- 40 BP	-8.0 o/oo	1170 +/- 40 BP
Beta - 261755 SAMPLE : PT185C263-97b ANALYSIS : AMS-Standard delivery MATERIAL/PRETREATMENT : (shell): acid etch 2 SIGMA CALIBRATION : Cal BC 800 to 720 (Cal BP 2750 to 2670) AND Cal BC 700 to 540 (Cal BP 2650 to 2490)	2240 +/- 40 BP	-6.8 o/oo	2540 +/- 40 BP

Dates are reported as RCYBP (radiocarbon years before present, "present" = AD 1950). By international convention, the modern reference standard was 95% the ¹⁴C activity of the National Institute of Standards and Technology (NIST) Oxalic Acid (SRM 4990C) and calculated using the Libby ¹⁴C half-life (5568 years). Quoted errors represent 1 relative standard deviation statistics (68% probability) counting errors based on the combined measurements of the sample, background, and modern reference standards. Measured ¹³C/¹²C ratios (delta ¹³C) were calculated relative to the PDB-1 standard.

The Conventional Radiocarbon Age represents the Measured Radiocarbon Age corrected for isotopic fractionation, calculated using the delta ¹³C. On rare occasion where the Conventional Radiocarbon Age was calculated using an assumed delta ¹³C, the ratio and the Conventional Radiocarbon Age will be followed by "**". The Conventional Radiocarbon Age is not calendar calibrated. When available, the Calendar Calibrated result is calculated from the Conventional Radiocarbon Age and is listed as the "Two Sigma Calibrated Result" for each sample.

CALIBRATION OF RADIOCARBON AGE TO CALENDAR YEARS

(Variables: C13/C12=-5.1:lab. mult=1)

Laboratory number: Beta-261753

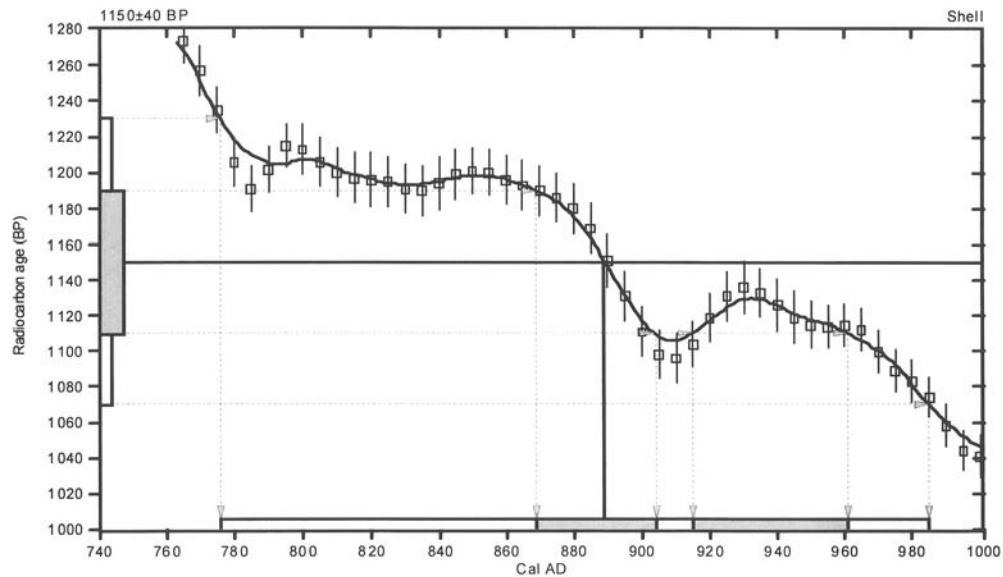
Conventional radiocarbon age: 1150±40 BP

2 Sigma calibrated result: Cal AD 780 to 980 (Cal BP 1170 to 960)
(95% probability)

Intercept data

Intercept of radiocarbon age
with calibration curve: Cal AD 890 (Cal BP 1060)

1 Sigma calibrated results: Cal AD 870 to 900 (Cal BP 1080 to 1050) and
Cal AD 920 to 960 (Cal BP 1040 to 990) (68% probability)



References:

Database used

INTCAL04

Calibration Database

INTCAL04 Radiocarbon Age Calibration

IntCal04: Calibration Issue of Radiocarbon (Volume 46, nr 3, 2004).

Mathematics

A Simplified Approach to Calibrating C14 Dates

Talma, A. S., Vogel, J. C., 1993, Radiocarbon 35(2), p317-322

Beta Analytic Radiocarbon Dating Laboratory

4985 S.W. 74th Court, Miami, Florida 33155 • Tel: (305)667-5167 • Fax: (305)663-0964 • E-Mail: beta@radiocarbon.com

CALIBRATION OF RADIOCARBON AGE TO CALENDAR YEARS

(Variables: C13/C12=-8;lab. mult=1)

Laboratory number: Beta-261754

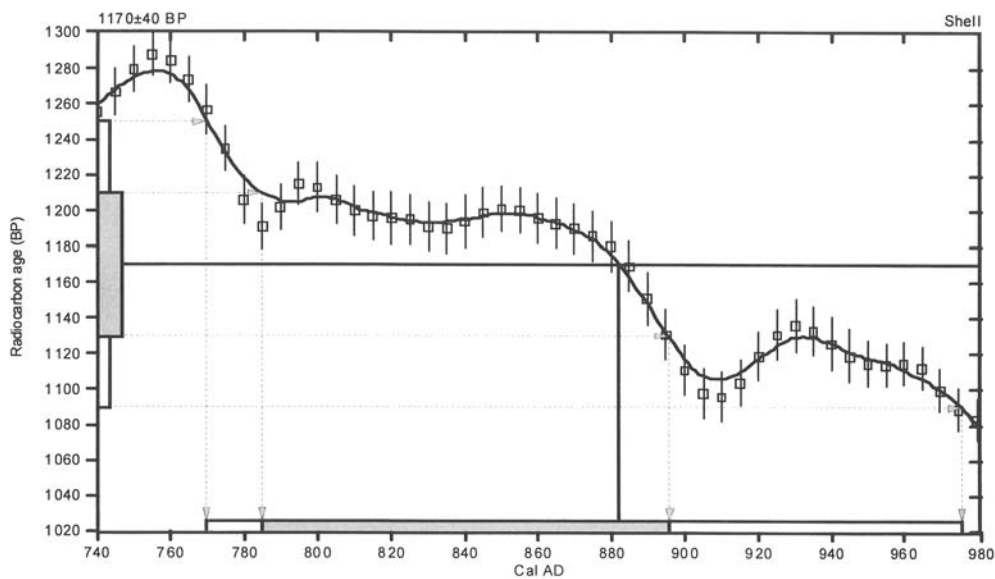
Conventional radiocarbon age: 1170±40 BP

2 Sigma calibrated result: Cal AD 770 to 980 (Cal BP 1180 to 970)
(95% probability)

Intercept data

Intercept of radiocarbon age
with calibration curve: Cal AD 880 (Cal BP 1070)

1 Sigma calibrated result: Cal AD 780 to 900 (Cal BP 1160 to 1050)
(68% probability)



References:

Database used

INTCAL04

Calibration Database

INTCAL04 Radiocarbon Age Calibration

IntCal04: Calibration Issue of Radiocarbon (Volume 46, nr 3, 2004).

Mathematics

A Simplified Approach to Calibrating C14 Dates

Talma, A. S., Vogel, J. C., 1993, Radiocarbon 35(2), p317-322

Beta Analytic Radiocarbon Dating Laboratory

4985 S.W. 74th Court, Miami, Florida 33155 • Tel: (305)667-5167 • Fax: (305)663-0964 • E-Mail: beta@radiocarbon.com

CALIBRATION OF RADIOCARBON AGE TO CALENDAR YEARS

(Variables: C13/C12=-6.8:lab.mult=1)

Laboratory number: Beta-261755

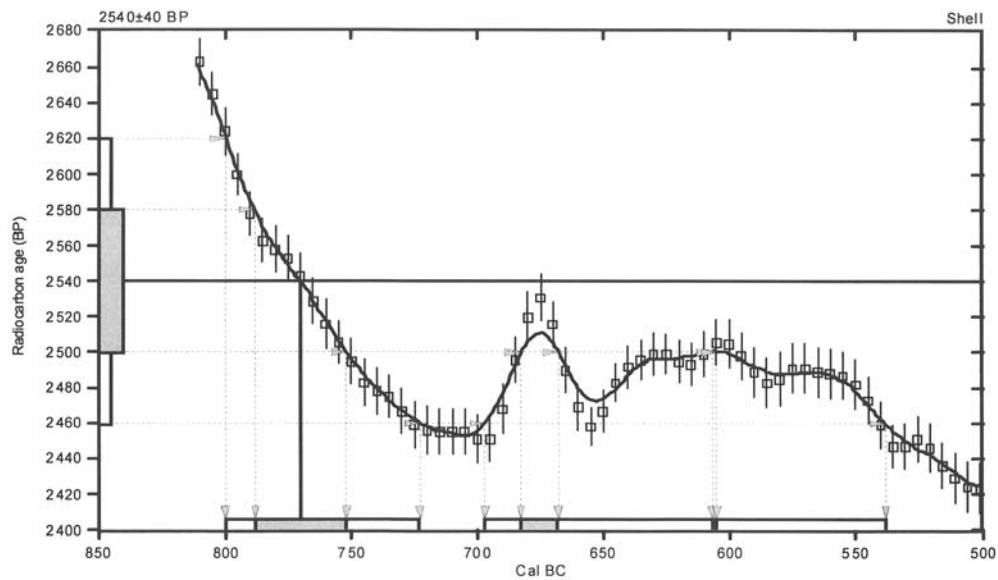
Conventional radiocarbon age: 2540±40 BP

2 Sigma calibrated results: Cal BC 800 to 720 (Cal BP 2750 to 2670) and
(95% probability) Cal BC 700 to 540 (Cal BP 2650 to 2490)

Intercept data

Intercept of radiocarbon age
with calibration curve: Cal BC 770 (Cal BP 2720)

1 Sigma calibrated results: Cal BC 790 to 750 (Cal BP 2740 to 2700) and
(68% probability) Cal BC 680 to 670 (Cal BP 2630 to 2620) and
Cal BC 610 to 600 (Cal BP 2560 to 2560)



References:

Database used

INTCAL04

Calibration Database

INTCAL04 Radiocarbon Age Calibration

IntCal04: Calibration Issue of Radiocarbon (Volume 46, nr 3, 2004).

Mathematics

A Simplified Approach to Calibrating C14 Dates

Talma, A. S., Vogel, J. C., 1993, Radiocarbon 35(2), p317-322

Beta Analytic Radiocarbon Dating Laboratory

4985 S.W. 74th Court, Miami, Florida 33155 • Tel: (305)667-5167 • Fax: (305)663-0964 • E-Mail: beta@radiocarbon.com

This page intentionally left blank.

APPENDIX L

**FUNCTIONAL ANALYSIS OF STONE TOOLS FROM BLM
PROJECT - LANDIS PROPERTY IN THE TEXAS PANHANDLE
(SITES 41PT186 AND 185/C)**

This page intentionally left blank.

**FUNCTIONAL ANALYSIS OF STONE TOOLS FROM BLM PROJECT -
LANDIS PROPERTY IN THE TEXAS PANHANDLE (SITES 41PT186
AND 185/C)**

Prepared for:



**TRC Environmental Corporation
505 East Huntland Drive, Suite 250
Austin, Texas 78752**

Prepared by:

**Bruce L. Hardy, Ph.D.
Department of Anthropology
Kenyon College
Gambier, OH 43022**

This page intentionally left blank.

L.1 INTRODUCTION

The Landis Property is situated in the Texas panhandle near Amarillo Texas. A sample of 42 stone tools from two sites was targeted for residue and use-wear analyses (Table L-1). Site 41PT185/C (Pipeline site, Locus C) represents a Late Archaic component radiocarbon dated between ca. 1600 and 2400 B.P. The second site, 41PT186 (Corral site), is a Protohistoric occupation radiocarbon dated to 200 to 300 B.P.

L.1.1 SAMPLE FROM 41PT185/C

This Late Archaic sample consisted of 31 artifacts that included flakes, bifaces and biface fragments, end and side scrapers, projectile points and point bases, and two large bifacial choppers (Table L-1). The projectile points comprise a corner-tang knife and a corner-notched point. None of the artifacts had been washed prior to analysis, although they had all been spot cleaned and labeled with ink and fingernail polish.

L.1.2 SAMPLE FROM 41PT186

The Protohistoric sample included 11 artifacts that consisted of flakes, end and side scrapers, and scraper fragments. These artifacts were not washed, but had been spot cleaned and labeled with ink and fingernail polish.

L.2 METHODS

Use-wear analysis gained popularity in the 1970s and 1980s under two primary approaches: the low-power approach with magnifications <100 diameters (e.g. Odell and Odell-Vereecken 1980) and the high-power approach with magnifications up to 500 diameters (e.g. Keeley 1980). The low-power approach focuses on edge damage, striations and edge rounding and is most useful at identifying use-actions and relative hardness of the use-material. The high-power approach was more specific, allowing the potential

identification of the use-material (wood, bone, hide, etc.) based on the formation of different characteristic micropolishes. However, further experimental work in the late 1980s suggested that these polishes were not distinct and were influenced by hardness of the material, silica content of the tool and the material, duration of use, and amount of water present (Fullagar 1991). A combination of these two techniques is used here, with a conservative interpretation of polishes to two broad categories, hard/high silica material (HHS) and soft materials (see below).

In the process of cleaning artifacts for use-wear analysis (often with hydrochloric acid or sodium hydroxide), many analysts cited the importance of removing “organics” in order to better see the polishes (e.g. Keeley 1980). Observation of unwashed artifacts revealed the presence of use-related residues on the artifacts surface. Briuer (1976) and Shafer and Holloway (1979) represent early applications of microscopic residue analysis to understanding stone tool function. Subsequent application of forensic identification techniques has allowed the identification of hair, feathers, blood, collagen, plant tissue, wood, starch grains, phytoliths and other microscopic structures (see Lombard, 2005 for a recent review).

By using a combination of use-wear and residue analysis, it is possible to arrive at a more complete understanding of a tool’s function as each method serves as a cross-check for the other.

The Landis Property samples were subjected to microscopic use-wear and residue analysis using established protocols described in Hardy et al. 2008.

All artifacts were examined with an Olympus BH microscope under bright-field incident light at magnifications ranging from 100 to 500 diameters. All wear patterns and residues were photographed using a Nikon Coolpix 995

digital camera, and their location on the surface was recorded on a line drawing of the artifact. Identifications of residues were made by comparison with published materials and a comparative collection of experimental stone-tool replicas (Brunner and Coman 1974; Catling and Grayson 1982; Beyries 1988; Anderson-Gerfaud 1990; Hoadley 1990; Fullagar 1991; Teerink 1991; Hather 1993; Hardy 1994; Brom 1986; Kardulias and Yerkes 1996; Williamson 1996; Hardy and Garufi 1998; Pearsall 2000; Haslam 2004; Dove et al. 2005; Fullagar et al. 2006; Hardy 2008). Residue recognition was the primary goal of the analysis; therefore, no special procedures were conducted to clean the tools for the sake of rendering use-wear patterns more visible. While this procedure may limit the use-wear information obtained, it serves to maximize the residues observed (Hardy and Garufi 1998; Hardy et al. 2001; Hardy 2004; Hardy 2008). Potentially identifiable residues include plant (plant tissue, plant fibers, starchy residue, epidermal cell tissue, wood, raphides, phytoliths, resin) and animal tissues (muscle tissue, collagen, fat, bone/antler, blood, hair, and feathers) (Hardy et al. 2001; Lombard 2004; Wadley et al. 2004). Distribution of residues and use-wear on the artifact surface were used to help demonstrate use-relatedness and to identify use-action (Hardy and Garufi 1998; Hardy et al. 2001; Lombard 2004).

Use-wear patterns recorded included edge damage (microflake scars, edge rounding), striations, and polishes. These were used to help identify use-action (Odell and Odell-Vereecken 1980; Mansur-Franchomme 1986). Due to the potential overlap of polishes produced by different materials, use-wear polishes were categorized as either “soft” or “hard/high silica” (e.g., Newcomer et al. 1986, 1988; Moss 1987; Bamforth 1988; Hurcombe 1988; Bamforth et al. 1990; Grace 1990; Fullagar 1991; Shea 1992). Soft polish often results from processing animal tissue

such as skin and meat. Hard/high-silica (HHS) polish is produced when processing soft plants with high silica content, such as reeds and grasses, and wood, bone/antler, and tilling soil. The amount of time a tool was used, silica content of the processed material, and presence of water are all factors that can influence polish formation (Fullagar 1991; Hardy 2004). A combination of residue and use-wear analysis can provide complementary and corroborative information, potentially producing more accurate results than either technique used alone (Hardy 1998; Hardy and Kay 1998; Hardy et al. 2001; Rots and Williamson 2004; Hardy et al. 2008:651-2).

In addition, artifacts that had sediment obscuring most of their surface were cleaned by briefly soaking in still water (still water immersion). This technique removes some of the adhering sediment without mechanical abrasion that might lead to loss of residues and alteration of use-wear patterns (Hardy et al. 2008). Artifacts were allowed to air dry before analysis.

One class of residues, starch grains, deserves further explanation. When viewed under cross-polarized light, starch grains exhibit extinction cross, the arms of which rotate as one of the polarizing filters is rotated (Figure L-1). This extinction cross is visible under both reflected and transmitted light. Recent work by Haslam (2006) and Loy (2006), however, demonstrates that there are several different particles which can exhibit extinction cross, including faecal spherulites, crystalline spherulites, and fungal spores such as conidia. For small starch grains in particular, Haslam recommends removal of the starch from the tool surface for observation under transmitted light for confirmation of the presence of starch grains. This analysis is limited to *in situ* observation of residues and the identification of starch grains on tool surfaces should be

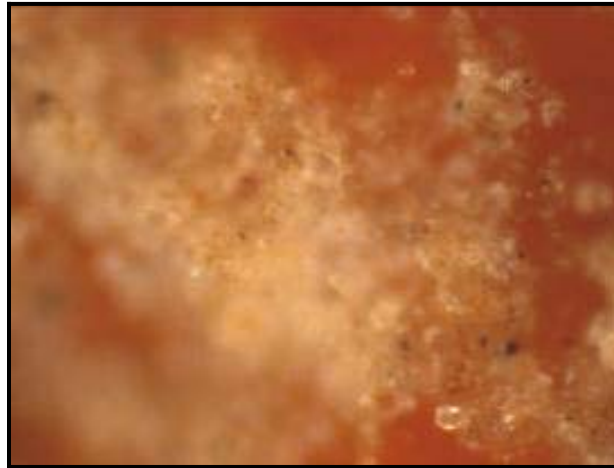


Figure L-1. Close-up of Starch Grains on Corner-Tang Knife Under Cross-Polarized Light.

treated as possible or probable. One advantage of *in situ* analysis of residues is the spatial information it provides about the distribution of the residue on the tool. It is also possible to observe use-wear patterns and other co-occurring residues which can strengthen the confidence of the starch identification. Examples include the presence of polishes and striae in direct association with the putative starch, the presence of raphides with the starch, or observation of starch grains within plant tissue adhering to the tool surface.

L.3 RESULTS

A visual summary of the evidence on all artifacts (except for those illustrated individually below, Figures L-2 through L-6) can be found at the end of the report (Figures L-7 through L-12).

L.3.1 41PT185/C LATE ARCHAIC

Over three-fourths of the sample (27/31, 87%) showed evidence of use either through use-wear or residues or both. The artifacts were used on a range of materials, including wood, plant, starchy plant, hide and bone (see Table

L-2). Four artifacts appear to have been used as projectiles and hafting was fairly common.

L.3.1.1 Plants

A variety of different plant types were processed at 41PT185/C. Woody plant tissue associated with HHS polish on a variety of different tool types including edge-modified flakes, bifaces, and a bifacial chopper. Wood is potentially identifiable to species level (Hoadley, 1990) if diagnostic anatomy is present. Although clearly identifiable as wood due to the presence of elongated rectangular parallel sided cells, anatomy diagnostic to a more specific taxonomic level was not observed. The presence of a large bifacial chopper (Figure L-2) along with smaller bifaces and edge-modified flakes used to process wood suggests that a range of woodworking activities, from procurement to fine-scale whittling and scraping, took place at the site.

Non-woody plant material was also processed. The presence of numerous artifacts with starch grains, both loose and within plant cells, attest to the processing of starchy plants, most likely underground storage organs for food. Five of the 31 artifacts (16.1%) from the sample had

starchy remains, including side scrapers (Figure L-2), a hafted corner-tang knife (Figure L-4), and a bifacial chopper (Figure L-5), and flakes (Figure L-6). Starch grains are identifiable under cross-polarized light by the presence of an extinction cross (Haslam 2005) and are potentially identifiable to taxon. The presence of large numbers of starch grains and starch-bearing plant tissue strengthens the confidence of identification. Further examination under transmitted light is warranted to confirm the presence of starches and to attempt to identify specific plants. The large bifacial chopper showed macroscopically visible residues that consisted of starch grains that may have been modified (Figure L-5). Heating of starches in the presence of water can cause changes to the extinction cross which are recognizable (Henry et al. 2009). Morphologically, these grains appear to have been altered, with the edges of the extinction cross becoming less distinct and faded. Further work to confirm this identification is warranted.

L.3.1.2 Animals

Evidence related to animal procurement and processing includes hair and bone fragments as well as impact fractures indicative of projectile use. The corner-tang knife, for example, was hafted and used to cut hide as well as starchy plant (see Figure L-4). An end and side scraper shows both HHS and bone fragments which suggest the scraping of bone. Overall, animal residues are much less frequent than plant residues. This may reflect a heavier emphasis on plant processing or may be due to preferential survival of plant residues (Hardy et al. 2008). Furthermore, the use of tools on multiple materials may obscure the wear and residue patterns of earlier uses. For example, if a tool is used to scrape hide and subsequently used to scrape wood, the latter activity may obscure or remove the traces of the former, particularly if the last material used is hard or high silica.

L.3.1.3 Hafting

Eleven of the 31 (36%) tools show evidence of hafting. Hafting traces include abraded ridges, striae, and polish which are confined to one portion of the tool. In general, hafting traces are bilateral, suggesting a split or notched haft as opposed to a juxtaposition haft. Wood and plant residues are observed in association with wear patterns and in two cases (#588-010 and #1104-010) resin is present and may have served as mastic (Figures L-8 and L-9). Hafting appears to have facilitated the processing of multiple materials (wood, starchy plant, hide) as well as projectile use.

L.3.2 41PT186, PROTOHISTORIC

Ten of the eleven tools (90.9%) from the Protohistoric occupation show evidence of use. Activities represented include cutting and scraping of plant, wood, and charred wood, as well as the scraping of hide (Table L-3). Use of tools on both plant and animal residues is common in this sample.

A distinctive feature of the functional evidence from this site is the high frequency of raphides (raphid phytoliths) found in association with plant remains and starch grains. The co-occurrence of starch and raphides strengthens the confidence level of the starch identification. Seven of eleven tools (63.6%) have raphides on them. Figure L-6 shows an edge-modified flake with a typical pattern of large numbers of raphides in association with starch grains and other tissues. Sobolik (1996) examined a sample of stone tools from the Archaic site of Hinds Cave (41VV456) and observed numerous artifacts with raphid phytoliths, “long rod-shaped cells with pointed ends” (p.463). The raphides observed by Sobolik are similar to the ones observed here and may derive from desert succulents such as yucca, stool, and agave (Piperno 1988). As with the Hinds Cave Archaic sample, these remains suggest that the inhabitants of 41PT186 were processing desert succulents with tools. Three of the six tools (50%) with

raphides and starch grains have hair fragments, suggesting that they were used in animal processing as well. The remaining tools with functional evidence were used for scraping wood, charred wood, and other plants (See Figures L-11 and L-12 for a visual summary).

L.4 DISCUSSION AND CONCLUSIONS

Combined, the samples from 41PT185/C and 41PT186 have 34 out of 41 (82.9%) with functional evidence. This high rate of return demonstrates excellent preservation of residues at these sites. Animal remains are also present in the form of hair and bone fragments. The range of residues includes numerous categories of plant remains: starch grains, wood, plant tissue, plant fibers, and raphides. These remains point to an important plant processing component to both assemblages. The presence of the raphides only in the Protohistoric sample is noteworthy as it underscores the integrity of the residue analysis. Processing of desert succulents is only seen in the later sample and may have been a major activity during the short occupation of this site.

The Late Archaic sample shows a wider range of tool functions and a similarly broad range of activities including both animal and plant processing. The frequency of starchy plant processing, points to the importance of plant foods in the diet. Further analysis of the starch assemblage may allow for more specific identification of these plants. With the notable exception of Hinds Cave (Sobolik 1996) and the Varga site (Hardy 2008), Archaic stone tool function is relatively poorly understood. In 1996, Sobolik wrote, following on work published by Shafer and Holloway (1979) “This study confirms that organic residue analysis can contribute significantly to a study of stone tool function and use, a fact that has been little heeded since the advent of such analyses over 15 years ago” (1996:468). Almost 15-years after that publication, I would echo those words and hope that more residue

analysis is conducted before another 15-years passes.

L.5 REFERENCES CITED

- Anderson-Gerfaud, P.
1990 Aspects of behavior in the Middle Paleolithic: Functional analysis of stone tools from southwest France. In: *The Emergence of Modern Humans: An Archaeological Perspective*, edited by P. Mellars, pp. 389-418. Cornell University Press, Ithaca.
- Bamforth, D.
1988 Investigating microwear polishes with blind tests: The institute results in context. *Journal of Archaeological Science* 15:11-23.
- Bamforth, D., G. Burns and C. Woodman
1990 Ambiguous use traces and blind test results: New data. *Journal of Archaeological Science* 17:413-430.
- Beyries, S.
1988 *Industries Lithiques: Traçéologie et Technologie*. British Archaeological Reports International Series, London.
- Brom, T.
1986 Microscopic identification of feathers and feather fragments of palearctic birds. *Bijdragen Tot De Dierkunde* 56:181-204.
- Briuer, F.
1976 New clues to stone tool function: plant and animal residues. *American Antiquity* 41(4):478-484.
- Brunner, H. and B. J. Coman
1974 *The Identification of Mammalian Hair*. Inkata Press, Melbourne.
- Catling, D., and J. Grayson.
1982 *Identification of Vegetable Fibers*. Chapman and Hall, New York.

- Dove, C.J., P. G. Hare, and M. Heacker
2005 Identification of ancient feather fragments found in melting alpine ice patches in southern Yukon. *Arctic* 58:38-43.
- Fullagar, R.
1991 The role of silica in polish formation. *Journal of Archaeological Science* 18:1-24.
- Fullagar, R., J. Field, T. Denham, and C. Lentfer
2006 Early and mid Holocene tool-use and processing of taro (*Colocasia esculenta*), yam (*Dioscorea* sp.) and other plants at Kuk Swamp in the highlands of Papua New Guinea. *Journal of Archaeological Science* 33:595-614.
- Grace, R.
1990 The limitations and applications of use-wear analysis. In *Review of The Interpretative Possibilities of Microwear Studies*, edited by B. Gräslund, H. Knutsson, K. Knutsson, and J. Taffinder, pp. 14:9-14. Proceedings of the International Conference on Lithic Use-wear Analysis, 15th-17th February 1989 in Uppsala, Sweden. Aun.
- Hardy, B. L.
1994 Investigations of stone tool function through use-wear, residue and DNA analyses at the Middle Paleolithic site of La Quina, France. Unpublished Ph.D. Dissertation, Indiana University.
1998 Microscopic residue analysis of stone tools from the Middle Paleolithic site of Starosele, Crimea, Ukraine. In: *The Middle Paleolithic of the Western Crimea*, Vol. 2, edited by K. Monigal and V. Chabai, pp. 179-196. Études et Recherches Archéologiques de l'Université de Liège.
- 2004 Neanderthal behaviour and stone tool function at the Middle Paleolithic site of La Quina, France. *Antiquity* 78:547-565.
- 2008 Results of Microscopic use-wear and Residue Analysis from the Varga Site 41ED28, Texas. In *The Varga Site: A Multicomponent, Stratified Campsite in the Canyonlands of Edwards County, Texas*, by J. M. Quigg, J. D. Owens, P. M. Matchen, G. D. Smith, R. A. Ricklis, M. C. Cody, and C. D. Frederick, Vol. II:777-819. TRC Environmental Corporation, TRC Technical Report No. 35319, and Texas Department of Transportation, Archeological Studies Program, Report No. 110.
- Hardy, B. L., and G. T. Garufi
1998 Identification of woodworking on stone tools through residue and use-wear analyses: Experimental results. *Journal of Archaeological Science* 25:177-184.
- Hardy, B. L. and M. Kay
1998 Stone tool function at Starosele. In: *Combining use-wear and residue analyses. The Middle Paleolithic of the Western Crimea*, Vol. 2, edited by K. Monigal and V. Chabai, pp. 197-209. Études et Recherches Archéologiques de l'Université de Liège.
- Hardy, B. L., M. Kay, A. E. Marks, and K. Monigal
2001 *Stone tool function at the Paleolithic sites of Starosele and Buran Kaya III, Crimea: Behavioral implications*. Proceedings of the National Academy of Sciences, U.S.A. 98:10972-10977.

- Haslam, M.
2004 The decomposition of starch grains in soils: Implications for archaeological residue analyses. *Journal of Archaeological Science* 31:1715-1734.
- 2006 Potential misidentification of in situ archaeological tool-residues: starch and conidia. *Journal of Archaeological Science* 33:114-121.
- Hather, J.
1993 *An Archaeobotanical Guide to Root and Tuber Identification*, Vol. I: Europe and South West Asia. Oxbow Books, Oxford.
- Henry, A.G., H. F. Hudson, and D. R. Piperno
2009 Changes in starch grain morphologies from cooking. *Journal of Archaeological Science* 36:915-922.
- Hoadley, R.
1990 *Identifying Wood: Accurate Results with Simple Tools*. Taunton Press, Newtown.
- Hurcombe, L.
1988 Some criticisms and suggestions in response to Newcomer, et al. (1986). *Journal of Archaeological Science* 15:1-10.
- Kardulias, N. and R. Yerkes
1996 Microwear and metric analysis of threshing sledge flints from Greece and Cyprus. *Journal of Archaeological Science* 23:657-666.
- Keeley, L. H.
1980 *Experimental Determination of Stone Tool Uses*. University of Chicago, Chicago.
- Lombard, M.
2004 Distribution patterns of organic residues on Middle Stone Age points from Sibudu Cave, Kwazulu-Natal, South Africa. *South Africa Archaeological Bulletin* 59:37-44.
- Lombard, M.
2005 Evidence of hunting and hafting during the Middle Stone Age at Sibudu Cave, KwaZulu-Natal, South Africa: A multianalytical approach. *Journal of Human Evolution* 48:279-300.
- Loy, T.
2006 Optical properties of potential look-alikes. In *Ancient Starch Research*, Torrence, R., Barton, H. (Eds.), p. 123. Walnut Creek, CA, Left Coast Press.
- Mansur-Franchomme, M. E.
1986 *Microscopie du Matériel Lithique Préhistorique: Traces d'Utilisation, Altération Naturelles, Accidentelles, et Technologiques*. National Centre for Scientific Research, Paris.
- Moss, E. H.
1987 A review of "Investigating microwear polishes with blind tests." *Journal of Archaeological Science* 14:473-481.
- Newcomer, M., R. Grace, and R. Unger-Hamilton
1986 Investigating microwear polishes with blind tests. *Journal of Archaeological Science* 13:203-217.
- 1988 Microwear methodology: A reply to E. H. Moss, L. Hurcombe, and D. Bamforth. *Journal of Archaeological Science* 15:25-33.
- Odell, G. and F. Odell-Vereecken
1980 Verifying the reliability of lithic usewear assessments by "blind tests": The low-power approach. *Journal of Archaeological Science* 7:87-120.

- Pearsall, D.
2000 *Paleoethnobotany: A Handbook of Procedures*. second ed. Academic Press, New York.
- Piperno, D.
1988 *Phytolith Analysis: An Archaeological and Geological Perspective*. New York: Academic Press.
- Rots, V., and B. S. Williamson
2004 Microwear and residue analyses in perspective: The contribution of ethnoarchaeological evidence. *Journal of Archaeological Science* 31:1287-1299.
- Shafer, H. J. and R. G. Holloway
1979 Organic residue analysis in determining stone tool function. In *Lithic Use-Wear Analysis*, edited by B. Hayden, pp.385-400, New York, Academic Press.
- Shea, J. J.
1992 Lithic microwear analysis in archaeology. *Evolution Anthropology* 1:143-150.
- Sobolik, K. D.
1996 Lithic organic residue analysis: An example from then Southwest Archaic. *Journal of Field Archaeology* 23:461-469.
- Teerink, B. J.
1991 *Hair of West European Mammals: Atlas and Identification Key*. Cambridge University Press, Cambridge.
- Wadley, L., M. Lombard, and B. Williamson
2004 The first residue analysis blind tests: Results and lessons learnt. *Journal of Archaeological Science* 31:1491-1501.
- Williamson, B. S.
1996 Preliminary stone tool residue analysis from Rose Cottage Cave. South Africa. *Journal of Field Archaeology* 5:36-44.

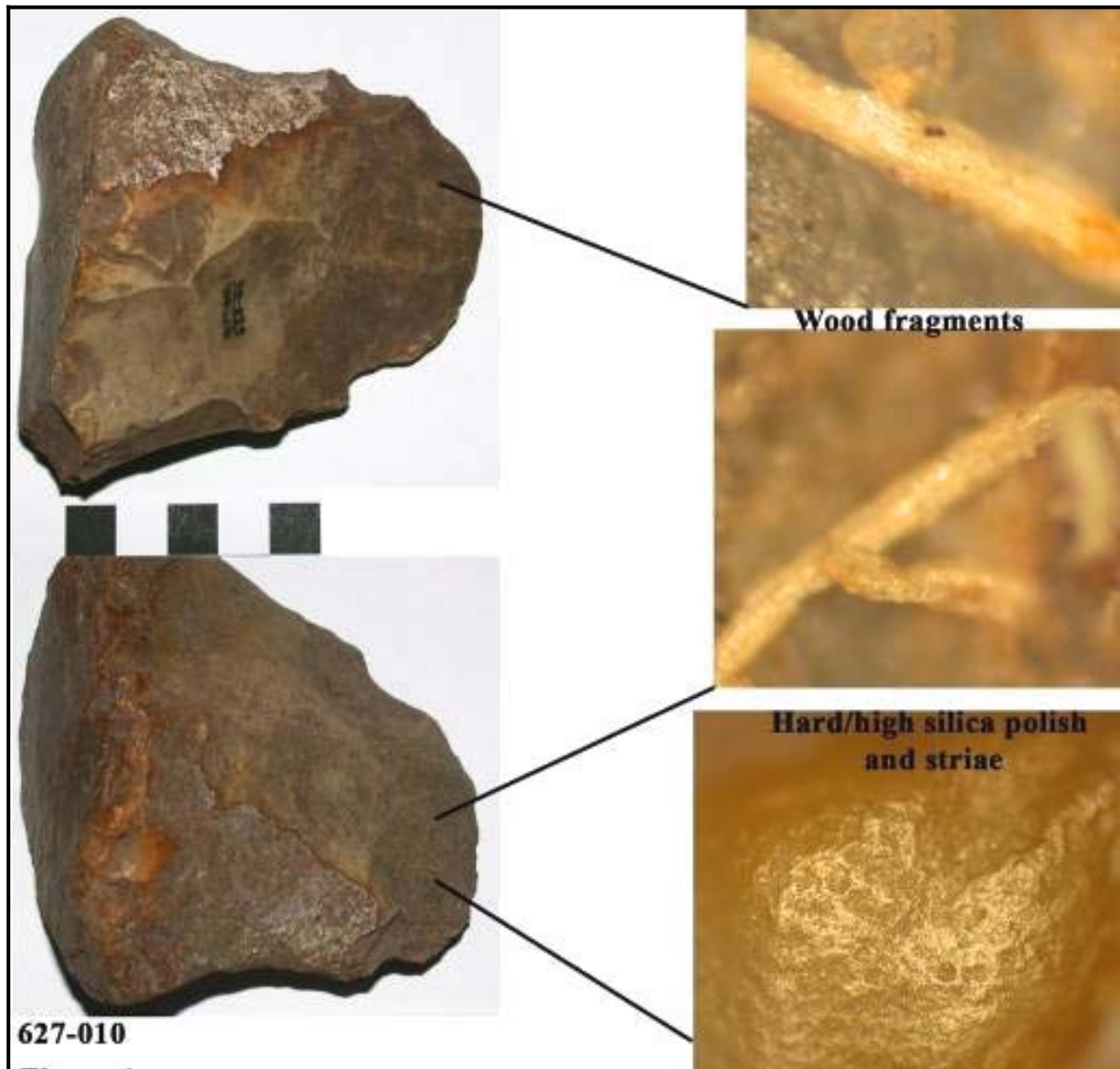


Figure L-2. Observations on Edwards Chert Chopper #627-010 from 41PT185/C.

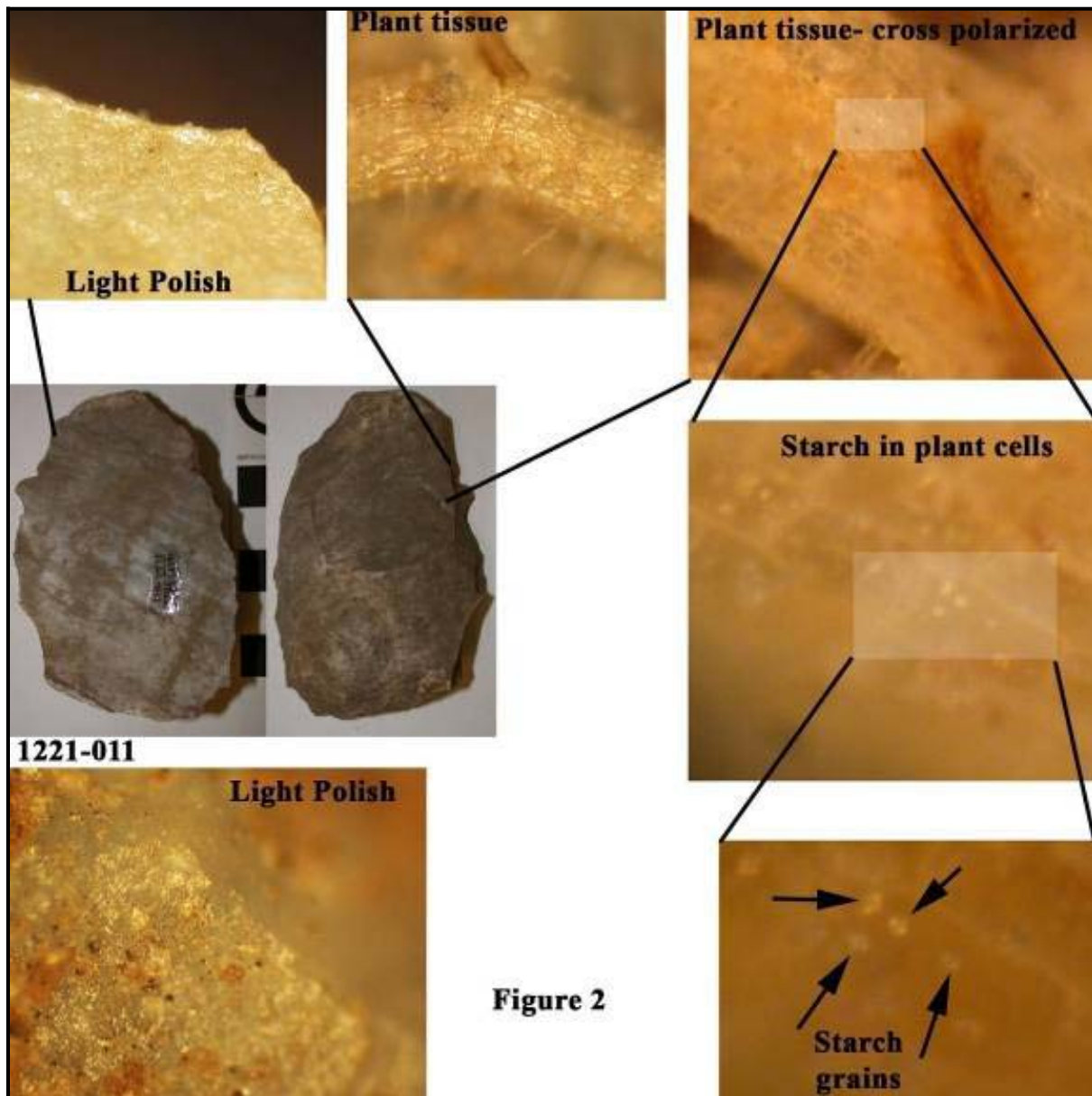


Figure L-3. Observations on Alibates Side Scraper #1221-011 from 41PT185/C.

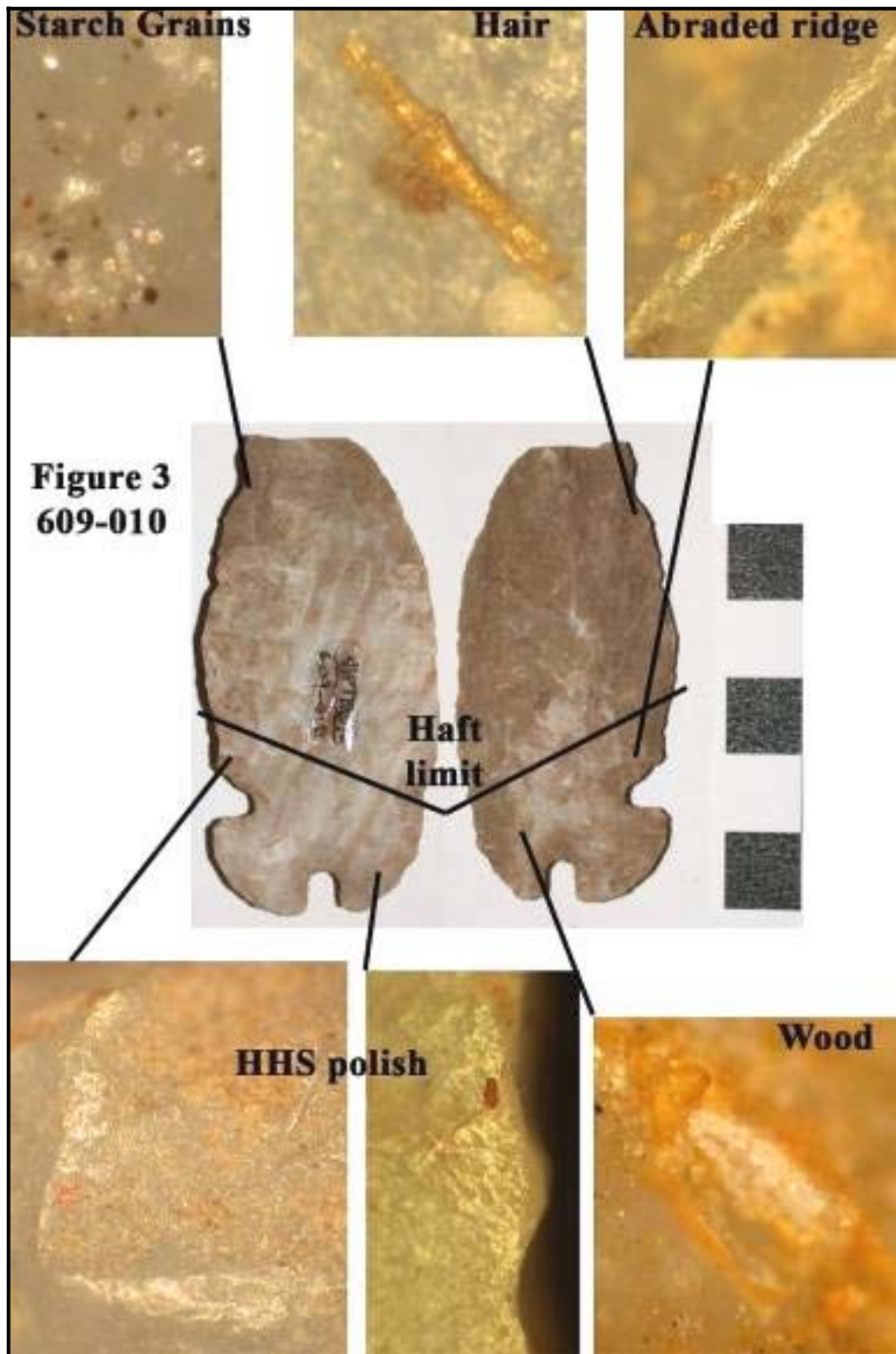


Figure L-4. Observations on Corner-Tang Knife #609-010 from 41PT185/C.

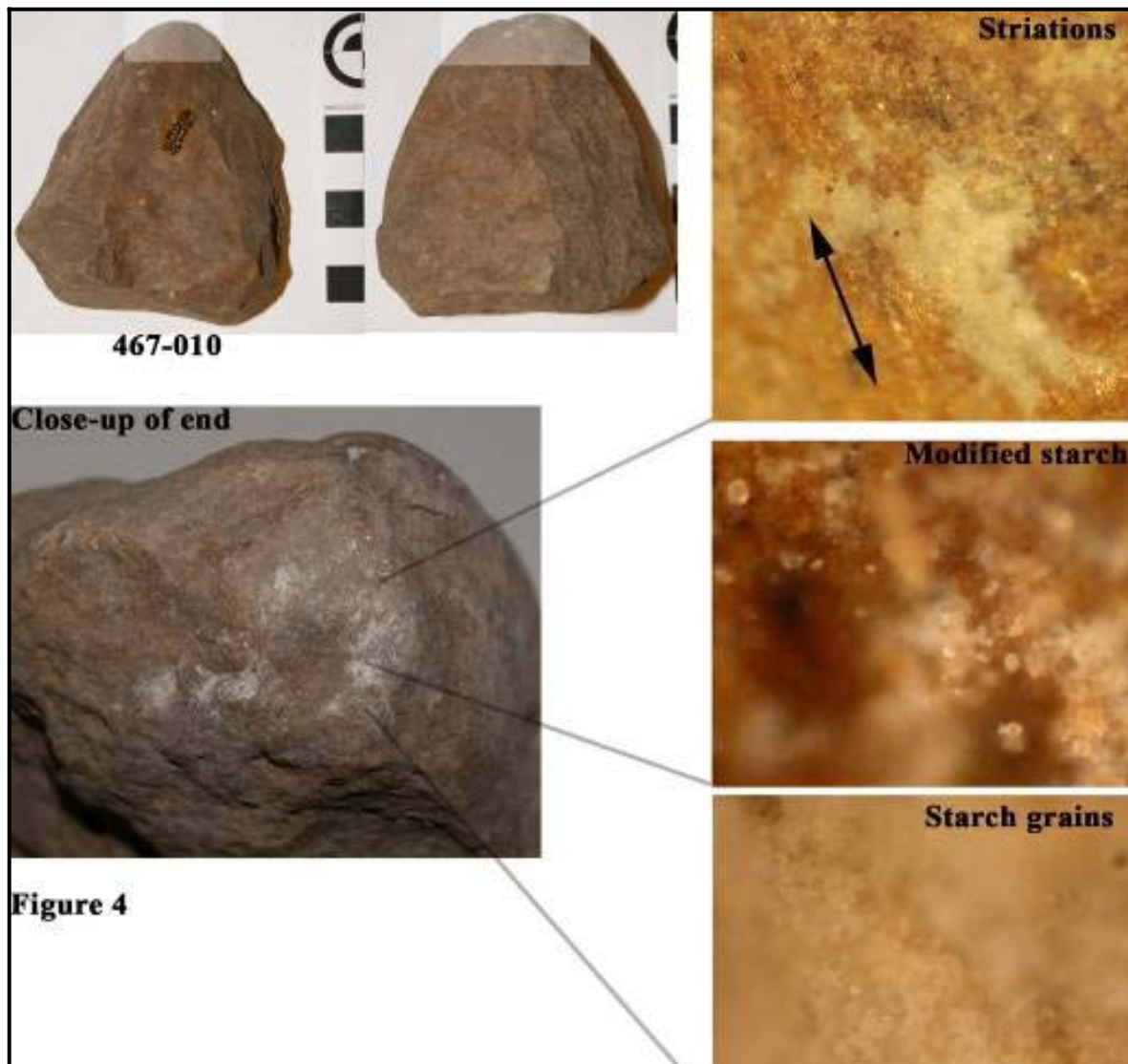


Figure L-5. Close-up of Observations on Potter Chert Hammerstone/Chopper #467-010 from 41PT185/C.

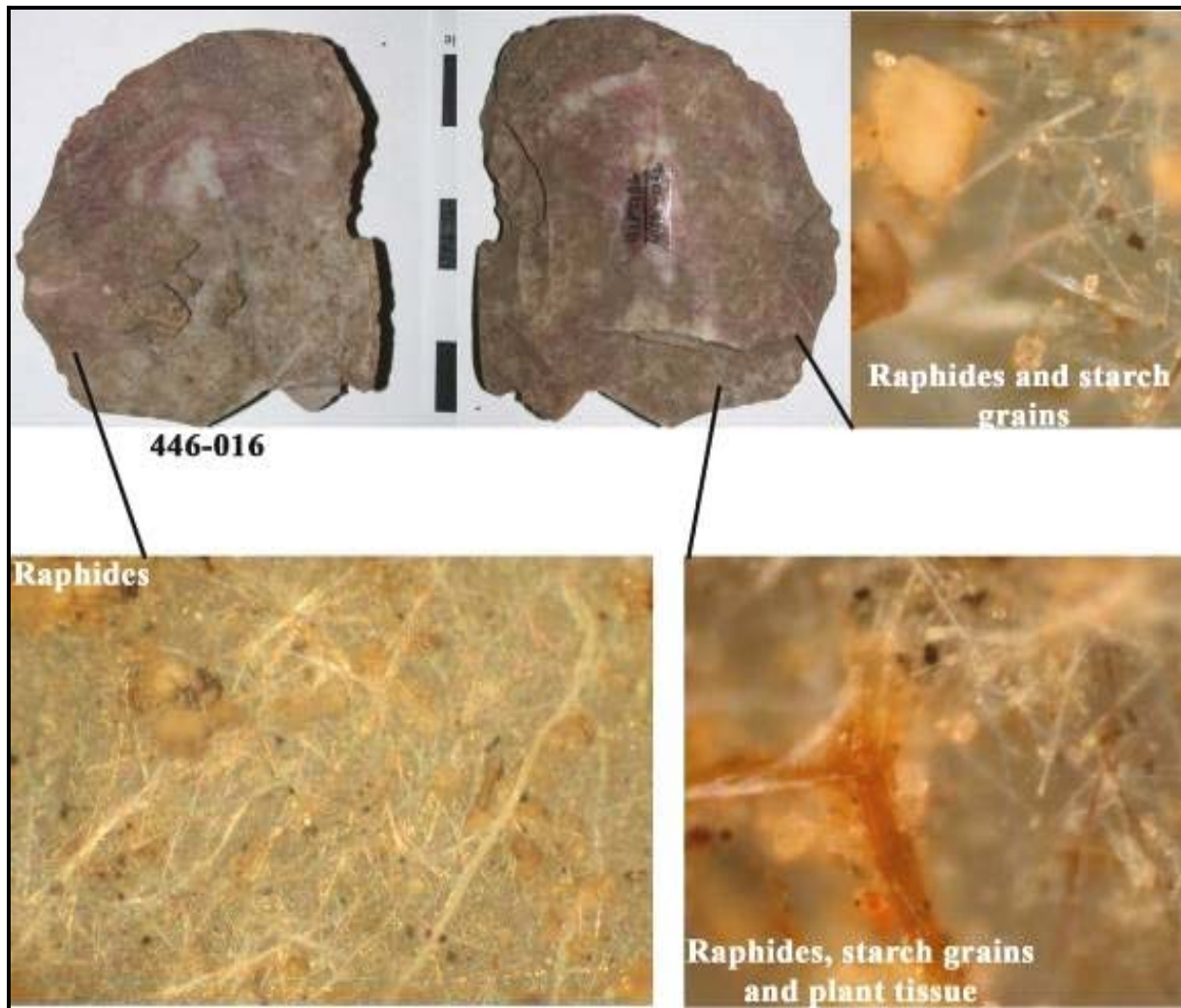


Figure L-6. Close-Up of Use-Wear Results and Microfossils Observed on Edge-Modified Flake #446-016 from 41PT186.

Table L-1. Summary of Sample by Tool Type

Tool type	41PT185/C	41PT186
Edge-modified flake	7	3
Flake	0	2
Biface midsection	1	0
Proximal biface	1	0
Biface	7	0
Biface edge	1	0
Side scraper	4	0
End and side scraper	3	4
Scraper fragment	0	2
Bifacial chopper	2	0
Corner-tang knife	1	0
Corner-notched point	1	0
Point stem and base	3	0
Total	31	11

Table L-2. Summary of Results from 41PT185/C

Catalog No.	Unit N/E	Depth (cmbs)	Artifact Type	Residues	Use-wear	Function
273-010	100/102	60-69	edge-modified flake	plant, starch grains, wood	HHS striae	slicing wood, starchy plant
317-010	101/108	65	biface midsection	plant fiber	abraded ridges	hafted, snapped
402-010	103/103	77	end and side scraper	hair, bone fragments, wood	HHS, abraded ridges	hafted, scraping bone
420-010	103/106	65	complete biface	plant tissue		unknown/unused
446-010	103/117	55	edge-modified flake	wood, starch grains	HHS	scraping wood
452-010	104/101	79	side scraper	starch grains, plant tissue	HHS	scraping starchy plant
467-010	104/104	62	complete biface chopper	starch grains-cooked?	striae	pounding cooked starch?
494-010	104/115	50-60	complete biface			unknown/unused
517-010	105/109	79	edge-modified flake		light polish	broken during use, unknown material
588-010	106/104	70-80	edge-modified flake	starch grains, resin	HHS, abraded ridges, striae	hafted with resin, used after break on starchy material
609-010	107-101	62	corner-tang knife	plant fiber, starch grains, wood, hair	HHS, soft	Hafted, cutting soft material, hide and starchy plant
627-010	107/106	35-50	biface chopper	wood	HHS	chopping wood
767-010	111/116	80-90	end and side scraper	wood, hair	abraded ridges	hafted, scraping hide
787-010	112/102	60-70	side scraper		light polish	unknown/unused
832-001	113/100	70-80	Edge-modified flake/core platform			unknown/unused
868-010	114/98	60-70	biface	plant, resin, starch grains	HHS, striae perpindic.	hafted, plant processing
957-010	116/99	50-60	edge-modified flake		HHS, microflake scars	slicing HHS
967-010	116/98	50-60	biface	wood	HHS	cutting wood
984-010	116/103	50-60	point stem and base		polished and abraded ridges	hafted
1033-010	117/98	45-50	point stem and base		light polish	unknown/unused
1064-010	117/106	46	biface	wood, plant, bark		cutting wood
1085-010	118/96	45-60	biface edge			unknown/unused

Catalog No.	Unit N/E	Depth (cmbs)	Artifact Type	Residues	Use-wear	Function
1104-010	118/100	60-70	Corner-notch point	plant fiber, resin	HHS, impact fracture	hafted proj. pt.
1128-010	118/105	58	large end and side scraper	starch grains	HHS	scraping HHS (starchy plant)
1163-010	119/99	50-60	proximal biface	wood	abraded ridges	hafted, proximal snap
1212-010	Dec-97	54-60	complete biface	wood fragments	impact fracture	hafted projectile
1220-011	120/99	37	drill stem base/biface	wood, plant fiber	HHS	scraping wood
1221-011	120/99	55	side scraper	plant w/starch grains	light polish	scraping soft starchy plant
1257-010	121/95	70-80	edge-modified flake	plant tissue, starch grains	HHS	slicing starchy plant
1288-010	121/104	60-70	complete point	plant frags	abraded ridges	hafted, use unknown
1348-010	110/105	50-60	point stem and base			unknown/unused

Table L-3. Summary of Results from 41PT186

Catalog No.	Unit N/E	Depth (cmbs)	Artifact Type	Residues	Use-wear	Function
360-010	484-494	90-100	edge-modified flake	plant tissue	HHS	cutting HHS plant
409-010	488/493	100-110	scraper fragment			unknown, unused
446-010	493/489	66	end and side scraper	charred wood, starch grains	striae	scraping charred wood
446-011	493/489	65	end and side scraper	Hair, raphides, starch grains	HHS	scraping hide, plant
446-012	493/489	67	end and side scraper	raphides, parenchyma		scraping plant
446-013	493/489	69	end and side scraper	hair, raphides, wood plant	abraded ridges	hafted, scraping hide
446-014	493/489	66	edge-modified flake	fragments, starch grains, raphides	edge rounding, striae	scraping plant
446-015	493/489	67	flake	hair, raphides	soft polish	cutting hide (raphides also present)
446-016	493/489	68	edge-modified flake	raphides, plant tissue, starch grains		cutting plant
446-017	493/489	68	flake	raphides, starch grains		cutting plant
501-010	497/496	100-110	scraper fragment	wood	HHS	scraping wood

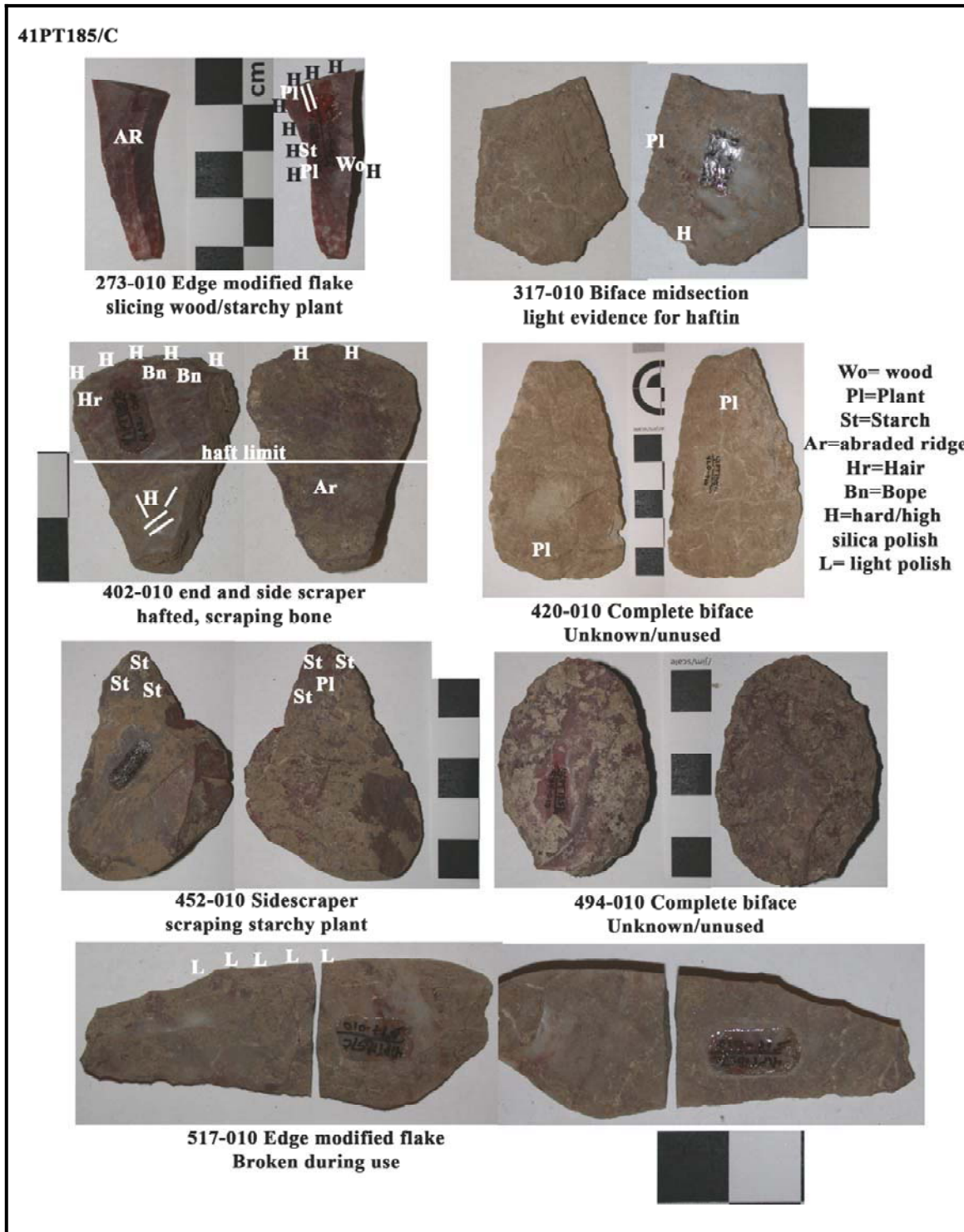


Figure L-7. Selected Artifacts from 41PT185/C Showing Location of Microfossils and Use-Wear.

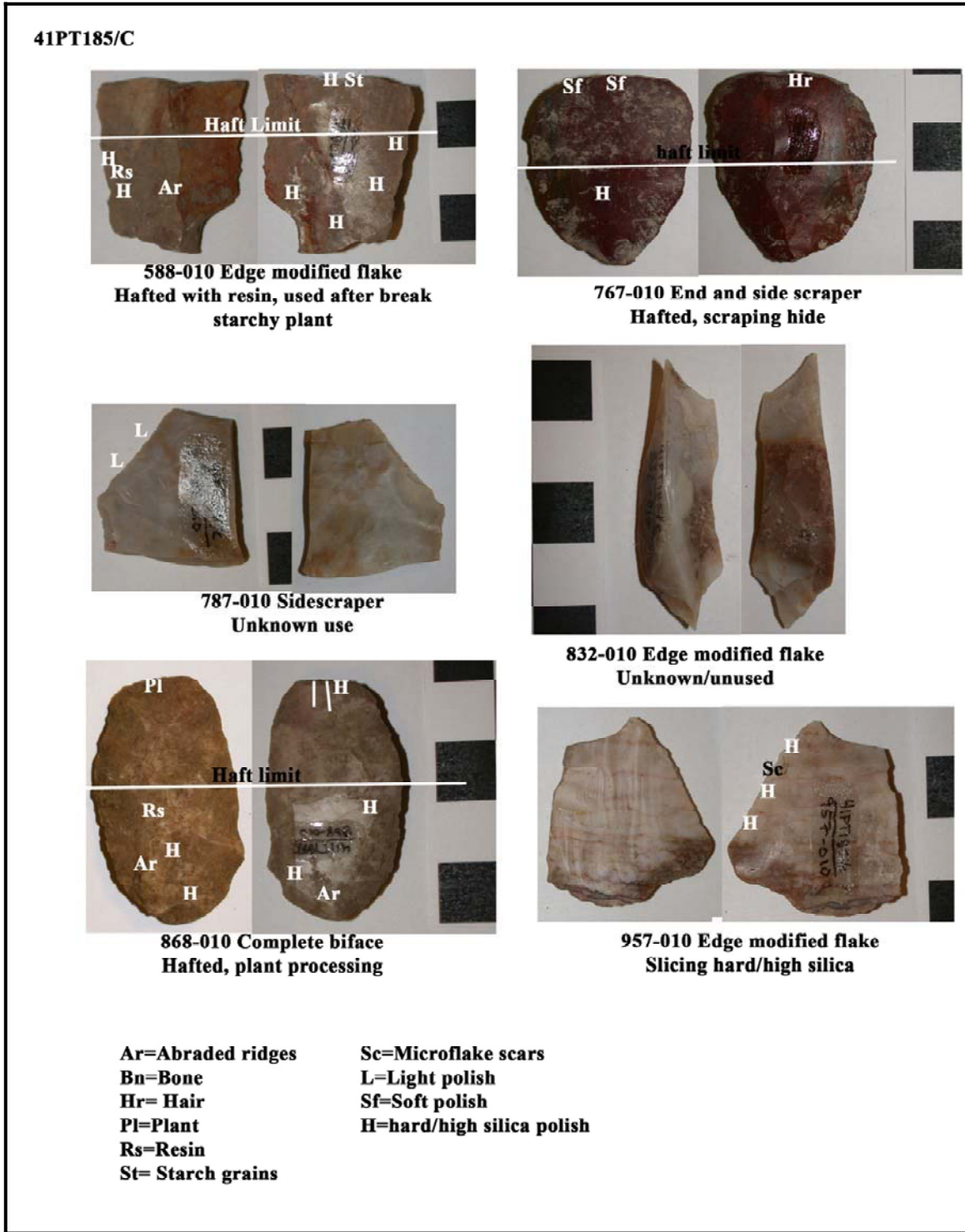


Figure L-8. Selected Artifacts from 41PT185/C
 Showing Location of Microfossils and Use-Wear.

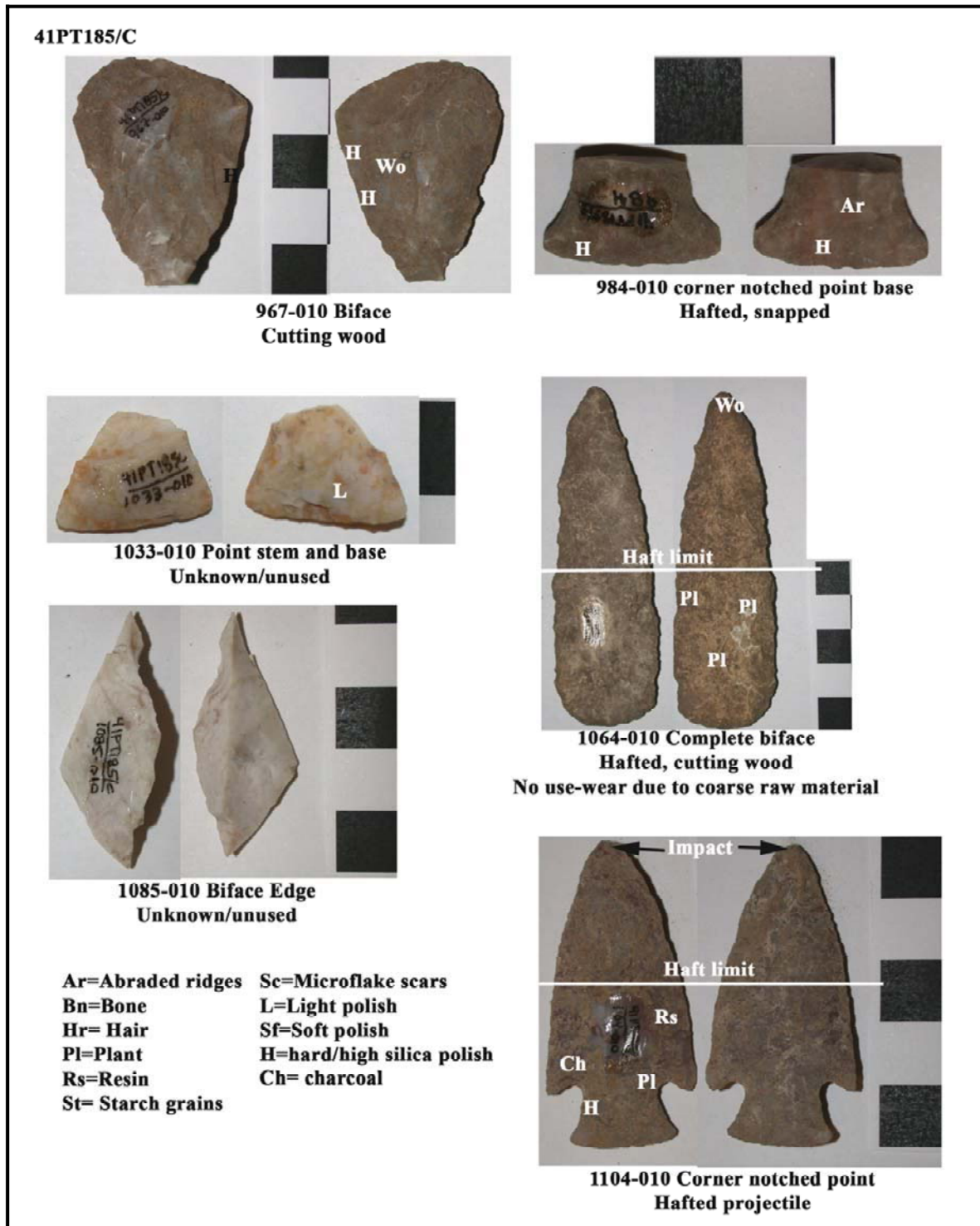


Figure L-9. Selected Artifacts from 41PT185/C
Showing Location of Use-Wear and Microfossils.

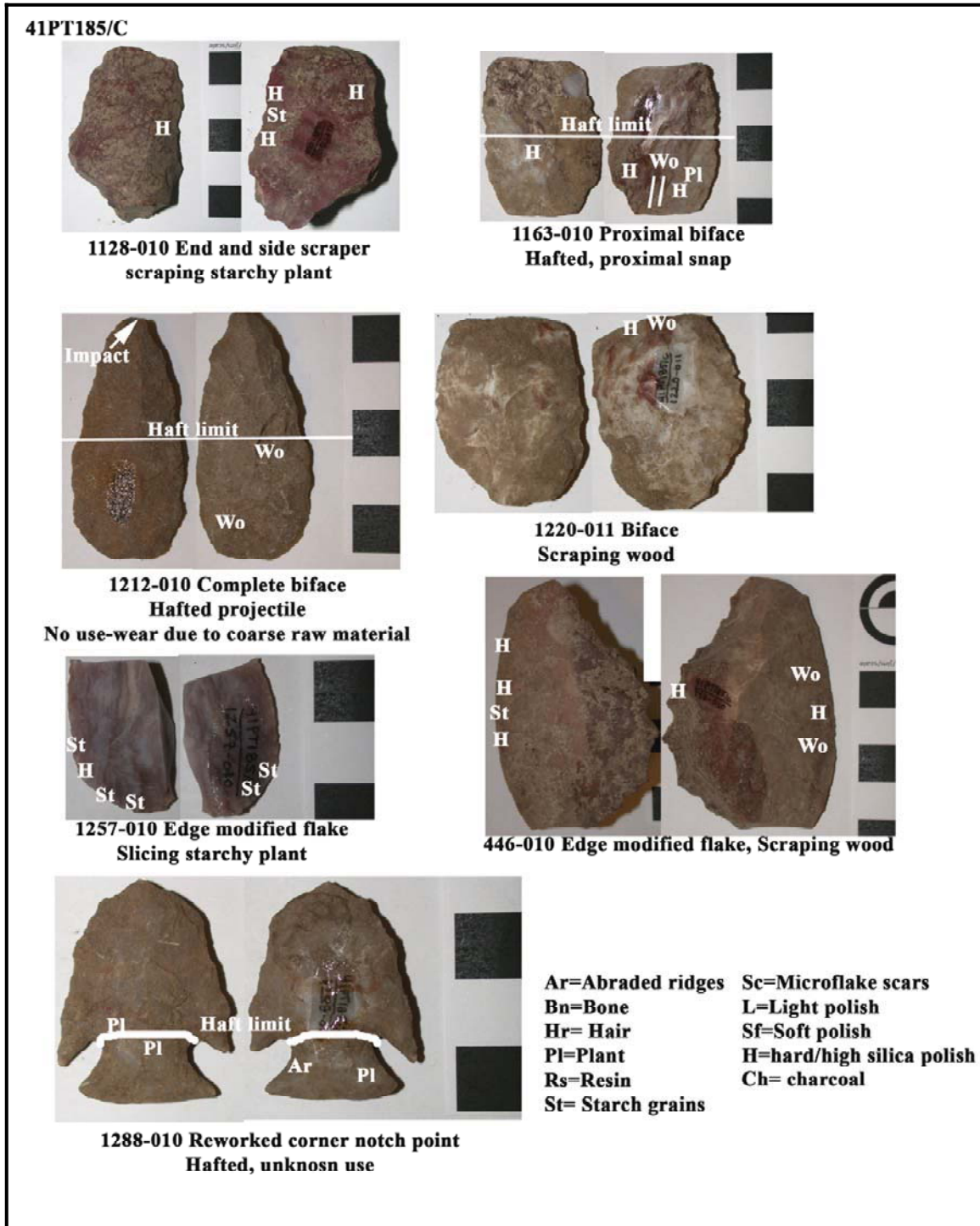


Figure L-10. Selected Artifacts from 41PT185/C
 Showing Location of Use-Wear and Microfossils.

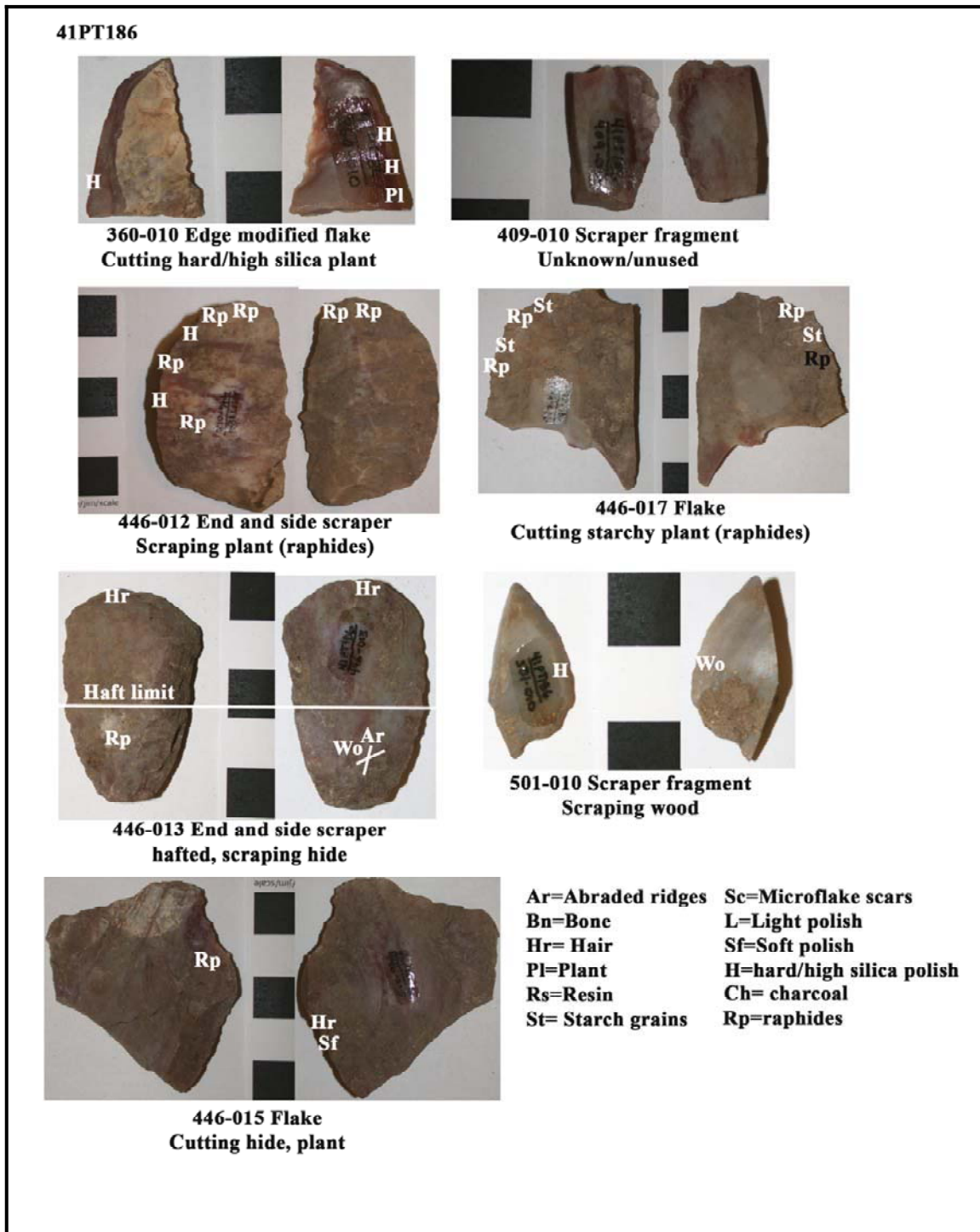


Figure L-11. Selected Artifacts from 41PT186, Showing Use-Wear and Microfossil Results.

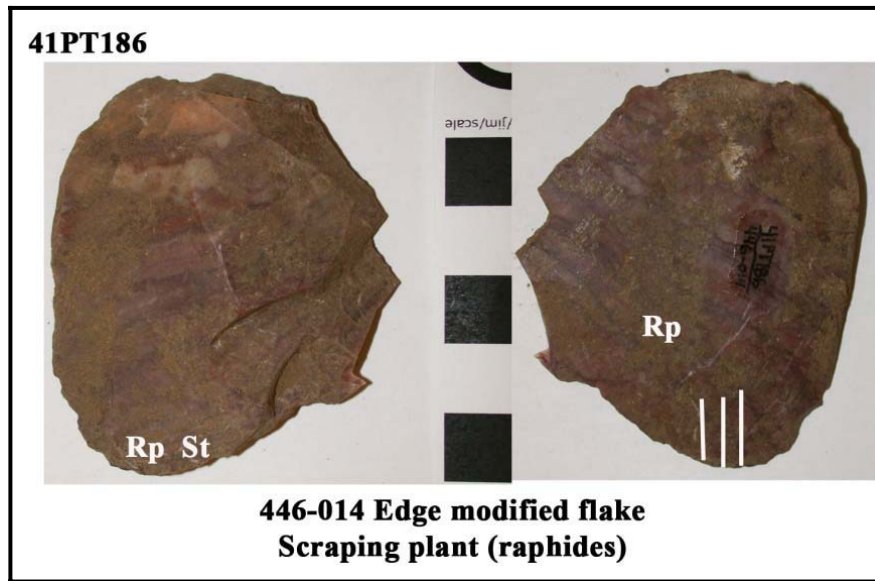


Figure L-12. Observed Use Areas and Microfossils on Edge-Modified flake #466-014 from 41PT186.

This page intentionally left blank.

APPENDIX M

**LATE HOLOCENE PALEOENVIRONMENTAL HISTORY OF
UPPER WEST AMARILLO CREEK VALLEY, TEXAS**

This page intentionally left blank.

LATE HOLOCENE PALEOENVIRONMENTAL HISTORY OF UPPER WEST AMARILLO CREEK VALLEY, TEXAS

Prepared for:



**TRC Environmental Corporation
505 East Huntland Drive, Suite 250
Austin, Texas 78752**

Prepared by:

**Manuel R. Palacios-Fest
with the contribution of
David L. Dettman
Department of Geosciences,
University of Arizona,
Tucson, AZ**

TNESR Report 09-05

This page intentionally left blank.

M.1 ABSTRACT

Micro-invertebrates, calcareous algae, and the stable isotopes from ostracodes and gyrogonites combine powerful tools for reconstructing paleoclimates. This study compares the paleoenvironmental signatures of land and aquatic mollusks, ostracodes, and charophyta with the stable isotope ($\delta^{18}\text{O}$ and $\delta^{13}\text{C}$) values of *Cypridopsis* sp. (ostracode) and *Chara globularis* and *Nitella flexilis* (gyrogonites). Each individual signature contributes its own evidence of environmental change between $1,890 \pm 40$ years B.P. and $\text{post-}750 \pm 40$ years B.P. The combined interpretation of the data permitted a more detailed reconstruction of paleoclimate variability at the transition of the Medieval Climatic Anomaly to the Little Ice Age.

M.2 INTRODUCTION

The reconstruction of ancient aquatic environments associated with human settlements allows paleolimnologists, geomorphologists, and geoarcheologists to understand both local and regional processes of environmental and climatic change, as well as the impact such change may have on human populations. The Texas Panhandle contains a rich record of human occupation and sedimentation spanning the past 11,500 years (Johnson and Holliday 2004). The paleontological and paleobotanical remains in the sediments provide evidence of the environmental history of the region. Numerous prehistoric sites are situated in the Texas Panhandle, including the upper West Amarillo Creek valley, near Amarillo where single- and multiple- occupation localities were identified by Charles Haecker (1999). Four prehistoric sites (41PT184, 41PT185, 41PT186, and 41PT 187) were considered potentially eligible for listing on the National Register Historic Place (NRHP: Haecker 1999). Several multiple-occupation sites with good stratigraphic context have provided useful

information on the stratigraphy, depositional environments, and paleoenvironments throughout the Holocene, including small lake basins and marshes (e.g., Cotter 1937; Howard 1935; Sellards 1952; Wendorf 1961; Wendorf and Hester 1975; Caran 1991).

The paleoecology of marshes is poorly known compared with that of lacustrine environments. Reconstructing the aquatic environment of a marsh discovered at the upper West Amarillo Creek valley during geoarcheological exploration is of the major significance because it will provide specialists understand the environmental background that affected northwestern Texas during the Late Holocene. Ostracodes (microcrustaceans), mollusks, and the gyrogonites of calcareous algae are used in this study to interpret the history of the marsh. In addition, stable isotopes ($\delta^{18}\text{O}$ and $\delta^{13}\text{C}$) from ostracodes and gyrogonites are used to integrate a more detailed paleoenvironmental history of the area.

Ostracodes are microscopic crustaceans characterized by a hinged bivalve carapace made of calcite and ranging in size between 0.5 and 2 mm. The carapace is the only body part that preserves to the geologic record (Pokorný 1978; Horne et al. 2002). In continental waters they are mostly benthic, although some species are organisms that swim under their own power (nektic) and may swim around the vegetation (Forester 1991). This group colonized continental aquatic systems as early as the Carboniferous but thrived in the oceans since the Cambrian. Today, ostracodes are diverse and abundant in marine and nonmarine environments. Paleontologists have devoted more time to the study of ostracodes than biologists, thus, the poorly understood ecology of ostracodes. However, recent progress on the application of ostracodes as indicators of hydrogeologic variations provide a rationale for studying the ecology of springs and seeps, as well as their associated wetlands or cienegas

(Forester 1983, 1986; De Deckker 1983; Palacios-Fest 1994, 2008; Palacios-Fest et al. 1994, 2001; Holmes and Chivas 2002).

Mollusks include the bivalve clams and mussels (Pelecypoda), and the univalve snails (Gastropoda). Mollusks are soft-bodied and unsegmented with a body organized into a muscular foot, a head region, a visceral mass, and a fleshy mantle that secretes a shell of proteinaceous and crystalline calcium carbonate (aragonite) materials. Marine and nonmarine species exist, as well. The nonmarine species, subject of this study, include several families of snails (Planorbidae, Ancyliidae, Lymnaeidae, Pupillidae) and at least one of clams (Sphaeridae). The associations of mollusks in the sediments reflect the water quality, salinity, and streamflow (Dillon 2003; Rutherford 2000). For example, the occurrence of only juveniles in a sample is interpreted as the introduction of early stage specimens during warm or warming months (Rutherford 2000). If the population reaches stability and adults are encountered, then, it is assumed that the feature held water for a relatively prolonged period. Some species require well-oxygenated, flowing (lotic) waters and prefer neutral to alkaline pH, but cannot be very tolerant to organic pollution, like *Pisidium* sp. and *Laevapex (Ferrisia) hendersoni*, present in the marsh. By contrast, other species can tolerate poorly-oxygenated (but not disoxic), standing (lentic) waters, and can tolerate some organic pollution and eutrophic conditions (Dillon 2003), like *Planorbella scalaris* and *Physa virgata*. The latter species prefer lakes, wetlands, ponds, and the calmest areas of coastal rivers. As the ostracode signatures, mollusks are used in this study to integrate the paleoecological characteristics of the upper West Amarillo Creek valley marsh (Unit D).

In addition to micro-invertebrates, the calcareous remains of the algae *Chara* and *Nitella* known as gyrogonites (fertilized female gametangia), may be used to

reconstruct the alkalinity, time of colonization, and paleohydraulics of the marsh. Charophytes are small branching algae, normally living in carbonate-rich freshwater. Modern examples are known as “stoneworts” because they have a partial carbonate skeleton. In appearance they look like small subaqueous “horsetails”. The Characeae or Charophyta are a strange and isolated group of aquatic plants growing entirely under water. Modern species prefer ponds or lakes, although they are occasionally found in running water, and have a partiality for somewhat brackish conditions such as freshly dug ditches in marshes near the sea. In overgrown waters they soon give way before more vigorous vegetation (like cattails). They commonly pioneer the colonization of habitats like recently dug canals and ditches (Allen 1950).

Ecologically, the Charophyta promote water clarity, enhance fish population and stabilize the bottom surface. In clear still water, masses of orange-red antheridia (the male reproductive organs) are abundant and visible (Allen 1950). The average height of these plants is from 30 to 46 cm, occasionally just a few centimeters. Usually, charophytes grow in shallow waters (less than 60 cm deep), but sometimes they may occur at much greater depths (Allen 1950). Many modern charophytes have a short season between spring and late summer just before the aquatic system dries-out (Allen 1950), therefore, they prefer warm to early warm temperatures (Allen 1950). Gyrogonites are used in this study to complement the micro-invertebrate record.

Stable isotope ($\delta^{18}\text{O}$ and $\delta^{13}\text{C}$) geochemistry is another approach to paleoclimatic reconstructions available from ostracode valves and the gyrogonites of Charophyta. Lister (1988) and Eyles (and Schwarcz 1991) have pursued the utility of carbon and oxygen isotopes in ostracodes, followed by numerous other researchers (e.g., Lewis et al. 1994; von Grafenstein et al. 2000;

Wrozyzna et al. 2009). The isotopic record from ostracode valves allowed these investigators to establish the rate and timing of climate change in time and space. For example, Lister (1988) determined the Alpine deglaciation, Holocene climatic changes, and changing lacustrine productivity of Lake Zurich, whereas Wrozyzna et al. (2009) utilized stable isotopes to identify lake level changes from Lake Nam County, southern Tibet during the past 600 years. Ostracode stable isotope studies have proven their significance in paleoenvironmental reconstructions, calcareous algae, however, they have been little explored.

In recent years, interest on the applicability of stable isotopes from calcareous algae has grown at a fast pace inducing researchers to analyze modern Charophyta to develop analogs for the geologic record. Coletta et al. (2001), Andrews et al. (2004), and Pentecost et al. (2006) have focused on the study of modern calcareous algae including the stems and gyrogonites to establish the trends in carbon and oxygen biofractionation in an attempt to use them in paleoecologic reconstructions. Becker et al. (2002), applied some of the results to one of the first applications to a geologic example from a Late Oligocene-Early Miocene lake in Switzerland (Brochene Fluh section) demonstrating that during the Late Oligocene the lake was a closed basin subject to seasonal changes that gradually diminished perhaps as the result of the ingression of the incoming Burdigalian sea.

The purpose of this investigation is to combine routine paleoecological analysis of micro-invertebrates and calcareous algae in combination with the stable isotope geochemistry ($\delta^{18}\text{O}$ and $\delta^{13}\text{C}$) of ostracodes and gyrogonites to reconstruct the late Holocene environmental history of the upper West Amarillo Creek valley marsh at Unit D (Figure M-1).

M.3 AREA OF STUDY

A brief summary of the area of study is presented in this section. The upper West Amarillo Creek valley is basically a small canyon cut into the Ogallala Formation, the source of the High Plains aquifer. It is located on the south side of the Canadian River (Figure 1 of Quigg 2008). In this area the Ogallala Formation rests unconformably upon Triassic sandstones and shales of the Trujillo and Tecovas formations. The prehistoric site 41PT185 at the Landis Property is on the valley floor near Amarillo, Texas.

Frederick (2008) describes a complex Holocene alluvial history in which six allostratigraphic units (A through F) have been recognized in the area (Figure 3 of Frederick 2008). Unit D, the source of materials for the present study, overlies the coarse sand Unit C and underlies Unit E characterized by coarse sediments indicating large flood events. Unit D consists of more than 4.5 m of fine-grained dark colored mud which appears to represent a period of presumably more humid climate when small ponds and marshes dominated the floor of the West Amarillo Creek valley.

The samples used for this study were obtained from backhoe trench (BT) 36, the most complete record of Unit D. The base of the unit was more than 5 m below the surface with bedrock encountered at the bottom. The period represented by Unit D appears to last a little more than 1,000 years, from roughly 1900 years B.P. to sometime after 800 years B.P. (see geochronology below and Frederick [2008]).

M.4 MATERIALS AND METHODS

A total of 24 sediment samples were selected for paleontological analysis. Nineteen of them provided information on micro-invertebrates (ostracodes and mollusks) and gyrogonites to reconstruct the

paleoenvironmental history of the upper West Amarillo Creek valley. In addition, five large floatation samples were analyzed for mollusks to integrate the paleoecologic record of the marsh. The samples were in stratigraphic sequence. The age control is discussed above. The sediment samples were prepared using routine procedures (Forester 1988) modified by Palacios-Fest (1994). Samples were air-dried, weighed, and soaked in boiling distilled water with 1 g of Alcanox to disaggregate the sediments. It sat at room temperature for five days stirring the samples once a day. Using a set of three-sieves, the samples were wet-sieved to separate the coarse (>1 mm), medium (>106 μm), and fine (>63 μm) sand fractions to help identify the system's paleohydraulics. The very fine sand and silt and clay fractions were washed out at this stage. Therefore, the particle-size analysis departs from the formal United States Department of Agriculture (USDA) procedure (USDA 2003) and it is used only as a rough reference in this study. It is important to highlight that the possible discrepancy between the approach used in this investigation and that of the USDA is the result of grouping the very fine sands with the finer fractions, which in fact change the total percentage of sand, but does not affect the actual behavior of sands in the ecosystem. The value of the approach used here is that it provides a quick and easy way to process the data and to estimate the patterns of water discharge into the marsh overtime. More detailed particle-size analysis may be conducted using the appropriate research methods. The data are shown in Table M-1. Table M-2 shows the mineralogical composition of the marsh.

The samples were analyzed under a low-power microscope. All samples were examined to identify fossil contents and faunal assemblages. All samples contained ostracodes, mollusks and/or gyrogonites (Table M-3). All 24 samples contained mollusks (Tables M-4 and M-5). Fifteen samples contained ostracodes (Tables M-6

and M-7) and gyrogonites (Tables M-8 and M-9). These microfossils were not recorded, but observed in the five floatation samples. Total and relative abundance was recorded from the sediment samples. Based on Delorme (1969, 1989), standard taphonomic parameters, like fragmentation, abrasion, disarticulation (carapace/valve = C/V ratios), and adulthood (adult/juvenile = A/J ratios) were recorded to establish the ecology of the communities (synecology) as opposed to the ecology of single species (autoecology) of the ecosystem (Adams et al. 2002). However, autoecology was implemented to integrate the environmental framework. The specimens were placed in micropaleontological slides or acrylic boxes and saved in Terra Nostra Earth Sciences Research, LLC collection.

Taphonomic parameters were used to recognize degrees of transport and/or burial characteristics like desiccation and sediment compaction. The rates of fragmentation, abrasion and disarticulation are realistic indicators of transport; commonly these parameters show increasing damage with increasing transport. One must be cautious in using this criterion, but the nature of the deposits suggests that micro-invertebrates may reflect the marsh's hydraulic properties. Other features like encrustation and coating were used to determine authigenic mineralization or stream action, respectively. The redox index and color of valves reflected burial conditions. The A/J and C/V ratios were used as indicators of biocenosis (Whatley 1983; Palacios-Fest et al. 2001). For example, Brouwers (1988) indicates that the ideal tanathocenosis should be composed of a 1:8 adult:juvenile ratio as ostracodes shed their skeletons eight to nine times. Juvenile valves, however, are more fragile than the adults and more readily subject to the physical and chemical effects of weathering, modifying that ratio to 1:5 or 1:6 (Brouwers 1988). Whatley (1983), on the other hand, describing the effects of transport and burial concluded that abundant disarticulated valves indicate

natural burial conditions; whereas abundance of carapaces indicates fast deposition and burial preventing the valves from separating. These taphonomic criteria may be applied to ostracodes and clams, and to a lesser extent to snails.

Fifty-two pristine valves of *Cypridopsis vidua* and *Cypridopsis okeechobei*, two of the most common ostracodes in the marsh were selected for stable oxygen ($\delta^{18}\text{O}$) and carbon ($\delta^{13}\text{C}$) isotope analysis along with 71 specimens of *Chara globularis* and *Nitella flexilis*, the most abundant gyrogonites recovered from the site. Grouped by species, in most cases two replicates for each stratigraphic interval were analyzed (see Tables M-10 and M-11). The specimens were thoroughly cleaned with pure (megohms18) water and a fine brush (000), and then submitted for stable isotope analysis to the Environmental Isotope Laboratory of the University of Arizona. Oxygen and carbon stable isotope ratios were measured using an automated carbonate preparation device (KIEL-III) coupled to a gas-ratio mass spectrometer (Finnigan MAT 252). Samples were reacted with dehydrated phosphoric acid under vacuum at 70°C. The isotope ratio measurement is calibrated based on repeated measurements of NBS-19 and NBS-18 and precision is $\pm 0.1\text{‰}$ for $\delta^{18}\text{O}$ and $\pm 0.06\text{‰}$ for $\delta^{13}\text{C}$ (1 sigma). Five replicates of *Cypridopsis* sp. produced questionable data due to low sample size (samples #74, #76, and one for #82). A low voltage correction factor was applied to test their applicability to the analysis. The corrected values shown in Table M-10 have an uncertainty of $\pm 0.2\text{‰}$ (Dettman, written communication, May 27, 2009) suggesting the viability of the data. Isotopic data for calcites are reported in delta notation relative to the VPDB international scale (Coplen 1994).

Paleoenvironmental indices were prepared for mollusks and ostracodes. The mollusk qualitative paleoenvironmental index (PI) groups the species in aquatic and terrestrial

clusters. Current literature was used to identify the mollusk species and their ecological requirements (Eversole 1978; Dillon 2000, 2003; Rutherford 2000; Sharpe 2003; Webb 1942). The equation (1) used in this study is:

$$\text{PI} = (\Sigma \% \text{ Terrestrial Species}) - (\Sigma \% \text{ Aquatic Species}) \quad 1$$

The index positively weighs the terrestrial species and negatively weighs the aquatic species. Aquatic mollusks inhabit waters of different hydrochemical composition (Sharpe 2003).

The qualitative salinity index (SI) for ostracodes takes into consideration the salinity tolerance of the species present in the marsh based on our current knowledge of their ecological requirements presented in the North American Nonmarine Ostracodes Database (NANODe) website (Forester et al. 2005) and other references (Delorme 1989; Palacios-Fest 1994; Curry 1999). The equation (2) used for the present study is:

$$\text{SI} = [8(\% \text{ Physocypria globula}) + 7(\% \text{ Candona patzcuaro}) + 6(\% \text{ Fabaeformiscandona caudata}) + 5(\% \text{ Cypridopsis vidua}) + 4(\% \text{ Ilyocypris bradyi}) + 3(\% \text{ Herpetocypris brevicaudata}) + 2(\% \text{ Potamocypris smaragdina}) + (\% \text{ Pseudocandona stagnalis})] - [(\% \text{ Darwinula stevensoni}) + 2(\% \text{ Eucypris meadensis}) + 3(\% \text{ Limnocythere floridensis}) + 4(\% \text{ Physocypria pustulosa}) + 5(\% \text{ Cypria ophthalmica}) + 6(\% \text{ Cavernocypris wardi}) + 7(\% \text{ Cypridopsis okeechobei})] \quad 2$$

The index positively weighs species with incrementally higher salinity tolerances and negatively weighs species with incrementally lower salinity tolerances.

The ecological requirements of calcareous algae are used in this study to generate an alkalinity index (AI), using the same model

as for mollusks and ostracodes. The equation (3) for the Charales is:

$$AI = (2 * \% Chara\ globularis + \% Chara\ filiformis) - \% Nitella\ flexilis \quad 3$$

The index positively weighs species with incrementally higher pH tolerance, and negatively species with incrementally lower pH tolerance. As indicated in Table M-8, the alkalinity range for calcareous algae is 7.5 to 10.5 (Coletta et al. 2001; Andrews et al. 2004; Pentecost et al. 2006).

Aquatic micro-invertebrates and calcareous algae inhabit waters of different hydrochemical composition, but at the species level many are very sensitive to water chemistry. Ostracode, mollusk, and calcareous algae assemblages can be used to recognize the three major water types defined by Eugster and Hardie (1978):

Type I: Ca²⁺, Mg²⁺, and HCO₃⁻ - dominated water; typically freshwater or very low salinity conditions.

Type II: Ca²⁺ -enriched/HCO₃⁻ - depleted water; additionally containing the combinations of Na⁺, Mg²⁺, SO₄²⁻, or Na⁺, Mg²⁺, Cl⁻; ranges from low salinity to hypersaline conditions.

Type III: Ca²⁺ -depleted/HCO₃⁻ + CO₃²⁻ (alkaline)-enriched water; usually containing combinations of Na⁺, Mg²⁺, Cl⁻, or Na⁺, Mg²⁺, SO₄²⁻; ranges from low salinity hypersaline conditions.

The application of this model to paleoenvironmental reconstructions is, to the best of my knowledge, better known for ostracodes. This spectrum clearly shows that water chemistry plays a major role in the geographic distribution of ostracodes. In addition to water chemistry, temperature is another factor that affects the distribution of these organisms, as the latitudinal distribution of ostracodes demonstrates. Many species respond to temperature

through both reproductive and survival ability (De Deckker and Forester 1988; Delorme and Zoltai 1984; Forester 1987). For example, *Cytherissa lacustris* is limited to water temperatures lower than 23°C, and is common in subpolar regions, whereas *Limnocythere bradburyi* is restricted to warm temperatures of low to mid-latitudes (Delorme 1978; Forester 1985). Their sensitivity to temperature makes ostracodes very useful for paleoclimate reconstructions (Cohen et al. 2000; Palacios-Fest 2002). Once the ecological requirements of ostracodes are determined, it is possible to reconstruct paleoenvironments from the geologic record (Delorme 1969; Holmes and Chivas 2002; Palacios-Fest 1994).

M.5 RESULTS

M.5.1 AGE CONTROL AND SEDIMENTARY RECORD

Frederick (2008) describes the stratigraphy of the upper West Amarillo Creek valley. In brief, six episodes of alluviation formed the West Amarillo Creek Valley, namely Units A through F. In a composite model Frederick (2008) hypothesizes on the origin and evolution of each unit (see Figure 3 of Frederick 2008). In this study, Unit D is the center of interest where the marsh developed. Overlying Unit C, a very distinctive deposit consisting of black (10YR 2/1) to dark grayish brown (10YR 4/2) or light brownish gray (10YR 6/2) silty sand to silty clay forms Unit D (Table M-1). The dominant minerals recognized in the marsh deposits are quartz and feldspars indicating its alluvial origin. Calcium carbonate nodules and root casts are common throughout the stratigraphic column indicating its alkaline nature. Other minerals are rare to very rare, but mollusk and ostracode shell fragments are moderately common (Table M-2). It is more than 4.5 m thick representing a period of presumably more humid climate that allowed the formation of small ponds and marshes in the area. The episode lasted

slightly more than 1,000 years. Unit D is capped by Unit E.

The geochronology, discussed in Frederick (2008), is based on four radiocarbon dates obtained from Unit D (Table M-1). The most detailed record was obtained from BT 36 which exposed a series of superimposed channels associated with the unit. At its base, is thicker than 5 m below the surface and not completely exposed during excavation of the trench. The earliest phase of sedimentation started sometime before 1890 ± 40 years B.P. (Beta-210070), a period characterized by more than 50% calcium carbonate deposited on the valley floor. The middle of the unit was dated to 1430 ± 40 years B.P. (Beta-239651); whereas the youngest date obtained for Unit D at BT 36 post-dates 750 ± 40 years B.P. (Beta-239652). Between 270 and 290 cm below ground surface (bgs), the dates obtained are in reverse order complicating the interpretation about the conclusion of the depositional history of Unit D. It undoubtedly terminates before 430 ± 40 years B.P., which is a radiocarbon age obtained from cultural material buried at the base of Unit E at the 41PT245 (Frederick 2008).

Based upon the geochronology of Unit D three sedimentation rates were obtained that permit identifying three paleoenvironmental phases during the unit's history: (1) the Lower Marsh phase (1890 ± 40 years B.P. to 1430 ± 40 years B.P.); (2) the Middle Marsh phase (1430 ± 40 years B.P. to 750 ± 40 years B.P.); and (3) the Upper Marsh phase (post- 750 ± 40 years B.P.). These rates indicate a gradual decrease in sediment accumulation from 0.32 cm yr⁻¹ during the Lower Marsh phase to 0.07 cm yr⁻¹ during Middle Marsh phase, back to 0.33 cm yr⁻¹ during the Upper Marsh phase (Table M-1). Coarsening upwards sediments mark the increasing sedimentation rate recorded at this interval.

Figure M-1 shows the composite chronostratigraphy including the trend of sand content distribution throughout the history of Unit D. For this study, roughly five stratigraphic horizons, occasionally interrupted by thin marly beds, were identified at BT 36. Based on field descriptions Horizon I, thicker than 60 cm, consists of dark gray to light gray clay with gravel and sand intervals. Horizon II, approximately 124 cm thick, consists of gray sand with gravel lenses. Horizon III, approximately 71 cm thick, consists of black clay. Horizon IV, approximately 50 cm thick, consists of marly, black clay; and Horizon V, more than 20 cm thick, consists of black clay (personal interpretation based on Frederick 2008).

M.6 THE BIOLOGICAL RECORD

Table M-3 summarizes the biological contents of the marsh and the overall taphonomic characteristics recorded. Ostracodes, mollusks, and calcareous algae are the groups present. Table M-4 shows the ecological characteristics of the mollusk species present at the upper West Amarillo Creek valley. Table M-5 shows the mollusk total population by sample and total and relative abundance by species per sample. Adulthood ratios by species are also listed to establish the biocenosis. Table M-6 lists the ostracode species recorded at Unit D including their ecological requirements; whereas Table M-7 summarize the total population by sample and total and relative population by species per sample. Adulthood and disarticulation ratios are included to assist in recognizing autochthony versus allochthony of the specimens. The calcareous algae record is documented in Tables M-8 and M-9. Table M-8 shows the ecological requirements of the species identified and Table M-9 presents the total and relative abundance of the species per sample.

Figure M-2 shows the total population of ostracodes, mollusks and gyrogonites recorded at Unit D of the upper West Amarillo Creek valley. The total number of specimens counted is presented in a logarithmic scale to facilitate identification of population trends by each group. Mollusks and gyrogonites are the most abundant. Ostracodes and mollusks the most diverse as described below.

M.6.1 MOLLUSKS

Mollusks are very rare to extremely abundant* (6 to 1,453 specimens) and diverse (20 species) (Figure M-2). The species identified are the Physidae *Physa virgata* (Gould 1855), *Physella gyrina aurea* (Say 1821), *Stagnicola elodes* (Say 1821), the Planorbidae *Gyraulus parvus* (Say 1817), *Planorbella scalaris* (Jay 1839), *Planorbella trivolvis intertextum* (Say 1817), *Planorbella trivolvis lenta* (Say 1817), *Micromenetus brogniartiana* (Lea 1842), the Lymnaeidae *Fossaria cubensis* (Pfeiffer 1839), *Pseudosuccinea columella* (Say 1825), the Ancyliidae *Laevapex (Ferrisia) hendersoni* (Walker 1908), the Hdyrobidae *Somatogyrus walkerianus* (Aldrich 1905), the Sphaeridae *Pisidium* sp. (Pfeiffer 1821), *Sphaerium transversum* (Say 1817), the Pupillidae *Pupoides* sp. 1, and *Pupoides* sp. 2, *Gastrocopta procera* (Gould 1840), *Gastrocopta tappaniana* (Adams, 1841), *Columella simplex* (Gould 1840), and the Polygyridae *Polygyra* ? sp. (Tables M-4 and M-5).

Figures M-3 and M-4 show the mollusk paleontologic and paleoecologic records for the upper West Amarillo Creek valley. Amongst the aquatic species, *G. parvus* is the dominant species throughout the stratigraphic column followed by *P. virgata* and to a lesser extent *S. walkerianus*, *Pisidium* sp. and *S. transversum*. Other

species occur sporadically. *Pupoides* sp. 1 and *G. procera* are the two most common terrestrial forms co-occurring with the aquatic forms. Other terrestrial gastropods seldom occur throughout the sedimentary record (Figure M-3).

The paleoenvironmental index generated from this faunal assemblage shows the fluctuations between terrestrial- and aquatic-dominated conditions overtime (Figures M-3 and M-4). For example, Figure M-2 indicates that Unit D was mostly an aquatic environment. Between 1890 ± 40 years B.P. and 1430 ± 40 years B.P. Unit D transformed from a terrestrial to an aquatic system as indicated by the dominance of *Pupoides* sp. 1, *G. procera*, and *M. brogniartiana* at the base, replaced by *G. parvus*, *L. (F.) hendersoni*, and *Pisidium* sp. towards the end of the Lower Marsh phase. Fluctuating conditions ranged from terrestrial to standing to flowing overtime.

At the Middle Marsh phase, between 1430 ± 40 and 750 ± 40 years B.P. co-occurrence of terrestrial and aquatic forms suggest the environment was mostly standing; ranging from stagnant to riparian conditions where some terrestrial forms thrived. *G. parvus* was the most common species alternating with the terrestrial snail *Pupoides* sp. 1. However, occurrence of *Pisidium* sp. and *L. (F.) hendersoni* at some intervals indicates a flowing environment at times. Fluctuations between flowing and standing conditions may have resulted from groundwater level changes or increasing effective precipitation or, more likely, a combination of both, suggesting mesic conditions. Figure M-3, as for the Lower phase shows a stronger terrestrial signatures due to the presence of *G. procera*, *G. tappaniana*, *Pupoides* sp. 1, *C. simplex*, and *M. brogniartiana*. The apparent discrepancy with Figure M-2 might be the result of sampling location with the large samples proceeding from a portion of the marsh closer to its edge.

* Abundance explanation: extremely abundant (>301), very abundant (>101<300), abundant (>51<100), common (>21<50), rare (>11<20), very rare (>6<10), and extremely rare (<5).

The Upper Marsh phase (post-750 ± 40 years B.P.) was characterized by the common occurrence of *Pisidium* sp. and *S. transversum* in an environment dominated by *G. parvus* and *P. virgata*. Mollusks reached their greatest concentrations (Figure M-2). Increasing flowing conditions prevailed in the marsh at this time. Some terrestrial species, however, occurred in the interval indicating the proximity of this environment to the sampling location. At this phase both Figures M-2 and M-7 show a strong aquatic signature suggesting increasing water discharge into the marsh generating a flowing environment. However, the overall record is not as diverse and abundant suggesting increasingly xeric conditions.

M.6.2 OSTRACODES

Ostracodes are extremely rare to extremely abundant (2 to 422 specimens) and diverse (15 species) (Figure M-2). The species identified are *Physocypria globula* (Furtos 1933), *Candona patzcuaro* (Tressler 1954), *Fabaeformiscandona caudata* (Kaufmann 1900), *Cypridopsis vidua* (Müller 1776), *Ilyocypris bradyi* (Sars 1890), *Herpetocypris brevicaudata* (Kaufmann 1900), *Potamocypris smaragdina* (Vavra 1891), *Pseudocandona stagnalis* (Sars 1890), *Darwinula stevensoni* (Brady and Robinson 1890), *Eucypris meadensis* (Gutentag and Benson 1962), *Limnocythere floridensis* (Keiser 1976), *Physocypria pustulosa* (Sharpe 1897), *Cypria ophthalmica* (Jurine 1820), *Cavernocypris wardi* ? (Marmonier et al. 1989), and *Cypridopsis okeechobei* (Furtos 1933) (Tables M-6 and M-7). *H. brevicaudata* as *E. meadensis*, *C. okeechobei*, and *C. vidua*, is a crenophilous species (thriving in springs).

Figure M-5 shows the paleontologic and paleoecologic records for the upper West Amarillo Creek valley. *C. vidua* and *P. pustulosa* are the dominant species over time. Other species occur intermittently throughout the geologic record. Their

occurrence, however, is used to determine environmental trends. *L. floridensis*, for example, is a species with stenotopic (restricted) preferences. Forester et al. (2005) reported this species from a few sites in eastern Texas where the total dissolved solids (TDS) ranged between 200 and 1,000 mg L⁻¹ and the carbonate alkalinity/Ca is about 1.00 meq L⁻¹. The species appeared at the end of the Lower Marsh phase and thrived through the lower part of the Middle Marsh phase to appear for the last time once in the lower portion of the Upper Marsh phase. Its occurrence is inferred to be associated with dilute water pulses entering the system, mesic conditions.

The *candonid* *P. stagnalis* occurred at the end of the Middle Marsh phase to disappear in the lower part of the Upper Marsh phase. This species is characterized by a wider salinity range than *L. floridensis* with which it did not co-exist in this study. The sporadic occurrence of other species indicates the limited variability of the environment. That is the case of *I. bradyi*, a streamflow indicator occurring at the transition from the Lower- to the Middle Marsh phase suggesting a period of increasing water discharge into the basin. *I. bradyi*, however, is not restricted to flowing waters but its presence in this interval is consistent with the interpretation of a flowing environment drawn in the mollusk section.

The salinity index created for this study indicates variations in water chemistry during deposition of Unit D associated with increasing water table and effective precipitation (Figure M-5). While mollusks indicate that most of the Lower Marsh phase (1890 ± 40 years B.P. to 1430 ± 40 years B.P.) was aquatic, the ostracode salinity index suggests dominantly saline waters prevailed overtime with minor fluctuations to more dilute conditions, except for the upper part where dilute conditions characterized the end of the phase. Occurrence of *L. floridensis*, *C. ophthalmica*, and *D.*

stevensoni, with the crenophilus species *E. meadensis*, *I. bradyi*, *C. okeechobei* and *C. vidua* towards the end of the phase imply rising water table and spring discharge. Salinity did not exceed 4,000 mg L⁻¹ TDS (the maximum salinity tolerance of *C. vidua*) during the saline periods. It was limited to less than 800 mg L⁻¹ TDS at the time *C. okeechobei* thrived in the environment. The mean TDS, however, roughly ranged around 1,000 mg L⁻¹, the optimal salinity for several species to complete their life-cycle.

During the Middle Marsh phase (1430 ± 40 years B.P. to 750 ± 40 years B.P.), rapid variations in the faunal assemblage containing up to nine species throughout the interval, indicate a period of alternating increasing and decreasing salinity in response to evapotranspiration during mesic conditions. Salinity ranged around 1,000 mg L⁻¹ TDS. *C. vidua* and *P. pustulosa* continued to dominate the environment. *L. floridensis* played a more significant role (as explained earlier in this section) at this time than before or after. Occurrence of *C. wardi* (a spring indicator) at the base of the Middle Marsh phase, is in good agreement with the conclusion of the former interval. The species identification, however, is uncertain. Increasing populations around 300 cm bgs indicate an ecological change that concludes with the accumulation of sediments during the Upper Marsh phase. Frequent occurrence of terrestrial snails in this phase is consistent with this interpretation.

The Upper Marsh phase (post-750 ± 40 years B.P.), experienced a less variable record with values indicating increasing salinity as *P. globula* (a high salinity tolerant species; Forester et al. 2005) appeared at about 245 cm bgs. The species was limited to that interval implying that rather than salinity it may indicate a spring source as groundwater table rose. *C. vidua* and *P. pustulosa* continued to dominate the environment this time associated with *P. globula*, *P. smaragdina*, *P. stagnalis*, *D.*

stevensoni, and *C. okeechobei*. Some crenophilus species, like *C. okeechobei* thrived in the lower portion of this phase, consistent with a spring source to the marsh. *C. okeechobei*, however, disappeared as more saline species entered the system. Occurrence of *P. smaragdina*, *P. stagnalis*, and *D. stevensoni* suggest salinity exceeded 1,000 mg L⁻¹ as *P. globula* disappeared from the marsh. During this interval, ostracodes reached their greatest concentration supporting the hypothesis of a flowing, stable environment as xeric conditions started to dominate (Figures M-2 and M-7).

M.6.3 CHAROPHYTA

The gyrogonites of Charales are extremely rare to extremely abundant (2 to 10,000+ specimens). Low diversity characterized the group (three species) including *Chara globularis* Thuillier, *Chara filiformis* (Herstch), and *Nitella flexilis* (Linnaeus, pro parte). While *C. globularis* and *C. filiformis* prefer high pH (>8.5), *N. flexilis* thrives in lower pH (<8.5) (Tables M-8 and M-9). The gyrogonites of *C. globularis* are the most common and abundant in the stratigraphic sequence. *C. filiformis* scatters throughout the record, whereas *N. flexilis* is limited to the Middle and Upper Marsh phases. Based on the species abundance and the alkalinity index developed for the group, Figure M-6 shows the variations in pH suggested by the gyrogonites.

At the base of the Lower Marsh phase (ca. 1890 ± 40 years B.P.), *C. globularis* and *C. filiformis* co-occurred in the system. To disappear for most of the record in response to increasing aridity. Rising water table introduced both species near the end of the period (Figure M-6). The transition from the Lower- to Middle Marsh phase (ca. 1430 ± 40 years B.P.) is marked by the appearance of *N. flexilis*, a species that prefers a pH lower than 8.5 dominating the early stages of the Middle Marsh phase. Lower pH may be the results of increasing

effective precipitation during more mesic conditions. *N. flexilis* declined as alkalinity rose to levels more favorable to *C. globularis* that remained the dominant species during the Upper Marsh phases more xeric conditions prevailed. The alkalinity index trend shown in Figure M-6 is consistent with the ostracode paleosalinity index implying a period of increasing salinity at the decline of *N. flexilis* to return to moderate salinity as discussed in the ostracode section. Similar to mollusks and ostracodes, gyrogonites reached their greatest concentration supporting the interpretation of a well-oxygenated, flowing, and stable environment (Figures M-2 and M-7).

In addition to the paleoecological signatures of ostracodes, mollusks, and calcareous algae, the stable isotope analyses of ostracodes and gyrogonites provided important information to reconstruct the environment. The geochemical results are discussed in the following section.

M.7 THE STABLE ISOTOPE DATA

Stable isotope values for *Cypridopsis* sp. and the gyrogonites are plotted in Figures M-7 and M-8. The Lower Marsh phase is mostly deprived of microfossils, occurring at the base and top of the interval, thus, stable isotope records are broken. The Middle and Upper phases generated valuable data. In *Cypridopsis* sp., $\delta^{18}\text{O}$ and $\delta^{13}\text{C}$ moderately covariant trends are evident at the base of the Lower Marsh phase and during the Middle Marsh phase, but not during the Upper Marsh phase. A secular isotopic trend for both the $\delta^{18}\text{O}$ and $\delta^{13}\text{C}$ values is discernible toward heavier values (Figure M-7). These values are consistent with Stable Isotope Stage 1 values recorded for the southern portion of the United States, especially Texas and the eastern states (Wright 2000).

The $\delta^{18}\text{O}$ in *Cypridopsis* sp. fluctuates between -3.5‰ and -6.25‰ just before the marsh coarse sediments limit the occurrence of microfossils. The moderately light $\delta^{18}\text{O}$ values suggest humid conditions at the Lower Marsh phase. The record resumes sometime around 1430 ± 40 years B.P. where $\delta^{18}\text{O}$ shows values around -6‰ increasing to heavier values towards the Middle Marsh phase where the values vary from -4‰ to 0.59‰; then, gradually declining to lighter values (-6‰) during the Upper Marsh Phase. The stable trend of the $\delta^{18}\text{O}$ during the Middle Marsh phase suggests the area was subject to steady aridity during a warm period equivalent to the Medieval Warm Period or Medieval Climatic Anomaly. The steady decline of the $\delta^{18}\text{O}$ values during the Upper Marsh phase indicates gradual cooling and wetter conditions at the onset of the Little Ice Age.

The $\delta^{13}\text{C}$ in *Cypridopsis* sp. (a nektonic species crawling on plants) are interpreted in terms of dissolved inorganic carbon (DIC) and alkalinity/salinity. Values of $\delta^{13}\text{C}$ in closed basins (as it is inferred Unit D was, at least during part of its environmental history) are less influenced by primary productivity than are open lakes (Stiller and Hutchinson 1980). The values fluctuate between -3.7‰ and -4.8‰ at the beginning of the record (Lower Marsh phase) to disappear with sediment coarsening implying more terrestrial influence into the basin. Increasing water table permitted the aquatic fauna and flora to thrive again in the system. At the end of the Lower Marsh phase (ca. 1430 ± 40 years B.P.) $\delta^{13}\text{C}$ values ranged around -3.5‰. During the Middle Marsh phase (1430 ± 40 years B.P. and 750 ± 40 years B.P.) $\delta^{13}\text{C}$ values fluctuated between the latter number and -2.3‰. As the marsh evolved into the Upper Marsh phase these values turned heavier (from -1.33‰ to 4.1‰) to return to lighter values towards the end of the record (-2‰ to -2.95‰).

$\delta^{18}\text{O}$ and $\delta^{13}\text{C}$ values are covariant during the Middle Marsh phase and the lower part

of the Upper Marsh phase suggesting a closed, shallow basin (Talbot 1990; Li and Ku 1997) as it may be expected during. Figure M-8 shows a moderate relationship ($r^2=0.58$) between $\delta^{18}\text{O}$ and $\delta^{13}\text{C}$ in *Cypridopsis* sp. supporting the close basin conditions of the marsh for most of its history (mostly during). Apparently, at about 250 cm bgs the marsh reached a breakpoint between $\delta^{18}\text{O}$ and $\delta^{13}\text{C}$. The covariance effect turns weaker or disappears towards the end of the record, consistent with the hypothesis of a deeper, more open system promoted by the cooling conditions of Little Ice Age.

In the gyrogonites $\delta^{18}\text{O}$ and $\delta^{13}\text{C}$ are covariant (Figure M-7) showing a moderate relationship ($r^2=0.60$) (Figure M-8). The secular isotopic trend for $\delta^{18}\text{O}$ and $\delta^{13}\text{C}$ fluctuate between lighter and heavier values. Similar to *Cypridopsis* sp. the $\delta^{18}\text{O}$ values at the base of the Lower Marsh phase (ca. 1890 \pm 40 years B.P.) start light (-6.7‰) to rapidly disappear due to terrestrial influence and lack of microfossils. At the end of the interval $\delta^{18}\text{O}$ values resumed more negative (greater than -7.0‰). It is significant to notice, that this is the interval where isotopic data were obtained from *N. flexilis* due to the absence of *C. globularis*. The trend, however, does not seem to disagree with other parameters like the alkalinity index derived from the gyrogonite paleoecologic data (Figure M-7).

At the transition to the Middle Marsh phase (1430 \pm 40 years B.P.) $\delta^{18}\text{O}$ values fluctuate between -5‰ and -6.9‰ remaining stable throughout the interval. The Upper Marsh phase (post-750 \pm 40 years B.P.) is also a stable episode with $\delta^{18}\text{O}$ values between -5.7‰ and -6.8‰ which makes impossible a distinction on environmental change.

At Unit D, $\delta^{13}\text{C}$ values ranged between -1.5‰ and -13.5‰. During the Lower Marsh phase (1890 \pm 40 years B.P.) the $\delta^{13}\text{C}$ ranged around -6.5‰ rapidly disappearing due to the lack of fossils and strong

terrestrial influence. As for the $\delta^{18}\text{O}$ at the transition to the middle marsh phase, *N. flexilis* was the gyrogonite present yielding lighter $\delta^{13}\text{C}$ values between -9.8‰ and -13.1‰. More importantly, at this interval a strong positive correlation exist between the $\delta^{13}\text{C}$ and alkalinity index diagrams suggesting the validity of the data. By contrast with the $\delta^{18}\text{O}$ trend at the Upper Marsh phase, the $\delta^{13}\text{C}$ show some variability in values ranging from -1.5‰ to -5.6‰.

Pentecost et al. (2006) demonstrated that in well-mixed environments, such as shallow streams the isotopic composition of charophytes is closer to equilibrium than samples taken from standing zones, such as shallow lakes. It is inferred in this study that the upper West Amarillo Creek valley marsh was a flowing system in which charophytes calcified gyrogonites near equilibrium. The stable isotope data, however, cannot be used to obtain reliable air temperature estimates because modern studies show a strong kinetic disequilibrium throughout the growth period of charophytes resulting from photosynthesis and chemical enhancement of the carbon dioxide.

M.8 DISCUSSION AND CONCLUSIONS

The combined paleoecologic and geochemical profiles provide a powerful tool for understanding the paleoclimatic history of Unit D. For the first time a complex record of mollusks, ostracodes, gyrogonites and stable carbon ($\delta^{13}\text{C}$) and oxygen ($\delta^{18}\text{O}$) isotopes are used to identify three paleoenvironmental phases in five stratigraphic horizons within Unit D of the upper West Amarillo Creek valley. The transition from terrestrial to aquatic conditions is delineated by the trends in mollusk populations and diversity. Occurrence of terrestrial gastropods throughout the record demonstrates the site was exposed to alternating episodes of wetter and drier conditions. Presence of

Pisidium sp. and *S. transversum* at some intervals advocate for flowing conditions associated with increasing water discharge into the basin as opposed to episodes of slow flowing (more standing) waters that favored the settlement of most of the gastropods identified in this study. During the Middle Marsh phase, abundant terrestrial mollusks indicate increasing aridity terminating near 750 ± 40 years B.P. at which time aquatic species invade the site implying wetter conditions during the Upper Marsh phase; a discrepancy with other signatures.

During aquatic stages, ostracodes and gyrogonites set the dominating conditions prevailing in the marsh. The occurrence of environmentally sensitive ostracode species like *L. floridensis*, *P. stagnalis*, *C. okeechobei*, and *C. ophthalmica* provide basic criteria to determine the paleohydrochemical changes in the upper West Amarillo Creek valley marsh. The paleosalinity index derived from the ostracode population and diversity allowed to infer that the marsh's salinity ranged between 300 mg L⁻¹ and 2,000 mg L⁻¹ TDS, mostly around 1,000 mg L⁻¹ TDS. The occurrence of *P. globula* (salinity tolerance up to 10,000 mg L⁻¹ TDS) suggests that at times salinity rose beyond 2,000 mg L⁻¹ TDS as aridity increased in the area. The introduction of *L. floridensis*, however, suggests that water salinity dropped below 800 mg L⁻¹ TDS (the species maximum tolerance), to rise and remain around 1,000 mg L⁻¹ TDS during the upper part of the Lower Marsh phase and all of the Middle Marsh phase. Rise and fall in salinity characterized the Upper Marsh phase suggesting increasing aridity followed by wetter conditions interpreted here as the transition between the and Little Ice Age.

The gyrogonites of charophytes provide significant information on the possible alkalinity of the marsh. The occurrence and sometimes co-occurrence of *C. globularis* (and *C. filiformis*) with *N. flexilis* advocates for fluctuating pH in the system. While

Chara thrives through waters with a high pH (>8.5) induced by rapid photosynthesis rates in small water bodies (Portie and Lijklema 1995), *Nitellas* are found growing in shallow to deep waters of soft (pH>8.5) or acid lakes and bogs (<http://www.ecy.wa.gov/programs/wq/plants/plantid2/descriptions/nit.html>). It is inferred in this study that alternating low to high alkalinity was driven by the reproduction rates of calcareous algae during the early warm to warm months of the year.

Charophyte fossils have proved valuable in the interpretation of sedimentary records throughout the Quaternary, Tertiary, and for parts of the Mesozoic and Paleozoic. Pentecost (1984) found a positive correlation of growth with water temperature in *Chara globularis*, consistent with the high productivity of gyrogonites recorded in this study. The relatively stable $\delta^{18}\text{O}$ trend overtime suggests the gyrogonites were produced mostly during the optimal growth season (late April-early July). Eutrophication and lake shallowing may have resulted from periods of high productivity as indicated by charophyte abundance and the alkalinity index.

The stable isotope signatures contributed to the paleoecological records to establish that the marsh was a closed basin most of the time as the $\delta^{13}\text{C}$ and $\delta^{18}\text{O}$ values of both *Cypridopsis* sp. and the gyrogonites co-varied throughout most of the time but turned weaker towards the upper part of the Upper Marsh phase. The change in the isotopic values over time is quite large (range of 6.8‰ $\delta^{18}\text{O}$ and 8.9‰ $\delta^{13}\text{C}$ in *Cypridopsis* and 2.8‰ $\delta^{18}\text{O}$ and 11.7‰ $\delta^{13}\text{C}$ in gyrogonites) indicating substantial climatic changes. The variations in isotopic values are interpreted as resulting primarily from changes in moisture conditions, affecting the abundance of drought-adapted CAM (Crassulacean acid metabolism) plant species (enriched in ^{13}C).

A correlation between the current stable isotope trends and those previously obtained from soil organic carbon (SOC) (Frederick 2008) is evident for the interval representing Unit D (Figure M-9). The main difference being that most of the Lower Marsh phase indicates an arid terrestrial environment deprived of aquatic forms; thus no direct correlation is available. The trend, however, suggests that as C₄ plants decrease, the $\delta^{13}\text{C}$ in SOC, the gyrogonites, and possibly *Cypridopsis* sp. become more negative implying increasing mesic conditions. By contrast, increasing C₄ plants in the area is associated with heavier $\delta^{13}\text{C}$ in SOC and gyrogonites, and somehow *Cypridopsis* sp. During the Middle Marsh Phase. The $\delta^{13}\text{C}$ of gyrogonites and SOC show increasingly heavier values; whereas the $\delta^{13}\text{C}$ of *Cypridopsis* sp. is variable. The Upper Marsh phase, however, shows a weak correlation.

In summary, it is interpreted that the upper West Amarillo Creek valley marsh at Unit D remained a year-round aquatic systems throughout most of its paleoenvironmental history. The marsh recorded, at least in part, the Medieval Climatic Anomaly and the transition into the Little Ice Age. This record is consistent with other studies across the nation (Petersen 1988; Stine 1990; Jones et al. 1999). The record is truncated by deposition of Unit E, preceded by arroyo-cutting sometime at or after 800 years B.P. The paleoecological signatures used for this study contributed diverse elements for the reconstruction of the marsh paleoenvironmental history. Radiocarbon dates younger than 750 ± 40 years B.P. are needed to close the geochronologic gap at the end of the record. A better understanding of the stable isotope signatures, especially of gyrogonites will permit a more precise interpretation of environmental change. This understanding will require the study of modern calcareous algae analogs in the vicinity of the Upper West Amarillo Creek valley.

M.9 REFERENCES

- Adams, K. R., S. J. Smith and M. R. Palacios-Fest
2002 Pollen and micro-invertebrates from modern earthen canals and other fluvial environments along the Middle Gila River, Central Arizona: Implications for archaeological interpretation. *Manuscript on file GRIC*, Sacaton, 61 pp.
- Allen, G. O.
1950 British stoneworts (Charophyta). Haslemere Natural History Society. Arbroath, T. Buncle and Co. Ltd. 52 pp.
- Andrews, J. E., P. Coletta, A. Pentecost, R. Riding, S. Dennis, P. F. Dennis, and B. Spiro
2004 Equilibrium and disequilibrium stable isotope effects in modern charophyte calcites: Implications for palaeoenvironmental studies. *Palaeogeography, Palaeoclimatology, Palaeoecology* 204:101-114.
- Becker, D., L. Picot, and J. P. Berger
2002 Stable isotopes ($\delta^{13}\text{C}$ and $\delta^{18}\text{O}$) of charophyte gyrogonites: example from the Brochene Fluh section (Late Oligocene-Early Miocene, Switzerland). *Geobios* 35:89-97.
- Bozarth, S.
2008 Appendix D: Opal phytolith analysis at 41PT186 and 41PT245 and palylonogical analysis at 41PT185/C. In *Final Interim Report for Phase I of the Data Recovery at Three Prehistoric Sites (41PT185, 41PT186, and 41PT245) Located within the Landis Property in Potter County, Texas*, edited by J. M. Quigg, C. D. Frederick, and K. G. Luedecke, pp. 138-151. Austin: TRC Project No. 150832.

- Brouwers, E. M.
1988 Sediment transport detected from the analysis of ostracod population structure: an example from the Alaskan Continental Shelf. In *Ostracoda in Earth Sciences*, edited by P. DeDeckker, J. P. Colin, and J. P. Peypouquet. Amsterdam: Elsevier, pp. 231-244.
- Caran, S. C.
1991 Cenozoic stratigraphy, southern Great Plains area. In *Quaternary Nonglacial Geology: Conterminous United States*, edited by R. B. Morrison, plate 5. Centennial vol. K-2. Boulder, Colorado: Geological Society of America.
- Cohen, A.S., M. R. Palacios-Fest, R. M. Negrini, P. E. Wigand and D. Erbes
2000 High resolution continental paleoclimate record for the middle-late Pleistocene from Summer Lake, Oregon, USA: II – Evidence of paleoenvironmental change from sedimentology, paleontology and geochemistry. *Journal of Paleolimnology*, 24:151-182.
- Coletta, P., A. Pentecost, and B. Spiro
2001 Stable isotopes in charophyte incrustations: Relationship with climate and water chemistry. *Palaeogeography, Palaeoclimatology, Palaeoecology* 173:9-19.
- Coplen, T. B.
1994 Reporting of stable hydrogen, carbon and oxygen isotopic abundances. *Pure Applied Chemistry* 66:273-276.
- Cotter, J. L.
1937 The occurrence of flints and extinct animals in pluvial deposits near Clovis, New Mexico, Part IV. Report on excavation at the gravel pit, 1936. *Proceedings of the Philadelphia Academy of Natural Sciences* 90:1-16.
- Curry, B. B.
1999 An environmental tolerance index for ostracodes as indicators of physical and chemical factors in aquatic habitats. *Palaeogeography, Palaeoclimatology, Palaeoecology* 148:51-63.
- De Deckker, P.
1983 The limnological and climatic environment of modern ostracodes in Australia - a basis for paleoenvironmental reconstruction. Proceedings of 8th International Symposia. Ostracoda edited by R. F. Maddocks, University of Houston, pp. 250-254.
- De Deckker, P. and R. M. Forester
1988 The use of ostracodes to reconstruct paleoenvironmental records. In *Ostracoda in the Earth Sciences*, edited by P. De Deckker, J. P. Colin, and J. . Peypouquet, pp. 175-200. Elsevier Scientific Publishers, Amsterdam, The Netherlands.
- Delorme, L. D.
1969 Ostracodes as Quaternary paleoecological indicators. *Canadian Journal of Earth Sciences* 6:1471-1476.
- 1978 Distribution of freshwater ostracodes in Lake Erie. *Journal Great Lakes Research, International Association Great Lakes Research* 4:216-220.
- 1989 Methods in Quaternary ecology #7: Freshwater ostracodes. *Geoscience Canada* 16(2):85-90.
- Delorme, L. D., and S. C. Zoltai
1984 Distribution of an arctic ostracode fauna in space and time. *Quaternary Research* 21(3):65-73.

- Dillon, R.T. Jr.
2000 *The ecology of freshwater molluscs*. Adobe eBook. Windows Vista/XP 2000.
- 2003 *The Freshwater gastropods of South Carolina*. College of Charleston, Charleston, SC. Website: <http://www.cofc.edu/~dillonr/FWG> SC
- Eugster H. P. and L. A. Hardie
1978 Saline lakes. In: Lerman, A. (ed.). *Lakes: Chemistry, geology, physics*. New York: Springer-Verlag, pp. 237-293.
- Eversole, A.
1978 Life cycles, growth and population bioenergetics of the snail, *Helisoma trivolvis* (Say). *J. Moll. Stud.*, 44:209-222.
- Eyles, N. and H. P. Schwarcz.
1991 Stable isotope record of the last glacial cycle from lacustrine ostracodes. *Geology* 19:257-260.
- Feist, M.
2003 Report on the Symposium, 1st International Symposium on Extant and Fossil Charophytes. Montpellier, France, July 4-8. 1989. School of Earth and Environmental Sciences. University of Wollongong. Website: <http://www.uow.edu.au/science/eesc/research/irgc/meeting1.html>
- Forester, R. M.
1983 Relationship of two lacustrine ostracode species to solute composition and salinity: Implications for paleohydrochemistry. *Geology* 11:435-438.
- 1985 *Limnocythere bradburyi* n. sp.: A modern ostracode from central Mexico and a possible Quaternary paleoclimate indicator. *Journal of Paleontology* 59:8-20.
- 1986 Determination of the dissolved anion composition of ancient lakes from fossil ostracodes. *Geology* 14:796-799.
- 1987 Late Quaternary paleoclimate records from lacustrine ostracodes, Chapter 12. In *The Geology of North America*, vol. K-3, North America and adjacent oceans during the last deglaciation, The Geological Society of America, pp. 261-276.
- 1988 Nonmarine calcareous microfossils sample preparation and data acquisition procedures. *U.S. Geological Survey Technical Procedure HP-78, R1*, pp. 1-9.
- 1991 Ostracode assemblages from springs in the western United States: Implications for paleohydrology. *Mem. ent. Soc. Can.* 155: 181-201.
- Forester, R. M., Smith, A. J., Palmer, D. F., and Curry, B. B.
2005 North American Non-Marine Ostracode Database "NANODE" Version 1, December, <http://www.kent.edu/NANODE>, Kent State University, Kent, Ohio, U.S.A.
- Frederick, C. D.
2008 Stratigraphic Overview of the Upper West Amarillo Creek Valley, Chapter 3. In *Final Interim Report for Phase I of the Data Recovery at Three Prehistoric Sites (41PT185, 41PT186, and 41PT245) Located within the Landis Property in Potter County, Texas*, edited by J. M. Quigg, C. D. Frederick, and K. G.

- Luedecke, pp. 18-30. Austin: TRC Project No. 150832.
- Garcia, A.
1994 Charophyta: Their use in paleolimnology. *Journal of Paleolimnology* 10:43-52.
- Haecker, C. M.
1999 *Phase I Archeological Survey: Amarillo and Exell Helium Plants and Landis Property, Potter and Moore Counties, Texas*. National Park Service, Intermountain Support Office, Anthropology Program, Santa Fe, New Mexico for the Bureau of Land Management, Helium Operations Unit, Amarillo, Texas.
- Holmes, J. A. and A. R. Chivas
2002 Ostracod shell chemistry- Overview. In *The Ostracoda: Applications in the Quaternary Research*, edited by J. A. Holmes and A. R. Chivas, pp. 185-204. Wasington, D.C.: American Geophysical Union, Geophysical Monograph 131.
- Horne, D. J., A. Cohen, and K. Martens
2002 Taxonomy, morphology and biology of Quaternary and living Ostracoda. In *The Ostracoda: Applications in the Quaternary Research*, edited by J. A. Holmes and A. R. Chivas, pp. 5-36. Wasington, D.C.: American Geophysical Union, Geophysical Monograph 131.
- Howard, C. D.
1935 Evidence of early man in North America. *The Museum Journal* (University of Pennsylvania) 24:61-175.
- Humphrey and R. Ferring
1994 Stable isotopic evidence for latest Pleistocene and Holocene climatic change in north-central Texas. *Quaternary Research* 41:200-213.
- Johnson, E. and V. T. Holliday
2004 Archaeology and late Quaternary environments of the Southern High Plains, Chapter 9. In *Prehistory of Texas*, edited by T. K. Perttula, pp. 283-295. College Station: Texas A&M University Press.
- Jones, T., G. Brown, M. Raab, L. Mark. McVickar, W. Spaulding, Geoffrey. Kennett, Douglas. York, Andrew. P. L. Walker
1999 Environmental Imperatives Reconsidered. *Current Anthropology* 40:137-170.
- Lewis, Michael, C. F., D. K. Rea, D. L. Dettman, A. M. Smith, and L. A. Mayer
1994 Lakes of the Huron basin: their record of runoff from the laurentide ice sheet. *Quaternary Science Reviews* 13(9-10):891-922.
- Li, H. C. and T. L. Ku
1997 $\delta^{13}\text{C}$ - $\delta^{18}\text{O}$ covariance as a paleohydrological indicator for closed-basin lakes. *Palaeogeography, Palaeoclimatology, Palaeoecology* 133:69-80.
- Lister, G. S.
1988 Stable isotopes from lacustrine Ostracoda as tracers for continental paleoenvironments. In *Ostracoda in Earth Sciences*, edited by P. De Deckker, J. P. Colin, and J. P. Peypouquet, pp. 210-218. Elsevier Science Publications, Amsterdam, The Netherlands.
- Palacios-Fest, M. R.
1994 Nonmarine ostracode shell chemistry from Hohokam irrigation canals in Central Arizona: A paleohydrochemical tool for the interpretation of prehistoric human occupation in the North American

- Southwest. *Geoarchaeology* 9(1):1-29.
- 2002 Significance of ostracode studies in geoarchaeology: A way to analyze the physical environment where ancient civilizations developed. *The Kiva* 68(1):49-66.
- 2008 Younger Dryas Ostracode Paleocology of Scholle Cienega, Abo Arroyo, New Mexico. Tucson: TNESR Report 08-10, 15 pp.
- Palacios-Fest, M. R., A. S. Cohen and P. Anadon
- 1994 Use of ostracodes as paleoenvironmental tools in the interpretation of ancient lacustrine records; *Revista Española de Micropaleontología*, 9(2):145-164.
- Palacios-Fest, M. R., J. B. Mabry, F. Nials, J. P. Holmlund, E. Miksa and O. K. Davis
- 2001 Early irrigation systems in Southeastern Arizona: The ostracode perspective. *Journal of South American Earth Sciences* 14(5):541-555.
- Palacios-Fest, M. R., A. L. Carreño, J. R. Ortega-Rámirez and G. Alvarado-Valdéz
- 2002 A paleoenvironmental reconstruction of Laguna Babícora, Chihuahua, Mexico based on ostracode paleoecology and trace element shell chemistry. *Journal of Paleolimnology*. 27(2):185-206.
- Pentecost, A.
- 1984 The growth of *Chara globularis* and its relationship to calcium carbonate deposition in Malham Tarn. *Field Studies* 6:53-58.
- Pentecost, A., J. E. Andrews, P. F. Dennis, A. Marca-Bell, and S. Dennis
- 2006 Charophyte growth in small temperate water bodies: Extreme isotopic disequilibrium and implications for the palaeology of shallow marl lakes. *Palaeogeography, Palaeoclimatology, Palaeoecology* 240:389-404.
- Petersen, K. L.
- 1988 Climate and the Dolores River Anasazi. *Univ. Utah Anthropological Papers* No. 113. 152 pp.
- Pokorný, V.
- 1978 Ostracodes. In *Introduction to marine micropaleontology*, edited by Bilal U. Haq and Anne Boersma, pp 109-149. Elsevier North Holland, New York.
- Portiele R. and L. Lijklema
- 1995 Carbon dioxide fluxes across the air-water interface and its impact on carbon availability in aquatic systems. *Limnol. Oceanogr.* 40:690-699.
- Quigg, J. M.
- 2008 Introduction, Chapter 1. In *Final Interim Report for Phase I of the Data Recovery at Three Prehistoric Sites (41PT185, 41PT186, and 41PT245) Located within the Landis Property in Potter County, Texas*, edited by J. M. Quigg, C. D. Frederick, and K. G. Luedecke, pp. 1-4. Austin: TRC Project No. 150832.
- Quigg, J. M., C. D. Frederick, and K. G. Luedecke
- 2008 Final Interim Report for Phase I of the Data Recovery at Three Prehistoric Sites (41PT185, 41PT186, and 41PT245) Located within the Landis Property in Potter County, Texas. Austin: TRC Project No. 150832.

- Rutherford, J.
2000 Ecology illustrated field guides. Wilfrid Laurier University, Waterloo, Ontario, website: <http://info.wlu.ca/~wwwbiol/bio305/Database>
- Sellards, E. H.
1952 Early man in America: A study in prehistory. Austin: University of Texas Press.
- Sharpe, S.
2002 Solute composition: a parameter affecting the distribution of freshwater gastropods. Conference proceedings: Spring-fed wetlands: Important scientific and cultural resources of the Intermontane Region. <http://wetlands.dri.edu>
- Stiller, M. and G. E. Hutchinson
1980 The waters of Merom: A study of Lake Huleh, part-1- Stable isotopic composition of carbonates of a 54 m core, paleoclimatic and paleotrophic implications. *Archiv für Hydrobiologie*, 89:275-302.
- Stine, S.
1990 Late Holocene fluctuations of Mono Lake, eastern California. *Palaeogeography, Palaeoclimatology, Palaeoecology* 78: 333 – 381.
- Talbot, M. R.
1990 A review of the paleohydrological interpretations of carbon and oxygen isotopic ratios in primary lacustrine carbonates. *Chemical Geology* (Isotope Geoscience Section) 80:261-279.
- Talbot, M. R. and K. Kelts
1990 Paleolimnological signatures from carbon and oxygen isotopic ratios in carbonates from organic carbon-rich lacustrine sediments. In *Lacustrine basin exploration: Case studies and modern analogs*, edited by B. J. Katz, pp. 99-112, AAPG Memoirs 50.
- United States Department of Agriculture (USDA)
2003 *Soils survey manual*. University Press of the Pacific, Honolulu, Hawaii, pp. 207-209.
- Von Grafenstein, U., U. Eicher, H. Erlenkeuser, P. Ruch, J. Schwander, and B. Ammann
2000 Isotope signature of the Younger Dryas and two minor oscillations at Gerzensee (Switzerland): palaeoclimatic and palaeolimnologic interpretation based on bulk and biogenic carbonates. *Palaeogeography, Palaeoclimatology, Palaeoecology* 159:215-229.
- Webb, W. F.
1942 United States Mollusca: A Descriptive Manual of Many of the Marine, Land and Fresh Water Shells of North America, north of Mexico. Walter Freeman Webb, 1st Edition, Bookcraft Press, New York.
- Wendorf, F.
1961 Paleoeology of the Llano Estacado. Santa Fe Museum of New Mexico Press.
- Wendorf, F. and J. J. Hester
1975 *Late Pleistocene environments of the Southern High Plains*. Publication of the Fort Burgwin Research Center 9. Dallas: Department of Anthropology, Southern Methodist University.
- Whatley, R.
1983 Some simple procedures for enhancing the use of Ostracoda in

- palaeoenvironmental analysis. *NPD Bulletin* (2):129-146.
- Wright, J. D.
2000 Global climate change in marine stable isotope records. (http://geology.rutgers.edu/~jdwright/JDWWeb/1999/JDWright_NUREG.pdf), downloaded May 18, 2009.
- Wrozyna, C., P. Frenzel, P. Steeb, L. Zhu, R. van Gelden, A. Mackensen and A. Schwalb.
2009 Stable isotope and ostracode species assemblage evidence for lake level changes of Nam Co, southern Tibet, during the past 600 years. *Quaternary International* 200(1-2)

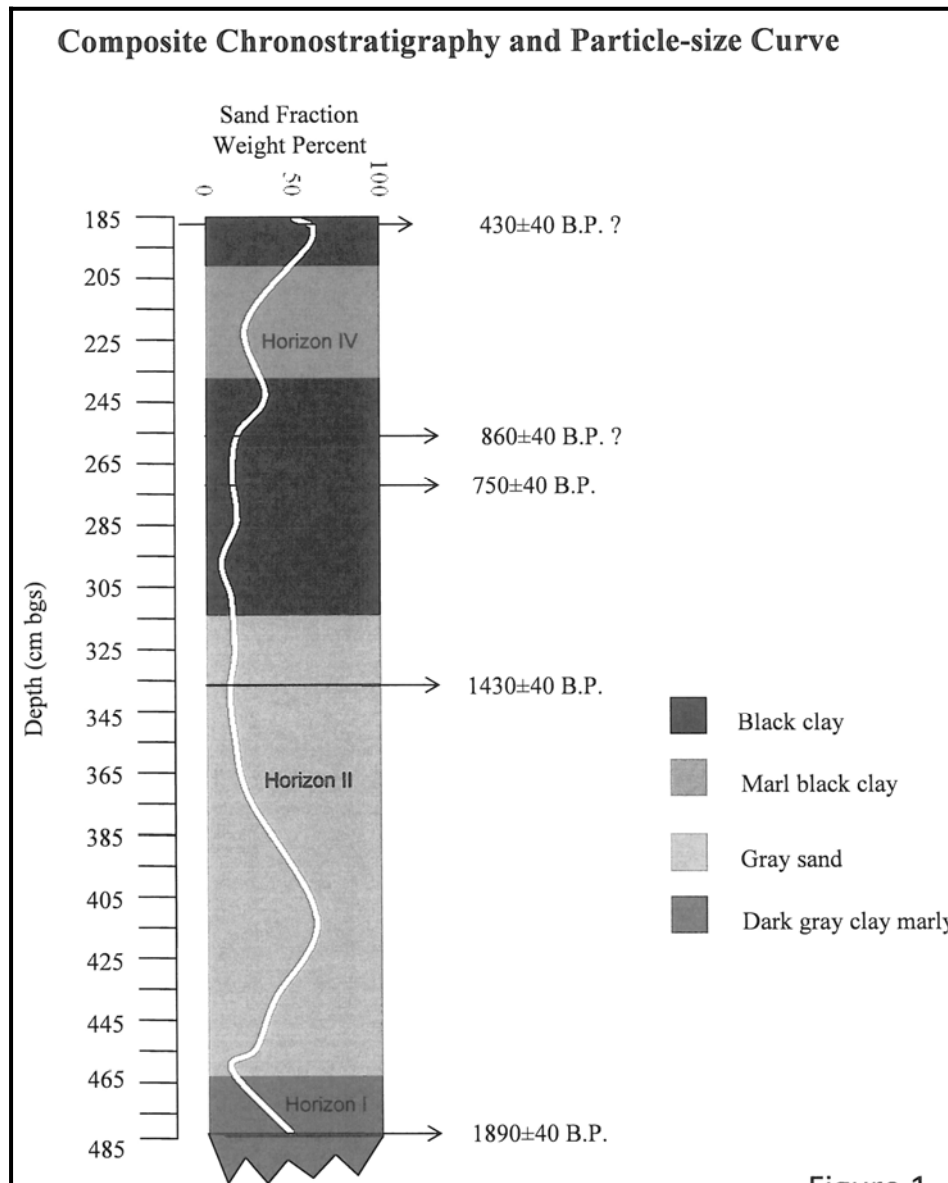


Figure M-1. Composite Chronostratigraphic Column and Sand Fraction-Size Curve

Note: Shows the trend of sediment input overtime for BT 36 at 41PT185/C, in Upper West Amarillo Creek valley, Texas. The upper age [430 ± 40 years. B.P.] is questionable because it is borrowed from Unit E. The 860 ± 40 years B.P. age is in reverse order with respect to the age below, considered a reliable date for this study [see Frederick 2008]. Based on the lithostratigraphy, five stratigraphic horizons are recognized in this study. The term "Horizon" is used to avoid confusion with the term "Unit" for Unit D of Frederick [2008].

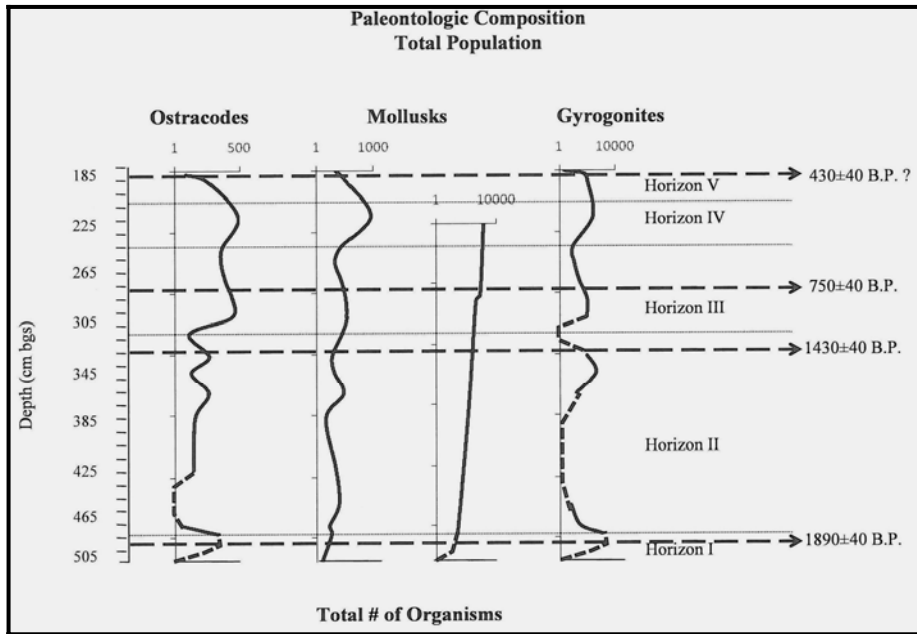


Figure M-2. Overall Faunal Composition Showing Total Population Trends Overtime.

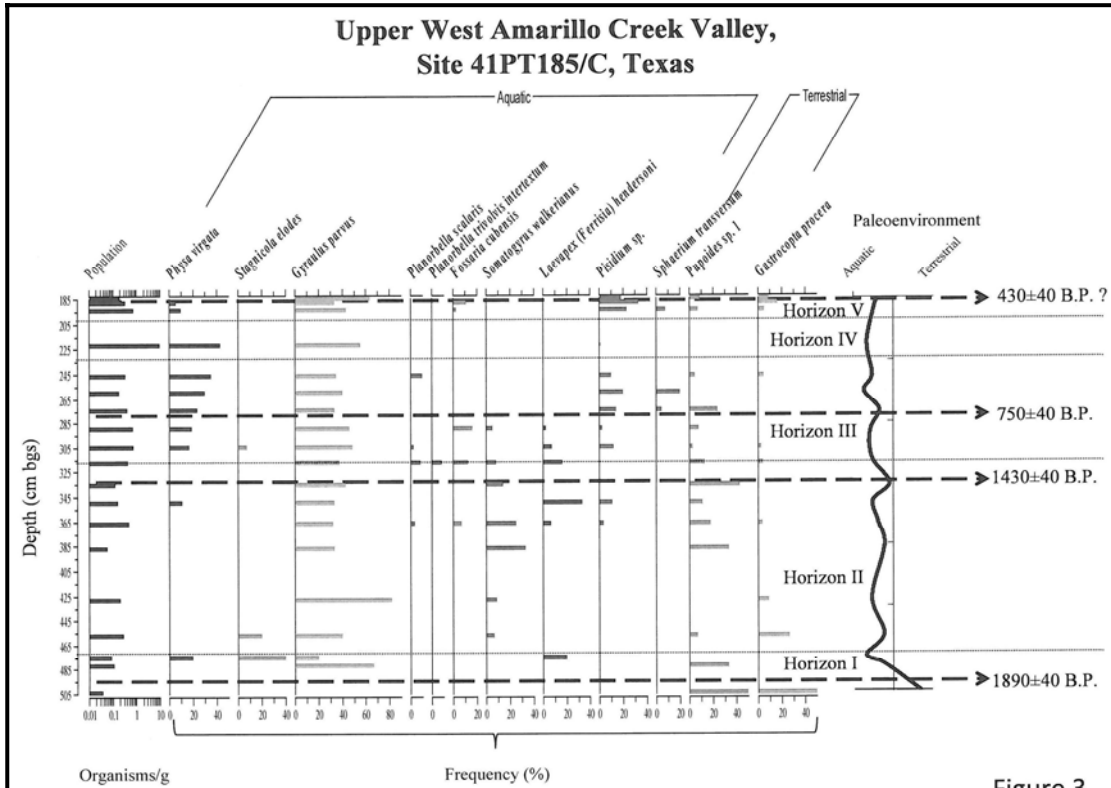


Figure M-3. Micro-Mollusk Paleoecology Obtained from 19 Sediment Samples.

Note: Relative abundance and the paleoenvironmental index [PI] curve show the transition from terrestrial to aquatic conditions overtime.

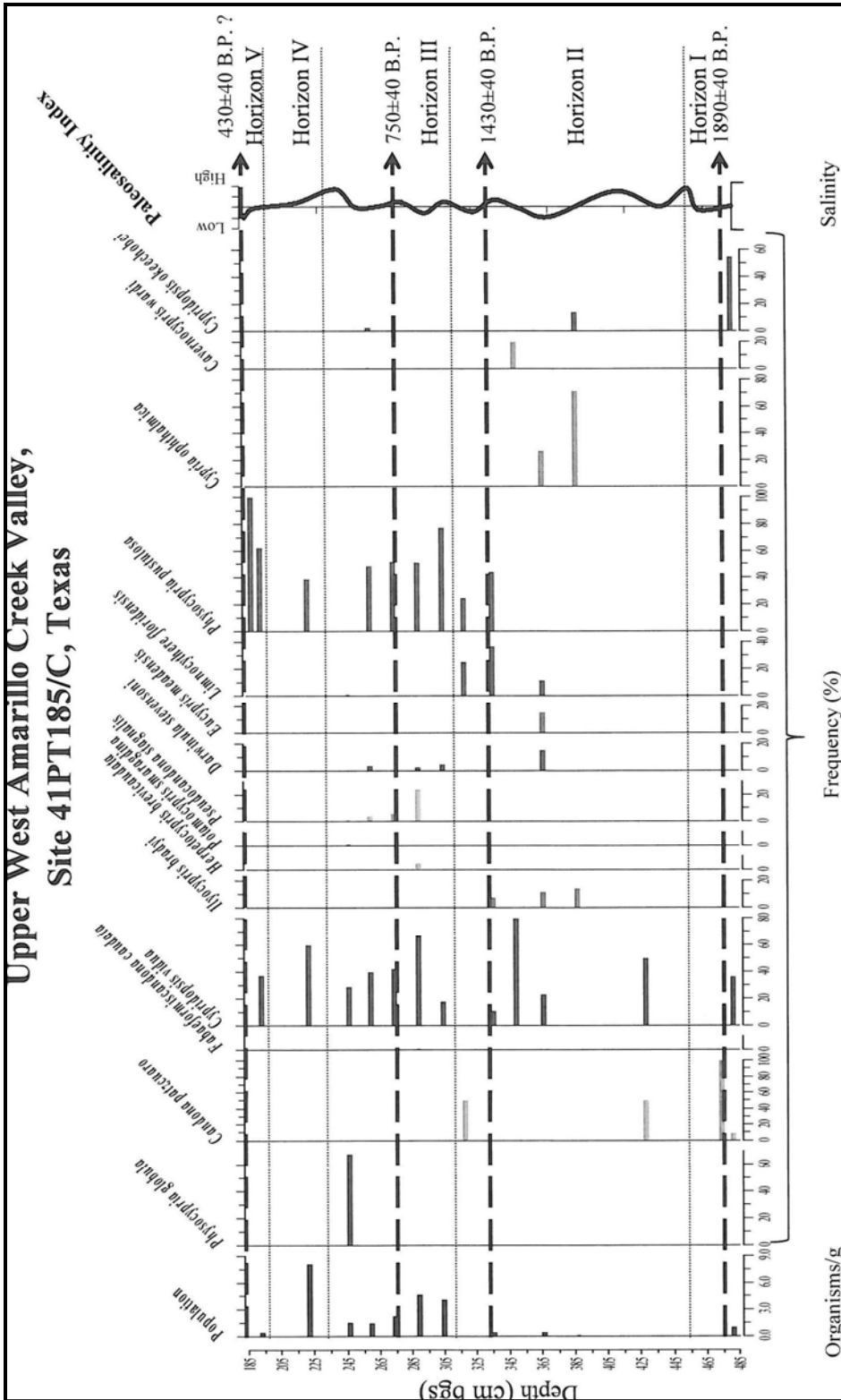


Figure M-5. Ostracode Paleocology and Relative Abundance Diagrams.

Note: Includes the paleosalinity index (SI) curve showing fluctuations between dilute and saline conditions affecting the marsh.

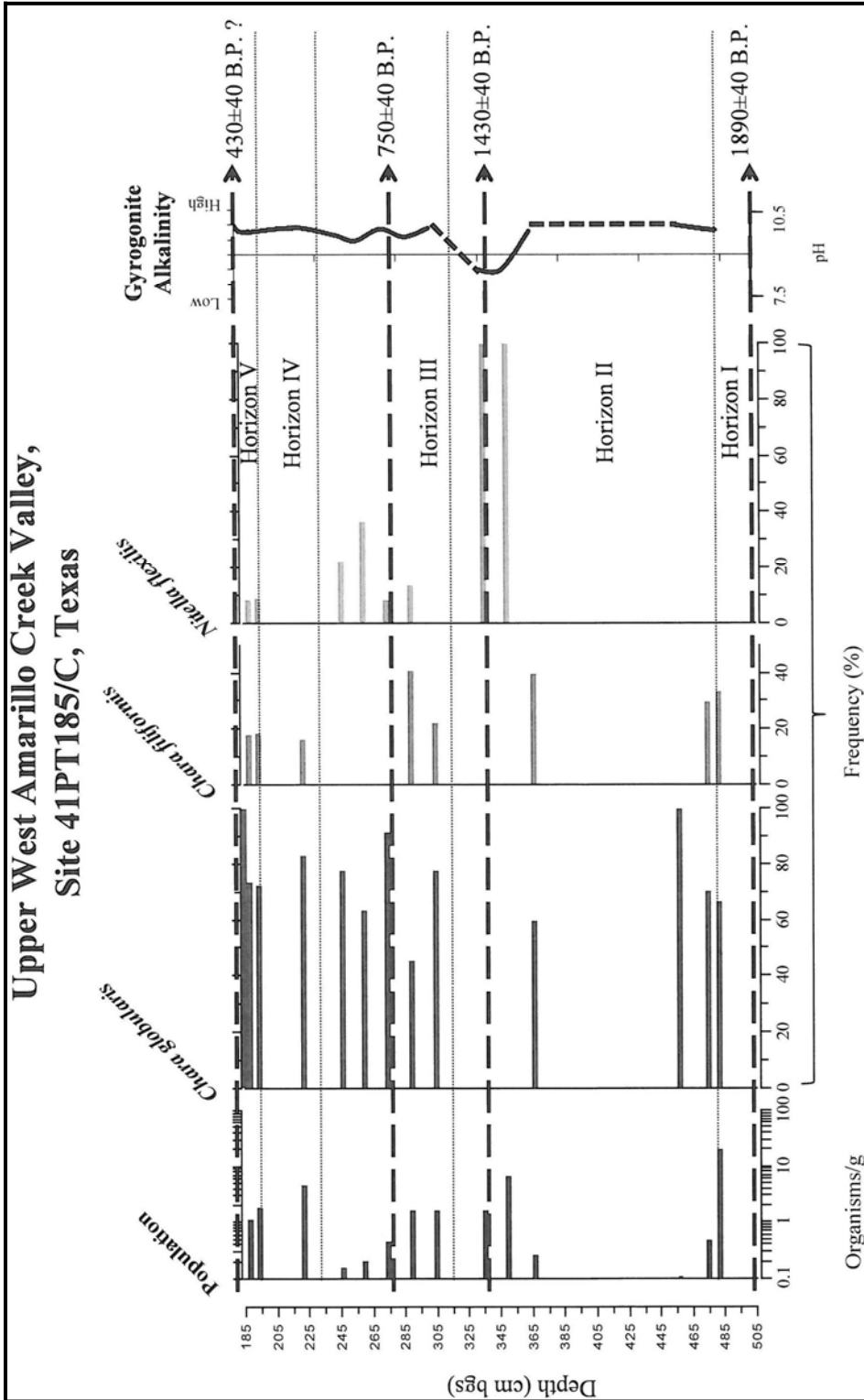


Figure M-6. Charophyta Paleoecology and Relative Abundance Diagrams Including the Alkalinity Index (AI) Curve Showing the Reconstructed Transition from Low to High Alkalinity Conditions Affecting the Marsh.

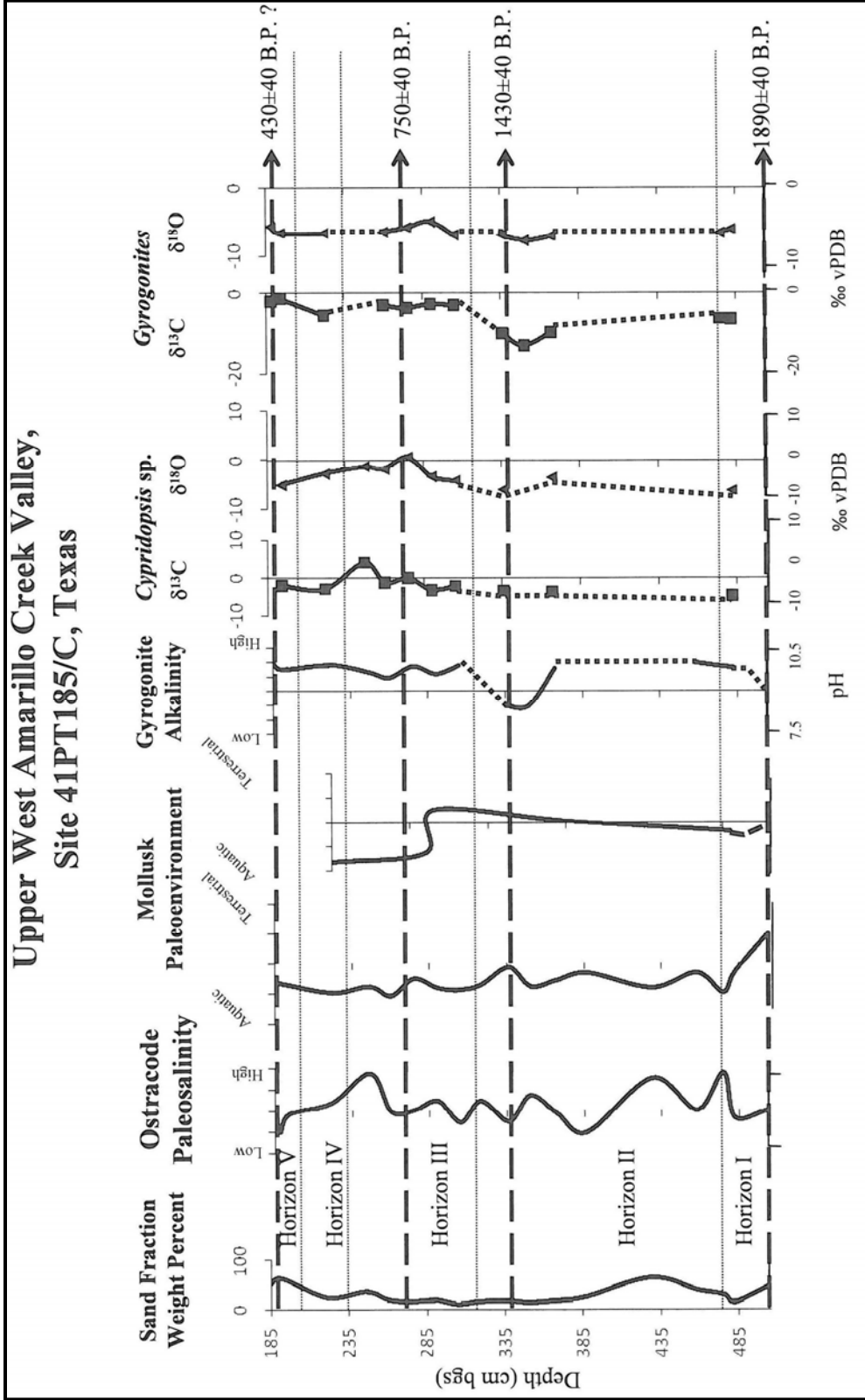


Figure M-7. Integrated Paleoeological Reconstruction Combining the Sand Fraction Curve, SI, PI, AI and Stable Isotope Records ($\delta^{13}\text{C}$ and $\delta^{18}\text{O}$) for the Ostracodes *Cypridopsis okeechobei* and *Cypridopsis vidua* and the Gyrogonites *Chara globularis* and *Nitella flexilis*.

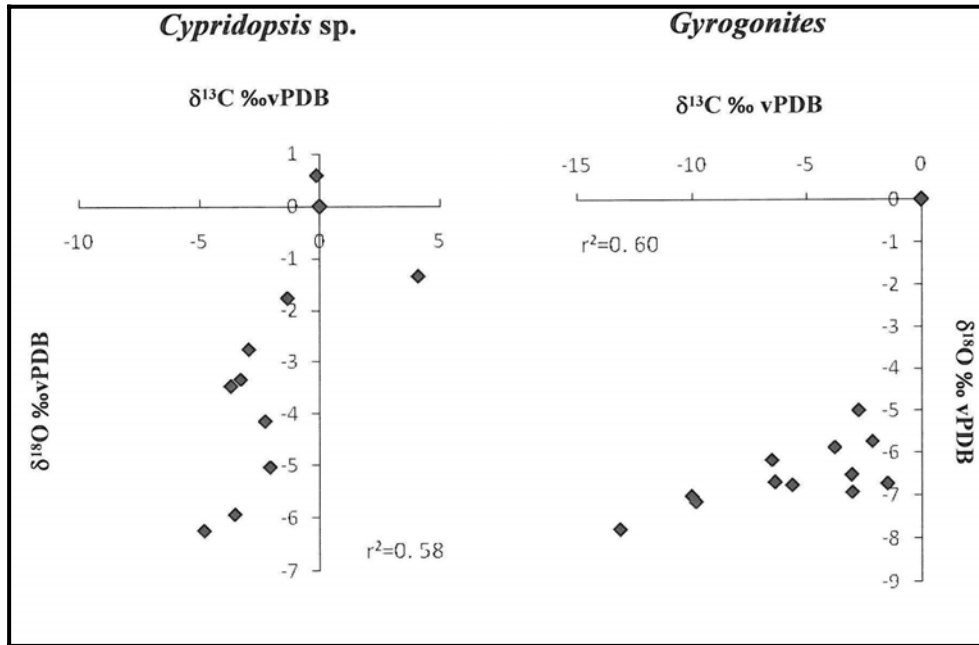


Figure M-8. Oxygen and Carbon Isotopes Show a Moderately Positive Correlation Coefficient for both Ostracodes and Gyrogonites, which is Consistent with a Closed Basin Interpretation for the Marsh from BT 36 at Site 41PT185/C.

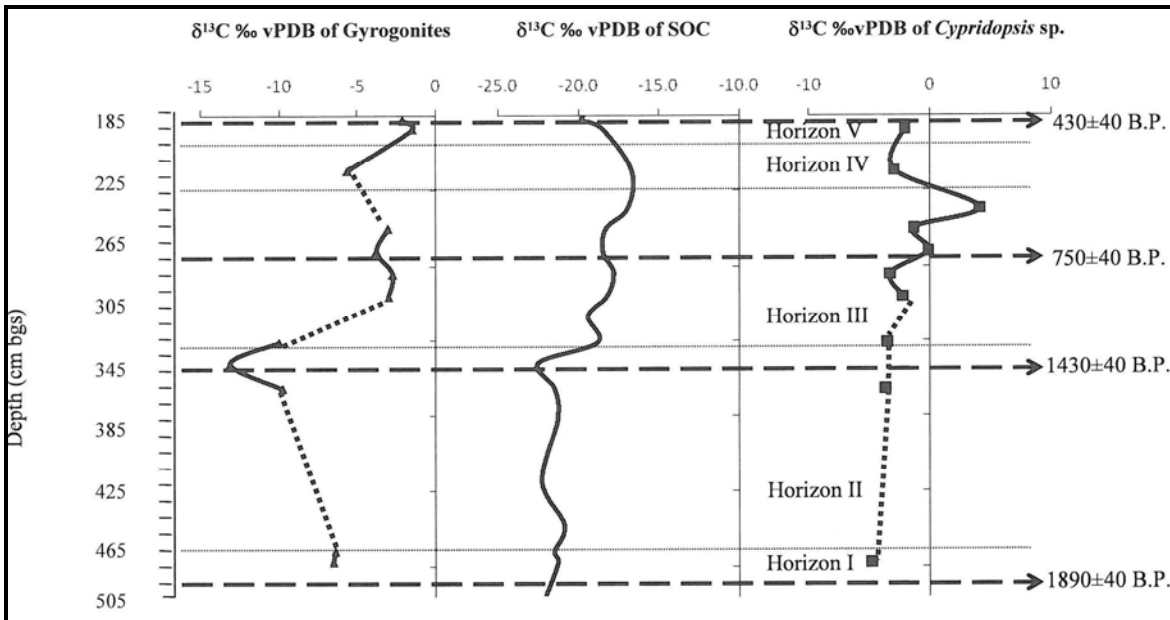


Figure M-9. Comparative Diagrams of $\delta^{13}\text{C}$ VPDB (per mil) Obtained from Gyrogonites, Soil Organic Carbon (SOC), and *Cypridopsis* sp.

Notice the positive correlation among the three signatures supporting the hypothesis of the transition between and Little Ice Age [LIA].

Table M-1. Sample Identification Numbers, Stratigraphic Position, Age Control, Sedimentation Rates, Bulk and Fraction Weight and Textural Classification of materials Analyzed from Unit D in BT 36 at Site 41PT185/C in the Upper West Amarillo Creek Valley.

Sample ID	Depth	Age	Sediment	Bulk	Fraction	>1 mm	>106	>63 mm	<63 mm	>1	>106	>63	<63	Texture	Color	Munsell
#	(cm bgs)	(Years B.P.)	ation Rate (cm Yr ⁻¹)	Wt. (g)	Wt. (g)	Wt. (g)	mm Wt. (g)	Wt. (g)	Wt. (g)	mm (%)	mm (%)	mm (%)	mm (%)			
BT 36-263-004-72	504-509			53.2	24.8	0.8	17.1	6.9	28.4	1.5	32.1	13.0	53.4	Silty sand	Light brownish gray	10YR 6/2
BT 36-263-004-68	482-486	1890 ± 40	0.32	52.4	7.2	0.2	5.8	1.2	45.2	0.4	11.1	2.3	86.3	Silty clay	Dark grayish brown	10YR 4/2
BT 36-263-004-69	475-479			54.0	14.8	0.6	8.8	5.4	39.2	1.1	16.3	10.0	72.6	Silty clay	Brown	10YR 5/3
BT 36-263-004-70	458-462			53.1	20.3	0.3	18.9	1.1	32.8	0.6	35.6	2.1	61.8	Silty sand	Light brownish gray	10YR 6/2
BT 36-263-004-71	429-432			53.3	33.3	0.7	27.7	4.9	20.0	1.3	52.0	9.2	37.5	Silty sand	Light brownish gray	10YR 6/2
BT 36-263-004-73	387-391			51.0	12.3	0.4	10.9	1.0	38.7	0.8	21.4	2.0	75.9	Sandy clay	Light brownish gray	10YR 6/2
BT 36-263-004-74	367-370			54.8	9.0	0.4	5.8	2.8	45.8	0.7	10.6	5.1	83.6	Sandy clay	Light brownish gray	10YR 6/2
BT 36-263-004-75	350-354			55.6	7.6	0.1	4.4	3.1	48.0	0.2	7.9	5.6	86.3	Silty clay	Light brownish gray	10YR 6/2
BT 36-263-004-76	336-340	1430 ± 40	0.07	52.9	8.8	0.1	8.5	0.2	44.1	0.2	16.1	0.4	83.4	Silty clay	Light gray	10YR 7/2
BT 36-263-004-77	318-321			54.4	8.0	0.3	6.5	1.2	46.4	0.6	11.9	2.2	85.3	Silty clay	Light gray	10YR 7/2
BT 36-263-004-78	305-309			53.2	5.0	0.4	4.1	0.5	48.2	0.8	7.7	0.9	90.6	Silty clay	Black	10YR 2/1
BT 36-263-004-79	290-293	750 ± 40	0.33	51.9	9.4	0.5	5.0	3.9	42.5	1.0	9.6	7.5	81.9	Silty clay	Black	10YR 2/1
BT 36-263-004-80	275-278	860 ± 40?		51.3	8.0	0.2	7.5	0.3	43.3	0.4	14.6	0.6	84.4	Silty clay	Black	10YR 2/1
BT 36-263-004-81	260-264			51.8	9.7	0.1	5.7	3.9	42.1	0.2	11.0	7.5	81.3	Silty clay	Black	10YR 2/1
BT 36-263-004-82	247-251			56.0	19.3	0.5	12.8	6.0	36.7	0.9	22.9	10.7	65.5	Sandy clay	Very dark brown	10YR 2/2
BT 36-263-004-83	222-227			51.9	12.1	0.7	10.0	1.4	39.8	1.3	19.3	2.7	76.7	Sandy clay	Very dark brown	10YR 2/2
BT 36-263-004-84	194-199			50.7	30.4	1.1	25.9	3.4	20.3	2.2	51.1	6.7	40.0	Silty sand	Very pale brown	10YR 7/3
BT 36-263-004-85	188-192			53.1	33.0	2.8	25.8	4.4	20.1	5.3	48.6	8.3	37.9	Silty sand	Very pale brown	10YR 7/3
BT 36-263-004-86	185-188	430 ± 40		55.8	28.8	1.4	24.9	2.5	27.0	2.5	44.6	4.5	48.4	Silty sand	Light brownish gray	10YR 6/2
BT 36-263-004-92	480-490	1890 ± 40	0.32	3300										Marly clay	Very dark brown	10YR 2/2
BT 36-263-004-93	375-385			3600										Clay	Black	10YR 2/1
BT 36-263-004-90	290-300			3600										Clay	Black	10YR 2/1
BT 36-263-004-89	285-289	750 ± 40	0.07	750										Clay	Black	10YR 2/1
BT 36-263-004-91	225-235			3800										Marly clay	Black	10YR 2/1

Table M-2. Mineralogical Composition of Samples Analyzed.

Sample ID #	Depth (cm bgs)	Bulk Wt. (g)	Fraction Wt. (g)	Quartz	Feldspars	CaCO ₃ Nodules	Root casts	Charcoal	Ostracode Frags.	Shell Frags.	Fish Scales	Bone Frags.
BT 36-263-004-72	504-509	53.2	24.8	VA	C	C	VR	R	VR	R		
BT 36-263-004-68	482-486	52.4	7.2	VA	C	C	VR	MC	R	MC		
BT 36-263-004-69	475-479	54.0	14.8	VA	C	C	R	R	R	MC		
BT 36-263-004-70	458-462	53.1	20.3	VA	C	C	VR	MC	VR	MC		
BT 36-263-004-71	429-432	53.3	33.3	VA	C	C	VR	VR	VR	MC		
BT 36-263-004-73	387-391	51.0	12.3	VA	C	C	R	R	VR	MC		
BT 36-263-004-74	367-370	54.8	9.0	VA	C	C	R	R	R	MC		
BT 36-263-004-75	350-354	55.6	7.6	VA	C	MC	VR	R	VR	MC		
BT 36-263-004-76	336-340	52.9	8.8	VA	C	C	VR	MC	VR	MC		
BT 36-263-004-77	318-321	54.4	8.0	VA	C	MC	R	R	VR	MC		
BT 36-263-004-78	305-309	53.2	5.0	VA	C	MC	VR	R	VR	MC		
BT 36-263-004-79	290-293	51.9	9.4	VA	C	A	R	R	VR	MC	VR	
BT 36-263-004-80	275-278	51.3	8.0	VA	C	C	R	MC	VR	MC		
BT 36-263-004-81	260-264	51.8	9.7	VA	C	C	R	R	VR	MC		
BT 36-263-004-82	247-251	56.0	19.3	VA	C			MC	VR	MC		VR
BT 36-263-004-83	222-227	51.9	12.1	VA	MC	C	A		VR	C		
BT 36-263-004-84	194-199	50.7	30.4	VA	C	A	C		R	MC		
BT 36-263-004-85	188-192	53.1	33.0	VA	C	A	MC		R	MC		
BT 36-263-004-86	185-188	55.8	28.8	VA	C	C	MC		R	MC		
BT 36-263-004-92	480-490	3300										
BT 36-263-004-93	375-385	3600										
BT 36-263-004-90	290-300	3600										
BT 36-263-004-89	285-289	750										
BT 36-263-004-91	225-235	3800										

Table M-3. Paleontological Composition and Taphonomic Characteristics of Mollusks, Ostracodes, and Gyrogonites.

Sample ID No.	Depth (cmbs)	Bulk Wt. (g)	Fraction Wt. (g)	Mollusks (#)	Ostracodes (#)	Gyrogonites (#)	Fragmentation	Abrasion	Encrustation	Coating	Redox	Color
BT 36-263-004-72	504-509	53.2	24.8	2			15	10	0	0	0	White
BT 36-263-004-68	482-486	52.4	7.2	6	55	1081	2	2	0	0	0	Clear
BT 36-263-004-69	475-479	54.0	14.8	5	2	27	15	10	0	0	0	Clear
BT 36-263-004-70	458-462	53.1	20.3	15		6	15	10	0	0	0	White
BT 36-263-004-71	429-432	53.3	33.3	11	6		5	5	0	0	0	White
BT 36-263-004-73	387-391	51.0	12.3	3	7		15	5	0	0	0	Clear
BT 36-263-004-74	367-370	54.8	9.0	28	26	15	5	5	0	0	0	Clear
BT 36-263-004-75	350-354	55.6	7.6	9	5	388	15	15	0	0	0	Clear
BT 36-263-004-76	336-340	52.9	8.8	7	27	86	5	5	0	0	0	Clear
BT 36-263-004-77	318-321	54.4	8.0	24	4		2	2	0	0	0	Clear
BT 36-263-004-78	305-309	53.2	5.0	41	222	86	2	2	0	0	0	Clear
BT 36-263-004-79	290-293	51.9	9.4	37	243	88	2	2	0	0	0	Clear
BT 36-263-004-80	275-278	51.3	8.0	21	119	24	2	2	0	0	0	Clear
BT 36-263-004-81	260-264	51.8	9.7	10	80	11	2	2	0	0	0	Clear
BT 36-263-004-82	247-251	56.0	19.3	20	90	9	2	2	0	0	0	Clear
BT 36-263-004-83	222-227	51.9	12.1	750	422	239	2	2	0	0	0	Clear
BT 36-263-004-84	194-199	50.7	30.4	39	24	98	5	5	0	0	0	Clear
BT 36-263-004-85	188-192	53.1	33.0	18	3	60	5	5	0	0	0	Clear
BT 36-263-004-86	185-188	55.8	28.8	11		2	15	10	0	0	0	White
BT 36-263-004-92	480-490	3300	NR	26	NR	1000+	2	2	0	0	0	White
BT 36-263-004-93	375-385	3600	NR	151	NR	1000+	2	2	0	0	0	White
BT 36-263-004-89	285-289	750	NR	865	NR	1000+	2	2	0	0	0	White
BT 36-263-004-90	290-300	3600	NR	464	NR	10,000+	2	2	0	0	0	White
BT 36-263-004-91	225-235	3800	NR	1453	NR	1000+	2	2	0	0	0	White

Table M-4. Ecological Requirements of Mollusks Species Recovered from BT 36 at Site 41PT185/C in the Upper West Amarillo Creek Valley.

Species	Habitat	Permanence	Salinity*	Chemistry (in HCO ₃ /Ca)*	
<i>Physa virgata</i> (Gould, 1855)	Streams, lakes, ponds, canals	Permanent or ephemeral	10-5,000 mg L ⁻¹	1-5 mg L ⁻¹	Freshwater to Ca- or HCO ₃ -rich
<i>Physella gyrina aurea</i> (Say, 1821)	Streams, lakes, ponds, swamps	Permanent or ephemeral	NA	NA	NA
<i>Stagnicola elodes</i> (Say 1821)	Streams, lakes, ponds, canals	Permanent or ephemeral	1,000-2,000 mg L ⁻¹	1-2 mg L ⁻¹	Freshwater to Ca- or HCO ₃ -rich
<i>Gyraulus parvus</i> (Say, 1817)	Streams, lakes, ponds, canals	Permanent or ephemeral or moist soil	10-5,000 mg L ⁻¹	1-5 mg L ⁻¹	Freshwater to Ca- or HCO ₃ -rich
<i>Planorbellascalaris</i> (Jay 1839)	Weedy species in swamps, ponds, lakes (lentic)	Permanent (oligotrophic environments)	NA	NA	NA
<i>Planorbella trivolvis intertexta</i> (Say, 1817)	Weedy species in swamps, ponds, lakes (lentic)	Permanent (eutrophic environments)	NA	NA	NA
<i>Planorbella trivolvis lenta</i> (Say, 1817)	Weedy species in swamps, ponds, lakes (lentic)	Permanent (eutrophic environments)	NA	NA	NA
<i>Fossaria cubensis</i> (Pfeiffer 1839)	Streams, ponds, lakes	Permanent or ephemeral	200-5,000 mg L ⁻¹	-2 to 1.5 mg L ⁻¹	Freshwater to Ca- or HCO ₃ -rich
<i>Laevapex (Ferrisia) hendersoni</i> Walker, 1908	Ditches, ponds, quiet backwaters in streams and lakes (stems of aquatic plants)	Permanent or ephemeral	NA	NA	NA
<i>Pisidium</i> sp. (Pfeiffer 1821)	Springs, lakes, streams	Permanent	~2,000 mg L ⁻¹	~2 mg L ⁻¹	Freshwater to Ca- or HCO ₃ -rich
<i>Sphaerium transversum</i> (Say)	Lakes, streams	Permanent	10-5,000 mg L ⁻¹	1-5 mg L ⁻¹	Freshwater to Ca- or HCO ₃ -rich
<i>Pseudosuccinea columella</i> (Say, 1825)	Amphibious, weedy, lakes, streams, swamps	Permanent	NA	NA	NA
<i>Micromenetus brognartiana</i>	Riparian, marshes	Moist soils	NA	NA	NA
<i>Somatogyrus walkerianus</i> (Aldrich, 1905)	Streams, lakes, ponds, swamps	Permanent	NA	NA	NA
<i>Pupoides</i> sp.	Open grassland, near springs, seeps, bogs	Moist soils	NA	NA	NA
<i>Columella simplex</i> (Gould 1840)	Deciduous leaf litter	Moist soils	NA	NA	NA
<i>Gastrocopta procera</i> (Gould 1840)	Prairie, savanna vegetation	Moist soils; supports drought	NA	NA	NA
<i>Gastrocopta tappaniana</i> (C.B. Adams, 1841)	Calcareous hygric conditions, frequent in alvars	Moist soils	NA	NA	NA
<i>Polygyra</i> sp.	Riparian, marshes	Moist soils	NA	NA	NA
Sources:					
Vokes and Miksicek, 1987					
Miksicek, 1989					
Bequaert and Miller, 1973					
Webb, 1942					
Sovell and Guralnick 2004					
*Sharpe 2002					
Dillon (2000: 123-135, 363)					
Eversole 1978					

Table M-6. Ecological Requirements of Ostracode Species Recovered from BT 36 at Site 41PT185/C in the Upper West Amarillo Creek Valley.

Species	Habitat	Permanence	Temperature	Salinity*	Chemistry*	Paleo/Biogeography**
<i>Physocypris globula</i> Furtos 1933	Springs, streams, lakes	Permanent	2-32°C Eurythermic	10-10,000 mg L ⁻¹	0.70-70.00 meq L ⁻¹ Freshwater to Ca-rich	Cosmopolitan; across North America but sparse
<i>Candona patzcuaro</i> Tressler 1954	Springs, streams, lakes	Permanent or ephemeral	2-32°C Eurythermic	200-5,000 mg L ⁻¹	0.5-30 meq L ⁻¹ Freshwater to Ca-rich	Cosmopolitan; worldwide
<i>Fabaeformiscandona caudata</i> (Kaufmann 1900)	Lakes, ponds	Permanent	2-32°C Eurythermic	10-5,000 mg L ⁻¹	0.5-10.0 meq L ⁻¹ Freshwater to Ca-rich	Cosmopolitan; across North America
<i>Cypridopsis vidua</i> (O.F. Müller, 1776)	Springs, streams, lakes	Permanent or ephemeral	2-32°C Eurythermic	100-4,000 mg L ⁻¹	0.10-50 meq L ⁻¹ Freshwater to Ca-rich	Cosmopolitan; worldwide
<i>Ilyocypris bradyi</i> Sars 1890	Streams, lakes, ponds	Permanent or ephemeral	6-18°C Cryophilic	100-4,000 mg L ⁻¹	0.10-50.0 meq L ⁻¹ Freshwater to Ca-rich	Cosmopolitan; across North America
<i>Herpetocypris brevicaudata</i> Kaufmann, 1900	Springs, streams, lakes	Permanent	14-28°C Thermophilic	100-4,000 mg L ⁻¹	0.10-50.0 meq L ⁻¹ Freshwater to Ca-rich	Western North America; from California to southern Nebraska
<i>Potamocypris smaragdina</i> Vavra 1891	Lakes, ponds	Permanent	2-32°C Eurythermic	40-3,000 mg L ⁻¹	0.20-5.0 meq L ⁻¹ Freshwater to Ca-rich	Cosmopolitan; across North America
<i>Pseudocandona stagnalis</i> (Sars, 1890) Meisch & Broodbakker 1993	Springs, streams, lakes	Permanent or ephemeral	2-32°C Eurythermic	200-2,000 mg L ⁻¹	0.10-5.0 meq L ⁻¹ Freshwater to Ca-rich	Cosmopolitan; across North America but scattered and limited to wetlands
<i>Darwinula stevensoni</i> (Brady & Robinson), 1890	Lakes, ponds	Permanent	2-32°C Eurythermic	100-2,000 mg L ⁻¹	0.10-5.0 meq L ⁻¹ Freshwater to Ca-rich	Cosmopolitan; worldwide
<i>Eucypris meadensis</i> Gutentag & Benson 1962	Springs, streams, lakes	Permanent	7-25°C Eurythermic	300-1,000 mg L ⁻¹	0.7-10.0 meq L ⁻¹ Freshwater to Ca-rich	Western North America; from California to southern Nebraska
<i>Limnocythere floridensis</i> Keiser 1976	Springs, streams, lakes	Permanent	NA	200-1,000 mg L ⁻¹	~1.00 meq L ⁻¹ Freshwater to Ca-rich	Limited to southeastern North America
<i>Physocypris pustulosa</i> Sharpe 1897	Lakes, ponds	Permanent	2-32°C Eurythermic	30-1,000 mg L ⁻¹	0.30-10.0 meq L ⁻¹ Freshwater to Ca-rich	Eastern North America; from Michigan to New York, south to Tennessee. Rare in western North America (Arizona, New Mexico, Texas)
<i>Cypris ophthalmitica</i> (Jurine 1820)	Lakes, ponds	Permanent	2-32°C Eurythermic	10-1,000 mg L ⁻¹	0.5-6.00 meq L ⁻¹ Freshwater to Ca-rich	Cosmopolitan; across North America but sparse
<i>Cavemocypris wardi</i> Marmontier & Meisch & Danielopol 1989	Springs, seeps, groundwater	Permanent	0-14°C Cryotopic	10-1,000 mg L ⁻¹	1-3 meq L ⁻¹ Freshwater to Ca-rich	Cosmopolitan; across North America but sparse
<i>Cypridopsis okeechobei</i> Furtos 1933	Springs, streams, lakes	Permanent	2-32°C Eurythermic	50-800 mg L ⁻¹	1.00-5.00 meq L ⁻¹ Freshwater to Ca-rich	Cosmopolitan; across North America but sparse
* Forester et al. 2005						
** Forester (1991), Anderson et al. (1998), Kulkoyutoglu et al. (2007)						

Table M-7. Total and Relative Abundance of Ostracode Species Recovered, Including Adult/Juvenile (A/J) and Carapace/Valve (C/V) Ratios.

BT 36 Sample ID No.	Depth (cnbs)	Ostracodes #	Ostracodes Weight (g)	Physocypris globata			Candona patzcuaro			Fabaeformiscand ona caudata			Cypridopsis vidua			Ilyocypris bradyi			Herpetocypris brevicaudata			Potamocypris smaragdina			Pseudocandona stagnatis				
				#		%		A/J C/V		%		A/J C/V		%		A/J C/V		%		A/J C/V		%		A/J C/V		%		A/J C/V	
				#	A/J	C/V	#	%	A/J	C/V	#	%	A/J	C/V	#	%	A/J	C/V	#	%	A/J	C/V	#	%	A/J	C/V	#	%	A/J
263-004-72	504-509																												
263-004-68	482-486	55	1.05			5	9.1	1	0																				
263-004-69	475-479	2	0.04			2	100.0	0	0																				
263-004-70	458-462																												
263-004-71	429-432	6	0.11			3	50.0	0	0																				
263-004-73	387-391	7	0.14																										
263-004-74	367-370	26	0.47																										
263-004-75	350-354	5	0.09																										
263-004-76	336-340	27	0.51																										
263-004-77	318-321	4	0.07																										
263-004-78	305-309	222	4.17																										
263-004-79	290-293	243	4.68																										
263-004-80	275-278	119	2.32																										
263-004-81	260-264	80	1.54																										
263-004-82	247-251	90	1.61			61	67.8	0.3	0.1																				
263-004-83	222-227	422	8.13																										
263-004-84	194-199	24	0.47																										
263-004-85	188-192	3	0.06																										
263-004-86	185-188																												
BT 36 Sample ID No.	Depth (cnbs)	Ostracodes #	Ostracodes Weight (g)	Darwinula stevensoni			Encypris meadensis			Limnocythere floridensis			Physocypris pustulosa			Cypria ophthalmica			Cavernocypris wardi			Cypridopsis okeechobei							
				#		%		A/J C/V		%		A/J C/V		%		A/J C/V		%		A/J C/V		%		A/J C/V					
				#	A/J	C/V	#	%	A/J	C/V	#	%	A/J	C/V	#	%	A/J	C/V	#	%	A/J	C/V	#	%	A/J	C/V			
263-004-72	504-509																												
263-004-68	482-486	55	1.05																										
263-004-69	475-479	2	0.04																										
263-004-70	458-462																												
263-004-71	429-432	6	0.11																										
263-004-73	387-391	7	0.14																										
263-004-74	367-370	26	0.47																										
263-004-75	350-354	5	0.09																										
263-004-76	336-340	27	0.51																										
263-004-77	318-321	4	0.07																										
263-004-78	305-309	222	4.17																										
263-004-79	290-293	243	4.68																										
263-004-80	275-278	119	2.32																										
263-004-81	260-264	80	1.54																										
263-004-82	247-251	90	1.61																										
263-004-83	222-227	422	8.13																										
263-004-84	194-199	24	0.47																										
263-004-85	188-192	3	0.06																										
263-004-86	185-188																												

* A = adult, J = juvenile, carapace, V = valve

Table M-8. Ecological Requirements of Charophyta Recovered from BT 36 at Site 41PT185/C in the Upper West Amarillo Creek Valley.

Species	Habitat	Permanence	Temperature	Optimal Seasonality	pH Preference
<i>Chara globularis</i> Thuillier	High pH; Ca-rich waters, slow lentic or lotic waters; occasionally in spring seeps; intolerant to high nutrient conditions	Permanent or ephemeral, prefer late spring-summer but may occur year-round	5-25°C; optimum: 17°C-22°C	Mid-January to late September. Peak between late April and mid-July	7.5-10.5; optimum: 9.5-10.5
<i>Chara filiformis</i> (Hertsch)	High pH; Ca-rich waters, slow lentic or lotic waters; occasionally in spring seeps; intolerant to high nutrient conditions	Permanent or ephemeral, prefer late spring-summer but may occur year-round	5-25°C; optimum: 17°C-22°C	Mid-January to late September. Peak between late April and mid-July	7.5-10.5; optimum: 9.5-10.5
<i>Nitella flexilis</i> (Linnaeus, pro parte)	Lower pH than <i>Chara</i> ; slow lentic to lotic waters; peaty bogs; intolerant to high nutrient conditions	Permanent or ephemeral, prefer late spring-summer but may occur year-round	5-25°C; optimum: 13°C-18°C	Mid-January to late September. Peak between late March and mid-June	7.5-10.5; optimum: 7.5-9.0

Sources: Coletta et al. 2001; Pentecost et al. 2006; Andrews et al. 2004.

Table M-9. Total and Relative Abundance of Charophyta Recovered from BT 36 at Site 41PT185/C in the Upper West Amarillo Creek Valley.

Sample ID No.	Depth (cmbs)	Bulk Wt. (g)	Fraction Wt. (g)	Gyrogonites #	Gyrogonites (g)	<i>Chara globularis</i>		<i>Chara filiformis</i>		<i>Nitella flexilis</i>	
						#	%	#	%	#	%
BT 36-263-004-72	504-509	53.2	24.8								
BT 36-263-004-68	482-486	52.4	7.2	1081	20.63	721	66.7	360	33.3		0
BT 36-263-004-69	475-479	54.0	14.8	27	0.50	19	70.4	8	29.6		0
BT 36-263-004-70	458-462	53.1	20.3	6	0.11	6	100		0		0
BT 36-263-004-71	429-432	53.3	33.3								
BT 36-263-004-73	387-391	51.0	12.3								
BT 36-263-004-74	367-370	54.8	9.0	15	0.27	9	60	6	40		0
BT 36-263-004-75	350-354	55.6	7.6	388	6.98		0		0	388	100
BT 36-263-004-76	336-340	52.9	8.8	86	1.63		0		0	86	100
BT 36-263-004-77	318-321	54.4	8.0								
BT 36-263-004-78	305-309	53.2	5.0	86	1.62	67	77.9	19	22.1		0
BT 36-263-004-79	290-293	51.9	9.4	88	1.70	40	45.5	36	40.9	12	13.6
BT 36-263-004-80	275-278	51.3	8.0	24	0.47	22	91.7		0	2	8.3
BT 36-263-004-81	260-264	51.8	9.7	11	0.21	7	63.6		0	4	36.4
BT 36-263-004-82	247-251	56.0	19.3	9	0.16	7	77.8		0	2	22.2
BT 36-263-004-83	222-227	51.9	12.1	239	4.61	199	83.3	40	16.7		0
BT 36-263-004-84	194-199	50.7	30.4	98	1.93	71	72.4	18	18.4	9	9.2
BT 36-263-004-85	188-192	53.1	33.0	60	1.13	44	73.3	11	18.3	5	8.3
BT 36-263-004-86	185-188	55.8	28.8	2	0.04	2	100		0		0
BT 36-263-004-92	480-490	3300	NR	1000+	NA	NR	NA	NR	NA	NR	NA
BT 36-263-004-93	375-385	3600	NR	1000+	NA	NR	NA	NR	NA	NR	NA
BT 36-263-004-90	290-300	3600	NR	10,000+	NA	NR	NA	NR	NA	NR	NA
BT 36-263-004-89	285-289	750	NR	1000+	NA	NR	NA	NR	NA	NR	NA
BT 36-263-004-91	225-235	3800	NR	1000+	NA	NR	NA	NR	NA	NR	NA

NR = not recorded; NA = not available

Table M-10. Ostracode Stable Isotope Data Obtained from *Cypridopsis okeechoebei* and *Cypridopsis vidua*. Two Replicates, the Mean and Standard Deviations are Shown for $\delta^{13}\text{C}$ and $\delta^{18}\text{O}$ Values.

Sample ID No.	Depth (cmbs)	Species	$\delta^{13}\text{C}$				$\delta^{18}\text{O}$			
			Replicate 1	Replicate 2	Average	Std. Dev.	Replicate 1	Replicate 2	Average	Std. Dev.
BT 36-263-004-72	504-509	---								
BT 36-263-004-68	482-486	<i>Cypridopsis okeechoebei</i>	-4.62	-4.97	-4.79	0.030	-6.43	-6.06	-6.25	0.044
BT 36-263-004-69	475-479	---								
BT 36-263-004-70	458-462	---								
BT 36-263-004-71	429-432	---								
BT 36-263-004-73	387-391	---								
BT 36-263-004-74	367-370	<i>Cypridopsis vidua</i>	-4.41	-2.96	-3.68	0.034	-3.73	-3.21	-3.47	0.069
BT 36-263-004-75	350-354	---								
BT 36-263-004-76	336-340	<i>Cypridopsis vidua</i>	-3.58	-3.45	-3.52	0.085	-6.59	-5.27	-5.93	0.114
BT 36-263-004-77	318-321	---								
BT 36-263-004-78	305-309	<i>Cypridopsis vidua</i>	-2.35	-2.18	-2.27	0.044	-3.45	-4.84	-4.14	0.057
BT 36-263-004-79	290-293	<i>Cypridopsis vidua</i>	-3.09	-3.48	-3.28	0.013	-3.01	-3.67	-3.34	0.037
BT 36-263-004-80	275-278	<i>Cypridopsis vidua</i>	-1.02	0.79	-0.11	0.026	-0.90	2.08	0.59	0.057
BT 36-263-004-81	260-264	<i>Cypridopsis vidua</i>	-2.58	-0.08	-1.33	0.033	-0.42	-3.11	-1.77	0.041
BT 36-263-004-82	247-251	<i>Cypridopsis vidua</i>	2.69	5.51	4.10	0.065	-1.67	-1.03	-1.35	0.057
BT 36-263-004-83	222-227	<i>Cypridopsis vidua</i>	-3.59	-2.31	-2.95	0.044	-3.18	-2.34	-2.76	0.045
BT 36-263-004-84	194-199	<i>Cypridopsis vidua</i>	-2.15	-1.97	-2.06	0.050	-4.09	-5.99	-5.04	0.078
BT 36-263-004-85	188-192	---								
BT 36-263-004-86	185-188	---								

Table M-11. Gyrogonite Stable Isotope Data Obtained from *Chara globularis* and *Nitella flexilis*. Two Replicates, the Mean and Standard Deviations are Shown for $\delta^{13}\text{C}$ and $\delta^{18}\text{O}$ Values.

Notice that three replicates were available for sample BT 36-#263-004-84.

Sample ID #	Depth (cmbs)	Species	d13C					d18O					
			Replicate 1	Replicate 2	Replicate 3	Average	Std. Dev.	Replicate 1	Replicate 2	Replicate 3	Average	Std. Dev.	
BT 36-263-004-72	504-509	---											
BT 36-263-004-68	482-486	<i>Chara globularis</i>	-6.70	-6.35		-6.52	0.022	-5.74	-6.59		-6.17	0.056	
BT 36-263-004-69	475-479	---	-6.18	-6.60		-6.39	0.022	-6.59	-6.77		-6.68	0.067	
BT 36-263-004-70	458-462	---											
BT 36-263-004-71	429-432	---											
BT 36-263-004-73	387-391	---											
BT 36-263-004-74	367-370	<i>Nitella flexilis</i>	-9.38	-10.28		-9.83	0.006	-7.12	-7.17		-7.14	0.028	
BT 36-263-004-75	350-354	<i>Nitella flexilis</i>	-12.83	-13.47		-13.15	0.015	-7.61	-7.95		-7.78	0.068	
BT 36-263-004-76	336-340	<i>Nitella flexilis</i>	-10.22	-9.84		-10.03	0.027	-6.97	-7.04		-7.01	0.023	
BT 36-263-004-77	318-321	---											
BT 36-263-004-78	305-309	<i>Chara globularis</i>	-2.37	-3.65		-3.01	0.028	-7.29	-6.55		-6.92	0.060	
BT 36-263-004-79	290-293	<i>Chara globularis</i>	-3.85	-1.62		-2.74	0.025	-3.57	-6.40		-4.99	0.052	
BT 36-263-004-80	275-278	<i>Chara globularis</i>	-4.38	-3.17		-3.78	0.037	-5.66	-6.08		-5.87	0.049	
BT 36-263-004-81	260-264	<i>Chara globularis</i>	-3.04			-3.04	0.016	-6.51			-6.51	0.026	
BT 36-263-004-82	247-251	<i>Chara globularis</i>											
BT 36-263-004-83	222-227	<i>Chara globularis</i>	-6.14	-5.13		-5.63	0.014	-6.42	-7.09		-6.75	0.050	
BT 36-263-004-84	194-199	<i>Chara globularis</i>	-1.24	-1.45	-1.74	-1.48	0.034	-6.05	-7.24	-6.87	-6.72	0.059	
BT 36-263-004-85	188-192	<i>Chara globularis</i>	-2.11	-2.15		-2.13	0.023	-5.47	-5.99		-5.73	0.045	
BT 36-263-004-86	185-188	---											

This page intentionally left blank.

APPENDIX N

PLANT REMAINS FROM 41PT185/C, 41PT186, AND 41PT245

This page intentionally left blank.

PLANT REMAINS FROM 41PT185/C, 41PT186, AND 41PT245

Prepared for:



**TRC Environmental Corporation
505 East Huntland Drive, Suite 250
Austin, Texas 78752**

Prepared by:

**Phil Dering, Ph.D.
Shumla Archeobotanical Services
Comstock, Texas**

This page intentionally left blank.

N.1 INTRODUCTION

The purpose of this analysis is to provide an assessment of the botanical assemblages from three sites, 41PT185/C, 41PT186, and 41PT245. A total of 14 flotation samples and 39 charcoal samples were submitted for analysis. The data will be utilized to assess the nature and condition of the plant remains from these sites and provide some evidence for plant utilization and local environmental conditions.

N.2 METHODS

Flotation is a method of recovering organic remains from archeological sediments by using water to separate heavy or soluble inorganic particles from plant parts and small animal bone. The material floating to the surface is called the light fraction, and this is caught on a fine mesh screen or strainer. The material that sinks to the bottom is the heavy fraction and it is also caught on a fine mesh screen. Most of the soil including clay and silt is suspended in water and passes through the screens and is either recycled or discarded. In this study, both the light and heavy fractions were submitted for analysis. In addition, point or screen-collected charcoal samples were submitted for identification.

The analysis followed standard archeobotanical laboratory procedures. The volume of the light fraction is first measured. In most cases up to 100 ml of light fraction from each sample is set aside for analysis. Then the portion to be analyzed is passed through a nested set of screens of 4 mm, 2 mm, 1 mm, and 0.450 mm mesh and examined for charred material, which is separated for identification. In the current study, charred plant material was so scarce that I sorted through the entire volume of each light fraction that was submitted for analysis.

Plant material is sorted into two categories – woody fragments, and seed/fruit fragments including maize or agave parts when present. Identification of carbonized wood was accomplished by using the snap technique, examining the fragments at 8 to 45 magnifications with a hand lens or a binocular dissecting microscope, and comparing the material to samples in the archeobotanical herbarium. All seed identifications were made using seed manuals and reference collections at Shumla Archeobotanical Services. Only charred plant material is included in the analysis, because uncarbonized material is consumed by insects, fungi and bacteria and does not survive more than a few years in the deposits of open sites.

Up to 25 wood charcoal fragments large enough to be manipulated are examined and identified from each flotation sample. Fragments smaller than 2 or 3 mm can not be manipulated. They are usually placed in the indeterminate category. When a sample contains more than 25 fragments, the rest of the material is scanned to make sure that no other taxa are present. Then the volume of the charcoal is measured and included along with its weight in the report. The results are presented in tabular format.

Sample content may be affected by various biological disturbance factors, including insect or small mammal activity, and plant root growth. In an effort to assess this impact, the amounts of roots, insect parts, leaves, and modern uncharred seeds are estimated for each flotation sample. These amounts are reported on a scale of 1-5 (+), 6-25 (++) , 26-50 (+++) , and over 50 (++++).

N.3 RESULTS AND DISCUSSION

Results of the analysis are presented in Tables N-1 through N-5. Table N-1 lists the flotation sample proveniences along with a summary of recovery and preservation indicators from each sample. Identifications

and counts of plant material recovered from each flotation and charcoal sample appear by site in Tables N-2 through N-5.

N.4 OVERVIEW

Recovery of charred plant material in the flotation samples was poor. The total charcoal in each sample varied from nothing to 2.5 g. Disturbance indicators were abundant, and several fresh, uncharred seeds occurred in samples from 41PT185/C. Roots and insect parts constituted the majority of the disturbance indicators, and some samples contained uncharred seeds, including sunflower, goosefoot/pigweed (cheno-am), and hackberry.

The worst recovery was noted at 41PT245, where 0.1 g of unidentifiable charred wood was found in a single sample. The Late Archaic site, 41PT185/C, also exhibited poor recovery or carbonized plant materials. Five of the seven flotation samples did not contain charred plant remains. Better results were noted at 41PT186, a Protohistoric site, from which 3.3 g of charred plant material was recovered. However, most of this material occurred in a single sample from Feature 8.

N.5 SITE SUMMARIES

41PT185/C. I examined seven flotation samples and 25 charcoal samples from this site. Mesquite was present in Feature 8 in relative abundance, and in Feature 11 cottonwood/willow-type. In contrast to the flotation samples, most of the identified wood was juniper in the individually collected charcoal samples. The majority of

these charcoal samples were collected from non-feature contexts. However, two were collected from Feature 9, and these samples yielded mesquite. Charcoal samples from Features 11 and 15 both contained juniper. No seed or fruit remains were noted in the samples.

The presence of cottonwood/willow indicates utilization of streamside vegetation, or vegetation near a spring. Mesquite grows either near a stream at slightly higher elevations or along the margins of open areas. At least today, sand plum grows on low dunes and mountain mahogany primarily along or at the base of the caprock, canyons, or on rocky breaks away from the caprock. Juniper is located on erosional breaks, slopes, and low hills.

All of the plant taxa in the archaeological assemblage grow in the region today. Woody materials found at the site reflect the utilization of several different ecological zones in the vicinity. Willow/cottonwood would have been selected from lower terraces, mesquite from margins of grasslands, and the Rosaceae-type wood from either low dunes or steeper, rocky slopes, and juniper from slopes. Without fire suppression and with pressure from use as fuel wood and structural material, woody plants were likely much less widespread in the region.

41PT186. I examined six flotation samples and 14 charcoal samples from this Protohistoric site. Charred wood or grass fragments occurred in all the flotation samples, an indication of somewhat better preservation. I did not find seed or fruit remains.

Table N-1. Flotation Sample Summaries.

Catalog No.	Feat.	Unit	Level	Light fraction vol. (ml), wt. (g)	Roots (r), Insect Parts (ip), Leaves (l)	Uncharred Seeds	Charred Seed Taxa	Total Charred Seeds/m size parts	Total Charcoal	Notes
Late Archaic 1600-2800 B.P.										
198-004	F3b	TU 20-b	80-90	57; 10.6	r+++	Sunflower (6)	--	--	0.0	
355-004	11	N102 E104	55-60	14; 5.2	r+++	--	--	--	0.0	
406-004	11	N103 E104	54-60	22; 1.2	r+++; ip+	--	--	--	<0.1	
471-004	8	N104 E105	41-50	18; 1.7	r+++	Sunflower (4)	--	--	0.0	
712-004	13	N110 E106	40-50	15; 1.6	r+++	Hackberry (1)	--	--	0.0	
1129-004	18	N118 E105	55-60	30; 3.8	r+++	Cheno-am (3), sunflower (5)	--	--	0.0	
1341-004	8a	N104 E105	56-61	70; 8.8	r+++	Cheno-am (6), sunflower (12)	--	--	0.1	
Protohistoric 200-300 B.P.										
259-004	1	TU 2	91-100	76; 26.9	r+++; ip++	--	--	--	0.2	
371-004	7	N486 E492	70-73	12; 4.8	r+++; ip++	--	--	--	<0.1	
372-004	7	N486 E493	70-80	110; 50.1	r+++; ip++	--	--	--	0.6	
405-004	8	N488 E489	63-78	22; 54.8	r+++; ip+	--	--	--	2.5	
407-004	8	N488 E490	66-80	92; 21.1	r+++	--	--	--	<0.1	
546-004	7	scraping	70-80	32; 4.5	r+++; ip++	Pocaceae (2)	--	--	<0.1	
Palo Duro/Woodland 1200-1400 B.P.										
348-004	2	TU 4 bulk	125-130	26; 7.6	r+++		--	--	0.0	Burned bone
348-004	2	TU 4 bulk	134-140	28; 6.1	r+++; ip+		--	--	0.1	Burned bone

	Site		41PT185/C	41PT185/C	41PT185/C	41PT185/C	41PT185/C	41PT185/C	41PT185/C		41PT186	41PT186	41PT186	41PT186	41PT186	41PT186		41PT245	41PT245
--	------	--	-----------	-----------	-----------	-----------	-----------	-----------	-----------	--	---------	---------	---------	---------	---------	---------	--	---------	---------

Table N-2. Flotation Samples from 41PT185/C, a Late Archaic Site.

Site	Catalog No.	Feature	Taxon	Common	Part	Count	Wt (g)
41PT185/C	198-004	3b	No identifiable plant remains	--	--	--	--
41PT185/C	355-004	11	No identifiable plant remains	--	--	--	--
41PT185/C	406-004	11	Salicaceae	Cottonwood/ willow-type	Wood	9	<0.1
41PT185/C	471-004	8	No identifiable plant remains	--	--	--	--
41PT185/C	712-004	13	No identifiable plant remains	--	--	--	--
41PT185/C	1129-004	18	No identifiable plant remains	--	--	--	--
41PT185/C	1341-004	8a	<i>Prosopis</i> sp.	Mesquite	Wood	16	0.1

Table N-3. Charcoal Samples from 41PT185/C, a Late Archaic Site.

Site	Catalog No.	Feature	Taxon	Common	Part	Count	Wt (g)
41PT185C	270-007	--	Indeterminate	NA	Flecks	--	--
41PT185C	299-007	--	<i>Juniperus</i> sp.	Juniper	Wood	2	0.1
41PT185C	348-007	--	Non botanical	NA	Burned bone	--	--
41PT185C	354-007	11	<i>Juniperus</i> sp.	Juniper	Wood	2	<.1
41PT185C	397-007	--	Indeterminate	NA	Flecks	--	--
41PT185C	452-007-1b	--	<i>Juniperus</i> sp.	Juniper	Wood	25+ (4ml)	1.7
41PT185C	464-007	--	<i>Juniperus</i> sp.	Juniper	Wood	1	0.2
41PT185C	490-007	--	Non botanical	NA	Burned bone	--	--
41PT185C	501-007	9b	<i>Prosopis</i> sp.	Mesquite	Wood	8	0.1
41PT185C	517-007	--	<i>Juniperus</i> sp.	Juniper	Wood	9	0.1
41PT185C	570-007	--	<i>Juniperus</i> sp.	Juniper	Wood	8	0.7
41PT185C	656-007	--	<i>Juniperus</i> sp.	Juniper	Wood	2	<.1
41PT185C	701-007	--	<i>Juniperus</i> sp.	Juniper	Wood	2	<.1
41PT185C	724-007	--	<i>Prosopis</i> sp.	Mesquite	Wood	3	0.1
41PT185C	774-007	--	<i>Juniperus</i> sp.	Juniper	Wood	3	0.2
41PT185C	909-007	--	Non botanical	NA	Burned bone	--	--
41PT185C	917-007	--	<i>Juniperus</i> sp.	Juniper	Wood	1	0.2
41PT185C	1045-007	--	<i>Juniperus</i> sp.	Juniper	Wood	2	<.1
41PT185C	1091-007	--	Non botanical	NA	Burned bone	--	--
41PT185C	1159-007	--	Indeterminate	NA	Slag	3	<.1
41PT185C	1170-007	--	<i>Juniperus</i> sp.	Juniper	Wood	11	0.4
41PT185C	1224-007	--	Non botanical	NA	Sooty sediment	--	--
41PT185C	1234-007	15	<i>Juniperus</i> sp.	Juniper	Wood	2	0.2
41PT185C	1270-007	--	<i>Prosopis</i> sp.	Mesquite	Wood	3	<.1
41PT185C	1337-007	9d	<i>Prosopis</i> sp.	Mesquite	Wood	7	0.2

Table N-4. Flotation Samples from 41PT186, a Protohistoric Camp.

Site	Catalog No.	Feature	Taxon	Common	Part	Count	Wt (g)
41PT186	259-004	1	Salicaceae	Cottonwood/ willow-type	Wood	24	0.1
41PT186	259-004	1	<i>Prosopis</i> sp.	Mesquite	Wood	2	<0.1
41PT186	259-004	1	Poaceae	Grass Family	Stem/culm	2	<0.1
41PT186	259-004	1	Indeterminate	N.A.	Wood	13	0.1
41PT186	371-004	7	Indeterminate	N.A.	Wood	16	<0.1
41PT186	372-004	7	<i>Prosopis</i> sp.	Mesquite	Wood	25+ (3 ml)	0.6
41PT186	405-004	8	Salicaceae	Cottonwood/ willow-type	Wood	24	0.9
41PT186	405-004	8	Rosaceae	Sand plum/mountain mahogany-type	Wood	19	1.1
41PT186	405-004	8	Indeterminate	N.A.	Root	22	0.4
41PT186	407-004	8	Rosaceae	Sand plum/mountain mahogany-type	Wood	8	<0.1
41PT186	546-004	7	Salicaceae	Cottonwood/ willow-type	Wood	5	<0.1
41PT186	546-004	7	Indeterminate	N.A.	Flecks	--	<0.1

Table N-5. Charcoal Samples from 41PT186, a Protohistoric Camp.

Site	Catalog No.	Feature	Taxon	Common	Part	Count	Wt (g)
41PT186	258-007		Salicaceae	Cottonwood-willow-type	Wood	6	<.1
41PT186	373-007	7	<i>Prosopis</i> sp.	Mesquite	Wood	13	0.3
41PT186	405-007-1	8	<i>Prunus</i> sp.	Sand plum/mountain mahogany-type	Wood	11	0.7
41PT186	421-007		Salicaceae	Cottonwood-willow-type	Wood	1	0.1
41PT186	425-007		<i>Prosopis</i> sp.	Mesquite	Wood	1	0.1
41PT186	440-007		<i>Juniperus</i> sp.	Juniper	Wood	1	0.1
41PT186	445-007		Salicaceae	Cottonwood-willow-type	Wood	9	<.1
41PT186	446-007	6	Indeterminate	NA	Wood	5	<.1
41PT186	466-007		Salicaceae	Cottonwood-willow-type	Wood	3	<.1
41PT186	478-007		Poaceae	Grass family	Culm/stalk	2	<.1
41PT186	478-007		Salicaceae	Cottonwood-willow-type	Wood	1	<.1
41PT186	493-007		Salicaceae	Cottonwood-willow-type	Wood	4	<.1
41PT186	504-007		Salicaceae	Cottonwood-willow-type	Wood	3	0.1
41PT186	520-007		Salicaceae	Cottonwood-willow-type	Wood	1	<.1
41PT186	547-007	8	Indeterminate	NA	Wood	5	<.1

Features 1 and 7 contained cottonwood/willow-type and mesquite wood, along with grass family culms/stems. Feature 8 contained an abundance of mesquite and sand plum/mountain mahogany type wood. Juniper was identified in only one charcoal sample. Cottonwood/willow is abundant along streamsides, and mesquite along the margins of open areas.

The abundance of cottonwood/willow-type at 41PT186 may be an indication of its use as a structural material. Grass stems may have been utilized in wall daub. The other wood types, especially juniper and mesquite, are more effective fuel woods. Cottonwood/willow is especially common at sites with structures, and posts have been identified as cottonwood/willow at the Hank site, 41RB106, (Dering 2005).

41PT245. Two samples were examined from this Palo Duro/Woodland site. Although very small fragments of charred wood were recovered from one of the samples, it was not identifiable. The other sample did not contain charred plant remains. The extreme reduction of plant material at this site is likely due to a combination of poor preservation conditions, the age of the site, and the small sample size.

N.6 CONCLUSION

The 14 flotation samples and 39 charcoal samples contained mesquite, cottonwood/willow-type, juniper, and indeterminate wood as well as some grass culm/stem fragments. Fruit or seed remains did not occur in samples from any site. Disturbance indicators were abundant, and the charred wood fragments in most of the samples were greatly reduced, making identification difficult.

Despite the poorly preserved nature of the botanical remains, there were recognizable differences in the assemblage from 41PT185 and 41PT186. The assemblage from 41PT185, the Late Archaic site, contained far more examples of juniper wood. At 41PT186 the assemblage contained only one example of juniper and abundant

cottonwood/willow-type material. Although the sample size is small, the assemblages suggest that patterns of wood selection changed in the area during the intervening time between the two occupations. It is, however, difficult to determine the cause of this change. It could indicate an environmental change, though this is unlikely because all three taxa (juniper, mesquite, and cottonwood) co-occur in the region today. It more likely indicates a very local shift in taxa abundance or the selection of wood for use in structures and/or as fuel. Juniper would have been utilized more for fuel and cottonwood/willow for structures. The difference is intriguing, but the sample size is too small to form any firm conclusions. What can be said is that the region contained mesquite at least by the Late Archaic period, and the abundance of cottonwood/willow was far greater in the Protohistoric samples from 41PT186.

N.7 REFERENCES

- Dering, J. P.
2005 Architecture and Subsistence at Hank's Site, 41RB106: Analysis of the Plant Remains. Draft submitted to Prewitt and Associates, Inc. Austin, Texas.

APPENDIX O

**MULTI-INSTRUMENT GEOPHYSICAL INVESTIGATIONS AT
41PT185, 41PT186, AND 41PT245**

This page intentionally left blank.

**MULTI-INSTRUMENT GEOPHYSICAL INVESTIGATIONS AT 41PT185,
41PT186, AND 41PT245**

Prepared for:



**TRC Environmental Corporation
505 East Huntland Drive, Suite 250
Austin, Texas 78752**

Prepared by:

**Chester P. Walker, Ph.D.
Archaeo-Geophysical Associates, LLC
Austin, Texas**

September 25, 2009

This page intentionally left blank.

O.1 MANAGEMENT SUMMARY

This report presents the findings from geophysical surveys at 41PT185/C, 41PT186, and 41PT245 in Potter County, Texas. A flux gradiometer, conductivity meter, magnetic susceptibility meter, and a Ground Penetrating Radar (GPR) were employed on an area totaling 650 m². A total of 210 m² was collected with the four geophysical technologies at 41PT245, 160 m² at 41PT185/C, and 280 m² at 41PT186. The geophysical surveys were conducted by Chester P. Walker of Archaeo-Geophysical Associates, LLC. Several geophysical anomalies were targeted for ground truthing, and subsequent archeological investigations demonstrated that several were thermal archeological features. There were, however, archeological features at 41PT185 and 41PT186 that were not located by the various geophysical techniques.

O.2 INTRODUCTION

This report presents findings from geophysical surveys at 41PT185/C, 41PT186, and 41PT245 in Potter County, Texas. A flux gradiometer, conductivity meter, magnetic susceptibility meter, and a ground penetrating radar (GPR) was used on an area totaling 650 m². A total of 210 m² was collected with the four geophysical technologies at 41PT245, 160 m² at 41PT185/C, and 280 m² at 41PT186.

Archeologists from TRC Environmental, Inc. (TRC) determined during the Phase I data recovery that the upper stratum at all three specific localities did not contain any cultural materials. The overburden was then stripped from all three sites and the geophysical surveys were conducted within the backhoe strip units. This final report expands on previous discussion of the geophysical survey (Walker 2008), and uses results from the archeological hand-excavations to correlate the geophysical data sets with the archeological findings.

Geophysical survey investigations have become an important part of the pursuit of North American archeology (Kvamme 2008). Several techniques have been derived from geophysical prospecting and adopted for archeological investigations (Clark 2000; Kvamme 2003). Techniques used mostly for archeological research include soil resistivity, soil conductivity, magnetic susceptibility, magnetometry, and GPR (Clark 2000; Kvamme 2003). All produce different results and require different equipment. The different geophysical techniques that have been used in archeology have been discussed in a number of seminal books and journal articles (Bevan 1998; Carr 1982; Clark 1990; Conyers 2004; Gaffney 2008; Gaffney and Gater 2003; Scollar et al. 1990; Weymouth 1986; Witten 2006).

Magnetic prospecting has proven to be one of the more useful geophysical technologies for locating buried architectural remains on archeological sites (Dabas and Tabbagh 2000:335-339). Magnetic prospecting is capable of measuring the magnetic properties of soils to the 0.1 nano Tesla (nT), which makes it possible to isolate subtle changes caused by earth moving or low heat firing (even when they occurred hundreds or thousands of years ago). These factors make magnetic prospecting a valuable tool to employ on sites with abundance of thermally altered features such as fire hearths, burned rock features, or burned houses, as well as on sites with features that extend through organic rich soils into more mature sub-soils. These examples, however, are also the major constraint of magnetic prospecting in archeological investigations, because if there are no magnetic contrasts between the archeological deposits and features and the surrounding sediments, then magnetometers lose their prospecting utility.

Similar to remote sensing of the natural environment, archeological prospecting is not meant to function as a solitary means of

investigation. Without a detailed understanding of the site-specific characteristics of archeological deposits, geophysical data are difficult to interpret and use in meaningful ways. This has been demonstrated by numerous case studies (Clark 2000; Weymouth 1986). This is not to say that it is not useful as a primary means of data acquisition when combined with extensive available data from manual subsurface archeological investigations. A growing body of literature addresses the use of geophysical prospecting as a primary means of data collection when coupled with other data from previous and/or current excavations: this has been described by Kvamme (2003) as the future of archeological geophysics.

In this report, I discuss the geophysical survey conducted by AGA at three prehistoric archeological sites located near Amarillo in Potter County, Texas. This work was conducted at the request of Mike Quigg of TRC primarily to locate and define geophysical anomalies on the site that may represent possible archeological features or archeological deposits of interest. As mentioned above, during the course of the geophysical survey at the three sites, a total of 650 m² was surveyed with each instrument, including magnetometry, magnetic susceptibility, electromagnetic conductivity; and GPR. The geophysical survey was limited to three very specific areas that had been previously laid out and stripped by TRC.

O.3 GEOPHYSICAL METHODS

Archeogeophysics employs a range of techniques for the non-destructive prospecting of archeological deposits (Gaffney and Gater 2003). These techniques have been developed for a range of applications, mostly geological in nature, but have been adapted for specific use in archeological research through rigorous field collection techniques and unique data

processing programs specifically developed for the study of the archeogeophysical record. The instruments used in this project record different properties. Magnetometers record the net sum of all magnetic fields both induced and remnant; GPR records relative dielectric permittivity; electromagnetic induction meters record both the conductivity of the soils as well as their induced magnetic properties (magnetic susceptibility). The geophysical instruments are differentially affected by variables such as moisture, metal trash or debris, and transmission of signals such as cell phones and transmission lines. Data collection is also impacted differently for each of the geophysical instruments by physical impediments such as trees, pavement, fences, and vegetation.

To address the complex matrix of variables that characterize the soil and the surroundings at a specific archeological site, it is important in the archeogeophysical investigations to come to the field prepared to collect data with several different instruments. The “multiple-technique” approach not only increases the likelihood of success in the ability to detect archeological features and archeological deposits of interest, but can often enhance the visibility of the archeological targets that may be present and preserved at archeological sites (Kvamme et al. 2006:251). Archeogeophysical data has a long history of success in helping to focus archeological excavations to specific targeted locations within sites to answer specific archeological questions, and under the right conditions can be used as a primary and stand-alone source of archeological data (Kvamme 2003).

O.3.1 MAGNETOMETER AND GRADIOMETER

Magnetometer and gradiometer surveys are non-invasive and passive techniques and measure slight variations in the magnetic properties of soil. Magnetometers and gradiometers have become the primary tool

for archeogeophysicists due in part to the fact that data can be collected and processed rapidly and efficiently, and when conditions are right, due to the properties of specific soils, magnetometers and gradiometers have proven useful in locating negative relief features such as pits and post holes, as well as thermally-altered features such as fire hearths and burned structures (Gaffney et al. 2000; Kvamme 2006a).

Magnetometers and gradiometers record the minute fluctuations that sediments and objects have on the earth's magnetic field. This is known as induced magnetism because the object does not maintain its own magnetic field. If the effects of this induced magnetism are strong enough compared to the magnetism of the surrounding soil matrix, even small pit features or post holes can be identified or resolved in the geophysical data along with the larger-sized features (i.e., structures). A second type of magnetism called remnant magnetism is created when an object maintains its own magnetic field. In prehistoric archeological examples, this occurs when objects are thermally altered, thus creating a magnetic state called thermoremanent magnetism (Kvamme 2006a:207). The properties of the specific magnetometer used in the current study—a Bartington 601-2 Fluxgate Gradiometer—is discussed in detail by Bartington and Chapman (2004).

0.3.2 GROUND PENETRATING RADAR

GPR data are acquired by transmitting pulses of radar energy into the ground from a surface antenna, reflecting the energy off buried objects, features, or bedding contacts in the soil, and then detecting the reflected waves back at the ground surface with a receiving antenna. When collecting radar reflection data, surface radar antennas are moved along the ground in transects, typically within a surveyed grid, and a large number of subsurface reflections are collected along each line. As radar energy moves through various materials, the

velocity of the waves will change depending on the physical and chemical properties of the material through which they are traveling (Conyers 2004). The greater the contrast is in electrical and magnetic properties between two materials at an interface, the stronger the reflected signal, and therefore the greater the amplitude of reflected waves (Conyers 2004). When the travel times of energy pulses are measured, and their velocity through the ground is known, distance (or depth in the ground) can be accurately measured (Conyers and Lucius 1996). Each time a radar pulse traverses a material with a different composition or level of water saturation, the velocity will change and a portion of the radar energy will reflect back to the surface and be recorded. The remaining energy will continue to pass into the ground to be further reflected, until it finally dissipates with depth.

The depths to which radar energy can penetrate, and the amount of resolution that can be expected in subsurface deposits, are partially controlled by the frequency (and therefore the wavelength) of the radar energy that is being transmitted (Conyers 2004). Standard GPR antennas propagate radar energy that varies in frequency from about 10 megahertz (MHz) to 1000 MHz. Low frequency antennas (10 to 20 MHz) generate long wavelength radar energy that can penetrate up to 50 m (164 ft.) below the surface in certain conditions, but are capable of resolving only very large buried features. In contrast, the maximum depth of penetration of a 900 MHz antenna is about 1 m or less (3.28 ft.) in typical materials, but its generated reflections can resolve features with a maximum dimension of a few cm or inches. A trade-off, therefore, exists between the depth of penetration and subsurface resolution. In this survey, a 400 MHz antenna was used, which produced data of good resolution at depths up to about 1.8 m (about 5.9 ft.).

The success of GPR surveys in archeological investigations is largely

dependent on soil and sediment mineralogy, clay content, ground moisture, depth of burial, and surface topography and vegetation. Electrically conductive or highly magnetic materials will quickly attenuate radar energy and prevent its transmission to a considerable depth. The best conditions for energy propagation are therefore dry sediments and soils without an abundance of clay. In this survey, the GPR data collection was concentrated in areas where the ground surface had been cleared of major vegetation and surface obstructions.

O.3.3 CONDUCTIVITY

Conductivity surveys measure the ability to conduct an electric current (Clay 2006:79). This measurement is the theoretical inverse to resistivity; however, measuring conductivity entails a much more complex set of procedures than does resistivity (Bevan 1983:51; Clay 2006:79). Conductivity instruments differ greatly from resistivity instruments in that no probes are inserted into the earth. The conductivity has a set of wire coils, one transmitting a low frequency signal and one receiving the signal. The conductivity meter is simply carried above the earth surface and data are logged automatically, making conductivity surveys time and labor efficient (although not as efficient as the magnetometer) for geophysical surveys.

Conductivity meters can resolve data at different depths by changing the separation of the transmission and receiving coil and by transmitting its signal at different frequencies. Some instruments allow for these variables to be changed and others, like the Geonics EM38—the most widespread conductivity meter used in American archeology—are not adjustable. The Geonics EM38B was employed for both the magnetic conductivity and magnetic susceptibility geophysical surveys. The EM38B will measure conductivity to approximately 1.5 m below the surface

when set in the vertical dipole mode (Ernwein 2008:133).

Conductivity has proven to be a useful tool at different scales in landscape archeology. Berle Clay's (2006) work at the Hollywood site in northern Mississippi demonstrates conductivity's ability to obtain detailed information about prehistoric Native American architecture by producing results that appear similar to those produced by magnetometer surveys. Grealy and Conyers (2008) have demonstrated a much more broad scale use for conductivity by mapping large tracts of land for geomorphological features (i.e., old channels, buried point bars and levee deposits, etc.) and revealing relict meander scars in major river floodplains (Grealy and Conyers 2008; Conyers et al. 2008).

O.3.4 MAGNETIC SUSCEPTIBILITY

Magnetic susceptibility is a measurement of a material's ability to be magnetized (Dalan 2006:161). Changes or contrasts in the magnetic susceptibility of sediments are the results of a conversion of weakly magnetic oxides and hydroxides to more strongly magnetic forms (Dalan 2006:162). The magnetic enhancement of anthropogenic soils can be caused by burning episodes (both natural and human-caused) as well as organic and inorganic pedogenic processes (Dalan 2006:162-163).

Magnetic susceptibility instruments differ from magnetometers in that they only measure fields resulting from induced magnetism, as compared to a magnetometer that records the net effect of induced and remnant magnetism (Dalan 2006:162; Kvamme 2006a:207-210). The differences between these two instruments produce data sets that are both complementary and unique. They are complementary in that magnetic susceptibility data can aid in the interpretation of magnetometer data (Dalan 2006:162-163), and magnetic susceptibility data is unique in that it can be used to

address entirely different research questions, such as tracking broad magnetic changes across the landscape (David 1995:20).

Magnetic susceptibility has the potential to, like magnetic conductivity, produce archeogeophysical results that are quite similar in appearance and information content to that obtained by magnetometer surveys. One of the best examples of this is from the Tom Jones site (3HE40), a 14th to 15th century Caddo mound center in southwestern Arkansas (Dalan 2006:182, Figure 8.9). Dalan has repeatedly demonstrated magnetic susceptibility's utility in both soil characterization and site formation issues (Dalan and Banerjee 1998; Dalan 2006, 2008).

O.4 FIELD METHODS

Field methods for archeogeophysical investigations vary in detail from technique to technique, but there are several factors that are consistent with all techniques. The density of the dataset is controlled by two factors: (1) traverse interval—the distance between the passes the instrument makes as it is passed back and forth across the collection area; and (2) sample interval—the distance between readings the instrument records as it passes along each traverse. To control for these two variables a survey grid was established inside the three scrape units established by TRC. These grids were marked with non-magnetic markers and allowed the surveyor to pass the various instruments across the sites in a series of systematic passes or traverses. The individual instruments control the second variable, the sample density. Readings are either collected in a known cycle (i.e., 5 readings per second) and the surveyor matches their sets to their gait to establish the desired sample density (this is the case with the magnetometer and EM meter), or a calibrated survey wheel is used to record readings at set intervals (as is the case with the GPR).

For all three sites the gradiometer data was collected with a traverse interval set at 0.5 m, and a 0.125 m sample interval; the traverse interval for the EM meter was 1.0 m, with a 0.25 m sample interval. GPR data was collected in 0.5 m transects with a sample rate of 32 readings per m.

O.5 DATA PROCESSING

The general goal of the data processing is to lessen the effects of background “noise” and to enhance the quality of the “signal” or “target” in the geophysical data. In field geophysics in general, and archeogeophysics in particular, the term noise is used to discuss any return that is not a direct result of the object under investigation, this being referred to as the “target” or “signal.” Hence, in some cases what is discussed as noise can in another case become the signal or target (Milsom 2005:13-14).

The general approach to data processing follows that advocated by Kvamme (2006b:236), namely to computer process the geophysical data to identify regular and culturally interpretable patterns using pattern recognition principles: “In general, anomalies exhibiting regular geometric shapes (lines, circles, squares, rectangles) tend to be of human origin” (Kvamme 2006b:236). After each processing step the results should be closely compared to their previous processed state to assure that data manipulation is not in fact decreasing the clarity and quality of the data, and thus avoiding the creation of processed images that are primarily products of the data processing itself.

The geophysical data from all three sites was surprisingly consistent. This is likely due to their close proximity to one another and the fact that TRC stripped off the overburden from all three sites. Stripping the overburden did introduce noise into the data (especially with the magnetometer data); however, it also aided in removing a

significant amount of potential noise from the upper portions of each site's deposits.

The magnetometer data was processed using ArchaeoSurveyor 2.0. The data was first clipped to ± 5 nT. Clipping the data replaces all values outside a specified minimum and maximum range. These minimum and maximum values are specified in either absolute values or \pm Standard Deviations (SD). This process is used to remove extreme data point values and aids in normalizing the histogram of the data. Archeological details are subtle, and having a normal distribution of data allows the fine detail to show through with clarity.

The data was then passed through a de-stripping filter using the zero median function. De-stripping is a process used to equalize the underlying differences between grids caused by instrument drift, inconsistencies during setup, delays between surveying adjacent grids, or heading error from magnetic instruments. The mean, mode, or median of each grid or traverse is subtracted from the grid or traverse, effectively zeroing the mean, mode, or median.

Finally the data was de-staggered as necessary. De-staggering is performed to correctly align readings from adjacent traverses. Data can become skewed if the surveyor incorrectly triggers the instrument. De-staggering data simply shifts the traverses a specified interval. A cubic spline algorithm is used to calculate the shifted data points to ensure a smooth curve from existing data.

The two EM datasets (conductivity and magnetic susceptibility) were also processed in ArchaeoSurveyor 2.0. Very little processing was done with the conductivity data other than simply importing the data and exporting images. Due to the high signal to noise ratio observed in all three magnetic susceptibility data sets, a low pass filter was used. A low pass filter calculates

the mean of a window of a specified size, and replaces the center value with the mean. This can use Uniform or Gaussian weighting. With Uniform weighting means, all values within the window are given equal weight. Gaussian weighting gives a higher weight to values closer to the center of the window. Low pass filters are more commonly applied to lessen the effects of background noise. As is the case with all data processing steps, low pass filters should be used with caution and close attention should be made to their resulting effects, assuring that no processing artifacts are created, or no significant anomalies removed as a result of their application (Kvamme 2006b).

GPR data was processed using GPR slice. The initial data processing for the project involved the generation of amplitude slice-maps (Conyers 2004). Amplitude slice-maps are a three-dimensional tool for viewing differences in reflected amplitudes across a given surface at various depths. Reflected radar amplitudes are of interest because they measure the degree of physical and chemical differences in buried materials. Strong, or high amplitude, reflections often indicate denser or different buried materials, such as archeological features. Amplitude slice-maps are generated through the comparison of reflected amplitudes between the reflections recorded in vertical profiles. In this method, amplitude variations, recorded as digital values, are analyzed at each location in a grid of many profiles where there is a reflection recorded. The amplitudes of all traces are compared to the amplitudes of all nearby traces along each profile. This database can then be "sliced" horizontally and displayed to show the variation in reflection amplitudes at a sequence of depths in the ground. The result is a map that shows amplitudes in map view, but also with depth. Often when this is done, changes in the soil related to disturbances such as trash pits or dense clusters of rocks can become visible, making many features visible to the human

eye that may not be visible in individual profiles.

O.6 GEOPHYSICAL DATA INTERPRETATION

Data at all three sites were collected in areas that were targeted for hand-excavations by TRC. These areas had all been stripped of their overburden and the geophysical surveys were conducted in large stripped areas. The geophysical surveys were

successful in locating thermally altered features as well as some more subtle features.

41PT185/C

41PT185/C was the most productive site in terms of recovered archeological features and was likewise the most productive site in terms of the archeogeophysical survey. There were a total of nine correlations between the geophysical anomalies and the excavated archeological features.

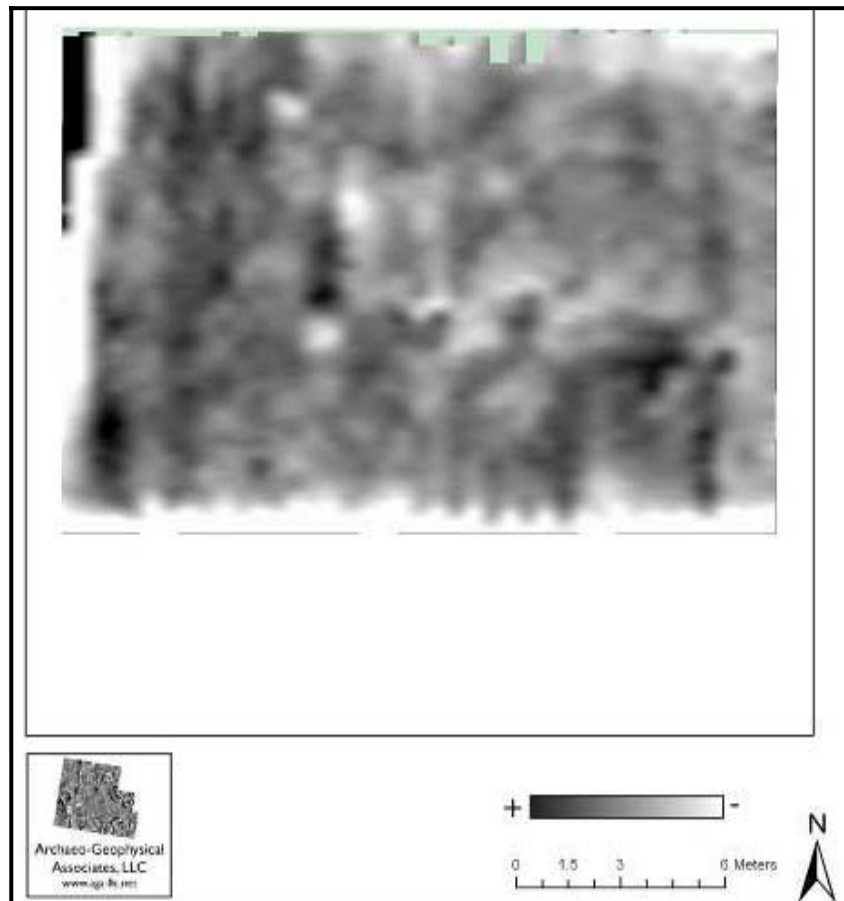


Figure O-1. Magnetometer Data from 41PT185/C.

Black Represents Positive Readings and White Represents Negative Readings. Data Range is ± 5 nT.

The magnetometer data (Figure O-1) consisted of a few pronounced positive magnetic anomalies scattered across the southern half of the collection area. The western edge of the collection area consists of strong negative magnetic trends, while in the northwest portion of the collection area there is a strong linear dipole. These signatures were due to the walls of the backhoe stripped block. There are also negative magnetic readings across both the southern edge and the northeastern corner of the collection area, which were also caused by the walls of the stripped block.

GPR data (Figures O-2 and O-3) from shallow time slices (5 to 9 cmbs and 9 to 14 cmbs) show large concentrations of median and high amplitude reflections in the south

central portion of the collection area, and then in the northeast part of the collection area in the lower slice. Conductivity data (Figure O-4) consists of a high conductive anomaly in the center of the northern edge of the collection area. A low conductive anomaly is located in the southwestern portion of the collection area. Along the southern edge of the grid is a homogeneous trend of median conductive values that are most likely due to feed back from the scrape unit walls that were also observable in the magnetometer data. The magnetic susceptibility data (Figure O-5) shows a trend that will continue at all three sites. The magnetic susceptibilities consist of low values (± 1.25 ppm) that alternate from low to high readings, creating a noisy dataset with little interpretive value.

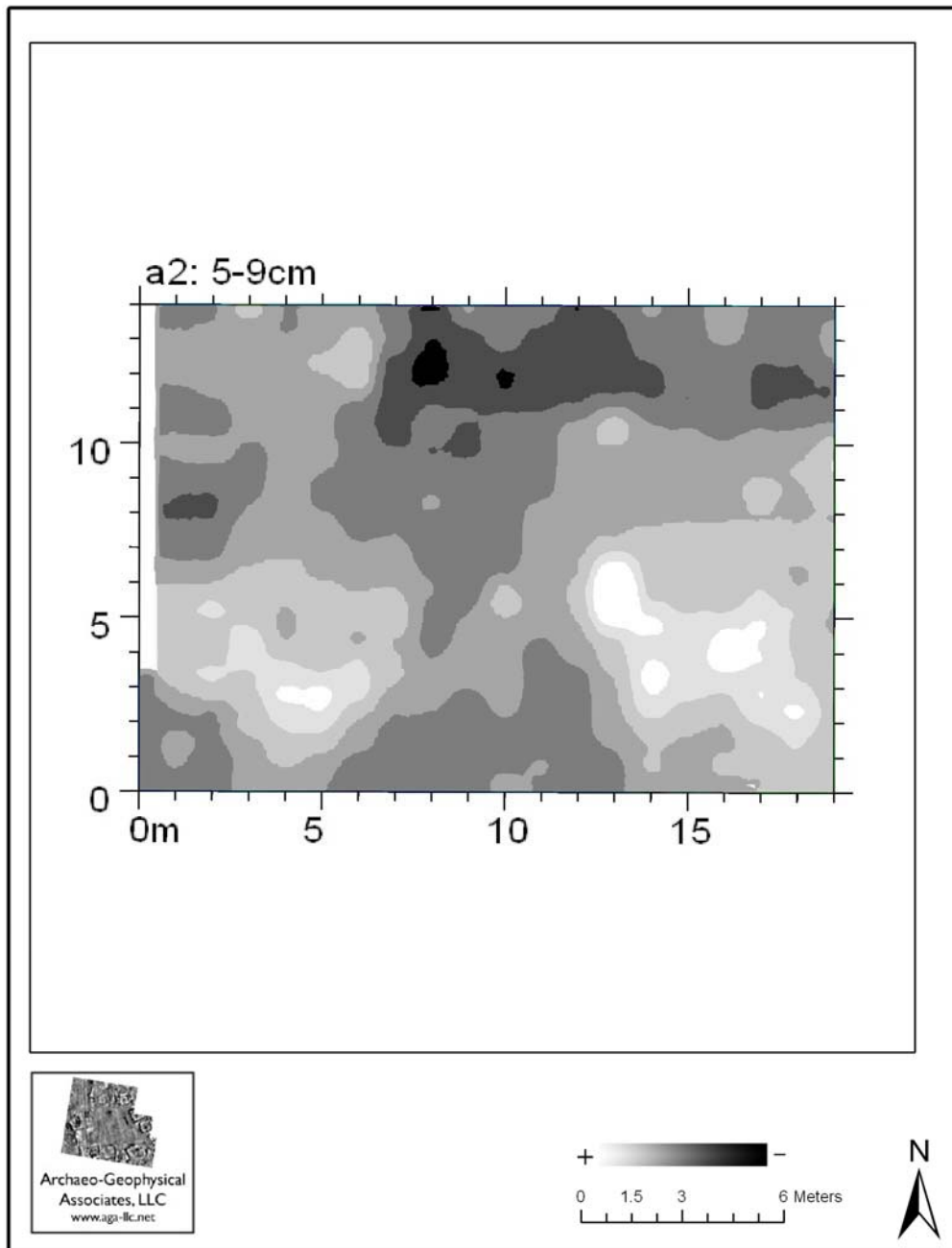


Figure O-2. GPR Time Slice from 5 to 9 cmbs from 41PT185/C.

White Represents High Amplitude Reflections and Black Represents Low Amplitude Reflections

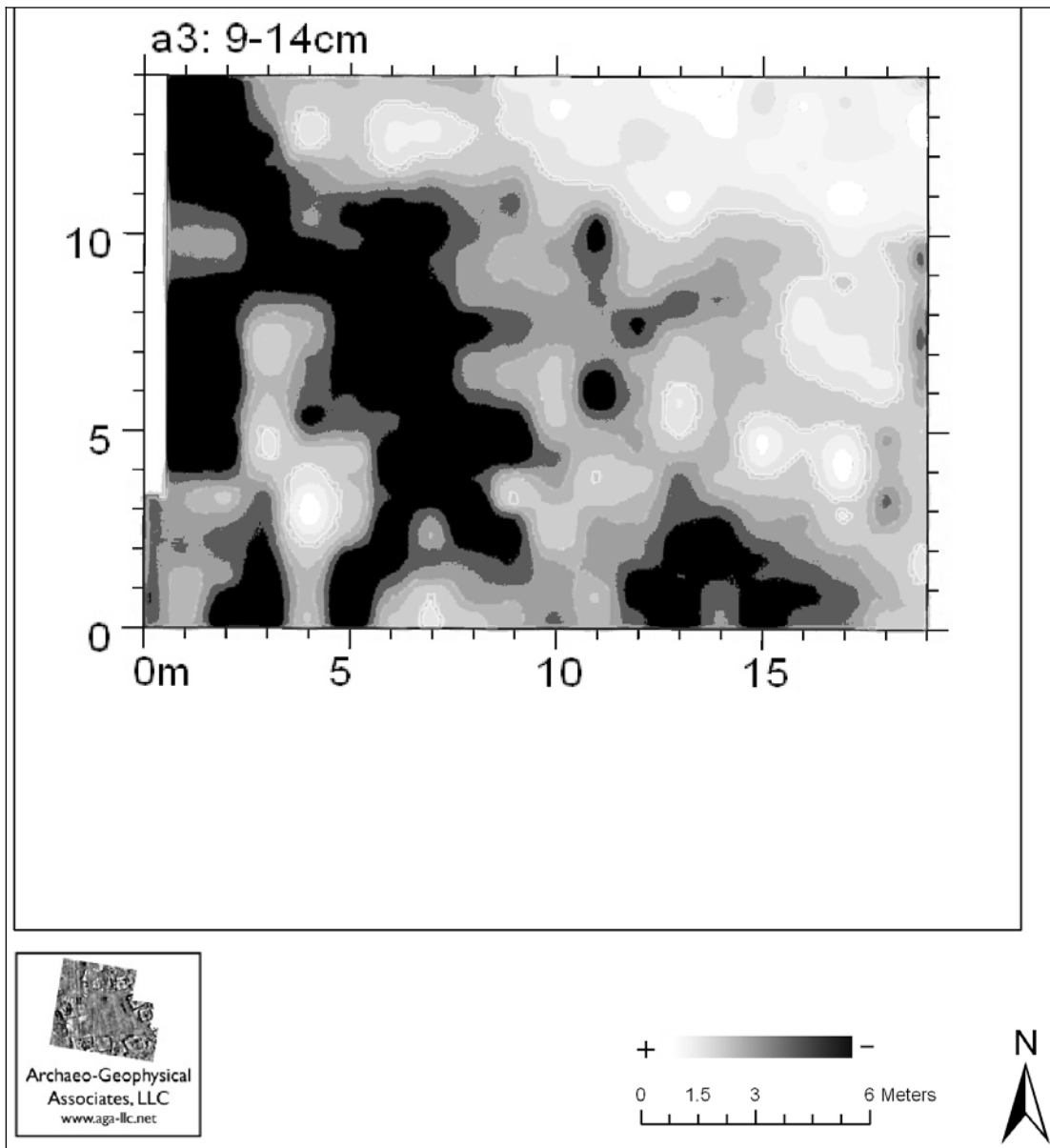


Figure O-3. GPR Time Slice from 9 to 14 cmbs from 41PT185/C.

White Represents High Amplitude Reflections and Black Represents Low Amplitude Reflections.

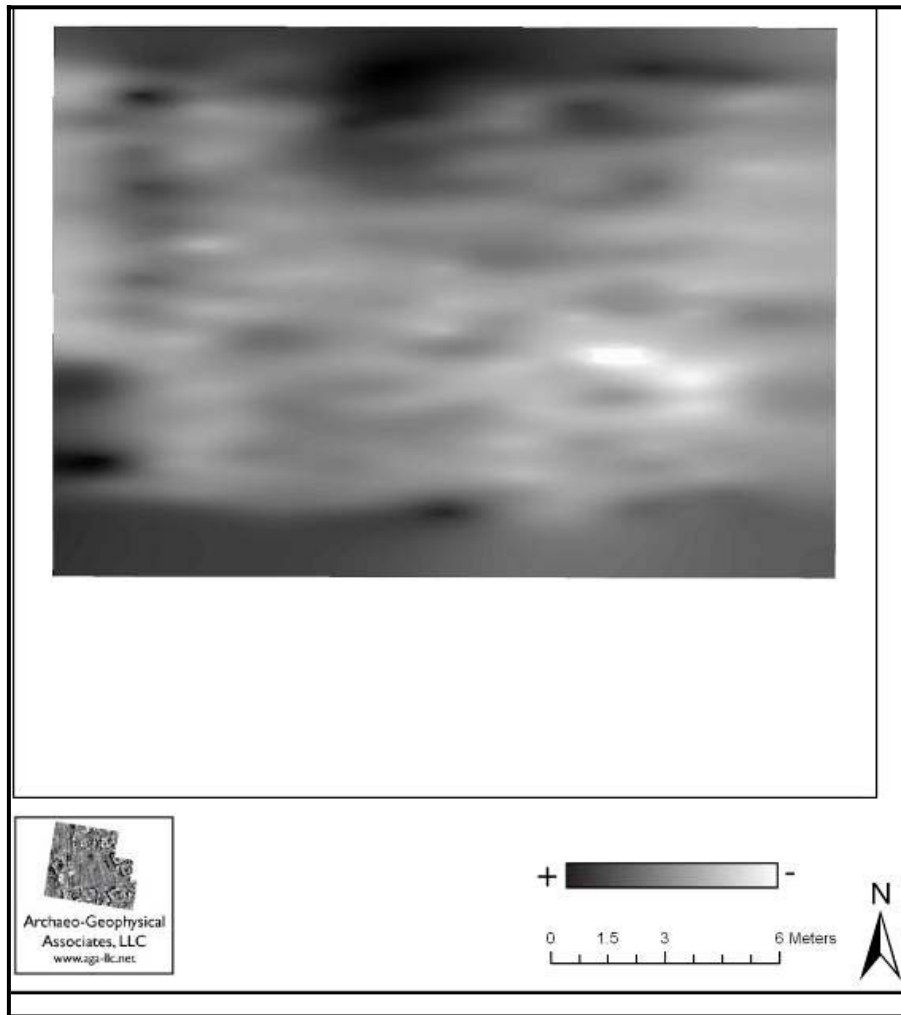


Figure O-4. Conductivity Data from 41PT185/C.

Black Represents High Conductivity and White Represents Low Conductivity.

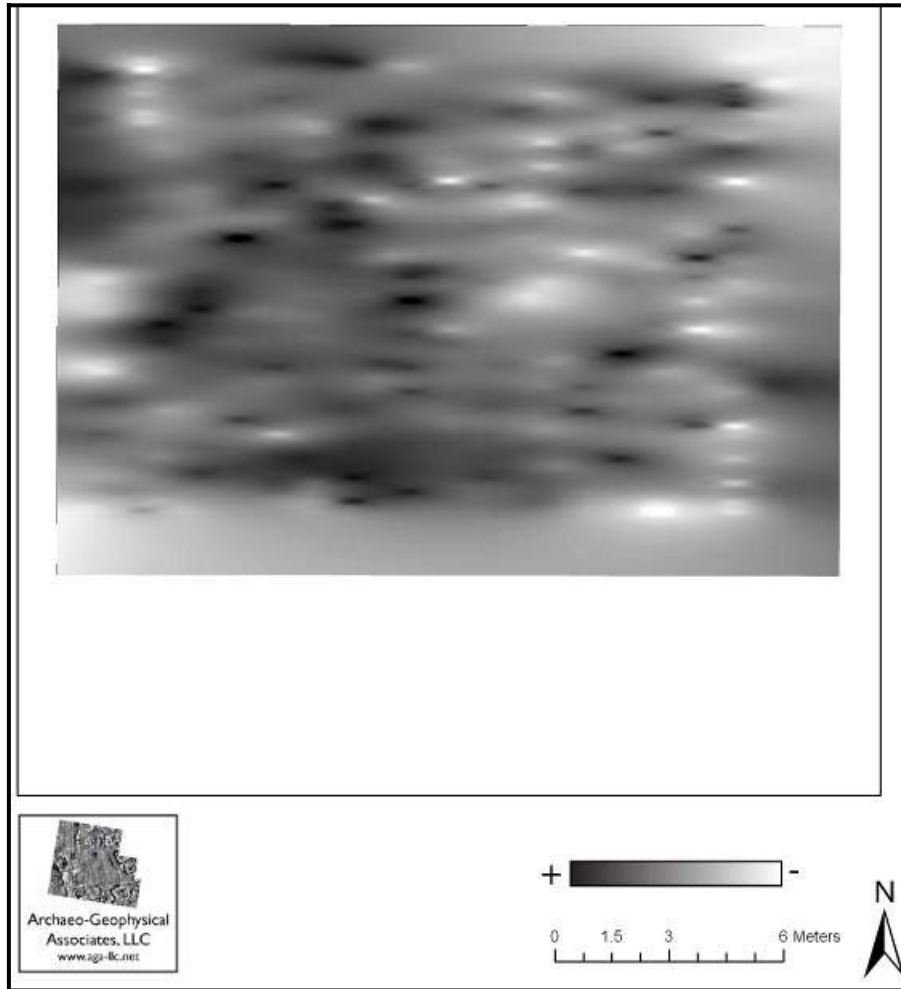


Figure O-5. Magnetic Susceptibility Data from 41PT185/C.

Black Represents High Magnetic Susceptibility and White Represents Low Magnetic Susceptibility.

TRC's excavations from site 41PT185/C contained features that consisted of concentrations of burned rocks (Figure O-6). These features did not show signs of intense oxidation or contain any charcoal concentrations (Mike Quigg, 2009 personal communication).

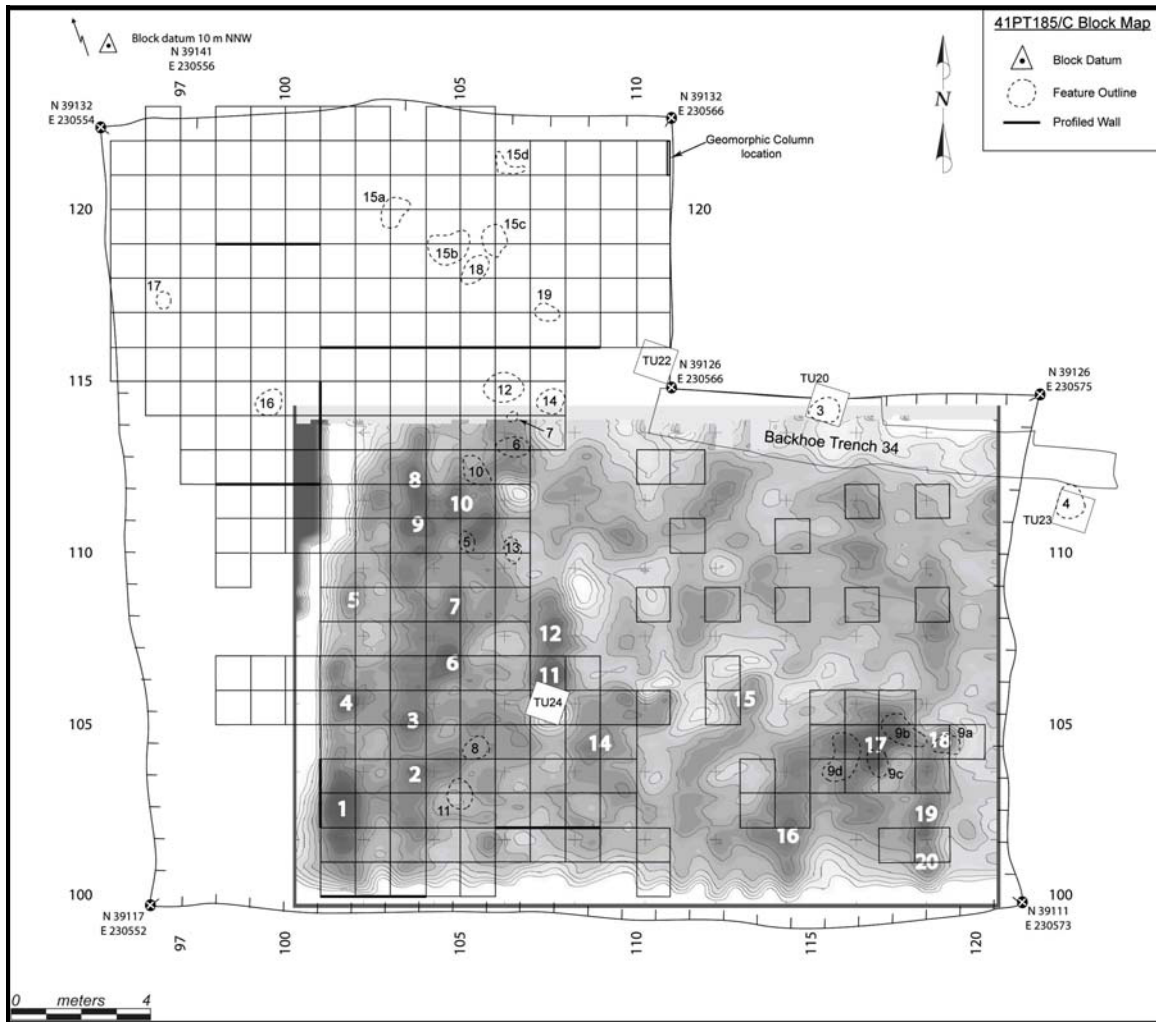


Figure O-6. Targeted Anomalies from 41PT185/C Overlaid with TRC's Excavation Units.

Table O-1 details the finding from TRC's field investigation at 41PT185/C (Figure O-7). Geophysical anomalies are listed and archeological materials recovered within a 50 cm radius of each anomaly are described. The strongest correlation between the geophysical anomalies and archeological materials is with anomalies 17 and 18 (see Figure O-7). At the locations of both of these anomalies, TRC's field crew recovered several pieces of burned rock that were recorded as Feature 9a through 9d. Figure O-8 shows the locations of the archeological features overlaid onto the magnetometer data. This image shows the strong correlation with the Feature 9 cluster (located in the southeast corner) with positive magnetic anomalies.

Table O-1. Results from Tested Anomalies from 41PT185/C.

Anomaly No.	Provenience North / East	Archeological Material	Distance from marked Spot
1	102 /101	1 small burned rock at 54 cm	over 1 small burned rock
2	104 /103	small burned rocks	on western edge of many burned rocks
3	105 /103	small scattered burned rocks	60-70 cm west of cluster of burned rocks
4	105 /101	none	possible rodent hole
5	108 /101	30 cm diameter rock	50 cm southeast of rock
6	112 /103		
7	108 /105	none	
8	112 /103	25 cm diameter rock	30 to 40 cm to east of rock
9	111 /103	none	nothing significant within 50 cm
10	112 /105	2 large rocks (17.5 kg)	50 cm northeast of 2 large rocks
11	106 /107	none	40-50 cm north of 1 x 1 m TU
12	no excavation		
13	skipped number		
14	104 /109	scattered burned rocks	over scattered burned rocks at 50-60 cm
15	106 /112	scattered burned rocks	over scattered burned rocks at 58-65 cm and rodent holes
16	102 /114	limited pieces	70 cm east of rodent hole
17	105 /117	lot of burned rocks	Top of Feature 9d burned rocks
18	104 /119	lots of burned rocks	Top of Feature 9a burned rocks
19	102 /117&118	None	possible rodent hole
20	101 /117&118	None	possible rodent hole

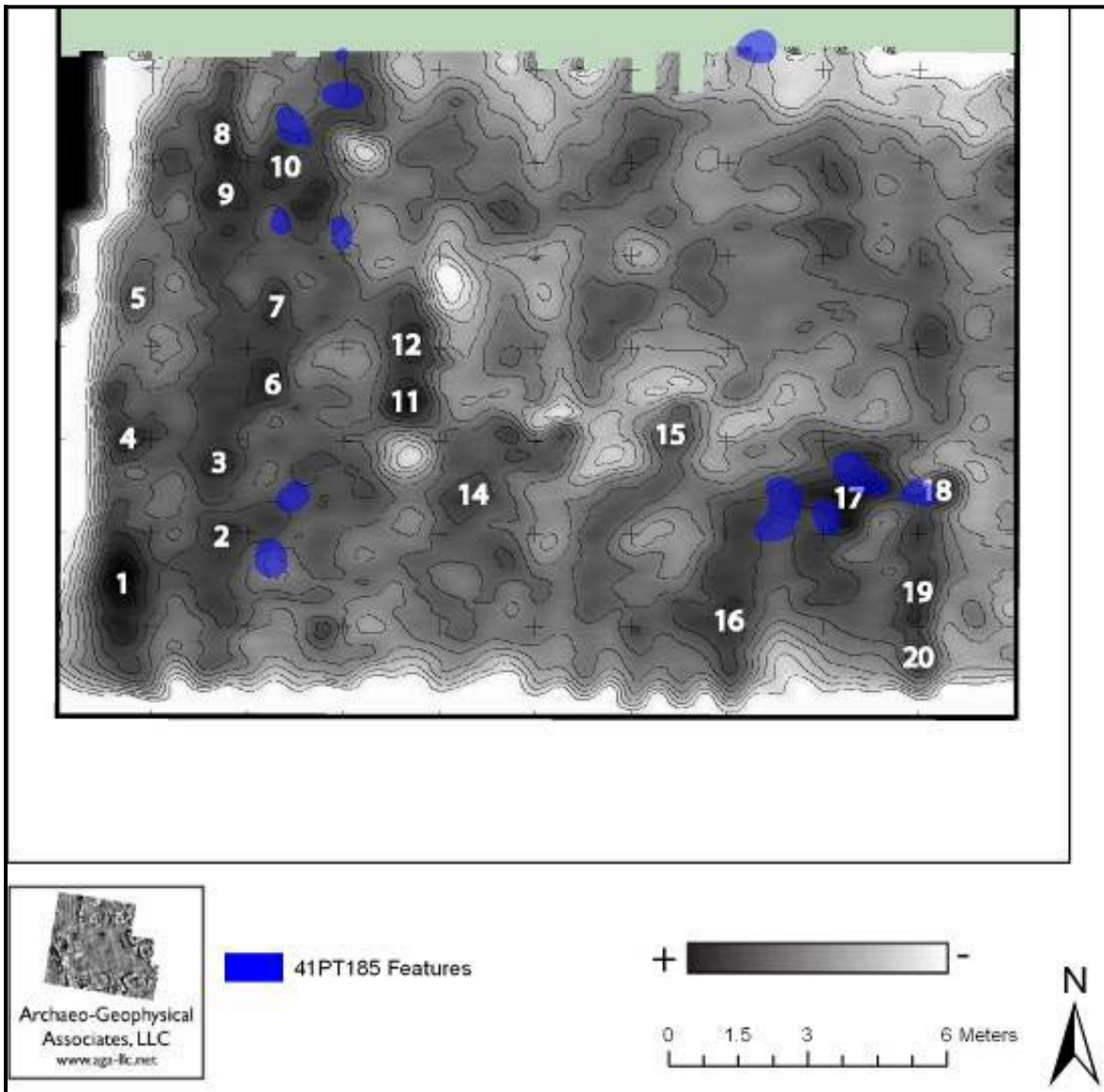


Figure O-7. Targeted Anomalies (1 to 20) from 41PT185/C Overlaid on a Contour Plot of the Magnetometer Data as Well as the Locations of TRC Identified Archeological Features.

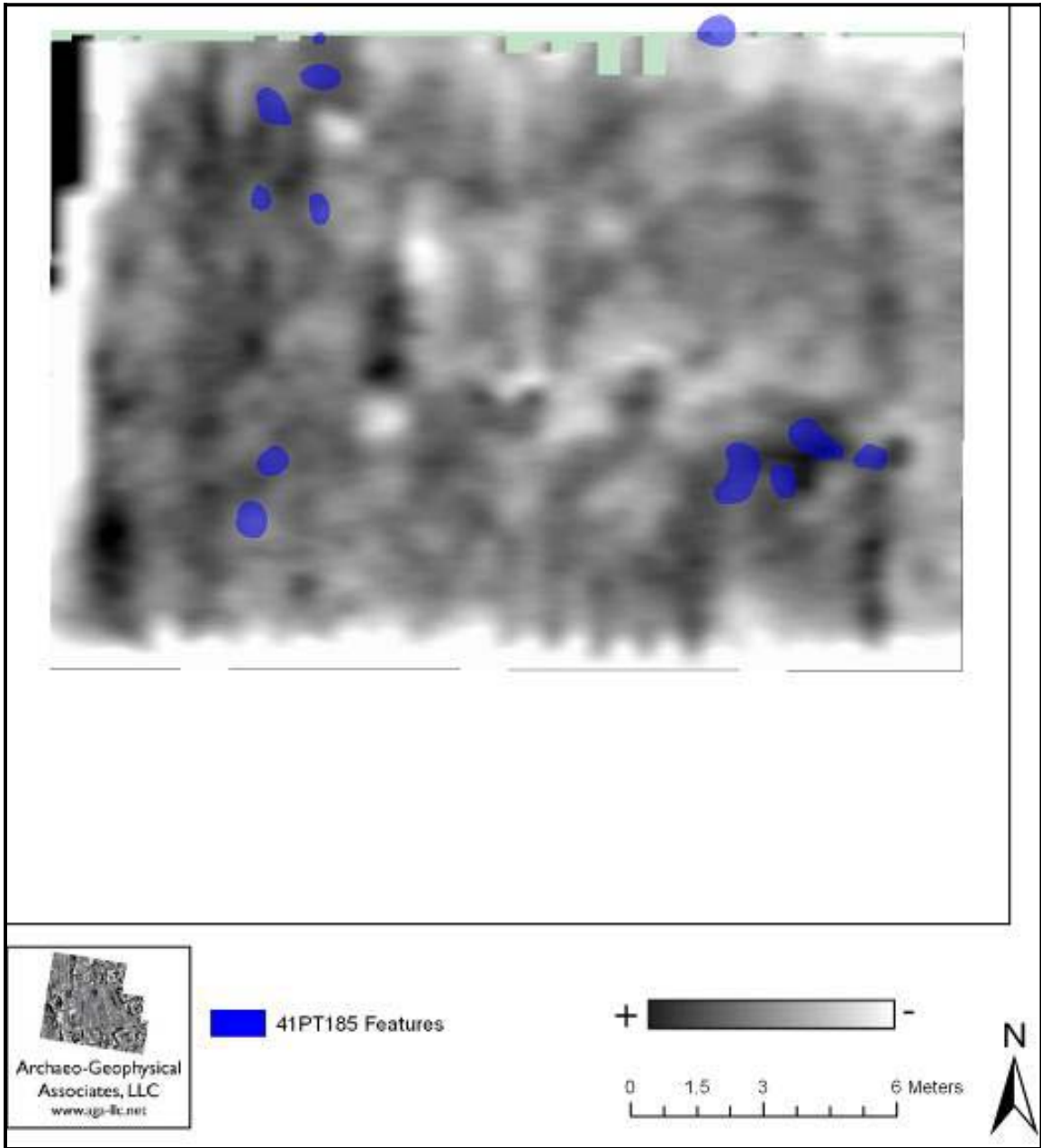


Figure O-8. Archeological Features from 41PT185/C Overlaid on the Magnetometer Data.

The best geophysical results from 41PT185/C were collected with the GPR. A total of 9 archeological features were recorded with the GPR, including Features 3, 6, 8, 9a through 9d, 10, and 11. These features are legible in GPR time slices ranging from 5 to 14 cmbs (Figures O-9 and O-10).

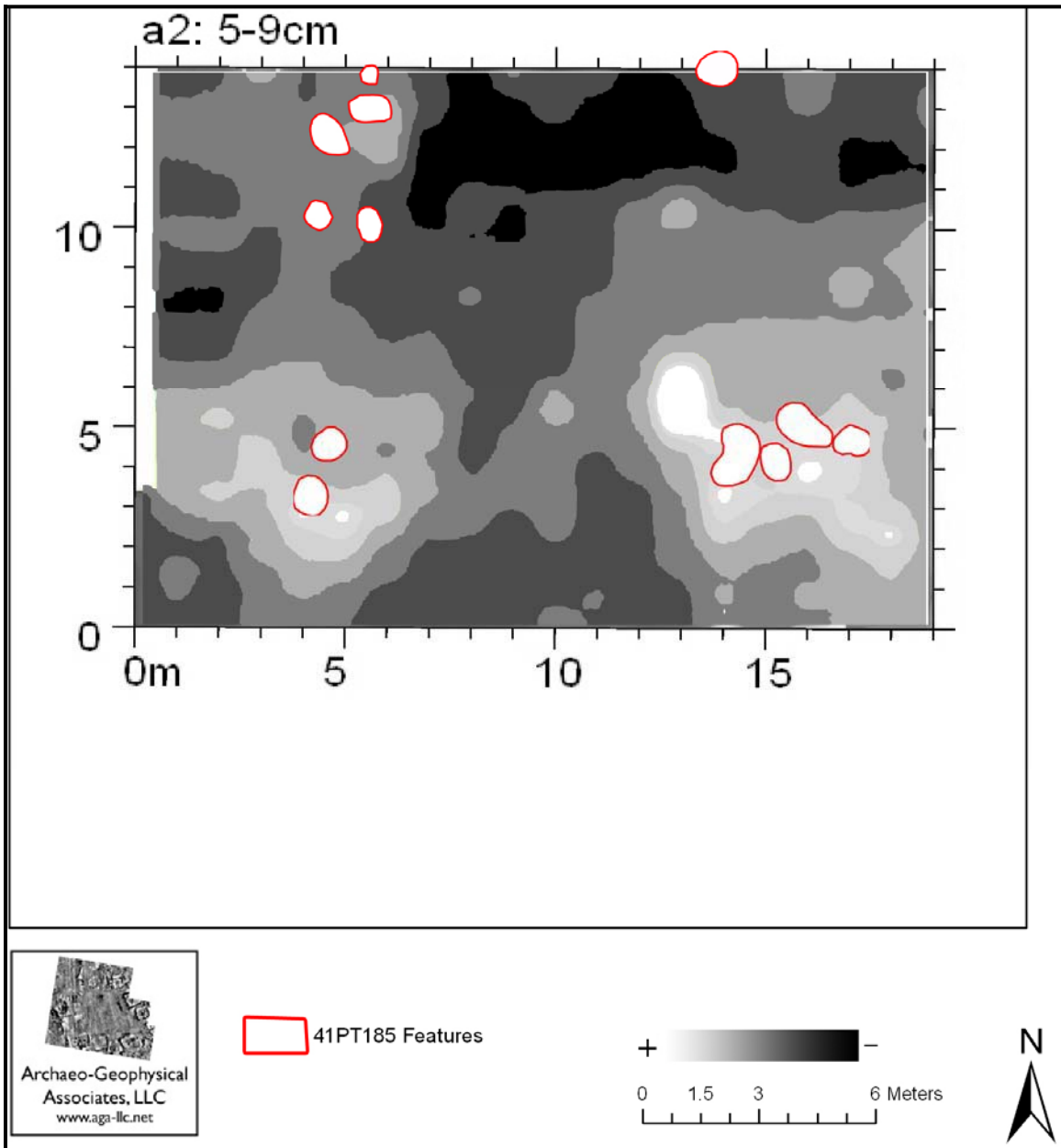
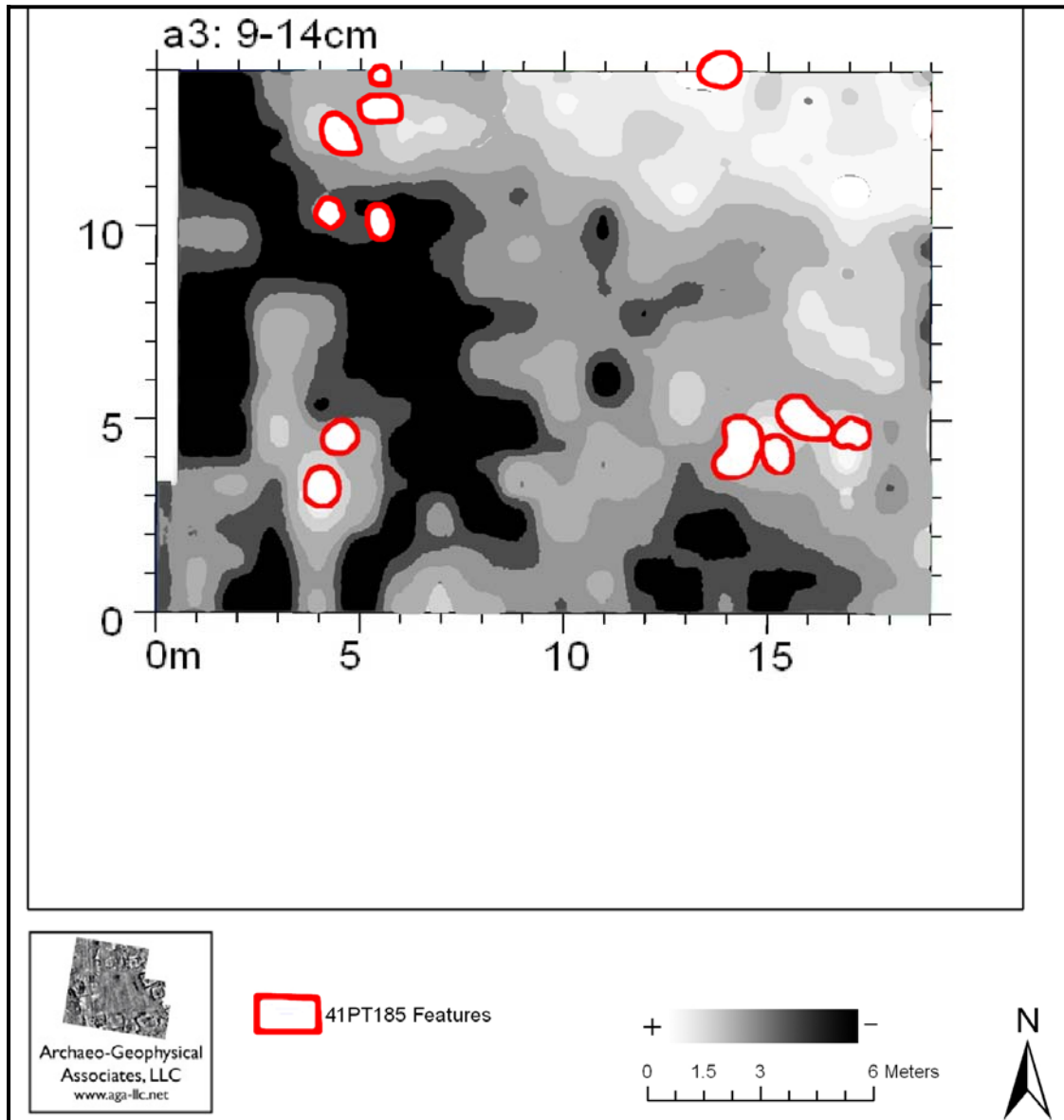


Figure O-9. Archeological Features from 41PT185/C
Overlaid on GPR Time Slice from 5 to 9 cmbs.



**Figure O-10. Archeological Features from 41PT185/C
Overlaid on GPR Time Slice from 9 to 14 cmbs.**

Conductivity also successfully identified the rock clusters from Features 9a through 9d or the tested locations of anomalies 17 and 18. These burned rock clusters are apparent geophysically as areas of low conductivity (Figure O-11). Features 9a through 9d were recorded by three of the four geophysical data sets used in the survey.

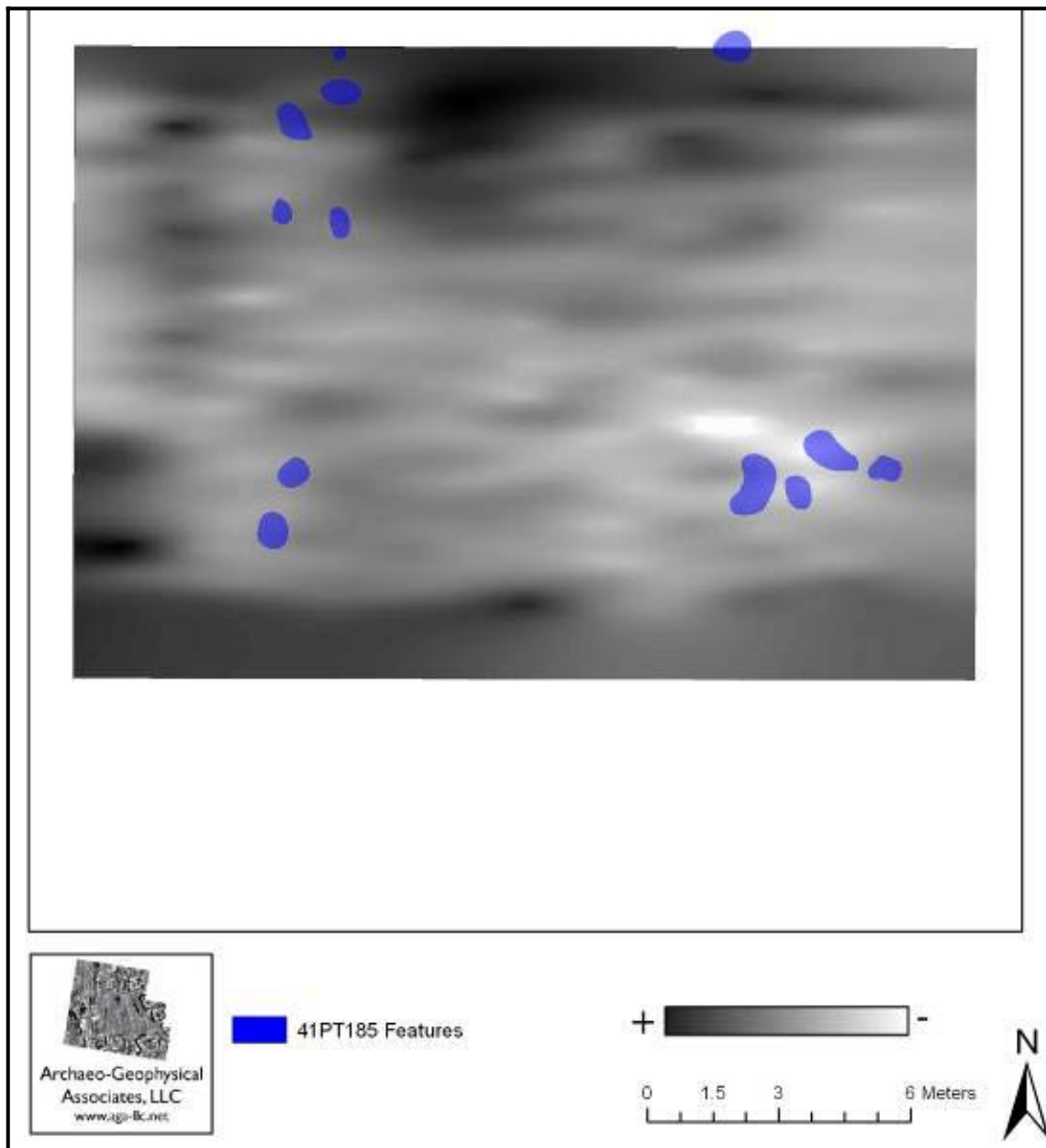


Figure O-11. Archeological Features from 41PT185/C Overlaid on the Conductivity Data.

41PT186

The geophysical data from 41PT186 consisted of a total of 280 m² covered with each of the technologies. The magnetometer data (Figure O-12) consisted of a relatively smooth data set with a few high magnetic anomalies in the western portion of the collection area. Most notable is the strong negative trends that surround the collection area. These low readings were caused by both the walls of the backhoe stripped block as well as the close proximity of the collection area to a large push pile from the stripping. This trend can be seen on the northeast edge of the collection area as well as the northwest edge.

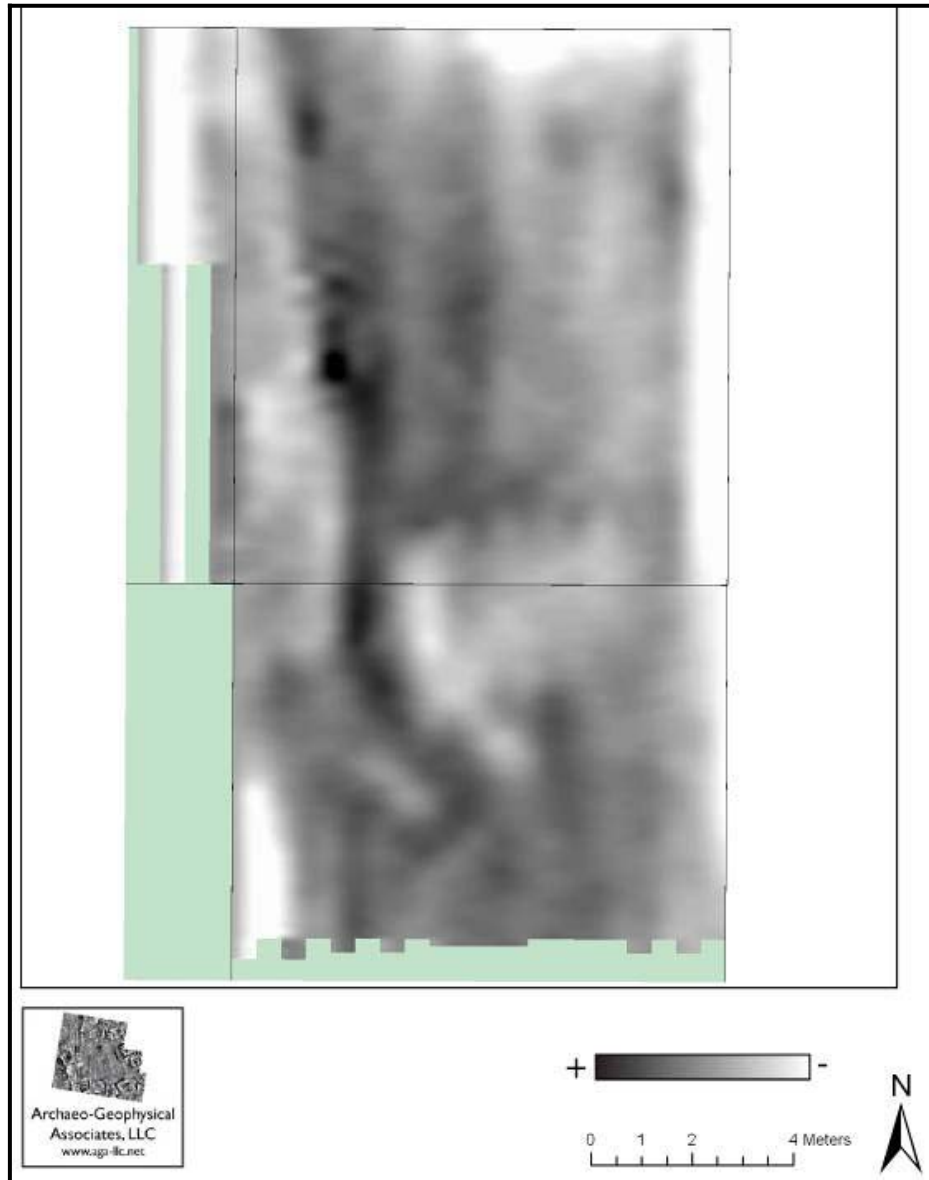


Figure O-12. Magnetometer Data from 41PT186.

Note: Black represents positive readings and white represents negative readings. Data range is ± 5 nT.

The GPR data (Figure O-13) consisted of several high amplitude reflections spread evenly across the dataset from north to south across the collection area. The conductivity data (Figure O-14) was noisy. The northwest edge of the collection area was adversely affected by its proximity to the large push pile, showing up as a high conductive trend. The magnetic susceptibility data (Figure O-15) was consistent with the data collected at the other two sites in that it contained little useful information, only a series of alternating high and low magnetic susceptibility readings. The data was noisy due primarily to the low overall range of the readings (± 1.25 ppm).

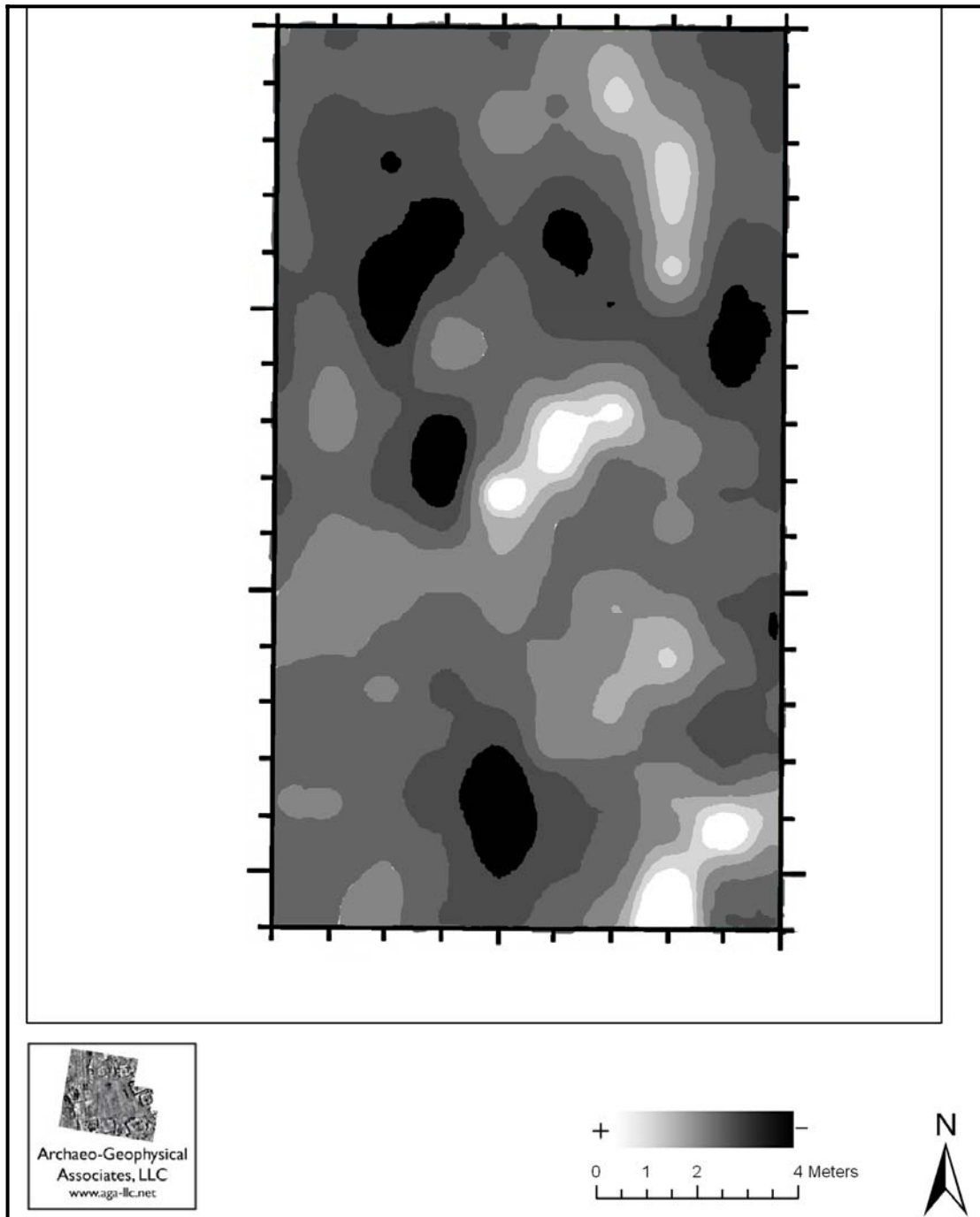


Figure O-13. GPR Time Slice from 10 to 20 cmbs from 41PT186. Dark Represents High Amplitude Reflections and Light Represents Low Amplitude Reflections.

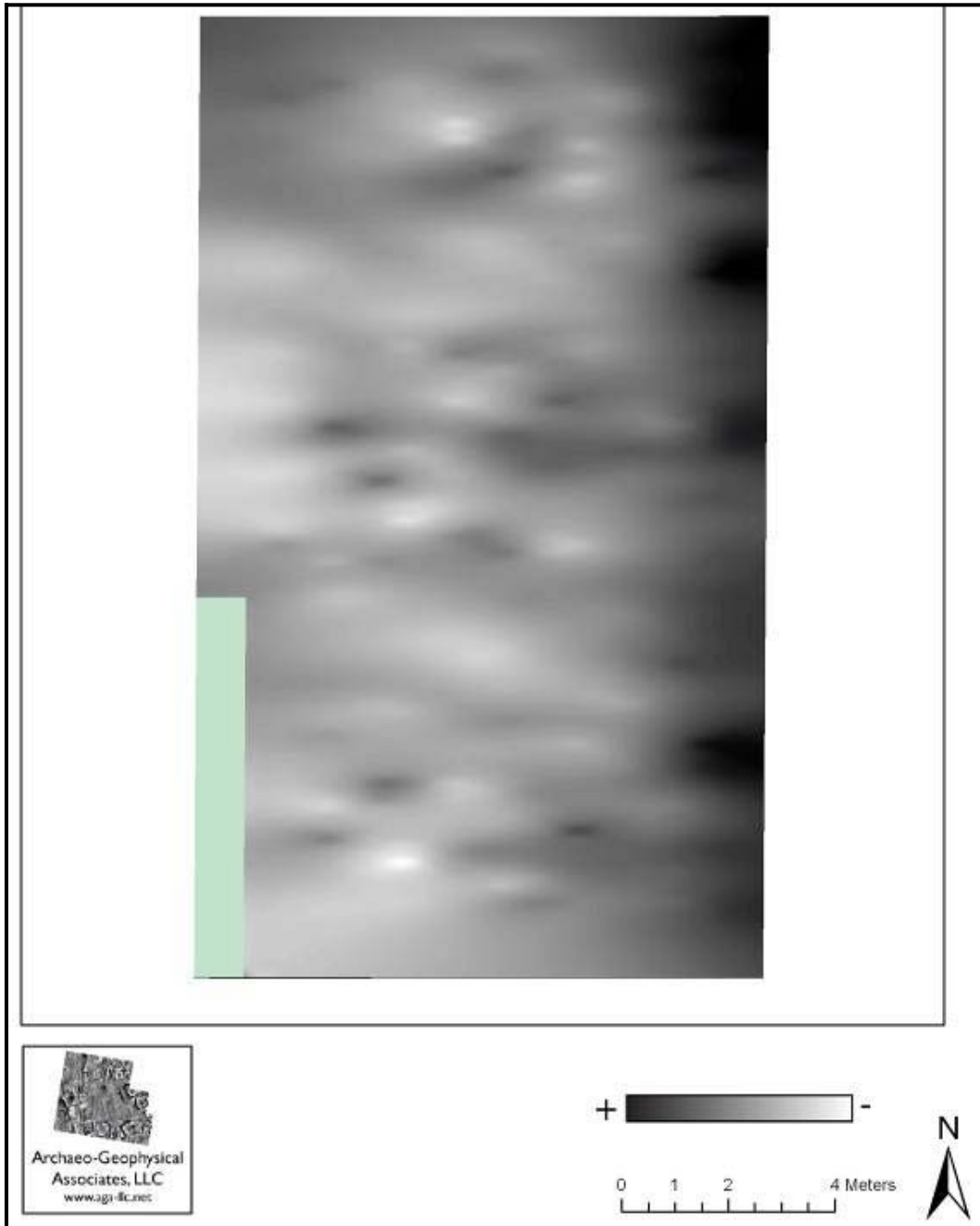


Figure O-14. Conductivity Data from 41PT186.

Note: Black represents high conductivity and white represents low conductivity.

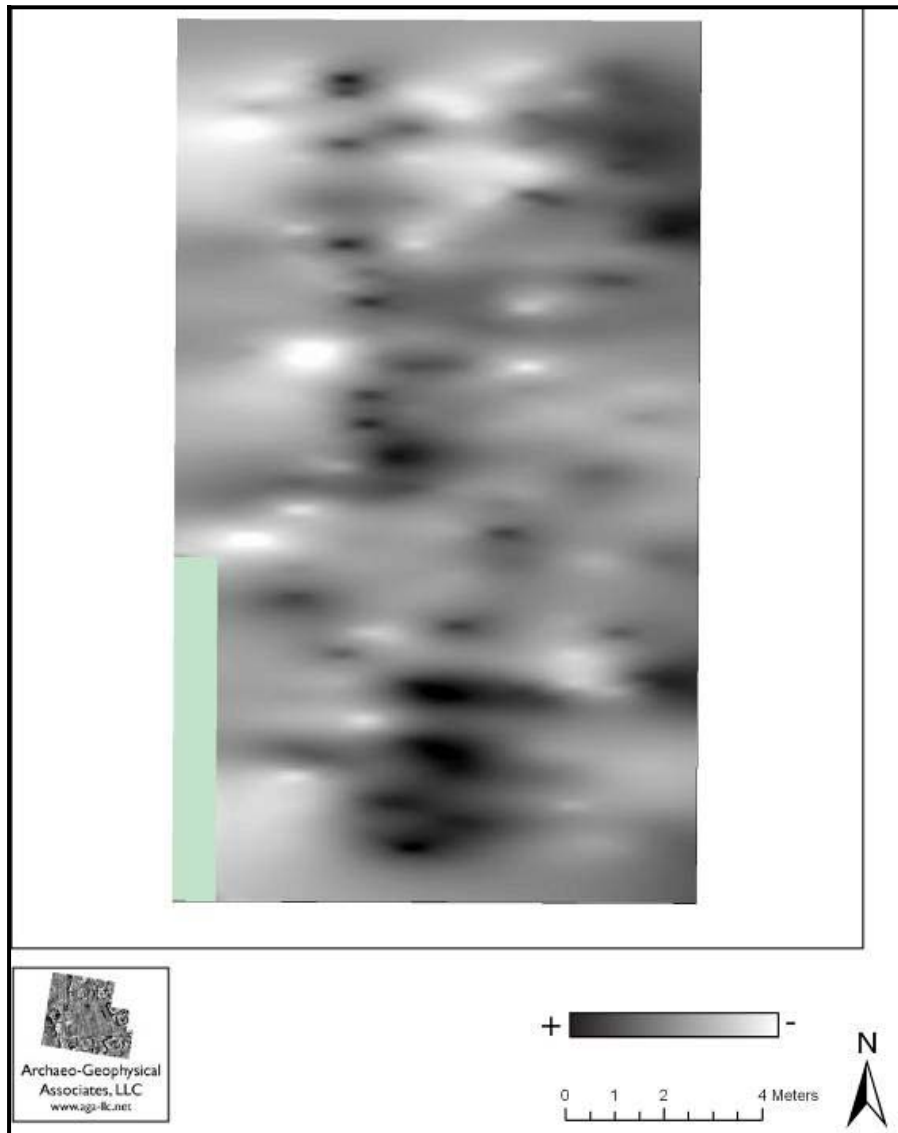


Figure O-15. Magnetic Susceptibility Data from 41PT186.

Note: Black represents high magnetic susceptibility and white represents low magnetic susceptibility.

Excavations at site 41PT186 (Figure O-16) documented a total of five features. Two features (Features 7 and 8) were shallow pits that were interpreted as heating elements with concentrations of ash, scattered charcoal, and light oxidation (Mike Quigg, 2009 personal communication). Feature 6, was a cluster of eight artifacts that measured 20 cm in diameter, and Feature 5 was a dark organic stain measuring 40 cm in diameter. Based largely on the results of the magnetometer data, 10 anomalies were chosen to be tested (Figure O-17). These anomalies were chosen were areas that showed a shift in the magnetic readings. Anomalies with high, median, and negative values were chosen.

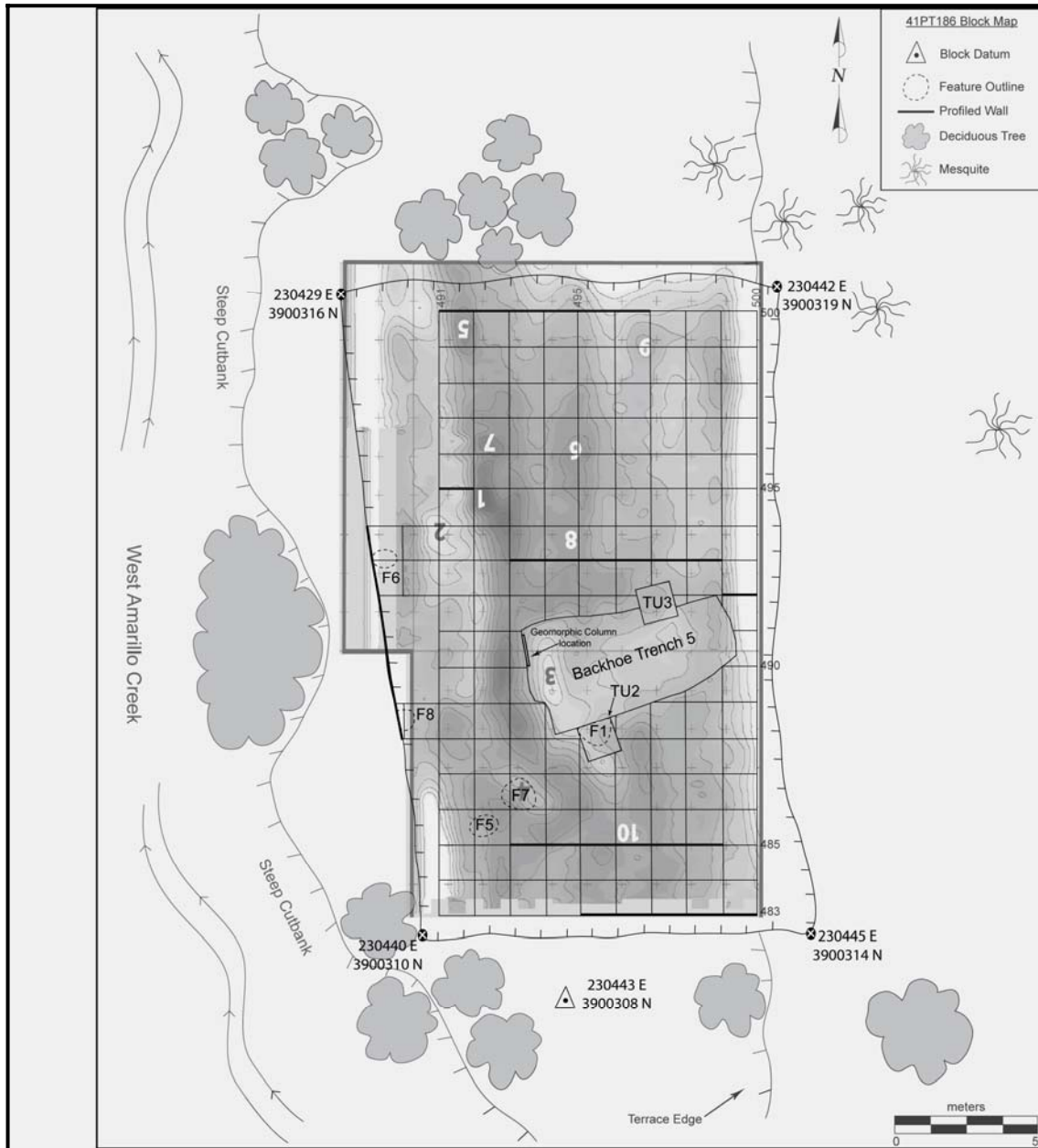


Figure O-16. Targeted Anomalies from 41PT186 (upside down numbers) Overlaid with TRC's Excavation Units and Locations of Identified Features.

Feature 7 is the only thermal feature that was recovered within the collection area and it was apparent in the magnetometer data as anomaly 4 (Figure O-17). Feature 8 was also a thermal feature, however, it was located almost completely outside of the geophysical collection area. Ironically, the area of Feature 7 was labeled for ground truthing in order to determine the source of a negative magnetic anomaly. Thermally altered features are usually identified in magnetometer surveys due to their enhanced magnetic fields, not due to low magnetic fields. These trends are also apparent in Figure O-18, where the locations of the excavated features are overlain on the magnetometer data. Two of the features (Features 6 and 8) are located outside of the collection area, two correspond with negative magnetic readings (Features 1 and 7) and one (Feature 5) is located in an area with median magnetic readings. The GPR data (Figure O-19) shows only one positive correlation, with Feature 1 in an area of reflections of median amplitude. Features 1, 5 and 7 occur in areas of low conductivity (Figure O-20).

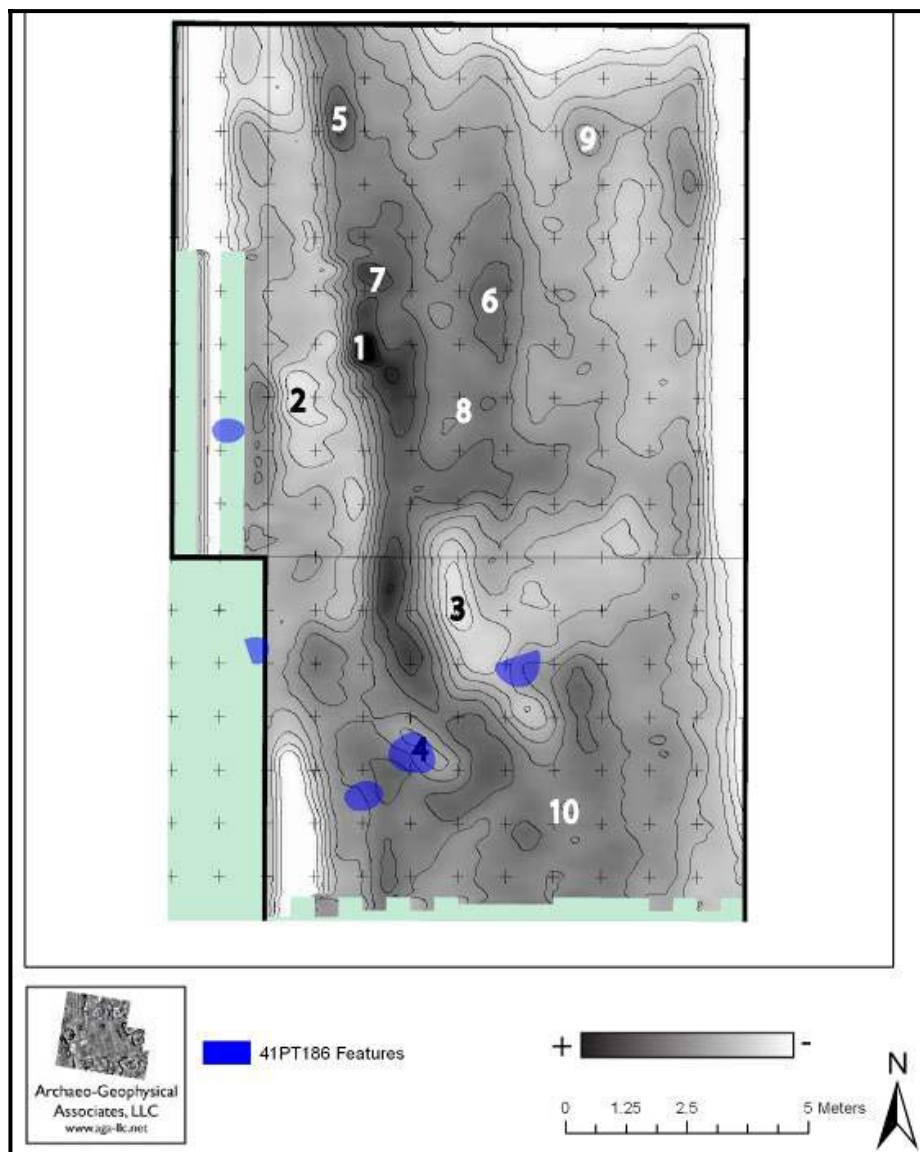


Figure O-17. Targeted Anomalies from 41PT186 Overlaid on a Contour Plot of the Magnetometer Data and the Locations of Archeological Features.

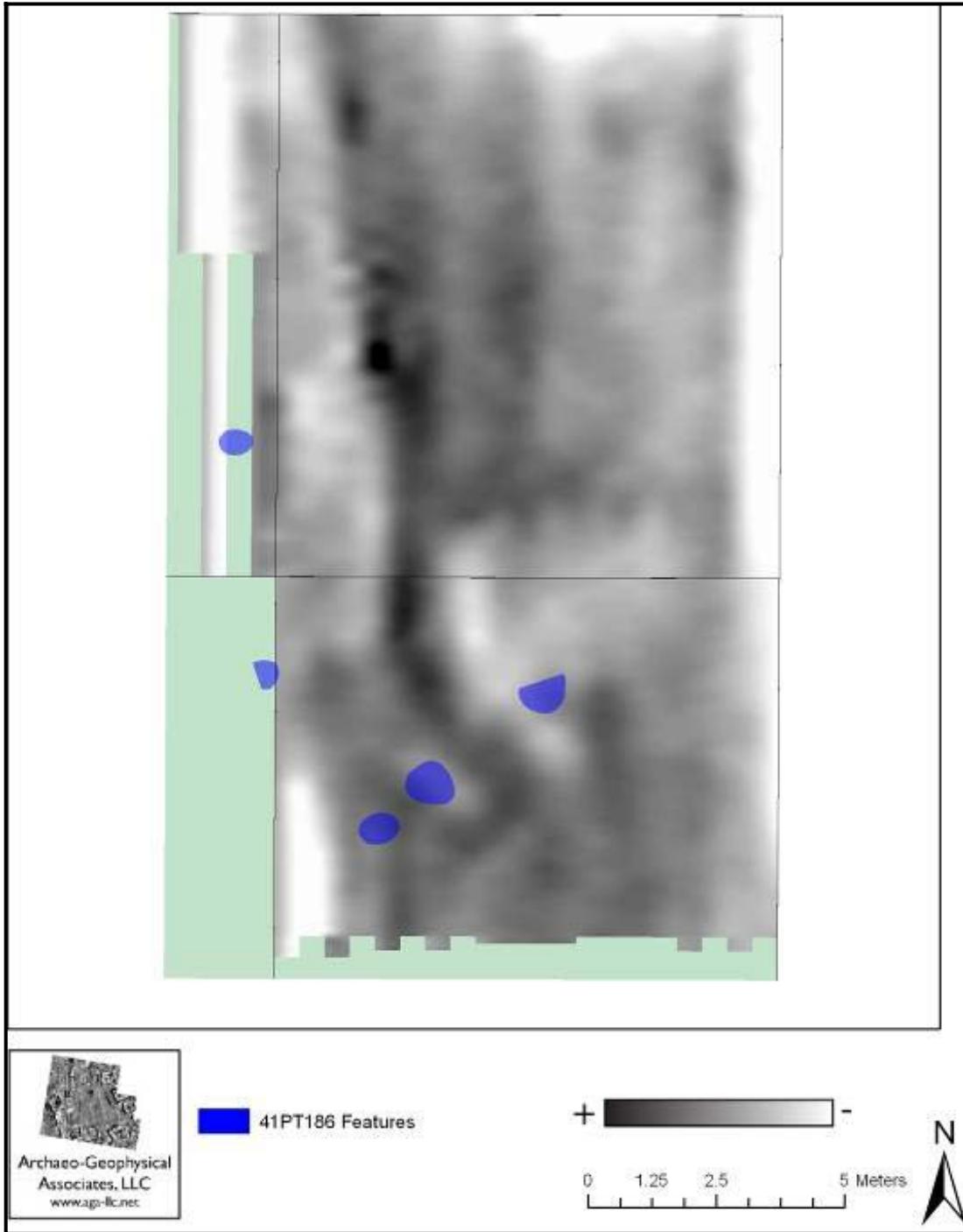


Figure O-18. Archeological Features from 41PT186 Overlaid on the Magnetometer Data.

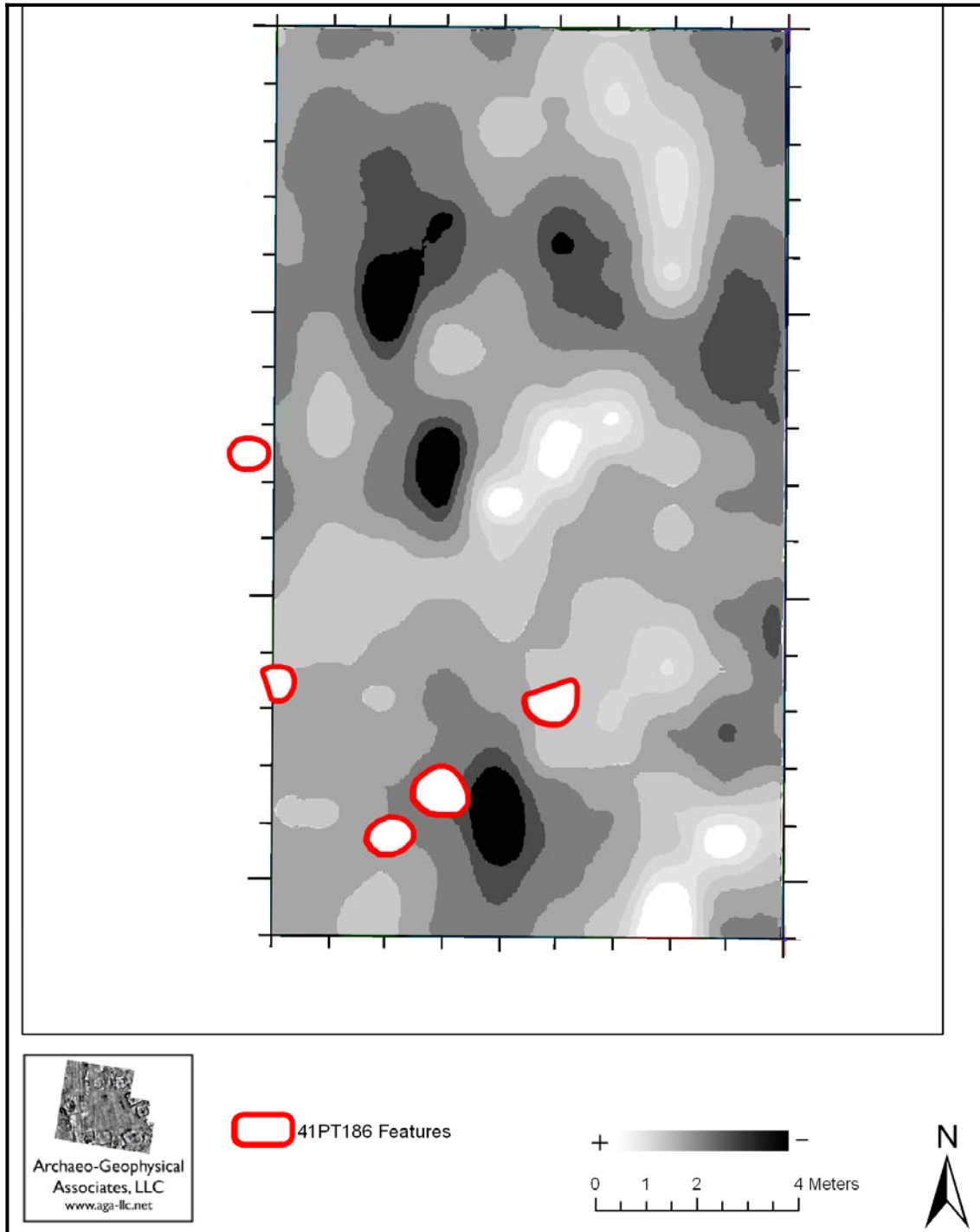


Figure O-19. Archeological Features from 41PT186 Overlaid on GPR Time Slice from 10 to 20 cmbs.

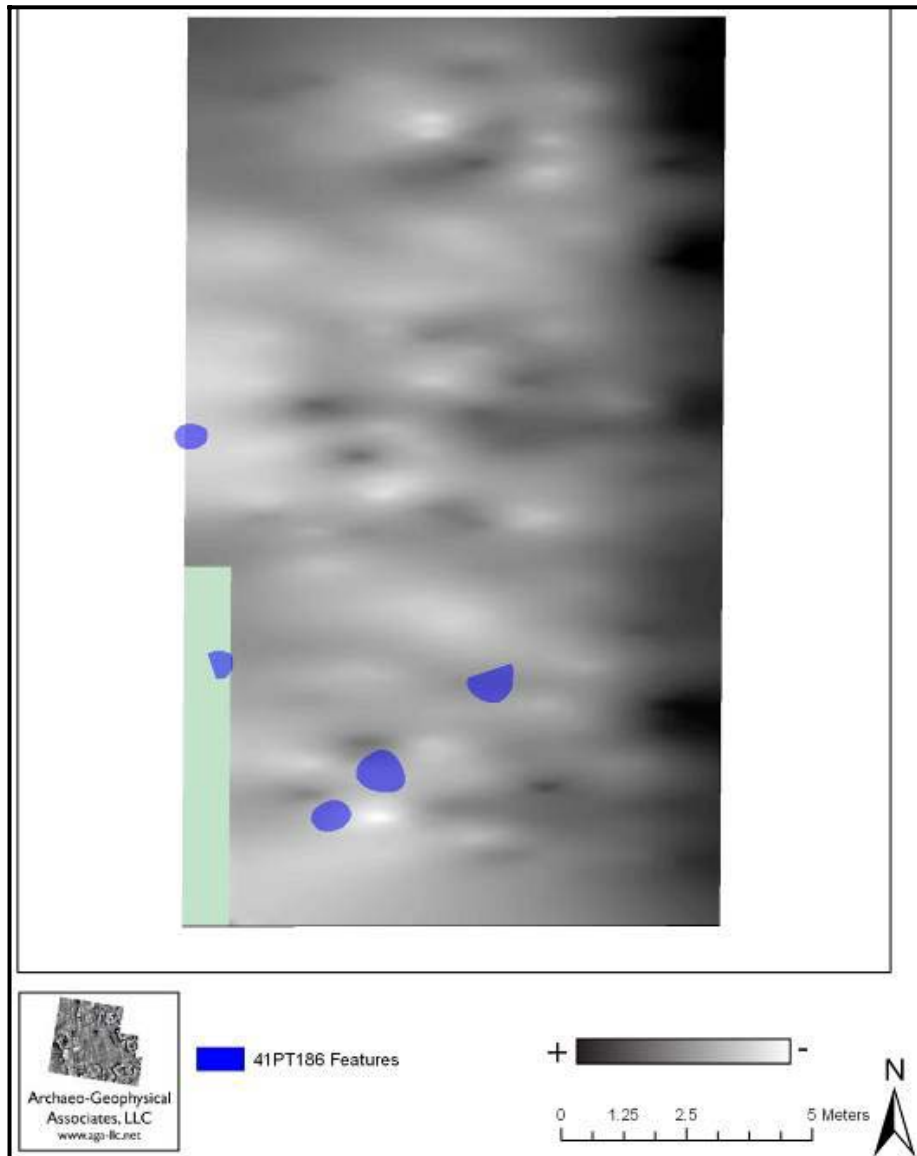


Figure O-20. Archeological Features from 41PT186 Overlaid on the Conductivity Data.

41PT245

The geophysical data from 41PT245 did not contain many obvious anomalies. The magnetometer data (Figure O-21) consisted of a relatively quiet background with the major magnetic values related to the filled backhoe trench in the northern portions of the collection area. In the GPR data (Figure O-22), there was a large high reflective anomaly in the southern portion of the collection area that was easily correlated with a low portion of the collection area that

was inundated with water directly preceding the geophysical survey. Conductivity data (Figure O-23) showed areas of low conductivity in the vicinity of the filled backhoe trench and a few high conductive anomalies in the central portion of the collection area. The magnetic susceptibility (Figure O-24) data was similar to that documented at 41PT185/C and 41PT186, and consisted of very low readings (± 1 ppm) that moved back and forth from low to high magnetic susceptibility, creating a noisy data set with little interpretive value.

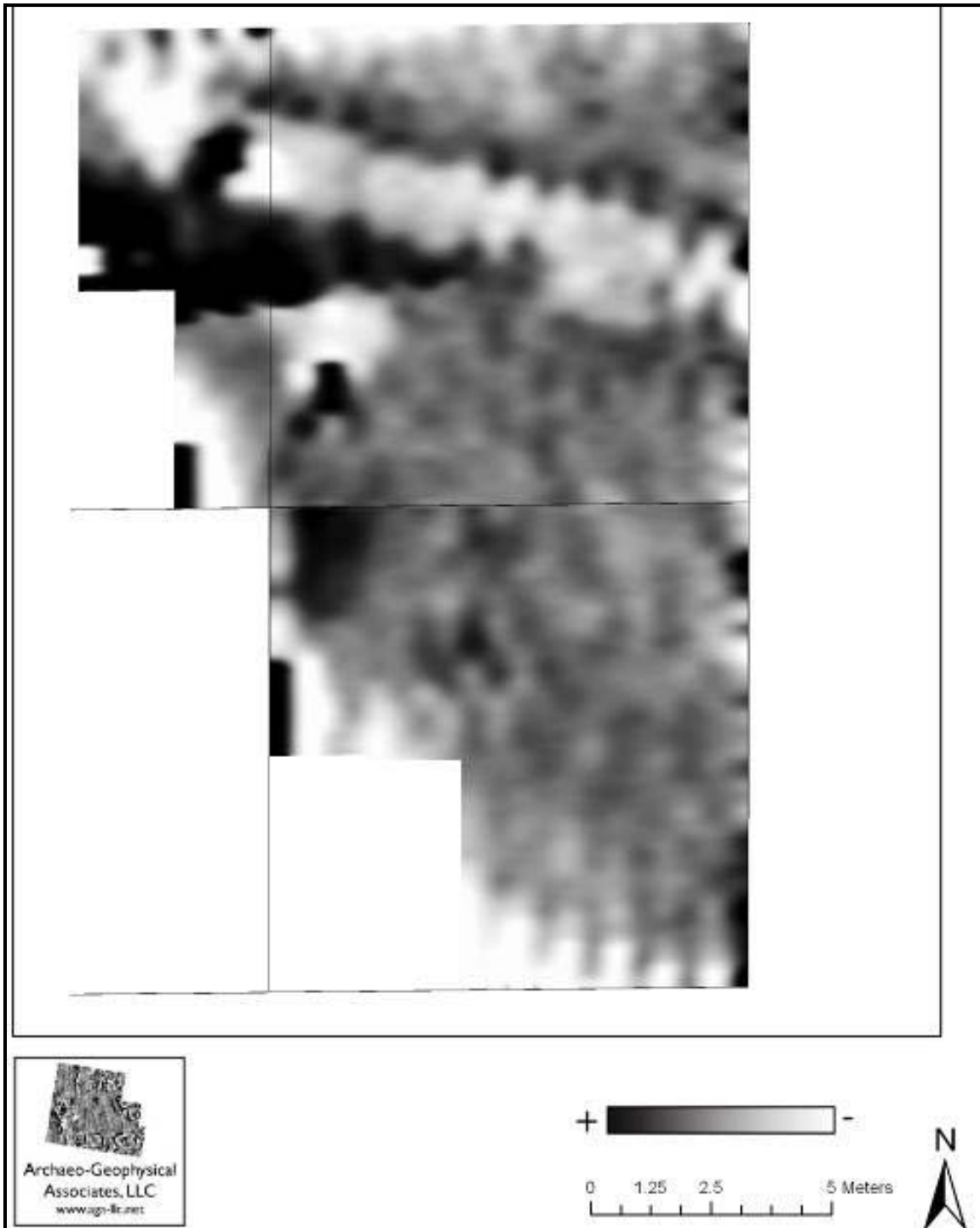


Figure O-21. Magnetometer Data from 41PT245.

Note: Black represents positive readings and white represents negative readings. Data range is ± 5 nT.

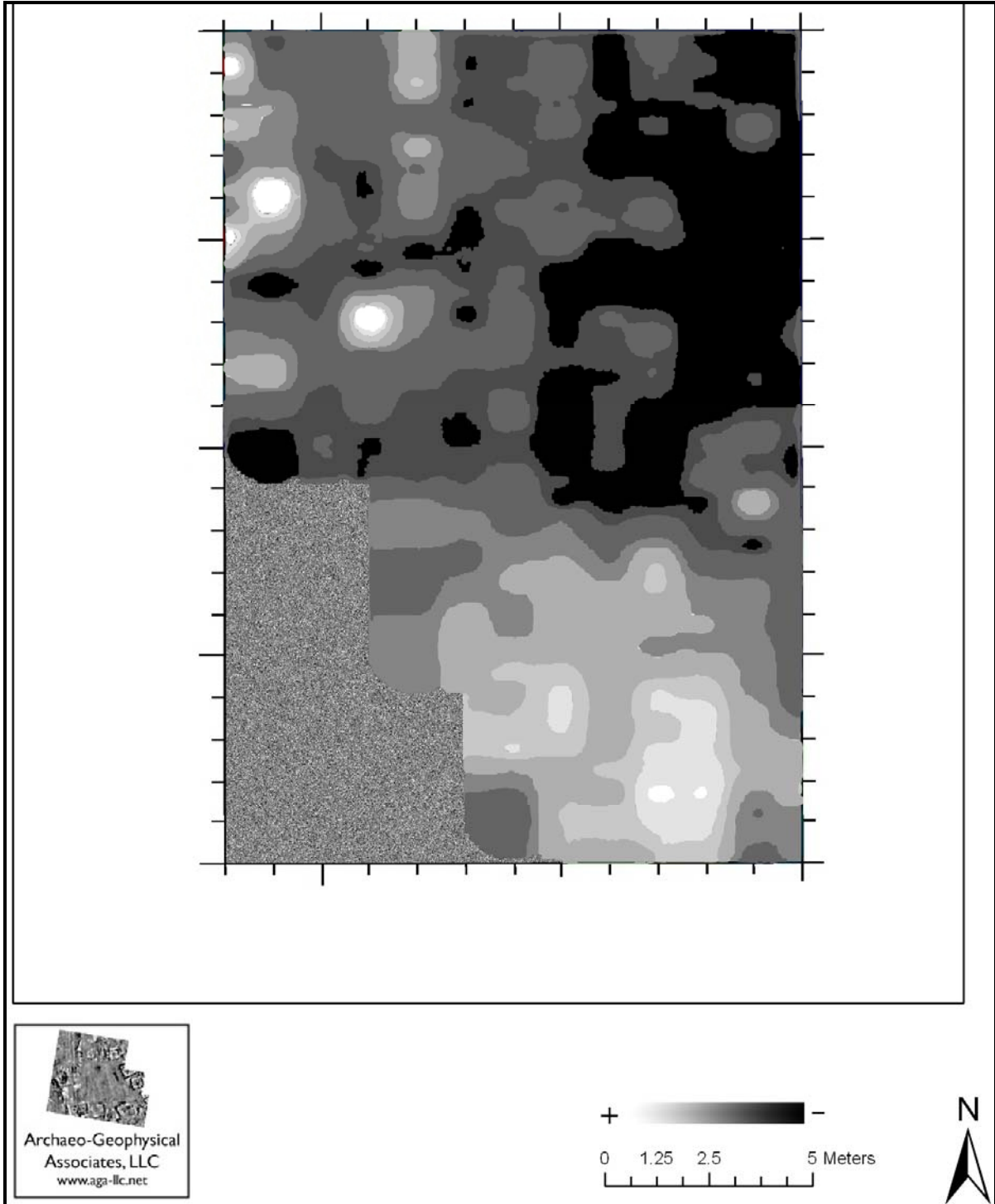


Figure O-22. GPR Time Slice from 14 to 21 cmbs from 41PT245.

Note: White represents high amplitude reflections and black represents low amplitude reflections.

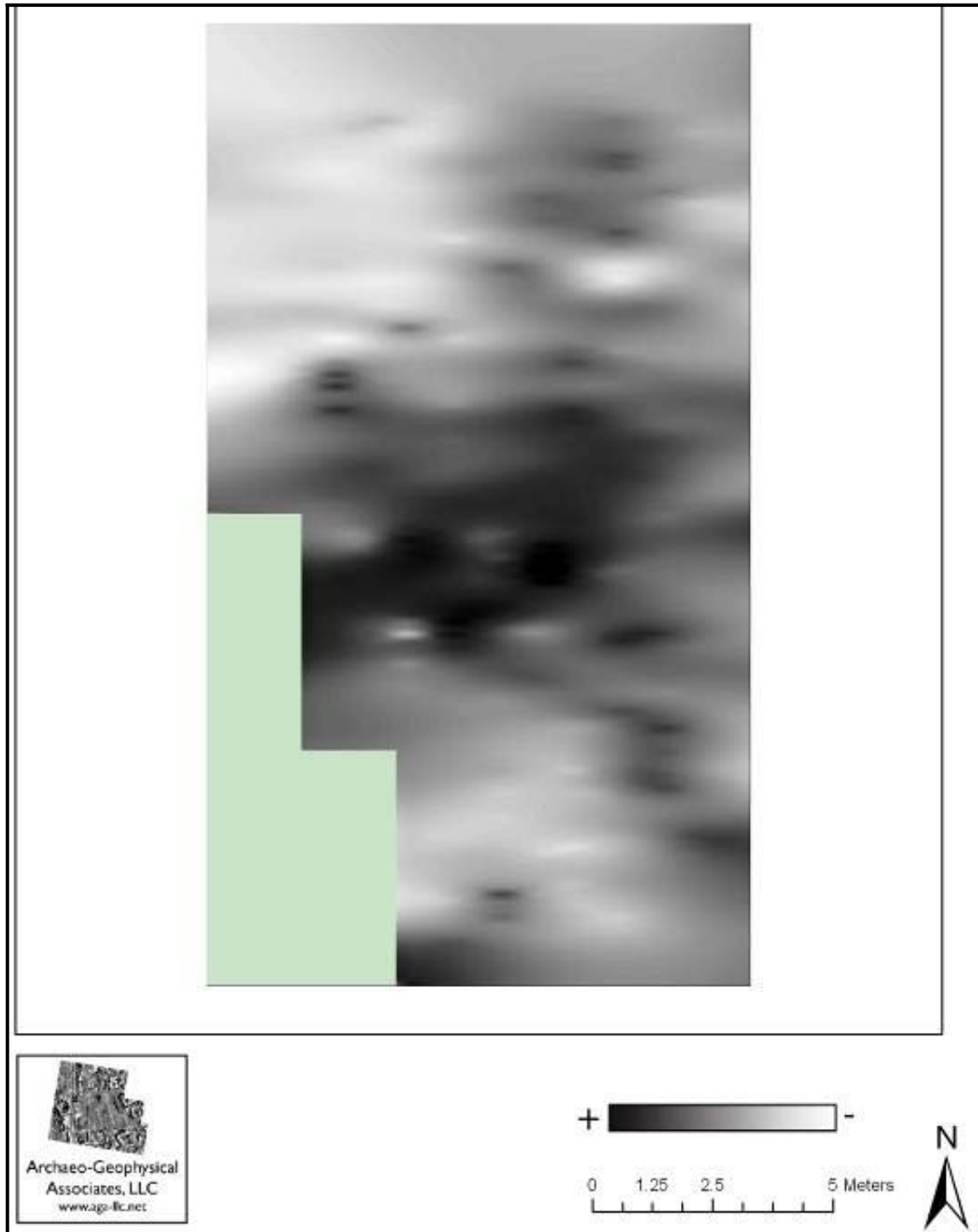


Figure O-23. Conductivity Data from 41PT245.

Note: Black represents high conductivity and white represents low conductivity.

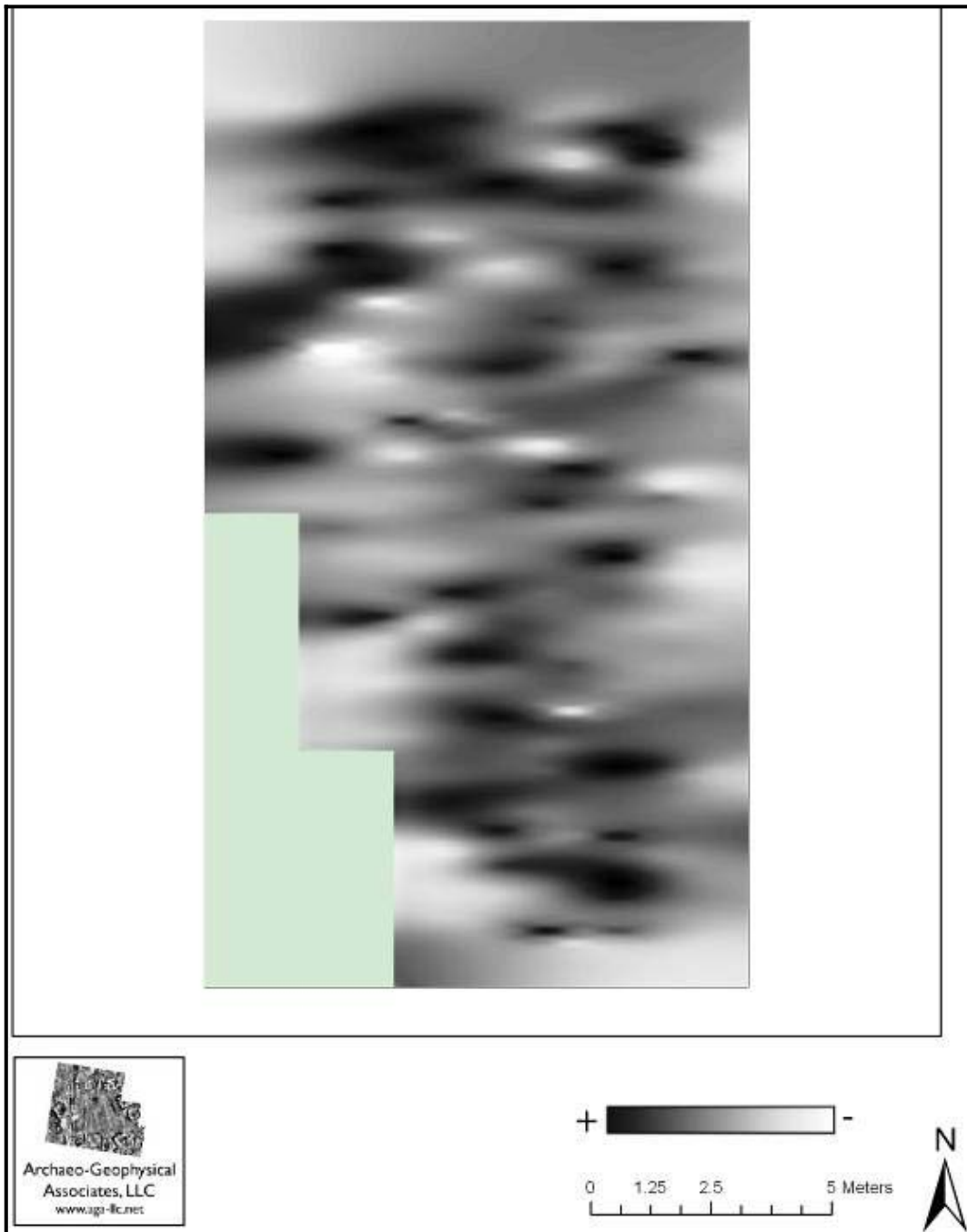


Figure O-24. Magnetic Susceptibility Data from 41PT245.

Note: Black represents high magnetic susceptibility and white represents low magnetic susceptibility.

Several areas (anomalies 1 through 7) were targeted for test excavations at 41PT245 based largely on the results of the magnetometer data (Figures O-25 and O-26). Subsequent excavations by TRC did not recover any cultural features or artifacts.

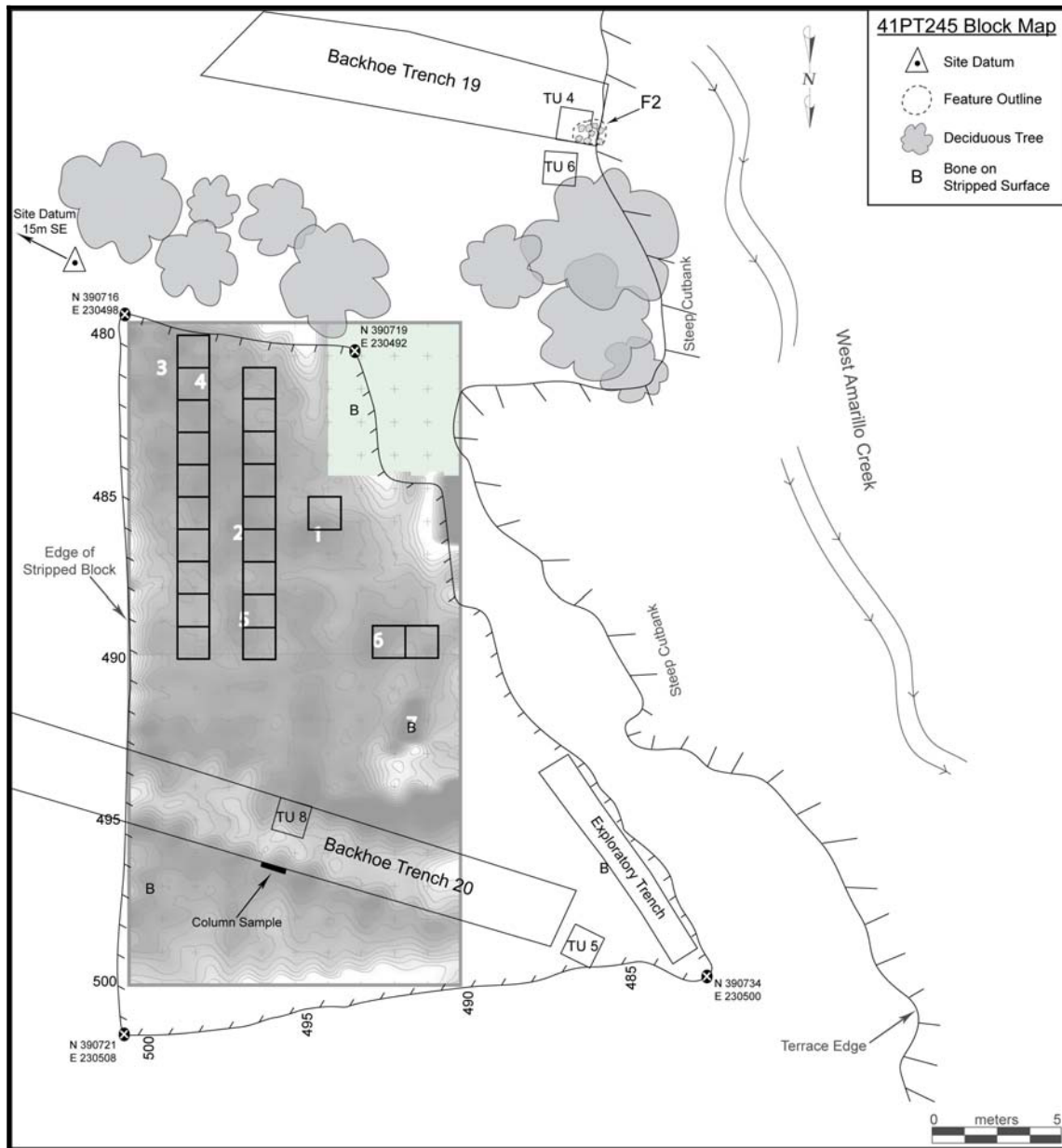


Figure O-25. Targeted Anomalies from 41PT245 Overlaid with TRC's Excavation Units.

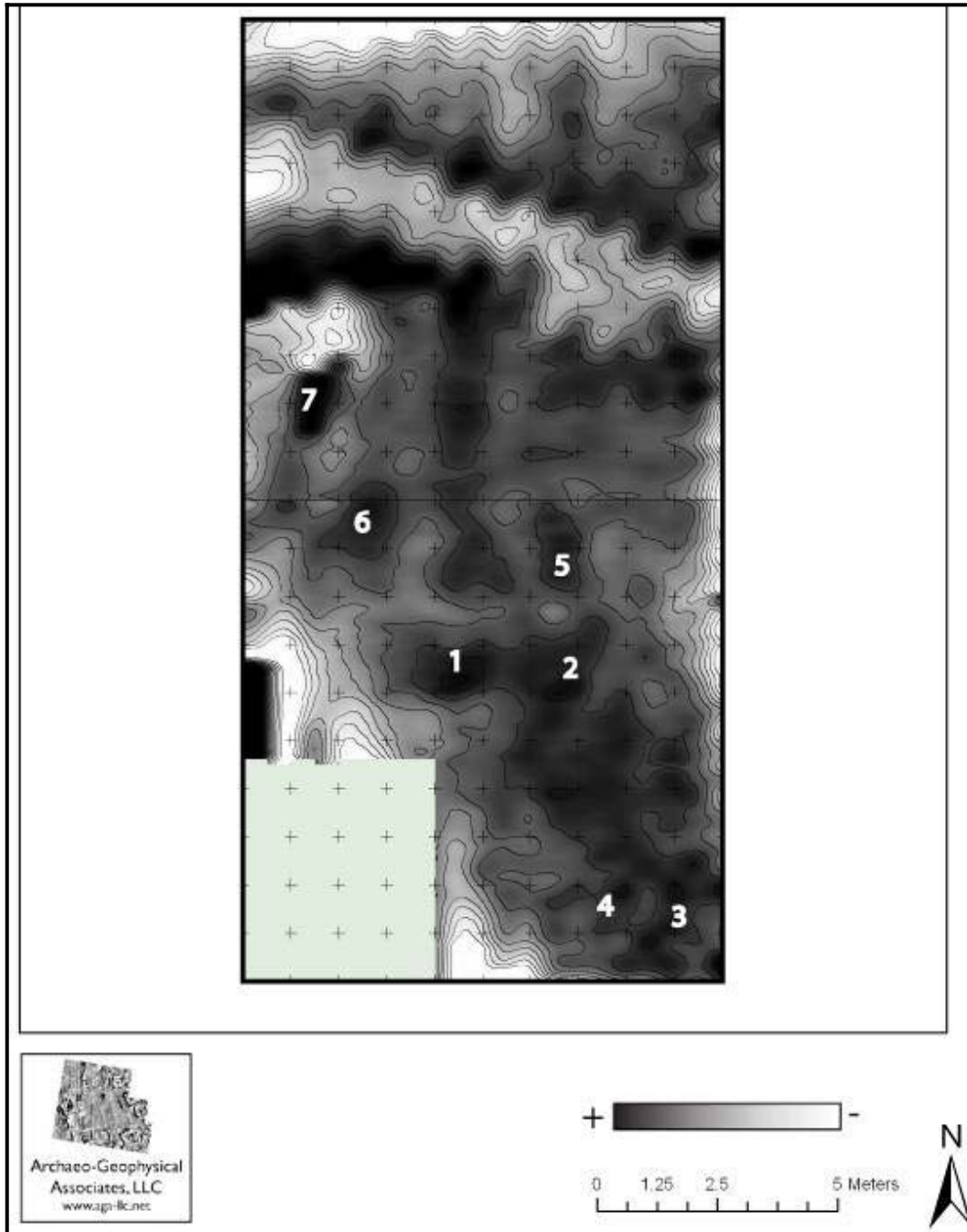


Figure O-26. Targeted Anomalies from 41PT245 Overlaid on a Contour Plot of the Magnetometer Data and the Locations of Archeological features

O.7 CONCLUSIONS

Results from the geophysical investigations and the subsequent archeological investigations conducted at 41PT185, 41PT186, and 41PT245 show the complex nature of archeogeophysical investigation. TRC recovered a total of 15 archeological features within the geophysical collection area. Of these 15 Features 11 were recorded with the various geophysical methods (see Table O-2). GPR alone recorded 10 of the 15 cultural features. There are clearly associations with burned rock features at 41PT185/C, as Features 9a through 9d was identified by the magnetometer, GPR, and the conductivity meter and at 41PT186, Feature 7 was recorded by the magnetometer and Feature 1 was recorded by the GPR.

Magnetometers are quite useful for locating thermally altered features and GPR is often useful for locating rock clusters. In the case of sites 41PT185/C and 41PT186 the lack of any well-defined features with extremely

high magnetic contrasts such as those proceed by an intact burned rock earth ovens with highly oxidized soils can help to explain the limited success of the magnetometer. The strongest correlation between the magnetometer data and the archeological data was from Feature 9a through 9d at site 41PT185/C. This feature consisted of a scattering of burned rock that was not associated with any burned sediments or a well-defined feature. Recovering features of this class with any great consistency will largely depend on the types of thermally altered material and the surrounding soils. The high success rate of the GPR collections was undoubtedly due to the fact that the over burden was cleared prior to the geophysical collection. It is hard to imagine finding a small cluster of rocks buried deeply beneath an alluvial overburden. GPR would, however, have a much greater chance of success targeting well-developed features such as storage pits and large rock filled pits, even if there was some over burden capping the site.

Table O-2. Archeological Features and Geophysical Techniques.

Geophysical Technique	Recorded Features at Site 41PT185/C	Recorded Features at Site 41PT186
GPR	3, 6, 8, 9 a – d, 10, 11	1
Magnetometer	9 a – d	7
Conductivity	9 a - d	

There were, however, several anomalies targeted that did not correlate with archeological features. This can be related to several issues. First and foremost is the manner in which the geophysical data were interpreted. This project was conducted with time constraints that did not permit the geophysicist to assist with the ground truthing, nor was there the opportunity to interact with the archeologists while they were in the field. Finding a way to insure dynamic interaction between the geophysicist and the archeologist conducting

the excavations would have greatly increased the success ratio of the geophysical survey, because it would allow both parties to address site specific issues and calibrate the archeogeophysical interpretations with the archeological observations to further hone the precision of the investigation. While there are many underlying principals that dictate the geophysical signatures of the various materials and objects, ultimately central interpretative step is made by analyzing the patterning of the geophysical trends and

anomalies. To this end, relative contrasts between the values and not the actual values themselves are most important. These relative contrasts can change from site to site depending on many factors such as local geologies, source material for the production of artifacts and features, as well as modern cultural disturbances such as surface trash. Keeping a dialogue open between the archeogeophysist and the archeologist can help to “recalibrate” the archeogeophysical interpretations.

This relationship would have been further strengthened if the geophysicist would have been able to revisit the sites during the excavation phase of the project. As archeologists gain experience working with the correlation of archeological and geophysical data, and the archeogeophysicist gains local experience in the character of archeological sites and their geophysical manifestations, archeogeophysical interpretive results will indeed be increase. The second issue that affected the success rate of the tested anomalies was the fact that due to some of the logistical constraints discussed above, anomalies were marked for testing with a fair amount of liberty. The excavation strategy dictated that large portions of the geophysical collection areas would be intensively investigated, and to take advantage of this situation, all anomalies of suspicion were targeted for ground truthing.

Collecting geophysical data over as large of an area as possible also can help increase the success of a geophysical survey. This allows for the identification of the larger geological trends in the data and more precisely focus on the anomalies that are believed to be cultural in origin within that trending data. If possible, it is often useful to collect data outside of the known boundaries of sites, because clear magnetic contrasts between the archeological site and its surrounding landscape help in identifying individual features within the site as well as

aiding in the delineation of the site boundaries.

All three collection areas at the three sites were mechanically stripped to remove the overburden prior to the geophysical collection. It was believed that this would help lessen the potential of noise created by the upper and culturally-sterile strata. This technique proved to have both positive and negative impacts on the geophysical survey. The positive impacts mainly pertained to the GPR collection from 41PT185/C, which was the data set that contained the highest number of positive correlation of geophysical anomalies to archeological features. The presence of a thick overburden would certainly have reduced the utility of this dataset. The negative impacts, increased noise due to walls and push piles of the scrape units, were observable primarily in the magnetometer data and to a lesser degree in the conductivity data for all three sites.

For future projects of this nature observations can be made that should increase the productivity of the geophysical component of the investigations. If possible, collect the geophysical data both before stripping and after stripping. This will aid in the quantification of the degree of magnetic disturbance from the overburden. In some geological deposits, it is quite possible to locate small burned rock features beneath non-cultural overburdens, even up to 2.5 mbs (Walker 2009). This could result in geophysical information that would allow the archeologists to scan the buried sites and place their backhoe stripped blocks systematically over or bisecting concentrations of features.

If stripping the overburden before the geophysical collection is needed, it would be advisable to strip as large of an area as possible. Situations that would dictate this would include sites where the upper strata contain ferrous soils or gravels, the archeological deposits are too deeply buried,

or the archeological deposits and features are too low in geophysical contrast to be identified through the noise of the upper strata. Noise from the strip unit walls and push piles will vary greatly depending on the make up of the sediments. However, even in magnetically passive soils, it is not realistic to collect geophysical data next to walls of a stripped block. Allowing as much room as possible (5 to 10 m) between the geophysical collection areas and stripped areas/backdirt piles would greatly increase the quality of the geophysical data around the parameters of the collection unit.

O.8 REFERENCES CITED

- Bartington, G. and C. E. Chapman
2004 A high-stability Fluxgate Magnetic Gradiometer for Shallow Geophysical Survey Applications. *Archaeological Prospection* 11:19-34.
- Bevan, B. M
1983 Electromagnetics for Mapping Buried Earth Features. *Journal of Field Archaeology* 10:47-54.
1998 *Geophysical Exploration for Archaeology: An Introduction to Geophysical Exploration*. Special Report No. 1. Midwest Archaeological Center, Lincoln, Nebraska.
- Carr, C.
1982 *Handbook on Soil Resistivity Surveying*. Center for American Archaeology Press, Evanston, Illinois.
- Clark, A.
2000 *Seeing Beneath the Soil: Prospecting Methods in Archaeology*. Routledge, London.
- Clay, B. R.
2006 Conductivity Survey: A Survival Manual. In *Remote Sensing in Archaeology: An Explicitly North American Perspective*, edited by J. K. Johnson, pp. 79-108. University of Alabama Press, Tuscaloosa.
- Conyers, L. B.
2004 *Ground-Penetrating Radar*. AltaMira Press, Walnut Creek, California.
- Conyers, Lawrence B. and Jeffrey E. Lucius
1996 Velocity Analysis in Archaeological Ground-Penetrating Radar Studies. *Archaeological Prospection* 3(1):25-38.
- Conyers, L. B., Eileen G. Ernenwein, M. Grealy, and K. M. Lowe
2008 Electromagnetic Conductivity Mapping for Site Prediction in Meandering River Floodplains. *Archaeological Prospection* 15:81-91.
- Dabas, M., and A. Tabbagh
2000 Magnetic Prospecting. In *Archaeological Method and Theory: An Encyclopedia*, edited by Linda Ellis, pp. 335-339. Garland, New York.
- Dalan, R. A.
2006 Magnetic Susceptibility. In *Remote Sensing in Archaeology: An Explicitly North American Perspective*, edited by J. K. Johnson, pp. 161-203. University of Alabama Press, Tuscaloosa.
2008 A Review of the Role of Magnetic Susceptibility in Archaeogeophysical Studies in the USA: Recent Developments and Prospects. *Archaeological Prospection* 15:1-31.

- Dalan, R. A. and S. K. Banerjee
1998 Solving Archaeological Problems Using Techniques of Soil Magnetism. *Geoarchaeology* 13:3-36.
- David, A.
1995 *Geophysical Survey in Archaeological Field Evaluation*. Ancient Monuments Laboratory, English Heritage Society, London.
- Ernenwein, E. G.
2008 A Geophysical View of Pueblo Escondido: Implications for the Pithouse to Pueblo Transition in the Jornada Mogollon. *Bulletin of the Texas Archeological Society* 79:125-145.
- Gaffney, C.
2008 Detecting Trends in the Prediction of the Buried Past: A Review of Geophysical Techniques in Archaeology. *Archaeometry* 50 (2):313-336.
- Gaffney, C. and J. Gater
2003 *Revealing the Buried Past: Geophysics for Archaeologists*. Tempus, Gloucestershire, England.
- Gaffney, C., J. A. Gater, P. Linford, V. Gaffney, and R. White
2000 Large-Scale Systematic Fluxgate Gradiometry at the Roman City of Wroxeter. *Archaeological Prospection* 7:81-99.
- Grealy, M. and L. B. Conyers
2008 EM31 Geophysical Survey Methods, Results, and Recommendations. In *Integrated Cultural Resources Investigations for the Bowie County Levee Realignment Project, Bowie County, Texas and Little River County, Arkansas*, by S. A. Sundermeyer, J. T. Penman, and T. K. Perttula, pp. 91-107. Miscellaneous Reports, Report of Investigations No. 29. LopezGarcia Group, Dallas, Texas.
- Kvamme, K.
2003 Geophysical Surveys as Landscape Archaeology. *American Antiquity* 68:435-457.
- 2006a Magnetometry: Nature's Gift to Archaeology. In *Remote Sensing in Archaeology: An Explicitly North American Perspective*, edited by J. K. Johnson, pp. 205-233. University of Alabama Press, Tuscaloosa.
- 2006b Data Processing and Presentation. In *Remote Sensing in Archaeology: An Explicitly North American Perspective*, edited by J. K. Johnson, pp. 235-250. University of Alabama Press, Tuscaloosa.
- 2008 Remote Sensing Approaches to Archaeological Reasoning: Pattern Recognition and Physical Principles. In *Archaeological Concepts for the Study of the Cultural Past*, edited by A. P. Sullivan III, pp. 65-84. The University of Utah Press, Salt Lake City.
- Kvamme, K., J. K. Johnson, and B. S. Haley
2006 Multiple Methods Surveys: Case Studies. In *Remote Sensing in Archaeology: An Explicitly North American Perspective*, edited by J. K. Johnson, pp. 251-268. University of Alabama Press, Tuscaloosa.
- Milsom, J.
2005 *Field Geophysics: The Geological Field Guide Series*. Third edition. Wiley, West Sussex, England.
- Scollar, I., A. Tabbagh, A. Hesse, and I. Herzog
1990 *Archaeological Prospecting and Remote Sensing*. Topics in Remote Sensing, No. 2, G. Hunt and M.

- Rycroft, series editors. Cambridge University Press, Cambridge.
- Walker, C. P.
2008 Preliminary Report of Technical Findings at sites 41PT185, 41PT186, and 41PT245. AGA Report 2008-10. Archaeo-Geophysical Associates, LLC, Austin. Submitted to TRC Companies, Inc. Austin, Texas.
- 2009 *Archaeogeophysical Survey at 41TR198*. AGA Report 2009-6. Archaeo-Geophysical Associates, LLC, Austin. Submitted to Geo-Marine, Inc. Plano, Texas.
- Weymouth
1986 Geophysical Methods of Archaeological Site Surveying. In, *Advances in Archaeological Method and Theory, Volume 9*, edited by M. B. Schiffer. Academic Press, Inc. New York.
- Witten, A. J.
2006 *Handbook of Geophysics and Archaeology*. Equinox Publishing, London.

This page intentionally left blank.

APPENDIX P

**DIATOM PALEOENVIRONMENTAL ANALYSIS OF SEDIMENTS
FROM ARCHAEOLOGICAL SITE 41PT185/C, BLM PROJECT-
LANDIS PROPERTY IN THE TEXAS PANHANDLE,
POTTER COUNTY, TEXAS**

This page intentionally left blank.

**DIATOM PALEOENVIRONMENTAL ANALYSIS OF SEDIMENTS FROM
ARCHAEOLOGICAL SITE 41PT185/C, BLM PROJECT-LANDIS
PROPERTY IN THE TEXAS PANHANDLE, POTTER COUNTY, TEXAS**

Prepared for:



**TRC Environmental Corporation
505 East Huntland Drive, Suite 250
Austin, Texas 78752**

Prepared by:

**Winsborough Consulting
Glen Ribbit
23606 Round Mountain Circle
Leander, Texas 78641
bwinsbor@io.com**

July 2009

This page intentionally left blank.

P.1 INTRODUCTION

This report describes the results of a diatom paleoenvironmental analysis of sediments from BLM Project- Landis Property in the Texas Panhandle. The site is in Potter County, on West Amarillo Creek, about 14 km from the Canadian River. As of 1923, West Amarillo Creek, fed by springs, maintained its stream throughout at least a part of its course during the entire year (Patton 1923). West Amarillo Creek is located on the southern edge of the semi-arid Canadian Breaks part of the Southwestern Tablelands ecoregion (Omernik 1987), and receives about 40.6 to 45.7 cm of rain on a topography characterized by the elevated, moderate-relief tableland, with broad valleys, sparse grassland and very few trees (Texas Commission on Environmental Quality 2004). About 16 km south of the site is the northern edge of the drier Llano Estacado part of the High Plains.

Diatoms are single-celled algae that have a silica cell wall and are therefore often preserved in stream and pond sediments. Diatoms are the most abundant algae in streams and are critically important to stream ecology as they stabilize the substrate and are primary producers and converters of inorganic nutrients into organic forms useable by other organisms. Diatoms that are common in an assemblage and sensitive to environmental characteristics can be used as indicator species in the interpretation of water quality and physical conditions. Many diatoms are cosmopolitan and their autecological characteristics have been well documented, particularly for the indicator species but there is a geographical component to the relationship between diatoms and environmental characteristics (Potapova and Charles 2007) due to floristic and environmental differences among ecoregions. Over the past few years regionally specific metrics, based on autecological (individual) attributes of diatom taxa, have been developed and are

being tested for use in monitoring the health of Wadeable streams throughout the United States. The goal is identify anthropogenic impacts causing degradation of water quality and aquatic life. These results can then be used to develop regionally specific analogs for paleoenvironmental interpretation.

Autecological indices use the relative abundance of species in assemblages and their ecological preferences, sensitivities, and tolerances to infer specific or general environmental conditions in an ecosystem (Lange-Bertalot 1979; Denys 1991; Lowe and Pan 1996; Stevenson and Pan 1999). Important attributes include trophic state, saprobity, pH, salinity, nitrogen uptake metabolism, oxygen requirements, moisture requirements, life forms (attached, motile, etc.), and habitat preferences including epiphytic (on plants), epilithic (on stones), epipellic (in mud), epipsammic (on sand), and planktonic (in water column). Metaphyton, another distinct habitat, are loose aggregates of benthic algae that become detached from the substrate and form dense, entangled or floating masses. Trophic state refers to the presence of inorganic nutrients such as nitrogen, phosphorus, silica and carbon, and saprobity refers to the presence of biodegradable organic matter and low oxygen concentrations (Van Dam *et al.* 1994). These attributes have been composited into various community level pollution metrics called trophic diatom indices that provide an indication of biotic integrity and human disturbance (Bahls 1993; Kelly and Whitton 1995; Lange-Bertalot and Genkal 1999; Mills *et al.* 2002; Musico 2002; Fore and Grafe 2002; Fore 2002; Potapova *et al.* 2004; Wang, Stevenson and Metzmeier 2005; Potapova and Charles 2007). Data from the above mentioned sources, and others, were consulted in determining diatom-based paleoenvironmental interpretations.

Porter *et al.* (2008) examined diatom data from 976 streams and rivers in the U.S. and found that algal metrics having significant

positive correlations with nutrient concentrations included indicators of trophic condition, organic enrichment, salinity, motility and taxa richness; and that the abundance of diatoms associated with high concentrations of dissolved oxygen was negatively correlated with both nitrogen and phosphorus concentrations. Nitrogen and phosphorus, essential nutrients for living organisms, may come from natural sources such as decomposition of plants and animals and dissolution of sediments. However, much of the phosphorus and nitrogen that enters streams is of human origin or related to human activities. Most algae use inorganic forms of phosphorous or nitrogen (such as nitrate, nitrite and ammonia), but some algae are able to use various forms of organic phosphorus or nitrogen.

Previous diatom investigations associated with archaeological sites or paleoecology in the region include the Clovis site in Blackwater Draw (Lohman 1936; Patrick 1938), the Llano Estacado (Hohn and Hellerman 1961), The Late Pleistocene on the Southern High Plains (Hohn 1975), the Lubbock Lake site (Compton 1975), prehistoric wells on the Southern High Plains (Winsborough 1988), the Mustang Springs site (Winsborough 1988; Meltzer 1991). A comprehensive regional paleoenvironmental study of marsh and pond deposition that covered the entire Holocene on the Southern High Plains, included a series of sections from sites on Running Water Draw, Blackwater Draw, Yellowhouse Draw and Mustang Draw (Winsborough 1995).

P.2 METHODS

Samples were cleaned of organic material and soluble salts with hydrogen peroxide and hydrochloric acid, rinsed to neutrality and mounted on permanent glass slides with Naphrax. A count of 500 diatom cells was done on each sample by counting random microscope fields, using an Olympus BH-2

at 1500x. The data was tabulated in EXCEL and figures were produced using Tilia and Tilia*Graph in TGView (Grimm, 2004).

P.3 RESULTS

Fourteen sediment samples were analyzed for diatom content. Thirteen of these were from Backhoe Trench 36 and one was from Feature 8 (N104/E105, 56-60 cmbs, catalog #1341-004-1a). The locations of individual samples from BT 36 are plotted on Figure P-1, a profile of BT 36. The trench samples represent a discontinuous stratigraphic sequence collected from the face of the backhoe trench. A complete set of diatom data, including provenience and catalog numbers is provided on Table P-1. A total of 160 diatom taxa were recorded during this study. The most abundant (dominant) diatoms in the backhoe column characterize the overall assemblage. The dominant taxa, in order of abundance, are *Rhopalodia gibba* (Ehrenberg) Müller, *Hantzschia amphioxys* (Ehrenberg) Grunow, *Epithemia turgida* (Ehrenberg) Kützing, *Synedra ulna* (Nitzsch) Ehrenberg, *Amphora copulata* (Kützing) Schoeman et Archibald, *Nitzschia amphibia* Grunow, *Aulacoseira crenulata* (Ehrenberg) Thwaites, *Luticola mutica* (Kützing) Mann, *Epithemia adnata* (Kützing) Brébisson, *Cocconeis placentula* var. *lineata* (Ehrenberg) Van Heurck. Subdominant taxa include *Rhopalodia gibberula* (Ehrenberg) Müller, *Sellaphora pupula* (Kützing) Mereschkowsky, *Diploneis puella* (Schumann) Cleve, and *Synedra acus* Kützing. These and other ecologically useful diatoms are illustrated on Figure P-2. The relative abundance of the ten most common diatoms is plotted on Figure P-3.

The structure and composition of the diatom assemblage in each sample varied as the environment changed, and the diatom flora adjusted to new habitat constraints. Because the samples in the present study are late Holocene in age, the flora is essentially a modern one and the ecological

characteristics of living diatoms can be used as analogs for paleoenvironmental interpretation. All but a couple of the diatom species found during this investigation have been reported from modern aquatic habitats in Texas.

Within the 13 samples in the column, species richness, the number of different species in a sample, was variable, and ranged from a low of 24 to a high of 70, with an average of 43.5 taxa per sample. Some samples exhibited dominance by one or a few taxa and other samples contained a more even distribution of species. Species richness in these samples was dependent on the kinds and number of habitats available for diatom colonization. The sand samples were less diverse because the unstable sand substrate limited diatom colonization to motile species.

For comparison with modern habitats, 73 modern benthic samples from wadeable streams in the Brazos River Basin, analyzed with the same protocols, had a species richness that ranged from 12-80 with an average of 42 taxa per sample (Winsborough unpublished data). As a system is stressed, species adapted to unfavorable conditions often become more abundant and sensitive forms disappear, leading to dominance by one or a few species. For example, eutrophic species generally increase in nutrient impacted sites and halophilic diatoms (those that prefer slightly elevated salt concentrations) increase under evaporitic conditions.

P.3.1 DESCRIPTION OF INDIVIDUAL SAMPLES, FROM OLDEST TO YOUNGEST

The oldest diatom sample in BT 36, #1 (catalog #263-004-4), 482-486 cmbs, dark gray marly clay, contains a moderately diverse diatom assemblage with 42 taxa, dominated by the epiphyte *Rhopalodia gibba* (160 cells out of 500). It and the other common diatoms, 57 *Synedra ulna*, 38

Epithemia turgida and 35 *Luticola mutica* are characteristic of alkaline, shallow, high conductivity fresh water with slightly elevated levels of carbonate or chloride and fluctuating water levels. *Synedra ulna* is an epiphyte but is also found on sediments and stones and has a rather broad tolerance range to salinity and drying. *Luticola mutica* is an aerophilic diatom found typically in brackish fresh water salinities. It probably thrived during the driest parts of the season. The habitat was probably a marsh with emergent macrophytes. There were motile sediment diatoms but none occurred in abundance suggesting that the macrophyte cover shaded the sediment surface. The presence of marl may indicate a relatively warm interval. The sample contained a limited amount of sediment and most of the diatoms were large epiphytic species, with the exception of *Luticola mutica*.

The next sample analyzed, proceeding up the section, #3 (cat. #263-004-6), at 458-462 cmbs was dark gray to grayish brown sandy loam. The diatom flora was slightly more diverse than the previous one (44 taxa), and was also dominated by the epiphyte *Rhopalodia gibba* (169 cells), followed by 45 *Sellaphora pupula*, 39 *Navicula libonensis*, and 24 *Hantzschia amphioxys* all motile sediment diatoms. These epipelagic forms were capable of moving up and down in the mud as necessary. *Rhopalodia gibba* was present in all the samples, but it was most abundant in these oldest two samples (Table P-1). This is the only interval in which the motile species *Sellaphora pupula* and *Navicula libonensis* were abundant. *Sellaphora pupula* is considered a good indicator of low nitrogen (Winter and Duthie 2000), in highly eutrophic, usually organically-polluted water (Kelly and Whitton 1995). There was probably a mixture of short and tall aquatic vegetation as there was a diverse epiphytic diatom flora, and exposed muds provided habitat for several species of aerophilic diatoms (forms found typically in soils and on damp or temporarily wet surfaces). The diatoms

were slightly diluted with clayey sediment and organic debris.

Sample #4 (cat. #263-007-7), at 429-432 cmbs, was grayish brown sand deposited some time after sample #3. There were 35 diatom taxa in the sample, and no single dominant, with 94 cells of *Hantzchia amphioxys*, 93 *Rhopalodia gibberula*, 70 *Rhopalodia gibba*, 28 *Luticola mutica*, and 26 *Amphora copulata*. *A. copulata* is epiphytic on other diatoms (Round and Lee 1989), and is also epilithic and epipelagic, motile and found in carbonate-rich freshwater streams, and brackish-marine habitats. The diatoms were heavily diluted with sediment and organic debris, including phytoliths. The diatoms suggest that there was some vegetation, possibly submerged, but also open muddy sand habitat, with a fluctuating water level. *H. amphioxys* and *L. mutica* are motile, aerophilic, sediment diatoms. *Rhopalodia gibberula*, a fresh-brackish species, called halophilic, is common in sediments of warm, alkaline, saline lakes with a pH of 8.3 (Hecky and Kilham 1973). Since the sand was probably a slope wash deposit, sediment stabilization would have taken some time.

The next sample, continuing up the section, #6 (cat. #263-004-9), collected at 387-391 cmbs, was black clay. The diatom assemblage was even more diverse, with 48 species. A shift in the diatom population, from the older samples, resulted in a new dominant, *Amphora copulata* (152 cells), followed by 48 *Hippodonta hungarica*, 43 *Hantzschia amphioxys*, 33 *Rhopalodia gibba* and 30 *Epithemia turgida*. The flora is a mixture of attached and motile species, and there is a trend toward increased nutrient levels, particularly nitrogen and phosphorous. This sample appears to represent a marshy area with both aquatic macrophytes and exposed sediment. As the sample represents a combination of diatoms, in a range of water quality characteristics and deposited over several years, it includes times of the year when vegetation had not

begun to grow. The mud was exposed to the sun, favoring diatoms such as *Amphora copulata* that are both motile and epiphytic, in a meso-eutrophic (moderate-substantial nutrient levels) environment (Levkov 2009). *A. copulata*, *R. gibba*, and *S. ulna* were considered indicators of eutrophic conditions, with high phosphorus and silica, in a study of epipelagic diatoms in South African rivers (Garcia-Rodriguez *et al.* 2007). (*Hippodonta hungarica* is also a motile form, found as an epiphyte in eutrophic water, as an aerophil on soils, and epipelagic in the sediments of springs, advantages that allow it to grow for much of the year rather than restricted to one or two seasonal growth periods (Round 1981). *H. hungarica* also showed a distinct association with sulphate dominated habitats (Blinn 1993) allowing it to grow in muds rich in hydrogen sulphide. *H. hungarica*, and *Hantzschia amphioxys* have been associated with turbid, alkaline conditions, in contrast to epiphytes such as *Epithemia turgida* that were most abundant in alkaline, clear pools with substantial macrophyte cover (Denys 2008). This set of autecological characteristics probably represents a complex benthic environment that contained many smaller, hydrologically connected, seasonally variable habitats.

Sample #8 (cat. #263-004-11), gray clay, collected at 350-354 cmbs, was unusually diverse with 67 taxa. There were no clear dominants as in previous sample. The most abundant diatoms were 30 *Rhopalodia gibba*, 27 *Synedra ulna*, and 22 *Cocconeis placentula*. There were aerophils, epiphytes, motile sediment forms and, for the first time, four centric, usually planktonic taxa. These data suggest that the environment may have been a wetland with relatively deeper areas of clear water, at least for part of the year. This type of environment would have supported a complex mosaic of deep and shallow habitats with vegetation limited to the shallower margins. Sediment deposition was very low.

Sample #9 (cat. #263-004-12) was black clay deposited from 336-340 cmbs. The diatom assemblage was diverse, with 60 taxa encountered. The assemblage was not only taxa rich but more even in distribution, dominated by 41 *Hippodonta hungarica*, 37 *Amphora copulata*, 32 *Diploneis puella*, and 30 *Rhopalodia gibba*. The water was somewhat shallow and clear, vegetated and contained diverse microhabitats. This sample may represent a more mature wetland than the previous sample and still contains a diverse mosaic of aquatic habitats. Microbial mats were well developed, and because of the significant number of motile taxa there was probably an increased accumulation of sediment, due in part to settling of suspended particles and detritus. A mixture of short and tall aquatic grasses allow for vertical distribution of different species, increasing the number of available microhabitats.

Sample #11 (cat. #263-004-13), collected above #9, was a thin marl black clay deposited at 305-309 cmbs. The organic-rich black clay was probably diluted by white calcium carbonate that was precipitated by salt tolerant algae such as *Chara* spp. and other green algae, cyanobacteria, and certain diatoms. This was the most species rich sample, with 70 diatom taxa. The most abundant diatoms include 50 *Rhopalodia gibba*, 41 *Cocconeis placentula*, 33 *Synedra ulna*, 28 *Epithemia adnata*, 24 *Epithemia turgida*, all commonly found as epiphytes in an alkaline marsh similar to the previous sample. The diatoms in this sample suggest a change in the water chemistry that made dissolved carbonates available. The rather even distribution of the diatom epiphytes in this sample suggests a mixture of vegetation types and possibly suspended algal mats. The sample was very diatomaceous and was not diluted by much sediment.

Sample #13 (cat. #263-004-16) was deposited some time later, above sample #11, from 275-278 cmbs, in the same

massive black clay. The composition of the diatom flora was different however. There were only 36 taxa. A centric diatom, *Aulacoseira crenulata* (154 cells) was the clear dominant appearing in large numbers for the first time, followed by 60 *Hantzschia amphioxys*, 49 *Nitzschia amphibia*, 41 *Epithemia turgida*, 35 *Synedra ulna*, 20 *Epithemia adnata* and 20 *Rhopalodia gibba*. Winter and Duthie (2000) found that *Nitzschia amphibia* is a good indicator of high phosphorus. *Aulacoseira crenulata*, the first planktonic diatom to dominate an assemblage in this study, has been described from fossil deposits in many parts of the world, and from living benthos of the littoral zone of small, oligotrophic, calcium rich water bodies (Krammer and Lange-Bertalot 1991). In a riverine-impounded wetland in Oregon, *Aulacoseira crenulata* was abundant when there was flooding from adjacent Willamette river (Weilhoefer and Pan 2003). This interval may represent a particularly wet period within a long dry episode, when the site was temporarily deeper, allowing *A. crenulata* to bloom (Figure P-3). Sedimentation was very low and there was not as much organic debris as in previous samples.

The next sample upsection, #15 (cat. #263-004-18), from 247-251 cmbs is a horizon of grayish brown clay within the massive black clay deposit. Species richness was similar with 38 diatom taxa. The assemblage was dominated by 160 cells of *Amphora copulata*, followed by 58 *Rhopalodia gibba*, 44 *Epithemia turgida*, 43 *Aulacoseira granulata* var. *angustissima*, and 21 *Hantzschia amphioxys*. These common taxa represent epiphytes, a planktonic form (*A. granulata* var. *angustissima*), motile species and aerophils, as does the remaining flora in the assemblage, suggesting a partially open wetland with a mixture of exposed sediment and macrophytes, possibly more turbid water and less overall productivity. Macrophyte growth may have been limited to low, salt tolerant grasses or sedges. The

sample was slightly diluted by very fine clay.

Sample #16 (cat. #263-004-19), at 222-227 cmbs, represents a slight shift in substrate composition to marl black clay. The diatom assemblage from this interval was moderately diverse and even in composition with 41 species, dominated by 72 *Cymbella excisa*, 56 *Epithemia turgida* var. *granulata*, 49 *Rhopalodia gibba*, 37 *Gomphonema subtile* var. *sagitta*, 29 *Aulacoseira crenulata*, and 28 *Synedra ulna*. All of these species are epiphytic, alkaliphilous and have a wide salinity tolerance. *Epithemia turgida* var. *granulata* was rare in this study, occurring only in two other samples and in small numbers. It is rather tolerant of pollution and, is halophilic (Porter 2008) suggesting that there was an accumulation of evaporitic salts. This sample was the one closest to being a pure diatomite.

The sample from the interval 188-192 cmbs, #18 (cat. #263-004-21) was grayish brown sand, deposited in a higher energy environment than the previous several samples. This sample had a relatively depauperate diatom assemblage with only 28 species. The diatoms were sparse and heavily diluted with sediment and phytoliths. Dominant taxa include 155 *Synedra ulna*, 138 *Epithemia turgida*, 75 *Hantzschia amphioxys*, 30 *Cocconeis placentula* and 14 *Luticola mutica*. The soil forms *H. amphioxys* and *L. mutica* were either washed in from the margins or were living on the sand surface when it was exposed. These epipsammic diatoms are capable of living on unstable substrates. *Synedra ulna* and *Cocconeis placentula* will attach to any firm surface and are early colonizers. This assemblage is suggestive of a rather flashy, muddy, drying, somewhat saline stream setting in which the diatom mats were restricted from maturing into a thick, diverse population by regular disturbance and, or low water levels.

Sample #19 (cat #263-004-22), from 185-178 cmbs, was a black clay deposit. This sample was the least species rich with only 24 taxa. The dominant diatoms were 183 *Synedra ulna*, 138 *Epithemia turgida*, 72 *Hantzschia amphioxys*, 33 *Epithemia adnata*, and 16 *Cocconeis placentula*. The remainder of the sample contained epiphytes and motile taxa tolerant of drying conditions. Some of the *Synedra ulna* cells were broken fragments, probably caused by grazers, and therefore the number is somewhat higher than it should be. This diatom assemblage is similar to the previous sample and appears to represent a damp, vegetated wetland. The diatoms were very diluted by sediments and phytoliths, and many of the diatoms are halophilic, indicating a concentration in salts due to evaporation.

The most recently deposited sample, #21 from 146-151 cmbs (cat. #263-004-24) was also black clay. There were 33 taxa, dominated by 183 *Hantzschia amphioxys*, 80 *Epithemia turgida*, 36 *Luticola mutica*, and 24 *Synedra ulna*. This sample contained at least 228 diatoms considered to be aerophils, 138 epiphytes and about 87 motile forms. This was an environment that probably dried out at least seasonally and was probably one of the driest samples in the section. The diatoms were diluted by phytoliths, and many chrysophycean statospores, another indicator of drying conditions.

The sample collected from under rock "ae" at the bottom of Feature 8 (56-60 cmbs, cat. #1341-004-1a) in 41PT185/C was very different in diatom composition. There were only 8 diatom taxa and two of them were only represented by fragments (*Eunotia* sp. and *Epithemia* sp.). The assemblage was heavily dominated by *Hantzschia amphioxys* with 402 cells out of 500, followed by *Luticola mutica* with 81 cells. These are both soil diatoms that are abundant in moist soil and mud. Of the other diatom taxa found in low numbers in the sample, *Diadesmis gallica* and *Pinnularia borealis*

are aerophils, and *Rhopalodia gibba* and *R. gibberula* were present in unusually low numbers. The most significant information from this sample is that it represents an area that was moist for long enough that sediment diatoms accumulated. There was very little evidence of aquatic diatoms and they could have been accidentally transported to the location.

P.4 DISCUSSION

The sediment diatom assemblage combines diatoms living on vegetation, the sediment surface and in the water column, at all times of the year and, depending on the thickness of the sample, over several years, thus integrating spatial and temporal variability in wetland diatom assemblages. Changes in water chemistry, light and temperature regimes over an annual cycle in this temperate location were significant to the composition of the diatom assemblage. For example, a study on the seasonal changes in the dominant diatoms on *Phragmites* found that the community change rate was very high, involving the replacement of many taxa every four weeks (Albay and Akcaalan 2003).

The sediment diatom flora in this study reflects a series of spatially and temporally different stages in stream channel/wetland development that fit into a conceptual model of wetland algae described by Goldsborough and Robinson (1996). The model describes four quasi-stable states: dry, open, sheltered, and lake. These states are dominated by epipelton, epiphyton, metaphyton, or phytoplankton respectively. Each state is determined by natural grazing pressure, water column stability, and anthropogenic influences. The dry wetland state exists during a drought when water levels are low and sediments are exposed and during a flood when sediments are again exposed and only limited grasses and sedges provide epiphyte habitat. Motile mud or clay (epipellic) species dominate, with few

macrophytes, except perhaps grasses or sedges. The amount of accumulated litter and macrophyte development determines how nutrient-rich the environment is. Marls were probably deposited as temperatures warmed.

An open wetland with submerged and emergent macrophytes develops as a dry wetland gradually fills with water. Epiphytic diatoms become dominant as epipellic forms are shaded out. A sheltered environment develops under conditions of high nutrient loading, high irradiance, alkaline pH, high calcium, high conductivity and a stable water column, without physical disturbance, leading to formation of dense metaphyton mats that can eventually shade out the macrophytes (Goldsborough and Robinson 1996). If the standing water dries out or becomes minimal before the end of the growing season and a dense, emergent macrophyte stands develop, and diatom growth is light inhibited.

Rapid water input into a previous wetland state leads to a lake state, with high water and nutrient levels, a turbid water column, a progressive loss of macrophytes and epiphytic diatom habitat. If enough time passes, depending on natural grazing pressure, water column stability and anthropogenic nutrient loading, there could be an eventual shift in dominance to phytoplankton. Common diatoms in the phytoplankton of isolated ponds in a wetland include many taxa that are typically epiphytes (tychoplankton), a lack of habitat fidelity noted by several diatom investigators working in wetlands (Goldsborough and Robinson 1996).

This model agrees with a recent study by Weihoefer and Pan (2007) who analyzed surface sediment diatoms, water quality, physical habitat and land use in 92 Oregon wetlands. They identified 4 statistically significant groups that corresponded to within-wetland water depth, nutrient levels and turbidity, the same variables that define

the model of Goldsborough and Robinson (1996). As in the models, each sample in this study integrated a set of contemporaneous but heterogeneous, interconnected habitats within a particular wetland state.

Several of the most abundant diatoms in the section belong to the genera *Epithemia* and *Rhopalodia* known to contain cyanobacterial endosymbionts capable of fixing elemental nitrogen in nitrogen-poor lakes, streams and marshes (Burkholder 1996). These epiphytes are known to dominate epiphytic habitats where the ratio of available nitrogen to phosphorus might be relatively low (Lowe 1996). Mayer and Galatowitsch (2001) also found that wetland sites with low diatom diversity were dominated by *Rhopalodia gibba*, *Epithemia adnata* and *Epithemia turgida* because they were superior competitors under low nitrogen, high phosphorus conditions. Pentecost (1998) noted a significant association between the presence of *Rhopalodia gibba* and calcite deposition in a thermal travertine-depositing spring where *R. gibba* was attached to the surface of moss and down to 20-30 mm below the surface of the moss, suggesting that it can thrive at low light levels (as would exist on stems in a dense macrophyte stand). *Rhopalodia gibba* was a dominant diatom in the littoral epilithon of Lake Tanganyika (Cocquyt 1999). These observations mean that in reality this diatom attaches to any available stable, solid surface, either plants or stones, under a wide range of light intensities, and has a competitive advantage in low nitrogen settings. The occurrence of these diatoms under low nitrogen and high phosphorous conditions in wetlands seems to be a universal phenomenon. Dominant diatoms on *Phragmites australis* stems in a eutrophic hardwater lake in Germany were stable from one year to the next and include *E adnata*, *E sorex*, *E turgida*, and *Rhopalodia gibba* (Müller 1999).

Salinity determines the potability of water, and diatoms have predictable responses to elevated ion concentrations, expressed as salinity when the ion is chloride, and as conductivity when there are mixed anion concentrations such as carbonate and sulfate. Some diatoms are sensitive to salts and others thrive on elevated concentrations. Diatom salinity classification schemes (Admiraal 1984; Denys and De Wolf 1999; Fritz *et al.* 1999) show that diatoms replace each other with increasing salinity and this series of species replacements along the salinity gradient make diatoms powerful indicators of chemical change driven by changes in hydrology and climate. In the present study the diatoms bracket the salinity gradient between freshwater forms that tolerate elevated ion concentrations and halophilic taxa that prefer conditions of elevated salt concentrations. The salt-tolerant taxa represent localized or seasonal evaporative conditions when salts accumulated. The amount of environmental stress at a particular time determined how many sensitive diatoms were eliminated in favor of a few very tolerant taxa.

Diatom paleoenvironmental studies, covering the same time interval as the present study, include the Mustang Springs site in Mustang Draw and the Lubbock Lake site on Yellow House Draw, both a short distance to the south on the Southern High Plains (Winsborough 1995). The diatom assemblages found in the draw studies were quite similar to the assemblages recorded in the present study and the paleoenvironmental interpretations were also similar. The paleoenvironments at Mustang Springs and Lubbock Lake were also well-aerated, alkaline, high conductivity freshwater to slightly saline, spring-fed marshes and marshy lakes, with shallow, marly, evaporative intervals, and fluctuating water tables. There was usually abundant aquatic vegetation, and a true phytoplankton population never developed at these sites, as was the case in the present study.

P.5 CONCLUSIONS

The diatom flora, although variable in the relative abundances of the most abundant taxa, remained rather consistent over time in the diatoms that characterize the various habitats distributed within the heterogeneous wetland complex. The assemblage as a whole was dominated by members of the Epithemiaceae family, including *Epithemia* and *Rhopalodia*, large epiphytic forms with internal siliceous supports thought to provide support during osmotic stress, and symbiotic algae that provides nutrients to the diatom in nitrogen-poor situations. Interpretation of individual samples should be viewed in the context of a complex system in which habitats typical of several phases of wetland evolution are present concurrently. General environmental characteristics, provided by the autecological traits of the common diatoms in BT 36, indicate that the water quality was characterized by high conductivity, derived from carbonates, sulfates and chlorides, depending on evaporation and precipitation conditions. The overall salinity was between fresh and brackish, with less than about 500 mg/L chloride or less than 0.9% ppt salinity (van Dam *et al.* 1994). The pH range was about 7 to 9. Water temperature varied seasonally and seasonal trends in primary productivity would have tracked seasonal air temperatures. The diatom assemblage reflects a shallow, alkaline, freshwater environment with slightly elevated alkalinity and salinity. Water depths were probably highly variable, with one and perhaps two relatively deep intervals (Figure P-3). Nutrient levels varied but the diatoms suggest that there was generally low nitrogen and moderate to high phosphorus levels.

Instream macrophyte growth and riparian vegetation cover varied over time and were particularly important in structuring the diatom communities in these late Holocene samples. Early in a growth season, submerged and emergent macrophytes,

provided colonizable substrates and nutrients for epiphytic diatoms, stabilized the sediment, and reduced turbidity and water velocity. Depending on local conditions during the growing period, macrophytes grew to dense stands and reduced algal growth by modifying the light regime. The diatoms suggest that overlain on a long, persistent black clay deposit accumulating in a wetland environment, were multiple brief episodes of erosion and deposition of coarser, sandy material. Because of the abundance of *Epithemia* and *Rhopalodia* species it is likely that the environment was low in nitrogen, and varying in phosphorus concentrations. The most consistently abundant diatom taxa were aerophils and epiphytes (Figure P-3).

This interpretation of late Holocene wetland conditions is comparable to paleoenvironmental reconstructions in wetland habitats on the Southern High Plains to the south, suggesting that there was a regional component to the paleoclimate. The common diatoms in this study are very similar to those found in late Holocene draws on the Southern High Plains where muds were deposited in spring-fed marshes (Winsborough 1995). Similar diatom assemblages have been recorded from late Holocene, shallow, slightly alkaline to saline, freshwater wetlands with well-developed macrophytes in other parts of the world, for example, in Northern Egyptian Delta lakes during warm, dry parts of the late Holocene (Zalat and Vildary 2007).

The diatoms in this study were characteristic of moderately good water quality. There was evidence of at least seasonally available water in some of the intervals, and there was the suggestion of limited availability in other intervals. The conclusions of this diatom study, when coupled with input from pollen, phytolith, sediment, geomorphology, and aquatic invertebrate studies should provide a more precise and comprehensive description of the aquatic and riparian paleoenvironments, and identify particular

constraints that would influence use of the site. Future work would benefit from close-interval sampling of a vertical column, to better refine the descriptions of the sequences in wetland evolution, and how they changed over time; and better distinguish between local individual wetlands under local topographic and hydrographic control and a larger, more regional signal of climate shifts.

P.6 REFERENCES CITED

- Admiraal, W.
1984 The ecology of estuarine sediment-inhabiting diatoms. In: *Progress in Phycological Research 3*, edited by F. Round and D.J. Chapman, pp. 269-322. Biopress Ltd., Bristol.
- Albay, M. and R. Akcaalan
2003 Comparative study of periphyton colonisation on common reed (*Phragmites australis*) and artificial substrate in a shallow lake, Manyas, Turkey. *Hydrobiologia* 506-509:531-540.
- Bahls, L. L.
1993 Periphyton Bioassessment Methods for Montana Streams. *Water Quality Bureau, Department of Health and Environmental Sciences, Helena, Montana*: 1-22.
- Blinn, D. W.
1993 Diatom community structure along physicochemical gradients in saline lakes. *Ecology* 74: 1246-1263.
- Burkholder, J. M.
1996 Interactions of benthic algae with their substrata. In: *Algal Ecology: Freshwater Benthic Ecosystems*, edited by R. J. Stevenson, M. L. Bothwell and R. L. Lowe, pp. 253-297. Academic Press, San Diego.
- Cocquyt, C.
1999 Seasonal variations of epilithic diatom communities in the northern basin of Lake Tanganyika. *Systematics Geography* 69:265-273.
- Compton, J. L.
1975 Diatoms of the Lubbock Lake Site, Lubbock County, Texas. Unpublished thesis, Texas Tech University, Lubbock.
- Denys, L.
1991 A check-list of the diatoms in the Holocene deposits of the western Belgian coastal plain with a survey of their apparent ecological requirements. In: Introduction, ecological code and complete list. Service Geologique de Belgique Professional paper 1991/2-No 246, 41pp.
- Denys, L.
2008 Diatoms. In: *Integrated management tools for water bodies in agricultural landscapes (mandscape), scientific support plan for a sustainable development policy, Final Report, Part 2: Global change, ecosystems and biodiversity*, edited by H. Hampel and K. Martens, pp. 28-32. Belgian Science Policy, Brussels.
- Denys, L. and H. De Wolf,
1999 Diatoms as indicators of coastal paleoenvironments and relative sea-level change. In *The Diatoms, Applications for the Environmental and Earth Sciences*, edited by E. F. Stoermer and J. P. Smol, pp. 277-297. Cambridge University Press, Cambridge, U.K.
- Fore, L. S.
2003 Response of diatom assemblages to human disturbance: development and testing of a multimetric index

- for the Mid-Atlantic Region (USA).
In: *Biological Response Signatures: Indicator Patterns Using Aquatic Communities*, edited by T. P. Simon, pp. 445-471. CRC Press, Hoboken.
- Fore, L. S. and C. Grafe
2002 Using diatoms to assess the biological condition of large rivers in Idaho (U.S.A.). *Freshwater Biology* 47:2015-2037.
- Fritz, S. C., B. F. Cumming, F. Gasse, and K. R. Laird
1999 Diatoms as indicators of hydrologic and climatic change in saline lakes. In: *The Diatoms, Applications for the Environmental and Earth Sciences*, edited by E. F. Stoermer and J. P. Smol, pp. 41-72. Cambridge University Press, Cambridge, U.K.
- Garcia-Rodriguez, F., G. C. Bate, P. Smailes, J. B. Adams and D. Metzeltin
2007 Multivariate analysis of the dominant and sub-dominant epipellic diatoms and water quality data from South African rivers. *Water SA* 33(5):653-658.
<http://www.wrc.org.za>
- Goldsborough, L. G. and G. G. C. Robinson
1996 Pattern in wetlands. In: *Algal ecology: freshwater benthic ecosystems*, edited by R. J. Stevenson, M. L. Bothwell and R. L. Lowe, pp. 77-117. Academic Press, San Diego.
- Grimm, E. C.
2004 TGView version 2.0.2. Illinois State Museum, Research and Collections Center, Springfield, Illinois.
- Hecky, R. E. and P. Kilham
1973 Diatoms in alkaline, saline lakes: ecology and geochemical implications. *Limnology and Oceanography* 18(1):53-71.
- Hohn, M. H.
1975 The diatoms. In: *Late Pleistocene environments of the Southern High Plains*, edited by F. Wendorf and J. J. Hester, pp. 197-200. Taos, Publication of the Fort Burgwin Research Center 9.
- Hohn, M. H. and J. Hellerman
1961 The diatoms. In: *Paleoecology of the Llano Estacado*, assembled by F. Wendorf, pp. 98-104. Santa Fe, The Museum of New Mexico Press, Burgwin Research Center Publication 1.
- Kelly, M. G. and B. A. Whitton
1995 The trophic diatom index: a new index for monitoring eutrophication in rivers. *Journal of Applied Phycology* 7:433-444.
- Krammer, K. and H. Lange-Bertalot
1991 Susswasserflora von Mitteleuropa Bd 2, Bacillariophyceae, Teil 3, Centrales, Fragilaceae, Eunotiaceae. In: H. Ettl, H. Gerloff, H. Heynig, D. Mollenhauer (Hrg.), Gustav Fischer Stuttgart, New York, 576 pp.
- Lange-Bertalot, H.
1979 Pollution tolerance of diatoms as a criterion for water quality estimation. *Nova Hedwigia* 64:285-304.
- Lange-Bertalot, H. and S. I. Genkal
1999 Iconographia Diatomologica. Annotated diatom monographs Vol. 6. *Diatoms from Siberia* 1. Koeltz Scientific Books, Königstein: 18-25.
- Levkov, Z.
2009 *Amphora sensu lato. Diatoms of Europe vol. 5*, A. R. G. Gantner Verlag and K. G., Liechtenstein: 49-51.

- Lohman, K. E.
1936 Diatoms from Quaternary lake beds near Clovis, New Mexico. *Journal of Paleontology* 9: 455-459.
- Lowe, R. L.
1996 Periphyton patterns in lakes. In: *Algal Ecology, Freshwater Benthic Ecosystems*, edited by R. J. Stevenson, M. L. Bothwell and R. L. Lowe, pp. 57-76. Academic Press, San Diego.
- Lowe, R. and Y. Pan
1996 Benthic algal communities as biological monitors. In: *Algal Ecology, Freshwater Benthic Ecosystems*, edited by R. J. Stevenson, M. L. Bothwell and R. L. Lowe, pp. 705-739. Academic Press, San Diego.
- Mayer, P. M. and S. M. Galatowitsch
2001 Assessing ecosystem integrity of restored prairie wetlands from species production-diversity relationships. *Hydrobiologia* 443:177-185.
- Meltzer, D. J.
1991 Altithermal archaeology and paleoecology at Mustang Springs, on the Southern High Plains of Texas. *American Antiquity* 56:236-267.
- Mills, M. R., G. V. Beck, J. F. Brumley, S. M. Call, M. C. Compton, E. C. Eisiminger, G. J. Pond, D. R. Peake, R. N. Pierce, and S. E. McMurray
2002 *Methods for Assessing Biological Integrity of Surface Waters in Kentucky, 2002*. Kentucky Department for Environmental Protection, Division of Water, Ecological Support Section, Frankfort, Kentucky. C-5 Diatom Master Taxa List:112-118.
- Müller, U.
1999 The vertical zonation of adressed diatoms and other epiphytic algae on *Phragmites australis*. *European Journal of Phycology* 34:487-496.
- Muscio, C.
2002 *The diatom pollution tolerance index*. City of Austin Watershed Protection and Development Review Department, Environmental Resource Management Division. SR-02-02: 1-17.
<http://www.ci.austin.tx.us/watershed/publications/default.cfm>
- Omernik, J. M.
1987 Ecoregions of the conterminous United States (map supplement): *Annals of the Association of American Geographers* 77(1):118-125, scale 1:7,500,000.
- Patrick, R.
1938 The occurrence of flints and extinct animals in pluvial deposits near Clovis, New Mexico, Part V: diatom evidence from the mammoth pit. *Proceedings of the Philadelphia Academy of Science* 90:15-24.
- Patton, L.
1923 *The geology of Potter County*. University of Texas Bulletin 2330, Bureau of Economic Geology and Technology, Division of Economic Geology.
- Pentecost, A.
1998 The significance of calcite (travertine) formation by algae in a moss-dominated travertine from Matlock Batch, England. *Archiv fur Hydrobiologie* 143(4):487-509.
- Porter, S. D.
2008 Algal attributes: an autecological classification of algal taxa collected by the National Water-Quality Assessment Program. *U.S.*

- Geological Survey Data Series 329,
(<http://pubs.usgs.gov/ds/ds329/>).
- Porter, S. D., D. K. Mueller, N. E. Spahr, M.
D. Munn and N. M. Dubrodsky
2008 Efficacy of algal metrics for
assessing nutrient and organic
enrichment in flowing waters.
Freshwater Biology 53:1036-1054.
- Potapova, M. G., D. F. Charles, K. C.
Ponader and D. M. Winter
2004 Quantifying species indicator values
for trophic diatom indices: a
comparison of approaches.
Hydrobiologia 517:24-41.
- Potapova, M. and D. F. Charles
2007 Diatom metrics for monitoring
eutrophication in rivers of the
United States. *Ecological
Indicators* 7:48-70.
- Round, F. E.
1981 *The ecology of algae*. Cambridge
University Press, Cambridge.
- Round, F. E. and K. Lee
1989 Studies on freshwater *Amphora*
species IV. The *Amphora* epiphytic
on other diatoms. *Diatom Research*
4(2):345-349.
- Stevenson, R. J. and Y. Pan
1999 Assessing environmental conditions
in rivers and streams with diatoms.
In: *The diatoms, applications for the
environmental and earth sciences*,
edited by E. F. Stoermer and J. P.
Smol, pp. 11-40. Cambridge
University Press.
- Texas Commission on Environmental
Quality
2004 Atlas of Texas Surface Waters.
*Texas Commission on
Environmental Quality* GI-316.
- Vam Dam, H., A. Mertens and J. Sinkeldam
1994 A coded checklist and ecological
indicator values of freshwater
diatoms from the Netherlands.
*Netherlands Journal of Aquatic
Ecology* 28(1):117-133.
- Wang, Yi-K., R. J. Stevenson and L.
Metzmeier
2005 Development and evaluation of a
diatom-based index of biotic
integrity for the Interior Plateau
Ecoregion, U.S.A. *Journal of North
American Benthological Society*
24(4):990-1008.
- Weilhoefer, C. L. and Y. Pan
2003 Wetland diatom assemblages as
indicators of flooding influence and
surrounding land use in the
Willamette Valley, Oregon.
Presented at the North American
Benthological Society Annual
Meeting, Athens, Georgia, In:
*Approaches for using Algae to
Monitor and Assess Freshwater
Ecosystems II*.
- 2007 Relationships between diatoms and
environmental variables in wetlands
in the Willamette Valley, Oregon,
U.S.A. *Wetlands* 27(3):668-682.
- Winsborough, B. M.
1988 Paleocological analysis of
Holocene algal mat diatomites
associated with prehistoric wells on
the Texas High Plains. *Geological
Society of America Abstracts with
Programs*, v. 20:132.
- 1995 Diatoms. In: Late Quaternary valley
fills and paleoenvironments of the
Southern High Plains, edited by V.
Holliday, pp. 67-83. *Geological
Society of America Memoir* 186.
- Winter, J. G. and H. C. Duthie
2000 Epilithic diatoms as indicators of
stream total N and total P
concentration. *Journal of North*

- American Benthological Society*
19(1):32-49.
- Zalat, A. and S. S. Vildary
- 2007 Environmental change in Northern Egyptian Delta lakes during the Holocene, based on diatom analysis. *Journal Paleolimnology* 37:273-299.

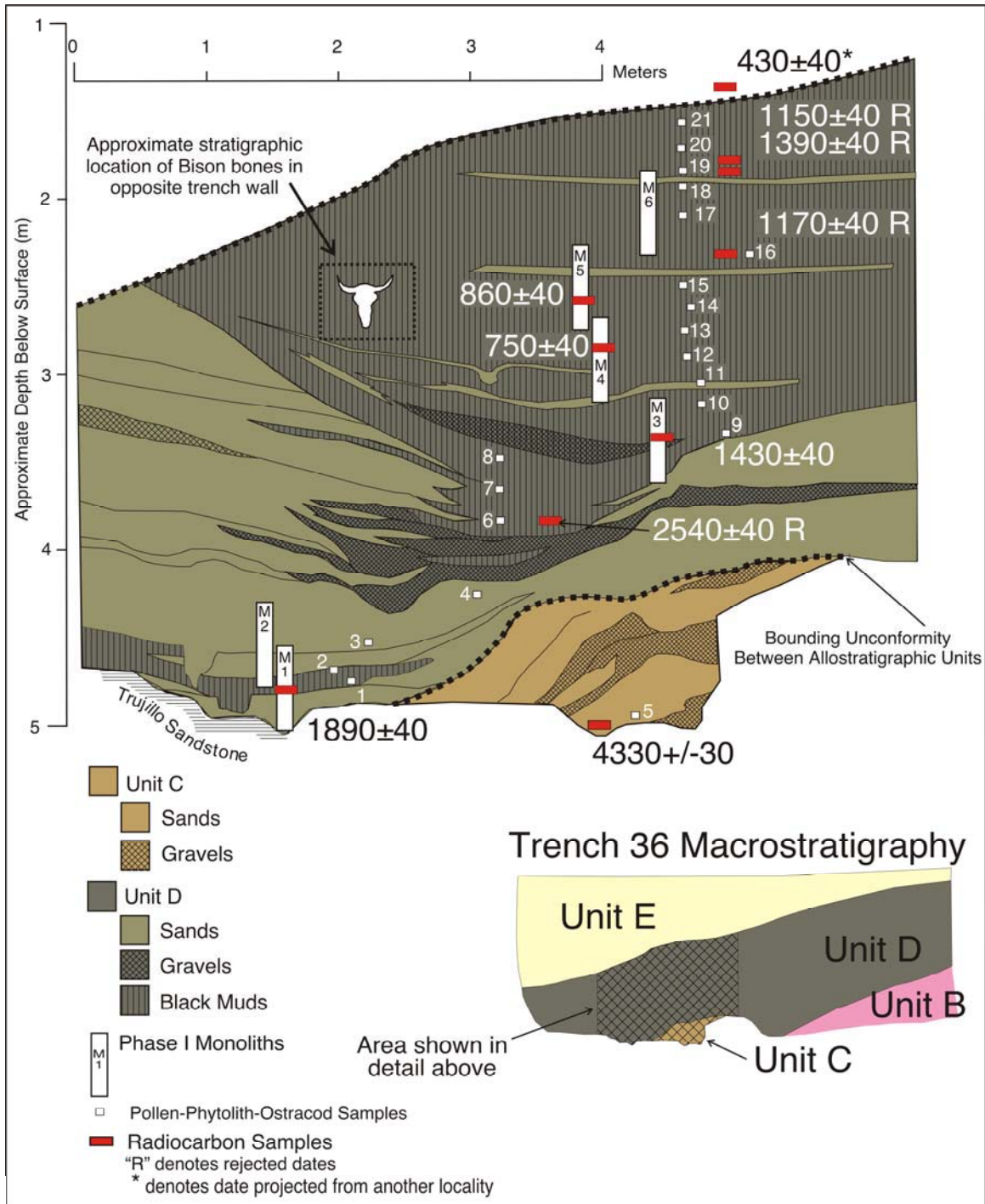


Figure P-1. Profile of Backhoe Trench 36 Showing Diatom Sample Locations.

(Note: Diatoms in same locations as pollen, phytolith, and ostracod locations.)

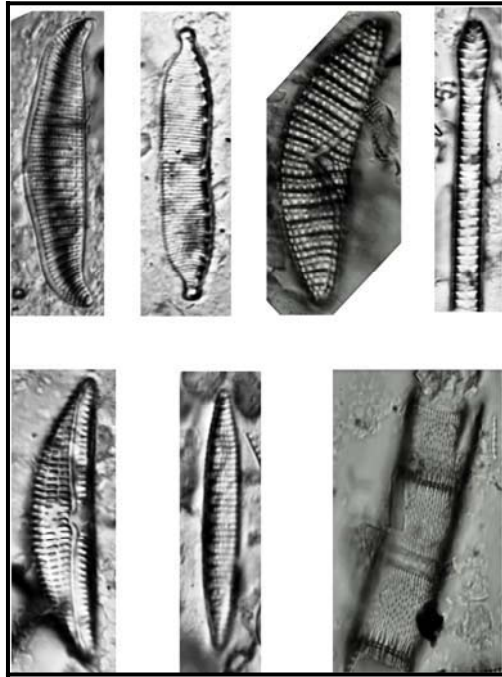


Figure P-2A. Diatoms. Top row left to right: *Rhopalodia gibba* 8x38, *Hantzschia amphioxys* 5x29, *Epithemia turgida* 12x44, *Synedra ulna* dia. 4; bottom row left to right: *Amphora copulata* 8x35, *Nitzschia amphibia* 3.5x26, *Aulacoseira crenulata* dia. 11.

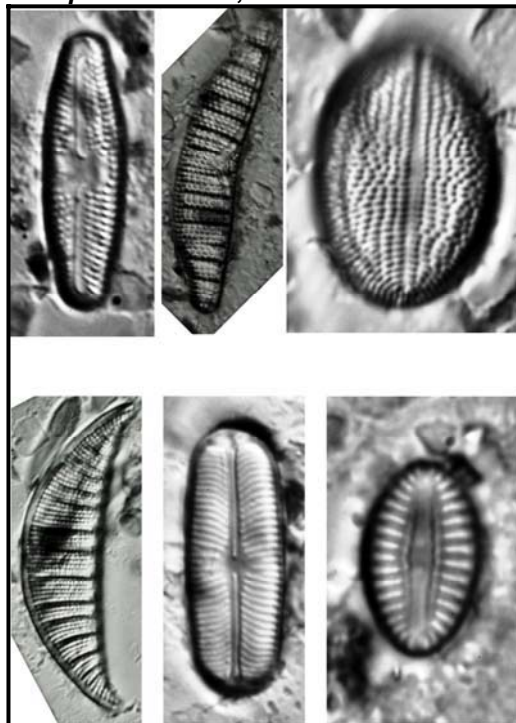


Figure P-2B. Diatoms. Top row left to right: *Luticola mutica* 5x20, *Epithemia adnata* 9x43, *Cocconeis placentula* var. *lineata* 10x15, *Rhopalodia gibberula* 10x41, *Sellaphora pupula* 7x20, *Diploneis puella* 7x11.

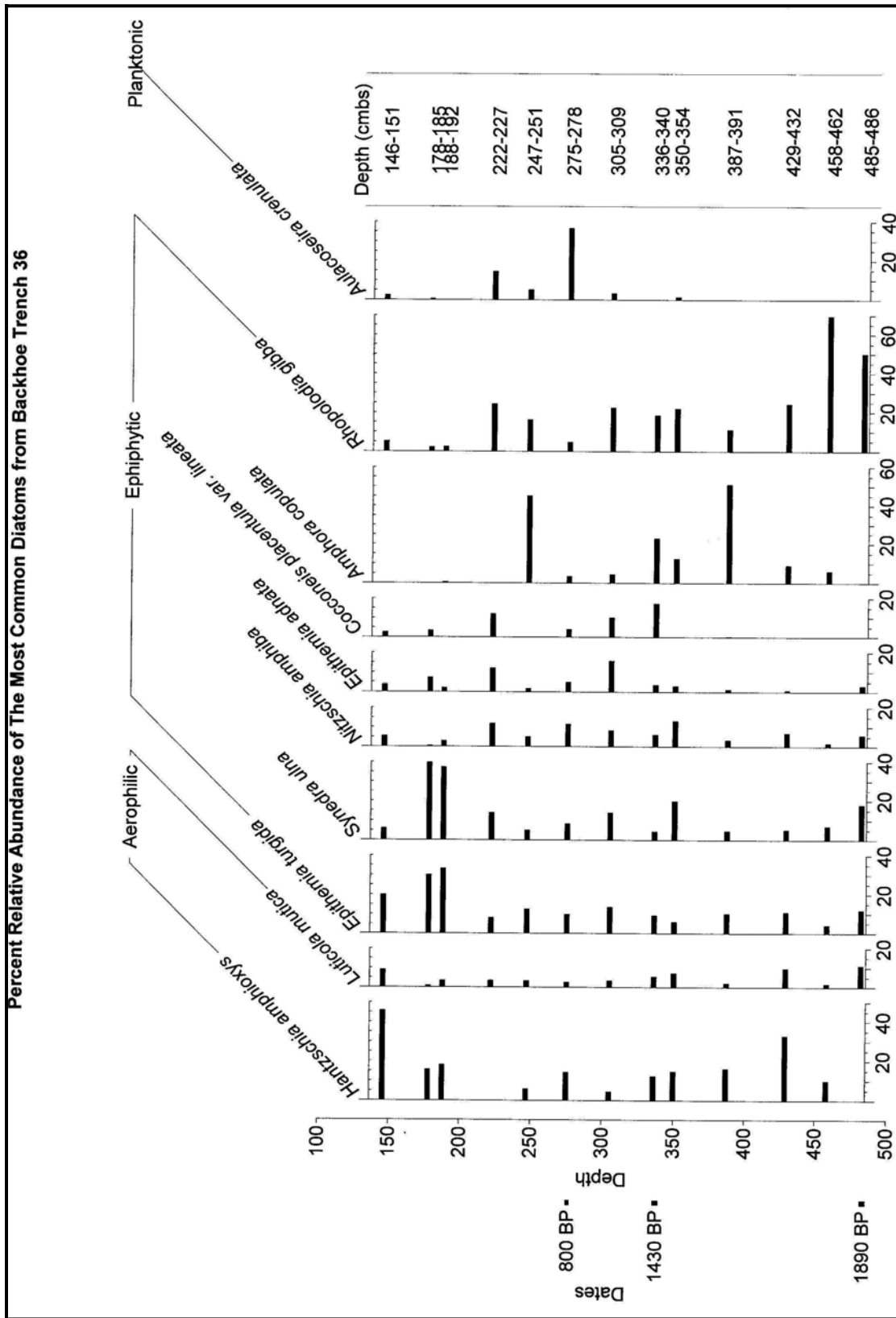


Figure P-3. Relative Abundance of Most Common Diatoms in Backhoe Trench 36

Table P-1. Diatom Abundance in Backhoe Trench 36

41PT185/C catalog numbers for BT 36 start with #263-4-	263-4-24	263-4-22	263-4-21	268-4-19	263-4-18	263-4-16	263-4-14	263-4-12	263-4-11	268-4-9	26304-7	263-4-6	263-4-4	1341-4-1a	
Collection sample numbers (bottom to top)	21	19	18	16	15	13	11	9	8	6	4	3	1	Feat. 8	
Depth (centemeter below surface), top to bottom	146-151	178-185	188-192	222-227	247-251	275-278	305-309	336-340	350-354	387-391	429-432	458-462	482-486	58-60	Total
Achnantheidium exiguum (Grunow) Czarnecki							2	1		4					7
Achnantheidium minutissimum (Kützing) Czarnecki				6			2	7	1						45
Adlafia bryophila (Petersen) Lange-Bertalot									2		3				5
Amphipleura pellucida (Kützing) Kützing							1								1
Amphora acutiuscula Kützing								3				2			5
Amphora coffeaeformis (Agardh) Kützing										1					1
Amphora coffeaeformis var aponina (Agardh) Kützing													5		5
Amphora copulata (Kützing) Schoeman et Archibald			2		16	14	8	7	1	15	2	1			43
Amphora inariensis Krammer				1						1					2
Amphora pediculus (Kützing) Grunow									1						1
Amphora veneta Kützing			2	4	1		7								14
Anomoeoneis costata (Kützing) Hustedt	2		4												6
Anomoeoneis sphaerophora (Kützing) Pfitzer		1	4		1		5	8		3		4			26
Aulacoseira crenulata (Ehrenberg) Thwaites	9	2		2	18	15	6		2						22
Aulacoseira granulata (Ehrenberg) Simonsen					2			1	8						11
Aulacoseira granulata var. angustissima (Müller) Simonsen					43			1							44
Biremis circumtexta (Meister ex Hustedt) Lange-Bertalot et Witkowski									4						4
Brachysira vitrea (Grunow) Ross							2								2
Caloneis bacillum (Grunow) Cleve	8	3	3	1		1	0	4	1	10	5	2	8		78
Caloneis leptosoma (Grunow) Krammer										2					2
Caloneis limosa (Kützing) Patrick									2						2
Caloneis molaris (Grunow) Krammer									2						2
Caloneis schumanniana (Grunow) Cleve								8	1	12		2	4		27
Caloneis silicula (Ehrenberg) Cleve						2									2
Cocconeis placentula Ehrenberg			3		10		3		2						92
Cocconeis placentula var. lineata (Ehrenberg) Van Heurck	1	1		2		17	1	2							11
Craticula cuspidata (Kützing) Mann	0	6		4			8	8		1					4
Craticula cuspidata (Kützing) Mann		6	7		3		4		2	5		5			32
Cyclostephanos tholiformis Stoermer, Håkansson et Theriot									1						13
Cyclotella meneghiniana Kützing				2						1					3

Table P-1 (continued)

41PT185/C catalog numbers for BT 36 start with #263-4-	263-4-24	263-4-22	263-4-21	268-4-19	263-4-18	263-4-16	263-4-14	263-4-12	263-4-11	268-4-9	26304-7	263-4-6	263-4-4	1341-4-1a	Feet. 8	Total
Collection sample numbers (bottom to top)	21	19	18	16	15	13	11	9	8	6	4	3	1			
Depth (centemeter below surface), top to bottom	146-151	178-185	188-192	222-227	247-251	275-278	305-309	336-340	350-354	387-391	429-432	458-462	482-486	58-60		
<i>Cyclotella pseudostelligera</i> Hustedt								1	3							4
<i>Cymatopleura elliptica</i> (Brébisson) Smith	1			2			5	2	3	5						18
<i>Cymatopleura solea</i> (Brébisson) Smith					10		14	24	8	9		1				66
<i>Cymbella cistula</i> (Ehrenberg) Kirchner	1						8					2				11
<i>Cymbella cymbiformis</i> Agardh				4			2									6
<i>Cymbella excisa</i> Kützing				72		2				1						75
<i>Cymbella kolbei</i> Hustedt									2							2
<i>Cymbella mexicana</i> (Ehrenberg) Cleve		5		13			3									21
<i>Cymbella proxima</i> Reimer									2							2
<i>Cymbella triangulum</i> (Ehrenberg) Cleve		1	2	22	22	2	4	16		14		3	2			68
<i>Denticula elegans</i> Kützing				2			4			2	5					13
<i>Denticula kuetingii</i> Grunow			2				4				4					10
<i>Denticula subtilis</i> Grunow											2					2
<i>Diadismis gallica</i> Smith														1		1
<i>Diploneis ovalis</i> (Hilse ex Rabenhorst) Cleve				2												2
<i>Diploneis puella</i> (Schumann) Cleve							8	32	21	28	1					90
<i>Diploneis subovalis</i> Cleve													10			10
<i>Encyonema kamtschaticum</i> Krammer									4							4
<i>Encyonema silesiacum</i> (Bleisch) Mann	2			1			1									4
<i>Encyonopsis microcephala</i> (Grunow) Krammer				18			8						2			28
<i>Eolimna minima</i> (Grunow) Lange-Bertalot	2								4							6
<i>Eolimna subminuscula</i> (Manguin) Moser									20							20
<i>Epithemia adnata</i> (Kützing) Brébisson	15	33	9	24	6	20	28	6	4	4	2		10	4		165
<i>Epithemia argus</i> (Ehrenberg) Kützing							4			1						5
<i>Epithemia sorex</i> Kützing			2	12	2		5	6	4							41
<i>Epithemia turgida</i> (Ehrenberg) Kützing	80	138	18	16	44	41	24	15	8	30	31	10	38			613
<i>Epithemia turgida</i> var. <i>granulata</i> (Ehrenberg) Hustedt	14			56							5					75
<i>Eunotia bilunaris</i> (Ehrenberg) Mills		1				2			0	4						17
<i>Eunotia</i> sp.														2		2
<i>Fallacia lenzii</i> (Hustedt) Lange-Bertalot							2									2

Table P-1 (continued)

41PT185/C catalog numbers for BT 36 start with #263-4-	263-4-24	263-4-22	263-4-21	268-4-19	263-4-18	263-4-16	263-4-14	263-4-12	263-4-11	268-4-9	26304-7	263-4-6	263-4-4	1341-4-1a	Feat. 8	Total
Collection sample numbers (bottom to top)	21	19	18	16	15	13	11	9	8	6	4	3	1			
Depth (centemeter below surface), top to bottom	146-151	178-185	188-192	222-227	247-251	275-278	305-309	336-340	350-354	387-391	429-432	458-462	482-486	58-60		
Fallacia pygmaea (Kützing) Stickle et Mann									4							4
Fragilaria capucina Desmazières				5	8	7		5								25
Fragilaria dilatata (Breb) Lange-Bertalot							3									3
Fragilaria nanana Lange-Bertalot							1									1
Fragilaria tenera (Smith) Lange-Bertalot							1		1							11
Frustulia vulgaris (Thwaites) deToni											5					5
Gomphonema acuminatum Ehrenberg				8			2					2				12
Gomphonema angustatum (Kützing) Rabenhorst	2	4				4		8		6			2			26
Gomphonema clavatum Ehrenberg			6		2	5		2					6			21
Gomphonema gracile Ehrenberg emend Van Heurck						8		2	4			3				17
Gomphonema intricatum var. vibrio (Ehrenberg) Cleve						1										1
Gomphonema maclaughlinii Reichardt				2			6									8
Gomphonema micropus Kützing																0
Gomphonema parvulum (Kützing) Kützing					2	1	4	3	1				2			22
Gomphonema pumilum (Grunow) Reichardt et Lange-Bertalot				4		2		8								24
Gomphonema sarcophagus Gregory							5									5
Gomphonema subtile var. sagitta (Schum)				3			4									41
Gomphonema truncatum Ehrenberg	2			2	1	2							2			9
Gyrosigma acuminatum (Kützing) Rabenhorst								2								2
Hantzschia abundans Lange-Bertalot				2									1			15
Hantzschia amphioxys (Ehrenberg) Grunow	1 8 3	7 2	7 5		2 1	6 0	8	2 0	2 0	4 8	9 4	2 4		4 0 2		10 27
Hippodonta hungarica (Grunow) Lange-Bertalot, Metzeltin et Witkowski				1	8			4	1	8						58
Luticola goeppertiana (Bleisch) Mann						2										2
Luticola mutica (Kützing) Mann	3 6	4	1 4	7	1 2	1 1	6	9	1 0	6	2 8	4	3 5	8 1		26 3
Mastogloia elliptica (Agardh) Cleve		5	4	5			1		2	6			9			46
Mastogloia smithii Thwaites	2	1				3							2			8
Navicula americana Ehrenberg											3					0
Navicula cari Ehrenberg																3
Navicula cincta (Ehrenberg) Ralfs	1						2	3				8				14
Navicula erifuga Lange-Bertalot							2					4	8			14

Table P-1 (continued)

41PT185/C catalog numbers for BT 36 start with #263-4-	263-4-24	263-4-22	263-4-21	268-4-19	263-4-18	263-4-16	263-4-14	263-4-12	263-4-11	268-4-9	26304-7	263-4-6	263-4-4	1341-4-1a Feat. 8	Total
Collection sample numbers (bottom to top)	21	19	18	16	15	13	11	9	8	6	4	3	1		
Depth (centemeter below surface), top to bottom	146-151	178-185	188-192	222-227	247-251	275-278	305-309	336-340	350-354	387-391	429-432	458-462	482-486	58-60	
Navicula incertata Hustedt												2			2
Navicula ingenua Hustedt									2						2
Navicula kotschy Grunow			2	2			5		2		2				13
Navicula libonensis Schoeman						2	2	7		3		3			53
Navicula menisculus Schumann									1 2						12
Navicula oblonga Østrup	6	1	3	2	1		7	1			9	1	8		49
Navicula recens Lange-Bertalot			1				5								6
Navicula radiosa Kützing				3			1 4		2			8	2		29
Navicula trivialis Lange-Bertalot						1									1
Navicula veneta Kützing				4								3			7
Neidium ampliatum (Ehrenberg) Krammer			3		2		5	2	3	1	1	5	2		39
Neidium bisulcatum (Lagerstedt) Cleve													2		2
Nitzschia amphibia Grunow	2 2	1 2	2 2	2 4	1 8	4 9	1 5	1 0	1 8	1 0	2 0	1 4	1 9		22 3
Nitzschia amphibioides Hustedt							3								3
Nitzschia angustata (Smith) Grunow	2				5	6	0	1 6	1 7	6	2	9			73
Nitzschia angustatula Lange-Bertalot					1			2							3
Nitzschia cf. subcommunis Hustedt												4			4
Nitzschia frustulum (Kützing) Grunow									6		2	4	6		18
Nitzschia inconspicua Grunow						1									1
Nitzschia linearis (Agardh ex Smith) Smith					1		1	2	7	2	2	5	7		27
Nitzschia microcephala Grunow													2		2
Nitzschia palea (Kützing) Smith								1	2			2	1		6
Nitzschia perminuta (Grunow) Peragallo							8	2 0							28
Nitzschia recta Hantzsch ex Rabenhorst													5		5
Nitzschia sigma (Kützing) Smith									2		1				3
Nitzschia solita Hustedt								3	2			2			26
Nitzschia tropica Hustedt							1	4	3			3	3		14
Nitzschia vitrea Norman	3		1												4
Pinnularia appendiculata (Agardh) Cleve						2				6			2		10
Pinnularia borealis Ehrenberg	9	2			2	2		5	2		2		4	5	33

Table P-1 (continued)

41PT185/C catalog numbers for BT 36 start with #263-4-	263-4-24	263-4-22	263-4-21	268-4-19	263-4-18	263-4-16	263-4-14	263-4-12	263-4-11	268-4-9	26304-7	263-4-6	263-4-4	1341-4-1a	
Collection sample numbers (bottom to top)	21	19	18	16	15	13	11	9	8	6	4	3	1	Feat. 8	
Depth (centemeter below surface), top to bottom	146-151	178-185	188-192	222-227	247-251	275-278	305-309	336-340	350-354	387-391	429-432	458-462	482-486	58-60	Total
Pinnularia cf. viridis (Nitzsch) Ehrenberg		5								3			1		9
Pinnularia divergentissima (Grunow) Cleve	6		1								6				13
Pinnularia gibba Ehrenberg	1				2	2									5
Pinnularia microstauron (Ehrenberg) Cleve	1 3						1 3	2		4					34
Pinnularia viridis (Nitzsch) Ehrenberg					5			1							6
Placoneis anglica (Ralfs) EJ Cox									2						2
Placoneis elginensis (Gregory) Cox						1		2			2				5
Placoneis exigua (Gregory) Mereschowsky										7		5			12
Placoneis gastrum (Ehrenberg) Mereschowsky		2													2
Placoneis placentula (Ehrenberg) Hienzerling							2								2
Placoneis pseudanglica (Lange-Bertalot) Cox									4						4
Planothidium lanceolatum (Breb. Ex Kützing) Round & Bukhtiyarova					4				7	1		5	4		21
Pseudostaurosira brevistriata (Grunow) Williams et Round													1		1
Rhoicosphenia abbreviata (Agardh) Lange-Bertalot	8		4	1		4		1 6		1			5		39
Rhopalodia brebissonii Krammer								2		4	2	4	12		24
Rhopalodia constricta (Smith) Krammer										1					1
Rhopalodia gibba (Ehrenberg) Müller	2 1	1 0	1 0	4 9	5 8	2 0	4 0	3 0	3 0	3 3	7 0	16 9	16 0		70 4
Rhopalodia gibberula (Ehrenberg) Müller	2									9 3	4	5	1		10 5
Sellaphora americana (Ehrenberg) Mann							4	5	2						11
Sellaphora laevisissima (Kützing) Mann	4			1		1		2	5						13
Sellaphora pupula (Kützing) Mereschowsky			3			4	8	1	1			45	3		95
Sellaphora seminulum (Grunow) Mann													2		2
Stauroneis borrichii (Petersen) Lund									1						1
Stauroneis phoenicenteron (Nitzsch) Ehrenberg	4	2	5	4	2		3	8	6		7	5			46
Stauroneis prominula (Grunow) Hustedt	4					2									6
Stauroneis pseudosubobtusoides Germain					3										3
Stauroneis smithii Grunow								1							1
Staurosira construens var. venter (Ehrenberg) Hamilton		1						3							4

Table P-1 (continued)

41PT185/C catalog numbers for BT 36 start with #263-4-	263-4-24	263-4-22	263-4-21	268-4-19	263-4-18	263-4-16	263-4-14	263-4-12	263-4-11	268-4-9	26304-7	263-4-6	263-4-4	1341-4-1a						
Collection sample numbers (bottom to top)	21	19	18	16	15	13	11	9	8	6	4	3	1	Feet. 8						
Depth (centemeter below surface), top to bottom	146-151	178-185	188-192	222-227	247-251	275-278	305-309	336-340	350-354	387-391	429-432	458-462	482-486	58-60	Total					
<i>Surirella angusta</i> Kützing									2											2
<i>Surirella bifrons</i> Ehrenberg								2												2
<i>Surirella brebissonii</i> Krammer et Lange-Bertalot							4	2	1	4	5	4								30
<i>Surirella elegans</i> Ehrenberg							3					2								5
<i>Surirella tenera</i> Gregory					2				4											6
<i>Synedra acus</i> Kützing			2	2			8	1	4	9	2	1	2							89
<i>Synedra ulna</i> (Nitzsch) Ehrenberg	2 4	1 8 3	1 5 5	2 8	1 8	3 5	2 5		2 7	1 4	1 5	1 7	5 7							60 5
<i>Synedra parasitica</i> (Smith) Hustedt									1 8											18
<i>Tryblionella acuminata</i> Smith			1					2	4		2									9
<i>Tryblionella apiculata</i> Gregory						4	2	0	2	1 8	2	9	8							65
<i>Tryblionella debilis</i> Arnott	1						2	6	6	1	1									17
<i>Tryblionella gracilis</i> Smith												2								2
<i>Tryblionella littoralis</i> (Grunow) Mann							2	2												14
Total counts	605	595	590	580	575	565	555	545	540	530	520	515	505	500	7720					

This page intentionally left blank.

APPENDIX Q

**METRIC AND NON-METRIC DATA FOR ARTIFACTS FROM THE
LANDIS PROPERTY SITES (41PT185, 41PT186, AND 41PT245) AND
PROJECT ARTIFACT DATABASE**

This page intentionally left blank

Q.1 METRIC AND NON-METRIC DATA

Individual observations, metric measurements, and provenience information on individual stone tools within each artifact classes (points, bifaces, scrapers, drills, unifaces, cores, and pottery) are presented in individual tables by class and component. The summaries of the observations and metric measurements that are presented in the body of the text for the different classes of artifacts by component were derived from these tables. The data in the tables is

presented in Microsoft Excel files with file names in italics.

Q.2 ARCHEOLOGICAL DATABASE

The entire Landis Property database from data recovery Phase I and II is presented in Microsoft Access format. The database includes all the information including the catalog numbers, provenience information, counts, weights, metric and non-metric observations on the various tools. The file names are in italics.

Table Q-1. 41PT185 Points

PNUM	#117-010	#193-010	#204-010	#208-010	#209-010
Unit	TU 9	TU 20	TU 22	TU 22	TU 22
Depth	40-50	40-50	10-20	50-60	60-70
Raw Material Type	Agatized Dolomite	Agatized Dolomite	Jasper	Agatized Dolomite	Jasper
Raw Material Source	Alibates	Alibates	Tecovas Formation (cherts and jaspers)	Alibates	Tecovas Formation (cherts and jaspers)
Max Length (mm)	17.34	8.08	12.57	14.49	13.21
Max Width (mm)	16.45	8.82	16.28	14.09	19.19
Max Thickness (mm)	4.71	3.07	5.62	2.00	4.69
Weight (g)	1.4	0.2	1.0	0.3	0.8
Long Cross-section	Indeterminate	Indeterminate	Indeterminate	Indeterminate	Indeterminate
Transverse Cross-section	Indeterminate	Indeterminate	Bi-Convex (Asymmetrical)	Indeterminate	Bi-Convex (Symmetrical)
Preform	Flake	Indeterminate	Indeterminate	Flake	Indeterminate
Shape	Indeterminate	Indeterminate	Indeterminate	Indeterminate	Indeterminate
Tool Class	Bifacial	Bifacial	Bifacial	Unifacial	Bifacial
Degree of Flaking	Complete	Marginal	Complete	Marginal	Complete
Cultural Period	Late Prehistoric	Indeterminate	Late Archaic	Late Prehistoric	Late Archaic
Flaking Pattern	Random Subparallel	Random Subparallel	Random Subparallel	Random Subparallel	Random Subparallel
Lateral Edge Angle (left)	60	68	—	45	52
Lateral Edge Angle (right)	—	60	—	45	55
Blade Length (mm)	—	—	—	14.50	—
Blade Width (mm)	—	—	—	14.10	—
Lateral Edge (left)	Excurvate	Indeterminate	Indeterminate	Excurvate	Straight
Lateral Edge (right)	Indeterminate	Indeterminate	Indeterminate	Straight	Straight
Shoulder Width (mm)	—	—	—	—	—
Notch Depth, left (mm)	—	—	—	—	—
Notch Depth, right (mm)	—	—	—	—	—
Notch Width, left (mm)	—	—	—	—	—
Notch Width, right (mm)	—	—	—	—	—
Ear Angle (left)	—	—	—	—	—
Ear Angle (right)	—	—	—	—	—
Stem Shape	Convex	—	Expanding	—	—
Stem Length (mm)	—	—	12.57	—	—
Stem Distal Width (mm)	—	—	13.07	—	—
Stem Proximal Width (mm)	15.89	—	16.28	—	—
Stem Thickness (mm)	—	—	5.62	—	—
Basal Shape	Excurvate	—	Incurvate	—	—
Basal Depth (mm)	—	—	0.88	—	—
Basal Notch Width (mm)	—	—	—	—	—
Form Completeness	Proximal	Fragment	Stem	Distal	Distal
Break Type	Thermal/Crenated	Use	Use	Use	Use
% of Cortex Remaining	0%	0%	0%	0%	0%
Thermal Alteration	Observed	Not Observed	Not Observed	Not Observed	Not Observed
Basal Grinding	None	None	heavy	—	—
Stem Grinding	None	None	Light	—	—

Table Q-1. continued

PNUM	#245-010	#375-010	#635-010	#895-010	#984-010	#1033-010
Unit	TU 28	N102 E109	N108 E103	N114 E105	N116 E103	N117 E98
Depth	70-80	40-50	42-50	40-50	50-60	40-50
Raw Material Type	Agatized Dolomite	Agatized Dolomite	Quartzite	Agatized Dolomite	Agatized Dolomite	Jasper
Raw Material Source	Alibates	Alibates	Dakota	Alibates	Alibates	Tecovas Formation (cherts and jaspers)
Max Length (mm)	12.44	28.43	23.34	11.30	12.54	12.61
Max Width (mm)	21.07	18.81	22.40	16.75	19.66	16.68
Max Thickness (mm)	5.91	5.07	5.69	4.44	5.66	4.72
Weight (g)	1.7	2.3	3.1	0.8	1.3	0.8
Long Cross-section	Indeterminate	Indeterminate	Indeterminate	Indeterminate	Indeterminate	Indeterminate
Transverse Cross-section	Bi-Convex (Asymmetrical)	Bi-Convex (Asymmetrical)	Bi-Convex (Asymmetrical)	Indeterminate	Bi-Convex (Asymmetrical)	Bi-Convex (Asymmetrical)
Preform	Indeterminate	Biface	Biface	Biface	Biface	Indeterminate
Shape	Indeterminate	Indeterminate	Indeterminate	Indeterminate	Indeterminate	Indeterminate
Tool Class	Bifacial	Bifacial	Bifacial	Bifacial	Bifacial	Bifacial
Degree of Flaking	Complete	Complete	Complete	Complete	Complete	Complete
Cultural Period	Late Archaic	Late Archaic	Late Archaic	Late Archaic	Late Archaic	Late Archaic
Flaking Pattern	Random Subparallel	Random Subparallel	Random Subparallel	Random Subparallel	Random Subparallel	Random Subparallel
Lateral Edge Angle (left)	—	45	38	—	—	—
Lateral Edge Angle (right)	—	60	45	—	—	—
Blade Length (mm)	—	—	—	—	—	—
Blade Width (mm)	—	—	—	—	—	—
Lateral Edge (left)	—	Straight	Indeterminate	—	—	—
Lateral Edge (right)	—	Straight	Indeterminate	—	—	—
Shoulder Width (mm)	—	—	—	—	—	—
Notch Depth, left (mm)	—	—	—	—	—	—
Notch Depth, right (mm)	—	—	—	—	—	—
Notch Width, left (mm)	—	—	—	—	—	—
Notch Width, right (mm)	—	—	—	—	—	—
Ear Angle (left)	—	—	—	—	—	—
Ear Angle (right)	—	—	—	—	—	—
Stem Shape	Expanding	—	Expanding	Expanding	Expanding	Expanding
Stem Length (mm)	10.51	—	7.03	9.93	12.54	12.61
Stem Distal Width (mm)	14.71	—	12.80	10.21	12.37	12.26
Stem Proximal Width (mm)	21.07	—	—	16.75	19.66	16.68
Stem Thickness (mm)	5.91	—	4.33	4.28	5.49	4.66
Basal Shape	Incurvate	Indeterminate	Indeterminate	Straight	Excurvate	Straight
Basal Depth (mm)	0.58	—	—	—	—	—
Basal Notch Width (mm)	—	—	—	—	—	—

Appendix Q
Lithic Analysis

Form Completeness	Stem	Distal	Proximal-Medial	Stem	Stem	Stem
Break Type	Use	Use	Use	Use	Use	Use
% of Cortex Remaining	0%	0%	0%	0%	0%	0%
Thermal Alteration	Not Observed	Not Observed	Not Observed	Not Observed	Not Observed	Not Observed
Basal Grinding	Light	—	None	None	Heavy	Light
Stem Grinding	Heavy	—	None	Light	Heavy	Light
PNUM	#1063-010	#1104-010	#1138-010	#1168-010	#1169-010	#1198-010
Unit	N117 E106	N118 E100	N118 E108	N119 E101	N119 E101	N119 E108
Depth	26-40	60-70	50-60	42-50	50-60	30-40
Raw Material Type	Unidentified Sedimentary	Agatized Dolomite	Jasper	Agatized Dolomite	Agatized Dolomite	Jasper
Raw Material Source	Unidentifiable	Alibates	Tecovas Formation (cherts and jaspers)	Alibates	Alibates	Tecovas Formation (cherts and jaspers)
Max Length (mm)	19.17	48.69	12.48	11.31	16.52	37.41
Max Width (mm)	11.99	24.13	16.64	16.52	12.63	16.54
Max Thickness (mm)	3.28	6.61	5.34	4.27	4.57	3.21
Weight (g)	0.6	7.1	1.1	0.8	0.9	1.8
Long Cross-section	Tapered Base/Tip	Tapered Base/Tip	Indeterminate	Indeterminate	Indeterminate	Flat
Transverse Cross-section	Bi-Convex (Asymmetrical)	Bi-Convex (Asymmetrical)	Bi-Convex (Asymmetrical)	Indeterminate	Indeterminate	Bi-Convex (Symmetrical)
Preform	Indeterminate	Biface	Indeterminate	Biface	Indeterminate	Biface
Shape	Triangular	Triangular	Indeterminate	Indeterminate	Indeterminate	Triangular
Tool Class	Bifacial	Bifacial	Bifacial	Bifacial	Bifacial	Bifacial
Degree of Flaking	Complete	Complete	Complete	Complete	Marginal	Complete
Cultural Period	Late Prehistoric	Late Archaic	Late Archaic	Late Archaic	Late Archaic	Late Prehistoric
Flaking Pattern	Random Subparallel	Random Subparallel	Random Subparallel	Random Subparallel	Random Subparallel	Random Subparallel
Lateral Edge Angle (left)	43	54	—	—	—	40
Lateral Edge Angle (right)	55	48	—	—	52	45
Blade Length (mm)	13.93	39.30	—	—	—	32.06
Blade Width (mm)	11.99	23.94	—	—	—	16.54
Lateral Edge (left)	Straight	Excurvate	—	—	Straight	Excurvate
Lateral Edge (right)	Recurvate	Excurvate	—	—	—	Excurvate
Shoulder Width (mm)	11.99	24.13	—	—	—	16.54
Notch Depth, left (mm)	2.0	5.00	—	—	—	2.53
Notch Depth, right (mm)	1.52	5.60	—	—	—	—
Notch Width, left (mm)	3.92	6.70	—	—	—	2.72
Notch Width, right (mm)	3.38	5.60	—	—	—	—
Ear Angle (left)	78	52	—	—	—	20
Ear Angle (right)	69	49	—	—	—	—
Stem Shape	Expanding	Expanding	Expanding	Expanding	Indeterminate	Expanding
Stem Length (mm)	5.43	10.27	12.48	—	—	5.05
Stem Distal Width (mm)	6.55	12.13	12.26	—	—	8.32

Landis Property: Data Recovery at 41PT185, 41PT186, and 41PT245, Potter County, Texas
Bureau of Land Management

Stem Proximal Width (mm)	8.54	16.94	16.64	16.52	—	9.08
Stem Thickness (mm)	1.81	4.39	5.34	4.27	—	1.95
Basal Shape	Straight	Excurvate	Excurvate	Excurvate	Indeterminate	Incurvate
Basal Depth (mm)	—	—	—	—	—	0.5
Basal Notch Width (mm)	—	—	—	—	—	—
Form Completeness	Complete	Complete	Stem	Stem	Edge Fragment	Complete
Break Type	Unbroken	Unbroken	Use	Use	Use	Indeterminate
% of Cortex Remaining	0%	0%	0%	0%	0%	0%
Thermal Alteration	Not Observed	Not Observed	Not Observed	Not Observed	Not Observed	Not Observed
Basal Grinding	None	Light	Light	Light	—	None
Stem Grinding	None	Light	Light	None	—	None

Table Q-1. continued

PNUM	#1226-010	#1279-010	#1288-010	#1348-010	#1355-010
Unit	N120 E101	N121 E101	N121 E104	N110 E105	N113 E108
Depth	44-60	60-70	40-50	50-60	54
Raw Material Type	Quartzite	Quartzite	Agatized Dolomite	Agatized Dolomite	Agatized Dolomite
Raw Material Source	Dakota	Dakota	Alibates	Alibates	Alibates
Max Length (mm)	24.95	13.17	32.84	17.55	24.08
Max Width (mm)	21.03	15.99	25.44	20.43	15.88
Max Thickness (mm)	5.36	4.77	6.33	6.56	5.66
Weight (g)	3.5	1.1	5.1	2.4	2.1
Long Cross-section	Wedged Base/Thick	Indeterminate	Wedged Base/Thick	Indeterminate	Indeterminate
Transverse Cross-section	Bi-Convex (Asymmetrical)	Bi-Convex (Asymmetrical)	Bi-Convex (Asymmetrical)	Bi-Convex (Asymmetrical)	Bi-Convex (Asymmetrical)
Preform	Biface	Indeterminate	Biface	Biface	Biface
Shape	Indeterminate	Indeterminate	Lanceolate	Indeterminate	Indeterminate
Tool Class	Bifacial	Bifacial	Bifacial	Bifacial	Bifacial
Degree of Flaking	Complete	Complete	Complete	Complete	Complete
Cultural Period	Late Archaic	Late Archaic	Late Archaic	Late Archaic	Late Archaic
Flaking Pattern	Random Subparallel	Random Subparallel	Random Subparallel	Random Subparallel	Random Subparallel
Lateral Edge Angle (left)	51	—	55	—	65
Lateral Edge Angle (right)	48	—	58	—	60
Blade Length (mm)	—	—	29.30	—	—
Blade Width (mm)	21.03	—	25.44	—	—
Lateral Edge (left)	Indeterminate	—	Excurvate	—	Straight
Lateral Edge (right)	Indeterminate	—	Excurvate	—	Straight
Shoulder Width (mm)	21.03	—	25.29	—	—
Notch Depth, left (mm)	0.83	—	5.58	—	—
Notch Depth, right (mm)	1.50	—	6.47	—	—
Notch Width, left (mm)	6.09	—	5.60	—	—
Notch Width, right (mm)	6.19	—	3.50	—	—
Ear Angle (left)	138	—	53	—	—
Ear Angle (right)	99	—	41	—	—
Stem Shape	Curved	Expanding	Expanding	Expanding	—
Stem Length (mm)	5.91	13.17	9.74	17.55	—
Stem Distal Width (mm)	10.21	12.55	12.49	13.68	—
Stem Proximal Width (mm)	8.77	15.99	20.25	20.43	—
Stem Thickness (mm)	4.98	4.77	4.62	6.56	—
Basal Shape	Excurvate	Straight	Excurvate	Excurvate	—
Basal Depth (mm)	—	—	—	—	—
Basal Notch Width (mm)	—	—	—	—	—
Form Completeness	Proximal-Medial	Stem	Complete	Stem	Distal

Landis Property: Data Recovery at 41PT185, 41PT186, and 41PT245, Potter County, Texas
Bureau of Land Management

Break Type	Use	Use	Unbroken	Use	Use
% of Cortex Remaining	0%	0%	0%	0%	0%
Thermal Alteration	Not Observed	Not Observed	Not Observed	Not Observed	Not Observed
Basal Grinding	Light	Light	Light	Light	—
Stem Grinding	Light	Light	Light	Light	—

Table Q-1. continued

PNUM	N/A
Unit	Site Surface
Depth	Surface
Raw Material Type	Agatized Dolomite
Raw Material Source	Alibates
Max Length (mm)	35.00
Max Width (mm)	23.00
Max Thickness (mm)	5.70
Weight (g)	3.8
Long Cross-section	Tapered Base
Transverse Cross-section	Bi-Convex (Asymmetrical)
Preform	Indeterminate
Shape	Triangular
Tool Class	Bifacial
Degree of Flaking	Complete
Cultural Period	Late Archaic
Flaking Pattern	Random Subparallel
Lateral Edge Angle (left)	60
Lateral Edge Angle (right)	55
Blade Length (mm)	28.00
Blade Width (mm)	23.00
Lateral Edge (left)	Straight
Lateral Edge (right)	Straight
Shoulder Width (mm)	23.00
Notch Depth, left (mm)	2.75
Notch Depth, right (mm)	—
Notch Width, left (mm)	5.07
Notch Width, right (mm)	—
Ear Angle (left)	60
Ear Angle (right)	—
Stem Shape	Expanding
Stem Length (mm)	8.03
Stem Distal Width (mm)	14.73
Stem Proximal Width (mm)	16.97
Stem Thickness (mm)	4.05
Basal Shape	Excurvate
Basal Depth (mm)	—
Basal Notch Width (mm)	—
Form Completeness	Complete

Break Type	Indeterminate
% of Cortex Remaining	0%
Thermal Alteration	Not Observed
Basal Grinding	None
Stem Grinding	None

Table Q-2. 41PT185 Bifaces

Provenience Number	#156-011	#159-010	#317-010	#347-010	#420-010
Unit	TU 15	TU 15	N101 E108	N102 E103	N103 E106
Depth (cmbs)	68-71	92	64-65	50-60	60-70
Raw Material Type	Agatized Dolomite	Quartzite	Agatized Dolomite	Agatized Dolomite	Quartzite
Raw Material Source	Alibates	Ogallala Gravels (Potter)	Alibates	Alibates	Ogallala Gravels (Potter)
Max Length (mm)	35.40	28.60	31.80	15.51	79.00
Max Width (mm)	27.10	38.20	26.50	20.60	46.70
Max Thickness	5.50	6.50	5.50	7.71	10.20
Weight (g)	5.5	8.6	4.6	2.9	44.4
Size Grade	>2.54 cm	>2.54 cm	>2.54 cm	<1.27 to >0.635 cm	>2.54 cm
Biface Stage	Late	Indeterminate	Late	Indeterminate	Early
Long Cross-section	Indeterminate	Indeterminate	Wedged Base/Flat	Indeterminate	Tapered Base/Tip
Transverse Cross-section	Plano-Convex	Indeterminate	Bi-Convex (Symmetrical)	Indeterminate	Plano-Convex
Degree of Flaking	Complete	Complete	Complete	Marginal	Complete
Flaking Pattern	Random Subparallel	Random Subparallel	Random Subparallel	Random Subparallel	Random Subparallel
Lateral Edge Angle (left)	60	55	40	68	68
Lateral Edge Angle (right)	55	50	35	—	50
Lateral Edge (left)	Straight	Excurvate	Straight	Indeterminate	Excurvate
Lateral Edge (right)	Straight	Excurvate	Straight	Indeterminate	Excurvate
% Cortex Remaining	0%	0%	0%	0%	0%
Cortical Type	Indeterminate	Indeterminate	Indeterminate	Indeterminate	Indeterminate
Tool Shape	Indeterminate	Indeterminate	Quadrilateral	Indeterminate	Teardrop
Flaked Edge Length, left (mm)	36.00	28.50	23.91	16.75	75.84
Flaked Edge Length, right (mm)	736.80	25.10	22.40	—	74.10
Flaked Edge Width, left (mm)	7.20	6.40	8.10	7.24	11.01
Flaked Edge Width, right (mm)	5.40	4.90	5.20	—	9.90
Form Completeness	Distal-Medial	Proximal	Proximal-Medial	Fragment	Proximal-Medial
Break Type	Indeterminate	Indeterminate	Indeterminate	Indeterminate	Indeterminate
Thermal Alteration	Not Observed	Not Observed	Not Observed	Not Observed	Not Observed

Table Q-2. continued

Provenience Number	#494-010	#609-010	#651-010	#653-011	#653-010
Unit	N104 E115	N107 E101	N108 E112	N108 E114	N108 E114
Depth (cmbs)	50-60	61.5	90-100	62-80	62-80
Raw Material Type	Agatized Dolomite	Agatized Dolomite	Agatized Dolomite	Quartzite	Quartzite
Raw Material Source	Alibates	Alibates	Alibates	Ogallala Gravels (Potter)	Ogallala Gravels (Potter)
Max Length (mm)	52.00	59.30	5.60	38.10	22.00
Max Width (mm)	35.00	28.90	15.00	46.90	34.00
Max Thickness	14.00	7.40	6.20	8.00	7.30
Weight (g)	26.3	15.1	0.5	14.0	4.7
Size Grade	>2.54 cm	>2.54 cm	<0.635 cm	>2.54 cm	>2.54 cm
Biface Stage	Late	Late	Indeterminate	Indeterminate	Indeterminate
Long Cross-section	Tapered Base/Tip	Wedged Base/Flat	Indeterminate	Indeterminate	Indeterminate
Transverse Cross-section	Bi-Convex (Asymmetrical)	Plano-Convex	Indeterminate	Bi-Convex (Symmetrical)	Indeterminate
Degree of Flaking	Complete	Complete	Complete	Complete	Complete
Flaking Pattern	Random Subparallel	Random Subparallel	Random Subparallel	Random Subparallel	Random Subparallel
Lateral Edge Angle (left)	55	45	—	55	55
Lateral Edge Angle (right)	60	50	62	50	55
Lateral Edge (left)	Excurvate	Excurvate	Indeterminate	Excurvate	Straight
Lateral Edge (right)	Excurvate	Excurvate	Indeterminate	Excurvate	Straight
% Cortex Remaining	0%	0%	0%	0%	0%
Cortical Type	Indeterminate	Indeterminate	Indeterminate	Indeterminate	Indeterminate
Tool Shape	Ovate	Lanceolate	Indeterminate	Indeterminate	Indeterminate
Flaked Edge Length, left (mm)	47.40	58.30	—	42.43	29.20
Flaked Edge Length, right (mm)	48.90	41.30	7.01	38.46	23.60
Flaked Edge Width, left (mm)	9.50	9.90	—	9.80	9.65
Flaked Edge Width, right (mm)	10.90	7.09	5.56	8.66	4.60
Form Completeness	Complete	Proximal-Medial	Fragment	Distal	Distal
Break Type	Unbroken	Use	Indeterminate	Indeterminate	Indeterminate
Thermal Alteration	Not Observed	Not Observed	Not Observed	Not Observed	Not Observed

Table Q-2. continued

Provenience Number	#737-010	#785-010	#800-010	#868-010	#967-010
Unit	N111 E102	N112 E102	N112 E105	N114 E98	N116 E98
Depth (cmbs)	40-50	37-50	60-70	60-70	50-60
Raw Material Type	Agatized Dolomite	Agatized Dolomite	Agatized Dolomite	Agatized Dolomite	Agatized Dolomite
Raw Material Source	Alibates	Alibates	Alibates	Alibates	Alibates
Max Length (mm)	29.49	58.30	23.67	39.93	42.40
Max Width (mm)	10.81	36.20	22.48	23.19	31.30
Max Thickness	2.79	19.00	8.20	6.60	7.80
Weight (g)	0.6	37.7	5.9	7.2	8.2
Size Grade	<1.27 to >0.635 cm	>2.54 cm	<2.54 to >1.905 cm	>2.54 cm	>2.54 cm
Biface Stage	Indeterminate	Early	Middle	Early	Indeterminate
Long Cross-section	Indeterminate	Tapered Base/Tip	Indeterminate	Tapered Base/Tip	Tapered Base/Tip
Transverse Cross-section	Indeterminate	Plano-Convex	Bi-Convex (Asymmetrical)	Plano-Convex	Plano-Convex
Degree of Flaking	Complete	Complete	Complete	Marginal	Complete
Flaking Pattern	Random Subparallel	Random Subparallel	Random Subparallel	Random Subparallel	Random Subparallel
Lateral Edge Angle (left)	50	70	75	50	60
Lateral Edge Angle (right)	—	65	75	48	40
Lateral Edge (left)	Excurvate	Excurvate	Incurvate	Excurvate	Excurvate
Lateral Edge (right)	Indeterminate	Excurvate	Excurvate	Excurvate	Excurvate
% Cortex Remaining	0%	0%	0%	0%	0%
Cortical Type	Indeterminate	Indeterminate	Indeterminate	Indeterminate	Indeterminate
Tool Shape	Indeterminate	Ovate	Indeterminate	Ovate	Teardrop
Flaked Edge Length, left (mm)	29.42	58.00	23.80	36.55	41.80
Flaked Edge Length, right (mm)	—	54.40	22.60	37.11	36.50
Flaked Edge Width, left (mm)	7.23	12.50	9.05	5.80	8.60
Flaked Edge Width, right (mm)	—	13.70	4.60	7.10	4.90
Form Completeness	Fragment	Complete	Proximal-Medial	Complete	Complete
Break Type	Indeterminate	Unbroken	Indeterminate	Unbroken	Unbroken
Thermal Alteration	Not Observed	Not Observed	Not Observed	Not Observed	Indeterminate

Table Q-2. continued

Provenience Number	#1038-010	#1064-010	#1085-010	#1107-010	#1163-010
Unit	N117 E99	N117 E106	N118 E96	N118 E101	N119 E99
Depth (cmbs)	30-40	46	45-60	60-70	50-60
Raw Material Type	Jasper	Unidentified Sedimentary	Agatized Dolomite	Chalcedony	Agatized Dolomite
Raw Material Source	Tecovas Formation (cherts and jaspers)	Unidentifiable	Alibates	Unidentifiable	Alibates
Max Length (mm)	29.86	98.90	39.70	15.30	41.40
Max Width (mm)	15.13	30.60	16.80	32.10	30.00
Max Thickness	6.85	7.90	6.80	7.20	8.50
Weight (g)	2.5	27.8	2.9	4.2	12.9
Size Grade	>2.54 cm	>2.54 cm	>2.54 cm	>2.54 cm	>2.54 cm
Biface Stage	Indeterminate	Late	Indeterminate	Middle	Indeterminate
Long Cross-section	Indeterminate	Tapered Base/Tip	Indeterminate	Indeterminate	Wedged Base/Flat
Transverse Cross-section	Indeterminate	Bi-Convex (Symmetrical)	Indeterminate	Plano-Convex	Plano-Convex
Degree of Flaking	Complete	Complete	Complete	Complete	Complete
Flaking Pattern	Random Subparallel	Random Subparallel	Random Subparallel	Random Subparallel	Random Subparallel
Lateral Edge Angle (left)	—	60	45	65	65
Lateral Edge Angle (right)	65	60	—	70	65
Lateral Edge (left)	Indeterminate	Excurvate	Excurvate	Straight	Excurvate
Lateral Edge (right)	Indeterminate	Excurvate	Indeterminate	Straight	Excurvate
% Cortex Remaining	0%	0%	0%	1-25%	0%
Cortical Type	Indeterminate	Indeterminate	Indeterminate	Indeterminate	Indeterminate
Tool Shape	Indeterminate	Teardrop	Indeterminate	Indeterminate	Indeterminate
Flaked Edge Length, left (mm)	—	97.20	37.90	15.70	41.26
Flaked Edge Length, right (mm)	9.80	95.09	—	8.20	39.10
Flaked Edge Width, left (mm)	—	7.90	4.40	7.22	6.60
Flaked Edge Width, right (mm)	9.00	7.40	—	1.70	5.20
Form Completeness	Fragment	Complete	Fragment	Medial	Proximal-Medial
Break Type	Indeterminate	Unbroken	Indeterminate	Indeterminate	Indeterminate
Thermal Alteration	Not Observed	Not Observed	Not Observed	Not Observed	Not Observed

Table Q-2. continued

Provenience Number	#1184-010	#1206-010	#1212-010	#1220-011
Unit	N119 E105	N120 E95	N120 E97	N120 E99
Depth (cmts)	29-43	50-60	54-60	37
Raw Material Type	Agatized Dolomite	Jasper	Quartzite	Agatized Dolomite
Raw Material Source	Alibates	Tecovas Formation (cherts and jaspers)	Dakota	Alibates
Max Length (mm)	24.25	17.30	52.40	41.10
Max Width (mm)	4.30	11.78	24.00	31.90
Max Thickness	3.51	4.56	10.20	8.40
Weight (g)	0.3	1.8	10.5	13.5
Size Grade	<2.54 to >1.905 cm	<1.905 to >1.27 cm	>2.54 cm	>2.54 cm
Biface Stage	Indeterminate	Indeterminate	Early	Indeterminate
Long Cross-section	Indeterminate	Indeterminate	Tapered Base/Tip	Wedged Base/Thick
Transverse Cross-section	Indeterminate	Indeterminate	Bi-Convex (Asymmetrical)	Bi-Convex (Asymmetrical)
Degree of Flaking	Complete	Complete	Complete	Complete
Flaking Pattern	Random Subparallel	Random Subparallel	Random Subparallel	Random Subparallel
Lateral Edge Angle (left)	50	—	65	60
Lateral Edge Angle (right)	—	58	70	65
Lateral Edge (left)	Excurvate	Indeterminate	Excurvate	Excurvate
Lateral Edge (right)	Indeterminate	Excurvate	Excurvate	Excurvate
% Cortex Remaining	0%	0%	0%	0%
Cortical Type	Indeterminate	Indeterminate	Indeterminate	Indeterminate
Tool Shape	Indeterminate	Indeterminate	Teardrop	Irregular
Flaked Edge Length, left (mm)	24.25	—	48.80	33.60
Flaked Edge Length, right (mm)	—	16.50	52.10	38.10
Flaked Edge Width, left (mm)	4.30	—	4.90	6.50
Flaked Edge Width, right (mm)	—	7.50	5.60	5.48
Form Completeness	Fragment	Fragment	Complete	Proximal-Medial
Break Type	Indeterminate	Indeterminate	Indeterminate	Indeterminate
Thermal Alteration	Not Observed	Not Observed	Not Observed	Not Observed

Table Q-3. 41PT185 Scrapers

Provenience Number	#332-010	#402-010	#452-010	#767-010	#1091-010
Unit	N101 E117	N103 E103	N104 E101	N111 E116	N118 E97
Depth	90-100	70-80	70-80	80-90	70-80
Raw Material Type	Jasper	Agatized Dolomite	Agatized Dolomite	Agatized Dolomite	Agatized Dolomite
Raw Material Source	Tecovas Formation (cherts and jaspers)	Alibates	Alibates	Alibates	Alibates
Max Length (mm)	44.35	37.06	54.41	38.98	24.41
Max Width (mm)	29.81	27.68	46.76	33.42	16.91
Max Thickness (mm)	6.18	8.72	12.80	9.74	6.29
Weight (g)	8.2	8.6	26.2	13.7	4.3
Size Grade	>2.54 cm	>2.54 cm	>2.54 cm	>2.54 cm	<2.54 to >1.905 cm
Long Cross-section	Flat	Bi-Wedge	Flat	Bi-Wedge	Indeterminate
Transverse Cross-section	Plano-Convex	Plano-Convex	Plano-Convex	Plano-Convex	Indeterminate
% of Cortex Remaining	0%	0%	0%	0%	0%
Cortical Type	Indeterminate	Indeterminate	Indeterminate	Indeterminate	Indeterminate
Tool Shape	Irregular	Teardrop	Irregular	Round	Indeterminate
Flaked Edge Length, left (mm)	—	34.40	54.60	23.40	23.30
Flaked Edge Length, right (mm)	42.30	35.70	37.90	32.20	—
Flaked Edge Length, distal (mm)	—	24.50	—	25.10	—
Flaked Edge Width, left (mm)	—	5.80	7.80	3.60	0.60
Flaked Edge Width, right (mm)	2.30	6.10	6.50	7.10	—
Flaked Edge Width, distal (mm)	—	5.10	—	2.80	—
Distal Edge Angle	80	70	65	70	—
Lateral Edge Angle (left)	60	65	60	60	50
Lateral Edge Angle (right)	65	65	50	60	—
Lateral Edge (left)	Incurvate	Straight	Incurvate	Excurvate	Excurvate
Lateral Edge (right)	Recurvate	Straight	Excurvate	Excurvate	Indeterminate
Edge Worked	Lateral - Right	Distal; Lateral - Right & Left	Distal; Lateral - Right & Left	Distal; Lateral - Right & Left	Lateral - Left
Form Completeness	Complete	Complete	Complete	Complete	Proximal-Medial
Break Type	Unbroken	Unbroken	Unbroken	Unbroken	Indeterminate
Thermal Alteration	Not Observed	Not Observed	Not Observed	Not Observed	Not Observed
Platform	Multi-Faceted	Flat	Multi-Faceted	Multi-Faceted	Multi-Faceted
Reduction Technique	Soft Hammer	Soft Hammer	Soft Hammer	Soft Hammer	Soft Hammer

Table Q-3. continued

Provenience Number	#1128-010	#1221-011	#1228-010	#1269-010
Unit	N118 E105	N120 E99	N120 E102	N121 E98
Depth	50-60	55	28-40	70-80
Raw Material Type	Agatized Dolomite	Agatized Dolomite	Agatized Dolomite	Agatized Dolomite
Raw Material Source	Alibates	Alibates	Alibates	Alibates
Max Length (mm)	53.77	49.92	44.95	22.65
Max Width (mm)	34.24	75.43	23.81	26.41
Max Thickness (mm)	19.79	25.07	11.09	6.72
Weight (g)	34.3	65.7	10.2	4.0
Size Grade	>2.54 cm	>2.54 cm	>2.54 cm	<2.54 to >1.905 cm
Long Cross-section	Wedged Base/Thick	Tapered Base/Tip	Bi-Wedge	Indeterminate
Transverse Cross-section	Plano-Convex	Plano-Convex	Plano-Convex	Plano-Convex
% of Cortex Remaining	0%	0%	0%	0%
Cortical Type	Indeterminate	Indeterminate	Indeterminate	Indeterminate
Tool Shape	Irregular	Irregular	Irregular	Indeterminate
Flaked Edge Length, left (mm)	31.10	—	30.10	22.30
Flaked Edge Length, right (mm)	31.69	—	22.10	23.70
Flaked Edge Length, distal (mm)	—	73.40	13.10	—
Flaked Edge Width, left (mm)	9.90	—	4.20	1.40
Flaked Edge Width, right (mm)	10.02	—	2.30	2.80
Flaked Edge Width, distal (mm)	—	14.10	4.80	—
Distal Edge Angle	75	60	50	—
Lateral Edge Angle (left)	70	80	50	50
Lateral Edge Angle (right)	70	60	60	60
Lateral Edge (left)	Recurvate	Straight	Excurvate	Excurvate
Lateral Edge (right)	Recurvate	Excurvate	Recurvate	Excurvate
Edge Worked	Lateral - Right	Distal	Distal; Lateral - Right & Left	Lateral - Right & Left
Form Completeness	Complete	Complete	Distal-Medial	Proximal-Medial
Break Type	None	Unbroken	Indeterminate	Indeterminate
Thermal Alteration	Not Observed	Not Observed	Indeterminate	Not Observed
Platform	Crushed	Crushed	None	Indeterminate
Reduction Technique	Hard Hammer	Hard Hammer	Pressure	Soft Hammer

Table Q-4. 41PT185 Edge-Modified Flakes

Provenience Number	#115-010	#152-010	#171-010	#173-010	#190-010	#199-010
Unit	TU 9	TU 15	TU 17	TU 17	TU 20	TU 20
Depth (cmbs)	20-30	20-30	10-20	30-40	10-20	90-100
Raw Material Type	Jasper	Agatized Dolomite	Agatized Dolomite	Agatized Dolomite	Agatized Dolomite	Agatized Dolomite
Raw Material Source	Tecovas Formation (cherts and jaspers)	Alibates	Alibates	Alibates	Alibates	Alibates
Max Length (mm)	24.80	19.80	44.60	41.40	9.50	28.10
Max Width (mm)	15.00	17.60	30.70	35.60	9.30	30.20
Max Thickness	8.30	4.40	6.80	11.80	1.40	4.70
Weight (g)	2.4	1.4	9.4	11.6	0.1	3.6
Size Grade	<2.54 to >1.905 cm	<1.905 to >1.27 cm	>2.54 cm	>2.54 cm	<0.635 cm	>2.54 cm
% of Cortex Remaining	0%	0%	0%	0%	0%	0%
Cortical Type	None	None	None	None	None	None
Tool Shape	Indeterminate	Indeterminate	Irregular	Irregular	Irregular	Indeterminate
Flaking Locus	Indeterminate	Distal/Lateral	Lateral Only	Distal	Distal	Lateral Only
Flaked Edge Angle (left)	55	55	60	55	45	55
Flaked Edge Angle (right)	—	60	65	—	—	
Flaked Edge Length, left (mm)	25.0	9.3	41.7	17.73	7.7	22.4
Flaked Edge Length, right (mm)	—	14.2	34.8	—	—	
Flaked Edge Width, left (mm)	5.3	2.8	7.4	2.15	0.78	2.2
Flaked Edge Width, right (mm)	—	2.1	9.5	—	—	—
Form Completeness	Fragment	Distal	Proximal-Medial	Distal-Medial	Complete	Medial
Break Type	Indeterminate	Indeterminate	Indeterminate	Indeterminate	Unbroken	Indeterminate
Thermal Alteration	Not Observed	Not Observed	Not Observed	Not Observed	Not Observed	Not Observed
Platform Type	None	None	Multi-Faceted	None	Crushed	None
Reduction Technique	None	None	Soft Hammer	None	Soft Hammer	None

Table Q-4. continued

Provenience Number	#206-010	#219-010	#242-010	#273-010	#312-010	#316-010
Unit	TU 22	TU 24	TU 27	N100 E102	N101 E107	N101 E108
Depth (cmbs)	30-40	50-60	60-70	60-70	50-60	50-60
Raw Material Type	Agatized Dolomite	Unidentified Sedimentary	Agatized Dolomite	Agatized Dolomite	Agatized Dolomite	Agatized Dolomite
Raw Material Source	Alibates	Unidentifiable	Alibates	Alibates	Alibates	Alibates
Max Length (mm)	13.00	31.40	41.60	39.00	44.70	12.00
Max Width (mm)	8.90	27.10	40.80	16.70	48.30	14.50
Max Thickness	2.20	10.40	11.20	6.70	17.90	3.80
Weight (g)	0.2	7.7	16.2	3.0	41.9	0.6
Size Grade	<0.635 cm	>2.54 cm	>2.54 cm	>2.54 cm	>2.54 cm	<1.27 to >0.635 cm
% of Cortex Remaining	0%	0%	0%	0%	0%	0%
Cortical Type	None	None	None	None	None	None
Tool Shape	Indeterminate	Irregular	Indeterminate	Irregular	Irregular	Indeterminate
Flaking Locus	Lateral Only	Distal	Proximal/Lateral	Lateral Only	Distal/Lateral	Lateral Only
Flaked Edge Angle (left)		55	65	60	65	65
Flaked Edge Angle (right)	70		65		60	
Flaked Edge Length, left (mm)		23.2	42.8	20.7	19.20	10.5
Flaked Edge Length, right (mm)	1.1		34.2		43.10	
Flaked Edge Width, left (mm)		10.9	3.5	1.6	2.50	1.5
Flaked Edge Width, right (mm)	0.70		2.0		2.60	
Form Completeness	Distal	Distal	Proximal-Medial	Medial	Proximal-Medial	Proximal
Break Type	Indeterminate	Indeterminate	Indeterminate	Indeterminate	Indeterminate	Indeterminate
Thermal Alteration	Not Observed	Not Observed	Not Observed	Not Observed	Observed	Not Observed
Platform Type	None	None	Flat	None	Multi-Faceted	Multi-Faceted
Reduction Technique	None	None	Soft Hammer	None	Hard Hammer	Soft Hammer

Table Q-4. continued

Provenience Number	#323-010	#346-010a	#356-010	#412-010	#446-010
Unit	N101 E109	N102 E103	N102 E104	N103 E105	N103 E117
Depth (cmbs)	80-90	40-50	60-70	53-60	55
Raw Material Type	Agatized Dolomite	Agatized Dolomite	Agatized Dolomite	Agatized Dolomite	Agatized Dolomite
Raw Material Source	Alibates	Alibates	Alibates	Alibates	Alibates
Max Length (mm)	44.00	20.00	25.00	13.90	70.30
Max Width (mm)	42.80	23.80	13.50	10.40	47.00
Max Thickness	04.00	4.60	4.50	3.40	24.30
Weight (g)	6.6	3.5	1.1	0.4	61.6
Size Grade	>2.54 cm	<2.54 to >1.905 cm	<1.905 to >1.27 cm	<1.27 to >0.635 cm	>2.54 cm
% of Cortex Remaining	0%	0%	0%	0%	0%
Cortical Type	None	None	None	None	None
Tool Shape	Irregular	Indeterminate	Indeterminate	Indeterminate	Irregular
Flaking Locus	Distal	Lateral Only	Indeterminate	Indeterminate	Lateral Only
Flaked Edge Angle (left)	70	60	62	50	68
Flaked Edge Angle (right)	—				
Flaked Edge Length, left (mm)	32.8	17	17.3	16.9	42.6
Flaked Edge Length, right (mm)	—				
Flaked Edge Width, left (mm)	0.5	2.32	0.5	5.5	3.1
Flaked Edge Width, right (mm)	—				
Form Completeness	Complete	Medial	Fragment	Fragment	Proximal-Medial
Break Type	Unbroken	Indeterminate	Indeterminate	Indeterminate	Indeterminate
Thermal Alteration	Not Observed	Not Observed	Not Observed	Not Observed	Not Observed
Platform Type	Multi-Faceted	None	None	None	Abraded
Reduction Technique	Soft Hammer	None	None	None	Soft Hammer

Table Q-4. continued

Provenience Number	#456-010	#493-010	#517-010	#522-010	#575-010
Unit	N104 E102	N104 E115	N105 E99	N105 E101	N106 E101
Depth (cmbs)	60-70	40-50	79	37-50	60-70
Raw Material Type	Agatized Dolomite	Quartzite	Agatized Dolomite	Agatized Dolomite	Agatized Dolomite
Raw Material Source	Alibates	Dakota	Alibates	Alibates	Alibates
Max Length (mm)	15.70	96.60	57.30	14.00	28.80
Max Width (mm)	16.80	57.50	21.60	13.00	20.30
Max Thickness	3.90	25.40	5.60	7.60	3.20
Weight (g)	1.0	131.0	6.5	2.9	1.9
Size Grade	<1.27 to >0.635 cm	>2.54 cm	>2.54 cm	<2.54 to >1.905 cm	<1.905 to >1.27 cm
% of Cortex Remaining	0%	76 - 100%	0%	0%	0%
Cortical Type	None	Nodular	None	None	None
Tool Shape	Indeterminate	Irregular	Irregular	Indeterminate	Ovate
Flaking Locus	Indeterminate	Lateral Only	Lateral Only	Indeterminate	Lateral Only
Flaked Edge Angle (left)	50	75	55	45	45
Flaked Edge Angle (right)					55
Flaked Edge Length, left (mm)	10.4	58.5	25.3		28.7
Flaked Edge Length, right (mm)					9.9
Flaked Edge Width, left (mm)	1.2	14	1.7	1.68	0.7
Flaked Edge Width, right (mm)					1.1
Form Completeness	Fragment	Complete	Medial	Fragment	Proximal-Medial
Break Type	Indeterminate	Unbroken	Indeterminate	Indeterminate	Indeterminate
Thermal Alteration	Not Observed	Not Observed	Not Observed	Not Observed	Not Observed
Platform Type	None	Flat	None	None	Multi-Faceted
Reduction Technique	None	Hard Hammer	Soft Hammer	None	Soft Hammer

Table Q-4. continued

Provenience Number	#585-010	#588-010	#595-010	#621-010a	#678-010
Unit	N106 E104	N106 E104	N106 E107	N107 E104	N109 E106
Depth (cmbs)	39-50	70-80	35-50	60-70	50-60
Raw Material Type	Agatized Dolomite	Agatized Dolomite	Agatized Dolomite	Agatized Dolomite	Agatized Dolomite
Raw Material Source	Alibates	Alibates	Alibates	Alibates	Alibates
Max Length (mm)	16.70	37.80	18.40	—	9.62
Max Width (mm)	20.00	31.30	26.60	9.7	11.60
Max Thickness	3.70	10.30	5.30	3.2	1.80
Weight (g)	0.7	13.5	2.6	1.5	0.1
Size Grade	<1.27 to >0.635 cm	>2.54 cm	<1.905 to >1.27 cm	—	<1.27 to >0.635 cm
% of Cortex Remaining	0%	0%	0%	0%	0%
Cortical Type	None	None	None	None	None
Tool Shape	Indeterminate	Irregular	Indeterminate	Indeterminate	Irregular
Flaking Locus	Indeterminate	Lateral Only	Distal	Indeterminate	Indeterminate
Flaked Edge Angle (left)	65	60	40	60	65
Flaked Edge Angle (right)		65		—	
Flaked Edge Length, left (mm)	16.2	26.5	12.3	—	8.1
Flaked Edge Length, right (mm)		32.7		—	
Flaked Edge Width, left (mm)	1.2	4.5	2.3	—	0.9
Flaked Edge Width, right (mm)		3.8		—	
Form Completeness	Fragment	Medial	Fragment	Medial	Fragment
Break Type	Indeterminate	Indeterminate	Indeterminate	Indeterminate	Indeterminate
Thermal Alteration	Not Observed	Not Observed	Not Observed	Not Observed	Not Observed
Platform Type	None	None	None	None	None
Reduction Technique	None	None	None	None	None

Table Q-4. continued

Provenience Number	#686-010	#696-010	#724-010	#724-011	#750-010
Unit	N110 E99	N110 E102	N111 E98	N111 E98	N111 E103
Depth (cmbs)	70-80	60-70	80-90	80-90	40-50
Raw Material Type	Agatized Dolomite	Jasper	Agatized Dolomite	Jasper	Agatized Dolomite
Raw Material Source	Alibates	Tecovas Formation (cherts and jaspers)	Alibates	Tecovas Formation (cherts and jaspers)	Alibates
Max Length (mm)	12.30	20.30	28.20	32.90	17.20
Max Width (mm)	12.00	13.00	16.50	26.40	24.10
Max Thickness	5.40	1.90	4.10	7.20	5.30
Weight (g)	1.2	0.6	1.8	6.7	2.2
Size Grade	<1.27 to >0.635 cm	<1.27 to >0.635 cm	<1.905 to >1.27 cm	>2.54 cm	<2.54 to >1.905 cm
% of Cortex Remaining	0%	0%	0%	0%	0%
Cortical Type	None	None	None	None	None
Tool Shape	Indeterminate	Indeterminate	Indeterminate	Irregular	Irregular
Flaking Locus	Indeterminate	Distal/Lateral	Lateral Only	Lateral Only	Proximal/Lateral
Flaked Edge Angle (left)	58	63	40	65	55
Flaked Edge Angle (right)			40		
Flaked Edge Length, left (mm)	8.3	20.2	12.7	28.5	20.8
Flaked Edge Length, right (mm)			10.9		
Flaked Edge Width, left (mm)	2.6	1.4	1.1	4.5	1.4
Flaked Edge Width, right (mm)			1		
Form Completeness	Fragment	Distal-Medial	Proximal-Medial	Proximal-Medial	Proximal-Medial
Break Type	Indeterminate	Indeterminate	Indeterminate	Indeterminate	Indeterminate
Thermal Alteration	Observed	Not Observed	Not Observed	Not Observed	Observed
Platform Type	None	None	Multi-Faceted	Multi-Faceted	Flat
Reduction Technique	None	None	Soft Hammer	Soft Hammer	Soft Hammer

Table Q-4. continued

Provenience Number	#754-010	#764-010	#787-010	#802-010	#821-010	#836-010a
Unit	N111 E104	N111 E106	N112 E102	N112 E105	N113 E98	N113 E102
Depth (cmbs)	40-50	60-70	60-70	70-80	50-60	50-60
Raw Material Type	Agatized Dolomite	Jasper	Agatized Dolomite	Agatized Dolomite	Agatized Dolomite	Unidentified Sedimentary
Raw Material Source	Alibates	Tecovas Formation (cherts and jaspers)	Alibates	Alibates	Alibates	Unidentifiable
Max Length (mm)	16.90	15.70	29.10	—	25.20	—
Max Width (mm)	5.90	16.80	26.50	—	19.80	—
Max Thickness	1.90	3.00	4.80	2.70	2.90	6.7
Weight (g)	0.2	0.6	5.8	1.7	1.7	2.6
Size Grade	<0.635 cm	<1.27 to >0.635 cm	>2.54 cm	>2.54 cm	<2.54 to >1.905 cm	—
% of Cortex Remaining	0%	0%	0%	0%	0%	0%
Cortical Type	None	None	None	None	None	None
Tool Shape	Indeterminate	Indeterminate	Indeterminate	Indeterminate	Indeterminate	Indeterminate
Flaking Locus	Indeterminate	Indeterminate	Indeterminate	Indeterminate	Indeterminate	Lateral Only
Flaked Edge Angle (left)	45	60	60	32	35	65
Flaked Edge Angle (right)				—		—
Flaked Edge Length, left (mm)	9.3	15.4	23.5	—	24.4	—
Flaked Edge Length, right (mm)				—		—
Flaked Edge Width, left (mm)	1	1.3	4.5	—	7.3	—
Flaked Edge Width, right (mm)				—		—
Form Completeness	Fragment	Fragment	Fragment	Fragment	Fragment	Medial
Break Type	Indeterminate	Indeterminate	Indeterminate	Indeterminate	Indeterminate	Indeterminate
Thermal Alteration	Not Observed	Not Observed	Not Observed	Not Observed	Not Observed	Not Observed
Platform Type	None	None	None	None	None	None
Reduction Technique	None	None	None	None	None	None

Table Q-4. continued

Provenience Number	#848-010	#916-010a	#942-010	#956-010	#957-010
Unit	N113 E105	N115 E97	N115 E105	N116 E96	N116 E96
Depth (cmbs)	60-70	60-70	38	40-50	50-60
Raw Material Type	Quartzite	Jasper	Unidentified Sedimentary	Jasper	Agatized Dolomite
Raw Material Source	Dakota	Tecovas Formation (cherts and jaspers)	Unidentifiable	Tecovas Formation (cherts and jaspers)	Alibates
Max Length (mm)	70.30	—	80.10	40.30	28.10
Max Width (mm)	51.90	—	53.40	38.70	32.90
Max Thickness	20.20	5.1	27.30	10.30	4.00
Weight (g)	46.6	2.2	125.0	15.4	3.9
Size Grade	>2.54 cm	—	>2.54 cm	>2.54 cm	>2.54 cm
% of Cortex Remaining	0%	0%	51 - 75%	26 - 50%	0%
Cortical Type	None	None	Nodular	Nodular	None
Tool Shape	Irregular	Indeterminate	Ovate	Irregular	Irregular
Flaking Locus	Lateral Only	Indeterminate	Distal/Lateral	Lateral Only	Lateral Only
Flaked Edge Angle (left)	65	45	50	68	55
Flaked Edge Angle (right)		—			55
Flaked Edge Length, left (mm)	43.9	—	136.2	8.7	12.9
Flaked Edge Length, right (mm)		—			13.8
Flaked Edge Width, left (mm)	6.1	—	20	2	1.1
Flaked Edge Width, right (mm)		—			0.8
Form Completeness	Complete	Medial	Complete	Proximal-Medial	Proximal-Medial
Break Type	Unbroken	Indeterminate	Unbroken	Indeterminate	Indeterminate
Thermal Alteration	Not Observed	Not Observed	Not Observed	Not Observed	Not Observed
Platform Type	Multi-Faceted	None	None	Multi-Faceted	Multi-Faceted
Reduction Technique	Hard Hammer	None	None	Hard Hammer	Soft Hammer

Table Q-4. continued

Provenience Number	#957-011	#958-010	#965-010	#980-010	#981-010	#982-010
Unit	N116 E96	N116 E96	N116 E98	N116 E102	N116 E102	N116 E103
Depth (cmbs)	50-60	60-70	30-40	40-50	50-60	32-40
Raw Material Type	Agatized Dolomite	Agatized Dolomite	Agatized Dolomite	Agatized Dolomite	Jasper	Agatized Dolomite
Raw Material Source	Alibates	Alibates	Alibates	Alibates	Tecovas Formation (cherts and jaspers)	Alibates
Max Length (mm)	24.40	29.80	26.00	45.70	32.70	21.40
Max Width (mm)	17.30	26.60	28.00	3.27	25.50	12.00
Max Thickness	4.70	5.20	7.20	9.80	7.60	6.80
Weight (g)	1.4	5.0	3.3	13.3	5.7	0.9
Size Grade	<2.54 to >1.905 cm	>2.54 cm	>2.54 cm	>2.54 cm	>2.54 cm	<1.27 to >0.635 cm
% of Cortex Remaining	0%	0%	0%	0%	0%	0%
Cortical Type	None	None	None	None	None	None
Tool Shape	Irregular	Indeterminate	Irregular	Irregular	Indeterminate	Irregular
Flaking Locus	Lateral Only	Indeterminate	Distal	Lateral Only	Lateral Only	Indeterminate
Flaked Edge Angle (left)		45	70	65	60	50
Flaked Edge Angle (right)	68			65		
Flaked Edge Length, left (mm)		21.16	8	46.3	21.4	7.8
Flaked Edge Length, right (mm)	12.8			43.4		
Flaked Edge Width, left (mm)		3.1	0.8	5.9	1.7	1.2
Flaked Edge Width, right (mm)	1.1			4		
Form Completeness	Complete	Fragment	Complete	Distal-Medial	Medial	Distal-Medial
Break Type	Unbroken	Indeterminate	Unbroken	Indeterminate	Indeterminate	Indeterminate
Thermal Alteration	Not Observed	Not Observed	Not Observed	Not Observed	Not Observed	Not Observed
Platform Type	Multi-Faceted	None	Crushed	None	None	None
Reduction Technique	Soft Hammer	None	Soft Hammer	None	None	None

Table Q-4. continued

Provenience Number	#983-010	#1022-010	#1065-010	#1083-010	#1085-011
Unit	N116 E103	N117 E96	N117 E106	N118 E95	N118 E96
Depth (cmbs)	40-50	60-70	50-60	60-70	45-60
Raw Material Type	Agatized Dolomite	Agatized Dolomite	Agatized Dolomite	Agatized Dolomite	Agatized Dolomite
Raw Material Source	Alibates	Alibates	Alibates	Alibates	Alibates
Max Length (mm)	20.30	24.60	20.70	13.80	—
Max Width (mm)	18.40	22.80	12.90	8.20	16.40
Max Thickness	4.40	3.60	3.60	2.00	6.00
Weight (g)	1.2	2.1	1.0	0.2	3.4
Size Grade	<1.905 to >1.27 cm	<2.54 to >1.905 cm	<1.27 to >0.635 cmch	<1.27 to >0.635 cm	<1.905 to >1.27 cm
% of Cortex Remaining	0%	0%	0%	0%	0%
Cortical Type	None	None	None	None	None
Tool Shape	Indeterminate	Indeterminate	Indeterminate	Irregular	Quadrilateral
Flaking Locus	Lateral Only	Indeterminate	Lateral Only	Distal	Lateral Only
Flaked Edge Angle (left)	60	50	45	70	45
Flaked Edge Angle (right)	55				45
Flaked Edge Length, left (mm)	9.2		8.6	5.3	—
Flaked Edge Length, right (mm)	9.2				—
Flaked Edge Width, left (mm)	0.6		0.5	0.8	—
Flaked Edge Width, right (mm)	1.1				—
Form Completeness	Medial	Distal	Medial	Complete	Medial
Break Type	Indeterminate	Indeterminate	Indeterminate	Unbroken	Indeterminate
Thermal Alteration	Not Observed	Not Observed	Not Observed	Not Observed	Not Observed
Platform Type	None	None	None	Multi-Faceted	None
Reduction Technique	None	None	None	Soft Hammer	None

Table Q-4. continued

Provenience Number	#1132-010	#1138-011	#1142-010	#1155-010	#1206-011
Unit	N118 E106	N118 E108	N118 E109	N119 E97	N120 E95
Depth (cmbs)	50-60	50-60	50-60	70-80	50-60
Raw Material Type	Agatized Dolomite	Agatized Dolomite	Agatized Dolomite	Agatized Dolomite	Agatized Dolomite
Raw Material Source	Alibates	Alibates	Alibates	Alibates	Alibates
Max Length (mm)	—	10.50	15.20	—	11.40
Max Width (mm)	—	11.10	14.30	31.90	11.70
Max Thickness	11.4	4.80	3.80	11.60	2.00
Weight (g)	3.7	0.3	0.7	10.2	0.2
Size Grade	<1.905 to >1.27 cm	<1.27 to >0.635 cm	<1.27 to >0.635 cm	>2.54 cm	<1.27 to >0.635 cm
% of Cortex Remaining	1 - 25%	0%	0%	0%	0%
Cortical Type	Nodular	None	None	None	None
Tool Shape	Irregular	Indeterminate	Indeterminate	Round	Indeterminate
Flaking Locus	Indeterminate	Indeterminate	Indeterminate	Lateral Only	Indeterminate
Flaked Edge Angle (left)	60	45	60	45	40
Flaked Edge Angle (right)	—			—	
Flaked Edge Length, left (mm)	17.9	4.8	8.7	20	7.3
Flaked Edge Length, right (mm)	—			—	
Flaked Edge Width, left (mm)	4.1	0.6	3.1	2	1.8
Flaked Edge Width, right (mm)	—			—	
Form Completeness	Fragment	Fragment	Fragment	Complete	Fragment
Break Type	Indeterminate	Indeterminate	Indeterminate	Unbroken	Indeterminate
Thermal Alteration	Not Observed	Not Observed	Not Observed	Not Observed	Not Observed
Platform Type	None	None	None	Multi-Faceted	None
Reduction Technique	None	None	None	Soft Hammer	None

Table Q-4. continued

Provenience Number	#1207-010	#1210-010	#1215-010	#1217-010	#1219-010
Unit	N120 E95	N120 E96	N120 E97	N120 E98	N120 E98
Depth (cmbs)	60-70	60-70	80-90	60-70	80-90
Raw Material Type	Agatized Dolomite	Agatized Dolomite	Agatized Dolomite	Agatized Dolomite	Agatized Dolomite
Raw Material Source	Alibates	Alibates	Alibates	Alibates	Alibates
Max Length (mm)	7.90	23.20	14.50	11.10	24.00
Max Width (mm)	13.70	32.50	8.50	9.68	14.90
Max Thickness	1.20	7.60	3.30	2.80	3.00
Weight (g)	0.2	3.5	0.3	0.3	0.9
Size Grade	<1.27 to >0.635 cm	>2.54 cm	<1.27 to >0.635 cm	<1.27 to >0.635 cm	<1.27 to >0.635 cm
% of Cortex Remaining	0%	76 - 100%	0%	0%	0%
Cortical Type	None	Indeterminate	None	None	None
Tool Shape	Irregular	Irregular	Indeterminate	Irregular	Irregular
Flaking Locus	Proximal Only	Distal	Indeterminate	Distal	Lateral Only
Flaked Edge Angle (left)	45	40	80	70	65
Flaked Edge Angle (right)					
Flaked Edge Length, left (mm)	11.5	14.1	5.3	5	11.8
Flaked Edge Length, right (mm)					
Flaked Edge Width, left (mm)	1.7	1.7	2.1	0.6	0.7
Flaked Edge Width, right (mm)					
Form Completeness	Complete	Complete	Fragment	Complete	Distal-Medial
Break Type	Unbroken	Unbroken	Indeterminate	Unbroken	Indeterminate
Thermal Alteration	Not Observed	Not Observed	Not Observed	Not Observed	Not Observed
Platform Type	Multi-Faceted	Flat	None	Multi-Faceted	None
Reduction Technique	Soft Hammer	Soft Hammer	None	Soft Hammer	None

Table Q-4. continued

Provenience Number	#1220-010	#1221-010	#1223-011	#1223-012	#1224-010
Unit	N120 E99	N120 E99	N120 E100	N120 E100	N120 E100
Depth (cmbs)	36-50	55	38-50	38-50	50-60
Raw Material Type	Agatized Dolomite	Jasper	Agatized Dolomite	Agatized Dolomite	Agatized Dolomite
Raw Material Source	Alibates	Tecovas Formation (cherts and jaspers)	Alibates	Alibates	Alibates
Max Length (mm)	25.00	34.40	14.00	13.20	24.10
Max Width (mm)	39.00	47.60	26.30	22.10	24.60
Max Thickness	10.30	13.20	3.80	5.10	7.90
Weight (g)	7.0	20.4	1.1	1.4	3.5
Size Grade	>2.54 cm	>2.54 cm	<1.905 to >1.27 cm	<1.27 to >0.635 cm	>2.54 cm
% of Cortex Remaining	1 - 25%	0%	0%	0%	0%
Cortical Type	Nodular	None	None	None	None
Tool Shape	Irregular	Irregular	Irregular	Indeterminate	Irregular
Flaking Locus	Lateral Only	Lateral Only	Lateral Only	Lateral Only	Lateral Only
Flaked Edge Angle (left)	50	50	60	48	55
Flaked Edge Angle (right)					60
Flaked Edge Length, left (mm)	17.9	13.1	8.4	7.8	5.7
Flaked Edge Length, right (mm)					11.1
Flaked Edge Width, left (mm)	0.7	2.6	1.1	0.8	0.6
Flaked Edge Width, right (mm)					0.8
Form Completeness	Proximal-Medial	Medial	Distal-Medial	Medial	Proximal-Medial
Break Type	Indeterminate	Indeterminate	Indeterminate	Indeterminate	Indeterminate
Thermal Alteration	Not Observed	Not Observed	Not Observed	Not Observed	Not Observed
Platform Type	Cortical	None	None	None	Multi-Faceted
Reduction Technique	Soft Hammer	None	None	None	Soft Hammer

Table Q-4. continued

Provenience Number	#1226-011	#1243-010	#1249-010	#1257-010	#1259-010
Unit	N120 E101	N102 E105	N120 E109	N121 E95	N121 E96
Depth (cmbs)	44-60	50-60	40-50	70-80	51-60
Raw Material Type	Opalite	Agatized Dolomite	Agatized Dolomite	Agatized Dolomite	Agatized Dolomite
Raw Material Source	Unidentifiable	Alibates	Alibates	Alibates	Alibates
Max Length (mm)	9.20	13.30	30.20	22.70	21.00
Max Width (mm)	13.60	14.60	33.50	15.00	14.40
Max Thickness	1.90	3.30	6.50	6.10	2.50
Weight (g)	0.3	1.2	6.6	2.8	0.9
Size Grade	<1.27 to >0.635 cm	<1.27 to >0.635 cm	>2.54 cm	<2.54 to >1.905 cm	<1.905 to >1.27 cm
% of Cortex Remaining	1 - 25%	0%	0%	0%	0%
Cortical Type	Nodular	None	None	None	None
Tool Shape	Irregular	Triangular	Indeterminate	Indeterminate	Irregular
Flaking Locus	Distal	Lateral Only	Indeterminate	Lateral Only	Lateral Only
Flaked Edge Angle (left)	60	48	65	60	55
Flaked Edge Angle (right)					50
Flaked Edge Length, left (mm)	7.7	8.7	26.6	17.6	10.2
Flaked Edge Length, right (mm)					10.1
Flaked Edge Width, left (mm)	0.9	1.1	0.8	1.6	1
Flaked Edge Width, right (mm)					0.9
Form Completeness	Complete	Complete	Fragment	Proximal-Medial	Distal-Medial
Break Type	Unbroken	Unbroken	Indeterminate	Indeterminate	Indeterminate
Thermal Alteration	Not Observed	Not Observed	Not Observed	Not Observed	Not Observed
Platform Type	Multi-Faceted	Multi-Faceted	None	Multi-Faceted	None
Reduction Technique	Soft Hammer	Pressure	None	Soft Hammer	None

Table Q-4. continued

Provenience Number	#1261-010	#1268-010	#1277-010	#1280-010	#1316-010
Unit	N121 E96	N121 E98	N121 E100	N121 E102	N122 E101
Depth (cmbs)	70-80	60-70	60-70	47-60	47-60
Raw Material Type	Agatized Dolomite	Agatized Dolomite	Agatized Dolomite	Agatized Dolomite	Agatized Dolomite
Raw Material Source	Alibates	Alibates	Alibates	Alibates	Alibates
Max Length (mm)	21.80	19.10	13.70	25.00	21.90
Max Width (mm)	18.40	11.30	14.20	11.90	15.70
Max Thickness	2.70	3.50	1.70	3.70	3.10
Weight (g)	1.0	0.7	0.3	0.9	0.7
Size Grade	<2.54 to >1.905 cm	<1.27 to >0.635 cm	<1.27 to >0.635 cm	<1.27 to >0.635 cm	<1.27 to >0.635 cm
% of Cortex Remaining	0%	0%	0%	0%	0%
Cortical Type	None	None	None	None	None
Tool Shape	Irregular	Indeterminate	Indeterminate	Indeterminate	Irregular
Flaking Locus	Lateral Only	Distal	Lateral Only	Indeterminate	Lateral Only
Flaked Edge Angle (left)	60	60	44	70	68
Flaked Edge Angle (right)					
Flaked Edge Length, left (mm)	14.9	5.5	4.6	12.7	15.7
Flaked Edge Length, right (mm)					
Flaked Edge Width, left (mm)	2	1.2	1.1	1	0.8
Flaked Edge Width, right (mm)					
Form Completeness	Complete	Distal	Proximal-Medial	Fragment	Proximal-Medial
Break Type	Unbroken	Indeterminate	Indeterminate	Indeterminate	Indeterminate
Thermal Alteration	Not Observed	Not Observed	Not Observed	Not Observed	Not Observed
Platform Type	Multi-Faceted	None	Dihedral Faceted	None	Crushed
Reduction Technique	Soft Hammer	None	Soft Hammer	None	Soft Hammer

Table Q-5. 41PT185 Tested Cobbles

Provenience Number	#174-001	#811-001
Unit	TU 17	N112 E110
Depth (cmbs)	40-50	70-80
Raw Material Type	Quartzite	Chalcedony
Raw Material Source	Dakota	Unidentifiable
Max Length (mm)	127.2	57.63
Max Width (mm)	119.24	42.41
Max Thickness	55.7	11.78
Weight (g)	1300	32.4
Size Grade	>1-inch	>1-inch
Flaking Pattern	Unidirectional (one platform)	Multidirectional (multiple platforms)
% Cortex Remaining	76 - 100%	0%
Cortex Type	Pebble/Cobble	Indeterminate/Type
Form Completeness	Complete	Complete
Break Type	Unbroken	Unbroken
Thermal Alteration	Observed	Not Observed

Table Q-6. 41PT185 Cores

Provenience Number	#130-001	#163-001	#226-001	#832-001
Unit	TU 11	TU 16	TU 25	N113 E100
Depth (cmbs)	90-100	27	80-90	70-80
Raw Material Type	Quartzite	Agatized Dolomite	Agatized Dolomite	Agatized Dolomite
Raw Material Source	Unidentifiable	Alibates (Llano Estacado)	Alibates (Llano Estacado)	Alibates (Llano Estacado)
Max Length (mm)	52.04	44.73	37.47	43.74
Max Width (mm)	35.14	28.61	14.79	10.61
Max Thickness	36.2	14.73	18.85	8.9
Weight (g)	76.5	13.2	12.1	3.8
Size Grade	>1-inch	>1-inch	<1 to >3/4-inch	>1-inch
Flaking Pattern	Unidirectional (one platform)	Multidirectional (multiple platforms)	Unidirectional (one platform)	Unidirectional (one platform)
Rejuvenated Edge	Absent	Absent	Absent	Absent
Lateral Edge Angle, left	—	—	—	—
Lateral Edge Angle, right	—	—	—	—
Lateral Edge, left	—	—	—	—
Lateral Edge, right	—	—	—	—
% Cortex Remaining	51 - 75%	0%	0%	0%
Cortex Type	Nodular	Indeterminate/Type	Indeterminate/Type	Indeterminate/Type
Flaked Edge Length (mm)	—	—	—	—
Flaked Edge Width (mm)	—	—	—	—
Form Completeness	Complete	Indeterminate Fragment	Indeterminate Fragment	Indeterminate Fragment
Condition	Non Exhausted	Indeterminate	Indeterminate	Indeterminate
Break Type	Unbroken	Indeterminate	Indeterminate	Indeterminate
Thermal Alteration	Not Observed	Not Observed	Not Observed	Not Observed

Table Q-6. continued

Provenience Number	#1089-001	#1352-001	#1354-001
Unit	N118 E97	N118 E105	—
Depth (cmts)	45-60	40-50	Backfill
Raw Material Type	Quartzite	Quartzite	Agatized Dolomite
Raw Material Source	Dakota	Ogallala Gravels (potter)	Alibates (Llano Estacado)
Max Length (mm)	81.18	131.6	38.34
Max Width (mm)	67.55	125.37	34.46
Max Thickness	23.87	74.09	22.6
Weight (g)	134.7	1186.6	29
Size Grade	>1-inch	>1-inch	>1-inch
Flaking Pattern	Multidirectional (multiple platforms)	Multidirectional (multiple platforms)	Multidirectional (multiple platforms)
Rejuvenated Edge	Present	Absent	Absent
Lateral Edge Angle, left	—	—	—
Lateral Edge Angle, right	60	—	—
Lateral Edge, left	—	—	—
Lateral Edge, right	Excurvate	—	—
% Cortex Remaining	1 - 25%	26 - 50%	0%
Cortex Type	Pebble/Cobble	Pebble/Cobble	Indeterminate/Type
Flaked Edge Length (mm)	77.64	—	—
Flaked Edge Width (mm)	18.3	—	—
Form Completeness	Complete	Complete	Complete
Condition	Non Exhausted	Non Exhausted	Exhausted
Break Type	Unbroken	Unbroken	Unbroken
Thermal Alteration	Not Observed	Not Observed	Not Observed

Table Q-7. 41PT186 Points

41PT186 Points			
Provenience Number	#277-010	#300-010	#326-010
Unit	TU 5	TU 6	TU 8
Depth (cmbs)	60-70	150-160	90-100
Raw Material Type	Agatized Dolomite	Jasper	Agatized Dolomite
Raw Material Source	Alibates	Tecovas Formation (cherts and jaspers)	Alibates
Max Length (cm)	26.00	37.60	21.00
Max Width (cm)	20.30	29.70	15.70
Max Thickness (cm)	4.00	7.10	2.70
Weight (g)	1.6	10.0	0.9
Long Cross-section	Indeterminate	Indeterminate	Indeterminate
Transverse Cross-section	Indeterminate	Bi-Convex (Symmetrical)	Indeterminate
Preform	Indeterminate	Biface	Flake
Shape	Triangular	Indeterminate	Triangular
Tool Class	Bifacial	Bifacial	Bifacial
Degree of Flaking	Complete	Complete	Marginal
Cultural Period	Late Prehistoric	Late Archaic	Late Prehistoric
Flaking Pattern	Random Subparallel	Random Subparallel	Random Subparallel
Lateral Edge Angle (left)	45	45	50
Lateral Edge Angle (right)	40	52	45
Blade Length (mm)	28.6	38.1	20.0
Blade Width (mm)	20.3	29.4	15.6
Lateral Edge (left)	Excurvate	Straight	Excurvate
Lateral Edge (right)	Excurvate	Excurvate	Excurvate
Stem Shape	Indeterminate	Indeterminate	Indeterminate
Basal Shape	Indeterminate	Indeterminate	Indeterminate
Form Completeness	Distal	Medial	Distal
Break Type	Indeterminate	Indeterminate	Indeterminate
% Cortex Remaining	0%	0%	0%
Thermal Alteration	Not Observed	Not Observed	Not Observed
Stem Grinding	Indeterminate	Indeterminate	Indeterminate

Table Q-8. 41PT186 Bifaces

Provenience Number	#280-010
Unit	TU 5
Depth	80-90
Raw Material Type	Agatized Dolomite
Raw Material Source	Alibates
Max Length (cm)	27.79
Max Width (cm)	18.95
Max Thickness (cm)	6.65
Weight (g)	3.9
Size Grade	<1.91 to >1.27
Biface Stage	Indeterminate
Long Cross-section	Indeterminate
Transverse Cross-section	Indeterminate
Flaking Pattern	Random
Degree of Flaking	Complete
Lateral Edge Angle (left)	—
Lateral Edge Angle (right)	55
Lateral Edge (left)	Indeterminate
Lateral Edge (right)	Excurvate
% of Cortex Remaining	0%
Cortical Type	Indeterminate
Tool Shape	Bipointed
Flaked Edge Angle (left)	23.66
Flaked Edge Angle (right)	—
Flaked Edge Width, left (mm)	10.37
Flaked Edge Width, right (mm)	—
Form Completeness	Fragment
Break Type	Indeterminate
Thermal Alteration	Not Observed

Table Q-9. 41PT186 Edge-Modified Flakes

Provenience Number	#264-010	#272-010	#282-010	#283-010	#285-010	#285-011	#289-010
Unit	TU 4	TU 5	TU 5	TU 6	TU 6	TU 6	TU 6
Depth (cmb)	10-20	10-20	110-120	0-10	20-30	20-30	60-70
Raw Material Type	Chert	Agatized Dolomite	Agatized Dolomite	Agatized Dolomite	Agatized Dolomite	Agatized Dolomite	Jasper
Raw Material Source	Edwards Chert	Alibates	Alibates	Alibates	Alibates	Alibates	Tecovas Formation (cherts and jaspers)
Max Length (mm)	10.3	19.2	25	14	23	24	31.8
Max Width (mm)	11.7	15.4	22	12	25	17	21
Max Thickness (cm)	3.1	3.6	4.9	2	3.1	4.2	6.7
Weight (g)	0.4	1.2	2.6	0.5	2.3	1.4	4.3
Size Grade (cm)	<1.27 to >0.635	<2.54 to >1.91	<2.54 to >1.91	<1.27 to >0.635	<2.54 to >1.91	<2.54 to >1.91	>2.54
% Cortex Remaining	0%	0%	0%	0%	0%	0%	0%
Cortical Type	Indeterminate	Indeterminate	Indeterminate	Indeterminate	Indeterminate	Indeterminate	Indeterminate
Tool Shape	Indeterminate	Indeterminate	Irregular	Indeterminate	Indeterminate	Irregular	Quadrilateral
Flaking Locus	Indeterminate	Indeterminate	Lateral Only	Indeterminate	Indeterminate	Lateral Only	Distal/Lateral
Flaked Edge Angle (left)	55	60	60	75	50	45	70
Flaked Edge Angle (right)	—	—	—	—	—	—	70
Flaked Edge Length, left (mm)	67.0	16.2	12.1	8.8	19.1	13.9	28.9
Flaked Edge Length, right (mm)	—	—	—	—	—	—	23.2
Flaked Edge Width, left (mm)	0.55	4.2	0.75	1.2	3.2	2.28	2.6
Flaked Edge Width, right (mm)	—	—	—	—	—	—	3.9
Form Completeness	Fragment	Medial	Medial	Fragment	Fragment	Complete	Complete
Break Type	Indeterminate	Indeterminate	Indeterminate	Indeterminate	Indeterminate	Unbroken	Unbroken
Thermal Alteration	Not Observed	Not Observed	Not Observed	Not Observed	Not Observed	Not Observed	Not Observed
Platform Type	Indeterminate	Indeterminate	Indeterminate	Indeterminate	Indeterminate	Multi-Faceted	Flat
Reduction Technique	Indeterminate	Indeterminate	Indeterminate	Indeterminate	Indeterminate	Soft Hammer	Soft Hammer

Table Q-9. continued

Provenience Number	#307-010	#342-011	#360-010	#425-010	#446-014
Unit	TU 7	BT 8	N484 E494	N491 E494	N493 E489
Depth (cmbs)	40-50	—	90-100	90-100	66
Raw Material Type	Agatized Dolomite	Quartzite	Agatized Dolomite	Agatized Dolomite	Agatized Dolomite
Raw Material Source	Alibates	Ogallala Gravels (potter)	Alibates	Alibates	Alibates
Max Length (cm)	25.10	55.00	28.80	12.00	60.00
Max Width (cm)	19.40	55.00	21.00	9.50	50.30
Max Thickness (cm)	5.70	15.00	5.00	2.90	12.40
Weight (g)	3.1	49.2	2.1	0.3	37.4
Size Grade (cm)	<2.54 to >1.905	>2.54	>2.54	<1.27 to >0.635	>2.54
% Cortex Remaining	0	0%	51 - 75%	0%	0%
Cortical Type	Indeterminate	Indeterminate	Nodular	Indeterminate	Indeterminate
Tool Shape	Irregular	Irregular	Irregular	Indeterminate	Irregular
Flaking Locus	Indeterminate	Whole Edge	Lateral Only	Indeterminate	Distal/Lateral
Flaked Edge Angle (left)	60	55	60	50	65
Flaked Edge Angle (right)	60	65	—	—	—
Flaked Edge Length, left (mm)	17.8	30.3	22.9	6.14	56.22
Flaked Edge Length, right (mm)	13.8	31.0	—	—	—
Flaked Edge Width, left (mm)	4.3	5.9	1.1	1.25	4.5
Flaked Edge Width, right (mm)	1.24	7.9	—	—	—
Form Completeness	Fragment	Complete	Distal	Fragment	Complete
Break Type	Indeterminate	Indeterminate	Indeterminate	Indeterminate	Unbroken
Thermal Alteration	Not Observed	Not Observed	Not Observed	Not Observed	Not Observed
Platform Type	Indeterminate	Indeterminate	Indeterminate	Indeterminate	Indeterminate
Reduction Technique	Indeterminate	Indeterminate	Indeterminate	Indeterminate	Indeterminate

Table Q-9. continued

Provenience Number	#446-016	#482-012	#552-010
Unit	N493 E489	N496 E495	—
Depth (cmbs)	68	100-110	Surface
Raw Material Type	Agatized Dolomite	Agatized Dolomite	Jasper
Raw Material Source	Alibates	Alibates	Tecovas Formation (cherts and jaspers)
Max Length (cm)	49.00	11.60	34.20
Max Width (cm)	56.00	9.30	37.10
Max Thickness (cm)	11.00	2.80	9.00
Weight (g)	26.7	0.3	11.1
Size Grade (cm)	>2.54	<1.27 to >0.635	>2.54
% Cortex Remaining	0%	0%	0%
Cortical Type	Indeterminate	Indeterminate	Indeterminate
Tool Shape	Irregular	Indeterminate	Triangular
Flaking Locus	Lateral Only	Indeterminate	Whole Edge
Flaked Edge Angle (left)	60	60	60
Flaked Edge Angle (right)	—	—	70
Flaked Edge Length, left (mm)	31.0	5.2	29.3
Flaked Edge Length, right (mm)	—	—	37.3
Flaked Edge Width, left (mm)	2.1	1.6	7.0
Flaked Edge Width, right (mm)	—	—	7.5
Form Completeness	Complete	Fragment	Complete
Break Type	Unbroken	Indeterminate	Indeterminate
Thermal Alteration	Not Observed	Not Observed	Not Observed
Platform Type	Dihedral Faceted	Indeterminate	Indeterminate
Reduction Technique	Hard Hammer	Indeterminate	Indeterminate

Table Q-10. 41PT245 Edge-Modified Flakes

PNUM	#347-010
Unit	TU 4
Depth	120-130
Raw Material Type	Jasper
Raw Material Source	Tecovas Formation (cherts and jaspers)
Max Length (mm)	33.20
Max Width (mm)	16.70
Max Thickness (mm)	7.20
Weight (g)	2.6
Size Grade	>2.54 cm
% of Cortex Remaining	0%
Cortical Type	Indeterminate
Tool Shape	Quadrilateral
Flaking Locus	Lateral Only
Flaked Edge Angle (left)	65
Flaked Edge Angle (right)	60
Flaked Edge Length, left (mm)	16.80
Flaked Edge Length, right (mm)	18.50
Flaked Edge Width, left (mm)	1.75
Flaked Edge Width, right (mm)	1.38
Form Completeness	Medial
Break Type	Indeterminate
Thermal Alteration	Not Observed
Platform Type	Indeterminate
Reduction Technique	Indeterminate

APPENDIX R

**ORGANIC RESIDUE (FTIR) ANALYSIS OF BURNED ROCK,
GROUNDSTONE, AND LITHIC SAMPLES FROM SITE 41PT185/C,
POTTER COUNTY, TEXAS**

This page intentionally left blank.

**ORGANIC RESIDUE (FTIR) ANALYSIS OF BURNED ROCK,
GROUNDSTONE, AND LITHIC SAMPLES FROM SITE 41PT185/C,
POTTER COUNTY, TEXAS**

Prepared for:



**TRC Environmental Corporation
505 East Huntland Drive, Suite 250
Austin, Texas 78752**

Prepared by:

**Melissa K. Logan
with Assistance from
R. A. Varney
PaleoResearch Institute, Inc. Golden, Colorado
PaleoResearch Institute Technical Report**

December 2009

This page intentionally left blank.

R.1 INTRODUCTION

Burned rock, ground stone, and lithic tools recovered from site 41PT185/C in Potter County, Texas were submitted for organic residue analysis. Samples were tested for organic residues using Fourier Transform Infrared Spectroscopy (FTIR). Specific artifact provenience data was not provided to PaleoResearch Institute in an effort to minimize bias in the analysis.

R.2 METHODS

FTIR (Fourier Transform Infrared Spectroscopy)

A mixture of chloroform and methanol (CHM) was used as a solvent to remove lipids and other organic substances that had soaked into the surface of the ground stone, burned rock, and lithic tools. This mixture is represented in the FTIR graphics as CHM. The CHM solvent and sample were placed in a glass container, and allowed to sit, covered, for several hours. After this period of time, the solvent was pipetted into an aluminum evaporation dish, where the CHM was allowed to evaporate. This process leaves the residue of any absorbed chemicals in the aluminum dishes. The residue remaining in the aluminum dishes was then placed on the FTIR crystal and the spectra were collected. The aluminum dishes were tilted during the process of evaporation to separate the lighter from the heavier fraction of the residue. The lighter and heavier fractions are designated Upper (lighter fraction) and Lower (heavier fraction) respectively in the subsequent analysis.

FTIR is performed using a Nicolet 6700 optical bench with an ATR and a silicon crystal. The sample is placed in the path of a specially encoded infrared beam. The infrared beam passes through the sample and produces a signal called an "inferogram." The inferogram contains information about the frequencies of infrared that are absorbed and the strength of the absorptions, which is

determined by the sample's chemical make-up. A computer reads the inferogram and uses Fourier transformation to decode the intensity information for each frequency (wave numbers) and presents a spectrum.

R.3 FTIR (FOURIER TRANSFORM INFRARED SPECTROSCOPY) REVIEW

Infrared spectroscopy (IR) is the study of how molecules absorb infrared radiation and ultimately convert it to heat, revealing how the infrared energy is absorbed, as well as the structure of specific organic molecules. Infrared spectroscopy has been experiencing a renaissance for identifying organic substances during the past few decades. It is currently considered one of the more powerful tools in organic and analytical chemistry. One of the primary advantages to the FTIR is that it measures all wave lengths simultaneously. It has a relatively high signal-to-noise ratio and a short measurement time. Each peak in the spectrum represents either a chemical bond or a functional group.

Since molecular structures absorb the vibrational frequencies or wavelengths of infrared radiation, the bands of absorbance can then be used to identify the composition of the materials under study. In the case of the current research, the portion of the electromagnetic spectrum between 4000-400 wave numbers is used for identifying organic materials. Carbohydrates, lipids, proteins and other organic molecules are associated with specific wave number bands (Isaksson 1999:36-39).

The infrared spectrum can be divided into two regions--the functional group region and the fingerprint region. These two groups are recognized by the effect that infrared radiation has on the respective molecules of these groups. The functional group region is located between 4000 and approximately 1500 wave numbers. The molecular bonds display specific characteristic vibrations that

identify fats, lipids, waxes, lignins, proteins, carbohydrates, etc. The fingerprint region, located below 1500 wave numbers, is influenced by bending motions, which further identify the molecules present.

Using the FTIR, it is possible to identify different types of organic compounds and eventually recognize different types of materials such as plant or animal fats or lipids, plant waxes, esters, proteins, carbohydrates, and more. Specific regions of the spectrum are important in identifying these compounds.

The results of the identification of specific wavelengths can be compared with commercial or laboratory created analytical standards to identify the specific types of bonds present in different materials. By combining the results of the analysis of individual samples with all of the reference materials in the PaleoResearch Institute (PRI) library, the percent match with individual reference items can be displayed. For instance, plant lipids or fats are identifiable between 3000 and 2800 wave numbers. A match might be obtained on this portion of the spectrum with nuts such as hickory, walnut, or acorn or with animal fats or corn oil. Recovery of high level matches with several types of nuts (in this example) indicates that nuts were processed. If the match with the PRI library is for meat fats, then the signature is more consistent with that produced by meat than plant parts such as nuts.

Samples containing many compounds are more difficult to identify – and many archaeological samples are complex mixtures. Multi-purpose artifacts, such as ground stone, which could have been used to crush or grind a variety of foodstuffs, or ceramic cooking vessels, which are expected to have been used to cook many different foods, might present a mixture problem. Mixtures sometimes have many absorption bands that overlap, yielding only broad envelopes of absorption and few distinctive

features. FTIR analysis is expected to be particularly valuable in examining fire-cracked rock (FCR), for which few other means of analysis exist, since the fats, lipids, waxes, and other organic molecules contained in liquids that seep out of the food being processed become deposited on the rocks during the baking process. Once again, these rocks might have been present in more than one cooking episode, thus having the potential to yield a complex signature. The PRI extraction method gently removes these organic molecules from the ground stone, ceramics, and/or rocks so that they can be measured with the FTIR and subsequently identified.

Organic molecules from sediments can be extracted and the sediments then characterized. This has the potential to be very useful in identifying signatures of the remains responsible for a dark horizon. For instance, if the dark horizons are the result of decaying organic matter (plant or animal), the FTIR will yield a signature of decaying organic remains. If the dark horizons are the result of blowing ash from cultural features, the FTIR signature will be considerably different. This is an affordable technique for making distinctions between horizons and identifying cultural horizons.

R.4 CARBOHYDRATES

Carbohydrates are a product of photosynthesis in green plants. This group of compounds is the most abundant found on earth. Carbohydrate is a term that encompasses three main groups of compounds: 1) sugars, 2) starches, and 3) fibers. To elaborate, sugars include the simple carbohydrates found in table sugar, honey, natural fruit sugars, and molasses. Starches and complex carbohydrates are present in legumes, grains, vegetables, and fruits. Fibers, including cellulose, hemicellulose, and pectin, are present in whole grains, legumes, vegetables, and fruits (Garrison and Somer 1985:13). Dietary carbohydrates provide energy for bodily

functions, including our ability to digest and absorb other foods. They are the body's preferred source of energy, although proteins and lipids also may be converted to energy. Carbohydrates are so important that an inadequate intake may result in nutritional deficiencies such as ketosis, energy loss, depression, and even loss of essential body protein. On the other hand, excess intake of carbohydrates causes obesity and dental decay.

To understand carbohydrates and their detection with the FTIR it is important to know that they are formed of carbon atoms coupled to "hydrates," such as water, resulting in empirical formulas of $C_nH_{2n}O_n$ where "n" represents the number of atoms for C, H, and O, respectively. "Biochemically, carbohydrates are polyhydroxy alcohols with aldehyde or ketone groups that are potentially active" (Garrison and Somer 1985:13). Since carbohydrates are classified according to their structure and the FTIR detects the bonds between molecules, we will review the simple sugars (monosaccharides), multiple sugars (oligosaccharides), and complex molecules (polysaccharides) that are made up of simple sugars.

R.4.1 Monosaccharides

Monosaccharides or naturally occurring simple sugars, contain 3 to 7 carbon atoms each. The most important monosaccharides for the diet are referred to as hexoses because they contain 6 carbon atoms ($C_6H_{12}O_6$). Although the formula is the same for simple sugars, variations in the arrangements of the atoms about the carbon chains creates different sugars.

Glucose

Glucose, dextrose, corn sugar, grape sugar, is the form that circulates in blood (blood sugar). It is also the form that cells use for energy. It is soluble in both hot and cold

water and crystallizes easily. Glucose is somewhat less sweet than cane sugar.

D-Glucose

D-glucose, or dextrorotatory glucose, is a biologically active form of glucose. In plants it results from photosynthesis; and in animals, it occurs from the breakdown of glycogen (Biology-online 2009a). Alpha and beta D-glucose are two specific forms of D-glucose, differing only in the placement of an OH-group in their molecular structure (Biology-online 2009a). As a result, the forms can easily shift back and forth between the two different alpha and beta states.

Fructose

Fructose, levulose, or fruit sugar is present in honey, ripe fruits, and a few vegetables. It is highly soluble, does not crystallize, is not absorbed directly into the blood, and is much sweeter than cane sugar. It is produced as a product of the hydrolysis of sucrose (an oligosaccharide).

Galactose

This monosaccharide is produced during digestion of lactose (milk sugar, an oligosaccharide).

Mannose

Mannose is a minor hexose carbohydrate present in aloe and probably other members of the lily family. Pentose carbohydrates (xylose and arabinose) are produced during digestion of certain fruits and meats. Ribose, another pentose produced during digestion, is also synthesized by the human body. Ribose is a constituent of riboflavin (a B complex vitamin), ribonucleic acid (RNA), and deoxyribonucleic acid (DNA).

R.4.2 Disaccharides

Disaccharides are formed when two monosaccharides are combined (Wardlaw 1996:72). Sucrose, lactose, and maltose are the three most common disaccharides found in nature (Wardlaw 1996:72).

Sucrose

Sucrose or common table sugar is derived from sugar cane, sugar beets, sorghum, molasses, or maple sugar. This disaccharide consists of one molecule of fructose and one molecule of glucose. It may be found in some vegetables and many fruits.

β-D-sucrose

β-D-sucrose is a specific form of D-sucrose most similar to table sugar. D-sucrose is only formed naturally by terrestrial plants, and is found in high concentrations in their fruits, seeds, and roots. The bodies of other organisms and animals cannot create it; however, D-sucrose can be chemically synthesized (Lemieux 1953).

Lactose

Lactose or milk sugar is unusual in its animal origin and is the only nutritionally significant sugar originating in animals. Lactose varies from 2% to 8% in mammalian milk, by volume.

Maltose

This short chain of glucose molecules is an intermediate product in the digestive hydrolysis of starch. It contributes its distinctive taste to malted beers.

R.4.3 Oligosaccharides

These carbohydrates have two or more hexoses combined with the loss of a water molecule (C₁₂H₂₂O₁₁). In other words, there will be one less oxygen than carbon and hydrogen will be double the quantity of

carbon, minus 2. Oligosaccharides are all water soluble and can crystallize, but are of varying sweetness. Raffinose and stachyose, both oligosaccharides found in beans and other legumes, are bonded together in a way that makes it impossible for human digestive enzymes to break them apart (Wardlaw 1996:80). Humans (and other monogastric animals) are missing the “-GAL enzyme. Therefore, raffinose and stachyose pass through the stomach and upper intestine, arriving in the lower intestine where they are fermented by gas-producing bacteria, which do possess the “-GAL enzyme. The result is manufacture of carbon dioxide, methane, and/or hydrogen in the lower intestine, leading to flatulence (and discomfort) commonly associated with eating beans and some other vegetables.

Raffinose

Raffinose is composed of three monosaccharides, or simple sugar units, galactose, glucose, and fructose, and is found in beans, as well as cabbage, brussels sprouts, broccoli, asparagus, other vegetables, and whole grains (Wardlaw 1996:80,G-14).

Stachyose

Stachyose is most abundant in beans, but is also present in smaller quantities in other vegetables and plants. This oligosaccharide is composed of four monosaccharides--galactose, galactose, glucose, and fructose (Wardlaw 1996:80,G-15).

R.4.4 Polysaccharides

These complex starchy compounds follow the empirical formula: C₆H₁₀O₅. They are not sweet, do not crystallize, and are not water soluble. Simply defined, polysaccharides are complex carbohydrates found in plants as starch and cellulose, and in animals as glycogen. Because the FTIR detects the bonds between atoms in molecules, it is important to know that

polysaccharides are formed of repeating units of mono- or disaccharides that are joined together by glycosidic bonds. Polysaccharides are often heterogeneous. The slight modifications of the repeating unit results in slightly different wave number signatures on the FTIR. Types of polysaccharides are descriptive and include storage (starches and glycogen), structural (cellulose and chitin), acidic (containing carboxyl groups, phosphate groups, and/or sulfuric ester groups), neutral (presumably without the acid features), bacterial (macromolecules that include peptidoglycan, lipopolysaccharides, capsules and exopolysaccharides), and more. The study of polysaccharides is an ever growing field and industry, since polysaccharides are important to proper immune function, bowel health, and a host of other factors that are important in human health. At present there is no comprehensive study of which plants and animal parts contain which polysaccharides. Research into this field is currently growing at a rapid pace. Some highlights for the purpose of our discussions are presented below.

Storage Polysaccharides

Storage polysaccharides are digestible polysaccharides. Starch and glycogen are the two primary groups of these polysaccharides (Wardlaw 1996:80-81).

Starch

Starch is the primary digestible polysaccharide in the human diet, and the most important carbohydrate food source (Murray, et al. 2000:155; Wardlaw 1996:80). Starch is composed of long chains of glucose units. "Cooking increases the digestibility of...starches...making them more soluble in water and thus more available for attack by digestive enzymes" (Wardlaw 1996:80). Amorphous starch granules encased in cell walls burst free when cooked because the granules absorb water and expand. The two primary

constituents of starch are amylose and amylopectin, both of which are a source of energy for plants and animals (Murray, et al. 2000:155; Wardlaw 1996:80). When the glucose chains are long and straight, the starch is labeled amylose. If the chains are short and branched, they are amylopectin. Shorter chains of glucose (dextrin) are the intermediate product of the hydrolysis of starch. Glucan, which is often found in association with pectin, resides in the cell walls of plants and trees and many forms of bacteria and fungi (Stephen 2006). Most people are familiar with beta glucans, which are a diverse group of molecules that occur commonly in the cellulose of plants, bran of cereals, cell walls of baker's yeast, and certain fungi, mushrooms, and bacteria. Some beta glucans may be useful as texturing agents and soluble fiber supplements. Beta glucans derived from yeast and medicinal mushrooms have been used for their ability to modulate the immune system.

Amylose and Amylopectin. The main difference between these types of starch are that amylose is composed of long straight chains of glucose, while amylopectin is defined by short, branched chains of glucose. Amylose and amylopectin "are found in potatoes, beans, breads, pasta, rice, and other starchy products" (Wardlaw 1996:82).

Glycogen

Glycogen is the storage polysaccharide of humans and other animals that is often referred to as animal starch (Murray, et al. 2000:155). Carbohydrates are converted to glucose, which circulated in the blood. Approximately 65% of this glucose feeds the brain, while the remainder is converted to glycogen in the liver and muscles, where it is stored. Glycogen stored in the muscles is for the exclusive use of muscle cells, while glycogen stored in the liver may be converted to glucose and distributed as needed for energy. Prolonged exercise

depletes muscles of glycogen, resulting in fatigue. The liver has a finite amount of room for glycogen, so excess quantities of carbohydrates that are not converted to glycogen are converted to triglycerides (fat) for storage. Structurally, glycogen is similar to amylopectin starch, but with more branches, making it quick and easy to convert for use as energy when the body needs blood glucose. Enzyme activity in the liver first converts glycogen to glucose-phosphate molecules, which are then converted to glucose, rather than releasing the molecules sequentially. This enzyme is present in the liver, but not in muscles, explaining why glycogen is available to be converted to glucose for the blood only from the liver and not the muscles. It is therefore, an ideal form of carbohydrate storage in the body (Wardlaw 1996:81). Glycogen is not present in meat that has been butchered (Wardlaw 1996:81) because an animal under stress converts glycogen to lactic acid and/or metabolizes the glycogen as part of the stress response (Green 2006; Nations 2009; Sheeler 2004). Hunting and/or chasing animals will also use up glycogen as the muscles fatigue.

Structural Polysaccharides

Structural polysaccharides, which are also known as dietary fiber, are indigestible by humans and other animals. Structural polysaccharides are primarily composed of cellulose, hemicellulose, pectin, gum, and mucilage (Wardlaw 1996:82). “The only noncarbohydrate components of dietary fiber are lignins, which are complex alcohol derivatives” (Wardlaw 1996:82). Lignins are complex alcohol derivatives that make up the non-carbohydrate components of insoluble plant fibers (Wardlaw 1996:82). As such, they cannot be digested by the enzymes animals produce (Carlile 1994). Lignin is found in all plants and is an important component of the secondary cell walls (Lebo 2001; Martone 2009; Wardlaw 1996:82). One of the important functions of lignin is to provide support through

strengthening of the xylem cells of wood in trees (Arms 1995; Esau 1977; Wardrop 1969). In linking plant polysaccharides, lignin provides strength to the cell walls and by extension to the entire plant (Chabannes 2001). Cellulose and chitin also provide structural support to animals and plants. Therefore, they are not water soluble. Cellulose, hemicellulose, and pectin are all comprised of simple sugars, and their differences are defined by the various inclusions, exclusions, and combinations of these sugars, as well as how the sugars are bonded, and their molecular structure.

Cellulose

Cellulose is comprised of a long linear chain of glucose, while hemicellulose consists of shorter branched chains of simple sugars in addition to glucose, including especially xylose, but also mannose, galactose, rhamnose, and arabinose (Crawford 1981; Updegraff 1969). Pectin, however, may be found in either a linear or branched form of simple sugars that are primarily composed of rhamnose.

β-D-cellulose. β-D-cellulose, which is found in the cell walls of plants, is one of three specific types of cellulose, alpha cellulose (true cellulose), beta cellulose, and gamma cellulose, which are differentiated by their molecular structures and properties (Gooch 2007; Kono 2006:318).

Hemicellulose

Hemicellulose resides in the cell wall structures of many plants, particularly grain and vegetable plants, and is a component of both insoluble and soluble fibers (Wardlaw and Paul M. Insel 1996:82). Some specific hemicelluloses include galactan, galactoglucomannan, glucomannan, glucuronoxylan (GX), and xyloglucan (Walker 2006; Wilkie 1985).

Galactan. Galactan is a structural polysaccharide, and hemicellulose,

composed of polymerized galactose, or repeating sugar units linked in unbranched or branched chains (Biology-online 2009b). Galactose is found predominantly in dairy products, but is also present in high quantities in sugar beets (a member of the Chenopodiaceae), and other gums and mucilages (Mayes 2000:149; McGee 1984:585; Mosby 2008).

Galactoglucomannan. Galactoglucomannan is a primary component of the woody tissue of coniferous plants (Gymnosperms) (Bochicchio 2003).

Glucomanan. Glucomanan, which may be very concentrated in some roots or corms and in the wood of conifers and dicotyledons (dicots), is a soluble fiber used to treat constipation by decreasing fecal transit time (Bochicchio 2003; Marzio 1989).

Glucuronoxylan. Glucuronoxylans, often abbreviated GX, “are one of the major hemicellulosic components found within the secondary cell walls of hardwoods” (Awano 2000:72). They have also been isolated from fruits and seeds, and found in various dicotyls including ground nutshells, sunflower hulls, and coneflower (Rudbeckia) (Ebringerova 2005:8).

Xyloglucan. Xyloglucan is the most abundant hemicellulose in the cell walls of most dicotyledonous plants, and all vascular plants (Fry 1989).

The primary cell wall of [these plants] is composed of cellulose microfibrils embedded in a matrix of hemicellulosic and pectic polysaccharides, of which the hemicellulose xyloglucan is a major component. Xyloglucan and cellulose together make up about two-thirds of the dry weight of primary cell walls and are the major tension-bearing components of the matrix. During cell expansion and elongation, the cell wall continually undergoes temporary loosening followed by

rapid reinforcement of wall structure. Xyloglucan endotransglycosylases (XETs) are unique enzymes in plants that are capable of modulating the chemistry of the matrix and therefore performing both of these functions (Eckardt 2004:792).

It is through this process that plant cell wall growth and repair occurs (Moore 1988).

Pectin, Gums, and Mucilages

Pectin, gums, and mucilages are soluble fibers found inside and around plant cells that help “glue” them together (Wardlaw 1996:82). Pectin is a structural heteropolysaccharide and common substance found in many plants (apples, plums, gooseberries, and citrus) often used for its gelling or thickening action. Plant derived gums and mucilages such as gum arabic, guar gum, and locus bean gum are also used for this same purpose. Arabinan, arabinogalactan, arabinoglucuronoxylan, and rhamnogalacturonan are some examples of these types of polysaccharides (Wilkie 1985).

Arabinan. In plants, arabinan is essential for the function of guard cells which “play a key role in the ability of plants to survive on dry land, because their movements regulate the exchange of gases and water vapor between the external environment and the interior of the plant” (Jones 2003:11783).

Arabinogalactan. Arabinogalactan is a sugar found in plant carbohydrate structures particularly gums and hemicelluloses. One of arabinogalactan’s many functions is to bond with proteins to repair damage when it occurs to a plant or its parts (Nothnagel 2000).

Arabinoglucuronoxylan.

Arabinoglucuronoxylan is found in the cell walls of softwoods and herbaceous plants (Sjostrom 1981).

Rhamnogalacturonan. Rhamnogalacturonans are specific pectic polysaccharides that reside in the cell walls of all land plants, and result from the degradation of pectin (Willats 2001). They are visible by the presence of peaks at 1150, 1122, 1070, 1043, 989, 951, 916, 902, 846, and 823 wave numbers.

Chitin

Chitin forms the exoskeleton of insects and related animals such as crayfish, shrimp, crabs, and lobsters. It is one of the most abundant natural materials in the world, and first appeared in the exoskeletons of trilobites and other Cambrian arthropods (Briggs 1999). Recent comparative studies on insect and shellfish chitin, indicate insect chitin, particularly from crickets, holds a higher dietary quality which may make cricket chitin an excellent polysaccharide resource for health and medical applications (Wang 2004).

Acidic Polysaccharides

Acidic polysaccharides are defined as containing carboxyl groups, phosphate groups, and/or sulfuric ester groups. Carboxylates, which are among the defining characteristics of acidic polysaccharides, are recognized in peaks located at 1560 cm⁻¹ and 1410 cm⁻¹.

Neutral Polysaccharides

These polysaccharides lack carboxyl groups, phosphate groups, and/or sulfuric ester groups. Examples of neutral polysaccharides cross other category boundaries of polysaccharides and include: chitin, chitosan, curdlan, dextran, glucan, inulin, arabinogalactan, arabinogalactorhamnoglycan, and other compounds that often either are contained within individual plants or are the result of fermentation.

Arabinogalactorhamnoglycan

Arabinogalactorhamnoglycan, is a specific polysaccharide, or complex carbohydrate, known as a neutral polysaccharide that is found in plant cell walls (Capek 1999; Kacurakova 2000). It exhibits peaks at 1049, 914, 837, and 810 wave numbers.

Bacterial Polysaccharides

These diverse macromolecules include peptidoglycan, lipopolysaccharides, capsules and exopolysaccharides. Their functions range from being structural cell wall components (peptidoglycan), virulence factors, and facilitating bacterium to survive in harsh environments (Pseudomonas in the human lung). Synthesis of these polysaccharides is both tightly regulated and an energy intensive process. Current research into the benefits of bacterial polysaccharides and their commercial exploitation is used to develop new applications for these products. Pathogenic bacteria often produce a thick, mucous-like, encapsulating layer of polysaccharide. This layer or capsule cloaks the antigenic proteins on the surface of the bacteria that would otherwise be identified by the host organism and provoke an immune response, leading to the destruction of the bacteria. Bacteria, fungi, and algae may secrete polysaccharides to help them adhere to surfaces and/or to prevent them from drying out. Humans have used some of these polysaccharides as thickening agents. The presence of these polysaccharides often may be identified by peaks at specific wave number locations using the FTIR.

Esters

Esters are an important functional group, as they are present as flavoring agents in food and are components of biological compounds such as fats, oils and lipids. In an ester, the basic unit of the molecule is known as a carbonyl. The presence of the double peak between 3000 and 2800 wave

numbers identifies the presence of the aldehyde functional group, which is present in fats, oils, lipids, and waxes.

There are two important groups of esters, saturated esters and aromatic esters. Aromatic esters take their name from their ability to produce distinctive odors, and are present as flavoring agents in food. In contrast, saturated esters do not produce distinctive odors. Esters are expressed in the FTIR spectrum by three distinct peaks (“the rule of three”) located at approximately 1700, 1200, and 1100 wave numbers, and a fourth peak in the region between 750 and 700 cm^{-1} , which represents the CH_2 bend associated with aromatic esters. The first peak for saturated esters falls in the 1750-1735 range, while the second peak lies between 1210 and 1160, and the third peak sits between 1100 and 1030. Saturated esters have a unique peak to acetates at 1240. This band can be very strong in the signature. The first peak for aromatic esters falls in the range between 1730 and 1715, followed by the second peak between 1310 and 1250, and finally the third peak between 1130 and 1100 (Smith 1999:110-112). Distinguishing between saturated and aromatic esters, which are both components of foods, is easy if all three bands are present, since they occupy different wave number regions.

Lipids

Lipids that are solid at room temperature are called “fats,” and those that are liquid at room temperature are referred to as “oils” (Wardlaw 1996:108). Both forms of lipids can be detrimental, as well as beneficial, to human health. Consumption of certain animal fats rich in saturated fatty acids can lead to heart disease, while ingesting omega-3 fatty acids such as EPA (eicosapentaenoic acid) and DHA (docosahexaenoic acid) found in fish and other plant sources are essential to good health.

Fatty Acids

Fatty acids are found in most lipids in the human and animal body, as well as in the lipids in foods (Wardlaw 1996:108). Long chains of carbons bonded together which are then bonded to hydrogens define the structure of fatty acids (Wardlaw 1996:109). A fatty acid is considered saturated if the carbons are connected by single bonds. Saturated fatty acids are high in animal fats. If the carbon chain has one double bond between two of the carbons then this fatty acid is called monounsaturated. If there are two or more double bonds between carbons than the fatty acid is polyunsaturated.

Essential Fatty Acids

Essential fatty acids, are those lipids critical to human health, such as omega-3 and omega-6 fatty acids, alpha-linolenic acid, and linoleic acid, that cannot be created within the body and must be obtained from dietary sources (Wardlaw 1996:110-111). These essential fatty acids are part of “vital body structures, perform vital roles in immune system function and vision, help form cell membranes, and produce hormone like compounds,” and are necessary to maintain good health (Wardlaw 1996:111). Diets high in essential fatty acids, like omega-3 and omega-6, reduce the risk of heart attacks because they minimize the tendency for blood to clot (Wardlaw 1996:112). Fish oils contain high concentrations of omega-3 and omega-6 fatty acids and may be administered as a dietary supplement.

Proteins

The human body uses protein from dietary plant and animal sources to form body structures and other constituents (Wardlaw 1996:152). “Proteins contribute to key body functions, including blood clotting, fluid balance, production of hormones and enzymes, vision, and cell growth and repair” (Wardlaw 1996:152). This constant regulation and maintenance of the body

requires thousands of different types of proteins that are not all available within the body (Wardlaw 1996:152). The majority of the building blocks for these proteins, which are also known as amino acids, are produced by plants.

Amino Acids

Within the body amino acids are linked to form the necessary proteins, making them not only essential for life, but key to nutrition. Amino acids can be combined in a multitude of ways to create a vast variety of proteins. Differences between these proteins are distinguished by the unique arrangements of amino acids. Proteins are created through a process called translation, in which amino acids are added, one-by-one, to form short polymer chains called peptides, or longer chains called polypeptides or proteins (Rodnina 2007). The order in which the amino acids are added is determined by the genetic code of the mRNA template, which is a copy of an organism's genes (Creighton 1993). Amino acids are divided into standard and non-standard types.

Standard Amino Acids

There are twenty naturally occurring amino acids on earth called standard amino acids (Creighton 1993). These amino acids are encoded by the standard genetic code and are found in all forms of life (Creighton 1993). The standard amino acids are broken down into two different types, essential and nonessential.

Essential Amino Acids

Eight of the standard amino acids are considered "essential amino acids" because they are necessary for normal human growth and cannot be synthesized by the human body (Young 1994). Essential amino acids must be obtained from food sources, and include histidine, isoleucine, leucine, lysine, methionine, phenylalanine, threonine,

tryptophan, and valine (Furst 2004; P. J. Reeds 2000; Wardlaw 1996:154).

Histidine. Histidine is an amino acid that is considered particularly indispensable, or essential, in infants, because they are unable to synthesize this amino acid until three to four years of age. Histidine is necessary for the growth and repair tissue, and is required for the manufacture of red and white blood cells. Histidine is also metabolized into histamine, a compound released by the immune system cells during an allergic reaction (Osiecki 2004). Sources of histidine include dairy, meat, poultry, fish, rice, wheat, and rye.

Isoleucine. Isoleucine is found in most common proteins. It is important for blood-clot formation and is concentrated in muscle tissues (Nelson 2005). Dietary sources of isoleucine include beef, poultry, fish, eggs, nuts, dairy, and legumes.

Leucine. Leucine is used in the liver, adipose tissue, and muscle tissue. In adipose and muscle tissue, leucine aids in the formation of sterols, and slows the degradation of muscle tissue by increasing the synthesis of muscle proteins (Combaret 2005; Rosenthal 1974). Common sources of leucine in the diet include beef, fish, shellfish, nuts and seeds, eggs, and legumes.

Lysine. Lysine is important for calcium absorption, building muscle, recovering from injuries or illnesses, and the production of hormones, enzymes, and antibodies (Nelson 2005). Plants that contain significant amounts of lysine include legumes, gourds/squash, spinach, amaranth, quinoa, and buckwheat (Wardlaw 1996:158). Other dietary sources of lysine include beef, poultry, pork, fish, eggs, and dairy.

Methionine. Methionine helps the body break down fats, and thus, prevents the build-up of fat in the arteries (Nelson 2005). It is found primarily in meat, fish, grains,

nuts and seeds (Wardlaw 1996:158); as well as in lower quantities in spinach, potatoes, and corn. Most fruits, vegetables, and legumes only contain small amounts of methionine.

Phenylalanine. Phenylalanine is essential for the developmental growth of infants, and is found naturally in the breast milk of mammals (Nelson 2005). As a result, dairy foods contain the highest concentration of phenylalanine in the diet. Other sources of phenylalanine include fish and seafood, poultry, meat, legumes, and nuts and seeds. One of the common uses of phenylalanine today is in the artificial sweetener aspartame, which is found in diet sodas and other sugar-free beverages and confections.

Threonine. Threonine is important for maintaining the proper balance of protein in the body (Nelson 2005). Foods high in threonine include poultry, fish, meat, legumes, seeds, and dairy (Wardlaw 1996:158).

Tryptophan. Tryptophan is important for normal growth in infants, and nitrogen balance in adults (Nelson 2005). It also increases brain levels of serotonin, a calming neurotransmitter when present in moderate levels, which causes relaxation and sleepiness (Wurtman 1980). This has led to the belief that consuming large amounts of turkey, which contains high levels of tryptophan, results in drowsiness, such as that experienced after traditional Thanksgiving and/or Christmas dinners. Dietary sources of tryptophan include poultry, beef, fish, eggs, dairy, cacao, oats, nuts and seeds, and legumes (Wardlaw and Paul M. Insel 1996:158).

Valine. Valine plays a role in muscle metabolism, repair and growth of tissue, and maintaining nitrogen balance in the body (Nelson 2005). It also preserves the use of glucose by providing an energy source for muscles. Nutritional sources of valine include fish, poultry, and some legumes.

Nonessential Amino Acids

The majority of the standard amino acids are considered “nonessential,” meaning that under normal circumstances these amino acids can be manufactured by the human body and are not required in the diet. However, some amino acids that are normally nonessential may become an essential part of the diet for a person whose health has been compromised (Wardlaw 1996:155). Nonessential amino acids include alanine, arginine, asparagine, aspartate (aspartic acid), cysteine, glutamate (glutamic acid), glutamine, glycine, proline, serine, and tyrosine (Furst 2004; P. J. Reeds 2000; Wardlaw 1996:154).

Alanine. Alanine plays an important role in the glucose-alanine cycle between tissues and liver (Nelson 2005). Common sources of alanine in the diet include such diverse things as meat, eggs, fish, legumes, nuts and seeds, and maize.

Arginine. Arginine is involved in cell division, the healing of wounds, immune function, and the release of hormones. Depending on developmental stage and health status, arginine can be considered a semi-essential, or conditionally essential amino acid. This is particularly true for children born preterm who cannot meet their requirements for arginine (Wardlaw 1996:155). Common dietary sources of arginine include dairy, beef, pork, poultry, wild game, seafood, wheat germ, hemp, buckwheat, oats, legumes, and nuts and seeds (Murray 1998).

Asparagine. Asparagine is one of the most common of the twenty natural amino acids, and is most abundant in asparagus, from which its name is derived (Nelson 2005). Although the characteristic smell observed in the urine of individuals after their consumption of asparagus is often attributed to asparagine, specific studies on this correlation suggest the odor might instead be due to the metabolization and oxidation of

asparagusic acid, also found in asparagus (Akers 1997; Vickery 1931; Waring 1987). Common sources of asparagine include asparagus, potatoes, legumes, nuts and seeds, dairy, beef, poultry, eggs, fish, and seafood.

Aspartate. Aspartate, also known as aspartic acid, is an important neurotransmitter in the brain (Nelson 2005). Common sources of aspartate include wild game, meat, oats, avocado, asparagus, and sprouted seeds.

Cysteine. Cysteine is classified as a non-essential amino acid; however, in rare cases, cysteine may be essential for infants, the elderly, and individuals with certain metabolic disease or who suffer from malabsorption syndromes (Nelson 2005). Dietary sources of cystine include pork, chicken, turkey, duck, eggs, dairy, red peppers, garlic and onions, broccoli, brussels sprouts, oats, and wheat germ.

Glutamate. Glutamate, or glutamic acid, is an important molecule in cellular metabolism. It is the most abundant excitatory neurotransmitter in the nervous system of mammals (Nelson 2005). Glutamate is found in dairy products, eggs, and all meats, such as beef, pork, poultry, wild meats, and fish (Reeds, et al. 2000).

Glutamine. Glutamine is the most abundant and naturally occurring, non-essential amino acid in the human body. It is one of the few amino acids which directly crosses the blood-brain barrier (Lee 1998). The blood-brain barrier is a collection of high density cells joined with almost impenetrable connections that protect the brain from being exposed to all elements in the blood, particularly bacteria (Lee 1998). Unlike many other substances, such as solutes, which are restricted from making this passage, glutamine in the blood can easily pass through these junctions (Lee 1998). Glutamine is not only found circulating in the blood, but is also stored in the skeletal muscles (Lee 1998). At times of illness or

injury, glutamine can be considered a conditionally essential amino acid that must be obtained temporarily from the diet because the body is unable to synthesize it on its own (Lee 1998). Glutamine is also beneficial in healing the cells of the gastrointestinal tract by stimulating regeneration and promoting new cellular growth. Common sources of glutamine in the diet include beef, chicken, fish, eggs, dairy, legumes, cabbage, beets, spinach, and parsley.

Glycine. Glycine is the smallest of the twenty standard amino acids (Nelson 2005). It is an inhibitory neurotransmitter in the central nervous system, particularly in the spinal cord, brainstem, and retina. Glycine is required to build protein in the body, synthesize nucleic acids, and for the construction of RNA, DNA, bile acids, and other amino acids in the body. It also aids in the absorption of calcium in the body. Dietary sources of glycine include poultry, pork, fish, eggs, beef, peanuts, seaweed, and a variety of seeds and nuts, such as sunflower, pumpkin, and sesame.

Proline. Proline is critical for the production of collagen and cartilage, and is produced in the liver from other amino acids (Nelson 2005). Nutritional sources of proline include most meats.

Serine. Serine is important in metabolic function (Nelson 2005). It serves as a neuronal signal by activating NMDA receptors in the brain, and helps to build muscle tissue (Mothet 2000). Common sources of serine in the diet are beef, eggs, nuts and seeds, legumes, and milk.

Tyrosine. Tyrosine assists and supports neurotransmitters in the brain, which help nerve cells communicate (Nelson 2005). It is found in casein, which is prevalent in dairy products. Other dietary sources of tyrosine include chicken, turkey, fish, almonds, avocados, bananas, legumes, and pumpkin and sesame seeds.

Non-standard Amino Acids

Non-standard amino acids are amino acids that are chemically altered after they have been incorporated into a protein, and/or amino acids that exist in living organisms, but are not found in proteins (Driscoll 2003).

Nucleic Acids

Millions of proteins exist in all living organisms to assist with the daily functions of these complex systems. Proteins are produced and assembled locally to exact specifications, and a large amount of information is necessary to properly manage the system. This information is stored in a set of molecules called nucleic acids. Nucleic acids not only contain the genetic instructions for the proper development and functioning of living organisms, but also play a role in copying genetic information to protein (Saenger 1984). The most common examples of nucleic acids are DNA (deoxyribonucleic acid) and RNA (ribonucleic acid).

R.5 ETHNOBOTANIC REVIEW

It is a commonly accepted practice in archaeological studies to reference ethnographically documented plant uses as indicators of possible or even probable plant uses in prehistoric times. The ethnobotanic literature provides evidence for the exploitation of numerous plants in historic times, both by broad categories and by specific example. Evidence for exploitation from numerous sources can suggest a widespread utilization and strengthens the possibility that the same or similar resources were used in prehistoric times. Ethnographic sources outside the study area have been consulted to permit a more exhaustive review of potential uses for each plant. Ethnographic sources document that with some plants, the historic use was developed and carried from the past. A plant with medicinal qualities very likely was discovered in prehistoric times and the usage

persisted into historic times. There is, however, likely to have been a loss of knowledge concerning the utilization of plant resources as cultures moved from subsistence to agricultural economies and/or were introduced to European foods during the historic period. The ethnobotanic literature serves only as a guide indicating that the potential for utilization existed in prehistoric times--not as conclusive evidence that the resources were used. Pollen and macrofloral remains, when compared with the material culture (artifacts and features) recovered by the archaeologists, can become indicators of use. Plants represented by organic residues will be discussed in the following paragraphs in order to provide an ethnobotanic background for discussing the remains.

R.5.1 Native Plants

Carya (Hickory)

Hickories (*Carya* sp.) trees are noted to be tall, common trees of rich, open woods and bottomlands. The nuts are recorded as the most important nut used by Indians of North America at the time of contact (Reidhead 1981:189). Several species of hickory are sweet and edible, although some are bitter. The nuts usually were harvested in the fall when the outer husks dried and split, and before competing animals harvested them all. Nuts usually were shelled by crushing, often using two rocks. Native groups in the eastern United States are noted to have placed shelled nuts in boiling water. Most of the shell fragments would sink to the bottom, while the nutmeats would float or be held in suspension. The nutmeats then could be skimmed off and used immediately or dried for storage. Hickory nuts are high in fat and provide protein, carbohydrates, iron, phosphorous, potassium, trace minerals, and vitamins A and C. Their high fat content makes them vulnerable to rancidity. Many ethnographic sources suggest that hickory nut oil and "milk" were the desired product.

The pulverized nuts were placed in slowly boiling water for a long period of time. The oil from the nutmeats (hickory butter) would separate and float to the surface where it was skimmed off and stored for later use. The rest of the nutmeats would dissolve into a milky fluid (hickory milk) that was drunk or used as stock for soup. Hickory sap can be used like maple sap. Leaves and green hulls yield tan, brown, and blackish dyes. Most species of *Carya* are found in the southeastern United States, with some species reaching parts of the Midwest. Hickory trees noted in Montgomery County include *C. aquatica* (water hickory), *C. cordiformis* (bitternut hickory), *C. leioderms* (swamp hickory), *C. myristicaeformis* (nutmeg hickory), *C. ovata* (shagbark hickory), *C. texana* (black hickory), and *C. tomentosa* (mockernut hickory) (Brill and Dean 1994:171-172; Gould 1962:35; McGee 1984:264, 271; Peterson 1977:190; Talalay, et al. 1984:338-359).

Euphorbiaceae (Spurge family)

Euphorbiaceae (spurge family) are annual or perennial herbs of varied habitats. Some of the genera found in the panhandle of Texas are *Acalypha* (copperleaf), *Argythamnia* (wildmercury), *Cnidoscolus*, *Croton* (croton), *Euphorbia* (spurge), *Phyllanthus* (leafyflower), *Reverchonia*, *Stillingia*, and *Tragia* (noseburn). Many of these plants are considered poisonous due to the presence of a resinous substance, euphorbin, in the plant juice. The sap is not water-soluble, but only fat-soluble (The Huntington Library 2009), and this feature, in combination with its poisonous properties, would have made it a clever adhesive and reinforcing agent for the haft of a spear and the fibers that secure it. A famed poison in the Spanish colonial era used by the Native Americans on arrow points was made from a species of *Euphorbia*. Spurge is also commonly used as a remedy for snakebite, a purge for stomachache, and as a powder for sore lips (Burlage 1968:71-; Gould 1962:56-58).

***Helianthus* (Sunflower)**

Helianthus (sunflower) is a member of the High-spine Asteraceae group. Sunflower seeds were an important and favorite food of the Indians, who ate the seeds raw or roasted. Seeds also were parched and ground into a meal used to make breads and cakes, or to thicken gravy. Ground seeds also were made into a paste similar to peanut butter. Oil was extracted by boiling crushed seeds and skimming the oil from the water. Indians used sunflower oil to grease their hair. Roasted shells and/or seeds were once used as a coffee substitute. Sunflower seeds contain 24% protein, 47% percent oil, and are good sources of vitamin B. Sunflowers also were commonly found in southwestern myths, art, and decorations. Purple and black dyes were obtained from sunflower seeds, and a yellow dye was made from the flowers.

H. tuberosus (Jerusalem artichoke) has large, edible tubers which were boiled, baked, or fried like potatoes. These bulbs are diuretic and used to treat diabetes. A tea made from sunflowers was used for lung ailments, malaria, coughs, high fevers, as an astringent, a diuretic, and as a poultice for snakebites and spiderbites. Sunflower seeds ripen from September to October, and plants can be found in waste places, fields, low meadows, prairies, and along roadsides and railroads (Burlage 1968:47; Foster and Duke 1990:132; Kindscher 1987:124-128; Kirk 1975:133; Sweet 1976:49). Other members of the Asteraceae family were used in a variety of ways, including medicinally and as food. Most Asteraceae seeds ripen in the late summer and fall.

***Juglans* (Walnut)**

Walnuts were used less intensively than either hickory nuts or acorns (Reidhead 1981:186), due to the sparse distribution and a more bitter taste. The roots of the walnut tree produce a substance called juglone, which is toxic to other walnut trees, and they

are intolerant of shade (Talalay, et al. 1984:340). Walnuts can be collected quickly and efficiently, as the entire crop stays on the ground for some time. Nuts are high in fat and protein and are commonly used as a food source. Animals provide little competition for this resource (Reidhead 1981:186). Black walnut (*Juglans nigra*), little walnut (*Juglans microcarpa*), and Arizona walnut (*Juglans major*) are native to Texas. Arizona walnut, or nogal, is a small to medium-sized tree. Medicinally, Arizona walnut leaves are dried and steeped in hot water to make a tea for the relief of irritable bowel syndrome, colitis, colon disorders, and dysentery (Moore 1990:60). Arizona walnut tends to grow in river bottoms, in valleys, from wet streambanks to dry terraces and hillsides, and in canyons and rocky ravines (Layser 1979; Minckley 1982; Stromberg 1990).

R.6 DISCUSSION

Site 41PT185/C is located in a creek valley in the panhandle of Texas in Potter County. During the site's occupation in the Holocene period it was situated within a creek valley in a Plains environment. Four burned rocks, two metates and a mano, and two choppers and a side scraper recovered from the site were tested for organic residues using Fourier Transform Infrared Spectroscopy (FTIR) (Table R-1). No additional information about the artifacts was provided in an effort to minimize bias in the analysis and interpretation. The results from this analysis will be discussed below by artifact type, but no interpretations will be made, as there is no provenience information to guide us as to which artifacts might be in a similar location. Interpretations of the influence of the matrix in which the artifacts were found and/or their association with features are, of necessity, omitted from this writing, as we have no access to the important provenience information.

R.6.1 Burned Rock

Sample #901-3-2b, representing a burned limestone rock, yielded peaks indicating the presence of absorbed water, fats/oils/lipids and/or plant waxes, aromatic esters, pectin, proteins including nucleic acids, cellulose and carbohydrates, starch, calcium oxalate, and the polysaccharides glucomannan and galactoglucomannan (Table R-2). Polysaccharides are complex carbohydrates including starch and cellulose found in plants, and glycogen found in animals. A peak at 872 wave numbers represents the presence of both glucomannan and galactoglucomannan. These polysaccharides are predominate in the woody tissue of coniferous plants (Gymnosperms), with galactoglucomannan being a primary component. Glucomannan is also present in the wood of dicotyledons, also known as dicots (Bohicchio 2003).

No matches were made with foods in the PaleoResearch signature reference library, nor did any matches occur with modern contaminants in the forensic libraries. Agricultural references were not included in the matching processes because of the absence of sufficient site information including local vegetation and temporal association. The lack of matches with modern contaminants suggests the signature obtained from the burned limestone rock represents organic residues. Fats, lipids, and water make a very minor contribution to the signal evidenced by the low amplitude peaks in these portions of the spectrum. Three prominent, high amplitude peaks are visible in the signature at 1410, 1025, and 872 wave numbers. In order, these peaks suggest protein, starch, and polysaccharides as the most heavily represented compounds in the sample, and likely represent the general presence of non-specific high protein plant materials. Similarities with this signature were also noted with the signature produced by calcium carbonate. Calcium carbonate is the primary component of limestone, so no

interpretive significance is attached to this finding.

A second burned limestone rock, represented by sample #1337-3-2b, yielded peaks indicating the presence of absorbed water, fats/oils/lipids and/or plant waxes, aromatic esters, pectin, protein, cellulose and carbohydrates, calcium oxalate, and the polysaccharides glucomannan, galactoglucomannan, and arabinogalactan. Arabinogalactan, represented in this sample by a peak at 1139 wave numbers, is a sugar found in plant carbohydrate structures particularly gums and hemicelluloses. One of arabinogalactan's many functions is to bond with proteins to repair damage when it occurs to a plant or its parts (Nothnagel 2000). No matches were obtained for the signature from the second limestone rock with any of the references in the PaleoResearch and forensic libraries, indicating the sample is representative of unidentifiable organic materials and not modern contaminants. Low amplitude peaks in the fats and lipids portion of the spectrum suggests these compounds make only a small contribution to the signature. Only water, represented by a relatively flat line in the respective range of the spectrum, makes almost no contribution to the signature at all. Proteins, polysaccharides, and aromatic esters display the most predominate peaks in the signal at 1395, 872, and 712 wave numbers respectively, suggesting these are the most heavily represented compounds in the sample. Moderately high amplitude peaks also are visible for the polysaccharide arabinogalactan at 1139 wave numbers and for starch at 1028 wave numbers. These specific peaks likely suggest the presence primarily of plant materials in the sample; however, this collection of peaks is not characteristic of any specific plant materials. Similarities were again noted with the signature from this sample and that of calcium carbonate, also representing limestone.

Two different signatures were obtained for sample #899-3-5b of organic residues extracted from a burned sandstone rock. With each organic residue sample there is the possibility of obtaining multiple signatures because our extraction process maximizes the separation of organic molecules based on their volatility. The most volatile organics evaporate first and are, thus, concentrated in the upper portion of the extraction dish. Less volatile organics remain in the sampling solution (CHM) and are recovered in the lower portion of the dish. This action is similar to that obtained using high performance liquid chromatography (HPLC), which separates molecules based on their molecular weight. It is through this principle that we recover different signatures from different parts of the extraction dishes. This process was developed to maximize the method. We sample multiple places on each dish to maximize our signature recovery. This sampling method was developed to attempt to separate the signature of foods from that of calcium carbonates and other compounds that might be considered to be "contaminants" and are present in some samples.

This technique acknowledges that many scientific procedures are, in fact, influenced by the scientific technique employed by individuals. It is, therefore, gratifying when the angle at which the sample was evaporated produces good matches with specific foods, because there is no way to determine, prior to extraction, which are the most volatile compounds in the sample.

The signatures for sample #899-3-5b yielded peaks indicating the presence of absorbed water, fats/oils/lipids and/or plant waxes, pectin, aromatic and saturated esters, proteins including nucleic acids, humates, cellulose and carbohydrates, starch, and polysaccharides including glucomannan and galactoglucomannan. The signature from the upper portion of the dish was very complex and as a result, difficult to tease out specific

plant matches. No matches were made with any foods in the PaleoResearch signature reference library or any modern contaminants in the forensic libraries suggesting the signature is representative of organic materials and not contaminants. The only match that was made was with the signature from the lower portion of the dish. This signature matched with deteriorated cellulose between 1062 and 964 wave numbers (Table R-3). The match with cellulose could indicate either plants processed that have deteriorated to the point they are only recognizable by their general cellulose signature, or the presence of the local environmental signal representing the natural decay of plant matter. Similarities were also noted between this signature and the signature for calcium carbonate, indicating deposition of calcium carbonate on this burned sandstone rock.

Another burned sandstone rock was also sampled (CE 14) for organic residues. Two signatures were also obtained for this sample. Sample #CE 14 yielded peaks representing the presence of absorbed water, fats/oils/lipids and/or plant waxes, aromatic rings, pectin, and protein. Matches with deteriorated cellulose were made with the signature from the lower portion of the dish, and *Euphorbia* (spurge) sap was matched with the signature from the upper portion of the dish. The presence of spurge sap on the burned sandstone rock could be the result of dripping the material as it was processed in the vicinity of the rock, or the rock could have served as a working platform. However, the environmental signal is always part of every organic residue sample, and without sufficient site information it is impossible to sort out the cultural signature from the environmental one. Therefore, the match with cellulose could either be interpreted as processed plants that have deteriorated to the point they are only recognizable by their general cellulose signature, or the presence of the local environmental signal representing the natural decay of plant matter in the

sediments from which the sandstone rock was recovered.

R.6.2 Ground Stone

A sandstone metate, represented by sample #405-10, yielded peaks indicating the presence of absorbed water, fats/oils/lipids and/or plant waxes, aromatic esters, pectin, protein, cellulose and carbohydrates, starch, and the polysaccharides glucomannan and galactoglucomannan (Table R-4). No matches were made with these peaks with foods in the PaleoResearch signature reference library, nor did any matches occur with modern contaminants in the forensic libraries. Agricultural references were not included in the matching processes because of the absence of sufficient site information including local vegetation and temporal association. The lack of matches with modern contaminants suggests the signature obtained from the sandstone metate represents organic residues. The presence of high amplitude peaks at 1417, 1009, and 872 wave numbers suggest proteins, cellulose and carbohydrates, and polysaccharides make the largest contributions to the signature. Fats and lipids also appear to be represented in this sample, but to a much lesser degree than the previously listed compounds. An almost horizontal line between 3600 and 3200 wave numbers indicates very little water in the sample suggesting, perhaps, that the materials ground with this tool were very dry. Similarities were also noted between this signature and the one produced by calcium carbonate, indicating a calcium carbonate deposition on the metate.

Sample #1129-10, representing a second sandstone metate, yielded peaks indicating the presence of absorbed water, fats/oils/lipids and/or plant waxes, aromatic esters, pectin, proteins including nucleic acids, cellulose and carbohydrates, starch, and the polysaccharides glucomannan, galactoglucomannan, and arabinoglucuronoxylan.

Arabinoglucuronoxylan, represented in this sample by a peak at 1161 wave numbers, is a polysaccharide found in the cell walls of softwoods and herbaceous plants (Sjostrom 1981). No matches were obtained for the signature from the second sandstone metate with any of the references in the PaleoResearch and forensic libraries, indicating the sample is representative of unidentifiable organic materials and not modern contaminants. Like the previous sample (#405-10), the high amplitude peaks in the protein, cellulose and carbohydrate, and polysaccharide portions of the spectrum suggest these compounds make the greatest contribution to the signature. Fats and lipids appear to make a minor contribution as well, but again, not to the same degree as proteins, cellulose and carbohydrates, and polysaccharides. Low amplitude peaks between 3600 and 3200 wave numbers indicate only a small amount of water in the sample. Based on the FTIR signatures produced from this sample (#1129-10), and that of sample #405-10, it appears these two sandstone metates were probably used to process similar materials, but without sufficient site information, further interpretations cannot be made. Similarities were also noted between this signature and the signature produced by calcium carbonate, indicating the presence of calcium carbonate deposition.

A quartzite mano, represented by sample #1175-10, yielded peaks indicating the presence of absorbed water, fats/oils/lipids and/or plant waxes, aromatic esters, pectin, protein, and cellulose and carbohydrates. No matches were made with this signature with any foods in the PaleoResearch reference library or any modern contaminants in the forensic libraries suggesting the signature is representative of organic materials and not contaminants. A high amplitude peak at 1001 wave numbers suggests cellulose and carbohydrates make the largest contribution to the signature, and might suggest processing plant materials of some kind with this groundstone; however, in the absence of

vital site information, no further interpretations can be made. Polysaccharides also appear to contribute to the signature, which is evidence by a moderate amplitude peak at 873 wave numbers. Proteins, fats, and lipids make only a small contribution (visible by low amplitude peaks between 1600 and 1400 wave numbers), while water (almost horizontal line between 3600 to 3200 wave numbers) makes little to no contribution to the signature. Only minor similarities were noted between this signature and the one produced by calcium carbonate suggesting that, if calcium carbonate is present in the sample, it is only in a small amount.

R.6.3 Lithic Tools

A Potter chert chopper was sampled (#467-10) for organic residues. Sample #467-10 yielded peaks representing the presence of absorbed water, fats/oils/lipids and/or plant waxes, pectin, aromatic rings, aromatic and saturated esters, proteins including nucleic acids, cellulose and carbohydrates, and the polysaccharide arabinan (Table R-5). Peaks at 1098 and 919 wave numbers indicate the presence of arabinan in the sample. In plants, arabinan is essential for the function of guard cells that “play a key role in the ability of plants to survive on dry land, because their movements regulate the exchange of gases and water vapor between the external environment and the interior of the plant” (Jones 2003:11783). Matches with these peaks were made with *Carya* (hickory) and *Juglans* (walnut) nutmeat, bird blood, and cooked rabbit (Table R-6). Although matches are made with specific nuts and meats, these matches are interpreted at a general, rather than specific level, suggesting the chopper could have been used to process any types of locally available nuts and meats. Drainages in the panhandle area of Texas and Oklahoma might well have supported hickory and/or walnut trees in the past, even if they are not part of the modern vegetation community. Other nut-bearing trees also might have been

part of the local vegetation in drainages and their associated riparian communities. However, without sufficient site information it is impossible to determine if these matches represent the cultural or environmental signal. As a result, other matches with deteriorated cellulose could be interpreted as other plants processed with the tool, or the local environmental signature representing the natural deterioration of plant matter.

Sample #627-10, representing an Edwards chert chopper, yielded peaks indicating the presence of absorbed water, fats/oils/lipids and/or plant waxes, pectin, aromatic rings, aromatic and saturated esters, protein, humates, cellulose and carbohydrates, β -D-cellulose, and polysaccharides including arabinogalactan, galactoglucomannan, rhamnogalacturonan, and glucan. A peak at 916 wave numbers indicates the presence of glucan. Glucan, often found in association with pectin, is also a polysaccharide that contains only glucose, or simple sugar, as a structural component (Stephen 2006). Glucans reside in the cell walls of plants and trees and many forms of bacteria and fungi (Stephen 2006). Most people are familiar with beta glucans, which are harvested from these sources and administered to humans as immune boosting supplements. Rhamnogalacturonans, also represented in this sample by a peak at 916 wave numbers, are specific pectic polysaccharides that reside in the cell walls of all land plants, and result from the degradation of pectin (Willats 2001). Finally, a peak at 916 wave numbers also indicates the presence of β -D-cellulose. β -D-cellulose, which is found in the cell walls of plants, is one of three specific types of cellulose, alpha cellulose (true cellulose), beta cellulose, and gamma cellulose, which are differentiated by their molecular structures and properties (Gooch 2007; Kono 2006:318).

An upper and lower signature were obtained for this sample. The upper signature yielded no matches to foods in the PaleoResearch

signature reference library, and it was not matched with modern contaminants in the forensic libraries suggesting the signature represents a complex organic signal from which specific foods cannot be teased out and identified. The lower signature matched strongly with *Helianthus* (sunflower) seeds. This match might suggest the chopper was used to process plant materials from members of the sunflower family, but in the absence of critical site information it is impossible to determine if these matches indicate foods processed with the tool or the local environmental signal. Choppers are not usually considered to have been used for processing seeds. Certainly, any association with seeds of the sunflower family might have introduced this signal. Storage of tools when they are not being used is one of several “unknown” factors that may contribute a signal, yet not be indicative of use of the tool.

An Alibates side scraper, represented by sample #452-10, yielded peaks indicating the presence of absorbed water, fats/oils/lipids and/or plant waxes, pectin, aromatic rings, aromatic and saturated esters, proteins including nucleic acids, humates, cellulose and carbohydrates, starch, and the polysaccharides galactoglucomannan, rhamnogalacturonan, glucan, and xyloglucan. Xyloglucan, represented in this sample by a peak at 1041 wave numbers, is the most abundant hemicellulose in the cell walls of most dicotyledonous plants, and all vascular plants (Fry 1989).

The primary cell wall of [these plants] is composed of cellulose microfibrils embedded in a matrix of hemicellulosic and pectic polysaccharides, of which the hemicellulose xyloglucan is a major component. Xyloglucan and cellulose together make up about two-thirds of the dry weight of primary cell walls and are the major tension-bearing components of the matrix. During cell expansion and elongation, the cell wall continually

undergoes temporary loosening followed by rapid reinforcement of wall structure. Xyloglucan endotransglycosylases (XETs) are unique enzymes in plants that are capable of modulating the chemistry of the matrix and therefore performing both of these functions (Eckardt 2004:792).

It is through this process that plant cell wall growth and repair occurs (Moore 1988).

Two signatures were also obtained for the organic residues extracted from the Alibates side scraper. No matches with the upper signature were made with foods in the PaleoResearch reference library, nor did any matches occur with modern contaminants in the forensic libraries.

The lack of matches with modern contaminants suggests the upper signature represents organic residues, but because of the complexity of the signal, specific foods cannot be identified. The lower signature matched well with Helianthus (sunflower) seed shells and duck skin, perhaps suggesting members of the sunflower family and meat were processed with this tool or that the tool was stored in close proximity to foods. However, without vital site information the cultural signal cannot be separated out from the environmental one.

R.7 SUMMARY AND CONCLUSIONS

As a whole, the FTIR record for the samples from site 41PT185/C yielded little information on the cultural utilization of plant and animal materials because of the absence of sufficient site information. FTIR analysis of the burned stone revealed matches with cellulose for samples #899-3-5b and #CE 14, and spurge sap for sample #CE 14, which could represent either a cultural or environmental component of the signature, but without additional information this cannot be determined. Specific foods could not be teased out and identified from the complex organic signatures obtained for the other two burned stone samples #901-3-2b and #1337-3-2b. Organic residue analysis of the ground stone yielded no matches, only complex organic signatures from which it was impossible to identify specific foods. The lithic tools examined for organic residues yielded matches with nuts, seeds, cellulose, and meat, which could represent the local environmental signature, or suggest the tools were used for processing both plant and animal materials. Without vital site information, which was withheld from PaleoResearch Institute because it was believed that it would bias the analyses, it is impossible to separate the cultural from the environmental signal and make any kind of interpretations.

TABLE R-1. PROVENIENCE DATA FOR SAMPLES FROM SITE 41PT185/C, TEXAS

Sample No.	Provenience / Description	Analysis
#901-3-2b	Burned rock, limestone	FTIR
#1337-3-2b	Burned rock, limestone	FTIR
#899-3-5b	Burned rock, sandstone	FTIR
#CE 14	Burned rock, sandstone	FTIR
#405-10	Metate, sandstone	FTIR
#1129-10	Metate, sandstone	FTIR

Sample No.	Provenience / Description	Analysis
#1175-10	Mano, quartzite	FTIR
#467-10	Chopper, Potter chert	FTIR
#627-10	Chopper, Edwards chert	FTIR
#452-10	Side scraper, Alibates	FTIR

TABLE R-2. FTIR PEAK SUMMARY TABLE FOR BURNED ROCK SAMPLES FROM SITE 41PT185/C, TEXAS

Peak Range	Represents	#901-3-2b Burned rock	#1337-3-2b Burned rock	#899-3-5b Burned rock	#CE 14 Burned rock
3600-3200	Absorbed Water	3576 3517 3484 3388 3372 3297	3431 3389 3341 3313 3290 3260 3234	3590 3486 3478 3392 3342 3293 3205	3360 3355
3371, 3342, 3334	O-H Stretch	3372	3341	3342	
3000-2800	Aldehydes: fats, oils, lipids, waxes	2922 2873 2851	2981 2971 2925 2889	2918 2849	2955 2920 2850
2974, 2968, 2965, 2962, 2956, 2872	CH3 Asymmetric stretch				2955
2959, 2938, 2936, 2934, 2931, 2930, 2926, 2924, 2922	CH2 Asymmetric stretch	2922	2925		
2879, 2875, 2873, 2871, 2870	CH3 Symmetric stretch	2873			
1750-1730	Saturated esters			1738	
Peak Range	Represents	901-3-2b Burned rock	1337-3-2b Burned rock	899-3-5b Burned rock	CE 14 Burned rock
1730-1705	Aromatic esters			1721 1711	

Peak Range	Represents	#901-3-2b Burned rock	#1337-3-2b Burned rock	#899-3-5b Burned rock	#CE 14 Burned rock
1700-1500	Protein, incl. 1650 protein	1655 1648 1638 1561	1654 1648 1636 1618 1577	1665 1655 1645 1574 1537	1631
1680-1600, 1260, 955	Pectin	1655 1648 1638	1654 1648 1636 1618	1665 1655 1645	1631
1660-1655	Proteins, Nucleic acids	1655		1655	
1500-1400	Protein	1410		1462 1420	1465
1465-1455	Protein/lipids			1462	1465
1490-1350	Protein	1410	1395	1462 1420 1376	1465
1394, 1379, 1366	Split CH3 umbrella mode, 1:2 intensity				1366
1377	Fats, oils, lipids, humates			1376	
1170-1150, 1050, 1030	Cellulose			1164	
Peak Range	Represents	901-3-2b Burned rock	1337-3-2b Burned rock	899-3-5b Burned rock	CE 14 Burned rock
1139	Arabinogalactan		1139		
1130-1100	Aromatic esters			1111	
1110	Starch			1111	
1028-1000	Cellulose Carbohydrates	1025	1028	1018 1016	

Appendix R
Organic Residue (FTIR) Analysis of Burned Rock, Ground Stone & Lithic Samples

Peak Range	Represents	#901-3-2b Burned rock	#1337-3-2b Burned rock	#899-3-5b Burned rock	#CE 14 Burned rock
1028	Ester O-C-C stretch		1028		
1026	Starch	1025			
1019	Primary alcohol CH ₂ -O stretch			1018	
931	Starch			931	
874	Polysaccharides			874	
872	CaCO ₃	872	872	872	
872	+Glucomannan (9:1, w/w), Glucomannan, Galactoglucomannan	872	872	872	
850	Starch			849	
830	Symmetric C-C-O stretch			831	
780	Calcium oxalate	780	781		
750	Out-of-plane C-H bend			750	
750-700	Aromatic esters	712	712	750 719 712	
719-22	CH ₂ Rock (methylene)			719	
692	Aromatic ring bend (phenyl ether)				693
660, 648	O-H Out-of-plane bend	647		649	

**TABLE R-3. MATCHES SUMMARY TABLE FOR FTIR RESULTS FROM BURNED ROCK
 SAMPLES FROM SITE 41PT185/C, TEXAS**

Match (Scientific Name)	Match (Common Name)	Part	#899-3-5b Burned rock (Range)	#CE 14 Burned rock (Range)
Deteriorated Cellulose	Deteriorated cellulose		#1062-964	#1073-926
<i>Euphorbia</i>	Spurge	Sap		#1695-1573

**TABLE R-4. FTIR PEAK SUMMARY TABLE FOR GROUNDSTONE
 SAMPLES FROM SITE 41PT185/C, TEXAS**

Peak Range	Represents	#405-10 Metate	#1129-10 Metate	#1175-10 Mano
3600-3200	Absorbed Water	3372	3519 3465 3427 3408 3326 3287	3527 3437 3382 3331 3305 3242
3371, 3342, 3334	O-H Stretch	3372		
3000-2800	Aldehydes: fats, oils, lipids, waxes	2918 2850	2921 2851	2953 2920 2850
2959, 2938, 2936, 2934, 2931, 2930, 2926, 2924, 2922	CH2 Asymmetric stretch		2921	
1730-1705	Aromatic esters	1727		
1700-1500	Protein, incl. 1650 protein	1645 1576 1538	1658 1645 1630 1578	1645 1578 1540
1680-1600, 1260, 955	Pectin	1645	1658 1645 1630	1645
1660-1655	Proteins, Nucleic acids		1658	
1500-1400	Protein	1417	1415	1420
1490-1350	Protein	1417	1415	1420
1170-1150, 1050, 1030	Cellulose		1161	

Peak Range	Represents	#405-10 Metate	#1129-10 Metate	#1175-10 Mano
1161, 1151	Arabinoglucuronoxylan + Galactoglucomannan		1161	
1028-1000	Cellulose Carbohydrates	1009	1018 1008	1001
Peak Range	Represents	405-10 Metate	1129-10 Metate	1175-10 Mano
1019	Primary alcohol CH ₂ -O stretch		1018	
872	CaCO ₃	872	872	
872	+Glucomannan (9:1, w/w), Glucomannan, Galactoglucomannan	872	872	
850	Starch	849	849	
750-700	Aromatic esters	712	712	712

TABLE R-5. FTIR PEAK SUMMARY TABLE FOR LITHIC TOOL SAMPLES FROM SITE 41PT185/C, TEXAS

Peak Range	Represents	#467-10 Chopper	#627-10 Chopper	#452-10 Side scraper
3600-3200	Absorbed Water	3538 3528 3422 3390 3295	3372 3350 3275	3423 3335 3207
3371, 3342, 3334	O-H Stretch		3372	3335
3000-2800	Aldehydes: fats, oils, lipids, waxes	2954 2920 2851	2987 2954 2918 2850	2985 2953 2921 2852
2959, 2938, 2936, 2934, 2931, 2930, 2926, 2924, 2922	CH ₂ Asymmetric stretch			2921
1750-1730	Saturated esters	1736	1739	
1730-1705	Aromatic esters	1712	1710	1725 1712

Peak Range	Represents	#467-10 Chopper	#627-10 Chopper	#452-10 Side scraper
1700-1500	Protein, incl. 1650 protein	1657 1647 1576 1539	1664 1626 1604 1576 1539	1659 1601 1553 1535 1517
1680-1600, 1260, 955	Pectin	1657 1647	1664 1626 1604	1659 1601
1660-1655	Proteins, Nucleic acids	1657		1659
1604, 1602, 1586, 1497, 1362	Aromatic ring mode		1604	1601
Peak Range	Represents	467-10 Chopper	627-10 Chopper	452-10 Side scraper
1500-1400	Protein	1464 1453 1435 1418	1465 1434 1419	1463 1456 1414
1465-1455	Protein/lipids	1464	1465	1463 1456
1453	Aromatic ring mode	1453		
1490-1350	Protein	1464 1453 1435 1418 1379 1364	1465 1434 1419 1377	1463 1456 1414 1378 1367
1394, 1379, 1366	Split CH3 umbrella mode, 1:2 intensity			1367
1384, 1364	Split CH3 umbrella mode, 1:1 intensity	1364		
1377	Fats, oils, lipids, humates		1377	1378
1170	Lipids			1169
1170-1150, 1050, 1030	Cellulose		1165	1169
1130-1100	Aromatic esters		1112	
1100-1030	Saturated esters	1098	1032	1071 1041
1028-1000	Cellulose Carbohydrates	1019 1004	1028 1011	1028 1026

Appendix R
Organic Residue (FTIR) Analysis of Burned Rock, Ground Stone & Lithic Samples

Peak Range	Represents	#467-10 Chopper	#627-10 Chopper	#452-10 Side scraper
1097	Arabinan	1098		
1059, 1033	Cellulose		1032	
1041, 1026	Glucan			1041 1026
1041	Xyloglucan			1041
1034, 960	Galactoglucomannan			961
Peak Range	Represents	467-10 Chopper	627-10 Chopper	452-10 Side scraper
1028	Ester O-C-C stretch		1028	1028
1026	Starch			1026
1019	Primary alcohol CH ₂ -O stretch	1019		
953	Pectin		953	
951, 916	Rhamnogalacturonan		916	950
934	Galactoglucomannan		935	
918	Arabinan	919		
916, 908	β-D-cellulose		916	
916	Arabinogalactan (Type II), Glucan		916	
874	Polysaccharides		874	
835	Pectin			835
813	Galactoglucomannan			812
750-700	Aromatic esters	721 712	721	721
719-22	CH ₂ Rock (methylene)	721	721	721
697	Aromatic ring bend		696	
692	Aromatic ring bend (phenyl ether)			692

Peak Range	Represents	#467-10 Chopper	#627-10 Chopper	#452-10 Side scraper
660, 648	O-H Out-of-plane bend			661

TABLE R-6. MATCHES SUMMARY TABLE FOR FTIR RESULTS FROM LITHIC TOOL SAMPLES FROM SITE 41PT185/C, TEXAS

Match (Scientific Name)	Match (Common Name)	Part	#467-10 Chopper (Range)	#627-10 Chopper (Range)	#452-10 Side scraper (Range)
<i>Carya</i>	Hickory	Nutmeat	3000-2800 1765-1699 1491-1385		
Deteriorated Cellulose	Deteriorated cellulose		3000-2800		
<i>Helianthus</i>	Sunflower seed	Nutmeat		3000-2800 1757-1691 1491-1405 1401-1344 988-919	
		Shell			3000-2800 1687-1630 1487-1417
<i>Juglans</i>	Walnut	Nutmeat	3000-2800		
Bird	Bird	Blood	3000-2800		
Duck	Duck	Skin			3000-2800 739-702
Rabbit	Rabbit	Meat (cooked)	3000-2800		

R.8 REFERENCES CITED

Akers, Hugh A. and S. Venkatasubramanian 1997 Stalking the Asparagus Trail. Food and Foodways 7(2):131-136.

Arms, Karen and Pamela S. Camp 1995 Biology. Saunders College Publishing, Fort Worth.

Awano, Tatsuya, Keiji Takabe, Minoru Fujita, and Geoffrey Daniel 2000 Deposition of Glucuronoxylans on the Secondary Cell Wall of Japanese Beech as Observed by Immuno-scanning Electron Microscopy. Protoplasma 212:72-79.

Biology-online 2009a D-glucose. Electronic document, www.biology-

- online.org/dictionary/D-glucose, accessed July 12, 2009.
- 2009b Galactan. Electronic document, www.biology-online.org/dictionary/Galactan, accessed July 29, 2009.
- Bohicchio, R. and F. Reicher 2003 Are Hemicelluloses from Podocarpus Lambertii Typical of Gymnosperms? Carbohydrate Polymers 53(2):127-136.
- Briggs, D.E.G. 1999 Molecular Taphonomy of Animal and Plant Cuticles: Selective Preservation and Diagenesis. Philosophical Transactions of the Royal Society B: Biological Sciences 354(1379):7-17.
- Brill, Steve and Evelyn Dean 1994 Identifying and Harvesting Edible and Medicinal Plants in Wild (and Not So Wild) Places. Hearst Books, New York, New York.
- Burlage, Henry M. 1968 Index of Plants of Texas with Reputed Medicinal and Poisonous Properties. Henry M. Burlage, Austin Texas.
- Capek, P., A. Kardosova, and D. Lath 1999 A Neutral Heteropolysaccharide from the Flowers of Malva mauritiana L. Chemistry Papers 52(2):131-136.
- Carlile, Michael J. and Sarah C. Watkinson 1994 The Fungi. Academic Press, San Diego.
- Chabannes, Matthieu, Katia Ruel, Arata Yoshinaga, Brigitte Chabbert, Alain Jauneau, Jean-Paul Joseleau, and Alain-Michel Boudet 2001 In Situ Analysis of Lignins in Transgenic Tobacco Reveals a Differential Impact of Individual Transformations on the Spatial Patterns of Lignin Deposition at the Cellular and Subcellular Levels. The Plant Journal 28:271-282.
- Combaret, Lydie, Dominique Dardevet, Isabelle Rieu, Marie-Noelle Pouch, Daniel Bechet, Daniel Taillandier, Jean Grizard, and Didier Attaix 2005 A Leucine-Supplemented Diet Restores the Defective Postprandial Inhibition of Proteasome-Dependent Proteolysis in Aged Rat Skeletal Muscle. Journal of Physiology 569(2):489-499.
- Crawford, R.L. 1981 Lignin Biodegradation and Transformation. John Wiley and Sons, New York.
- Creighton, Thomas E. 1993 Proteins: Structures and Molecular Properties. 2nd ed. W. H. Freeman and Company, Ltd., San Francisco.
- Driscoll, D. and P. Copeland 2003 Mechanism and Regulation of Selenoprotein Synthesis. Annual Review of Nutrition 23:17-40.
- Ebringerova, Anna, Zdenka Hromadkova, and Thomas Heinze 2005 Hemicellulose. In Polysaccharides I: Structure, Characterization, and Use, edited by T. Heinze, pp. 1-67. Springer-Verlag, Berlin.
- Eckardt, Nancy A. 2004 Inside the Matrix: Crystal Structure of a Zyloglucan Endotransglycosylase. The Plant Cell 16:792-793.
- Esau, Katherine 1977 Anatomy of Seed Plants. John Wiley and Sons, New York.
- Foster, Steven and James A. Duke 1990 A Field Guide to Medicinal Plants: Eastern and Central North America. Houghton Mifflin Company, Boston.
- Fry, S.C. 1989 The Structure and Functions of Xyloglucan. Journal of Experimental Biology 40:1-11.
- Furst, P. and P. Stehle 2004 What are the Essential Elements Needed for the Determination of Amino Acid Requirements

- in Humans? *Journal of Nutrition* 134(6):1558S-1565S.
- Garrison, Robert, Jr. and Elizabeth Somer 1985 *The Nutrition Desk Reference*. Keats Publishing, Inc., New Canaan, Connecticut.
- Gooch, Jan W. 2007 *Encyclopedic Dictionary of Polymers*. Springer Science+Business Media, LLC, New York.
- Gould, F. W. 1962 *Texas Plants: A Checklist and Ecological Summary*. Texas Agricultural Experiment Station. Submitted to M.P. 585.
- Green, N. P. O., G. W. Stout, and D. J. Taylor 2006 *Biological Science 1 & 2*. 3rd ed. Cambridge University Press, Cambridge.
- Isaksson, Sven 1999 *Guided By Light: The Swift Characterisation of Ancient Organic Matter by FTIR, IR-Fingerprinting and Hierarchical Cluster Analysis*. *Laborativ Arkeologi* 12:35-43.
- Jones, Louise, Jennifer L. Milne, David Ashford, and Simon J. McQueen-Mason 2003 *Cell Wall Arabinan is Essential for Guard Cell Function*. *Proceedings of the National Academy of Sciences of the United States of America* 100(20):11783-11788.
- Kacurakova, A., P. Capek, V. Sasinkova, and A. Ebringerova 2000 *FT-IR Study of Plant Cell Wall Model Compounds: Pectic Polysaccharides and Hemicelluloses*. *Carbohydrate Polymers* 43:195-203.
- Kindscher, Kelly 1987 *Edible Wild Plants of the Prairie*. University Press of Kansas, Lawrence, Kansas.
- Kirk, Donald R. 1975 *Wild Edible Plants of Western North America*. Naturegraph Publishers, Happy Camp, California.
- Kono, Hiroyuki and Yukari Numata 2006 *Structural Investigation of Cellulose I' and I\$ by 2D RFDR NMR Spectroscopy: Determination of Sequence of Magnetically Inequivalent D-glucose Units Along Cellulose Chain*. *Cellulose* 13:317-326.
- Layser, Earle F.; Schubert, Gilbert H. 1979 *Preliminary classification for the coniferous forest and woodland series of Arizona and New Mexico*. U.S. Dept. of Agriculture, Forest Service, Rocky Mountain Forest and Range Experiment Station.
- Lebo, Stuart E. Jr., Jerry D. Gargulak, and Timothy J. McNally 2001 *Lignin*. In *Encyclopedia of Chemical Technology*. 4th ed. John Wiley and Sons, Inc.
- Lee, Wha-Joon, Richard A. Hawkins, Juan R. Vina, and Darryl R. Peterson 1998 *Glutamine Transport by the Blood-Brain Barrier: A Possible Mechanism for Nitrogen Removal*. *American Journal of Physiology Cell Physiology* 274(4):C1101-C1107.
- Lemieux, R.U. and G. Huber 1953 *A Chemical Synthesis of Sucrose*. *Journal of the American Chemical Society* 75(16):4118.
- Martone, Patrick T., Jose M. Estevez, Fachuang Lu, Katia Ruel, Mark W. Denny, Chris Somerville, and John Ralph 2009 *Discovery of Lignin in Seaweed Reveals Convergent Evolution of Cell-Wall Architecture*. *Current Biology* 19(2).
- Marzio, L., R. Del Bianco, M.D. Donne, O. Pieramico, and F. Cucurullo 1989 *Mouth-to-Cecum Transit Time in Patients Affected by Chronic Constipation: Effect of Glucomannan*. *The American Journal of Gastroenterology* 84(8):888-891.
- Mayes, Peter A. 2000 *Carbohydrates of Physiologic Significance*. In *Harper's Biochemistry*, edited by D.
- K. F. Robert K. Murray, Peter A. Mayes, and Victor W. Rodwell, pp. 149-159. McGraw-Hill, New York.

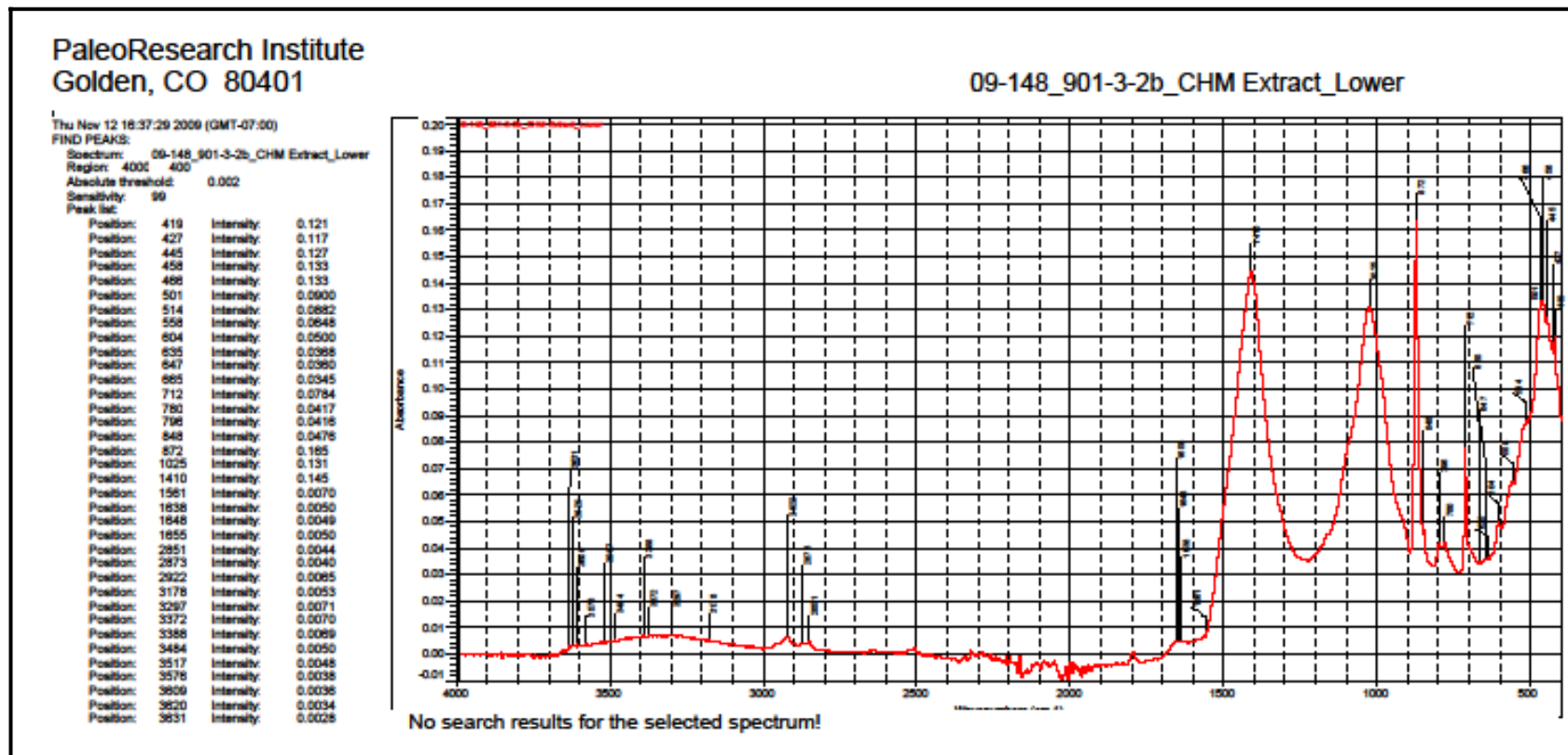
- McGee, Harold 1984 *On Food and Cooking*. Charles Scribner's Sons, New York, New York.
- Minckley, W. L. ; Brown, David E. 1982 Wetlands. In Brown, David E., ed. *Biotic Communities of the American Southwest--United States and Mexico*. *Desert Plants* 4(1-4):223-287.
- Moore, Michael 1990 *Los Remedios: Traditional Herbal Remedies of the Southwest*. Red Crane Books, Santa Fe, New Mexico.
- Moore, P.J. and L.A. Saehelin 1988 Immunogold Localisation of the Cell Wall Matrix Polysaccharides Rhamnogalacturonan_I and Xyloglucan During Cell Expansion and Cytokinesis in *Trifolium pratense* L. - Implications for Secretory Pathways. *Planta* 174:433-445.
- Mosby 2008 *Mosby's Medical Dictionary*. Mosby/Elsevier, St. Louis.
- Mothet, Jean-Pierre, Angele T. Parent, Herman Wolosker, Roscoe O. Brady, Jr., David J. Linden, Christopher D. Ferris, Michael A. Rogawski, and Solomon H. Snyder 2000 D-serine is an Endogenous Ligand for the Glycine Site of the N-methyl-D-aspartate Receptor. *Proceedings of the National Academy of Sciences* 97(9):4926-4931.
- Murray, N. D., Michael and Pizzorno, N. D., Joseph 1998 *Encyclopedia of Natural Medicine*. Random House Inc., New York.
- Murray, Robert K., Daryl K. Granner, Peter A. Mayes and Victor W. Rodwell 2000 *Harper's Biochemistry*. 25th Edition ed. McGraw-Hill, New York.
- Nations, Food and Agriculture Organization of the United 2009 *Effects of Stress and Injury on Meat and By-product Quality*. Electronic document, www.fao.org/docrep/003/X6909E/x6909e04.htm, accessed November 17, 2009.
- Nelson, D. L. and M. M. Cox 2005 *Lehninger Principles of Biochemistry*. 4th ed. W. H. Freeman and Company, New York.
- Nothnagel, Eugene A., Antony Bacic, and Adrienne E. Clarke 2000 *Cell and Developmental Biology of Arabinogalactan-proteins*. Kluwer Academic, New York.
- Osiecki, Henry, Fiona Meeke, and Jenny Smith 2004 *The Encyclopedia of Clinical Nutrition*. Volume 1, *The Nervous System*. Bio Concepts Publishing, Eagle Farm Qld., Australia.
- Peterson, Lee A. 1977 *Edible Wild Plants*. Collier Books, New York, New York.
- Reeds, P.J. 2000 Dispensable and Indispensable Amino Acids for Humans. *Journal of Nutrition* 130(7):1835S-1840S.
- Reeds, Peter J., Douglas G. Burrin, Barbara Stoll, and Farook Jahoor 2000 Intestinal Glutamate Metabolism. *Journal of Nutrition* 130(4):978S-982S.
- Reidhead, Van A. 1981 *A Linear Programming Model of Prehistoric Subsistence Optimization: A Southeastern Indiana Example*. *Prehistory Research Series VI (1)*. Indiana Historical Society, Indianapolis, Indiana.
- Rodnina, M. V., M. Beringer, and W. Wintermeyer 2007 How Ribosomes Make Peptide Bonds. *Trends in Biochemical Sciences* 32(1):20-26.
- Rosenthal, J., A. Angel, and J. Farkas 1974 Metabolic Fate of Leucine: A Significant Sterol Precursor in Adipose Tissue and Muscle. *American Journal of Physiology* 226(2):411-418.

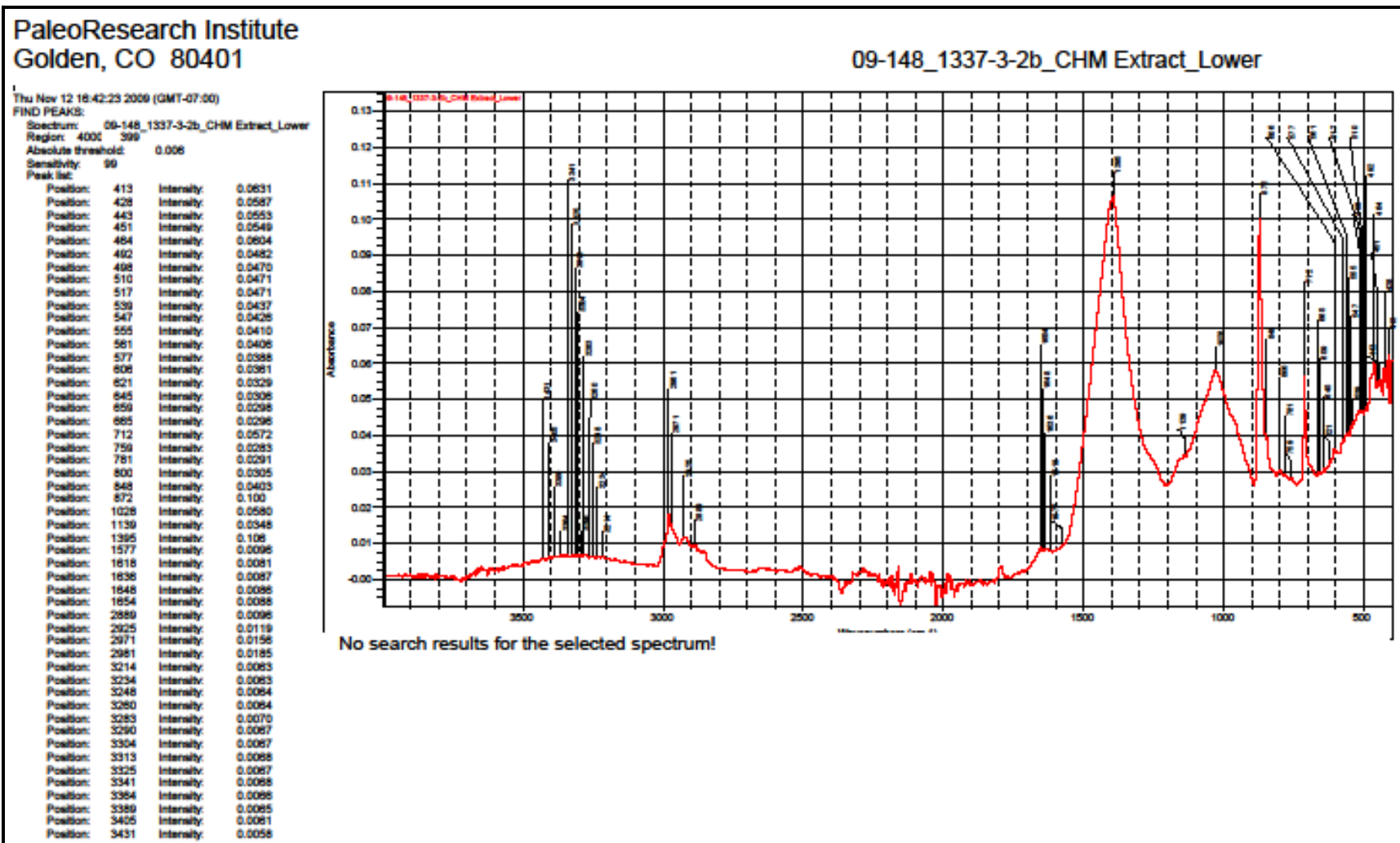
- Saenger, Wolfram 1984 Principles of Nucleic Acid Structure. Springer, New York.
- Sheeler, Phillip and Donald E. Bianchi 2004 Cell and Molecular Biology. 3rd ed. John Wiley and Sons, New York.
- Sjostrom, J. 1981 Wood Chemistry: Fundamentals and Applications. Academic Press, New York.
- Smith, Brian 1999 Infrared Spectral Interpretation, A Systematic Approach. CRC Press, New York.
- Stephen, Alistair M., Glyn O. Phillips, and Peter A. Williams 2006 Food Polysaccharides and Their Applications. Taylor & Francis, Boca Raton.
- Stromberg, Juliet C., Patten, Duncan T. 1990 Flower Production and Floral Ratios of a Southwestern Riparian Tree, Arizona walnut (*Juglans major*). *American Midland Naturalist* 124(2):269-277.
- Sweet, Muriel 1976 Common and Useful Plants of the West. Naturegraph Company, Healdsburg, California.
- Talalay, Laurie, Donald R. Keller and Patrick J. Munson 1984 Hickory Nuts, Walnuts, Butternuts, and Hazelnuts: Observations and Experiments Relevant to their Aboriginal Exploitation in Eastern North America. In *Experiments and Observations on Aboriginal Wild Plant Food Utilization in Eastern North America*, edited by P. J. Munson, pp. 338-359. Prehistory Research Series. vol. VI (2). Indiana Historical Society, Indianapolis, Indiana.
- The Huntington Library, Art Collections, and Botanical Gardens 2009 International Succulent Introductions: Plant Introductions of the Huntington Botanical Gardens. Electronic document, www.huntington.org/BotanicalDiv/ISI2003/isi/2003-26.html, accessed October 1, 2009.
- Updegraff, D.M. 1969 Semimicro Determination of Cellulose in Biological Materials. *Analytical Biochemistry* 32:420-424.
- Vickery, H. B. and C.L. Schmidt 1931 The History of the Discovery of the Amino Acids. *Chemical Reviews* 9:98-207.
- Walker, J. C. F. 2006 Primary Wood Processing: Principles and Practice. Springer, Dordrecht, The Netherlands.
- Wang, Dun, Yao-yu Bai, Jiang-hong Li, and Chuan-xi Zhang 2004 Nutritional Value of the Field Cricket (*Gryllus testaceus walker*). *Entomologia Sinica* 11(4):275-283.
- Wardlaw, Gordon M., Ph.D., R.D., L.D. and Paul M. Insel, Ph.D. 1996 Perspectives in Nutrition. Mosby-Year Book, Inc., St. Louis, Missouri.
- Wardrop, A.B. 1969 The Structure of the Cell Wall in Lignified Collenchyma of *Eryngium* sp. (Umbelliferae). *Australian Journal of Botany* 17:229-240.
- Waring, R.H., S.C. Mitchell, and G.R. Fenwick 1987 The Chemical Nature of the Urinary Odour Produced by Man After Asparagus Ingestion. *Xenobiotica* 17:1363-1371.
- Wilkie, K. C. B. 1985 New Perspectives on Non-Cellulosic Cell-Wall Polysaccharides (Hemicellulose and Pectic Substances) of Land Plants. In *Biochemistry of Plant Cell Walls*, edited by C. T. a. J. R. H. Brett. Cambridge University Press, Cambridge.
- Willats, William, Lesley McCartney, William Mackie, and J. Paul Knox 2001 Pectin: Cell Biology and Prospects for Functional Analysis. *Plant Molecular Biology* 47:9-27.
- Wurtman, R. J., F. Hefti, and E. Melamed 1980 Precursor Control of Neurotransmitter

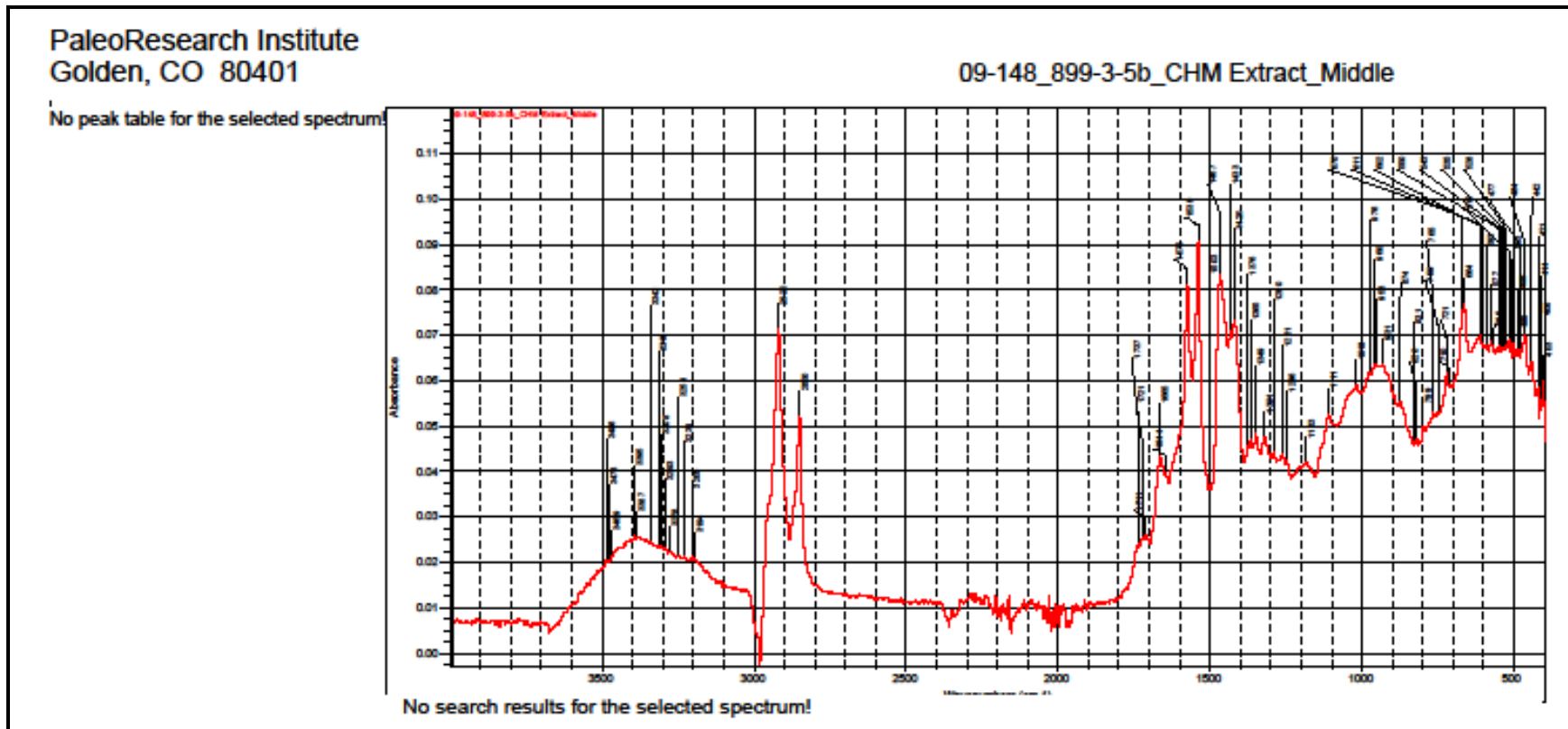
Synthesis. Pharmacological Reviews
32(4):315-335.

Young, V.R. 1994 Adult Amino Acid
Requirements: The Case for a Major
Revision in Current Recommendations.
Journal of Nutrition 124(8):1517S-1523S.

This page intentionally left blank.







PaleoResearch Institute
Golden, CO 80401

09-148_899-3-5b_CHM Extract_Upper

Thu Nov 12 16:36:45 2009 (GMT-07:00)

FIND PEAKS:

Spectrum: 09-148_899-3-5b_CHM Extract_Upper

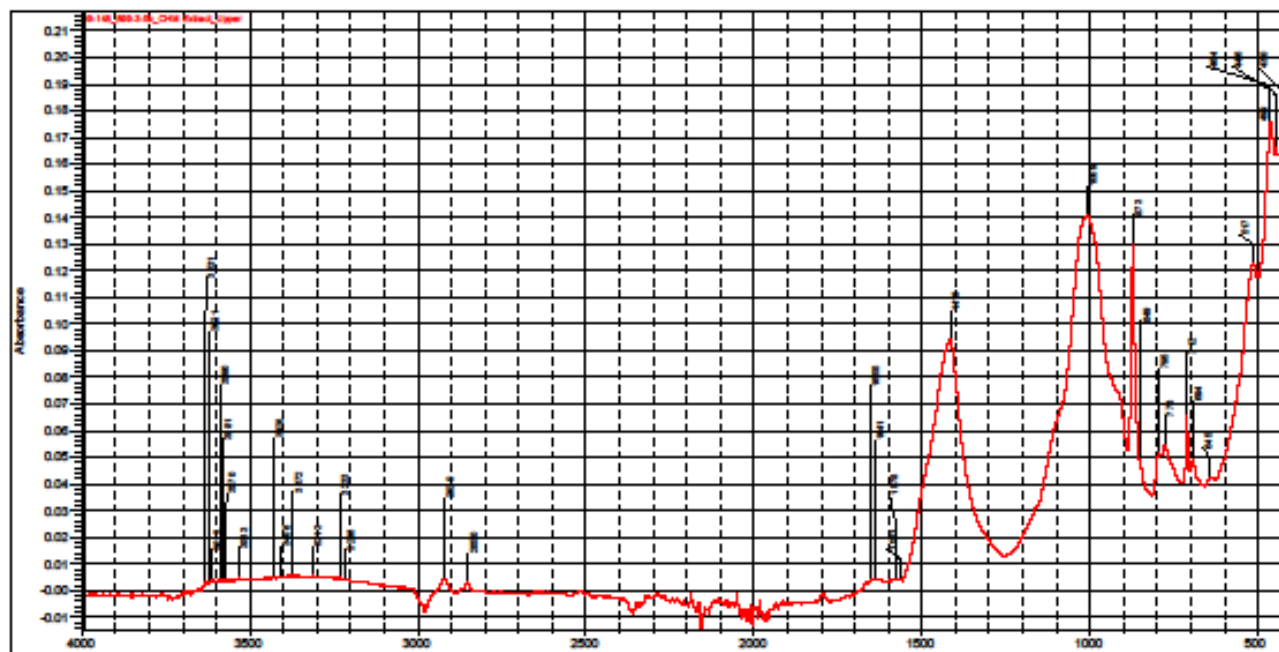
Region: 4000 400

Absolute threshold: 0.003

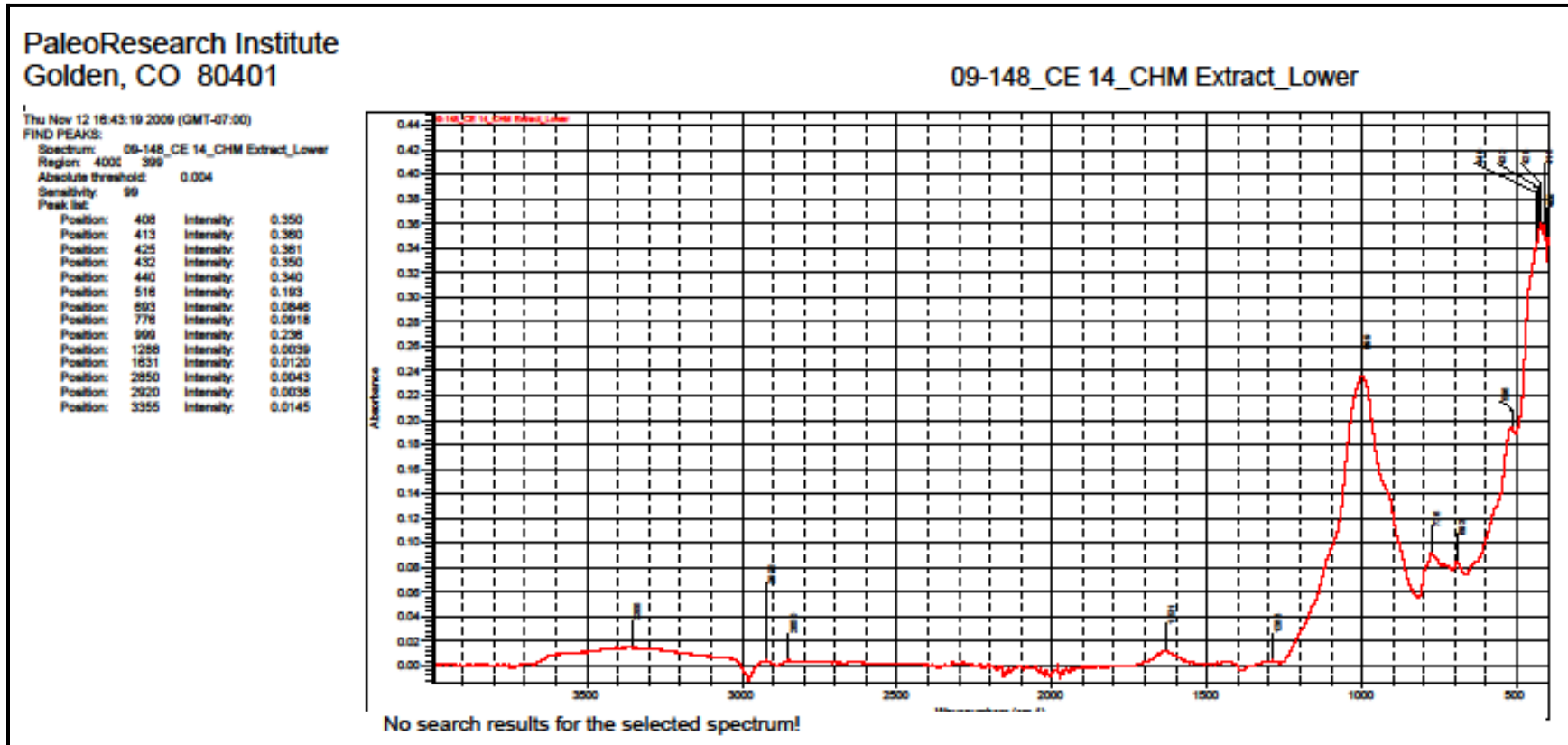
Sensitivity: 99

Peak list:

Position: 401	Intensity: 0.137
Position: 419	Intensity: 0.158
Position: 423	Intensity: 0.159
Position: 430	Intensity: 0.168
Position: 448	Intensity: 0.168
Position: 484	Intensity: 0.178
Position: 499	Intensity: 0.119
Position: 517	Intensity: 0.122
Position: 645	Intensity: 0.0423
Position: 694	Intensity: 0.0489
Position: 712	Intensity: 0.0681
Position: 778	Intensity: 0.0548
Position: 795	Intensity: 0.0515
Position: 840	Intensity: 0.0489
Position: 873	Intensity: 0.131
Position: 1009	Intensity: 0.141
Position: 1418	Intensity: 0.0038
Position: 1561	Intensity: 0.0044
Position: 1578	Intensity: 0.0044
Position: 1841	Intensity: 0.0041
Position: 1855	Intensity: 0.0038
Position: 2850	Intensity: 0.0028
Position: 2920	Intensity: 0.0041
Position: 3218	Intensity: 0.0043
Position: 3233	Intensity: 0.0047
Position: 3313	Intensity: 0.0054
Position: 3372	Intensity: 0.0056
Position: 3408	Intensity: 0.0053
Position: 3428	Intensity: 0.0050
Position: 3533	Intensity: 0.0045
Position: 3570	Intensity: 0.0040
Position: 3581	Intensity: 0.0037
Position: 3590	Intensity: 0.0039
Position: 3613	Intensity: 0.0040
Position: 3621	Intensity: 0.0037
Position: 3631	Intensity: 0.0032



No search results for the selected spectrum!



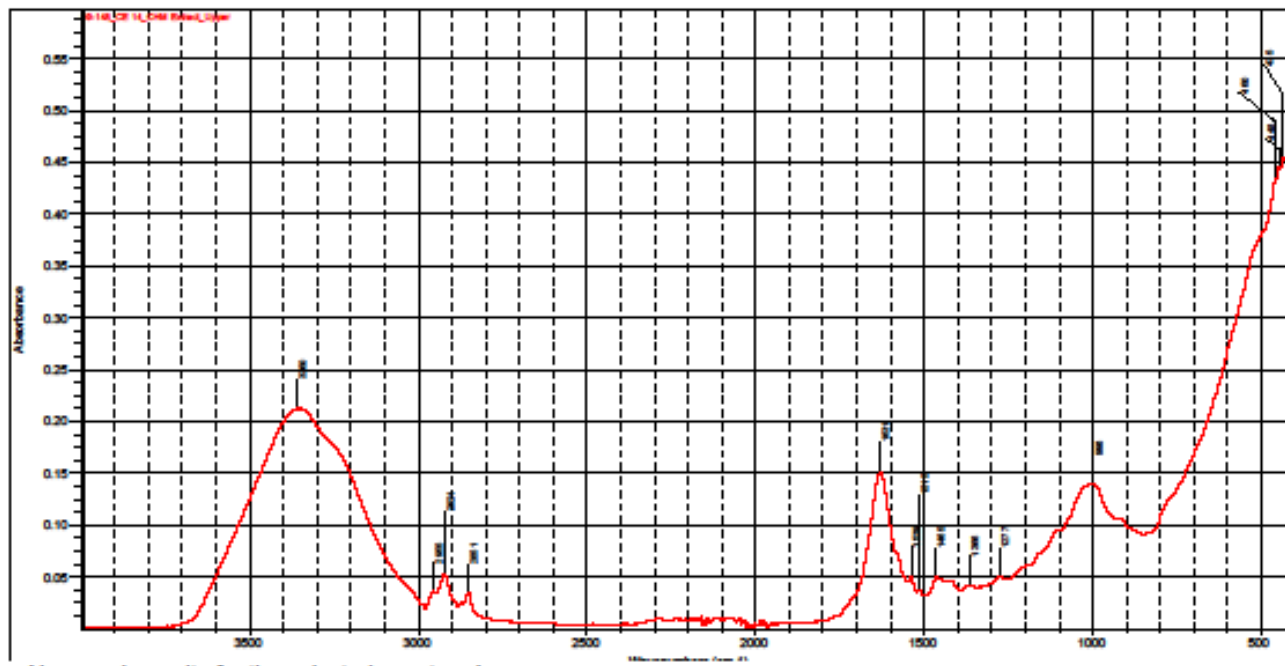
PaleoResearch Institute
Golden, CO 80401

09-148_CE 14_CHM Extract_Upper

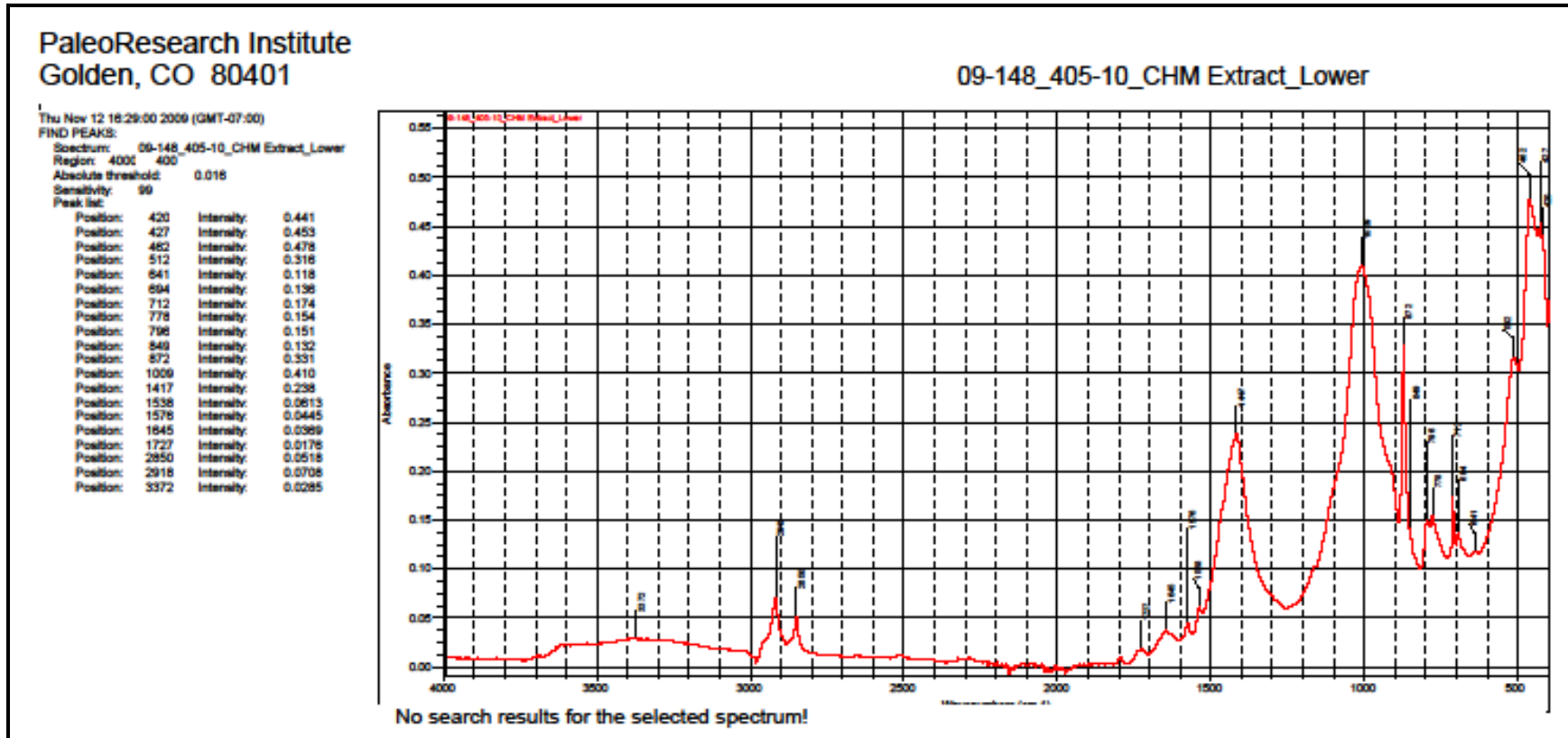
Thu Nov 12 16:43:49 2009 (GMT-07:00)

FIND PEAKS:

Spectrum:	09-148_CE 14_CHM Extract_Upper	
Region:	4000	399
Absolute threshold:	0.020	
Sensitivity:	99	
Peak list:		
Position:	405	Intensity: 0.471
Position:	418	Intensity: 0.475
Position:	435	Intensity: 0.456
Position:	448	Intensity: 0.445
Position:	480	Intensity: 0.434
Position:	908	Intensity: 0.140
Position:	1277	Intensity: 0.0502
Position:	1368	Intensity: 0.0423
Position:	1485	Intensity: 0.0503
Position:	1515	Intensity: 0.0378
Position:	1539	Intensity: 0.0510
Position:	1831	Intensity: 0.152
Position:	2851	Intensity: 0.0348
Position:	2921	Intensity: 0.0329
Position:	2955	Intensity: 0.0380
Position:	3360	Intensity: 0.213



No search results for the selected spectrum!



PaleoResearch Institute
Golden, CO 80401

Thu Nov 12 18:40:21 2009 (GMT-07:00)

FIND PEAKS:

Spectrum: 09-148_1129-10_CHM Extract_Lower

Region: 4000 400

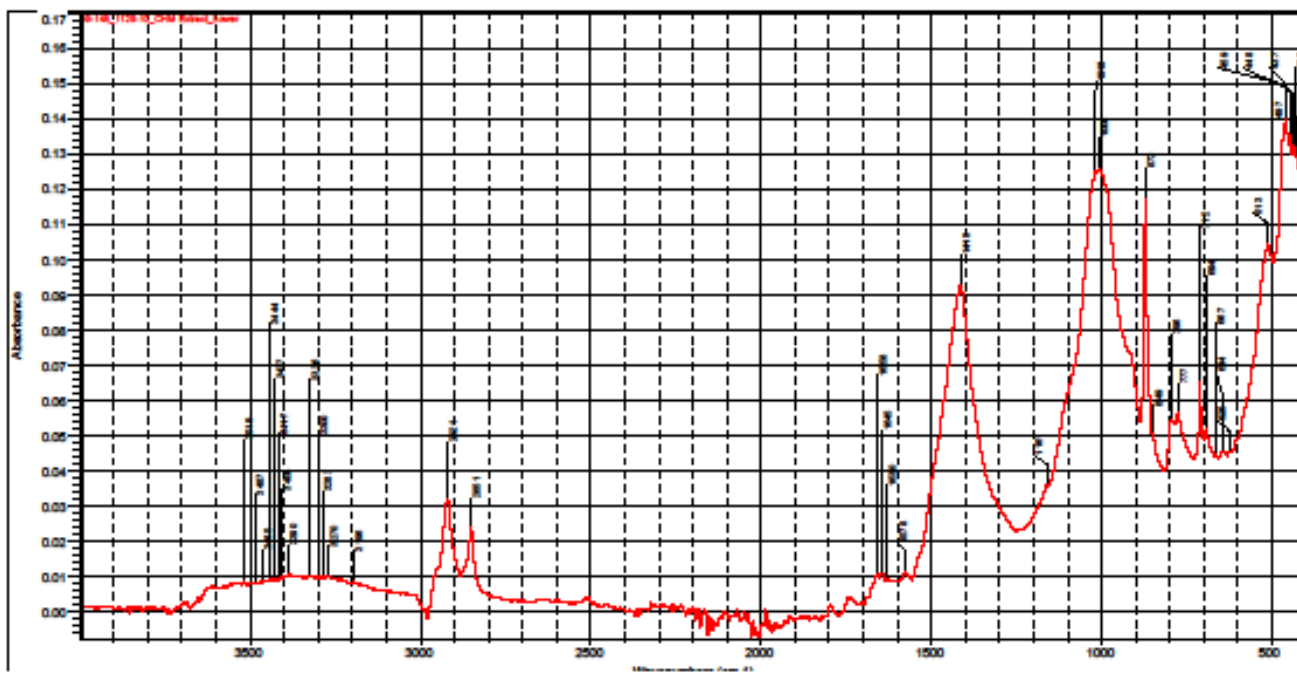
Absolute threshold: 0.008

Sensitivity: 99

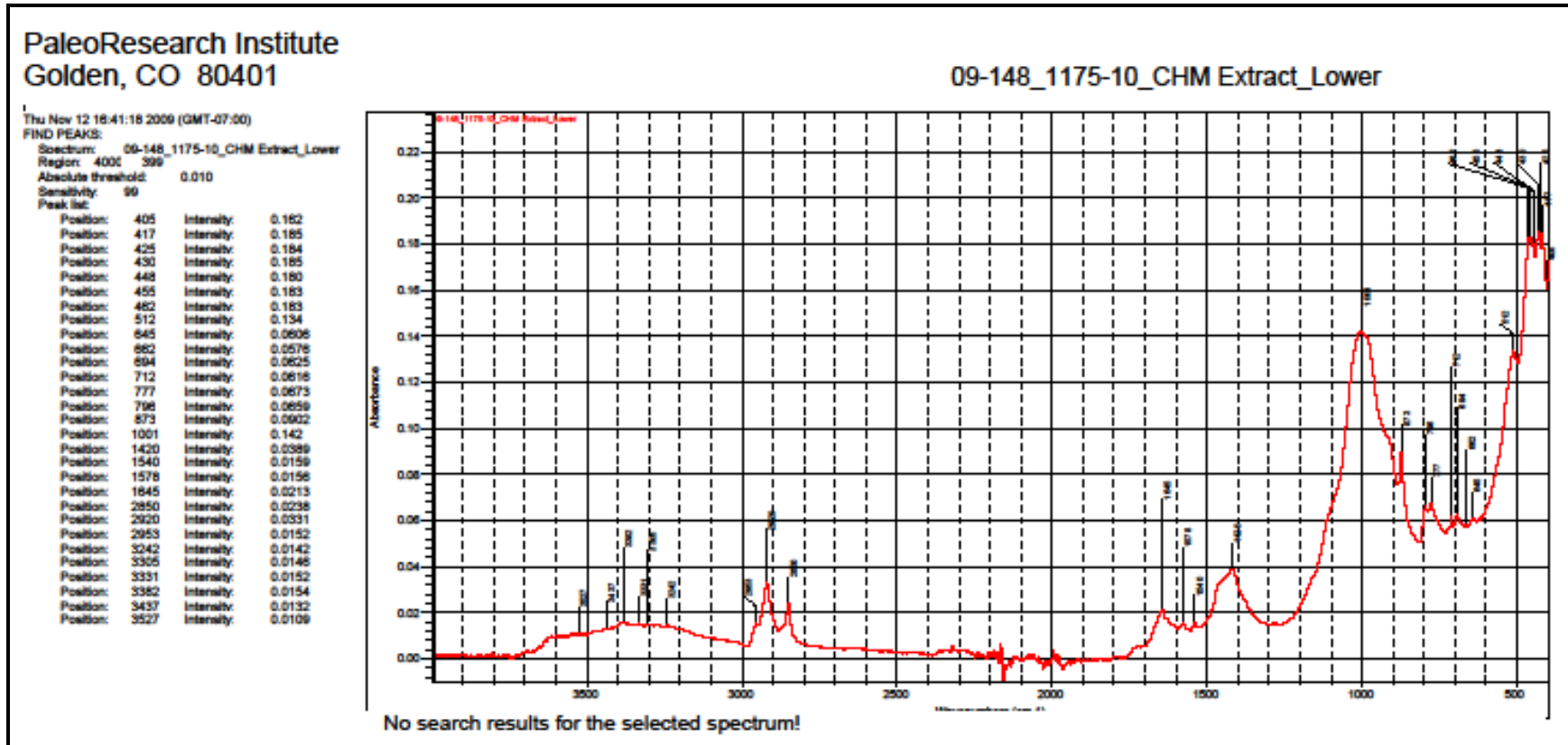
Peak list:

Position: 411	Intensity: 0.119
Position: 423	Intensity: 0.128
Position: 432	Intensity: 0.132
Position: 437	Intensity: 0.132
Position: 448	Intensity: 0.135
Position: 459	Intensity: 0.140
Position: 497	Intensity: 0.0999
Position: 513	Intensity: 0.105
Position: 625	Intensity: 0.0458
Position: 644	Intensity: 0.0458
Position: 667	Intensity: 0.0447
Position: 694	Intensity: 0.0524
Position: 712	Intensity: 0.0655
Position: 777	Intensity: 0.0598
Position: 796	Intensity: 0.0548
Position: 849	Intensity: 0.0502
Position: 872	Intensity: 0.118
Position: 1008	Intensity: 0.128
Position: 1018	Intensity: 0.125
Position: 1181	Intensity: 0.0361
Position: 1415	Intensity: 0.0931
Position: 1578	Intensity: 0.0113
Position: 1630	Intensity: 0.0097
Position: 1845	Intensity: 0.0110
Position: 1858	Intensity: 0.0106
Position: 2851	Intensity: 0.0240
Position: 2921	Intensity: 0.0325
Position: 3196	Intensity: 0.0088
Position: 3270	Intensity: 0.0102
Position: 3287	Intensity: 0.0101
Position: 3300	Intensity: 0.0101
Position: 3328	Intensity: 0.0102
Position: 3390	Intensity: 0.0105
Position: 3408	Intensity: 0.0098
Position: 3417	Intensity: 0.0097
Position: 3427	Intensity: 0.0094
Position: 3444	Intensity: 0.0095
Position: 3485	Intensity: 0.0089
Position: 3487	Intensity: 0.0083
Position: 3519	Intensity: 0.0088

09-148_1129-10_CHM Extract_Lower



No search results for the selected spectrum!

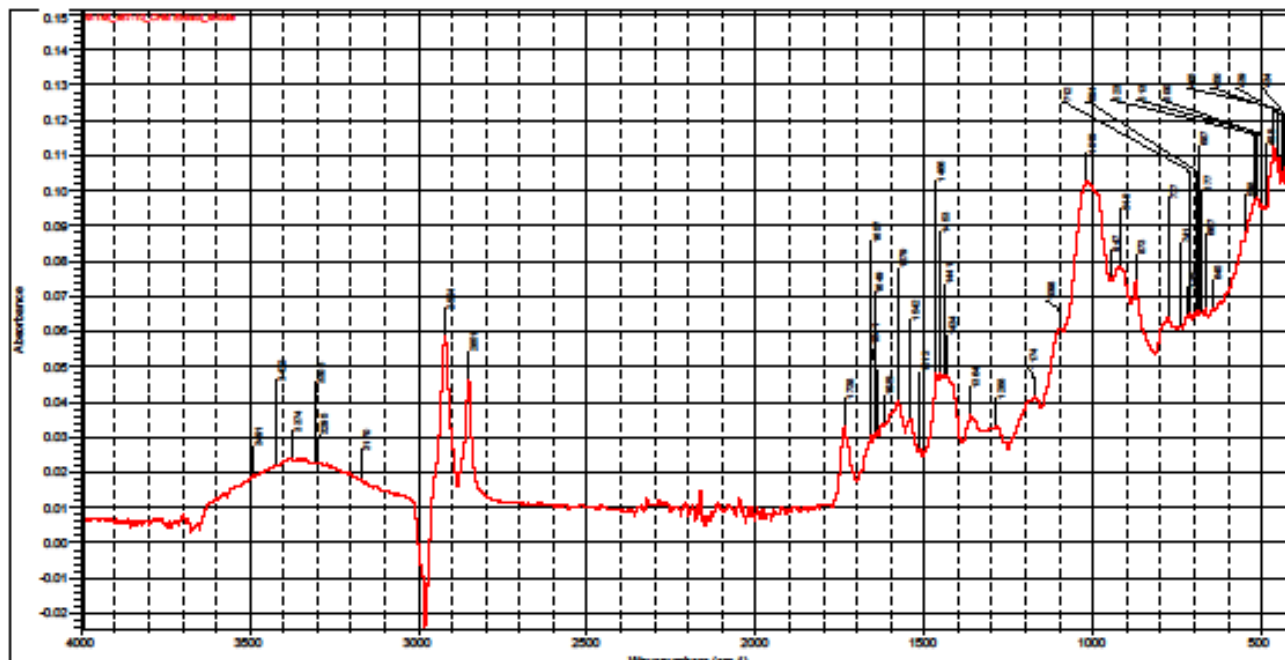


PaleoResearch Institute
 Golden, CO 80401

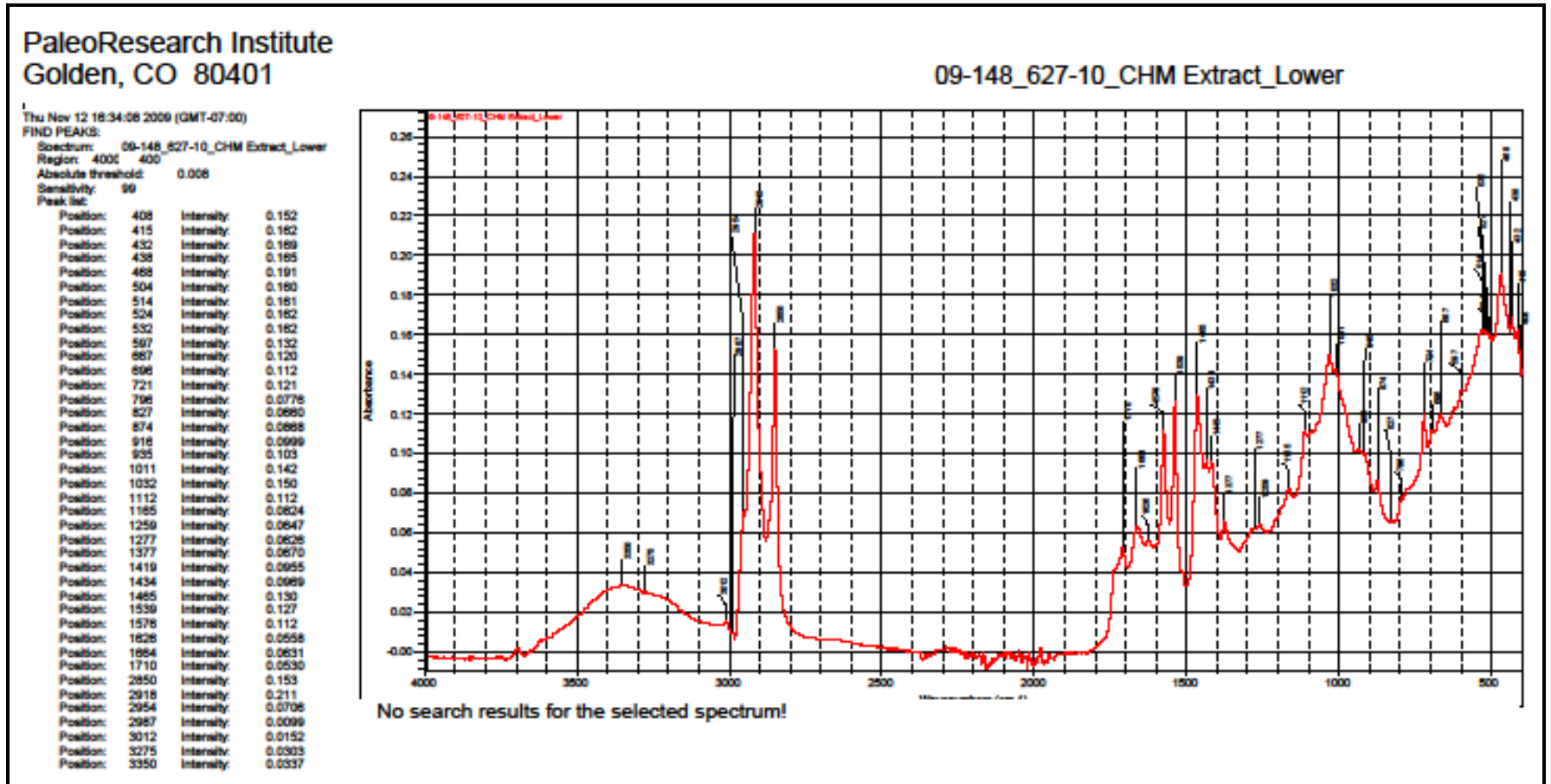
09-148_467-10_CHM Extract_Middle

Thu Nov 12 18:32:44 2009 (GMT-07:00)
 FIND PEAKS:
 Spectrum: 09-148_467-10_CHM Extract_Middle
 Region: 4000 400
 Absolute threshold: 0.017
 Sensitivity: 99
 Peak list:

Position	Intensity
403	0.0981
412	0.105
424	0.108
434	0.107
439	0.108
450	0.110
485	0.113
489	0.0951
500	0.0982
513	0.0982
523	0.0989
548	0.0898
645	0.0898
667	0.0895
677	0.0853
687	0.0857
694	0.0858
712	0.0855
719	0.0847
741	0.0818
777	0.0839
873	0.0743
919	0.0783
947	0.0752
1019	0.103
1098	0.0809
1174	0.0418
1288	0.0330
1384	0.0382
1434	0.0474
1441	0.0474
1453	0.0480
1488	0.0481
1513	0.0285
1542	0.0351
1579	0.0402
1619	0.0339
1641	0.0318
1649	0.0301
1657	0.0303
1738	0.0330
2851	0.0483
2921	0.0585
3170	0.0182
3295	0.0227
3308	0.0229
3374	0.0238
3422	0.0222
3491	0.0192



No search results for the selected spectrum!



PaleoResearch Institute
 Golden, CO 80401

09-148_452-10_CHM Extract_Lower

Thu Nov 12 16:30:33 2009 (GMT-07:00)

FIND PEAKS:

Spectrum: 09-148_452-10_CHM Extract_Lower

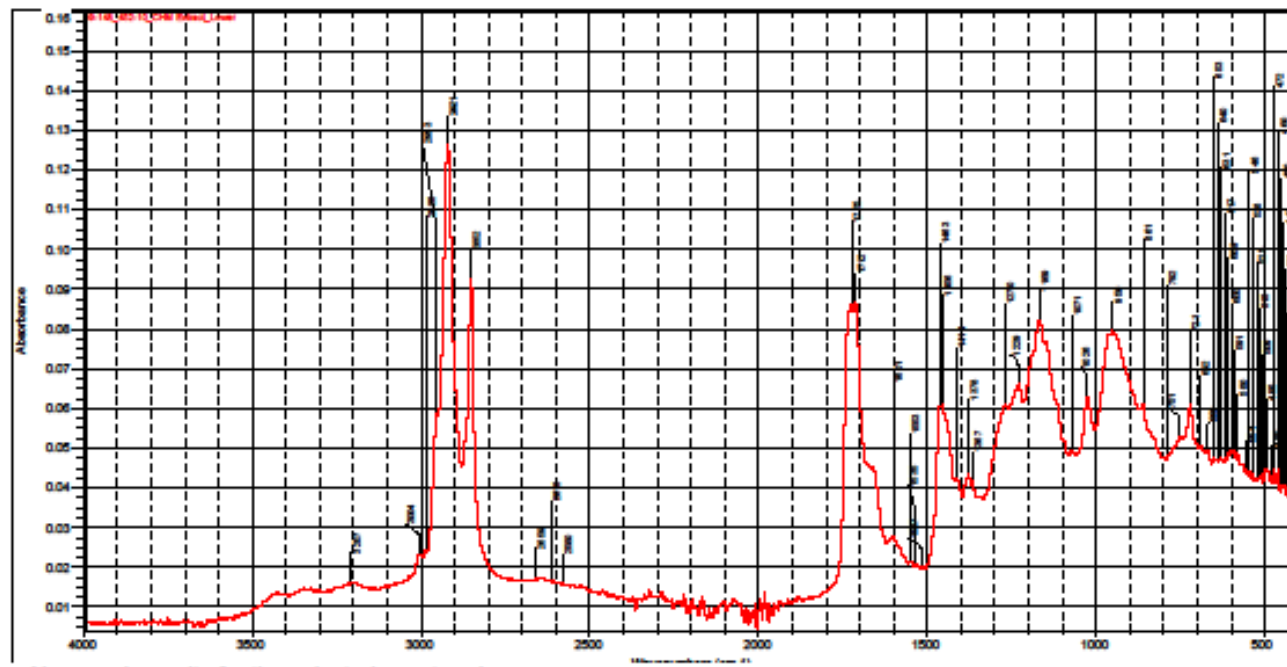
Region: 4000 400

Absolute threshold: 0.016

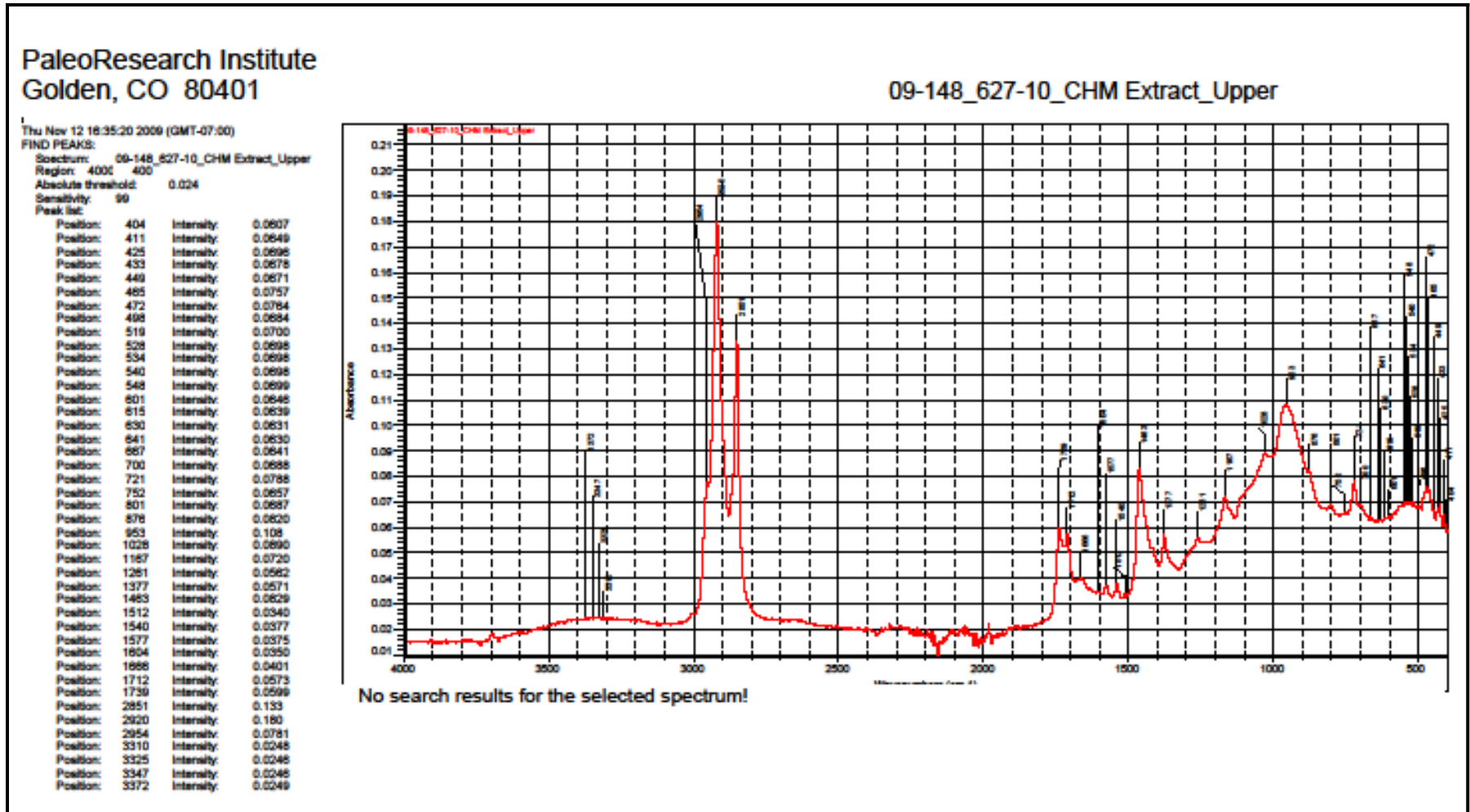
Sensitivity: 99

Peak list:

Position: 405	Intensity: 0.0419
Position: 411	Intensity: 0.0449
Position: 419	Intensity: 0.0449
Position: 431	Intensity: 0.0400
Position: 438	Intensity: 0.0406
Position: 443	Intensity: 0.0406
Position: 450	Intensity: 0.0410
Position: 460	Intensity: 0.0452
Position: 472	Intensity: 0.0451
Position: 480	Intensity: 0.0432
Position: 495	Intensity: 0.0447
Position: 509	Intensity: 0.0433
Position: 515	Intensity: 0.0432
Position: 525	Intensity: 0.0426
Position: 538	Intensity: 0.0438
Position: 548	Intensity: 0.0443
Position: 554	Intensity: 0.0445
Position: 580	Intensity: 0.0485
Position: 591	Intensity: 0.0494
Position: 600	Intensity: 0.0491
Position: 609	Intensity: 0.0487
Position: 617	Intensity: 0.0475
Position: 631	Intensity: 0.0473
Position: 640	Intensity: 0.0472
Position: 653	Intensity: 0.0476
Position: 689	Intensity: 0.0492
Position: 692	Intensity: 0.0506
Position: 721	Intensity: 0.0608
Position: 751	Intensity: 0.0530
Position: 792	Intensity: 0.0479
Position: 861	Intensity: 0.0611
Position: 950	Intensity: 0.0795
Position: 1026	Intensity: 0.0631
Position: 1071	Intensity: 0.0491
Position: 1169	Intensity: 0.0623
Position: 1229	Intensity: 0.0661
Position: 1270	Intensity: 0.0612
Position: 1367	Intensity: 0.0417
Position: 1376	Intensity: 0.0436
Position: 1414	Intensity: 0.0424
Position: 1456	Intensity: 0.0610
Position: 1463	Intensity: 0.0606
Position: 1517	Intensity: 0.0201
Position: 1535	Intensity: 0.0206
Position: 1553	Intensity: 0.0216
Position: 1601	Intensity: 0.0277
Position: 1712	Intensity: 0.0669
Position: 1725	Intensity: 0.0661
Position: 2580	Intensity: 0.0181
Position: 2615	Intensity: 0.0169
Position: 2659	Intensity: 0.0173
Position: 2652	Intensity: 0.0626
Position: 2621	Intensity: 0.127
Position: 2953	Intensity: 0.0587
Position: 2985	Intensity: 0.0246
Position: 3004	Intensity: 0.0234
Position: 3207	Intensity: 0.0162



No search results for the selected spectrum!

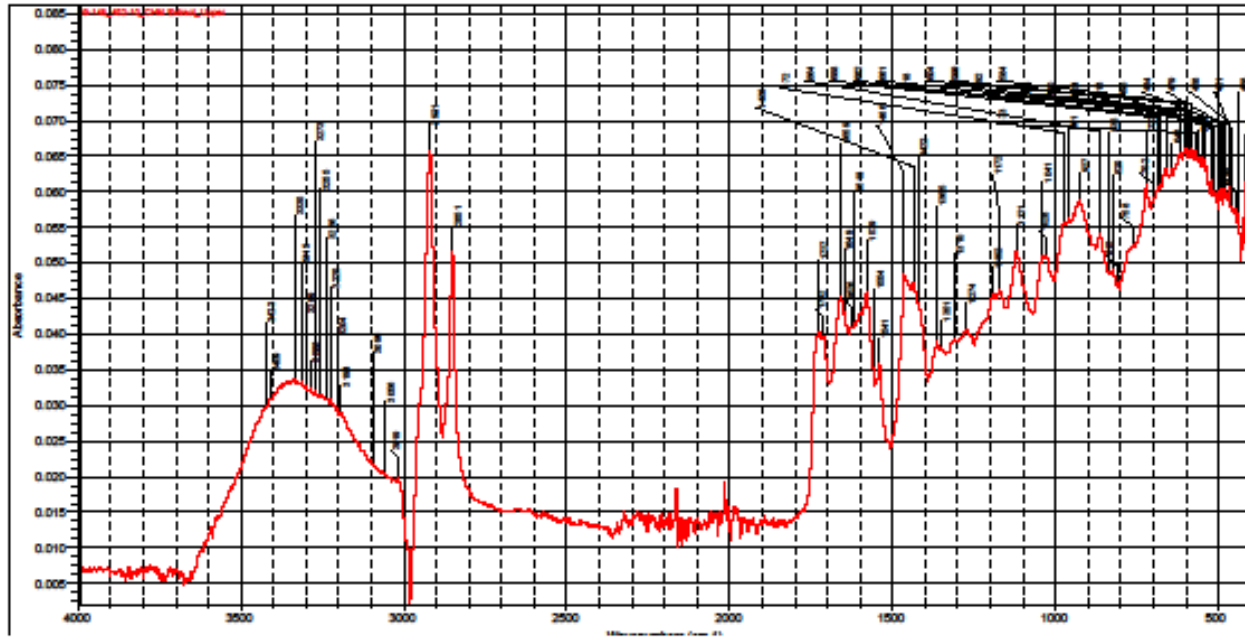


PaleoResearch Institute
Golden, CO 80401

09-148_452-10_CHM Extract_Upper

The Nov 12 10:31 AM 2009 (GMT-07:00)
FIND PEAKS:
Spectrum: 09-148_452-10_CHM Extract_Upper
Reaction: 4000 400
Absolute threshold: 0.0196
Sensitivity: 99
Peak list:

Position	Intensity
406	0.0593
418	0.0516
436	0.0570
448	0.0577
461	0.0578
486	0.0608
476	0.0566
484	0.0606
492	0.0604
513	0.0600
524	0.0617
542	0.0638
548	0.0647
590	0.0646
573	0.0656
594	0.0656
590	0.0654
596	0.0661
604	0.0660
618	0.0654
643	0.0633
661	0.0633
663	0.0606
686	0.0603
703	0.0586
723	0.0612
758	0.0526
813	0.0473
826	0.0460
832	0.0489
864	0.0541
927	0.0590
961	0.0564
973	0.0557
1038	0.0506
1041	0.0510
1121	0.0516
1173	0.0483
1192	0.0457
1274	0.0406
1310	0.0390
1351	0.0391
1382	0.0390
1423	0.0444
1436	0.0471
1486	0.0487
1541	0.0326
1554	0.0334
1576	0.0461
1616	0.0415
1628	0.0410
1646	0.0431
1686	0.0422
1712	0.0396
1721	0.0404
2021	0.0516
2821	0.0629
3016	0.0196
3056	0.0333
3096	0.0318
3194	0.0390
3204	0.0396
3222	0.0397
3236	0.0310
3252	0.0315
3271	0.0321
3296	0.0324
3296	0.0326
3312	0.0333
3332	0.0337
3426	0.0310
3421	0.0300



No search results for the selected spectrum!

This page intentionally left blank.